

AD-A037 223

SINGER CO BINGHAMTON N Y SIMULATION PRODUCTS DIV
AVIATION WIDE-ANGLE VISUAL SYSTEM (AWAVS). DESIGN ANALYSIS REPO--ETC(U)
APR 75

F/G 1/2

N61339-75-C-0009

UNCLASSIFIED

AWAVS-1

NAVTRAEQUIPC-75-C-0009-1 NL

1 OF 5
AD
A037223



AD A037223



Technical Report: NAVTRAEQUIPCEN 75-C-0009-1

AVIATION WIDE-ANGLE VISUAL SYSTEM (AWAVS)
DESIGN ANALYSIS REPORT (Study Report)

SINGER-Simulation Products Division
Binghamton, New York 13902

14 April 1975

Final Report for period September - December 1974

DoD Distribution Statement

Approved for public release;
distribution unlimited.



NAVAL TRAINING EQUIPMENT CENTER
ORLANDO FLORIDA 32813

NAVTRAEQUIPCEN 75-C-0009-1

GOVERNMENT RIGHTS IN DATA STATEMENT

Reproduction of this publication in whole or in part
is permitted for any purposes of the United States
Government.

UNCLASSIFIED

SECURITY CLASSIFICATION OF THIS PAGE (When Data Entered)

REPORT DOCUMENTATION PAGE		READ INSTRUCTIONS BEFORE COMPLETING FORM	
1. REPORT NUMBER NAVTRAEQUIPC 75-C-0009-1	2. GOVT ACCESSION NO.	3. RECIPIENT'S CATALOG NUMBER	
4. TITLE (and Subtitle) AVIATION WIDE-ANGLE VISUAL SYSTEM (AWAVS) / DESIGN ANALYSIS REPORT (STUDY REPORT)		5. TYPE OF REPORT & PERIOD COVERED Final Report September - December 74	
7. AUTHOR(s) VISUAL ENGINEERING DEPARTMENT SINGER-SIMULATION PRODUCTS DIVISION		6. PERFORMING ORG. REPORT NUMBER AWAVS-1	
9. PERFORMING ORGANIZATION NAME AND ADDRESS Singer-Simulation Products Division Binghamton, New York 13902		8. CONTRACT OR GRANT NUMBER(s) N61339-75-C-0009	
11. CONTROLLING OFFICE NAME AND ADDRESS Naval Training Equipment Center Orlando, Florida 32813		10. PROGRAM ELEMENT, PROJECT, TASK AREA & WORK UNIT NUMBERS Program Element 63720N Project W4308 Work Unit 4781	
14. MONITORING AGENCY NAME & ADDRESS (if different from Controlling Office) N4308 / N4308		12. REPORT DATE 14 Apr 75	13. NUMBER OF PAGES 427
		15. SECURITY CLASS. (of this report) Unclassified	
16. DISTRIBUTION STATEMENT (of this Report) Approved for public release; distribution unlimited.		15a. DECLASSIFICATION/DOWNGRADING SCHEDULE	
17. DISTRIBUTION STATEMENT (of the abstract entered in Block 20, if different from Report)			
18. SUPPLEMENTARY NOTES			
19. KEY WORDS (Continue on reverse side if necessary and identify by block number) Target Image Generator Large Screen Raster Computer FLOLS Fresnel Lens Optical Landing System Digital-Analog Background Image Generator Optical Probe Target Insetting Carrier Model Special Effects Generator TV Projector			
20. ABSTRACT (Continue on reverse side if necessary and identify by block number) This study report covers the analysis efforts performed on the research and engineering effort spent in developing feasible data by which to design the Aviation Wide Angle Visual System (AWAVS). The ten foot radius display screen system employs two real image large screen black & white TV projectors mounted behind and above the observer. Both a camera model image generator and a flying spot scanner image generator are employed for TV image along with a real image FLOLS generator.			

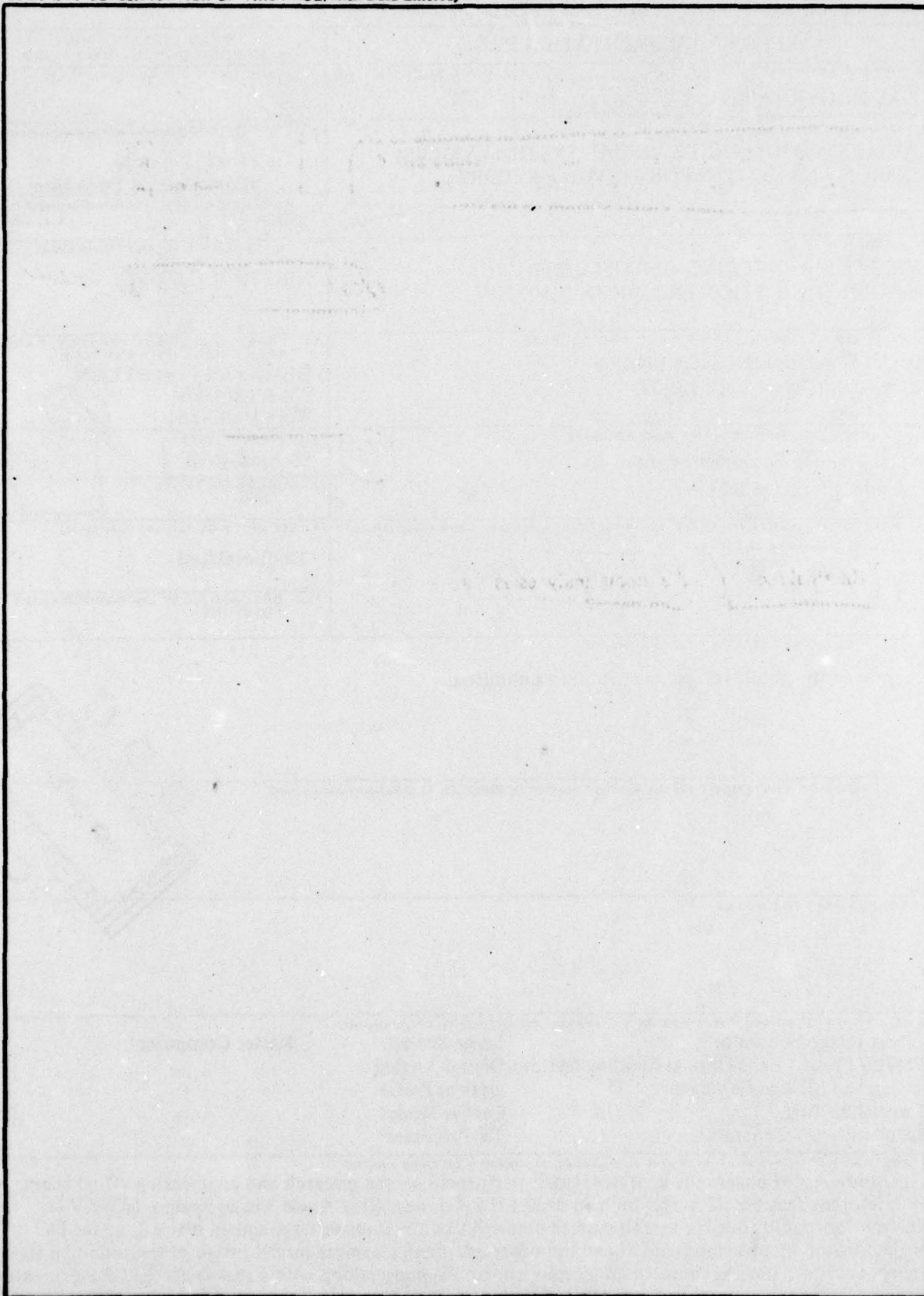
DD FORM 1 JAN 73 1473

EDITION OF 1 NOV 65 IS OBSOLETE

UNCLASSIFIED

SECURITY CLASSIFICATION OF THIS PAGE (When Data Entered)

SECURITY CLASSIFICATION OF THIS PAGE(When Data Entered)



SECURITY CLASSIFICATION OF THIS PAGE(When Data Entered)

PREFACE

This final technical report is generated in response to NTEC Contract N61339-75-C-0009 (DD 1423 item A001) and documents the study and design analysis effort that has been performed in achieving the technical requirements that have been specified for the Aviation Wide Angle Visual System (AWAVS).

The report describes and analyzes the original concept and alternate approaches to meeting the requirements for image generation and display formatting and providing additional system flexibility. The impact of the various technical approaches, each upon one another, is discussed and evaluated. Determinations of the overall system performance and recommendations as to which approaches should be pursued are made and justified. Detailed analyses of anticipated problem areas such as servo drive and control, target inseting and projected scene keying are presented together with a rigorous mathematical treatment for all areas of design.

The provisions and capabilities for system expansion that have been included in the design in order to increase the scope of simulation and training value of the ultimate device are also described.

The final section of the report analyzes as a total system, the preferred alternate approaches and describes the recommended implementation.

ACCESSION for	
NTIS	White Section <input checked="" type="checkbox"/>
DTC	Buff Section <input type="checkbox"/>
UNANNOUNCED	<input type="checkbox"/>
JUSTIFICATION	
BY	
DISTRIBUTION/AVAILABILITY CODES	
Dist.	AVAIL. and/or SPECIAL
A	

TABLE OF CONTENTS

Section		Page
I	INTRODUCTION	
	General Description	15
II	TARGET IMAGE GENERATOR	
	Methods Considered	17
	Proposed Method	17
	Alternate Methods	17
	Target Model Board Assembly	17
	Model Scale Factor	17
	Target Model Illumination	18
	Target Model Illumination System	21
	Carrier Deck Lighting	21
	Carrier Lights	24
	Target Model Motion	27
	Target Optical Probe	27
	Target Television Camera	39
	Target Camera Gantry	45
	X Drive	45
	Y Drive	45
	Z Drive	45
	Performance Requirements for X, Y, Z	46
	Target Model Board Assembly	54
	Target Television Camera	55
III	TARGET PROJECTOR	
	Methods Considered	58
	Target TV Projector	58
	Target Projector Optics	63
	Target Projector Lens	67
	Target Projector Gimbal	76
	Target Projector Support Structure	76
	Resolution	80
IV	FLOLS (FRESNEL LENS OPTICAL LANDING SYSTEM)	
	Methods Considered	82
	Alternate Methods	85
	FLOLS Model	87
	FLOLS Motion System	87
	X, Y Displacement Servo Requirements	90
	Zoom Servo Requirement Determination	92
	FLOLS Roll Servo Requirement	92
	FLOLS IRIS Servo Requirements	92
	FLOLS Registration of Carrier	93

TABLE OF CONTENTS (Cont)

Section	Page
IV (Cont) FLOLS Optics	94
Optimization Of Fiber Illumination	99
Condenser-Arc Lamp Optimization	100
Resolution	102
FLOLS Luminance	102
Range Simulation	105
FLOLS Image Movement	106
FLOLS Support Structure	107
Alternates	108
Closed-Loop Probe to Model	108
Light-Emitting Source With Position-Sensitive Detector	110
V BACKGROUND IMAGE GENERATOR	
Methods Considered	112
Proposed Method	112
Alternate Methods	112
Digital-Analog Raster Computer (DARC)	112
FSS Raster Shape Derivation	115
Raster Shapes	119
FSS. DARC Functional Hardware	134
Flying-Spot Scanner System	136
Deflection Amplifier	136
Cathode Ray Tube	136
Linearity Circuits	136
Remaining Circuits	136
Wave Pattern Film Transparency	136
System Scaling	140
Background Optics	140
Signal Detection and Processing	142
Flight Envelope	142
Background Image Generator Modulation Transfer Function	144
Flying-Spot Scanner Lens (MTF ₄)	145
BIG System Visual Resolution	148
Effects of Contrast Enhancement of Film	155
Alternates	157
Altitude Cues	157
Velocity Cues	165
Synthetic Wake Generation	166
VI BACKGROUND PROJECTOR	
Methods Considered	169
Proposed Method	169
Alternate Methods	170

TABLE OF CONTENTS (Cont)

Section	Page
VI (Cont)	170
TV Projector	170
Projector Optics	178
Background Projector Support Structure	186
Background Image System MTF Analysis	187
BIG System MTF Analysis	187
Alternates	187
Background TV Projector	187
VII	
DISPLAY SCREEN	
Methods Considered	189
Proposed Method	189
Alternate Methods	189
Display Screen Details	189
Screen Gain	190
VIII	
SERVO SYSTEMS	
Methods Considered	191
Proposed Method	191
Alternate Methods	191
Model Servos	191
Probe Servos	193
Gantry Servos	195
FLOLS ΔX , ΔY Displacement Servos	196
FLOLS Zoom Servo	196
FLOLS Iris Control	198
Target Projector Servo Systems	198
IX	
TARGET INSETTING	
Methods Considered	199
Proposed Method	199
Alternate Methods	199
Proposed Target Insetting Design	199
Method of Blanking	199
System Tolerance	199
Analog Elliptical Blanking	200
Digital Elliptical Blanking	203
Elliptical Equation	206
Implementation	207
Error Terms On Video Insetting	208
Assumption	209
Error Analysis	211
Mapping Errors	211
Time and Temperature Projector Mapping Errors	211

TABLE OF CONTENTS (Cont)

Section		Page
IX (Cont)	Target Projector Servo Pointing Error	213
	Insetting Method	214
	Summary	216
	Alternates	217
	Background Seascape Scanning	217
X	MATHEMATICAL MODELS*	
	Methods Considered	223
	Summary	223
	Software System Flow Chart	227
	Discussion of Frames of Reference	227
	Target Image Generator	231
	Overall Description	231
	Carrier Model Drive Signal Module	232
	Wake Disk Drive Signal Module	233
	Gantry Drive Signal Module	236
	Probe Drive Signal Module	239
	Camera Raster Shaping Module	240
	Target Projector Optics	242
	Overall Description	242
	Point of Interest Selection	242
	Target Projector Optics Drive Signal Module	244
	FLOLS	245
	Overall Description	245
	Meatball Drive Signal Module	245
	Wave-Off Lights Drive Signal Module	246
	Cut Lights Drive Signal Module	246
	Optics Drive Signal Module	246
	Background Image Generator	247
	Overall System Description	247
	Desired FSS Raster Shapes	247
	BIG Drive Signal Development	248
	Target Insetting	248
	Determination of Desired Target Projector Video Blanking	249
	Special Effects Generator	251
	Overall System Description	251
	Visibility Effects Drive Signal Module	251
	Other Program Modules	252
	Aircraft Position and Altitude Module	252
	Ground Track Module	252
	Carrier Simulation	253
	Arresting Hook Module	253

TABLE OF CONTENTS (Cont)

Section		Page
X (Cont)	Arrested Landing Module	254
	Crash Conditions Module	255
	Catapult Launch Module	256
XI	SPECIAL EFFECTS GENERATORS	
	Methods Considered	257
	System Block Diagrams	257
	Principle of Operation	260
	Operational Controls	262
	Conclusion	262
XII	FUTURE ADDITION	
	Requirements	263
	Air to Air Combat	263
	Formation Flying	262
	Shore-Based Airport Operation	264
	Air-to-Ground Weapon Delivery	265
	Camera Model Ground Image Generators	266
	Application	268
	Limitations	268
	Camera Model (Gimballed Aircraft Model)	268
	TV Scanned Vamp	269
	Scanned Transparency	269
	Electronic Image Generation	269
	Computer-Generated Imagery	269
	Calligraphic Day/Nite Visual System	270
	Synthetic Terrain Generator	270
	Haze/Horizon	270
	Sun Image Generator	270
	VASI Generator	270
	Background Projector	270
	Inset Projector	271
XIII	SYSTEM CONTROLS	
	Methods Considered	275
	Location and General Arrangement	275
	Instructor Station Controls and Displays	276
	Servo Systems	276
	Operation and Maintenance	276
XIV	RECOMMENDED SYSTEM	
	General Description	281
	Target Image Generator	281
	Target Projector	281
	FLOLS	281
	Special Effects Generator	282

TABLE OF CONTENTS (Cont)

Section	Page
XIV (Cont) Target Image Generator	282
Target Model Board Assembly	282
Perspective Distortion Analysis	282
Scale Factor of Model	289
Range vs. Altitude for Correct Aspect Angle	289
Wake Cutoff Analysis	295
XYZ Performance Requirements	301
Deck Lighting	301
Model Illumination	302
Television Line Scan Rates	307
Target Television Camera	309
Conventional Probe	321
Target Projector System	325
Eidophor Light Output	325
Target Project Zoom Optical Invariant	327
Target Projector System Optics	327
Television Line Scan Rates	332
Target System Resolution	332
FLOLS	336
FLOLS Optics	336
FLOLS Range Simulation	341
Light-Emitting Source with Position-Sensitive Detector	341
Development of Simulation	352
FLOLS Tracker Light-Emitting Source	354
Background Image Generator	357
Raster Reset	357
Cathode Ray Tube	357
Film Plate	359
Wake Image Generation	368
Method of Implementation	368
For the Obscured-Target, Visible Near-End of Wake Condition	374
Error Involved With WIG Attachment	375
Projected Scene Keying	377
System Design	377
TV Camera and Optical Considerations	379
Scene-Keying Camera Image Analysis	382
Target Insetting Error Summary	391
Smearing Effects Due To Isocon Lag	391
Comparator Reference Levels Without System Shading Considerations ...	394
Shading Effects	394
Comparator Reference Levels For Raster Edge	395
Total System Comparator Reference Levels	395
Signal Detection for the Carrier Edge	397
Summary on SKI	399

TABLE OF CONTENTS (Cont)

Section		Page
XIV (Cont)	Special Effects Generator	399
	Target SEG	399
	Generation of Sea Merge	400
XV	CONCLUSIONS	
	Target Image Generation	402
	Background and Wake Image Generation	403
	Special Effects Generation	403
	Target Scene Keying	403
XVI	RECOMMENDATIONS	404
XVII	SUMMARY	
	Target Image Generator	405
	Target Model	405
	Target Model Illumination	405
	Target Model Motion	405
	Target Optical Probe	405
	Target Television Camera	405
	Target Camera Gantry	405
	Target Projector	405
	Projector	405
	Target Projector Lens	406
	Target Projector Gimbals	406
	FLOLS (Fresnel Lens Optical Landing System) Image Projector	406
	FLOLS Motion System	406
	FLOLS Illumination	406
	Background Image Generator	406
	Image Content	407
	Background Projector	407
	Background Projector Lens	407
	Background Projector Support Structure	407
	Display Screen	407
	Servo Systems	407
	Target Insetting	407
	Math Model	408
	Special Effects Generator	408
	Future Additions	408
	REFERENCE MATERIAL	
	Reference Footnotes List	409
	List of Abbreviations	412
	Symbol Dictionary	413
	Distribution List	

LIST OF ILLUSTRATIONS

Figure		Page
1	Model Board Assembly	19
2	Disc and Model Dimensions	20
3	Lighting Fixture Configuration	22
4	Carrier Light System	23
5	Plan View of Flight Deck With Required Lights	25
6	Prismatic Fibre Light Distribution	26
7	Deck Edge Light	28
8	Vertical "Dropline" Light	28
9	Relationship of Geometrical Blur B to Defocus δ	30
10	Required Probe MTF For 5% Target System Response	32
11	MTF vs Spatial Frequency	33
12	System Resolution vs Geometrical Blur	34
13	Probe Geometrical Blur & System Resolution vs Distance From Eye Point	36
14	Geometrical Blur vs Range to Touchdown	38
15	Vidicon Modulation Transfer Function	41
16	Vidicon Faceplate Illumination Characteristics	42
17	Digital-Analog Raster Computer Functional Diagram	44
18	X_G, Y_G , to X_C, Y_C Relationship	48
19	Simulated Straight-Line Fly-By Trajectory	49
20	Target Projector Optical System	59
21	Projector Pointing Straight Ahead	60
22	Projector Center-Set, -50° AZ., -10° EL.	60
23	Projector Center-Set, -50° AZ., $+30^\circ$ EL.	61
24	Eidophor Modulation Transfer Function	62
25	Total Scan Lines On 3 x 4 Raster	64
26	Target Projector Optics Schematic	68
27	Aperture Geometry	70
28	Bar Mirror and Relay Lens Relationship	70
29	Extreme Ray-Schematic	71
30	Illustration of Tan θ_4 Equation	74
31	Telecentric Lens Pair	75
32	Exit Aperture Location	77
33	Azimuth and Elevation Drive	78
34	Display System Side View	79
35	FLOLS and Target Projector Optics	83
36	FLOLS Optical System Schematic	84
37	FLOLS Model Board	86
38	FLOLS Image Generator	88
39	Tracking Angle/Rate	90

LIST OF ILLUSTRATIONS (Cont)

Figure		Page
40	FLOLS Optics	95
41	Collimating Lens Aperture Calculations	98
42	Collimating Lens Data for Calculation	98
43	FLOLS Collimating and Field Lens Schematic	100
44	Model Board With Meatball Lights	101
45	FLOLS Lamp and Condensing Lens Schematic	101
46	FLOLS Image Generator	103
47	FLOLS Optical Chain	108
48	Simplified System To Point Probe At FLOLS Board	109
49	Probe-Pointing System, Simplified	110
50	Background Image Generator	113
51	Background Projector, Position 2	120
52	Required Raster for Position 1	126
53	FSS DARC Functional Block Diagram	135
54	Flying-Spot-Scanner System	137
55	Tentative Spectral Energy Distribution for LP202 Phosphor	141
56	Background Optics Schematic	141
57	Scanner Rectification	142
58	Resolution Improvement/Nadir Requirements Comparison	143
59	Background Image Generator Modulation Transfer Function Flow Diagram	145
60	Cascaded Results of f(MTF) Equation	146
61	Resolution On CRT Face of Film	146
62	Modulation Transfer Function of Cathode Ray Tube Spot	147
63	Resolution, FSS Film System (MTF _B)	149
64	Resolution Requirements Relative to Visual Dimensions	150
65	Background Image Generator System Revolution Vs. MTF	153
66	Signal Processor System Background Image Generator	154
67	Enhanced Video Effects	156
68	Angle For Nadir Vs. Aircraft Alt and Film Diameter, 25-Ft. Waves	158
69	System Resolution Vs. MTF, @ 156 ft.	162
70	System Resolution Vs. MTF, @ 100 Ft.	163
71	System Resolution Vs. MTF, @ 81 Ft.	164
72	AWAVS Display System	171
73	Projector System MTF	173
74	Image Plot for Projector Position No. 1	174
75	Image Plot for Projector Position No. 2	175
76	Screen FOV For Projector Position No. 2	176
77	Eidophor MTF Data	177
78	Light Output and Total Scan Lines Relationship	177
79	Projector Lens Axis Level	180
80	Projection Lens Axis Tilted Down	180
81	Projector Position No. 1	181

LIST OF ILLUSTRATIONS (Cont)

Figure		Page
82	Position No. 1 With Azimuthal Rotation	183
83	Observer's Field In Azimuth and Elevation	184
84	Image Plot On Projector Raster	185
85	Background System	188
86	Typical Model Servos Signal Flow Diagram	192
87	XYZ Servo Signal Flow Diagram	197
88	ΔX , ΔY Displacement Servo	197
89	Simple Analog Circular Blanking Circuit Function Block Diagram	201
90	Error Terms in Figure 93 Circuit	202
91	FOV Elliptical Blanking Block Diagram	204
92	A Video Signal	205
93	Time Domain Ellipse on X-Y Plane	205
94	Video Blanking	206
95	Simple Video Chopper Circuit	207
96	Position of Projector Relative to the Display Screen	210
97	System Mapping Error	212
98	A Simple Blanking Circuit	215
99	Worst Case Video Blanking Without Delay Circuit	216
100	Insetting of Seascape Along The Ellipse	217
101	Typical S-20 Spectral Response	219
102	Visual Response	219
103	Possible Conditions	222
104	Blanking Circuit	222
105	AWAVS Software System Flow Chart	229
106	Aircraft Position and Altitude Module	252
107	Ground Track Module	252
108	Carrier Simulation Module	253
109	Arresting Hook Module	253
110	Arrested Landing Module	254
111	Crash Conditions Module	255
112	Catapult Launch Module	256
113	Special Effects Generator, Simplified Block Diagram	257
114	Visibility and Special Effects Generator Block Diagram	259
115	AWAVS Display System, Future Addition	273
116	Instructor Station Panel	277
117	Model Board Assembly, Corrected View	283
118	Model vs. World Carrier Dimensions Comparison	284
119	Probe Slant Range vs. Slant Range Sim.	292
120	Persp. Error & Disp. Reso. vs. Slant Range	293
121	Max. Altitude vs. Slant Range	294
122	Carrier Wake and Field of View	300
123	Definition of Variables for Illumination Program	304
124	Lighting Configuration	305

LIST OF ILLUSTRATIONS (Cont)

Figure		Page
125	Illumination Levels	306
126	Target Image Generator Television Functional Diagram	308
127	Camera Raster Plots	310
128	Spot Size vs. Resolution	319
129	Camera Modulation Transfer Function	322
130	Light Output vs. Aperture Size	326
131	Projector Optics	329
132	AWAVS Target Projection System MTF	333
133	Uniform Screen Illumination	334
134	Cross-Screen Reflectance Measurement Experiment	336
135	FLOLS Optics (Corrected)	337
136	Probe Pointing System Simplified	343
137	Optical Probe Tracking of IR Source, Block Diagram	344
138	Light Source Transfer Function	346
139	Illustration of Quadrature Logic	347
140	Combining M+ and M- Functions	348
141	Deadband	348
142	Block Diagram for Computer Simulation	349
143	Computer Simulation	350
144	Error Plot For Sweep of 2700 Arc-Min/Sec Deadband of ± 6 Arc-Min	351
145	Probe Friction Level	352
146	Representation of Probe Friction Level	353
147	Simulation of Gantry Velocity Input	353
148	Comparison of Two Light Sources	355
149	Raster Reset BIG Block Diagram	358
150	BIG Film Plate	359
151	Angle From Nadir vs. Aircraft Altitude	363
152	Resolution of Film Referenced to CRT Face	365
153	Carrier Circling Pattern	367
154	BIG and WIG Coverage In Sea Plane	370
155	Wake Transparency	371
156	Example of Plotted Digitized Points	373
157	Algorithm to Find "Stub" Wake Corner Point	373
158	Wake Attachment Zone Box	376
159	Display Configuration	378
160	Spectral Characteristics of Various Display Components	379
161	Typical Transfer Characteristic	384
162	Typical Signal to Noise-in-Signal Ratio as a Function of Faceplate Illuminance or Irradiance From Flux Levels Within a Given Scene. (Beam Adjustment Fixed at 2 x Knee Setting)	384
163	Day Signal & Noise Levels and Discriminator	387
164	Dusk Signal & Noise Levels and Discriminator	387
165	Residual Signal (Lag) Characteristic of Isocon Image Tube	392
166	Keying Camera Active Region	394
167	Pictorial Representation of Table 39	396
168	Block Diagram of Signal Detection	398
169	Projected Dot Sampling	398
170	Error Sampling with Mini-Raster Generator	398
171	Target Image SEG	400
172	Background Image SEG	401

LIST OF TABLES

Table		Page
1	Carrier Model Motions Required	27
2	AWAVS Television Camera Characteristics Summary	40
3	Slant Range Versus Zoom	47
4	Gantry Positions, Velocities, and Accelerations	51
5	Values of X_G , ϕ , $\dot{\phi}$	53
6	Scan Line Trade-Off Study	56
7	FLOLS Zoom Focal Length And Iris Size Relationships	66
8	Net Lens Transmission	75
9	Basis of MTF Estimates	80
10	Component and System MTF On-Axis, 100 MM Probe Altitude	81
11	Scanning Trade Off	81
12	FLOLS Servo Requirements	89
13	Component Estimated Transmission Value	105
14	FLOLS Zoom and Iris Change	107
15	State of Sea Description	138
16	Scan Line Data	187
17	Probe Req'd Performance (Estimated)	194
18	FLOLS Servo Requirements	198
19	Target Projector Servo Requirements	198
20	Required Cues For Image Generators	267
21	Instructor Station Controls and Indicators	278
22	Probe Parameters vs. Slant Range Simulated	290
23	Display Parameters vs. Slant Range Simulated	291
24	Viewing Angles	297
25	Field of View	299
26	Examples of Gantry Performance Requirements	301
27	Region Area vs. Luminosity	327
28	Comparison of Available Zoom Lenses	328
29	FLOLS Zoom	342
30	Simulation Results	352
31	Raster Reset BIG Design Goals	361
32	X-Y Table Performance	366
33	Summary of Scene Keying Errors	375
34	Summary of WIG Attachment Errors Under Dynamic Conditions	377
35	Static Errors For WIG Attachment	377
36	Summary of Errors (First Detection Criteria)	390
37	Target Insetting Error Summary	392
38	Signal Current Vs. Residual Signal and S_B	393
39	Shading Data Associated With SKI	394
40	Signal Current (I_S) Vs. S_B For the Edge of the Raster Plane	395
41	Comparator Reference Levels	397

SECTION I

INTRODUCTION

GENERAL DESCRIPTION.

The visual simulation system described herein is in response to the requirements established for the Aviation Wide-Angle Visual System (AWAVS). The system provides the pilot with a realistic view of an external scene which responds to the simulated operation of the aircraft, and enables the following flight tasks to be accomplished:

- 1) Circling carrier traffic patterns under daylight, dusk, and night conditions.
- 2) Circling carrier arrested landing under daylight, dusk, and variable ceiling conditions.
- 3) Catapult takeoff and bolter under daylight, dusk, and variable ceiling conditions.

The visual system will be designed in such a way that, without modification of the display system, additional image generation equipment can be added to simulate the following:

- 1) Shore traffic patterns under day, dusk, and night conditions.
- 2) Approaches to, landing on, and takeoff from a runway, under day, dusk, night, and variable ceiling conditions.
- 3) Night touch-and-go landings on a runway under variable ceiling conditions.
- 4) Air-to-air combat.
- 5) Air-to-ground weapon delivery.
- 6) Formation flight.

On a single wraparound spherical screen must be combined the relatively bright images of a televised wide-angle seascape, a televised very-high-quality "area-of-interest" carrier and wake, and a high-brightness FLOLS presentation, in color. The detailed performance requirements and specifications structured about these fundamental requirements function in an interlocking and mutually-consistent manner so as to impose rigorous demands on the character and behavior of these images. Moreover, the impact of many of the AWAVS specifications upon the implementation of subsidiary system functions (e.g., FLOLS/carrier image registration, image inseting, etc.) requires design sophistication as much as or even more than implementing the fundamental functions noted earlier. Indeed, because of the specified aspects of some of these secondary system functions, it would be dangerously easy to stray from the central purpose of the AWAV system, which is to generate and present to the eye a carrier image of outstanding quality, with the ability to preserve that quality through a very large dynamic range, and with a dynamic motion performance (both translational and rotational) capable of faithfully reproducing the characteristics of a broad range of high-performance aircraft.

NAVTRAEQUIPCEN 75-C-0009-1

A close examination of Table 1 in paragraph 3.7.4.3 of Specification 212-102 is very revealing in this regard. Table 1 specified carrier image resolution in TV lines as a function of slant range. The conversion of TV resolution to angular resolution, based on an assumed carrier length of 1039 feet, results in the following tabulation:

Target Range (NM)	Minimum Number of Resolution Elements TV Lines	Equivalent Angular Resolution Arc-Minutes Per TV Lines
0	700	5.15
1.5	600	0.65
2	400	0.74
3	300	0.64
4	200	0.72
6	150	0.64

It is obvious from this representation of Table 1 that the angular resolution called for constitutes a design challenge. To meet this challenge, Singer's design places primary emphasis on achieving the resolution goals for the target and background system, and avoids, in its implementation of secondary functions, the use of any techniques inimical to the displayed target image.

As shown in this report, in order to meet the specified goals and the depth of focus requirement, an optical probe with tilt optics and an adjustable pupil from 0.5 to 2mm (rather than a conventional probe) is used. In addition, with the minimum probe pupil height of 7.4mm, the Scheimpflug-corrected probe, designed by the Farrand Optical Company, is used. The only modification required is to change the field of view from 120° to 60° and add a zoom lens and a servo-controlled iris.

As a consequence of selecting a minimum probe pupil height of 7.4mm for a scaled eye-height of 7.5 ft, the scale of the aircraft carrier is 309:1. In order to provide carrier heading changes, the carrier is positioned approximately on the center of a rotating disk and the wake, which is twice the length of the carrier, is laid out from the carrier to the edge of the disk. The diameter of the disk is therefore 16 feet.

It is theoretically possible to simulate all flight paths using only one translational degree of camera gantry freedom, plus rotation of the model. However, for close flybys of the carrier at high speed, the rotational velocity requirement on the carrier and wake model is high. Therefore, in order to limit the rotational rate to a reasonable figure, Singer uses a camera gantry which has two translational degrees of freedom. This is discussed in more detail later in this report. The component parts of the system are briefly described in the following paragraphs.

SECTION II

TARGET IMAGE GENERATOR

The target image generator will consist of four major assemblies, grouped together to provide the video signals to the video processing equipment. These four components are:

- 1) A model board assembly, containing the carrier model, which is driven to simulate heading, heave, pitch and roll motions, and with carrier deck lighting.
- 2) A gantry structure which includes the cable takeup mechanism, the rail on which the tower rides, and the tower which holds the camera, camera electronics, probe, probe electronics, the X,Y,Z translation servo assemblies, and the necessary control circuit components.
- 3) A flood lighting structure to provide the required ambient lighting levels.
- 4) An electronics cabinet which contains a local maintenance control panel, gantry position readouts and electronics, misc power supplies, isolation amplifiers, and power control and protection circuit breakers.

METHODS CONSIDERED.

Proposed Method. Figure 1 illustrates the method selected to represent, illuminate, and generate the target image.

Alternate Methods. Alternate methods are discussed beginning on page 44.

TARGET MODEL BOARD ASSEMBLY.

The target model board will be 16 ft. high and 32 ft. long mounted on a framework approximately 3½ ft. off the floor. The support assembly will be approximately 8 ft. longer (40' total) to provide the upper guide rail for the gantry tower.

The carrier model will be mounted at the center of a 16 ft dia. disc, which will be located at the left end of the model board as viewed from camera side. The disc will contain the painted wake and carrier support assembly. Disc rotation will provide carrier heading rotation, relative to the line-of-sight from the probe to the carrier. The carrier model support plate will support the model drive assemblies for heave, pitch, and roll, as well as the light box, which provide carrier deck lighting fiber optics illumination.

The carrier model will be constructed of suitable, light-weight material to enable attachment of the drive assemblies, to rigidly hold the fiber optics in position, and withstand the scuffing of the flexible fill material around the waterline, and not distort from ambient heat. The model will contain conical-typed fiber optics for the omnidirectional deck edge lights. The runway center-line, runway edge, and athwartship lights will have prism cuts at the end to provide higher intensity unidirectional (directed aft) lighting. The vertical drop line lights will also be directed aft. The fiber bundles will be brought out to the light source box on the support assembly.

The gap between the model and disc cutout of the waterline surface will be filled with a thin, flexible material for several inches around the carrier with extension arms at the lower edge of the model to pull the flexible material up when the carrier motion is above the disc water line. When the carrier model pitches or heaves downward, the material will be depressed below the disc water level surface by the model.

The carrier wake is painted on the disc along a line extending from the carrier stern to the edge of the disc with wake fading out at the disc edge.

Model Scale Factor. (Figure 2 illustrates disc and model dimensions.) A model scale factor of 309:1 has been selected to provide a wake length of at least double the carrier water line length on 16 ft. disc. To reduce the motion of the FLOLS position on the carrier model as it pitches and rolls, the carrier model will be pitched and rotated in heading about the 37-ft. draft waterline, at the fore and aft position of the FLOLS (417.25 ft. forward of the aft position). This corresponds to 77.5 ft. aft of the limit amidships location, using 990-ft. waterline dimension. The wake length for an 8-ft. radius (2472 ft.) disc is 2054.75 ft. which provides a wake length/carrier length ratio of:

$$\frac{2054.75}{990} = 2.075:1$$

TARGET MODEL ILLUMINATION.

The zoom range over which the probe will operate is 165.24 mm focal length (for 10.37°) to 25.98 mm focal length (for 60°). The pupil sizes corresponding to these focal lengths will be 2.9 mm to 0.5 mm. This means the f/No.'s will range from f/56.98 at the long focal length to f/51.96 at the short focal length. The f/No. is not perfectly constant; this means the illumination on the faceplate of the camera tube will change as the probe is zoomed. To compensate for this 20% change in illumination it may be necessary to decrease the camera gain as a function of focal length. It is not possible to decrease the pupil size below 0.5 mm to compensate for this because of the decrease in MTF that would be experienced because of diffraction.

The illumination required at the camera tube faceplate to give a white 46-db signal-to-noise ratio, as derived from the Westinghouse specification data of the tube, is 0.048 foot candles of spectrally modified halide light. However, to account for unknown reflection characteristics of the model, a more conservative illumination at the faceplate of 0.074 foot candles will be provided.

To compute the illumination required on the model, the following formula is used:

$$I_m = \frac{4 I_i N^2}{R T M}$$

Where: I_m = Illumination required on the carrier model.

I_i = Worse case illumination required on the camera tube faceplate = 0.074 foot candles.

N = Worst case f/No. = 56.98.

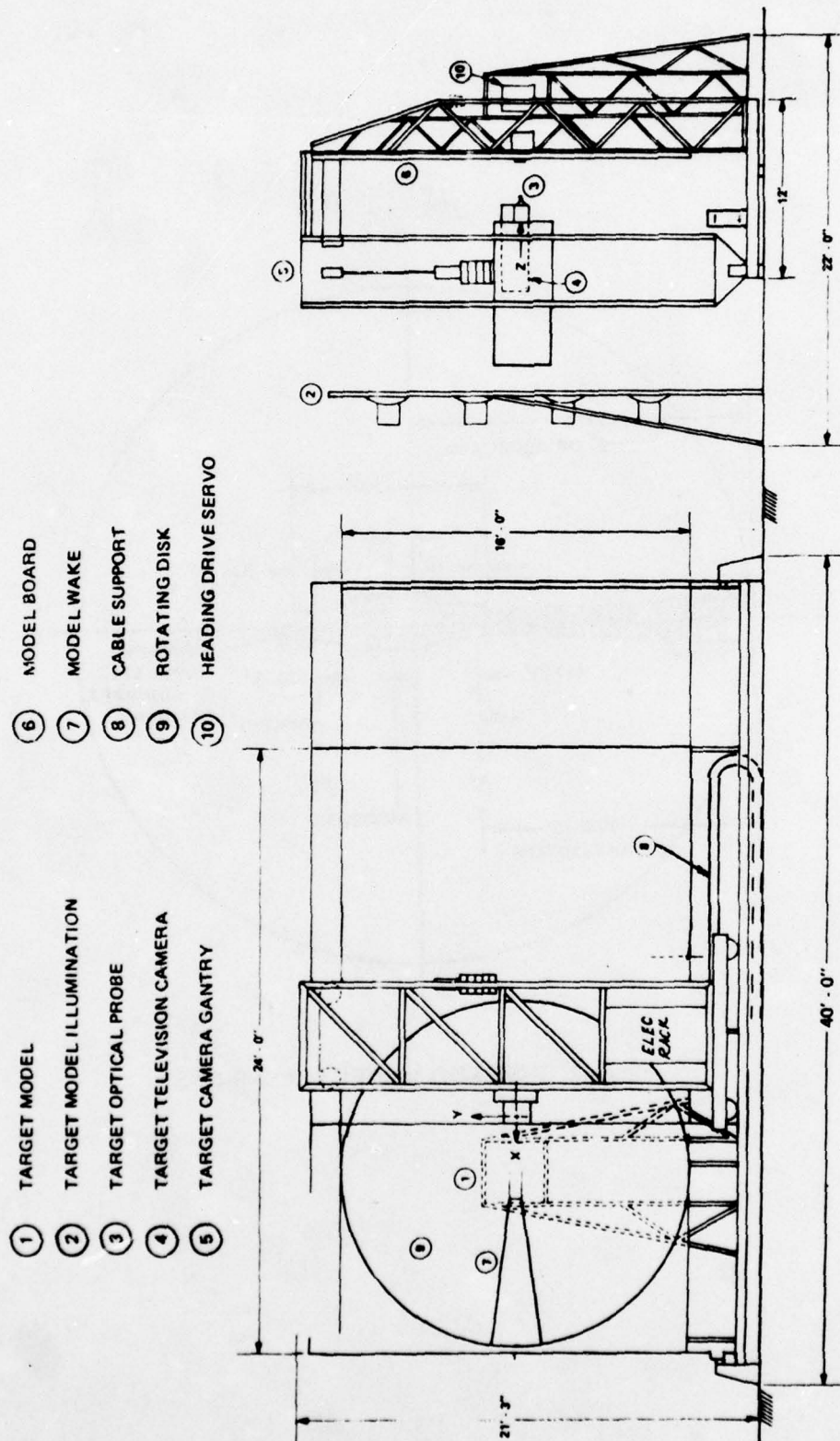


Figure 1. MODEL BOARD ASSEMBLY

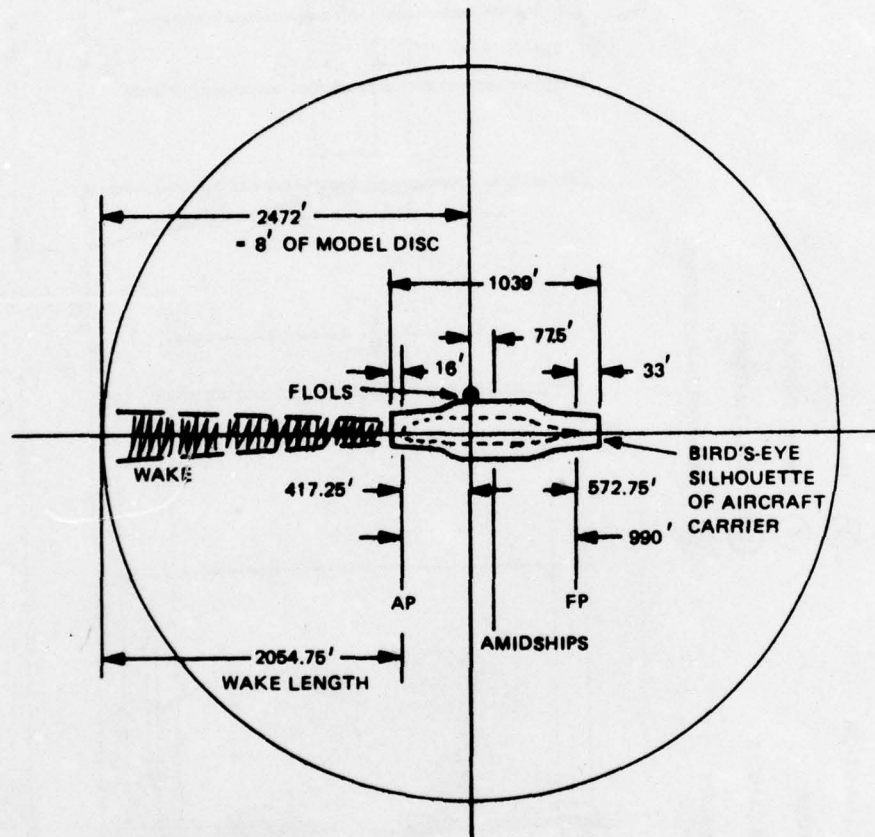


Figure 2. DISC AND MODEL DIMENSIONS

- R = Average highlight reflectance of the carrier model = 0.60
- T = Probe transmission = 0.25
- M = Maintenance factor to allow for lamp and camera tube aging = 0.8.

Using these numbers, the carrier illumination requirement (I_m) is 7910 foot-candles.

Target Model Illumination System. The 16' x 32' carrier and seascape will be illuminated by a 16' x 24' lighting board, located approximately 13 feet away, containing 96, 1000-watt metal halide lamps and fixtures.

It is estimated that a 2-ft vertical x 2-ft horizontal fixture spacing, the lighting level at the model surface, at a point 8 ft. high and 12 ft. from the left, will be approximately 9000 foot-candles.

The carrier model will be illuminated by approximately 8500 foot-candles. This predicted 8500 foot-candle power exceeds the required level of 7910 foot-candles. These estimates are based on the 6240 foot-candle center illumination that was achieved on the F4E-18 system, with a 16-foot by 44-foot model board, a lighting bank with a 13-foot spacing, and a fixture spacing of 4 ft. vertically by 2 ft. horizontally.

Wide beam enclosed fixtures with a beam spread of, approximately, $116^\circ \times 113^\circ$ will be used. Day will be simulated with all 96 lights on. Dusk will be simulated by turning alternate lights off in a checkerboard pattern as shown in figure 3. Night will be simulated by turning all the lamps off. The metal halide lamps require approximately 4 minutes to reach operating level from a "cold" start. From a "hot" start (i.e., from turning off the light bank until subsequently reaching back on) approximately 20 minutes is required. This inconvenience is justified in that metal halide-type lamps are the only lighting system capable of giving good color rendition and providing sufficient illumination level.

Flourescent lamps, even packed as tight as practically possible, could not give the required illumination level. The 76 lamps and ballasts on the main lighting bank will draw approximately 82 kw (86.3 KVA) during day simulation. Gantry fill-in lighting will be minimal, and should draw no more than 2 kw.

Carrier Deck Lighting. Light fibers are assembled in five bundles that will have masking capability to yield an on-off condition for each bundle. One light is the sole source for all bundles. The light system is shown in figure 4 depicting a stationary source and optical components. A five-sided, pyramidal mirror system is attached to a cylindrical structure, symmetrically about its axis.

The fibers are mounted on five, special-metal plates that are adjusted to the five images formed by the mirror configuration. To vary light levels, proper filters will be attached. Five individually-controlled masks and their hardware are also mounted to the cylindrical fixture for the purpose of masking each set of bundles independently.

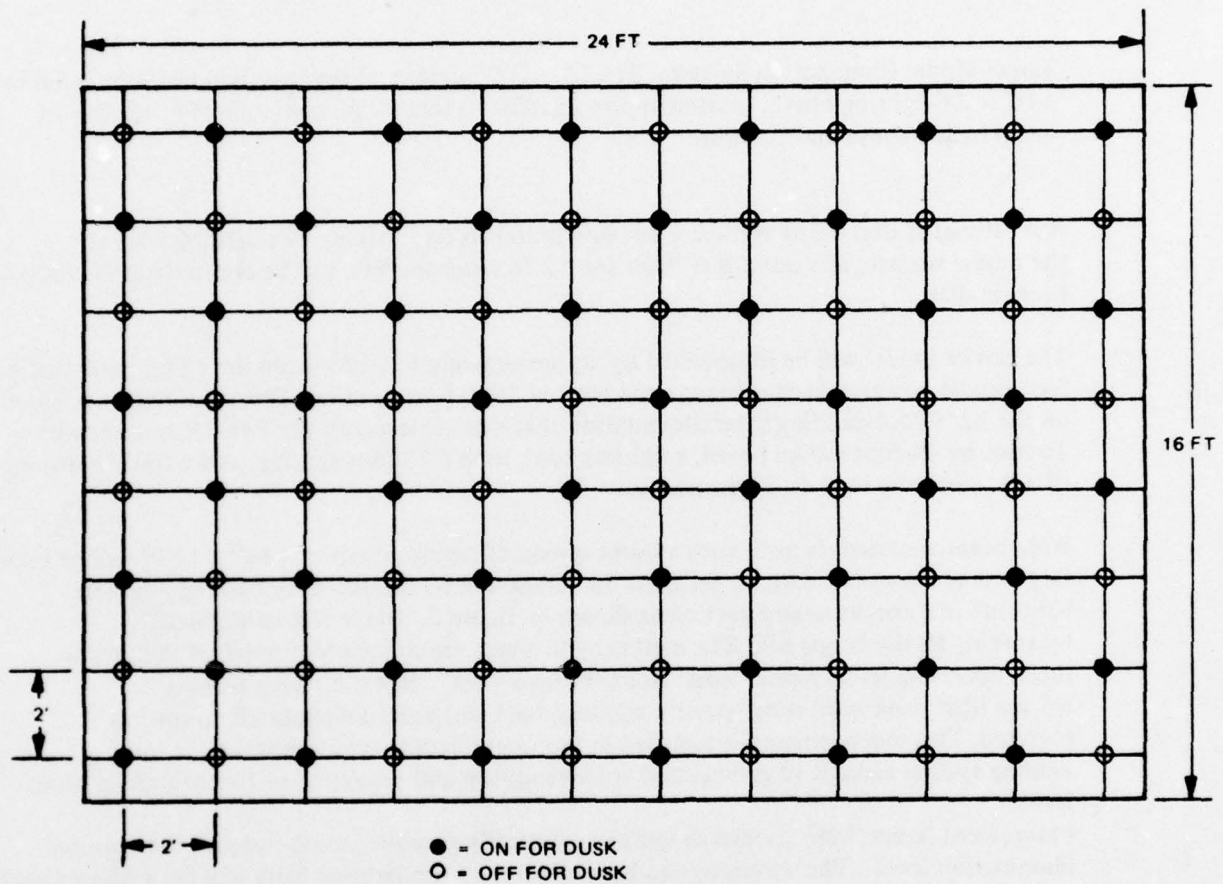


Figure 3. LIGHTING FIXTURE CONFIGURATION

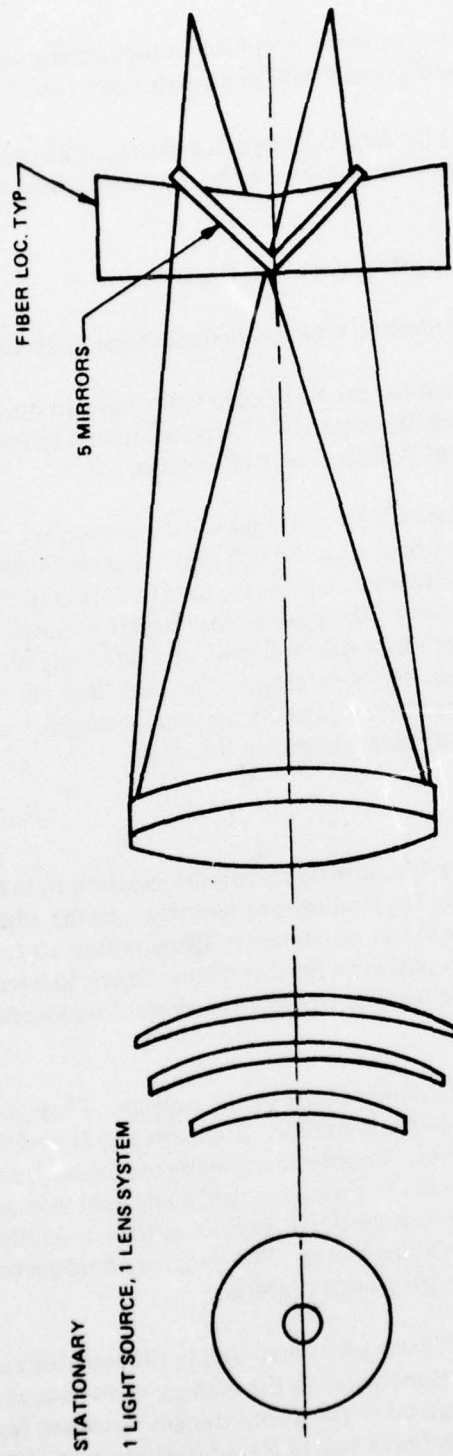


Figure 4. CARRIER LIGHT SYSTEM

The entire mirror and fiber assembly is permanently attached to the bearing and gear drives housing that controls the angular rates and position of the aircraft carrier model board disc.

The fibers that are attached to the light pipe fixture are guided through the center clearance of the drive, and then onto their allotted positions, on the carrier model deck and fan tail vertical "Dropline" lights adapter.

A sketch of the carrier with the required lights is shown in figure 5.

Figure 6 is a graph showing the light distribution from a prismatic fiber in elevation angles.

The polished cone fibers that are to be used for the deck edge lights have an omnidirectional distribution in azimuth peaked at a nominal elevation of 12 degrees with a fall off down to 80 percent of the peak at elevated angles of 2 degrees and 22 degrees.

The polished prismatic fibers that are to be used for the angled deck centerline, edge, and athwartship lights are unidirectional. The prism angle is such that the peak output occurs on a plane normal to the polished prism face elevated at 6 degrees from the plane of the deck. The projected illumination will be 90 percent of the peak at zero degree elevation and 12 degree elevation. The azimuth illumination profile will peak at a line lying on the aircraft approach angle (plane) parallel to the angled deck centerline. The projected illumination will be 90 percent of the peak at 10 degrees left or right, and 58 percent of the peak at 20 degrees left or right of the main beam rotated about a line normal to the deck.

Carrier Lights.

Runway Centerline Lights. These lights provide primary lineup information to incoming pilots. They are located on the centerline of the landing area (runway) on the angled deck at intervals of approximately 45 feet. There will not be simulated lights within 10 feet aft of any arresting-gear wires. There are fourteen positions for directional fibers, located with the beam axis facing aft and parallel to the angle deck centerline to represent real-world configuration.

Runway Edge Lights. These lights define the lateral limits of the runway. They are located in two rows parallel to and equidistant from the runway centerline. The rows are 35 feet from the centerline, and form a runway width of 70 feet. Twenty-seven lights are located, so that a line perpendicular to the runway centerline and passing through a centerline light also passes through each of two edge lights. In this manner, a symmetrical, rectangular pattern is exhibited. The twenty eighth light would fall outside the flight deck area. The lights are unidirectional, aligned with the beam facing aft and parallel to the angled deck centerline.

Runway Athwartship Lights. The purpose of these lights is to define the longitudinal limits of the runway. They will be placed on lines perpendicular to the runway centerline at the extremities of the landing area. The ramp lights will be spaced at five-foot intervals outboard from the aft centerline light. The outermost athwartship lights in this line are 5 feet inboard of the runway edge lights. The forward athwartship lights are spaced at approximately 5-foot intervals outboard from the forward runway centerline light. The 12 lights for the ramp and 7 lights for the forward will be unidirectional and aligned with the beam axis, facing aft, and parallel to the angled deck centerline.

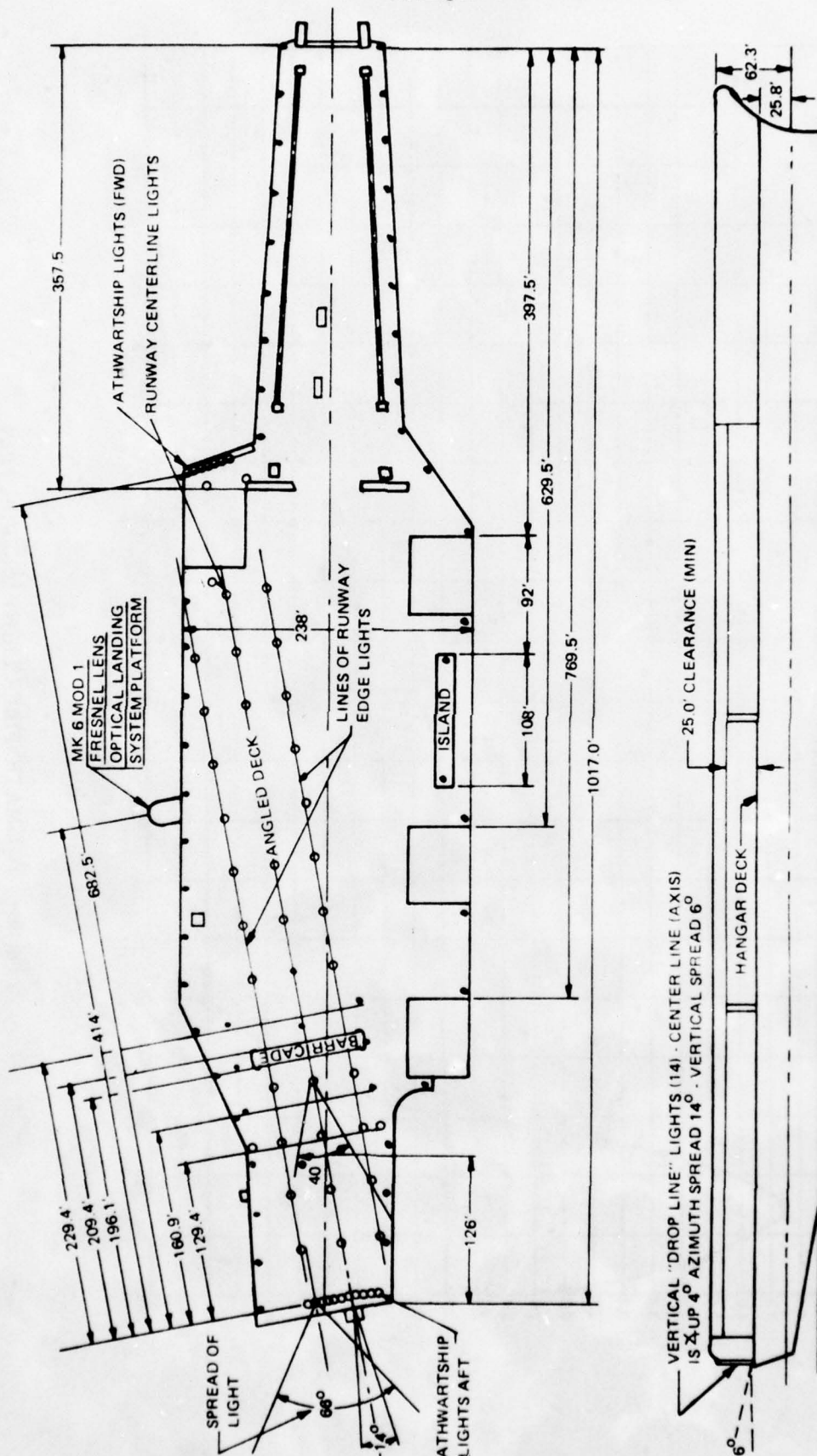


Figure 5. PLAN VIEW OF FLIGHT DECK WITH REQUIRED LIGHTS

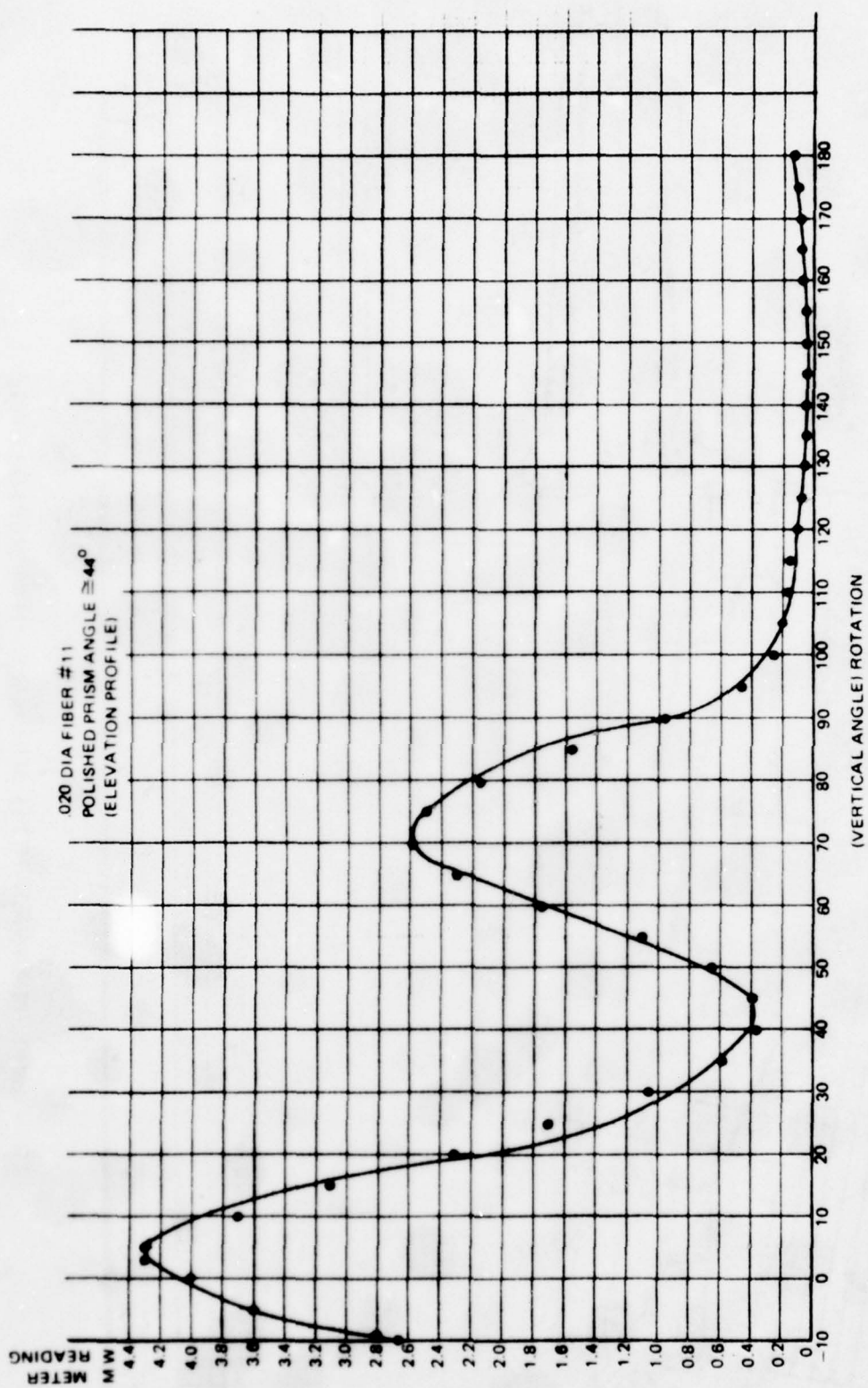


Figure 6. PRISMATIC FIBER LIGHT DISTRIBUTION

Deck Edge Lights. The purpose of these lights is to outline the edge of the flight deck. The lights will be spaced at 40-foot intervals around the perimeter of the flight deck. The lights will be omnidirectional and of low intensity. Figure 7 shows ground cones to simulate omnidirectional lights and the graphs show the relative distribution. There will be approximately 47 deck edge lights on the model.

Vertical "Dropline" Lights. These lights are at the aft section, mounted in a vertical row, below the deck level at the ramp. To simulate the proper azimuthal and vertical spread angles, flat ground and polished ends of fibers (see figure 8) will be used as a source for each light, and a prefabricated mask will be developed to contain the bundles within the angular boundaries.

There will be fourteen of these lights assembled as a vertical "dropline" light assembly.

TARGET MODEL MOTION.

The carrier model motions required are as shown in table 1. The pitch, roll and heave of excursions of the carrier model relative to the disc are the numbers from the specification. The rates and accelerations are computed from the range and periods specified, assuming sinusoidal motions over the range. Carrier Heading parameters have been derived from an analysis of the required model heading with respect to the LOS from the probe (X, Y, Position of the Gantry) to the model AOI, during various maneuvers of the aircraft around and about the carrier.

Table 1. CARRIER MODEL MOTIONS REQUIRED

AXIS	RANGE	PERIOD	RATE	ACCEL	ACC Y POSIT
Pitch	± 5 Deg	10 Sec	$3.14^{\circ}/\text{Sec}$	$1.98^{\circ}/\text{Sec}^2$	0.1% of 10° *
Roll	± 12 Deg	16 Sec	$4.7^{\circ}/\text{Sec}$	$1.85^{\circ}/\text{Sec}^2$	0.2% *
Heave	± 30 Ft	10 Sec	$18.8 \text{ Ft}/\text{Sec}$	$11.9 \text{ Ft}/\text{Sec}^2$	0.2% of $60'$ *
Heading	Continuous	NA	$42^{\circ}/\text{Sec}$	$26^{\circ}/\text{Sec}^2$	0.01% of 360°

*Based on holding carrier Deck F.P. point to within $1/8$ ft. during motion excursion.

**Based on holding FLOLS point to within $1/8$ ft. during roll motion.

TARGET OPTICAL PROBE.

The optical probe is Scheimpflug-type. (See figure 4.) This permits the carrier deck to be in perfect focus. However, the superstructure and fantail will be out of focus, during the maneuver which uses the Scheimpflug compensation.

OMNIDIRECTIONAL FIBERS FOR
TARGET IMAGE GENERATOR
GRIND & POLISH CONE α
LENGTHS TO BE DETERMINED
 $\theta = 55^\circ \begin{smallmatrix} +0 \\ -15 \end{smallmatrix}$
 $\alpha = 10^\circ$ (ANGLE OF PEAK OUTPUT)

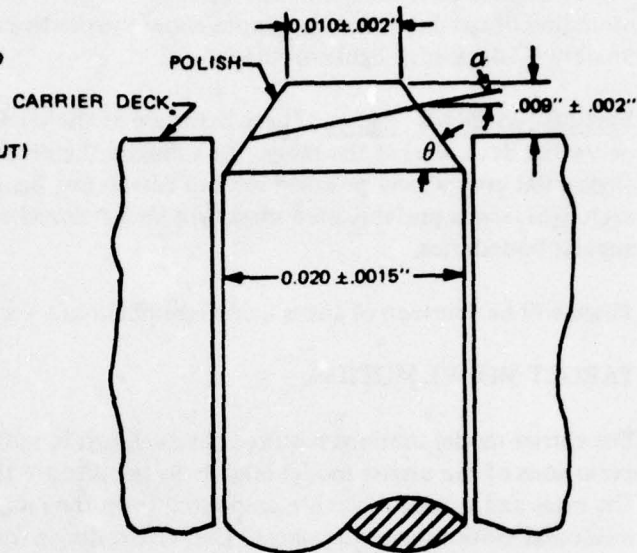


Figure 7. DECK EDGE LIGHT

STANDARD SQUARE CUT FIBER
FOR TARGET IMAGE GENERATOR
DIA. - A - .020"
LENGTHS TO BE DETERMINED
 $\theta = 35^\circ$ (MAXIMUM FOR THE GLASS MEASURED)

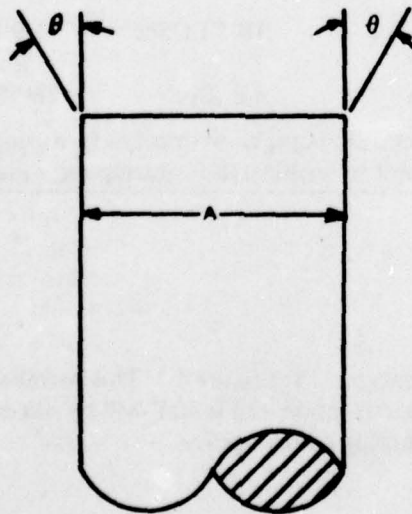


Figure 8. VERTICAL "DROPLINE" LIGHT

Since a large part of the carrier will be out of focus, as a result of the Scheimpflug correction, a study was undertaken to compare a Scheimpflug probe with a conventional probe. To discuss the comparative performances, the effects of defocus on system resolution must be considered. In presenting graphical data pertaining to defocus, defocus is expressed in terms of the angular size of the geometrical blur.

Refer to figure 9 for the definition of the term "geometrical blur" as used herein. An image point viewed in a plane defocussed by a distance δ from the plane of best focus will have a blur circle of diameter B. As can be seen from the geometry of the figure, the blur size can be expressed as:

$$B = \frac{D\delta}{q},$$

where q is the effective image distance, and D is the diameter of the aperture of the imaging system. The object distance in this application is large enough that the image distance is well approximated by f, the effective focal length of the imaging system. Thus:

$$B \approx \frac{D}{f} \delta,$$

so that B is proportional to δ , with D and f as constants. The blur B can be expressed in terms of its apparent angular subtense:

$$B' \approx \frac{B}{f} \approx \frac{D}{f^2} \delta \text{ (in radians),}$$

or;

$$B'' = \left(\frac{180}{\pi} \cdot 60 \right) B' \approx 3437.7 \frac{D}{f^2} \delta \text{ (in arc minutes).}$$

The quantities B' or B'' provide a rough guide to the resolution capability of the imaging device when it is defocussed enough that defocus effects contribute the bulk of the image degradation. However, a substantial part of the image degradation in the target image probe results from diffraction as a result of the pupil diameter of only 0.5mm. A convenient approach to evaluating the effect of defocus when diffraction plays a significant role is to use a theoretical calculation of the MTF of a defocussed perfect lens. Although this approach does not account for image degradation due to optical aberrations, it does permit one to judge whether a given amount of defocus significantly increases image degradation above that resulting from diffraction. Further, if an amount of defocus is found to increase degradation insignificantly above that due to diffraction alone, it will certainly increase it insignificantly in comparison to the effects of diffraction plus aberrations. The approach is convenient since tabulations of the MTF of a defocussed perfect lens have been published, whereas an exact calculation cannot be made for an actual optical system until its detailed design is complete.

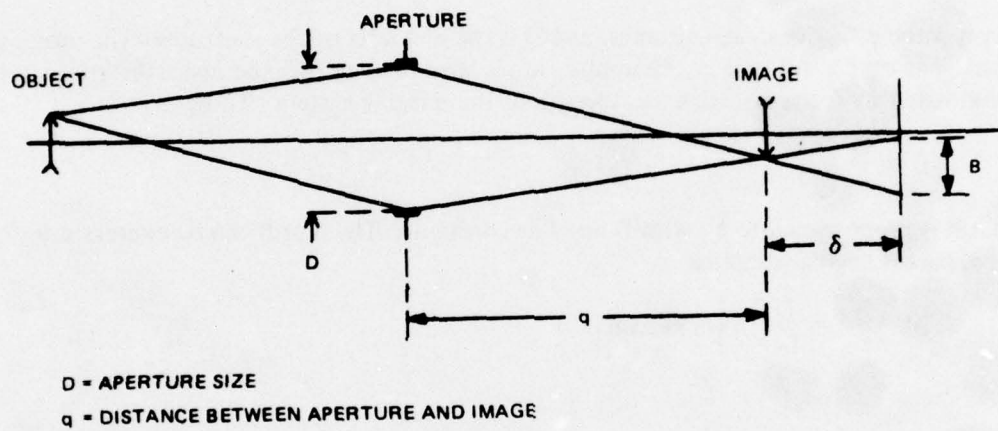


Figure 9. RELATIONSHIP OF GEOMETRICAL BLUR B TO DEFOCUS δ

The curves of figure 10 are plotted using "Tables of the Modulation Transfer Function of a Defocussed Perfect Lens".¹ The dimensionless defocus parameter Δ (units of $\lambda/4$ or Rayleigh units) for which these tabulations are made is related to the defocus distance in image space δ by equation (2) of that reference:

$$\Delta = \frac{\delta}{2F^2 \lambda},$$

where F is the f-number $\frac{f}{D}$, and λ is the wavelength of light considered. This is rewritten as follows:

$$\Delta = \frac{\delta}{2 \left(\frac{f}{D}\right)^2 \lambda} = \frac{1}{2} \frac{D}{\lambda} \left(\frac{D}{f^2} \delta\right) = \frac{1}{2} \frac{D}{\lambda} B',$$

$$\Delta = \frac{1}{2(3437.7)} \frac{D}{\lambda} B'' = 1.4544 \left(\frac{D}{\lambda}\right) B'' \times 10^{-4}$$

The curves of figure 10 were plotted using a pupil diameter of 0.5 mm and a wavelength of 550 nm, giving values of 1.32, 2.64, 3.31, 3.97, and 5.29 Rayleigh units of defocus for geometrical blurs of 10, 20, 25, 30, and 40 arc minutes, respectively. These curves were plotted using a computation which follows the method described in reference 1 and which was checked against the tabulations of that reference. The curves give MTF's for the probe (considered as aberration-free) as a function of spatial frequency. The spatial frequency, in units of ν_o (the cutoff frequency of 1 cycle per λ/D radians) is converted to cycles per arc-min. by substituting for λ and D and converting to arc minutes, giving $\nu_o = 0.2644$ arc-min., using $D = 0.5$ mm and $\lambda = 550$ nm.

To examine the effect on system resolution, consider the MTF's of the remainder of the system. Assume that the limiting resolution is reached when the product of all the MTF's falls to 5%. Multiplying MTF estimates for the target image camera, the target projector Eidophor, and the target projection optics, and dividing this product into 5%, the MTF required of the probe is obtained if an overall MTF of 5% is to result. This is shown in figure 11.

Laying figure 11 over figure 10, graphical solutions are obtained for the spatial frequency where the curve of figure 11 intersects the curves of figure 10. Thus, the spatial frequency at which the overall MTF reaches 5% for probe defocus corresponding to blur circle diameters of 0, 10, 20, 25, 30 and 40 arc minutes. The angular resolution that corresponds to each of these frequencies ν is $1/\nu$. Using these points, resolution vs. defocus can be plotted (expressed as blur circle angular diameter). Passing a smooth curve through these points, the solid curve is obtained in figure 12.

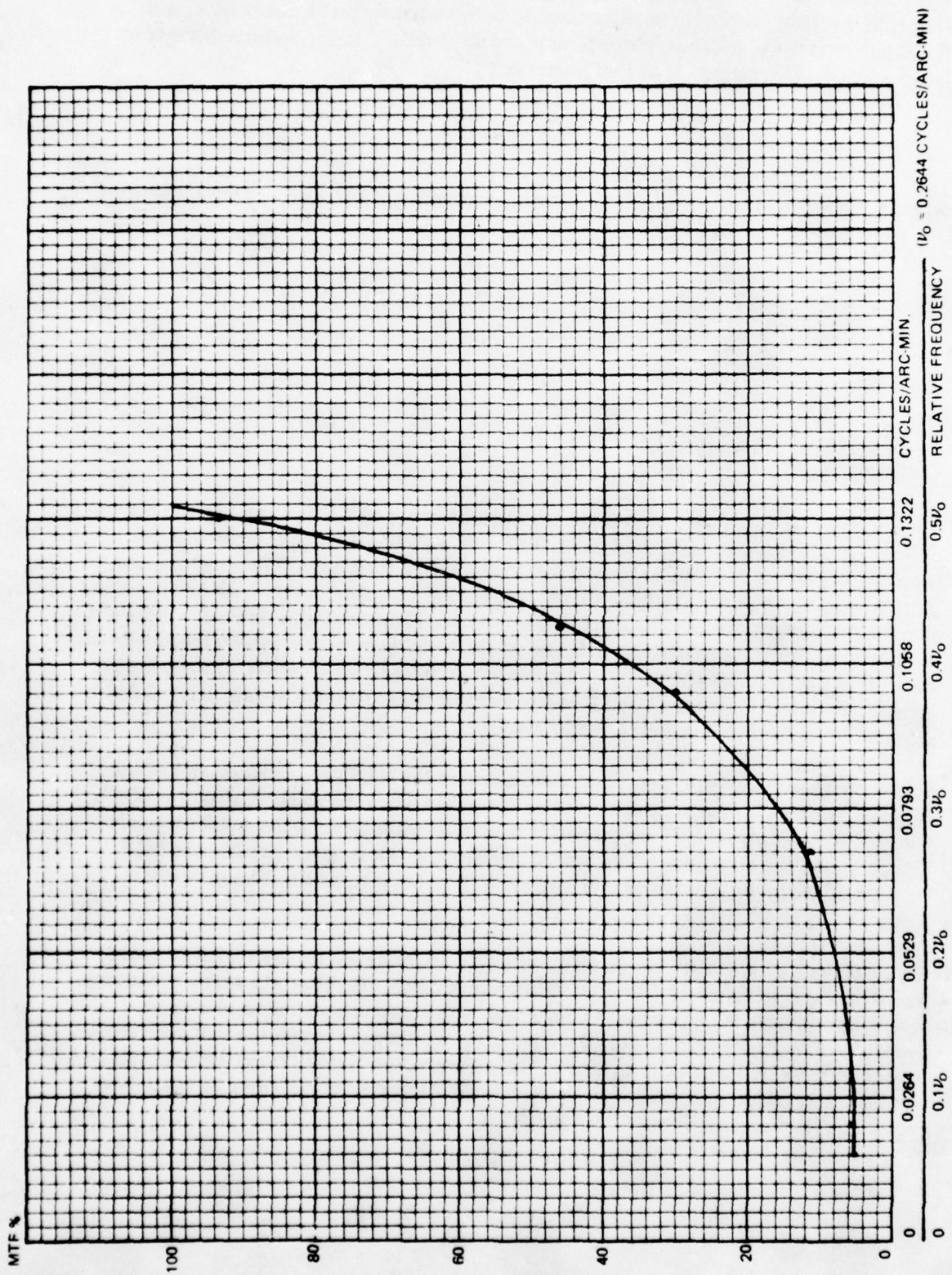


Figure 10. REQUIRED PROBE MTF FOR 5% TARGET SYSTEM RESPONSE

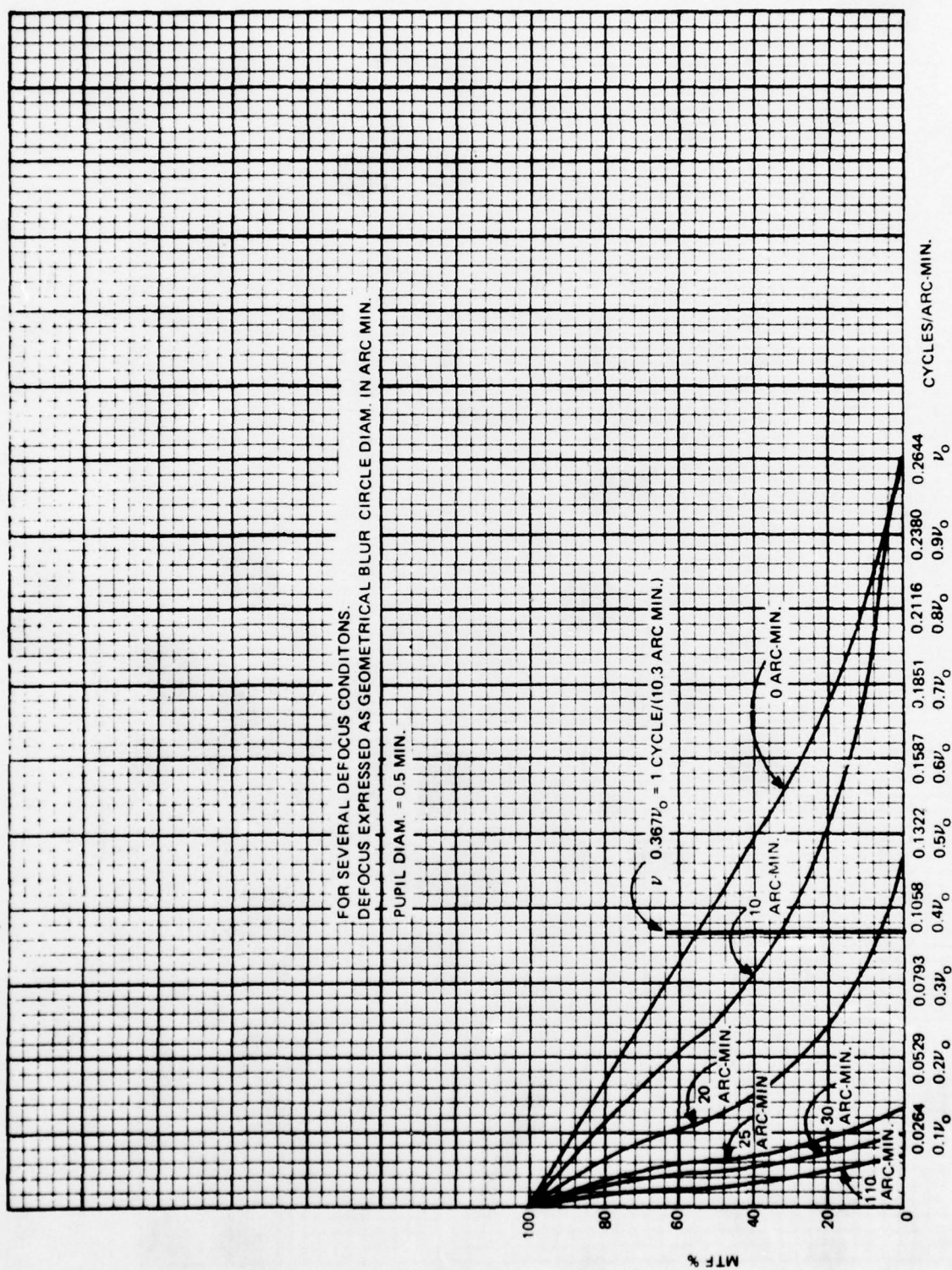


Figure 11. MTF VS SPATIAL FREQUENCY

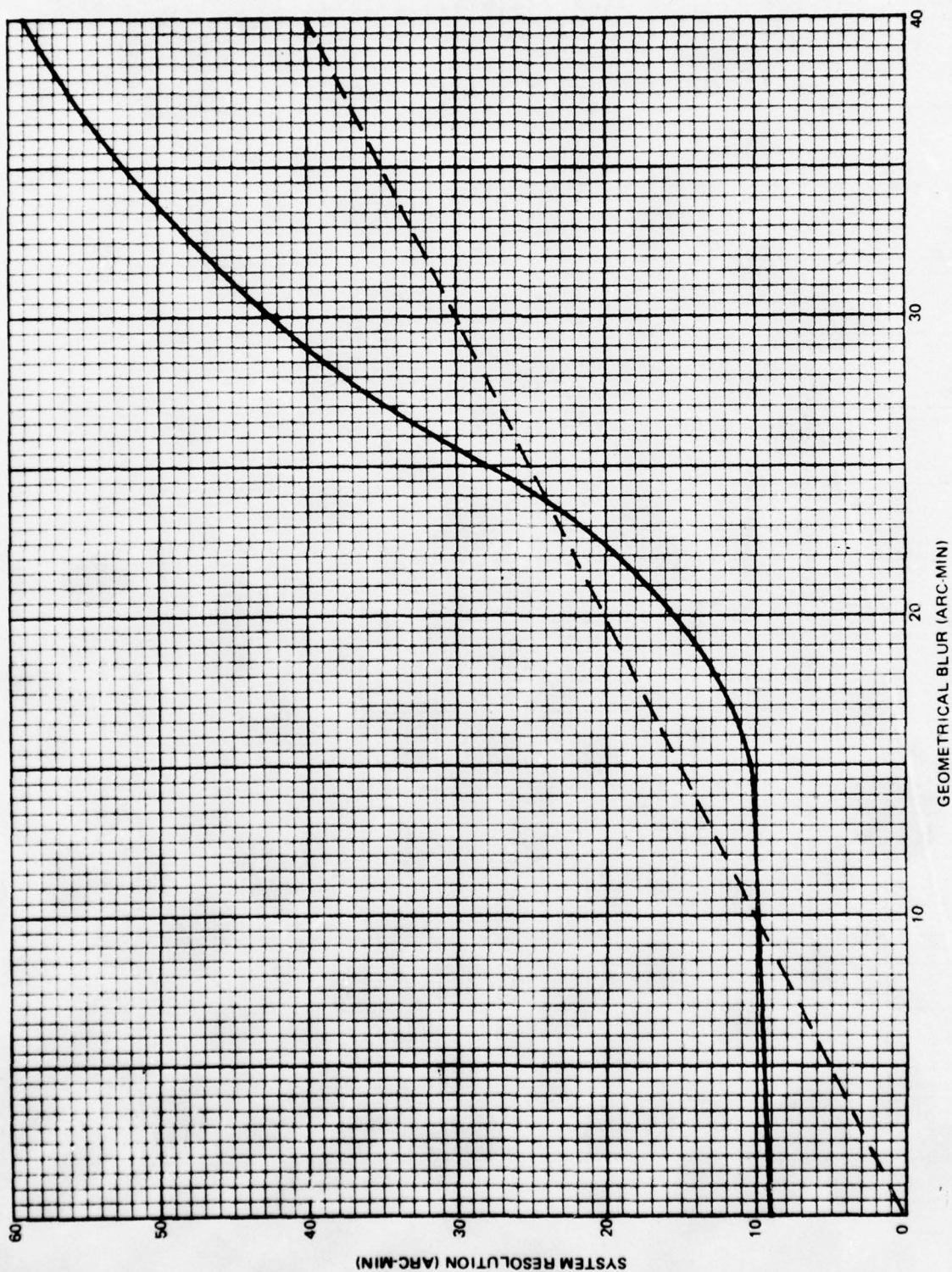


Figure 12. SYSTEM RESOLUTION VS GEOMETRICAL BLUR

Examining figure 12, see that the system resolution does not degrade very rapidly as a function of defocus for blur circles up to about 18-20 arc minutes, after which it increases very rapidly (the dashed line, a plot of resolution = blur circle diameter, is shown for comparison). Hence, if no useful imagery is defocused to a blur circle diameter greater than 18-20 arc minutes, it is pointless to go to extraordinary means (such as Scheimpflug compensation) to bring it into better focus.

Figure 13 is a plot for a conventional probe showing defocus and system resolution (as determined from figure 12) for a conventional probe as a function of the component parallel to the optical axis of the distance (in scale ft.) from the probe eyepoint to the viewed object. This curve is for a scale factor of 370:1 and a pupil diameter of 0.5 mm. The probe is adjusted for sharpest focus at 107 scale ft. This was considered to be at or near the optimum setting (to a certain extent this is subject to personal preference) for simulating aircraft touchdown, which is the task which shows the conventional probe in the most unfavorable light.

Figure 13 shows that for objects at ranges from 60 to 500 scale ft., there is only a slight relative increase in the resolved angle relative to the in-focus case. The resolved angle is still rising only gradually at 500 ft. The geometrical blur rises to an asymptote of 19.5 arc minutes for an object at infinity which, from figure 16, gives a resolved angle of 13.5 arc minutes. Below 60 feet, the situation deteriorates rapidly. At 20 ft., the imagery is grossly degraded. The imagery at 20 ft. could be improved by focussing closer than 107 ft., but only at the expense of the image quality of distant points. Points as close as 20 ft. may be in the field of view at touchdown, but presumably the pilot has more important places to direct his attention at touchdown than 20 ft. in front of his eyepoint.

For the Scheimpflug probe (with the servos appropriately driven) the entire plane of the deck is in sharp focus. The geometrical blur is zero for all objects in the plane of the deck, and for such objects the plot of resolved angle would be a horizontal line tangent to the curve for the conventional probe at its minimum point. Herein lies the sole advantage of the Scheimpflug probe which, although formidable for scale factors such as 2000:1, is slight for a scale factor of 370:1.

This advantage must be weighed against several disadvantages. The complication of several additional stages of intermediate images, complete with tilting lenses and optical path compensators (the servos of which must move them in proper synchronism) has the result that performance of an actual probe is degraded from the ideal of the "perfect lens" approximation (for which our MTF calculations were made) much more in the case of the Scheimpflug probe than it is for the conventional probe, which has a relatively simple optical train. This is true even when the Scheimpflug probe is adjusted for high altitude operation; i.e., with the tilting relay lenses in the untilted position. When the probe is adjusted for low altitude compensation, the tilting lenses are operated at the extreme edges of their fields of view, with a resulting loss of resolution. Although the extreme near and far objects are rendered more sharply than the conventional probe can image them, the best points in the field of the Scheimpflug probe will not be imaged as well as the best portions in the field of the conventional probe. In fact, for a scale factor of 370:1 and a range of object distances restricted to 60 to 500 scale feet, these effects may very well wipe out the theoretical improvement which the Scheimpflug probe provides, even at the extremes of 60 and 500 feet.

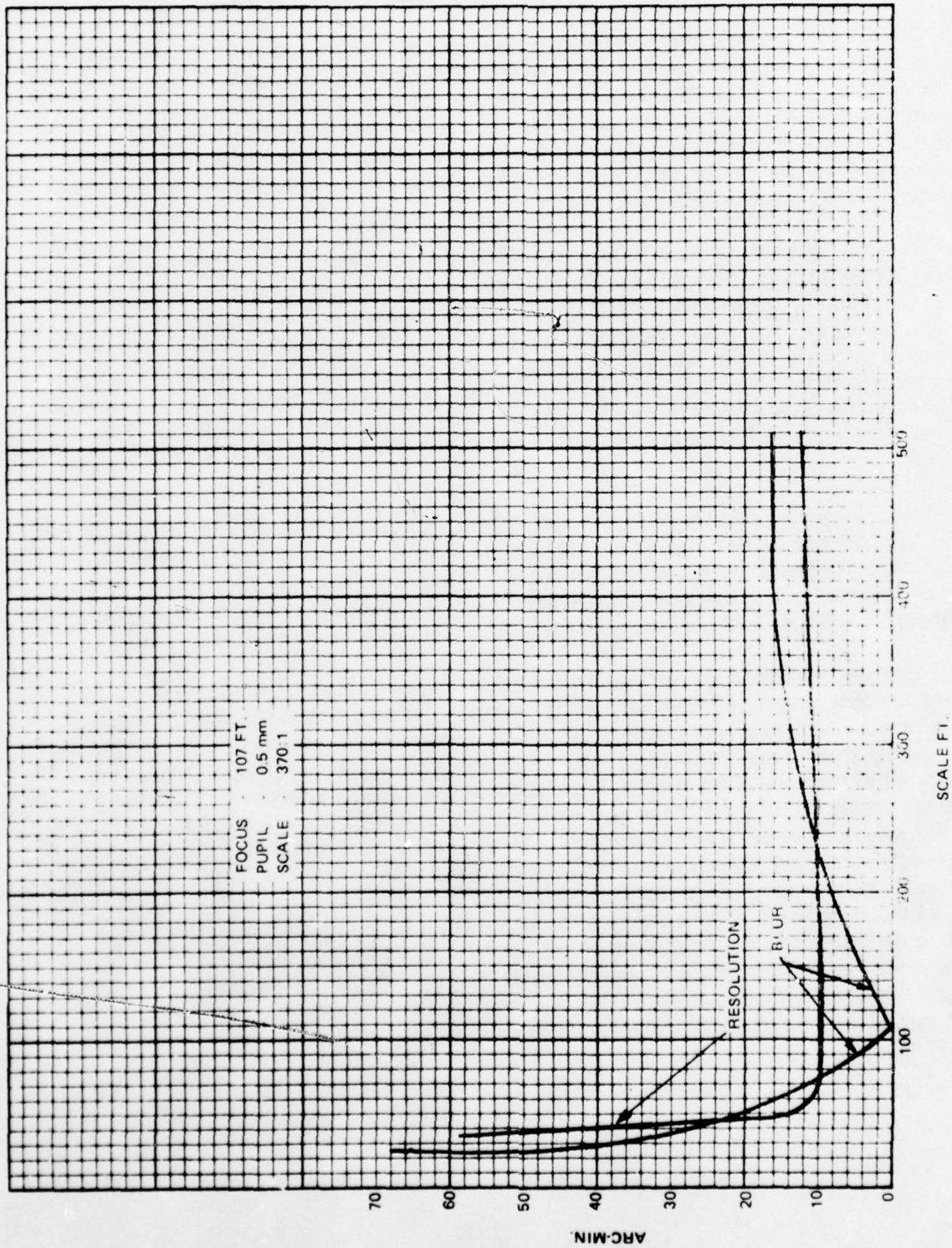


Figure 13. PROBE GEOMETRICAL BLUR & SYSTEM RESOLUTION VS. DISTANCE FROM EYE POINT

The vertical height of the carrier island results in yet another problem in using a Scheimpflug probe. The plane of best focus of a probe is just that - a plane. The tilting lenses of a Scheimpflug probe enable the plane of best focus (which is perpendicular to the optical axis of a conventional probe, or essentially vertical) to be brought into coincidence with the landing surface. Objects above and below this plane will be defocussed. For a terrestrial model, this is still ideal - with a little planning, large vertical objects can be excluded from the field of view from the vantage point of a landing approach. In the carrier landing application, it is not possible to exclude the carrier island which is a large (58.6 ft.) vertical object. Figure 14 shows the geometrical blur and the corresponding system resolution as a function of aircraft range to touchdown for the top of the carrier island. The curve for angular blur was calculated assuming that the island is 58.6 ft. high and 112.5 ft. away at touchdown, and that approach is on a 40° glide slope. The curve for angular blur, which goes off-scale on figure 14, reaches 114 arc minutes at touchdown. For points on the island lower than the top, the angular blur is less, being in direct proportion to the height of the viewed point above the deck. It is obvious that the top of the island is unacceptably blurred some distance from touchdown, and nearly all of the island will be unacceptably blurred at touchdown.

These technical considerations aside, the greater mechanical and optical complexity of the Scheimpflug probe has undesirable maintenance and alignment consequences. This burden, as well as the significantly higher cost, cannot be justified without a significant performance advantage in the intended application.

If future applications include use of terrestrial scale models of highly reduced scale factors such as 2000:1, the balance shifts in favor of the Scheimpflug probe for such applications. At such scale factors, the limitations of the conventional probe are more severe. One can quickly see the nature of these limitations by scaling the graphs of figure 13, which is drawn to a scale factor of 370:1. If the numbers (scale feet) on the horizontal scale of the graph are increased in proportion to the scale factor, the curves are correct for the case in which the distance to the plane of best focus (in scale feet) is increased in proportion to the scale factor. The actual distances on the model are the same; just letting the same distance represent more scale feet. The asymptotes of the curves at infinity are the same. Thus, the distance to the nearest usable imagery, by whatever criterion one chooses, is increased in proportion to the scale factor. If a conventional probe is chosen for the present application, it may be desirable to replace it with a Scheimpflug probe for some future application of the AWAVS system.

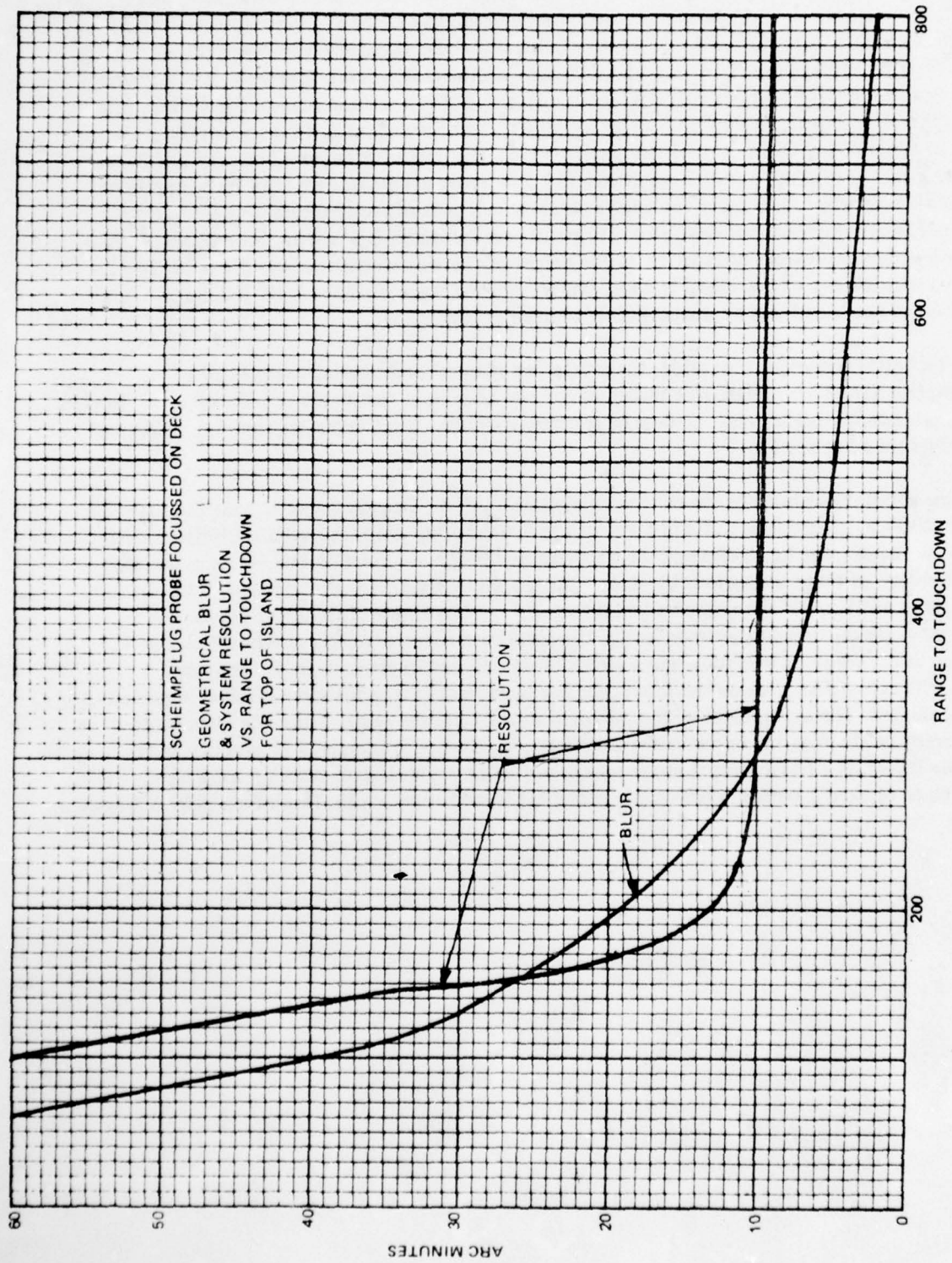


Figure 14. GEOMETRICAL BLUR VS. RANGE TO TOUCHDOWN

Since a large part of the carrier will be out of focus, as a result of the Scheimpflug correction, a study was undertaken to compare a Scheimpflug probe with a conventional probe.

TARGET TELEVISION CAMERA.

The design analysis of "Target TV Projector"², shows that in order to meet the system resolution of 700 horizontal lines by 500 vertical lines for a 60-degree by 40-degree field of view, an 825 scan line, 30-Hz frame, 2:1 interlace television format is required. Due to limitations in the TV projector, the camera will over-scan the required field of view. By properly applying the camera raster computer and field of view blanking an improvement in the camera MTF can be realized, which will tend to offset the MTF losses in the projector, due to the increased line-scan requirement by the projector design analysis.

Singer has developed a state-of-the-art, high-resolution camera for the luminance channel of the color camera of the F-4E No. 18 Weapon System Trainer capable of meeting the resolution, sensitivity, and deflection requirements outlined herein. Since the bandwidth of the F-4E camera is greater than required for this application (30 MHz), it will be reduced to improve signal-to-noise ratio. The existing camera was designed with a 2-inch image tube, optically coupled to an image intensifier, and operates with a Scheimpflug-corrected optical probe in a camera-model system. This design is based on utilizing such a camera, modified for reduced bandwidth and mechanically repackaged for this application.

Table 2 summarizes the characteristics of the AWAVS television camera.

The Westinghouse intensified WX5168 Vidicon is used because its superior resolving power and sensitivity provide optimum performance in a very critical area. Figures 15 and 16 illustrate the modulation transfer characteristic and sensitivity curves for this vidicon.

The vidicon/intensifier MTF at 770 TV lines/width for the nominal 4:3 aspect ratio would be 0.75. By over-scanning of the target FOV by 10%, the MTF will improve to about 0.79, as shown in figure 15. It is intended to operate the Vidicon target at 0.75 μ amp target current which would require 0.048 foot candles. For a margin of safety and future expansion capability, a more conservative faceplate illumination of 0.075 foot candles will be used. The signal-to-noise ratio of the F-4E No. 18 luminance channel was 40 db at a 30 MHz bandwidth. The AWAVS target camera requires an 11.5 MHz bandwidth which results in a 12.4 db improvement given by the relationship:

$$\Delta S/N = 20 \log \left(\frac{f_0}{f_1} \right)^{3/2}$$

$$\Delta S/N = 20 \log \left(\frac{30}{11.5} \right)^{3/2} = 12.4 \text{ db}$$

Table 2. AWAVS TELEVISION CAMERA CHARACTERISTICS SUMMARY

ITEM	SPECIFICATION
Image Tube Type	Intensified, Westinghouse WX-31836/WX5168, 2-inch Vidicon, with Selenium photoconductor
Modulation Transfer Function	See Figure 15
Limiting Vertical Resolution	590 TVL/height
Limiting Horizontal Resolution	770 TVL/width
Deflection System	Linear
Deflection Amplifier Bandwidth, Small Signal	500 KHz
Gamma	1.0
Lag (after 3rd field)	25%
Scan Rate	825 Lines, 60 Fields, 2:1 interlace
Video Bandwidth	11.5 MHz

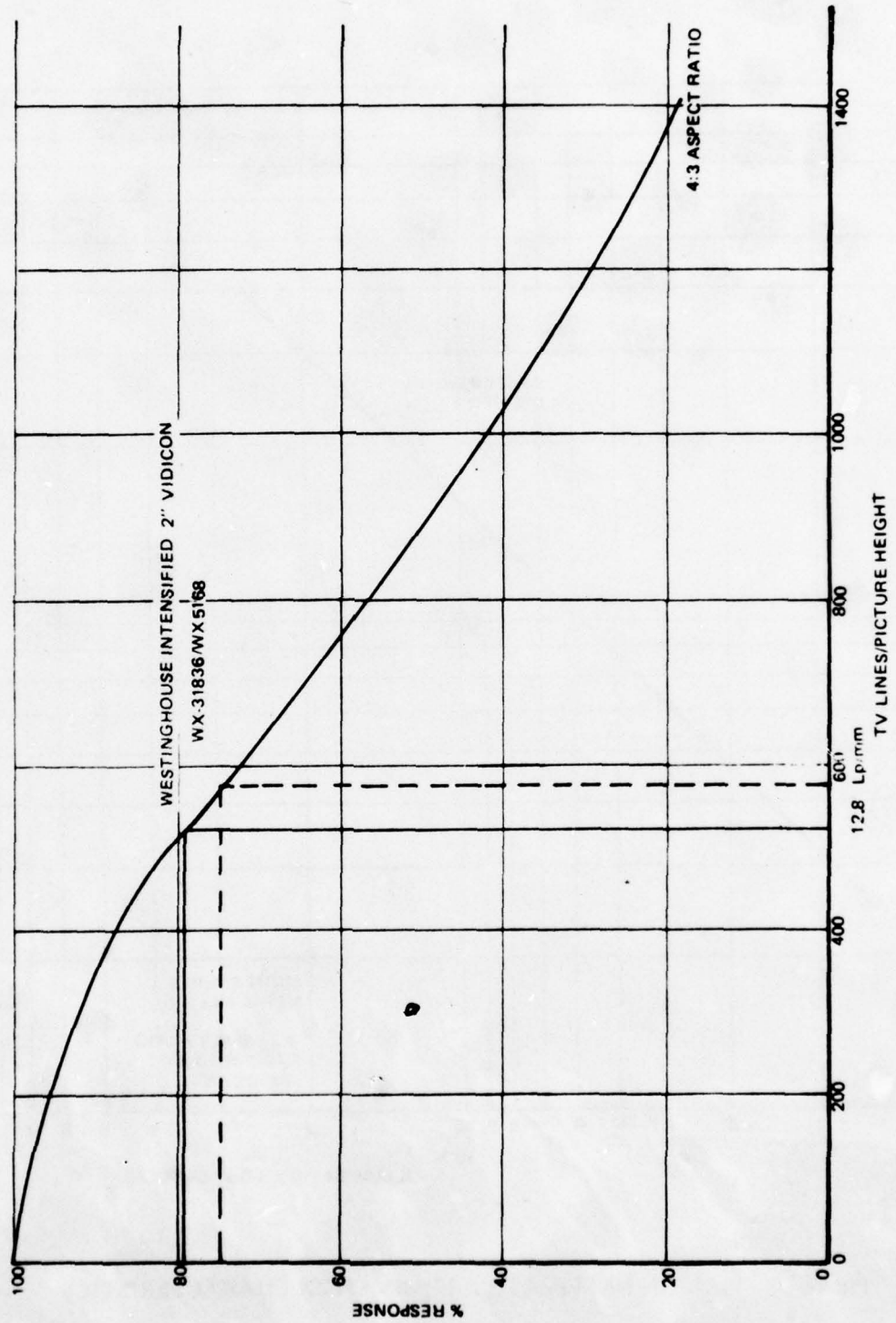


Figure 15. VIDICON MODULATION TRANSFER FUNCTION

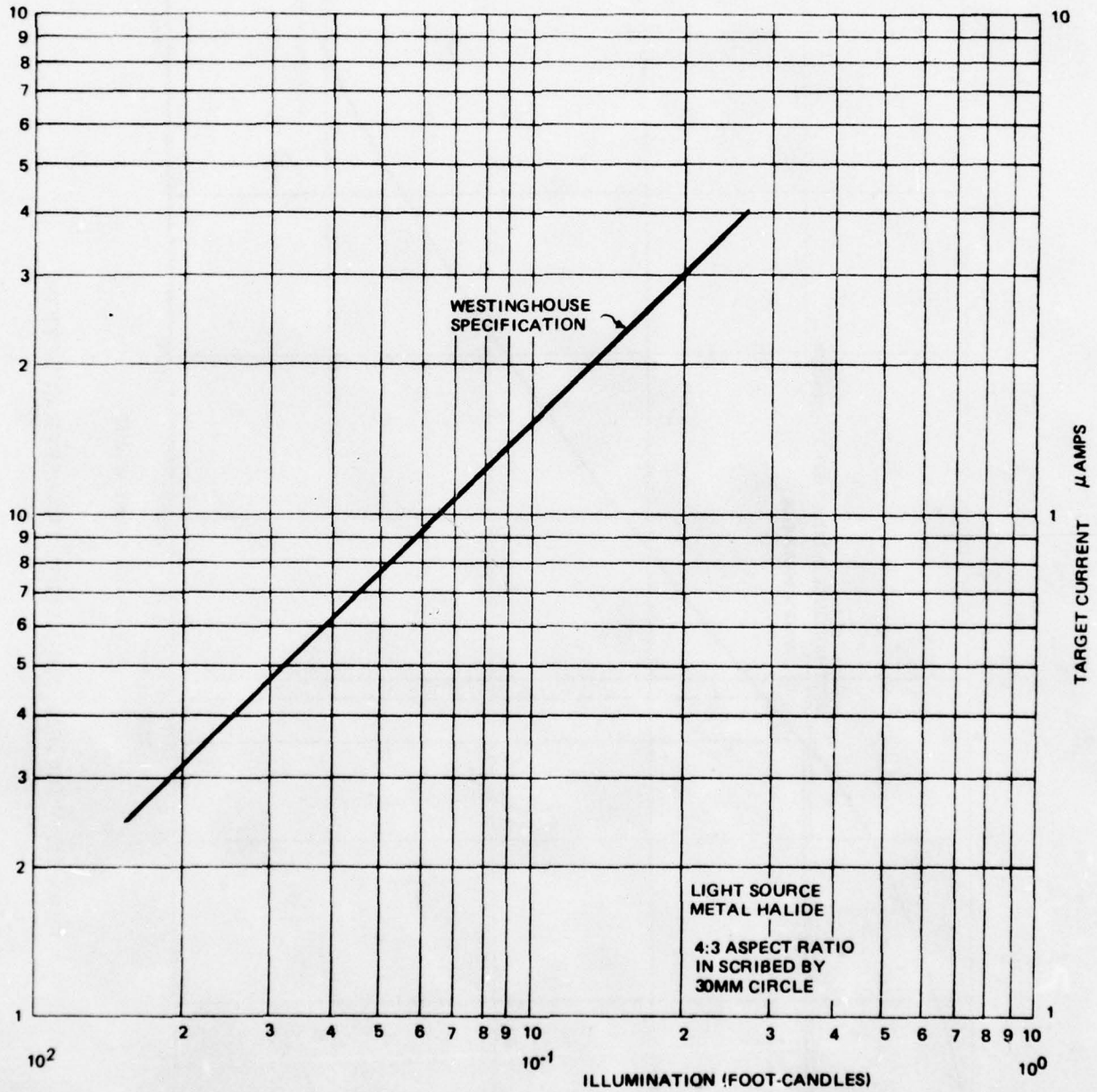


Figure 16. VIDICON FACEPLATE ILLUMINATION CHARACTERISTICS

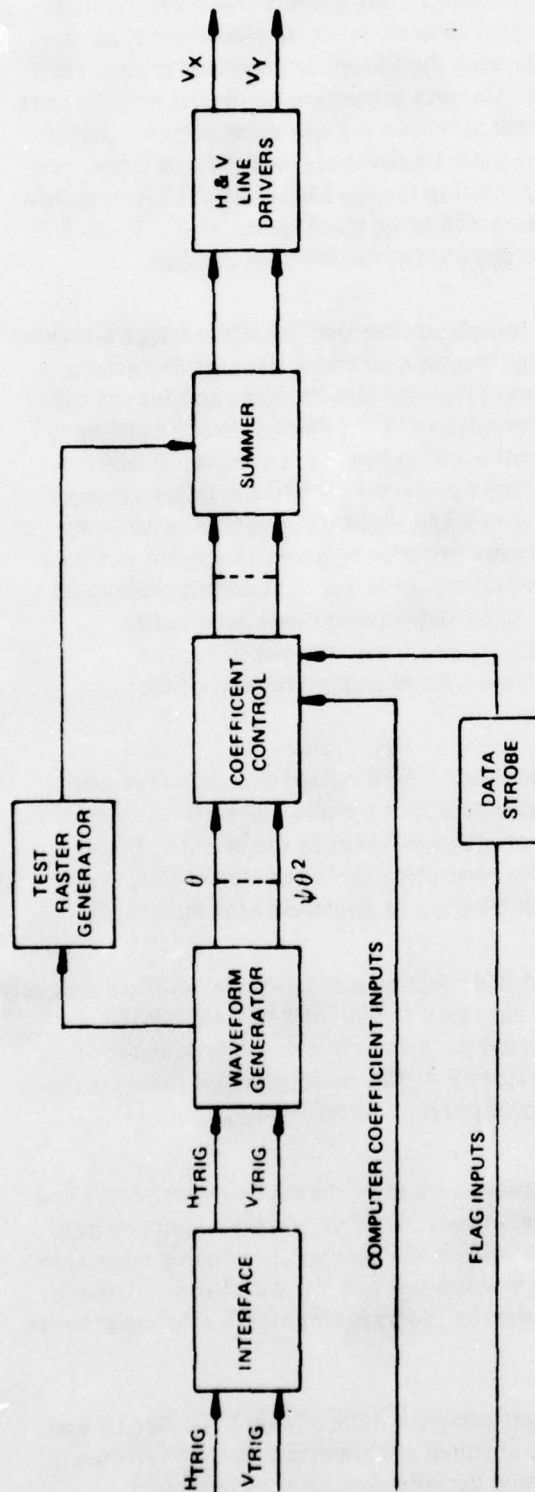
The expected S/N ratio will be reduced by 6 db, due to smaller signal current, resulting in a total camera S/N ratio of 46 db.

- 1) Vidicon - The WX5168 vidicon exhibits a unity gamma characteristic and, in order to maintain the 46-db signal-to-noise ratio, no electronic gamma correction will be used to complement the Eidophor projector gamma for realistic, gray scale reproduction. Gamma correction amplifiers amplify dark picture areas more than white areas accentuating any noise present. Rather than using gamma correction, the model reflectances will be controlled over a low, dynamic range, thus compensating for the Eidophor. This will provide a very good image generator system S/N ratio, since (generally) a 40-db S/N ratio is considered acceptable for most video display applications.
- 2) Camera Raster Shaping - Camera complex raster shaping at the target television camera is required for proper image mapping on the system display screen. Corrections for both the camera and projector lens systems, and for the off-axis position of the target projector relative to the display screen must be incorporated. All raster shaping will occur in the target camera. Raster shaping cannot be applied at the target projector, due to the inflexibility of the Eidophor raster format. Horizontal and vertical deflection waveforms will be generated by a dynamic camera raster computer and applied to linear deflection amplifiers driving a low-inductance yoke. A relatively wide-band linear amplifier with a small signal (non-slew-rate-limited) bandwidth of at least 10 times the horizontal scan frequency is required for the horizontal deflection field to maintain a faithful reproduction of the camera raster computer waveform.
- 3) Camera Digital-Analog Raster Computer - The function of a digital analog raster computer DARC is to generate complex V_X and V_Y waveforms which are used to control the trajectory of electron beams in the camera. Figure 17 outlines the general equation for generating these waveforms (V_X and V_Y), and illustrates a general block diagram to implement the equations.

Waveform coefficients are the so-called "mapping coefficients" and are uniquely determined for given azimuth and elevation coordinates of field of view. That is, for a given target projector azimuth and elevation, a unique set of values is input from the simulator system digital computer, and these coefficients in turn scale their various corresponding waveforms.

The DARC waveform generator forms a variety of shapes from horizontal and vertical triggers by successive analog integration. Digital coefficients operate on these waveforms through MDAC's (multiplying digital-to-analog converters). The results are summed to form composite V_X and V_Y waveforms. There is a practical limit to the number of waveform terms, imposed by the error terms in the analog integration process.

The DARC associated with the target camera will be a basic F-4E No. 18 unit, extended in complexity, to achieve required system accuracy and dynamic range. Section 5 contains a functional description of the technology³.


 K_{1j} = COEFFICIENT

 θ = INTEGRATION FORMED BY FIELD TRIGGER

 ψ = INTEGRATION FORMED BY LINE TRIGGER

 $P(i), Q(j)$ = INTEGERS DEPENDENT ON i, j

$$V_x = \sum_{j=0}^m K_{1j} \theta^{P(i)} \psi^{Q(i)}$$

$$V_y = \sum_{j=0}^m K_{2j} \theta^{P(i)} \psi^{Q(i)}$$

Figure 17. DIGITAL-ANALOG RASTER COMPUTER FUNCTIONAL DIAGRAM

TARGET CAMERA GANTRY.

The target camera gantry provides the motion of the camera probe assembly relative to the carrier. The gantry will have 3 degrees of freedom as follows:

- X - Along floor - approx 28 ft.
- Y - Vertical - approx 14 ft.
- Z - Parallel to floor, mutually perpendicular to X and Y, approx 3 ft.

X-Drive. The gantry tower on the trolley will ride on the rail mounted on the floor. The trolley has two concave cross-section wheels riding on a circular cross section rail to provide alignment at the base. The upper part of the gantry is held in alignment by a guide wheel riding on a rail at the top of the model support structure. The trolley-tower assembly is driven by a dc torque motor dc tachometer, built integrally on the wheel axle of one of the trolley wheels.

Y-Drive. The tower has two guide rails mounted vertically on one end and a counter-weight guide assembly on the opposite end. The Y-carriage is attached to these two guide rails with Round-way bearings. The Y-carriage is counter-balanced by counter weights connected to it by a steel cable running over two pulleys at the top of the tower. Drive for the Y carriage is provided by a Rohlix rotary to linear motion drive from a vertically-mounted shaft parallel to the two guide rails. This shaft is driven by dc torque motor, dc tachometer assembly mounted at the top of the tower.

Z Drive. The carriage supports a similar (but smaller) drive shaft, dc torque motor, dc tachometer, and guide rail to position the Z carriage frame work. The Z-carriage carries the optical probe, TV camera, mechanical crash sensor, and fill-in lighting assemblies.

The Z carriage, tower and lower rail have precision racks attached which are geared to the feedback position transducers for the respective axis. In addition, electrical-limit switches are provided on each axis to prevent the respective motors from driving the carriage into the bearings or mechanical stops at full torque.

The tower electronics rack carries the servo-amplifiers, and power supplies for the X-Y-Z drive systems, the probe drive servos, and control-circuit components.

Power, control and video signal cables are routed to the moving tower-trolley by a cable tow assembly.

NAVTRAEQUIPCEN 75-C-0009 -1

Performance Requirements For X, Y, Z. The performance requirements for there axes of motion have been computed from an analysis of the required flight maneuvers near the carrier with the 309:1 scale factor. The accuracy and resolution requirements listed below, have been established to meet the specified 1/8-ft. positioning requirement.

	<u>Range*</u>	<u>Velocity</u>	<u>Acceleration</u>	<u>Resolution</u>	<u>High Speed Tracking Error</u>
X	28(+) Ft (8343)	2.186 Ft/Sec (400 Kts)	0.4168 Ft/Sec ² (4G)	0.000427' ≅ (1/8 Ft)	0.028 Ft @ 2.186'/Sec
Y	14 Ft (4326)	2.186 Ft/Sec (400 Kts)	0.4168 Ft/Sec ² (4G)	0.000427' ≅ (1/8 Ft)	0.014 Ft @ 2.186'/Sec
Z	2.912 Ft (900)	0.260 Ft/Sec (6100 Ft/Min)	0.3126 Ft/Sec (3G)	0.000427' ≅ (1/8 Ft)	0.0029 Ft @ 0.26 Ft/Sec

*Max Range to Ctr Rot Target = 20.55 ft (6360 ft)

These performance requirements are based on a computer program that will control the gantry position, probe attitude, and zoom ratios such that the presently defined maneuvers at the defined altitude and velocities can be performed without picture degradation. Flight maneuvers of the aircraft near the carrier will be constrained within a velocity, distance, and altitude envelope.

The slant range versus zoom table (table 3) is consistent with a 400-kt (scaled) relative range rate and a 4g (scaled) gantry capability. With this range-zoom schedule, aspect distortion will not occur due to limited Z-gantry travel for flight maneuvers below the following altitudes:

<u>Simulated Slant Range</u>	<u>Maximum Altitude</u>
(1) $R \leq 4560$ ft	900 ft
(2) $R \geq 8100$ ft	$(\frac{900}{6360} R)$ ft

For $4560 \text{ ft} \leq R \leq 8100 \text{ ft}$, a smooth, maximum-altitude transition between 900 ft. and 1146 ft. is provided.

With this range-zoom schedule, perspective distortions due to zoom are zero for ranges out to 4560 ft. Beyond this range, the maximum perspective distortion occurs at about 2-nm range and is less than 2 arc-minutes of error (3 resolution elements) for the near end of the carrier deck.

Table 3. SLANT RANGE VERSUS ZOOM

DISPLAY					PROBE				
"R" SIMULATED RANGE (NM)	θ CARRIER ANGULAR WIDTH	ℓ TV LINES OVER ANGULAR WIDTH	RESOLUTION PER TV LINE (ARC MINUTES)	Z_D DISPLAY ZOOM POWER	R_P PROBE RANGE	R SIMULATED RANGE	θ_P PROBE CARRIER ANGULAR WIDTH	ℓ TV LINES OVER ANGULAR WIDTH	Z_P PROBE ZOOM POWER
6	1.6°	150	.64	10:1	6360	6	9.3°	150	1.77:1
4	2.4°	200	.72	10:1	6360	4	9.3°	200	2.61:1
3	3.2°	300	.64	10:1	6360	3	9.3°	300	3.46:1
2	4.9°	400	.74	10:1	6360	2	9.3°	400	5.23:1
1.5	6.5°	600	.65	9.1:1	6360	1.5	9.3°	600	6.36:1
8100 FT	7.3°	600	.73	8.1:1	6360	8100	9.3°	600	6.36:1
4560 FT	13.0°	600	1.3	4.56:1	4560	4560	13.0°	600	4.56:1
1000 FT	55.0°	600	5.5	1:1	1000	1000	55.0°	600	1:1
PROBE STARTS MOVING 8100 FT SCALE RANGE									
PROBE IS TRAVELING AT CORRECT VELOCITY AT 4560 FT SCALE RANGE (3/4 NM)									

The following is an analysis of two, possible techniques to drive the X, Y gantry and disk rotation. One technique is to minimize the X and Y gantry accelerations by using an optimized ellipse to create the gantry drive commands. The second technique is simply a piston technique, driving only the X-gantry axis and maintaining the Y-gantry centered. The first technique allows maximum velocity and minimum fly-by distances. However, as the aircraft velocity and/or flight path exceeds the gantry drive capability the system will lag with the possible result that the gantry will be "trapped in the corner." The gantry cannot be trapped in the second technique, but the X gantry accelerations, required by the algorithm of the second technique, are unachievable, even with major X-gantry redesign.

Let the coordinates of the aircraft in the frame of the carrier axes be X_C, Y_C, Z_C , and the coordinates of the probe in the frame of the gantry axes be X_G, Y_G, Z_G . The rotation of the disk on which the carrier model is mounted requires a transformation between these coordinates. The rotation ϕ of the disk does not affect the Z coordinate, so that, assuming X_G, Y_G , and Z_G are in scale dimensions then $Z_G = Z_C$. Figure 18 shows the relationship of X_G, Y_G to X_C, Y_C .

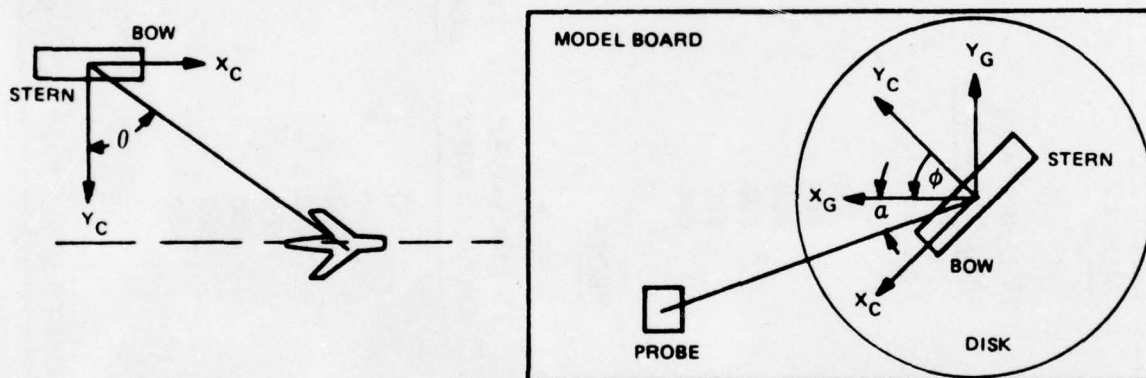


Figure 18. X_G, Y_G TO X_C, Y_C RELATIONSHIP

From figure 18, we can write:

$$\alpha = -\tan^{-1} \left(\frac{Y_G}{X_G} \right), \quad \theta = \tan^{-1} \left(\frac{X_C}{Y_C} \right),$$

$$\theta = \phi + \alpha.$$

$$(1) \quad \phi = \theta - \alpha = \tan^{-1} \left(\frac{X_C}{Y_C} \right) + \tan^{-1} \left(\frac{Y_G}{X_G} \right).$$

We must also have:

$$(2) \quad X_C^2 + Y_C^2 = X_G^2 + Y_G^2.$$

This does not determine X_G, Y_G , since we have just one equation (eq. (2)) to determine two variables. Once we have chosen X_G, Y_G (consistent with eq. (2)), ϕ will be whatever eq. (1) requires it to be. This freedom is used to select a trajectory that will not require excessive accelerations and will not allow the gantry to get trapped on the negative X_G side of the gantry.

Figure 19 shows a trajectory that was found to simulate the straight-line fly-by indicated by the dotted line in the left half of figure 18 without requiring excessive gantry accelerations \ddot{X}_G and \ddot{Y}_G .

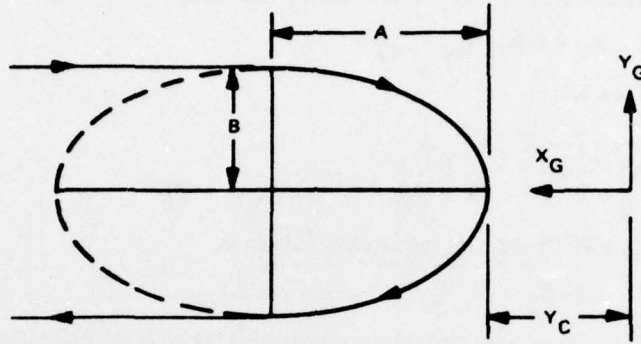


Figure 19. SIMULATED STRAIGHT-LINE FLY-BY TRAJECTORY

Figure 19 shows an ellipse with semi-major axis A and semi-minor axis B, with one vertex, a distance Y_C from the center of the disk (origin of gantry axes). At the points where the ellipse crosses the minor axis, we have $X_G = A + Y_C$, $Y_G = B$. Substituting these values into (2) and solving for X_C we obtain the special value X_{CO} :

$$(3) \quad X_{CO}^2 = (A + Y_C)^2 + B^2 - Y_C^2.$$

Now for $X_C^2 > X_{CO}^2$, the gantry is made to traverse the lines $Y_G = -\text{SIGN}(X_C) \cdot B$. For these cases, we have, from eq. (2), $X_G = +\sqrt{X_C^2 + Y_C^2 - B^2}$. As the gantry and disc accelerations are relatively small for those cases, we are more interested in the case $X_C^2 \leq X_{CO}^2$, for which the gantry traverses the right hand side of the ellipse. By combining the equation of the ellipse with eq. (2), X_G and Y_G are determined. The equation of the ellipse is:

$$(4) \quad \frac{(X_G - (A + Y_C))^2}{A^2} + \frac{Y_G^2}{B^2} = 1.$$

Hence we may write:

$$(5) \quad Y_G^2 = B^2 \left\{ 1 - \frac{[X_G - (A + Y_C)]^2}{A^2} \right\};$$

or:

$$(6) \quad Y_G = -\text{SIGN}(X_C) \cdot B \sqrt{1 - (X_G - (A + Y_C))^2 / A^2}.$$

The sign choice allows a continuous time derivative of Y_G as X_C crosses the origin. Substituting (5) into (2) gives:

$$(7) \quad X_G^2 + B^2 (1 - (X_G - (A + Y_C))^2/A^2) - (X_C^2 + Y_C^2) = 0.$$

This is a quadratic equation in X_G , and assumes the form:

$$(8) \quad A_Q X_G^2 + B_Q X_G + C_Q = 0.$$

If we let:

$$(9) \quad \begin{aligned} A_Q &= 1 - B^2/A^2 \\ B_Q &= 2(A + Y_C) B^2/A^2 \\ C_Q &= B^2 (1 - (A + Y_C)^2/A^2) - (X_C^2 + Y_C^2). \end{aligned}$$

In terms of these coefficients, the required solution is:

$$(10) \quad X_G = (-B_Q + \sqrt{B_Q^2 - 4A_Q C_Q})/2A_Q.$$

The positive sign for the square root is required in order to have $X_G = 0$ for $X_C = Y_C = 0$.

Equation (10) determines X_G , and with this known, equation (6) determines Y_G . Hence the gantry motion is determined, and with this known, Eq.(1) determined the disc rotation, the choice of B is $7 \times 309 = 2163$ scale ft., the maximum the gantry will allow. The value of A was adjusted by trial and error, so that for a straight-line fly-by at $Y_C = 500$ ft., $|\ddot{X}_G|_{\max} = |\ddot{Y}_G|_{\max}$. The trial and error process stopped at $A = 2658$.

For an ellipse, optimized in this way for 500' fly-by, the following table 4 gives gantry positions, velocities, and accelerations for such positions of X_C that the gantry moves from the point $X_G = A + Y_C$, $Y_G = B$ to the point $X_G = Y_C$, $Y_G = 0$, simulating a fly-by at $Y_C = 500$ ft., at a velocity of 320 knots. For larger values of Y_C , maximum accelerations and velocities will be less in magnitude, but $|\ddot{X}_G|_{\max}$ will not equal $|\ddot{Y}_G|_{\max}$. The gantry velocities at a given gantry position are directly proportional to the fly-by velocity, and the accelerations are proportional to the square of the fly-by velocity. Therefore, for velocities in excess of 320 knots at 500' fly-by, the gantry acceleration performance limit of 4 scale g's for \ddot{X}_G and \ddot{Y}_G will be exceeded. Also, as the pilot alters his path from a straight fly-by at these close in ranges, velocity must be reduced in order not to exceed the gantry velocities.

Table 4. GANTRY POSITIONS, VELOCITIES, AND ACCELERATIONS

X_C	X_G	Y_G	ϕ	\dot{X}_G KNOTS SCALE	\dot{Y}_G KNOTS SCALE	$\dot{\phi}$ RADIANS/ SEC	\ddot{X}_G SCALE G'S	\ddot{Y}_G SCALE G'S	$\ddot{\phi}$ RADIANS/ SEC ²
SCALE FT	SCALE FT	SCALE FT	DEGREES	SCALE	SCALE	SEC	SCALE	SCALE	SEC ²
-3794.9	3158	2163	-48.09	-384.5	0	0.1143	1.480	-4.035	-0.00281
-3415.4	2714.2	2132.6	-43.51	-363.3	-50.1	0.1132	1.713	-3.522	-0.00040
-3035.9	2297.5	2046.5	-38.95	-338.8	-94.3	0.1136	1.978	-3.148	0.00124
-2656.5	1912.1	1910.7	-34.36	-310.6	-134.1	0.1149	2.274	-2.837	0.00236
-2277.0	1562.6	1730.0	-29.70	-278.2	-169.9	0.1168	2.595	-2.543	0.00306
-1897.5	1254.0	1509.3	-24.96	-241.4	-201.7	0.1191	2.932	-2.234	0.00337
-1518.0	991.7	1253.3	-20.12	-200.2	-229.2	0.1214	3.265	-1.886	0.00332
-1138.5	780.8	967.7	-15.19	-154.7	-251.7	0.1236	3.570	-1.486	0.00290
-759.0	626.2	658.7	-10.18	-105.5	-268.5	0.1254	3.818	-1.030	0.00215
-379.5	531.8	333.5	-5.10	-53.5	-278.9	0.1266	3.981	-0.529	0.00116
0	500	0	0	0	-282.4	0.1270	4.038	0	0

g = 32 ft/sec² assumed

$$\dot{X}_C = 320 \text{ kts.}$$

$$Y_C = 500 \text{ ft.}$$

$$h = 0$$

For a straight-line fly-by with \dot{X}_C constant and Y_C constant, and with no Y_G gantry motion, the gantry acceleration \ddot{X}_G is:

$$\ddot{X}_G = \frac{d^2}{dt^2} \sqrt{X_C^2 + Y_C^2} \quad (\text{in scale ft/sec}^2)$$

which has a maximum value of $\frac{\dot{X}_C^2}{Y_C}$, at the point $X_C = 0$.

For this case, the disc rotation rate is $\dot{\phi} = \dot{\theta} = \frac{d}{dt} \tan^{-1} \left(\frac{X_C}{Y_C} \right)$ which has a maximum value of $\frac{\dot{X}_C}{Y_C}$ at the point $X_C = 0$ the angular acceleration $\ddot{\phi}$ has the maximum absolute value of $\frac{3}{8} \sqrt{3} \left(\frac{\dot{X}_C}{Y_C} \right)^2 \cong 0.65 \left(\frac{\dot{X}_C}{Y_C} \right)^2$ at the points $X_C = \pm \frac{1}{3} \sqrt{3} Y_C$.

Values of \ddot{X}_G , $\dot{\phi}$, and $\ddot{\phi}$ are listed in table 5 for several values of \dot{X}_C and Y_C .

Table 5. VALUES OF $\dot{X}_G, \dot{\phi}, \ddot{X}_G, \ddot{\phi}$

\dot{X}_C (SCALE KNOTS)	Y_C (SCALE FEET)	\ddot{X}_G (SCALE G'S)	$\dot{\phi}$ RADIANS/SEC	$\ddot{\phi}$ RADIANS/SEC ²
212	1000	4	.358	.083
250	1393	4	.303	.060
350	2730	4	.217	.030
300	500	16	1.013	.667
320	570	16	.948	.584
320	1000	9.13	.540	.190
350	1000	10.92	.591	.227
350	500	21.84	1.182	.908

 $Y_G = 0$

ALTERNATES.

Target Model Board Assembly. The wake length may be as long as a mile or more depending on carrier velocity and sea state, which in turn is a function of wind velocity and duration of wind. For the simulation approach defined, the wake length cannot exceed the length from the carrier fantail to the disc (approximately 2055 ft.).

The wake length on the disc can be varied by having a thin tape on the disc assembly that is above the disc (carrier side) from carrier stern to the edge of the disc with a takeup assembly below the disc. This tape can have a wake pattern painted on it that fades out at approximately 2000 ft. This tape can then be positioned to provide the fade-out portions at the necessary location astern of the carrier to simulate carrier velocities from 0 (no wake) to max velocity (2000 ft.) wake.

An alternate-size gantry has been investigated which would not contain the disc for ~~rotating~~ the carrier heading. The basis for this gantry structure is to use a higher ~~structure~~ (24 ft. high by 24 ft. long) that would have the carrier model located at the ~~center~~ of the model. The carrier will have pitch, roll and heave motions only. The gantry would move around the carrier model which would remain fixed in heading. The painted wake or alternate variable length wake would not be constrained to appear two times carrier length.

Advantages of this arrangement would be less complex software, longer wake, one less large motor-generator and ~~slipping~~ assembly, and fewer constraints on flight path over carrier.

Disadvantages of this arrangement would be the scale factor would be changed to approximately 520:1, and the model deck lighting will be more difficult to implement to scale.

Standard probe dimensions at this scale factor will interfere with the model superstructure when the pilot lands on the carrier deck. In order to prevent this problem, a probe will be used with a small circular snout that protrudes from the main body of the probe. Consequently it will clear the model superstructure. The snout will extend 7 inches from the base of the model. The width from the line of sight to the starboard side is 1.5 inches, and the width to the port side is 2.06 inches.

This probe equals or exceeds the originally-proposed probe performance specifications, except that it has a restricted pitch range of +25° to -40°. The minimum altitude is:

$$\left[1.9 \text{ mm } \left(\frac{520 \times 3.3}{1000} \right) \right] = 3.3 \text{ ft. at this scale factor.}$$

Target Television Camera. The following discussion addresses the effect of operating the TV scan at rates of 525 or 1023 lines, rather than the required scan rate. NTEC specification 212-102, requires 700 TV lines per picture width by 500 TV lines per picture height. The standard formula for arriving at the necessary scan line rate for a given vertical resolution is:

$$(1) N_T = \frac{N_V}{K} + 2 N_R.$$

Where: N_T = Total no. scan lines
 N_V = Vertical resolution in TV lines
 K = Kell factor taken to be 0.75
 N_R = No. of scan lines required for vertical retrace, which is approximately 1200 uses per retrace

Thus:

$$(1) N_T = \frac{500}{.75} + 2 \times 26 = 719 \text{ TV lines.}$$

The closest standard TV line rate is 729 lines. The time required for each scan line is given by:

$$T_T = \frac{1}{N_T \times 30} = \frac{1}{729 \times 30} = \frac{1}{21,870}$$

$$T_T = 45.7 \mu \text{ sec.}$$

If the practical limit of 7 μ sec is allowed for horizontal retrace, then the active time for each scan line is 38.7 μ sec.

$$T_a = T_T - T_R$$

T_a - active scan time

T_T - total scan time per line

T_R - retrace time = 7 μ sec

The required bandwidth for a given horizontal resolution is given by the equation:

$$B_W = \frac{N_H}{2 \times T_a}$$

Where:

B_W - Bandwidth

N_H - Horizontal resolution in TV lines/width.

T_a - Active scan time.

Then:

$$B_W = \frac{700}{2 \times 38.7} = 9.04 \text{ MHz.}$$

Table 6 lists a comparison of the 729 line-scan standard with two alternate scan rates, 525 and 1023. The vertical resolution was determined via equation (1) and the horizontal resolution set at 1.4 times the vertical resolution to maintain the same proportion as the original specification. That is:

$$\frac{N_H}{N_V} = \frac{700}{500} = 1.4.$$

The last column of table 6 lists the signal-to noise ratio, associated with each line-scan systems. The S/N is related to signal bandwidth by the following equation:

$$(2) \quad S/N_1 = S/N_0 + 20 \log \left(\frac{f_0}{f_1} \right)^{3/2}$$

Where:

S/N_1 = New ratio

S/N_0 = Original S/N

f_1 = Bandwidth of new system

f_0 = Bandwidth of original system

Table 6. SCAN LINE TRADE-OFF STUDY

N_T	N_V	N_H	N_R^*	T_T	T_a	B_W	S/N
729 LINES	500	700	26	45.7 μ s	38.7 μ s	9.04 MHz	48db
525 LINES	365	511	19	63.5 μ s	56.5 μ s	4.52 MHz	54db
1023 LINES	715	1001	35	32.6 μ s	25.6 μ s	19.55 MHz	41db

$$* N_R = \frac{1200}{T_T} = 1200 \times N_T \times 30$$

$$N_V = (N_T - 2N_R) K$$

The signal-to-noise ratio is 46 db for a 11.5 MHz bandwidth.⁴ Therefore, equation (2) gives a S/N of 48 db for a 729-line system, and 54 db for a 525-line system, and 41 db for the 1023-line system. It can be observed that as resolution is increased, the S/N ratio is decreased; and therefore, the optimum system performance is a tradeoff between resolution and S/N ratio.

As the resolution is increased, not only does the reduced signal-to-noise ratio affect final picture quality, but also the system's modulation transfer function will fall off at the extended spatial frequencies.

Therefore, in considering the extension of resolution by increased-line scan rates, it became necessary to consider the total system performance and not just the TV camera performance. In general, as in this design, the TV chain (camera and projector) will limit the resolution before the optical system. Since the proposed TV camera employs wideband dc deflection amplifiers, operation throughout the range of 525 to 1023 scan lines is completely feasible. It would be necessary to provide proper synchronous-drive signals to the camera sweep generator and to appropriately limit the video bandwidth for each selected line rate.

SECTION III

TARGET PROJECTOR

The target projector will display the aircraft carrier, wake, and FLOLS in any position in the required field of view.

METHODS CONSIDERED.

Proposed Method. The proposed target projector subsystem consists of an Eidophor TV projector, optics, bearing and elevation prisms, and associated servos. These are illustrated in figure 20.

Alternate Methods. Alternate methods are discussed beginning page 80.

TARGET TV PROJECTOR.

The proposed target projector is an Eidophor model EP8. This includes the projector and the power supply for the lamp. The standard magnetic deflection electronics provide a uniform, rectangular raster, capable of static, keystone correction for projection angles between + 10 and -20 degrees. For this design analysis, Singer intends to use this raster without modification in the initial configuration, and provide the necessary mapping modification for the entire system in the raster computer equipment which is associated with the target image camera. An analysis has been made of the $f(\tan \theta)$ mapping of the field of view of the observer back onto the Eidophor raster surface plane. It demonstrates that in order to meet the 700 horizontal by 500 vertical resolution elements, over the full 60° by 40° field of view, the raster will have to be over-scanned. Figures 21 through 23 illustrate the mapping for three different projector-pointing directions.

The amount of raster overscan involves a compromise between FOV and the required number of V scan lines and bandwidth. The figures show how a standard 4:3 aspect ratio, when allowed to round off the FOV corners up to a 60° FOV diagonal, effects the system resolution. These raster plots demonstrate that the raster over-scans the required FOV by 18 percent, vertically and 10 percent, horizontally. In effect, the projector resolution requirements become 770 horizontal by 590 vertical resolution elements. Taking into account a 0.75 Kell factor, and 38 lines for vertical retrace, a total scan-line count of 825 is required, in order to attain 590 vertical-resolution elements. The horizontal frequency is 24,750 Hz and, allowing for a 7-μ sec retrace line, the active scan time per horizontal line is 33.4 μ sec. Thus the minimum bandwidth requirement is given by

$$\beta\omega = \frac{\text{Horizontal resolution elements}}{2 \times \text{active scan line}}$$

$$\beta\omega = \frac{770}{2 \times 33.4} = 11.5 \text{ MHz}$$

The projector bandwidth is 15 MHz, so as to not limit the total system response. Figure 24 shows the modulation transfer function of an Eidophor projector derived from actual measurements⁵. Note that the plotted MTF includes the effects of an unknown lens. The projector MTF for 770 resolution elements per picture width is 0.55.

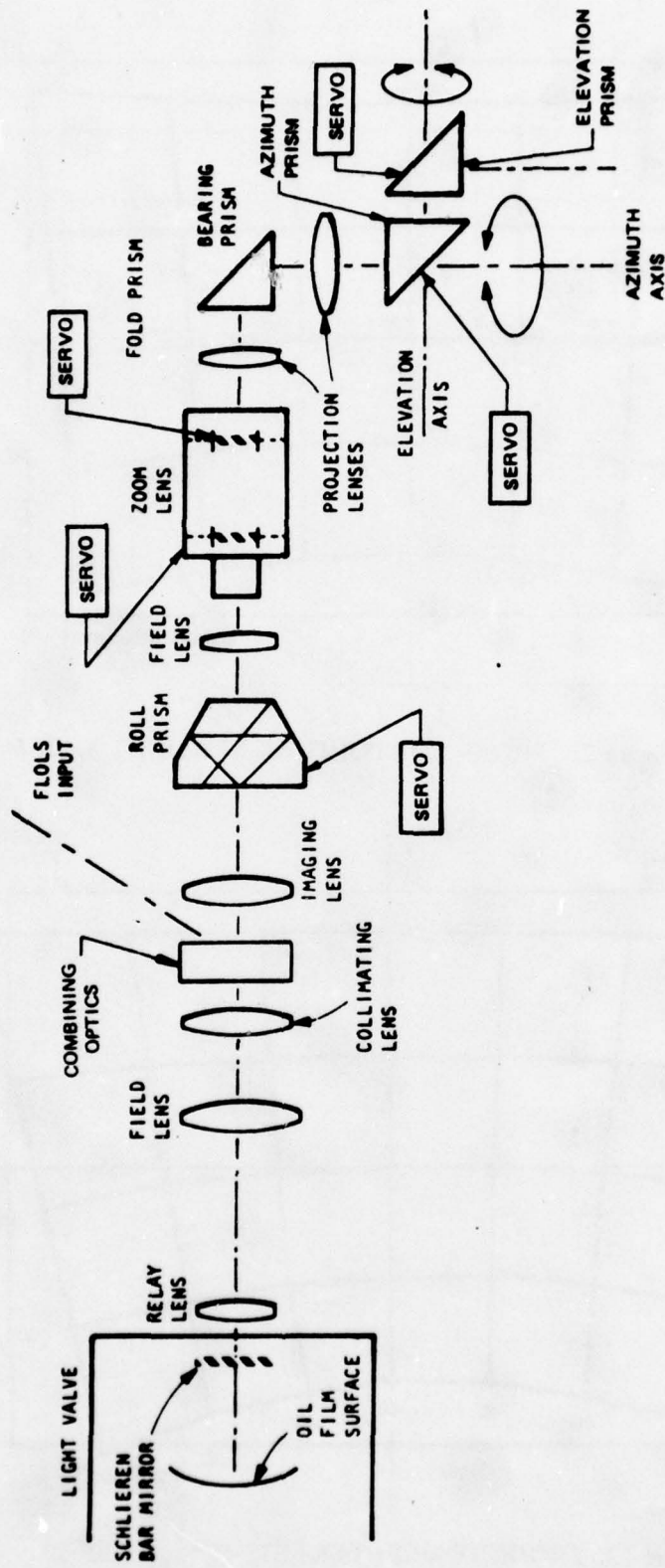


Figure 20. TARGET PROJECTOR OPTICAL SYSTEM

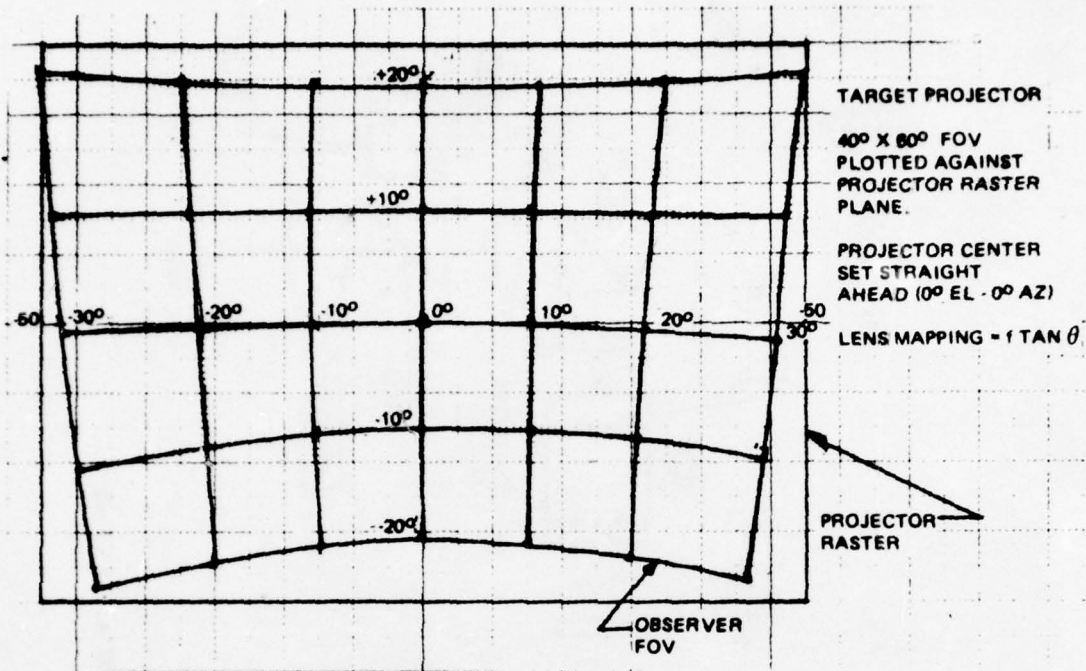


Figure 21. PROJECTOR POINTING STRAIGHT AHEAD

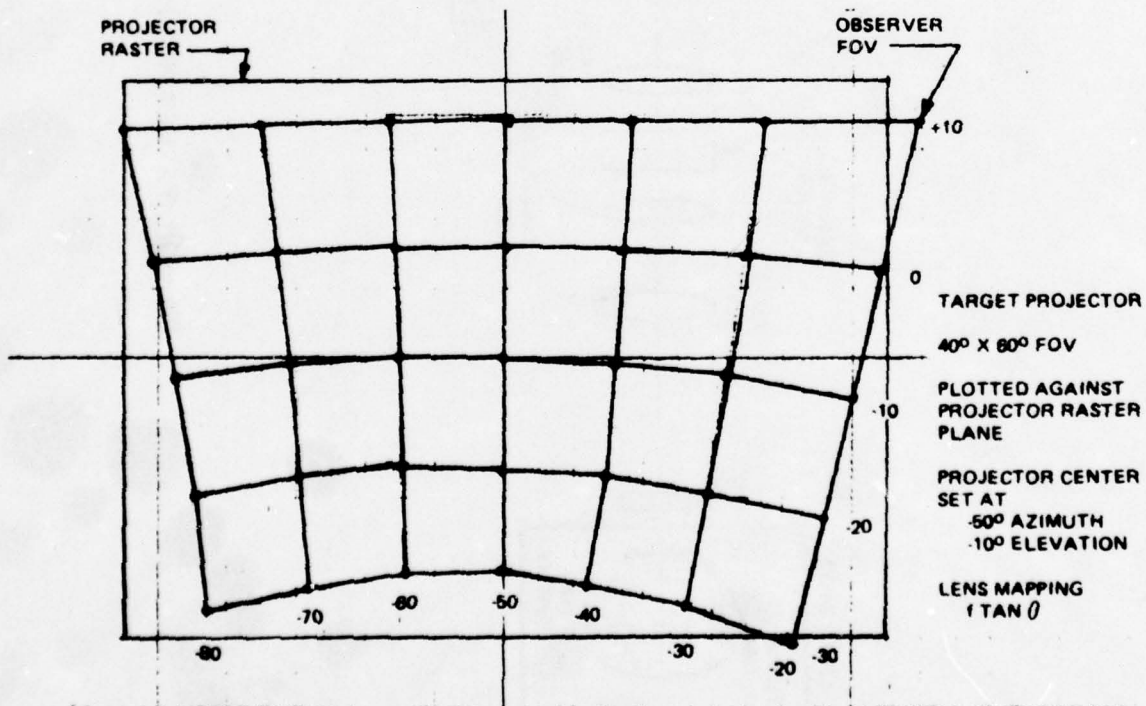


Figure 22. PROJECTOR CENTER-SET, -50° AZ., -10° EL.

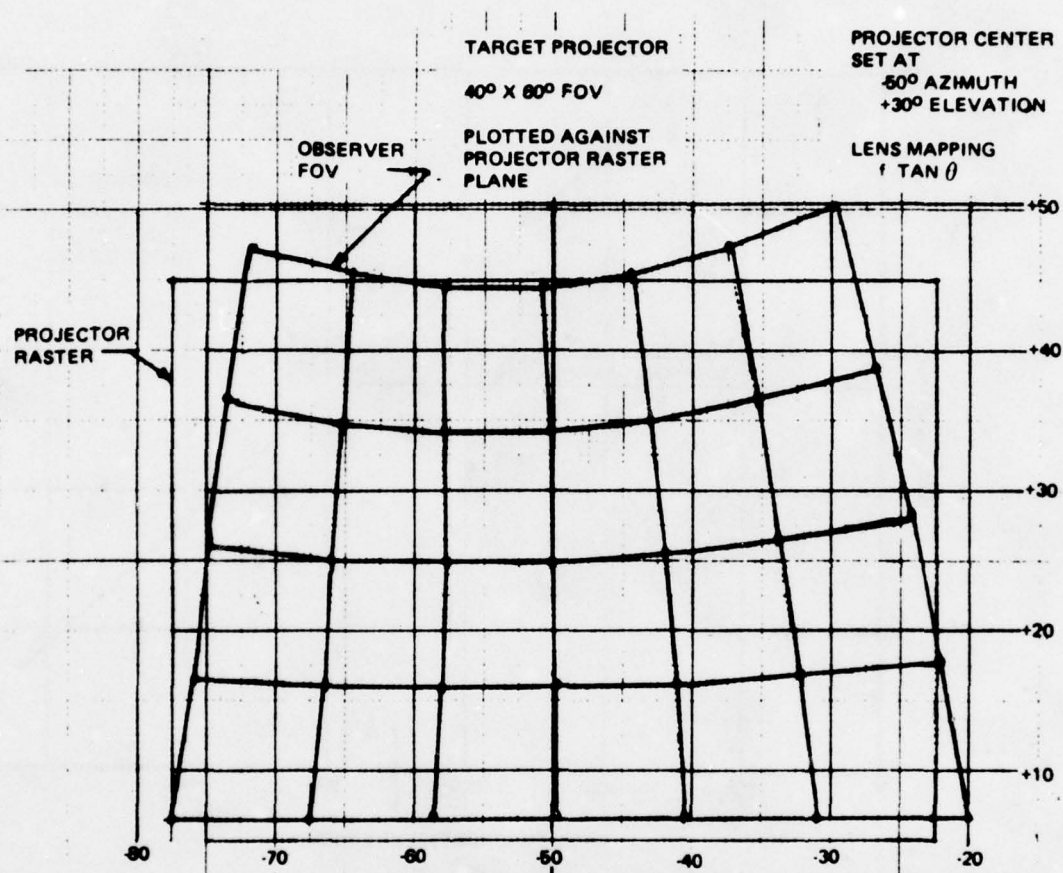


Figure 23. PROJECTOR CENTER-SET, -50° AZ., +30° EL.

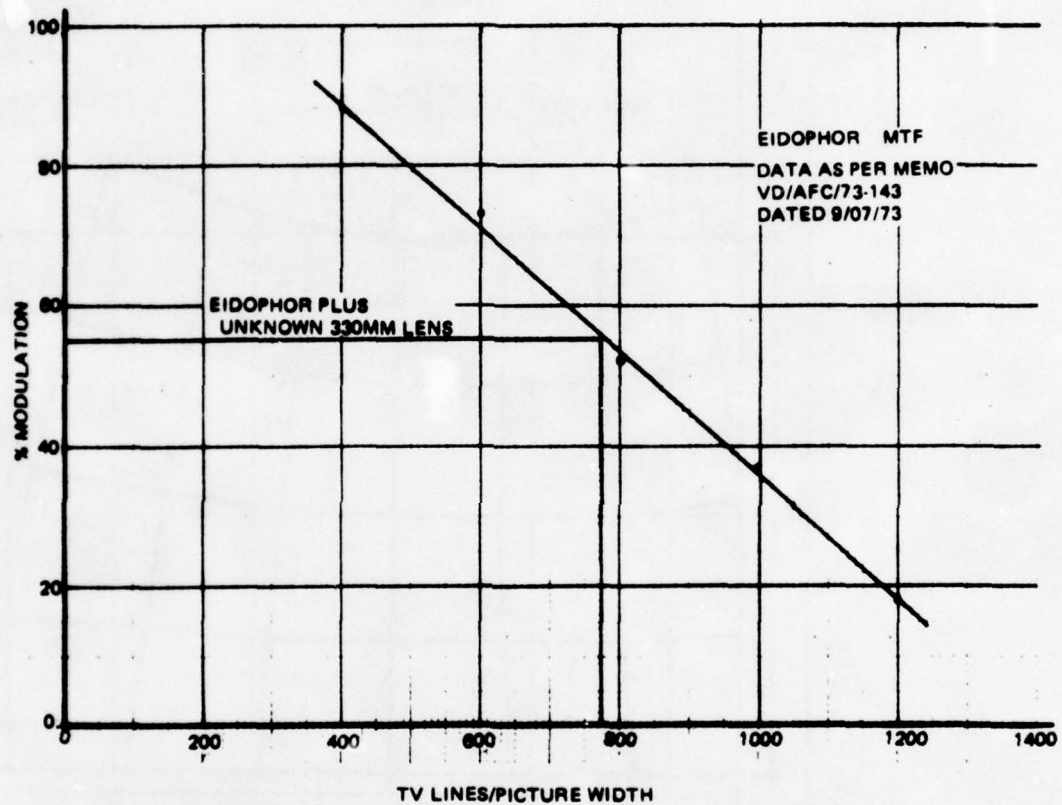


Figure 24. EIDOPHOR MODULATION TRANSFER FUNCTION

To accomplish target insertion into the background, special projector blanking is applied. This is discussed in detail in section 9.

Figure 25 shows the relationship between light output and total scan lines⁶. This is specified as 4000 lumens, $\pm 10\%$, at the raster center, with less than 35% brightness distribution over the raster area. It can be seen that essentially-constant light output can be expected for line rates up to about 800 scan lines with a very sharp roll-off in light output above 900 scan lines. Thus the use of 825 scan lines will not influence the brightness at the screen.

TARGET PROJECTOR OPTICS.

The roll prism introduces the correct roll orientation relative to the pilot and compensates for the roll introduced by the azimuth and elevation prism motions.

The zoom lens changes the image's apparent size so that ranges greater than 0.75 nautical miles from the aircraft carrier can be simulated. The projector and camera zooms are used in synchronism to maximize the target resolution, as discussed in section 5.

The projection lenses are approximately a symmetrical pair. They have external pupils to pick up the pupil from the zoom lens and relay it to a position midway between the azimuth and elevation prisms. This type of lens is used in optical probes and optical comparators. It is usually difficult to design without distortion, but by using a pair that is at least approximately symmetrical the distortion can be virtually eliminated. These lenses are required if one uses azimuth and elevation prisms to move the target image. These lenses are very light in comparison to the whole projector. The prisms use instrument servos which are more precise and less costly than torque motors, which would be required to drive the whole projector in azimuth and elevation.

The pupil must be between the elevation and azimuth prisms, otherwise the larger fields of view would be vignetted.

Because the light level is low, everything possible must be done to preserve it. A special combining optical system was chosen to combine the images of the target and FLOLS. The zones of transmission within the combining optics are aligned coincidentally with the Schlieren mirror bars of the Eidophor projector.

Because the transmission zone of the combining optics is discontinuous, the FLOLS and target image must be collimated prior to the combining optics to prevent multiple images due to the varying optical path.

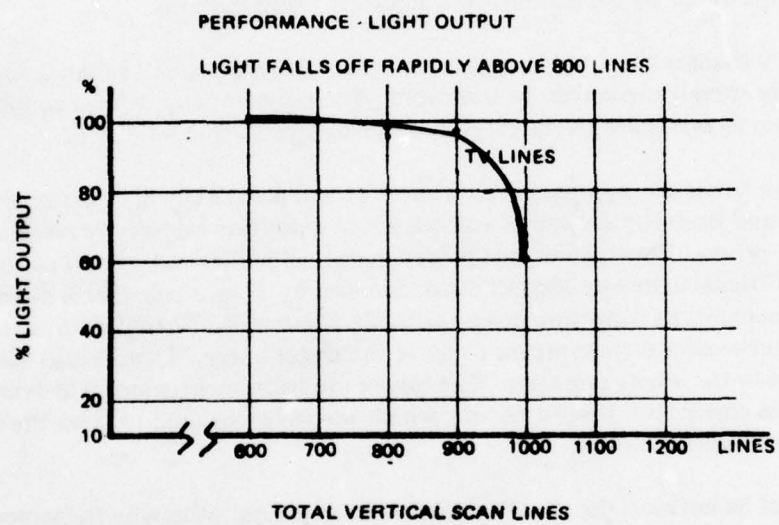


Figure 25. TOTAL SCAN LINES ON 3 x 4 RASTER

Following the combining optics, an image must be formed at the zoom object plane. This is done using an imaging lens. The back-focal of this lens is quite long and permits the insertion of a roll prism in its path. This prism is necessary to reduce roll rate of the roll prism in the probe. It also permits both fixed-roll and fixed ΔX , ΔY in the FLOLS during the simulated FLOLS approach. As a result, the inaccuracies of the FLOLS servos and the accompanying noise will not affect the relative position of the FLOLS and carrier.

The zoom lens both restores the magnified target to the correct size and simulates greater range by further reduction of the image size. The zoom will be an Angenieux (10 x 35, f/3.8) lens.

The entrance pupil of the zoom lens is fixed in position, but not necessarily in size. This pupil is conjugate with the pupil within the combining optics.

The zoom exit pupil does move. This presents a problem for the final projection lenses. This problem would not exist if the image were projected directly to the screen from the zoom lens. But this technique requires heavy servos to be able to move the whole projector to the correct position. These servos and mechanics are not as precise as the small-instrument servos in the proposed design.

This design uses a pair of telecentric lenses to relay the zoom exit pupil to a point midway between the elevation and azimuth prisms and to project the image at the correct size onto the screen. It is necessary to have a pupil which corresponds to the 60° field of view, located between the prisms, so that there is no vignetting.

The pupil for a "zoomed" field of view moves closer to the zoom lens, but the field of view becomes smaller. At the other extreme, the pupil has moved back, near the last lens, but the field has decreased to 7°. This size field can easily pass through the prisms, since the exit pupil size is constant, being driven by a servo.

The azimuth motion of the target image on the screen is achieved by rotating the azimuth and elevation prism assembly about the azimuth axis.

The elevation prism is offset from this axis, which is aligned with the simulated aircraft centerline. This introduces some small distortion in the images, and was discussed in the previous section.

Table 7 shows the relationship of the target and probe zoom focal lengths, resolution, and sizes as a function of simulated range.

Table 7. FLOLS ZOOM FOCAL LENGTH AND IRIS SIZE RELATIONSHIPS

"R" SIMULATED RANGE (NM)	DISPLAY			Z_D DISPLAY ZOOM POWER
	θ CARRIER ANGULAR WIDTH	TV LINES OVER ANGULAR WIDTH	RESOLUTION PER TV LINE (ARC MINUTES)	
6 n.m.	1.6°	150	.64	10:1
4	2.4°	200	.72	10:1
3	3.2°	300	.64	10:1
2	4.9°	400	.74	10:1
1.5	6.5°	600	.65	9.1:1
8100 FT	7.3°	600	.73	8.1:1
4560 FT	13.0°	600	1.3	4.56:1
1000 FT	55.0°	600	5.5	1:1

R_P PROBE RANGE	R SIMULATED RANGE	θ_P PROBE CARRIER ANGULAR WIDTH	TV LINES OVER ANGULAR WIDTH	W CARRIER WIDTH ON FRACTION OF CAMERA	Z_P PROBE ZOOM POWER
6360	6 n.m.	9.3°	150	.25	1.77:1
6360	4	9.3°	200	.37	2.61:1
6360	3	9.3°	300	.49	3.46:1
6360	2	9.3°	400	.74	5.23:1
630	1.5	9.3°	600	.90	6.36:1
6360	8100	9.3°	600	.90	6.36:1
4560	4560	13.0°	600	.90	4.56:1
1000	1000	55.0°	600	.90	1:1

PROBE STARTS MOVING 6360 FT SCALE RANGE

PROBE IS TRAVELING AT CORRECT VELOCITY AT 4560 FT SCALE RANGE (3.4 NM)

Target Projector Lens. Figure 26 shows a schematic of the target projector optics from the Eidophor projector through the zoom lens. The figure also contains typical first-order optical data for the major lens units used in the system.

Within the Eidophor projector are Schlieren bar mirrors. The relay and field lens image this Schlieren bar at the combining optics, while simultaneously collimating the image from the Eidophor.

The decollimating lens is located sufficiently far from the bar mirror to clear the input light from the FLOLS projector. Following the decollimating lens is the field lens which images the bar mirrors onto the zoom lens pupil. The zoom lens pupil is approximately 1 inch in diameter and is located approximately 95 mm from the zoom object plane.

The diagonal size of the zoom lens image is 42 mm. The zoom lens is an Angenieux 10 x 35, f/3.8 lens. The image size relative to the Eidophor object is 1:2.14. This means that the f number of the zoom lens projected back to the Eidophor bar mirror is f/8. Therefore, only an f/8 bundle of light will be accepted from the optical system following the Schlieren bar mirror. This will eliminate light scatter from that portion of the pupil which is occluded by the zoom pupil.

The Schlieren bar mirror is 350 mm from the Eidophor raster surface. The f/8 effective cone subtends, at the bar mirror, a circle of $350 \div 8 \cong 44$ mm.

The first lens is located approximately 404 mm from the object. This distance is as close as is practical to the bar mirrors for first lens location.

It is preferable to relay the images at magnifications other than unity, because of the difficulty in focusing and in aligning them. The first relay lens will magnify the image to a larger size, so that the bar mirror can be easily relayed.

The focal length of this fast-enlarging lens should be 210 mm since there are many standard lenses with this focal length available from Schneider, Optique Boyer, and Christof Friedrich. The f/No. of this lens is about 4.5, therefore, the aperture is 46.7 mm.

This aperture can be used to calculate the largest object distance possible. See figure 27.

Using similar triangles with the lens aperture and bar mirror as bases, the following relation can be written:

$$\frac{S_0}{\frac{46.7}{2} \quad \frac{90}{2}} = \frac{350}{\frac{42}{2} \quad \frac{90}{2}}$$

$$S_0 = 389 \text{ mm}$$

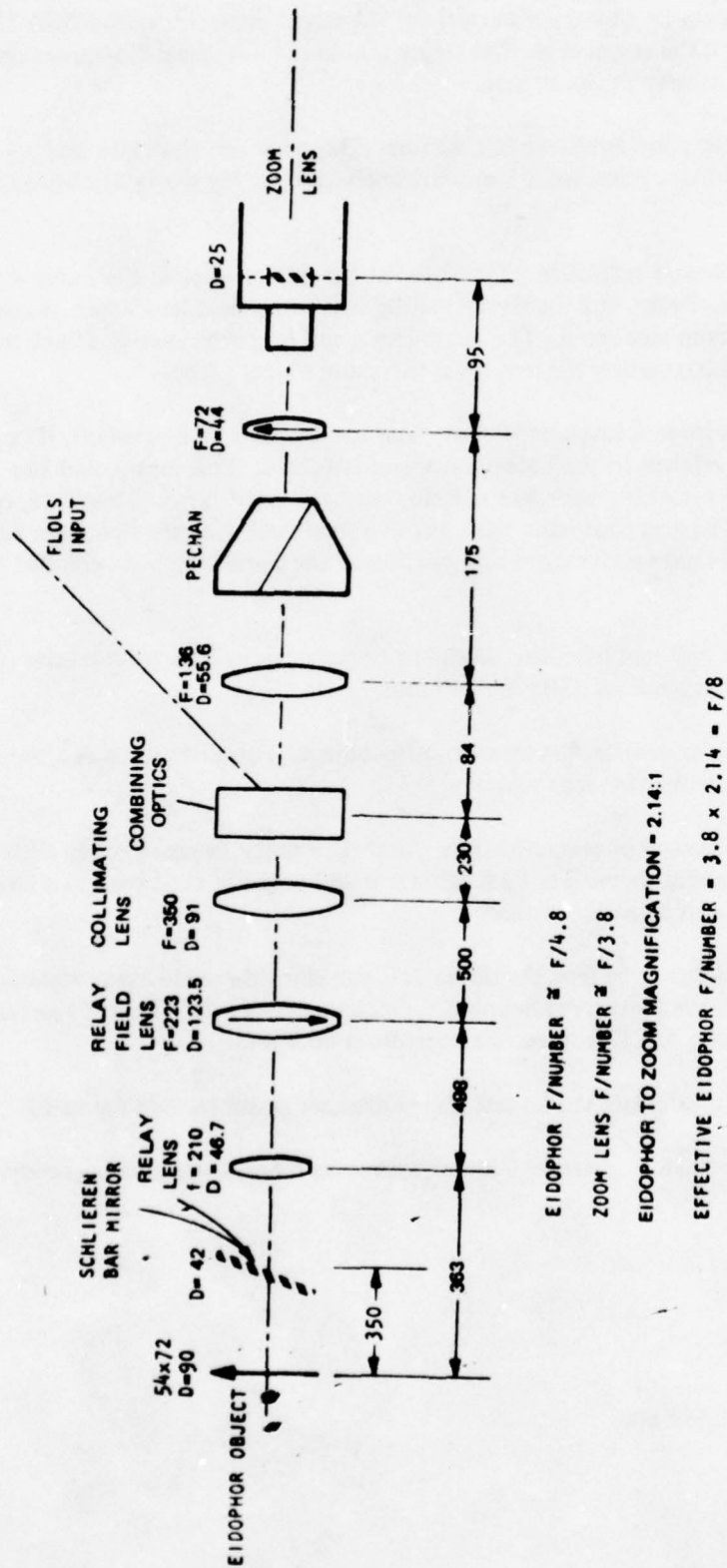


Figure 26. TARGET PROJECTOR OPTICS, SCHEMATIC

The approximate image distance is found using the equation:

$$S'_0 = \frac{S_0 f}{S_0 - f}$$

Substituting values:

$$S'_0 = \frac{389 \times 210}{389 - 210}$$

$$S'_0 = 456 \text{ mm}$$

The magnification is simply $m = -456/389 = -1.17$. The image size is $-90 \times 1.37 = -105.6 \text{ mm}$. The relay field lens is then 123.5 mm in diameter.

The collimating lens has a focal length of 500 mm. This is available from Schneider as a tele-zenon. The object for this lens is 123.5 mm. This represents a field of view of

$$\theta = 2 \tan^{-1} \frac{105.6}{2 \times 500}$$

$$\theta \cong 12^\circ$$

The decollimating lens must image the field in the 44 mm diameter of the zoom lens. The focal length is:

$$f = \frac{22}{\tan 6^\circ} \cong 209$$

The image of the Projector Schlieren Bar is derived from the equation:

$$S'_1 = \frac{S_1 f}{S_1 - f}$$

For the meanings of the terms of the equation shown above, see figure 28. Therefore:

$$S_1 = \frac{13 \times 210}{13 - 210} ;$$

$$S_1 = -13.9 \text{ mm.}$$

The aperture of the collimating lens is found from its $f/\text{No.}$, which is 5.5. The aperture is $500 : 5.5 \approx 91 \text{ mm}$.

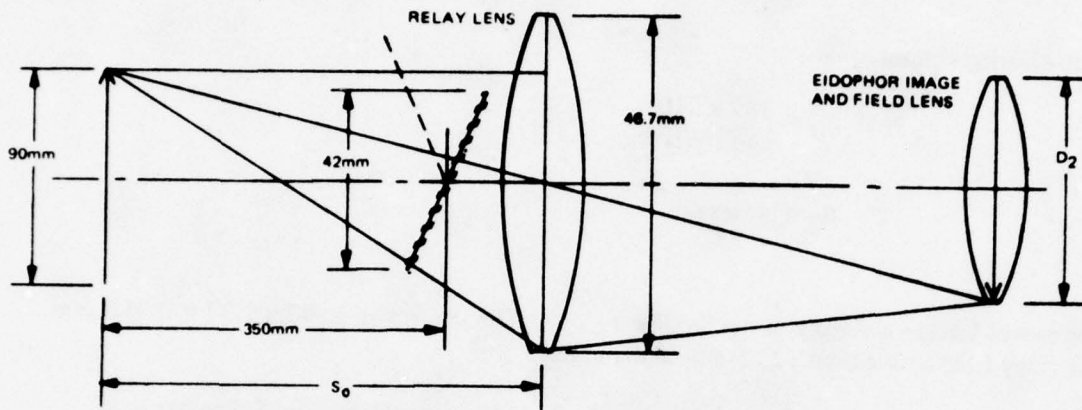


Figure 27. APERTURE GEOMETRY

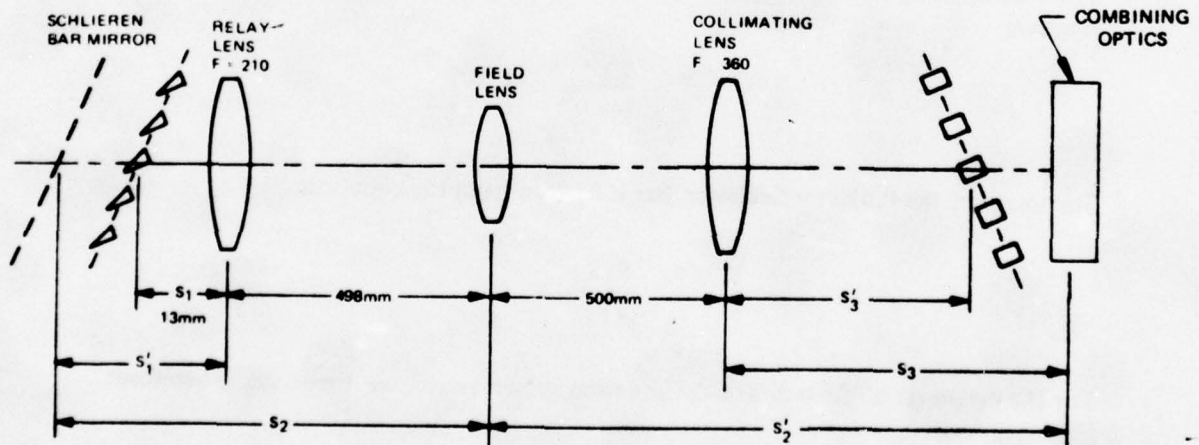


Figure 28. BAR MIRROR AND RELAY LENS RELATIONSHIP

The pupil's chief rays which pass from the edge of the bar mirror through the center of the field lens will hit the collimating lens within its aperture. Therefore, the focal length of the field lens can be chosen so that the collimating lens will not vignette any of the image.

The extreme ray from the top of the Schlieren bar mirror passes through the bottom edge of the field lens, and the bottom edge of the collimating lens. This is shown on figure 29.

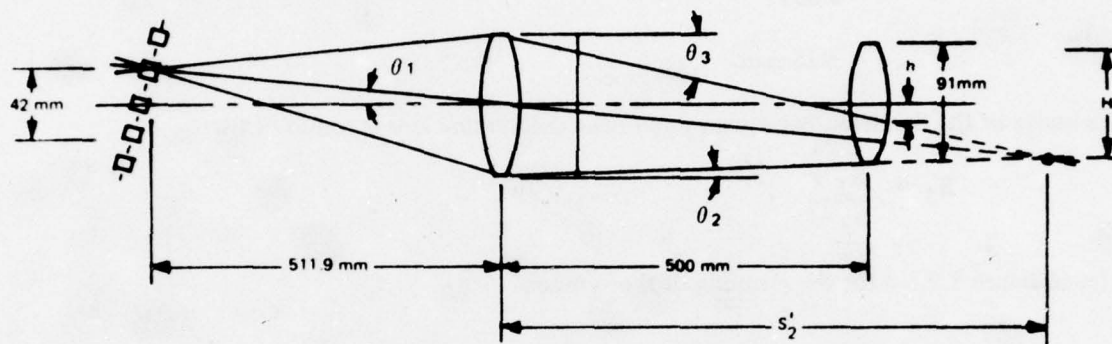


Figure 29. EXTREME RAY SCHEMATIC

From the figure the following equations can be written.

$$\tan \theta_1 = \frac{-2.12/2}{495} = 0.0425$$

$$\tan \theta_2 = \frac{(105.6 - 91)/2}{500} = 0.0146$$

$$\frac{H}{2} = S'_2 \tan \theta_1 = -0.0425 S'_2$$

$$\frac{H}{2} = S'_2 \tan \theta_2 - 123/2 = 0.0146 S'_2 - 52.8$$

combining these last two:

$$-0.0425 S'_2 = 0.0146 S'_2 - 52.8$$

$$S'_2 = \frac{52.8}{0.0571}$$

$$= 925 \text{ mm}$$

The image of the Schlieren bar mirror due to the collimating lens is found below:

$$S'_3 = \frac{S_3 f}{S_3 - f} ;$$

refer to figure 3.2.1-3 for the meaning of the symbols.

$$S'_3 = \frac{(500 - 925)(500)}{(500 - 925) - (500)} ;$$

$$= 230 \text{ mm};$$

this is the location of the Fresnel bar mirror where the FLOLS imagery is inserted.

The height of the image is:

$$\begin{aligned} H &= 2 S'_2 \tan \theta_1 \\ &= -2 \times 925 \times 0.0425 = 78.6 \text{ mm} \end{aligned}$$

The height H' of it after leaving the collimator:

$$H' = 78.6 \times \frac{230}{925 - 500} = 42.5 \text{ mm};$$

the value of $\tan \theta_3$ can be calculated:

$$\begin{aligned} \tan \theta_3 &= \frac{(105.6 + 78.6)/2}{925} \\ &= 0.0995 \end{aligned}$$

The height h on the collimating lens of the upper extreme ray from the top of the bar mirror through the top of the field lens is:

$$\frac{h}{2} = \frac{-105.6}{2} + 500 \tan \theta_3;$$

$$\frac{h}{2} = 3.05 \text{ mm}$$

The angle the ray has after leaving the collimator is found from the equation below.

$$\tan \theta_4 = \frac{\frac{h + H'}{2}}{S_3'}$$

Refer to figure 30 for the meaning.

Therefore:

$$\tan \theta_4 = \frac{\frac{h + H'}{2}}{S_3'};$$

$$\text{then, } \tan \theta_4 = \frac{3.05 + 21.25}{230} = 0.1056$$

The choice of an ISCO, 175 mm f.l., $f/2.7$ lens permits locating the lens about 84 mm from the combining optics. The aperture of this lens is calculated below:

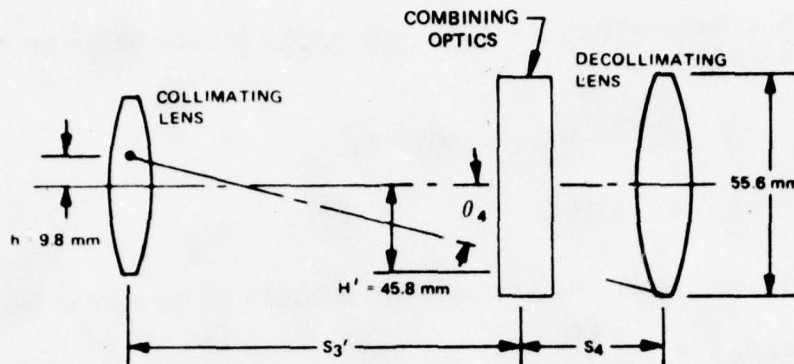
$$175/2.7 = 55.6 \text{ mm}$$

$$S_4 = \frac{(55.6 - 42.5)/2}{0.0995} = 65.8$$

$$S_4 \cong 65.8 \text{ mm}$$

This provides plenty of room to insert the FLOLS image.

The back-focus of this lens is 105 mm. The back-focus of the zoom lens is about 50 mm. This provides about 158 mm of path which is sufficient to insert a Pechan roll prism.

Figure 30. ILLUSTRATION OF TAN θ_4 EQUATION

Following the Angenieux 10 x 35 zoom is a pair of projection lenses which must be designed. They are like the objective in an optical comparator, or optical probe. They are used as a pair to relay the exit pupil of the zoom to a point inbetween the azimuth and elevation prisms for the 60° field of view. Figure 31 shows the arrangement of these lenses.

Image Luminance - The luminance is determined by three factors. They are the output of the Eidophor - the actual acceptance f/No. and the optical transmission.

The output is 4000 lumens at f/4.8 at the Eidophor. However, as determined in figure 26, the actual accepted f/No. is f/8. Therefore the flux available is

$$\left(\frac{4.8}{8}\right)^2 \times 4000 = 1440 \text{ lumens.}$$

The transmission can be estimated for the various optical elements. Table 8 shows the values ascribed to the various lenses. These are estimates based on experience and are conservative.

The flux delivered to the screen is $0.077 \times 1440 = 110$ lumens

The field of view is 40° x 60° over which the flux is more or less uniformly distributed. The screen is approximately 10 ft. away. The area this corresponds to is approximately:

$$\frac{40}{57.2} \times \frac{60}{57.2} \times 10^2 = 73 \text{ ft.}^2$$

The illumination is $110 \div 73 = 1.5$ ft. candles.

This requires a screen gain of 4 to meet the 6 foot-lambert requirement, which is not considered acceptable, due to difficulties in obtaining uniform brightness over the large screen field of view.

Table 8. NET LENS TRANSMISSION

Relay Lens	80%
Field Lens, Collimator	90%
Collimating Lens	75%
Combining Optics	95%
Decollimating Lens	70%
Roll Prism	60%
Field Lens, Zoom	90%
Zoom Lens	70%
1st Projection Lens	80%
Prism	95%
2nd Projection Lens	80%
Prism	95%
Net Transmission	7.7%

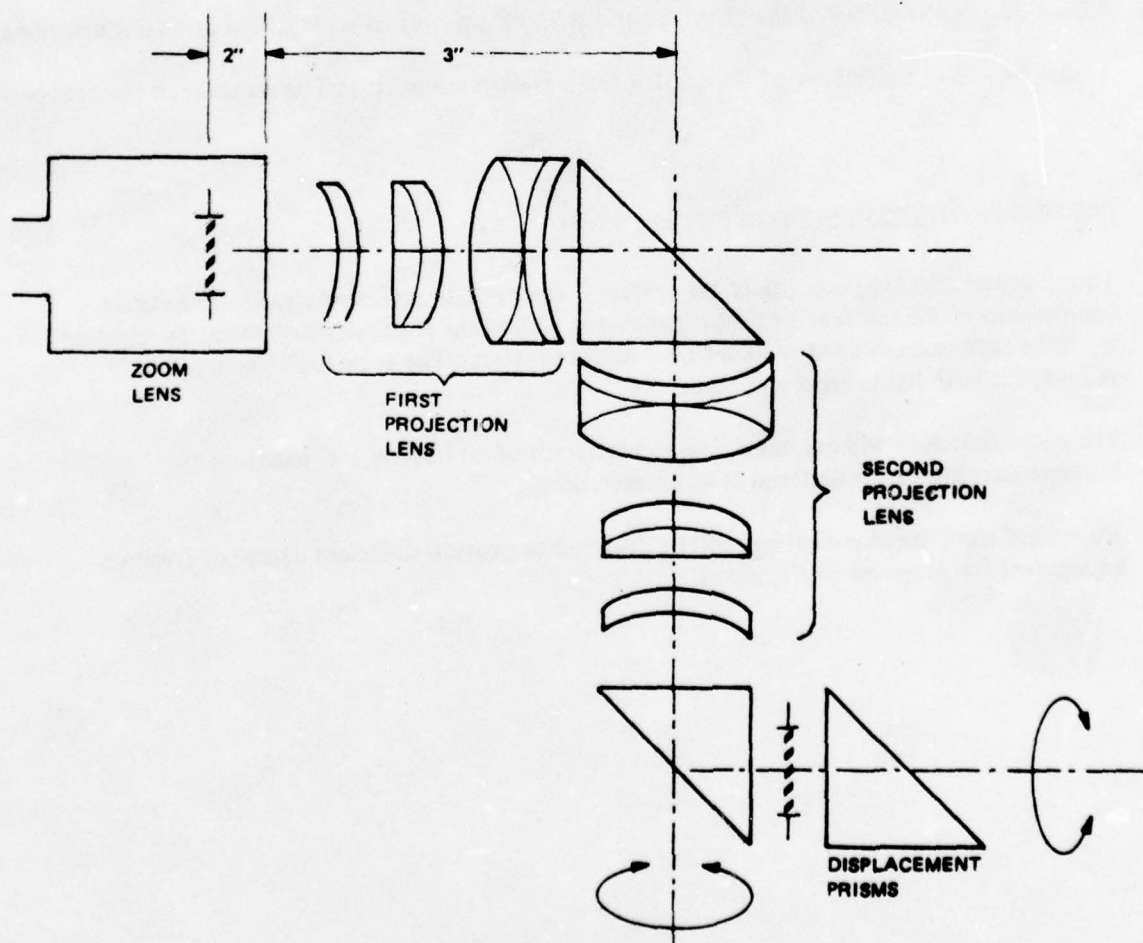


Figure 31. TELECENTRIC LENS PAIR

TARGET PROJECTOR GIMBAL.

The structure that supports the target projector and gimbal must provide sufficient rigidity to hold all components in the required optical alignment as well as the required electronics. In addition, it must be light enough to be installed on a motion system. The truss-type construction proposed is both lightweight and rigid. The entire structure will exhibit a final safety factor of no less than 4 based on the ultimate strength of the material at 4g acceleration. All optical component mountings will be designed to provide adequate adjustment for purposes of alignment.

The proposed gimbal system will consist of two prisms that rotate together about a vertical axis to give continuous azimuth or relative bearing, while the final prism in the optical path rotates $\pm 90^\circ$ to give elevation. As a protective measure there will be no components, stationary or otherwise, located in the excursion envelope of the projector gimbals.

Figure 32 shows the location of the exit aperture relative to the cockpit from the front.

Figure 33 shows a detail of the elevation and azimuth prisms and some of the critical dimensions.

Figure 34 shows a side view of the display systems with many critical dimensions to the exit pupil.

TARGET PROJECTOR SUPPORT STRUCTURE.

The structure that supports the target projector will provide sufficient rigidity to hold all components in the required optical alignment as well as the required electronics. In addition, it will be light enough to be installed on a motion system. The truss-type construction proposed is both lightweight and rigid.

The entire structure will exhibit a final safety factor of no less than 4 based on the ultimate strength of the material at 4g acceleration.

All optical component mountings will be designed to provide sufficient degree-of-freedom adjustment for purposes of alignment.

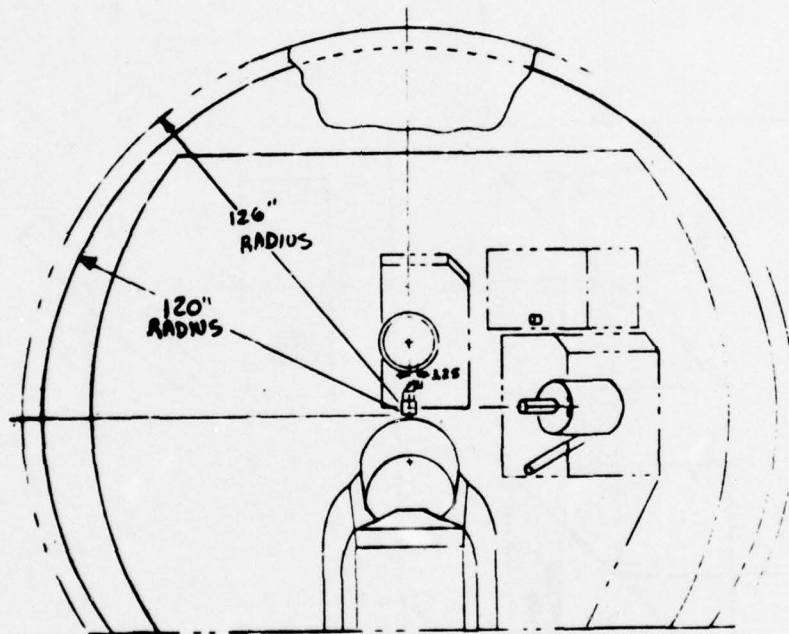


Figure 32. EXIT APERTURE LOCATION

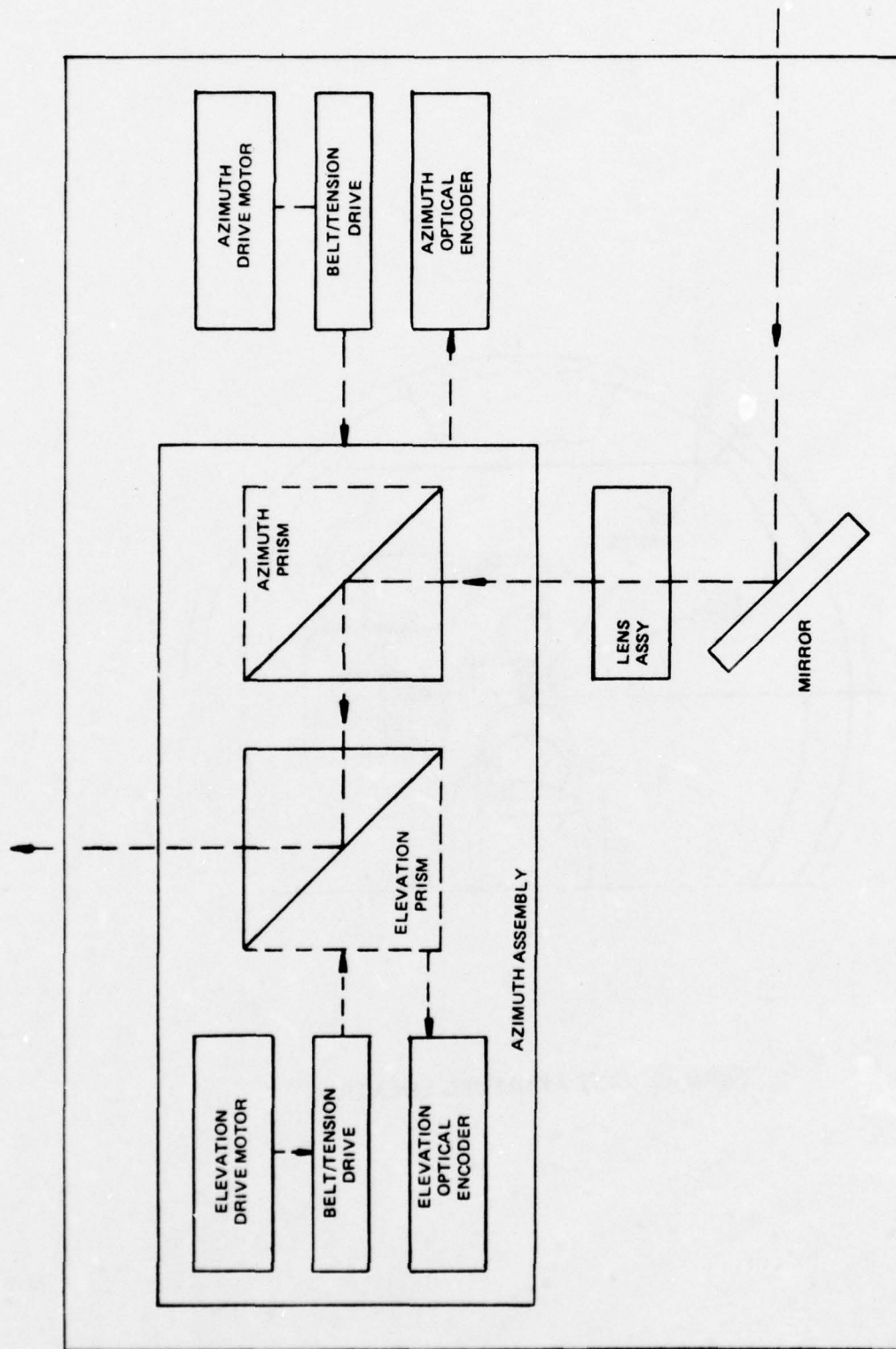


Figure 33. AZIMUTH AND ELEVATION DRIVES

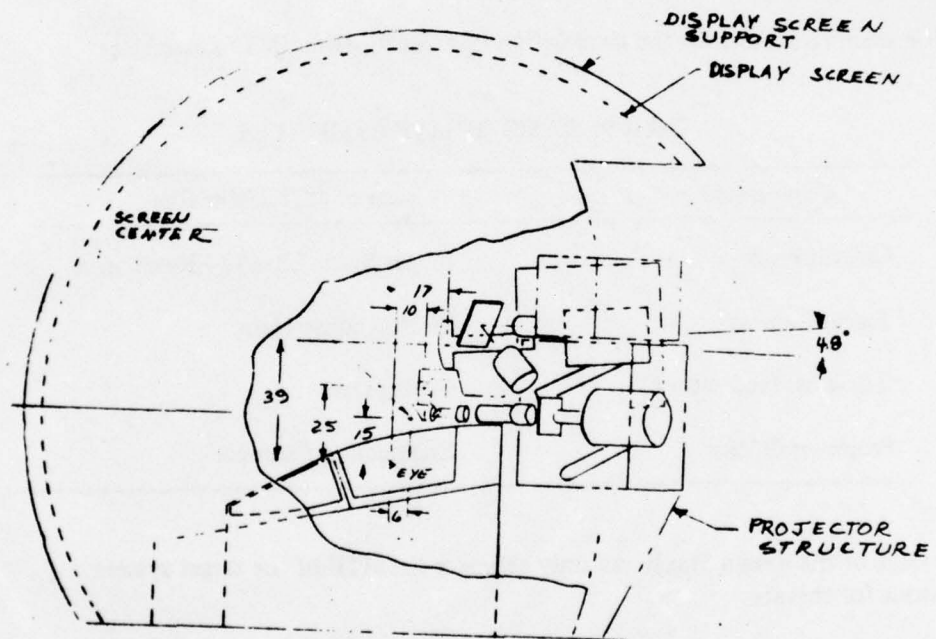


Figure 34. DISPLAY SYSTEM SIDE VIEW

RESOLUTION

The target system resolution is comprised of the cascaded transfer function of four components. There are:

- a) Optical Probe
- b) Target Camera
- c) Eidophor Projector
- d) Projector Optics

Table 9 presents the basis for the modulation transfer function (MTF) estimates.

Table 9. BASIS OF MTF ESTIMATES

Component	Basis of MTF Estimates
Optical Probe	Singer Spec. LR-632 - Revision A
Target Camera	Westinghouse Data
Eidophor Projector	Gretag Data
Projector Optics	Engineering Estimate

At this stage of the design Singer can only estimate the MTF of the target system. The reasons for this are:

- a) Several commercial lenses are being used in the design. While they are the best available, nevertheless their MTF performance is not known until they are procured and tested.
- b) Due to the large number of optical surfaces, scattering of light will have a significant unspecified effect on MTF.
- c) Probe vendor has not yet agreed to deliver resolution per LR 632-A

Table 10 presents the on-axis MTF of the components of the target system and the target system for resolutions of 60, 30, 20 and 10 arc-minutes per line pair.

Table 10. COMPONENT AND SYSTEM MTF ON-AXIS, 100 MM PROBE ALTITUDE

	Resolution (Arc-Minutes/Line Pair)			
	60	30	20	10
Optical Probe	91	80	70	46
Target Camera	99	97	93	78
Eidophor Projector	99	95	90	60
Projector Optics	99	95	80	33
Target System	81	70	47	7

ALTERNATES.

Target TV Projector. The target projector may be operated at the same range of line scan rates between 525 and 1023 lines as the target camera. Table 10 summarizes the resultant resolution and required bandwidth. The analysis for the task parallels that of analysis for performance requirements for X, Y, Z will not be repeated. The big difference between the Eidophor projector and the TV camera is that changing line scan ratio is not easily accomplished at the projector as they are at the camera. Since the projector operates on the principle of an equilibrium between electron charge and oil surface tension, the projector manufacturer has recommended that we limit the range of scan lines from between 525 and 825 lines. Over this range, the available light output is relatively constant, and switching between line rates can be accomplished by the changing of circuit card modules. It is therefore, reasonable that the target image system (camera and projector) employs a scan rate from between 525 and 825 lines rates. Table 11 exhibits scan line tradeoffs.

Table 11. SCANNING TRADE OFF

NT	NV	NN	NR	γ_T	γ_a	MINIMUM BW	PROJECTOR LIGHT OUTPUT
729 Lines	500	700	26	45.7 μ s	38.7 μ s	9.04MHz	4000 Lumens
525 Lines	365	511	19	63.5 μ s	56.5 μ s	4.52MHz	4000 Lumens
1023 Lines	715	1001	35	32.6 μ s	25.6 μ s	19.55MHz	2000 Lumens

SECTION IV

FLOLS (FRESNEL LENS OPTICAL LANDING SYSTEM)

The FLOLS must be simulated in such a way that when viewed from the cockpit, the lights appear in the correct position and attitude with respect to the carrier and present the correct size, color, and configuration for all altitudes and range.

Of the several different methods considered for generating a FLOLS image and inserting it into the target image, an optical coupling of a scaled FLOLS model into the target projection path was chosen as providing the best compromise of performance, complexity, and flexibility.

METHODS CONSIDERED.

Proposed Method. Figure 35 shows a simplified illustration of the selected method of composite image generation for the target and the FLOLS. To achieve high brightness and de-emphasize the tracking requirements, a separate FLOLS image generator with high intensity light sources (Xenon arc lamps) is optically coupled into the path of the target projector. The FLOLS image generator consists of a scaled model (about 30:1) of the FLOLS Board with the necessary optics for imaging and motion to project a high intensity image at the Fresnel mirror. The model board is fixed with respect to the target projector, thus eliminating errors due to differences between the target projector and the FLOLS projector. Central to this approach is the reduction in the size of the servos from those required to move a whole projector to instrument size servos where higher accuracies are easier to obtain.

The FLOLS image and the carrier image are combined at the Fresnel mirror and projected from that point as a composite image, thus reducing relative errors between the FLOLS and carrier.

Figure 36 shows the schematic of the optical system. The optical system is capable of varying the FLOLS apparent range by use of both the zoom lens and variable iris. The image will always appear as a projection of the FLOLS on a plane perpendicular to the ideal glide slope, even though the actual viewing point may be to the side.

The range simulation begins at six nautical miles by the iris. Since the FLOLS light size is below the resolution limit of the eye, varying the brightness of the light with the iris will cause an apparent change in range. The FLOLS size will remain constant in to about 5200 ft. The iris opening as a function of range is calculated in the range simulation paragraph (page 95). At 5200 feet the semi-height of the outer Fresnel lens, from the datum line, subtends one minute of arc which is the average visual resolution limit.

From this point, the pilot can begin to clearly detect movement of the meatball relative to the datum line. Therefore, the zoom lens will begin to change the apparent size of FLOLS model. The zoom range is 2.78:1, and so will operate up to approximately 450 feet from the FLOLS. From this

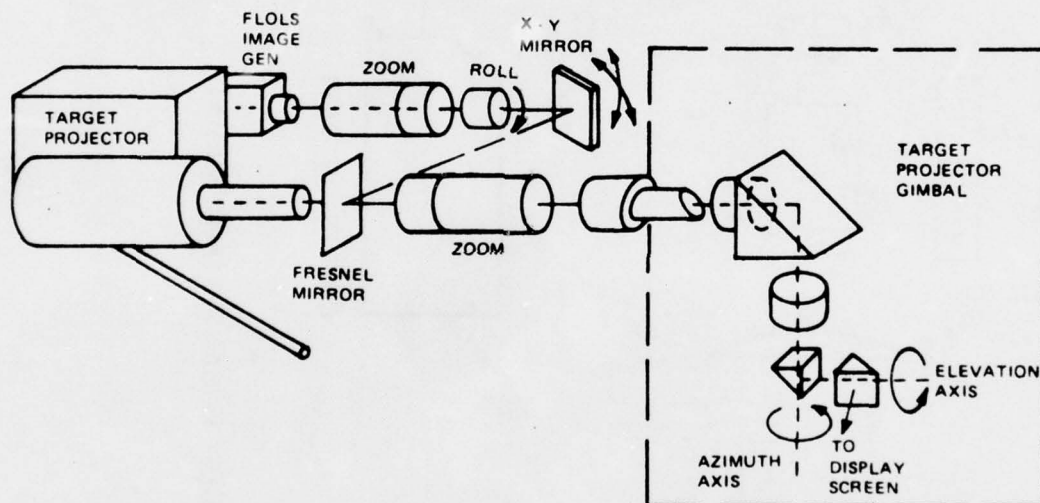


Figure 35. FLOLS AND TARGET PROJECTOR OPTICS

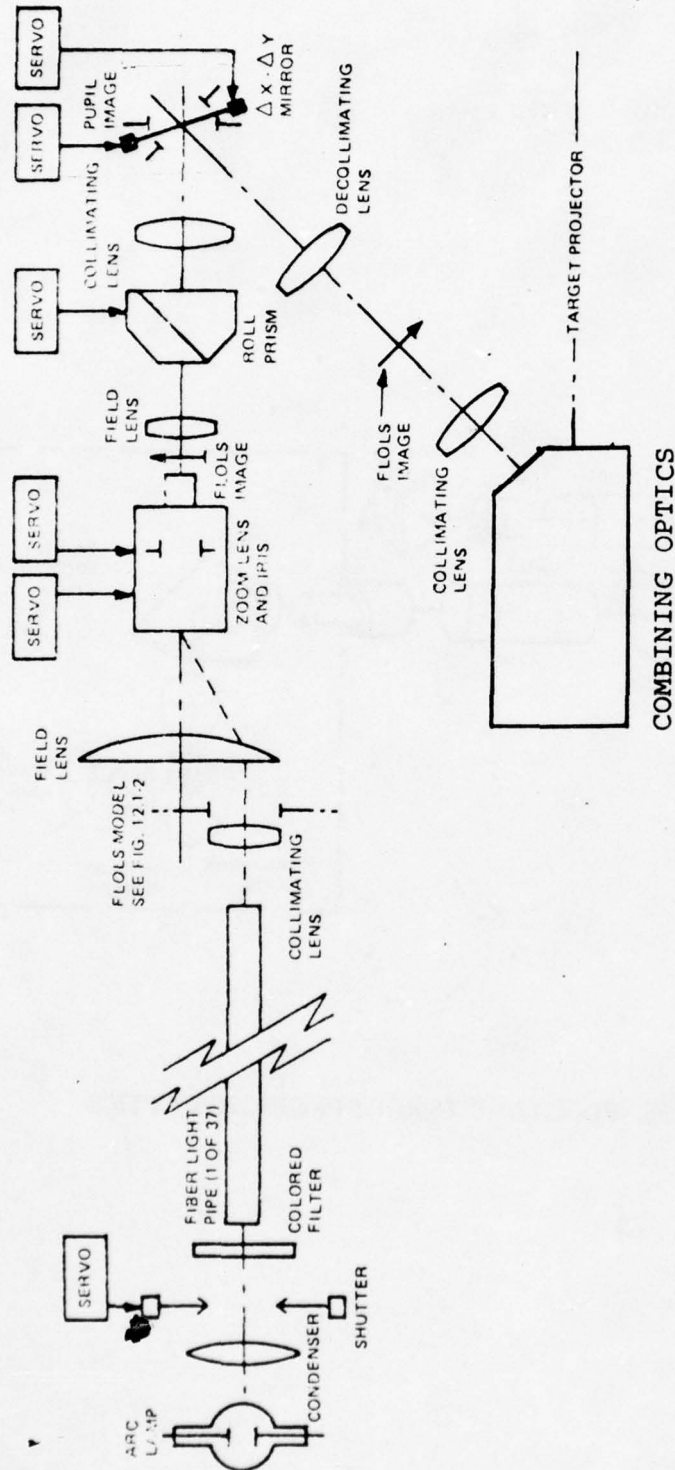


Figure 36. FLOLS OPTICAL SYSTEM SCHEMATIC

point, it will cease to zoom. At this point, though, the aircraft is usually hooked or has bolted. The meatball is probably no longer visible, since this point is about 20° relative to the FLOLS center, and the luminous range of the meatball is only 20° .

The roll prism will provide the correct FLOLS orientation with respect to the Eidophor-carrier image. The $\Delta X - \Delta Y$ FLOLS mirror will be locked to position the center of the image correctly on the roll prism axis, but ΔX and ΔY servos, and gimbals will be provided for flexibility.

The individual FLOLS lights are each modeled by a fiber and lens. The fiber conducts the light from an arc lamp and shutter system to a model board which appears just like the FLOLS system. (See figure 37.) Each lens on the model collimates the output end of its fiber and is cut to the size and shape of the particular FLOLS light. All the individual lights on the FLOLS are collimated and have their axis parallel to the system axis. This is so that when the zoom lens is at its greatest focal length, the FLOLS field lens images or decollimates the pupil of the zoom through the fiber end and projects all onto the same surface. The size of this image is sufficiently large, so of it that there is no vignetting when the zoom is at its shortest focal length. Therefore, the luminosity of the FLOLS image is constant over the zoom range. The field lens which is located near the zoom image must relay the zoom exit pupil to the $\Delta X - \Delta Y$ mirror. The pupil will not move then the image is translated by the $\Delta X - \Delta Y$ mirror. Therefore, the FLOLS lights will not be vignetted during movement.

The iris in the zoom lens will be modified to a new type which can be closed to no opening. This can be used to shut off the FLOLS lights when they are out of range without extinguishing the arc lamps. Otherwise, one would face the problem of frequent restarting of the arc lamps. An alternate design may be to include a shutter at this point and reduce the servo requirements.

The FLOLS image is centered at the center of the roll device, so that the effects of misalignment of the roll device are eliminated. The input errors are cancelled by oppositely-signed output errors. The Fresnel mirror is used to combining the FLOLS and target imagery. It is positioned so that its mirrored portions line up with the shadow image cast by the Schlieren bar mirror of the Eidophor. This is done so the Fresnel mirror will not significantly alter the luminosity of the target image. The pupil image of the FLOLS is formed at the Fresnel bar mirror. This minimizes the size of the Fresnel mirror and insures uniform image luminance. The FLOLS image is collimated at this point, so the the discontinuity of the mirror will not cause a splitting up of the final, projected FLOLS image into as many separate images as there are bar mirrors. The only requirement which the Fresnel mirror must meet is a parallelism of the bar mirror surface.

Once the FLOLS image passes from the Fresnel mirror, it is projected by the target projector optics, along with the target image. Any servo motion after this point affects both FLOLS and target images alike.

Alternate Methods.

- 1) Video inseting or visual keying of a FLOLS image into the target projector image. This was rejected because of its inability to provide adequate FLOLS intensity relative to the target background.

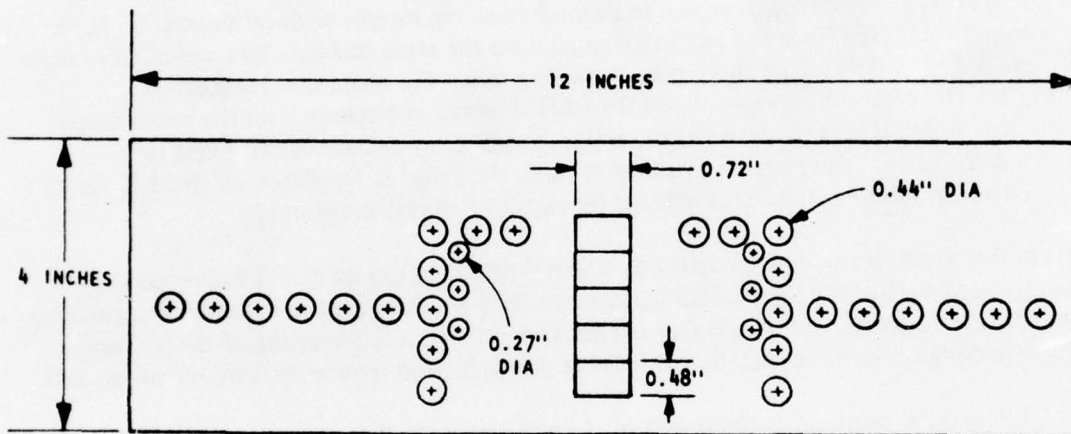


Figure 37. FLOLS MODEL BOARD

- 2) Including FLOLS on target model. This was rejected because it required adopting a color TV system for target image generation and it also provided inadequate intensity relative to the target.
- 3) Separate FLOLS projector. This was rejected because of the complexity associated with accurately tracking the target image throughout the total field of view.
- 4) Optically-coupled CRT or laser FLOLS projector. This was rejected because of the complexity of the supporting electronics required to generate the colored, FLOLS signals.

FLOLS MODEL. Figure 38 shows the illumination system. Two arc lamps are used. One is used for the meatball, cut, and emergency waveoff. Rings of lenses surround each arc and image it onto the ends of the fibers. They are coaxially aligned with the optical axes of the lenses.

Mounted with the lenses are colored filters to simulate the various colors on the FLOLS. The fibers terminate at the FLOLS board, which is shown in detail in figure 37. Near the ends of all the fibers, except the datum fibers, are cylinders with apertures cut in them to switch lights on and off. These apertures are driven to simulate the light patterns of the FLOLS and the movement of the meatball light.

A practical size for the FLOLS model is about 12 inches, which must subtend about 3° from the zoom lens. This locates the FLOLS about 55 inches from the zoom. The maximum zoom lens aperture is about 3 inches, and it is virtual, appearing about 25 inches behind the first element of the lens.

The required control signals for the FLOLS generator are:

- 1) LAMP IGNITING.
- 2) LAMP POWER.
- 3) SIGNALS FOR CUT and EMERGENCY WAVEOFF.
- 4) COMMAND SIGNAL WITH SEVEN DIFFERENT POSITIONS FOR THE MEATBALL.
- 5) WAVEOFF CONTROL SIGNAL.

FLOLS MOTION SYSTEM.

The motion system must provide the capability of placing the FLOLS image at the Fresnel mirror so that the FLOLS will appear in the proper position with respect to the target image. The specified error level is a maximum of 5% of the carrier image width as the image is positioned over the display screen. Since the carrier width is 252 feet, the FLOLS image must be within 12.5 feet (scaled) of the true position. The constraints on the FLOLS motion system are such that the FLOLS image must be properly placed on the projected target over a range in target size of 2.78:1. The images will automatically track each other at the screen, because both are processed by the same optics and projector motion system from the point of insertion, as shown in figure 35. The servos used on the roll prism and the X-Y tilting mirror will be designed to meet these motion requirements, even though the X-Y mirror will be locked in one position in the basic design.

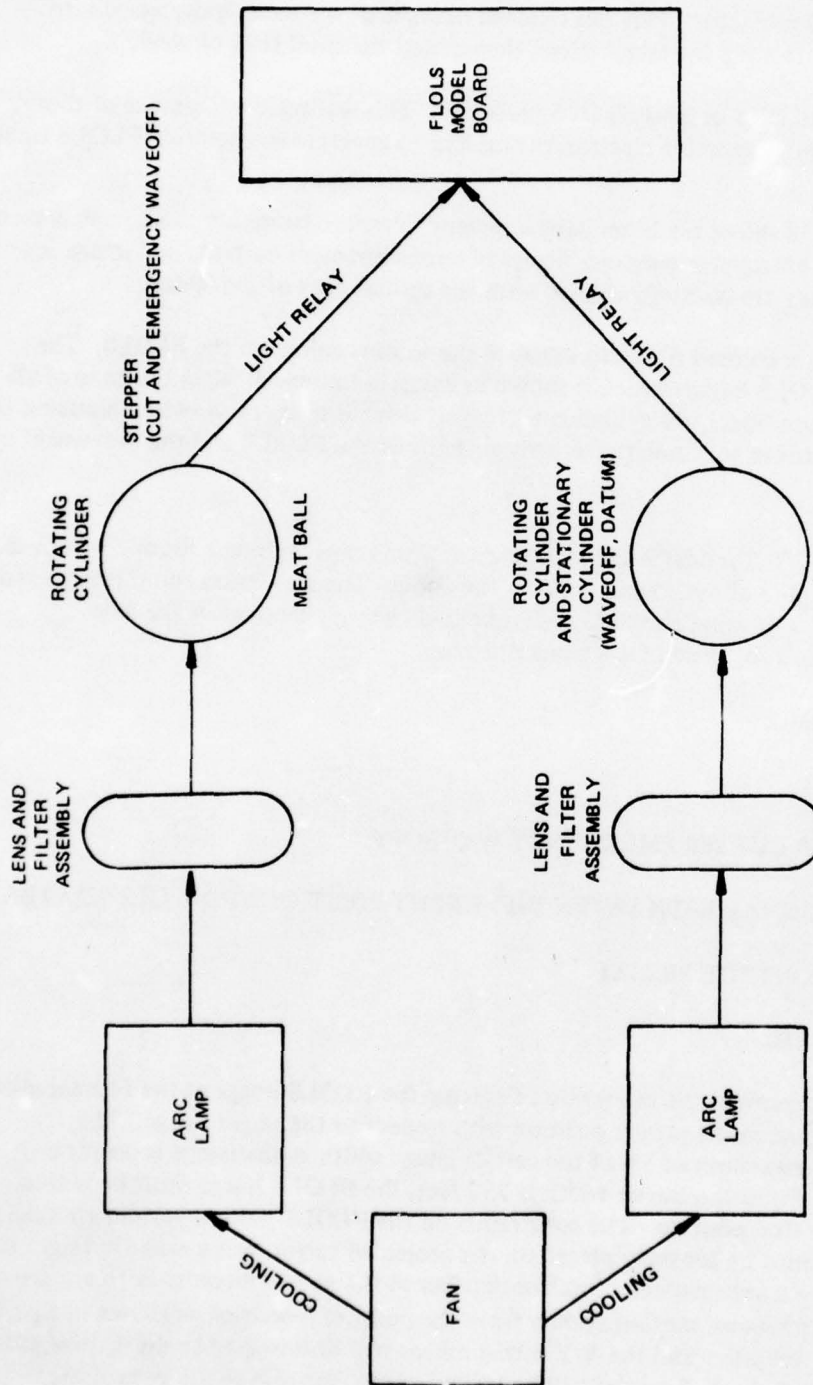


Figure 38. FLOLS IMAGE GENERATOR

NAVTRAEQUIPCEN 75-C-0009-1

The AWAVS computer will control the FLOLS motion system by computing the probe pointing vectors (line of sight) to be at the carrier FLOLS location, whenever FLOLS is seen by the pilot. The slow movement of the carrier relative to the computer iteration rate of 30 per second makes the dynamic tracking of ship's motion and FLOLS position entirely feasible. The frequency response of the FLOLS motion servos must be sufficient to follow the ship's motion.

The FLOLS Motion System consists of five servos as shown on figure 36: Zoom, X Displacement, Y Displacement, IRIS, and Roll.

The zoom changes the size of the image and only contributes small errors to the positional accuracy of the FLOLS.

The iris servo controls the light intensity for range simulation and brightness control. This servo will also shut off the FLOLS when they are not required. The ΔX and ΔY mirror servos, if used would cause displacement of the FLOLS at the Fresnel mirror. The roll servo rolls the FLOLS image. Table 12 shows a summary of the servo requirements in table form.

Table 12. FLOLS SERVO REQUIREMENTS

SERVO	LINEARITY %	RESOLUTION %	EXCURSION RAD	RATE RAD/SEC	ACCELERATION RAD/SEC SEC
X DISP	0.05	0.01	0.1	0.5	1
Y DISP	0.05	0.01	0.1	0.5	1
ZOOM	1.0	0.3	1.0	1.0	0.1
ROLL	0.05	0.01	π	2π	15.0
IRIS	1.0	1.0	2.0	10.0	40.0

X, Y Displacement Servo Requirements. While it is recognized that the specifications for X and Y displacement servos would be different, the two servos will be similar in design. For this analysis, the two servos will be considered to be the same and the X displacement will be considered to be the requirement for both. Therefore, only the X servo is discussed.

The following paragraphs discuss the tracking rate analysis. (For illustration, see Figure 39.)

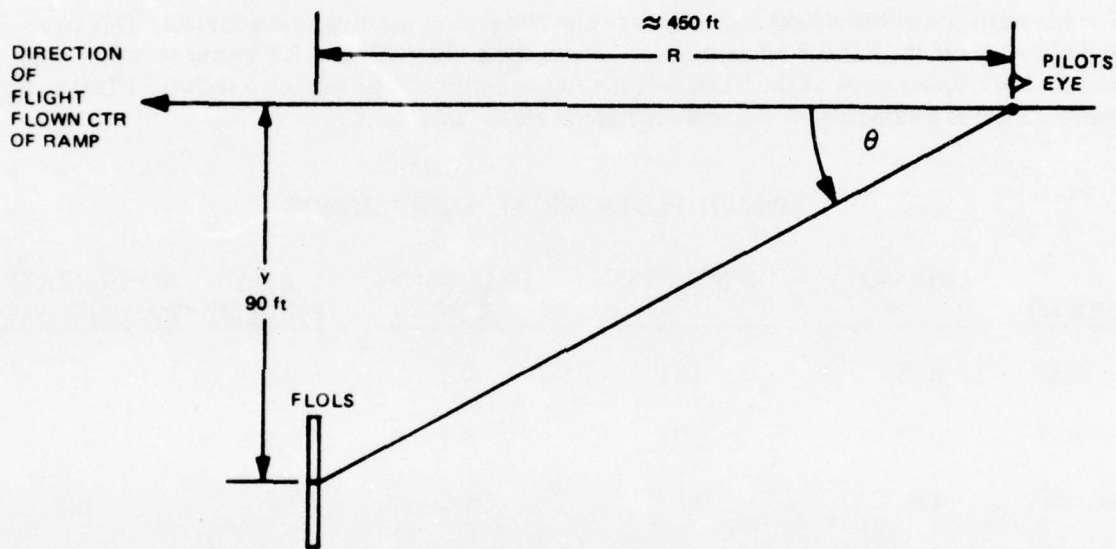


Figure 39. TRACKING ANGLE/RATE

To determine the rate of change of θ (ω) as pilot lands and hooks or bolters, we assume that the FLOLS goes out of pilot's FOV at $R_{\min} \approx 450$ ft.. Then the FLOLS is 90 ft. from center of ramp.

In General:

$$\tan \theta = \frac{y}{R} ; R = y \cot \theta ;$$

$$\text{and } \frac{dR}{dt} = y \frac{d}{dt} (\cot \theta).$$

Let velocity of eyepoint = v :

$$\text{and, } \frac{d\theta}{dt} = \omega ;$$

$$v = y \frac{d}{d\theta} (\cot \theta) \omega ;$$

and,

$$-\csc^2 = - \frac{R^2 + y^2}{y^2}$$

$$\omega = - \frac{y}{R^2 + y^2} v ;$$

where:

v is relative velocity of aircraft with respect to FLOLS.

y is constant 90 ft.

R_{\min} is assumed to be 450 ft. (range at which FLOLS is turned off).

$$\omega = -0.2 \text{ RAD/sec for}$$

$$v = 150 \text{ knots} = 253 \text{ ft./sec.}$$

With some design margin, let X-Y mirror require a rate of 0.5 rad/sec.

Because changes in rates on final approach are so slow, and because the FLOLS is extinguished at 450 ft. from touchdown, an acceleration of 1 rad/sec. sec. was assumed.

Zoom Servo Requirement Determination. The full zoom range is accomplished by rotation of the zoom control through about 180° . Since the zoom is only going to use about $\frac{1}{4}$ of this, the required excursion will only take about 45° . With some design margin, let this be considered to be 0 to 60° .

Since the zoom function is nonlinear with the rotation of the zoom control, conformity of 1% to the analytic function will be considered adequate.

The resolution requirements are more difficult to determine. For a minimum size of the FLOLS at the Fresnel mirror a range of 1000 ft. is computed with a FLOLS board of 30 ft. The FLOLS board occupies about 100 arc-min. of angular subtense at the pilot's eyepoint. Resolution of the zoom determines apparent changes in range by size changes of the image viewed. At 1000 ft simulated range, the zoom resolution is considered to be most critical. If the angular subtense determined above is used, and a 10% change is considered tolerable, then a resolution of 10 arc-min. is required. This translates to a drive accuracy (for a ring driven by a 1:4 gear), at the zoom mechanical control, of 40 arc-min. This requires a resolution of approximately 0.3%.

FLOLS ROLL SERVO REQUIREMENT.

The FLOLS roll servo is required to roll the FLOLS image about the FLOLS axis. Therefore, the requirements for this servo are somewhat reduced from that of a more general case. The dynamic requirements are those of the F4 simulated aircraft which has a roll rate of 2π rad/sec and a roll acceleration of 30 rad/sec sec. Since the angular displacement of the control ring on the roll prism causes the image to roll at twice that displacement, the servo is only required to easily seen up to a near range of 450 ft., a linearity of 0.5% and a resolution of 0.01% will insure smooth, accurate motion in roll.

FLOLS IRIS Servo Requirements. The iris servo will be used to control the light intensity and simulation of range. The servo demands are not very stringent for this application. The iris will also be used to extinguish the FLOLS, when the simulated aircraft is outside the FLOLS envelope. The closing command to extinguish the FLOLS is considered to be the most demanding on the iris servo. The extinguishing at approximately 450 ft. from the FLOLS as the simulated aircraft comes over the ramp is used to determine closure rate, with a full closure requiring about 135 deg. of travel in about $\frac{1}{4}$ second (about 60 ft. at 250 ft/sec airspeed). This gives a closure rate of about 10 rad/sec and an acceleration requirement of at least 40 rad/sec (reaching 10 rad/sec in about $\frac{1}{4}$ second). An alternate design of a shutter in the zoom may be used to reduce the servo requirements, if the rate on acceleration became a design difficulty.

The linearity and resolution are considered not be to demanding on the servo.

A linearity of 1%, with a resolution of 1% is judged to be adequate.

FLOLS Registration of Carrier. To estimate the tracking capability and errors of the FLOLS with respect to the carrier, the precision, resolution, and accuracy of the separate subsystems will first be determined. For a logical approach, the total system has been separated into the following subsystems:

- 1) FLOLS ΔX , ΔY and Roll Errors.
- 2) TV Camera Projector Errors.
- 3) Optical Probe Pointing Errors.
- 4) Gantry X, Y, Z, Position Errors.

In each of the subsystems above, the contributing errors are identified and magnitudes are assigned. A simple error model is constructed for each subsystem and the interrelation of error is assumed to be RSS. This allows a simplified mathematical relationship between subsystems and a most probable magnitude of the composite errors. The assumption is made that the command to each element in the subsystem does not contain errors (i.e., the computer will command all elements independently, and to a higher resolution and accuracy than the controlled element is capable). This establishes a reference for all commands. The initial models will assume all alignment errors to be negligible or to be calibrated well below the actual or final control variable.

FLOLS ΔX , ΔY and Roll Errors. The provision has been made to move the FLOLS in ΔX and ΔY with roll. However, initially, the ΔX and ΔY will be fixed, and only the rotational errors (due to roll) will contribute to the FLOLS registration. The analysis of these errors, due to ΔX and ΔY , is included in FLOLS image movement for referenced capability, if it is decided to use them at a later date⁸. With ΔX and ΔY fixed, the FLOLS will be projected to a fixed point with only size change due to zoom, brightness change due to iris control, and roll capability due to roll prism. The error contribution due to ΔX and ΔY and zoom will be considered zero, and the roll error is considered negligible in the first level of analysis. Therefore, the FLOLS will be considered to contribute no errors to the composite image and is considered the reference for carrier image registration.

TV Camera and Projector Errors. After considering the magnitude of errors in the total system, the contributing errors of the TV raster (both camera and projector) were considered not to be significant. These capabilities will be listed here for possible, future reference.

The TV camera has a raster position stability at the vidicon plate of approximately 0.1%. If the raster is considered to subtend approximately 10 degrees at 1 nm, the errors due to raster drift would be approximately 1 arc min at the pilot's eyepoint, at that particular range.

Using the same approach as above, and considering the electronics in the projector, it was decided to use an error of 0.2% for the TV projector.

These errors will be considered negligible in the first level of analysis.

AD-A037 223

SINGER CO BINGHAMTON N Y SIMULATION PRODUCTS DIV
AVIATION WIDE-ANGLE VISUAL SYSTEM (AWAVS). DESIGN ANALYSIS REPO--ETC(U)
APR 75

F/G 1/2

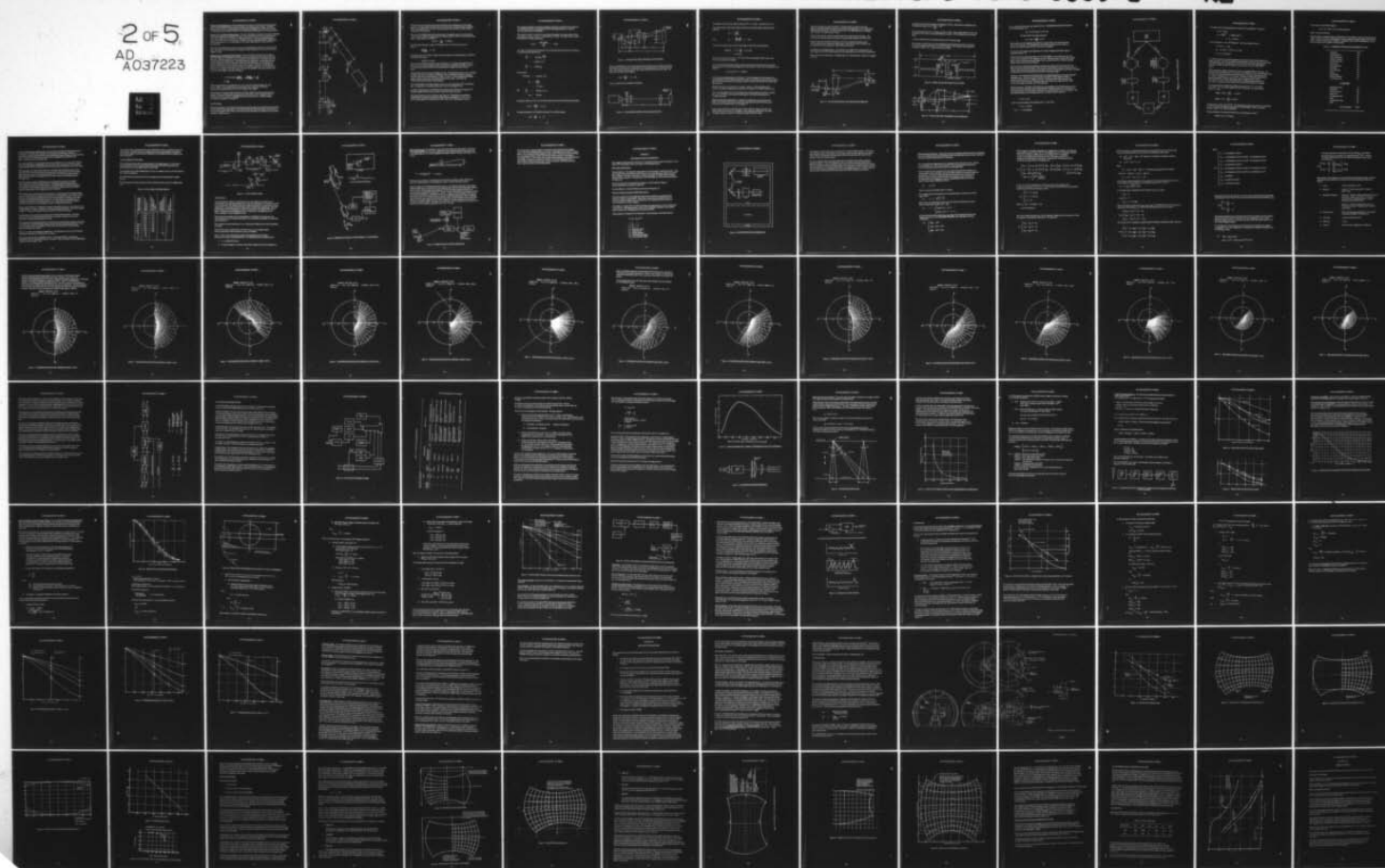
N61339-75-C-0009

UNCLASSIFIED

AWAVS-1

NAVTRAEQUIPC-75-C-0009-1 NL

2 OF 5
AD
A037223



Optical Probe Pointing Errors. The best estimate of the errors to be expected in the optical probe came from past efforts and experiences with similar type optical probes at Singer. At present a design is under way for a current program, and the expected capability has an RSS of 45 arc-min. It is realized from the outset that this error is the single-most contributing error in the entire system.

Gantry X, Y, Z, and Model Position Errors. The error attributable to the gantry and those attributable to the carrier model were considered at the same time, because these errors were considered to be of the same magnitude. In the gantry, the three parameters X, Y, and Z were assigned position errors in the order of 0.05 in. in each axis. The RSS of the three axis (neglecting the orthogonality of the axis) is about 0.1 in. If a scale factor of 310 is used, this is almost 31 inches of error in the real world.

The carrier model has heading, roll, pitch, and heave parameters that contribute to the total system error. Since the motion is compatible to the gantry motion a similar error of about 30 inches was assigned to these.

Composite Error of Relative FLOLS Position. Since the FLOLS is combined with the target at the Fresnel mirror in the projector, the projector azimuth and elevation servos effect both in the same way. Therefore, these servos do not contribute to the relative error. The relative error will be determined at the Fresnel mirror. The FLOLS Projector will project a fixed image with only zoom to change size and roll to rotate the image about the FLOLS axis. For this analysis the FLOLS contributes no errors at this point (i.e., it will be used as a reference to determine the relative error). Since the optical probe contributes the majority of all errors, it is considered first. The error of the image at the Fresnel mirror, due to the 45 min RSS⁹, will cause a position error (ϵ) at the carrier image as a function of Range, R:

$$\epsilon = R (45 \text{ min}) \times \frac{(\text{DEG})}{(60 \text{ min})} \frac{(\text{RAD})}{(57.3 \text{ DEG})} \cong \frac{R}{80}$$

$$R = 80\epsilon$$

If the max specified error is considered to be 12.5 ft. than the maximum Range at $R = 80$ ($12.5 = 1000$ ft. Thus considering only the pointing errors of the probe, the FLOLS exceeds the maximum relative error of 12.5 at a range of only 1000 ft.

Some method of closing a feedback loop from the carrier model to the optical probe should be explored. The errors of the probe pointing must be reduced by a factor of approximately 10 to make this error contribution compatible with the rest of the system. A possible method of doing this is discribed in Alternates ¹⁰.

FLOLS OPTICS.

First order description. The FLOLS optical system relays the image of the FLOLS model and inserts it into the path of the target projector. The zoom lens will vary the FLOLS size so that it matches the size of the carrier on the camera. The iris will vary the luminosity for calibration as well as range simulation. (See Figure 40.)

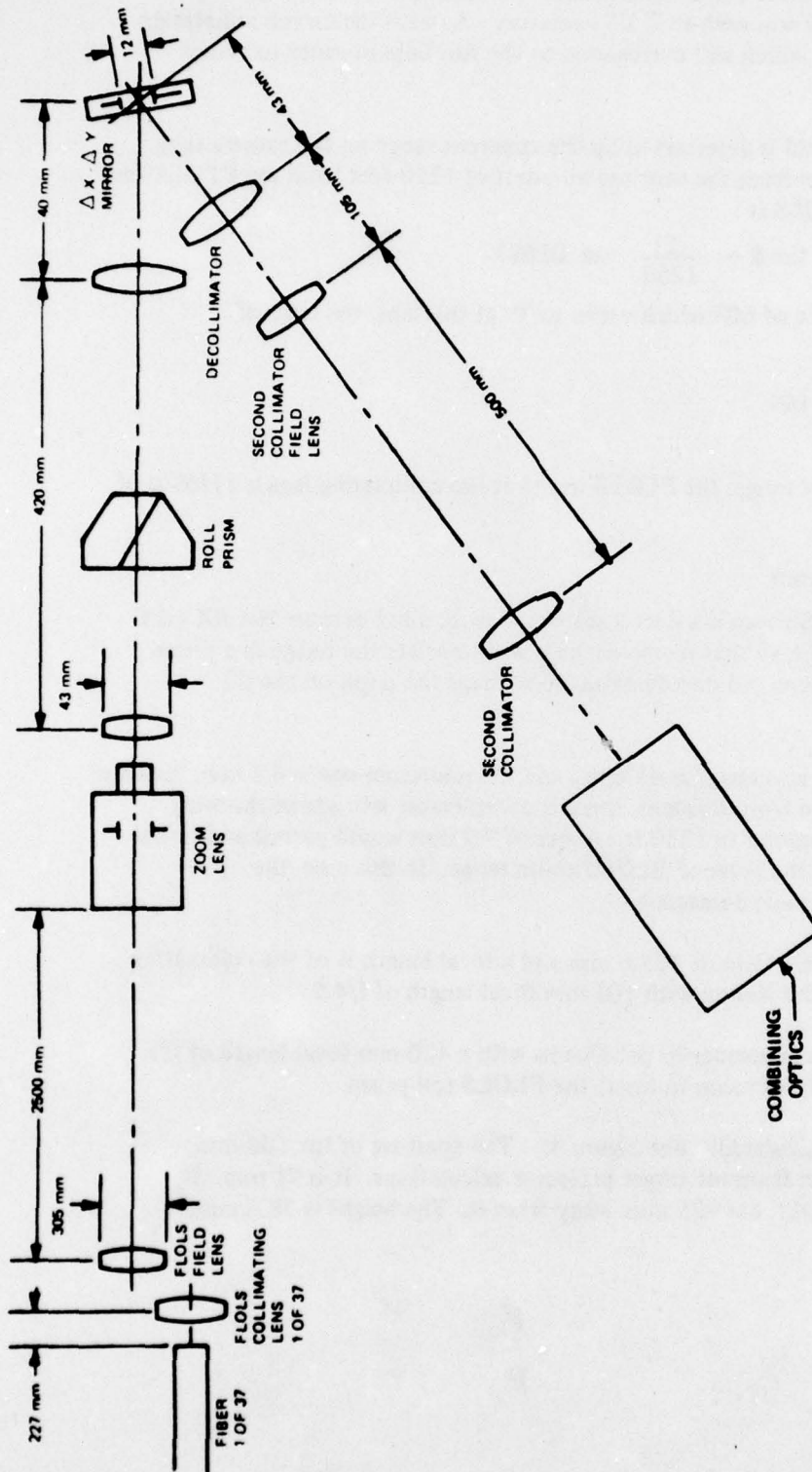


Figure 40. FLOLS OPTICS

The first lens from the Fresnel mirror will be identical to the collimating lens in the target projector. Its focal length is 500 mm with an f/5.5 aperture. As with the target collimating lens, its image will be 105.6 mm which will correspond to the full field in order to accept FLOLS $\Delta X - \Delta Y$ movement.

The size of the FLOLS in this field is determined by the apparent range on the camera tube. For the case of a 1000-foot range from the touchdown point of 1250 feet from the FLOLS the angle 2θ subtended by the FLOLS is :

$$2 \tan \theta = \frac{21}{1250} \cong .01683.$$

The whole field subtends an angle of 60° which varies to 7° at this lens, the ratio of sizes is :

$$\frac{2 \tan 30}{.01683} \cong 69;$$

this implies that at the 1250 foot range, the FLOLS image at the collimating lens is 11/69th of the field of 105.6 mm, or:

$$123/69 \cong 1.53 \text{ mm}$$

The next lens toward the FLOLS zoom is a decollimator. It is required because the $\Delta X - \Delta Y$ mirror must be in collimated light, so that its movements will translate the image in a plane. It is also required that the field lens and decollimating lens image the pupil on the tilt mirror.

The maximum size of the zoom lens image is 43 mm., and the minimum size is 4.3 mm. Because a range of only 2.78:1 is required from this lens, there is considerable latitude in choosing the zoom point which will correspond to 1250 ft. A size of 7.2 mm would permit additional change in range on both ends of the planned FLOLS zoom range. In this case, the collimating-decollimating lenses must demagnify.

The decollimating lens must have a field of 105.6 mm and a focal length $\frac{1}{4}$ of the collimating lens. A suitable lens is a Schneider Xenon with 105-mm focal length of f/4.5.

A suitable collimating lens is the Schneider Repro-Claron with a 420-mm focal length of f/9. This path length will allow plenty of room to insert the FLOLS roll prism.

The required apertures can be calculated. (See figure 41) The aperture of the 500-mm, collimating lens is already known from the target projector calculations. It is 91 mm. It forms a virtual image of the FLOLS bar 925 mm away from it. The height is 78.6 mm.

The longest focal length for the second collimator field lens is calculated from the aperture of the decollimator since the extreme rays must pass through its aperture. Figure 41 shows the data needed for calculation.

The values of the $\tan \theta_1$ and $\tan \theta_3$ were already determined in the target projector first-order analysis. They are: $\tan \theta_1 = 0.0425$; $\tan \theta_3 = 0.0146$. The value of $\tan \theta_5$ can be determined by the following equation:

$$\tan \theta_5 = \frac{23.3 - 105.6}{\frac{2}{105}} = -0.473.$$

The image is located where the paraxial, chief ray and extreme rays have the same frequency. The equations describing them are:

$$\begin{aligned} \frac{H_2}{2} &= -\tan \theta_5 S_6 - \frac{105.6}{2} \\ &= 0.392 S_6 - 52.8 \end{aligned}$$

$$\frac{H_2}{2} = -0.0425 S_6.$$

Equating these:

$$-0.0425 S_6 = 0.392 S_6 - 52.8;$$

$$\begin{aligned} S_6 &= \frac{52.8}{0.435} \\ &= 121.5 \text{mm;} \end{aligned}$$

$$\text{and, } \frac{H_2}{2} = -0.0425 \times 121.5;$$

$$H_2 = 10.3 \text{mm.}$$

The angular movement of the $\Delta x, \Delta y$ mirror required to move the FLOLS across the field is:

$$2 \tan^{-1} \frac{52.8}{105} = 53.4^\circ.$$

The angle subtended by the FLOLS at the mirror for a 1250-ft. range is:

$$\tan^{-1} \frac{1.8}{105} \cong 1^\circ.$$

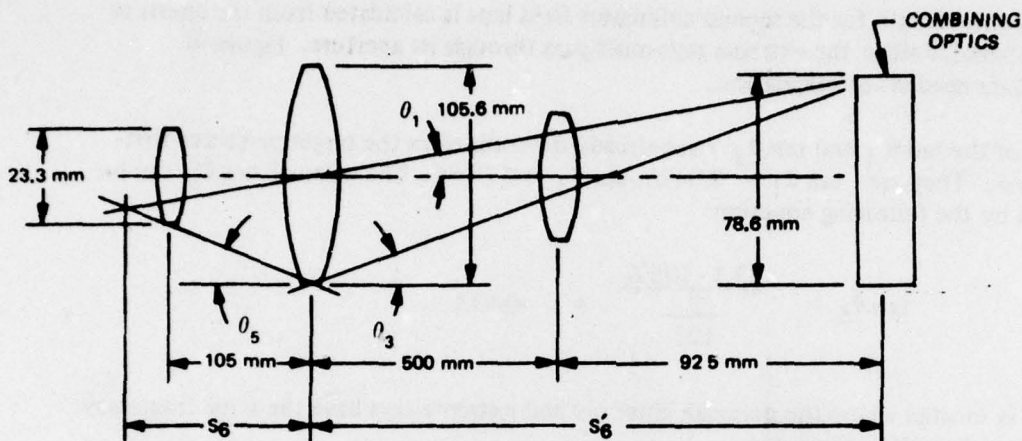


Figure 41. COLLIMATING LENS APERTURE CALCULATIONS

The next collimating lens can be located approximately 40 mm from the pupil on the mirror. The aperture of the lens must be larger than the 12-mm pupil diameter, by the growth of the beam. The maximum growth occurs at short ranges when the full zoom may be used. The field, then, is 43 mm, and the angle is:

$$2 \tan^{-1} \frac{43/2}{420} \cong 5.9^\circ.$$

Figure 42 shows the data needed for calculation.

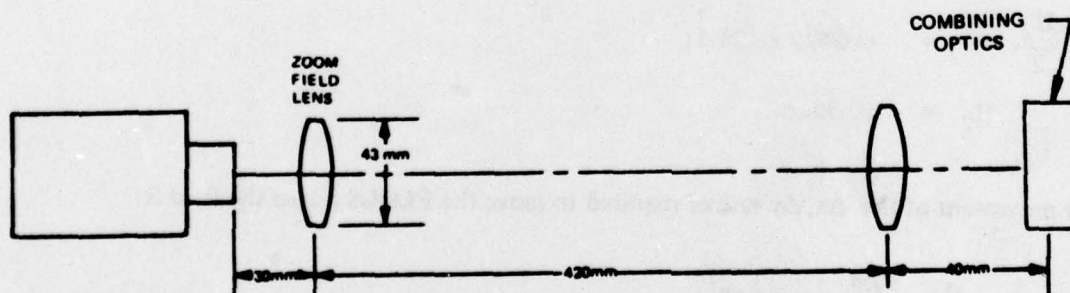


Figure 42. COLLIMATING LENS DATA FOR CALCULATION

The aperture must be 12 mm, plus $2 \times 40 \tan 2.95^\circ \cong 4.12$ mm. The aperture is 16.12.

The image distance of the pupil or mirror, as seen from the zoom image is formed from the equation:

$$S_7 = \frac{f_7 S_7'}{S_7 - f_7} ;$$

then,
$$S_7 = \frac{420 \times 40}{40 - 420} \cong -44.2.$$

The size of the pupil as seen from the zoom image is found from the magnification:

$$\begin{aligned} \text{Pupil size} &= 12 \times \frac{44}{40} \cong 13.2 \text{ mm} \\ &\approx 13.2 \text{ mm.} \end{aligned}$$

This implies a zoom f No. of $420 \div 13.2$, or $f/32$. The zoom normally will not close to this size, so a new iris must be installed.

In the case of the FLOLS image filling the whole zoom field, the FLOLS model will subtend approximately 7° at 350 mm focal length with a model board 12 inches wide. The distance to the board is:

$$6 \times 25.4 / \tan 3.5^\circ = 2500 \text{ mm}$$

For this case, the paraxial aperture is $350/32=11$. This is the largest the pupil becomes. The combined effects of the FLOLS lens and FLOLS field lens will image the end of the fiber bundle (in the FLOLS model board) onto the pupil. These two lenses must merge all the FLOLS lights. (See figure 43.)

The field lens will have an aperture of 12 inches, or 305 mm. The focal length will be 2500mm. The angle subtended by the pupil from the field lens is $11/2500 \cong 0.0044$ radians.

This is the same angle that the end of the fiber in the FLOLS model must subtend. The fiber size is 1 mm. Therefore, the maximum focal length of the FLOLS collimating lens is $1/0.0044 = 227$ mm.

Optimization Of Fiber Illumination. A review of the calculations concerning the focal length of the FLOLS collimating lenses and fiber size shows that the field of view of this collimating lens is 0.0044 radians, or 0.25 degrees ¹¹.

These lenses and fibers are quite small, and so will be difficult to align so that all 37 are parallel within a few percent of 0.25 degrees. In fact, alignment would have to be about .01 degree to assure no vignetting or variation in brightness between lights.

This is not practical for optics of this size. A better solution is to shorten the focal length of the collimating lens so that the end of the fiber subtends about 1.4° . This permits alignment errors of about 1.15° which are achievable. The collimating lens focal length is then $75/14/57.3$ or approximately 30 mm.

The only affect this has is that the image of fibers at the probe pupil will be larger. This increase in size will also eliminate any chance of vignetting as the pupil moves with zoom.

Singer is currently using fibers of 0.030 in. or 0.75 mm, and has found these to have very low insertion loss, compared to smaller fibers. They still retain good flexibility, and so can be bent from the light house to the FLOLS model board.

Condenser-Arc Lamp Optimization. The insertion cone of light can be calculated from the focal length of the FLOLS collimating lens and the largest aperture on the FLOLS model board.

Figure 44 shows the model board. The largest light is the FLOLS meatball. Each has a diagonal of 22 mm.

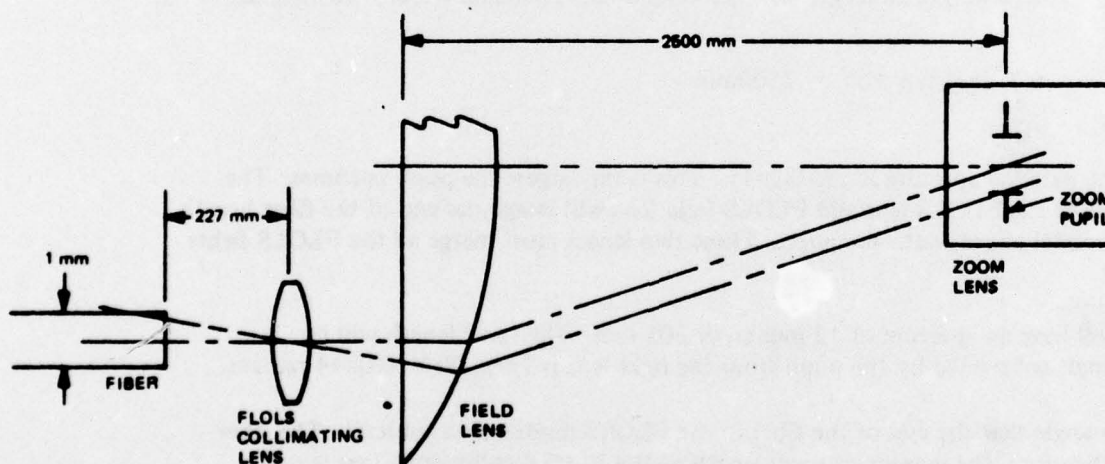


Figure 43. FLOLS COLLIMATING AND FIELD LENS SCHEMATIC

The lenses on the model board have a focal length of 30 mm. This makes the semi-field of the collimating lens equal to $\tan^{-1} \frac{22/2}{30} = 20^\circ$.

This is a practical number for a condenser as well as a fiber. Tests at Singer-SPD have shown that the fall-off at 20° off axis never exceeds 50% and is closer to 75% of the peak value for shorter fibers.

It is also a relatively simple condenser which has a 20° semi-cone angle.

The condenser will pick up an arc from the Hanovia 500-watt lamp of about 0.35 mm square which has an average luminosity of 1.02×10^9 ft lamberts. The condenser must magnify the arc about $0.75/0.36 = 2.1 \times$. Figure 45 shows the scheme.

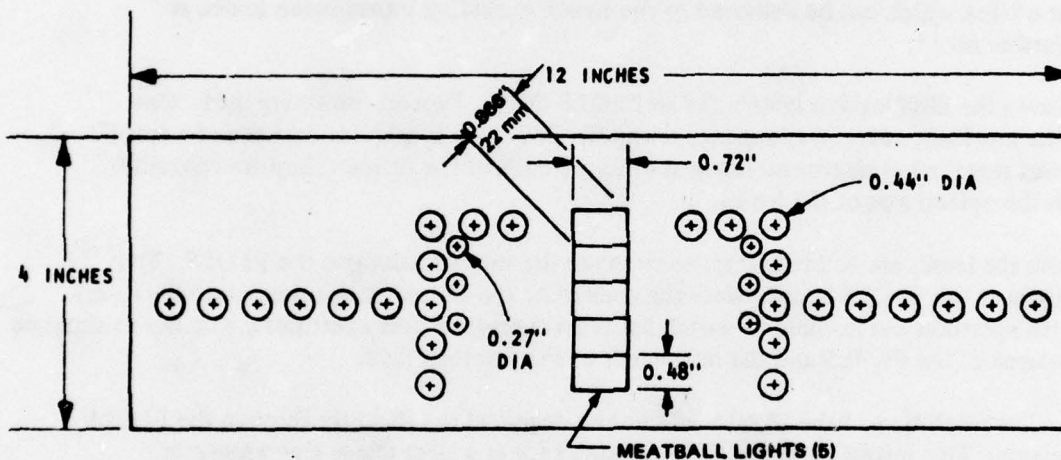


Figure 44. MODEL BOARD WITH MEAT BALL LIGHTS

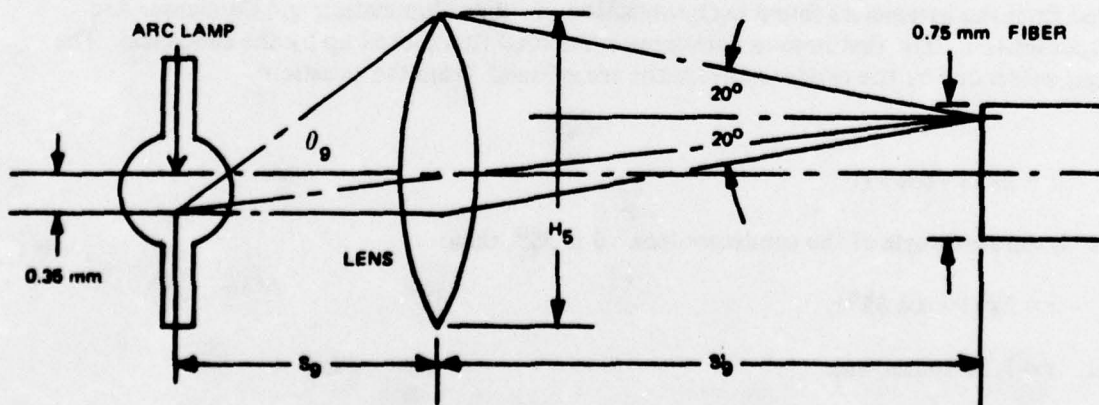


Figure 45. FLOLS LAMP AND CONDENSING LENS SCHEMATIC

If s_9 is chosen as 50 mm, then s_5 must be 105 mm. This immediately specifies the aperture H_5 of the condenser. It is

$$H_5 = 2 \times 105 \tan 20^\circ \cong 76^\circ \text{ mm.}$$

The input field is then easily calculated.

$$\theta_9 = 2 \tan^{-1} \frac{76/2}{50} \cong 70^\circ$$

These members are all consistent with what the arc lamp will do. The calculations were done for the worst case. The other lights on the FLOLS are smaller and will require an insertion cone angle less than the 40° required for the meatball.

The amount of flux which can be delivered to the screen excluding transmission losses, is calculated farther on ¹².

Figure 46 shows the illumination system for all FLOLS lights. Two arc lamps are used. One is used for the meatball, cut, and emergency waveoff. The other is used for datum and waveoff. Rings of lenses surround each arc and image it onto the ends of the fibers. They are coaxially aligned with the optical axis of the lenses.

Mounted with the lenses are colored filters to simulate the various colors on the FLOLS. The fibers terminate at the FLOLS board. Near the ends of all the fibers, except the datum fibers, are cylinders with apertures cut in them to switch lights on and off. These apertures are driven to simulate the light patterns of the FLOLS and the movement of the meatball light.

Resolution. The resolution of the FLOLS will not be degraded significantly through the FLOLS image generation. This results from the FLOLS being kept at a large image size while it is presented on the screen at 2.5 degrees, maximum. At this size, the FLOLS subtends about 20 mm in the FLOLS zoom lens. The loss in resolution occurs in the target projector, where its size at the target zoom lens is 1/25 of the target size.

FLOLS Luminance. Estimates of the luminance and transmission of the FLOLS projector can be calculated from the parameters found in Optimization of Fiber Illumination and Condenser Arc Lamp Optimization. The first item to determine is the total flux picked up by the condenser. The solid angle subtended by the condenser from the arc is found from the equation:

$$r = 2\pi (1 - \cos \theta);$$

where θ is the semi-angle of the condenser lens. θ is 35° , then:

$$r = 2\pi (1 - \cos 35^\circ);$$

and, $r = 1.14$ Steradians.

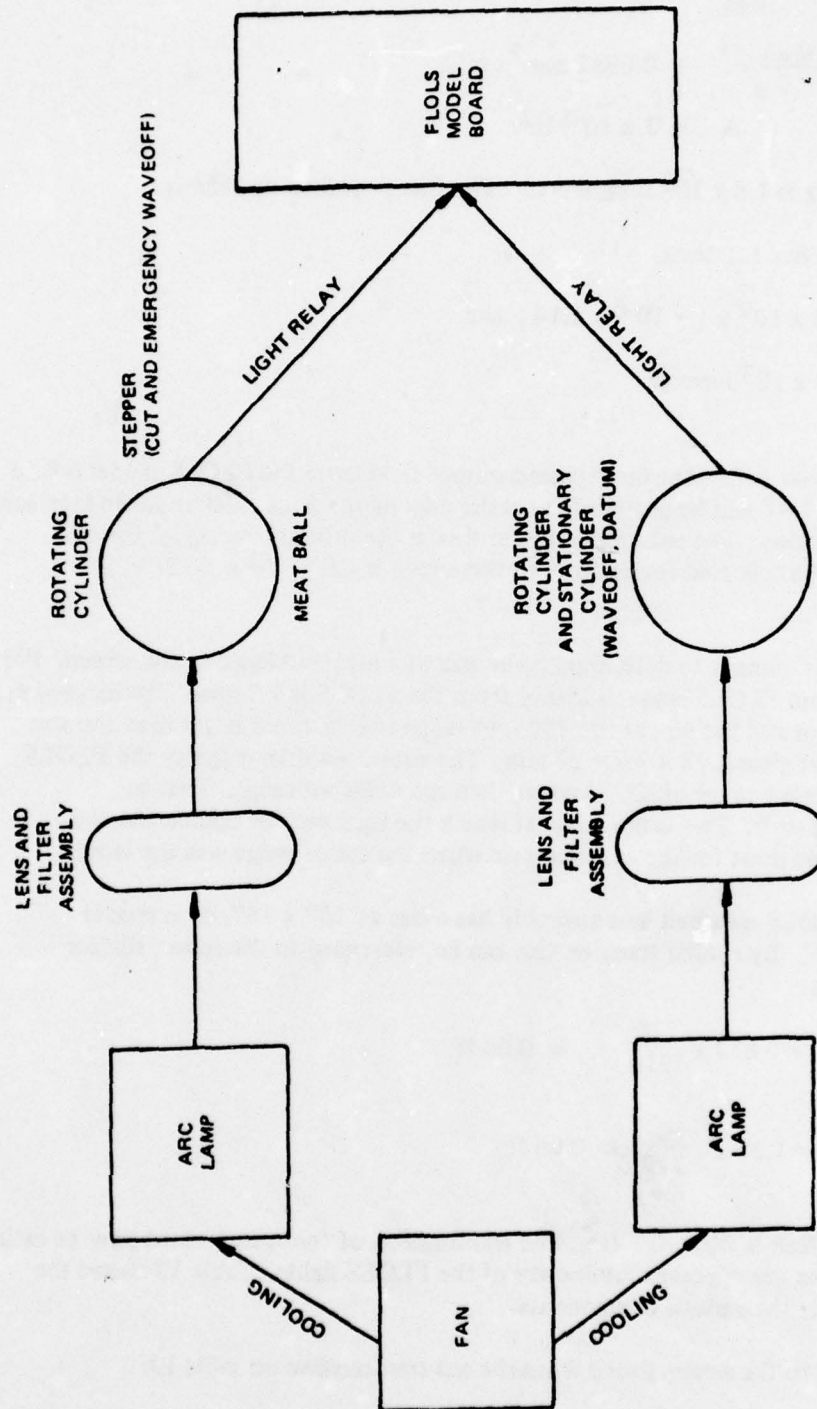


Figure 46. FLOLS IMAGE GENERATOR

The region of the arc being picked up is a circle of 0.35 mm diameter. The area is:

$$A = \pi r^2. \text{ Then,}$$

$$A = \pi \left(\frac{0.35}{2} \right)^2 = 0.0962 \text{ mm}^2; \text{ or,}$$

$$A \cong 1 \times 10^{-6} \text{ ft}^2.$$

The arc luminosity is 1.8×10^9 ft-lamberts. The flux ϕ picked up then is:

$$\phi = B \times A \times r; \text{ then,}$$

$$\phi = 1.8 \times 10^9 \times 1 \times 10^{-6} \times 1.14; \text{ and}$$

$$\phi \cong 1.9 \times 10^3 \text{ lumens.}$$

It is stated in section 4.4.2 that the required output field from the FLOLS model is 0.25 degrees, whereas; 1.4° will be provided for easier alignment. This must be taken into account in the light calculation. The reduction, due to this, is the ratio of the angles squared: the amount of light collected for delivery to the screen is $1.9 \times 10^3 \times .0327 \cong 62$ lumens.

The last geometric number to determine is the size of a meatball light on the screen. For reference, the zoom-FLOLS size at 1250 ft. from the FLOLS is 7.2 mm. The maximum size at the zoom is 43 mm and the size at the 450-foot range is 2.78 times larger than the size at 1250 feet. That gives $2.78 \times 7.2 = 20$ mm. The zoom can then magnify the FLOLS meatball to simulate a range of 43/20 closer than the 450-foot range. That is, $450 \div (43/20) = 210$ ft. This is the range at which the light pickup calculation was done above. It was done for the extreme case when the zoom image was the largest.

An individual FLOLS meatball lens assembly has a size of 10" x 15", or in model size 0.833' x 1.25'. By similar triangles, this can be referenced to the screen surface which is 10' away:

$$\text{Height} = 0.833 \times \frac{10}{210} \cong 0.04 \text{ ft.}$$

$$\text{Width} = 1.25 \times \frac{10}{210} \cong 0.06 \text{ ft.}$$

The area on the screen is $24 \times 10^{-4} \text{ ft}^2$. The transmission of the system must now be estimated in order to calculate the apparent luminosity of the FLOLS lights. Table 13 shows the estimated values for the various components.

The flux delivered to the screen found from the net transmission on table 13:

$$0.0027 \times 62 = 0.16 \text{ lumens.}$$

The luminosity of the FLOLS image is:

$$(0.16 \div 24 \times 10^{-4}) \times 1.43 = 100 \text{ foot-lamberts;}$$

where 1.43 is the screen gain.

Range Simulation. Range simulation is implemented by two methods. They are zoom lens and iris control. The zoom is used at closed ranges to correctly present the angular height of the meatball lights. At greater range, where it is difficult to distinguish which of the meatball lights are on, the iris will be used to dim the lights to simulate range.

Table 13. COMPONENT ESTIMATED TRANSMISSION VALUE

Condenser	65%
Insertion Factor	80
Fiber Transmission	80
FLOLS Condenser	85
FLOLS Field Lens	80
Zoom Lens	70
Zoom Field Lens	90
Roll Prism	60
First Collimator	80
Mirror	95
Decollimator	80
Second Collimator	75
Combining Optics	35

In Target Path

Decollimating Lens	70
Roll Prism	60
Field Lens Zoom	90
Zoom Lens	70
1st Projection Lens	80
Prism	95
2nd Projection Lens	80
Prism	95

Net Transmission 0.27%

In order to determine the optimum use of the zoom lens, the closest and farthest use must be determined. At 1250 feet, the carrier size on the Eidophor stops changing. This size is maintained constant by the probe zoom which magnifies the image as the gantry recedes from the model. Since the TV camera limits the resolution, the magnification brings the carrier size to a maximum size on the camera tube.

The closest approach for the zoom drive can be set at 100 feet for a 10:1 zoom lens. However, servo rate-limits demand a higher figure. For the present, this is being set at the ramp, which is approximately 450 feet from the FLOLS. This means the zoom will drive over a 2.78:1 range.

The target image size at the probe camera tube is constant from a simulated range of 1250 feet to 9370 feet. The 9370-foot point is beyond the point when the extreme-most meatball light subtends one minute arc, the visual resolution limit. The one-minute point occurs at approximately 6200 feet. During this interval, the size is varied on the viewing screen by the target zoom.

Further increases in range from 9370 feet can be simulated by a reduction in intensity. This is identical with the physiological effects of increasing an observer's range from an object which is smaller than his visual resolution. This phenomenon is easily understood by knowing that the visual resolution limit can be referred to as a small area on the eye which produces a signal equal to the average stimuli over a small area.

The intensity can be reduced by the iris in the zoom lens. The amount of flux passing through the iris is proportional to the square of the diameter, since it is dependent on the area of the iris. However, the physiological intensity falls off in inverse proportion to the square of the range. Therefore, the range simulation from 9370 feet to the outer limit can be simulated by just changing the iris diameter in inverse proportion to the range. Table 14 shows the manner in which the FLOLS zoom and iris change as a function of range from the FLOLS.

FLOLS Image Movement. It is planned to design the simulator so that $\Delta x - \Delta y$ movement of the FLOLS image is not required. However, it is included for future flexibility. The motion is shown in figure 47. Roll is also included to correctly orient the FLOLS to the carrier.

The sensitivity of the roll device is the same as the target and probe roll servos. The upper and lower limiting velocities and stall acceleration is the same. This stems from the fact that object and image azimuth angle are the same.

The collimator and decollimator lenses surrounding the roll prism produce an image in the center of the roll device. This will eliminate image movement due to roll prism assembly errors. These errors will only affect the pupil position. There will be no vignetting, since the following apertures are larger than needed.

The $\Delta x - \Delta y$ Servos are affected by magnification. The final field of view is 60° but the same information covers about $17\frac{1}{2}^\circ$ at the $\Delta x - \Delta y$ mirror.

On the final screen image, it is desirable to have a 1 arc-minute sensitivity. This reflects a sensitivity at the $\Delta x - \Delta y$ mirror of about $\frac{1}{4}$ arc-minute. This is computed from the magnification required to achieve the 60° field.

The accuracy is also calculated from the screen requirements. For a 5 arc-minute error at the screen the $\Delta x - \Delta y$ mirror must have a positional accuracy of approximately 5 arc-minutes. The positional range of the mirror must correspond to the maximum field as it appears at the mirror, that is 61° .

FLOLS SUPPORT STRUCTURE

The FLOLS optical chain will be located along side of the target projector. It is felt that a flat plate optical bench with suitable stiffness will support the FLOLS model board and associated optics out to the target projector optical chain.

The remainder of the FLOLS image generator can be on a separate mount to minimize vibration due to motor and shutters.

The FLOLS flat plate optical bench will be an integral part of the target projector support structure.

With this approach the optics and servos will be accessible with the removal of a light-and-dust cover.

Table 14. FLOLS ZOOM AND IRIS CHANGE

SIMULATED RANGE FROM TOUCHDOWN	SIMULATED RANGE FROM FLOLS	FRACTIONAL WIDTH OF CARRIER ON CAMERA	FLOLS ZOOM FOCAL LENGTH MIN FOCAL LENGTH = 1	IRIS SIZE MAX DIAMETER = 1
6 nm	36730 ft	0.25	1	0.255
4	24570	0.37	1	0.382
3	18490	0.49	1	0.507
2	12410	0.74	1	0.755
1.5	9370	0.90	1	1
8100 ft	8350	0.90	1	1
4950	5200	0.90	1	1
4560	4810	0.90	1	1
1000	1250	0.90	1	1
200	450		2.78	1
0	250			
-250	0			

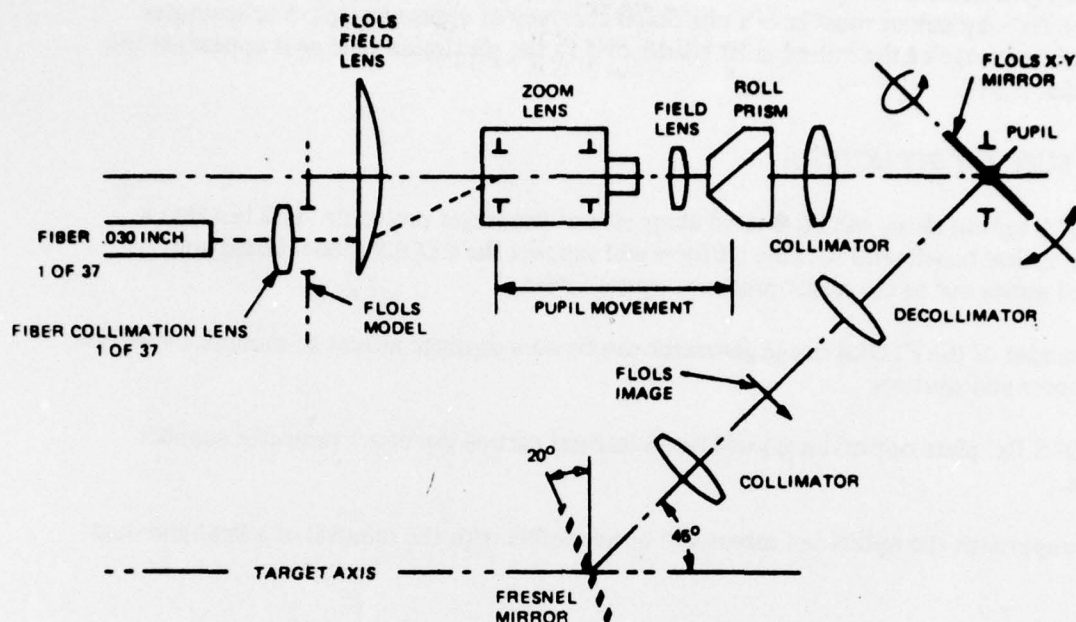


Figure 47. FLOLS OPTICAL CHAIN

ALTERNATES.

Closed-Loop Probe to Model. A closed loop between the model and the probe may be accomplished by putting a light-emitting source (spectral compatible to TV system) in the FOV of the optical probe. By using the raster of the image received from the optical probe to sense pointing error, a horizontal and vertical displacement command may be generated. The most probable place for the emitting source would be in the center of the FLOLS board on the model. (Eliminates roll and displacement, due to off-axis roll). If the light spot in the FOV is objectionable, it may be blanked out later.

Since the probe is supposed to be looking straight at the FLOLS, the necessary drive for the probe servos may be computed and added to the commanded probe signal for minimizing the pointing errors.

Effort should be made to keep the servo error computational algorithm fast (wide bandwidth) and simple.

Since roll, iris, zoom, focus, and tilt do not affect the e_x , e_y , in an aligned system, the only required error drives would be for pitch, and heading.

Figure 48 shows a very simple system schematic illustrating the above principle. Maximum use is made of proposed hardware. The additional hardware requirements are:

- 1) e_x , e_y decode electronics
- 2) Computer program to compute corrected drive signals for pitch and heading servo

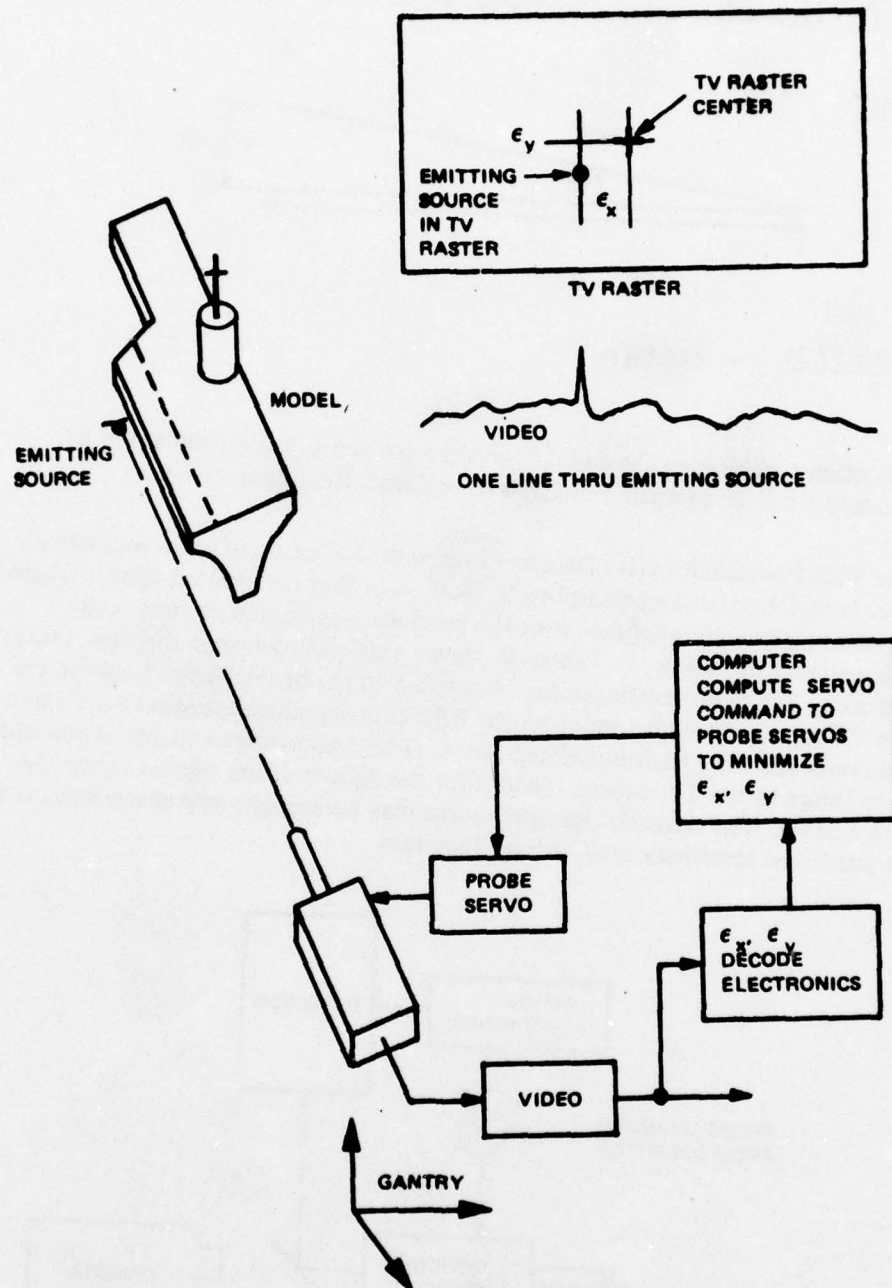
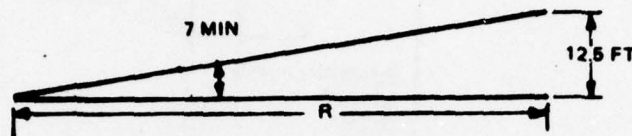


Figure 48. SIMPLIFIED SYSTEM TO POINT PROBE AT FLOLS BOARD

System Requirements. The sensitivity of each optical probe servo is in the order of 1-2 arc-min., if a pointing capability of 6-7 arc min. is assumed for best overall pointing of optical probe, and, if the AWAVS spec of 12.5 ft error is assumed, the range at which a 7 arc-min. error causes a 12.5 ft error:



$$R = \frac{12.5 (60 \times 57.3)}{7} = 6138.8 \text{ ft.}$$

This allows the specification (positioning the FLOLS within 5 percent of carrier width) to be met, out to approximately 1 nm, as compared to 1000 ft. without closed-loop control.

Light-Emitting Source With Position-Sensitive Detector. An approach exists where a very narrow bandwidth light source is matched with a beamsplitting filter, such that the emitted light is filtered from the scene. The advantage of this approach over the previously-explained method is the removal the keying signal from the scene¹³. Figure 49 shows a simplified system diagram, showing the fundamental approach. The light-emitting diode is matched to the beamsplitter, between the optical probe and the TV camera, in such a way that the light-emitting-diode emission is reflected into the detector and removed from the transmitted image. The beamsplitter will not appreciably affect the transmission image to the TV camera. Diodes for the light-emitting sources in the low red range are readily available. The image of the light source may be brought into sharp focus at the detector, so that the positional sensitivity may be 2 or 3 arc-min.

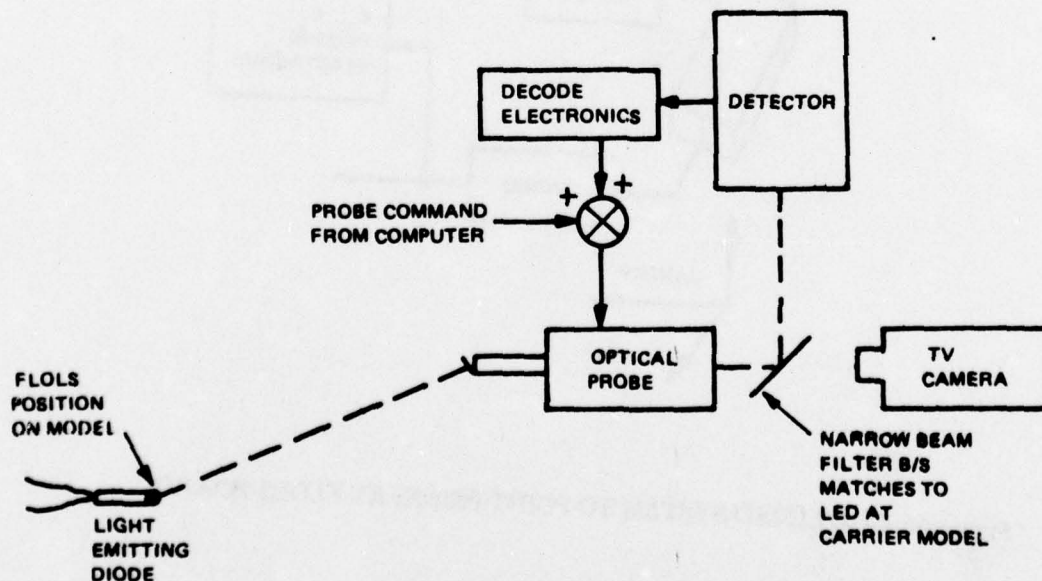


Figure 49. PROBE-POINTING SYSTEM, SIMPLIFIED

The detector has to sense the position of the emitted spot and generate error signals to drive the pitch and heading servos in the probe. These signals may be used as a lock-on signal, or as a command plus error signal for probe control. The detector may be as simple as a four-quadrant detector, which will drive the decode electronics in the classical "bang-bang" mode, or may require more complex position-sensitive, or scanning techniques. More design is necessary to determine if the limit cycle of the "bang-bang" servo is objectionable or detectable in the image. However, a hierarchy of detectors does exist and one can be selected to meet the requirement.

SECTION V

BACKGROUND IMAGE GENERATOR

The background image generator will produce a background that will consist of sea state 2 or 3 to within 10° of the horizon, haze to the horizon, and amorphous clouds.

METHODS CONSIDERED.

Proposed Method. The background image generator will be housed in a light-tight cabinet. A flat plate, suitably stiff, will provide the optical bench to mount the flying spot scanner, optics and photomultiplier. This plate will mount in a vertical plane inside the cabinet with lower space allocated for the electronics. This approach is used successfully on our F4 land mass simulation (see figure 50.)

All optical component mountings will be designed to provide sufficient degree-of-freedom adjustment for purposes of alignment.

Alternate Methods. Alternate Methods are discussed starting page 156.

DIGITAL-ANALOG RASTER COMPUTER (DARC).

The raster computer for this background image generator will provide mapping function detailed in section X, math models. These math models describe mapping functions to correct for projector displacement eye displacement, lens mapping, aircraft attitude and vertical transform for the film imagery.

The DARC to be employed in the AWAVS background image generator was first implemental on the F4E-18. This implementation utilizes a two dimensional description of this desired shape in terms of the orthogonal axis of the projector surface.

Raster shapes are developed by the DARC from a series expansion of the following form:

$$V_x, V_y = K_i \psi^j \theta^k$$

$$i = 1, \dots, l$$

$$j = 0, \dots, m$$

$$k = 0, \dots, n$$

$$\psi = \text{horizontal sweep}$$

$$\theta = \text{vertical sweep}$$

$$K = \text{scaling constants}$$

$$V_x = \text{x-axis deflection signal}$$

$$V_y = \text{y-axis deflection signal}$$

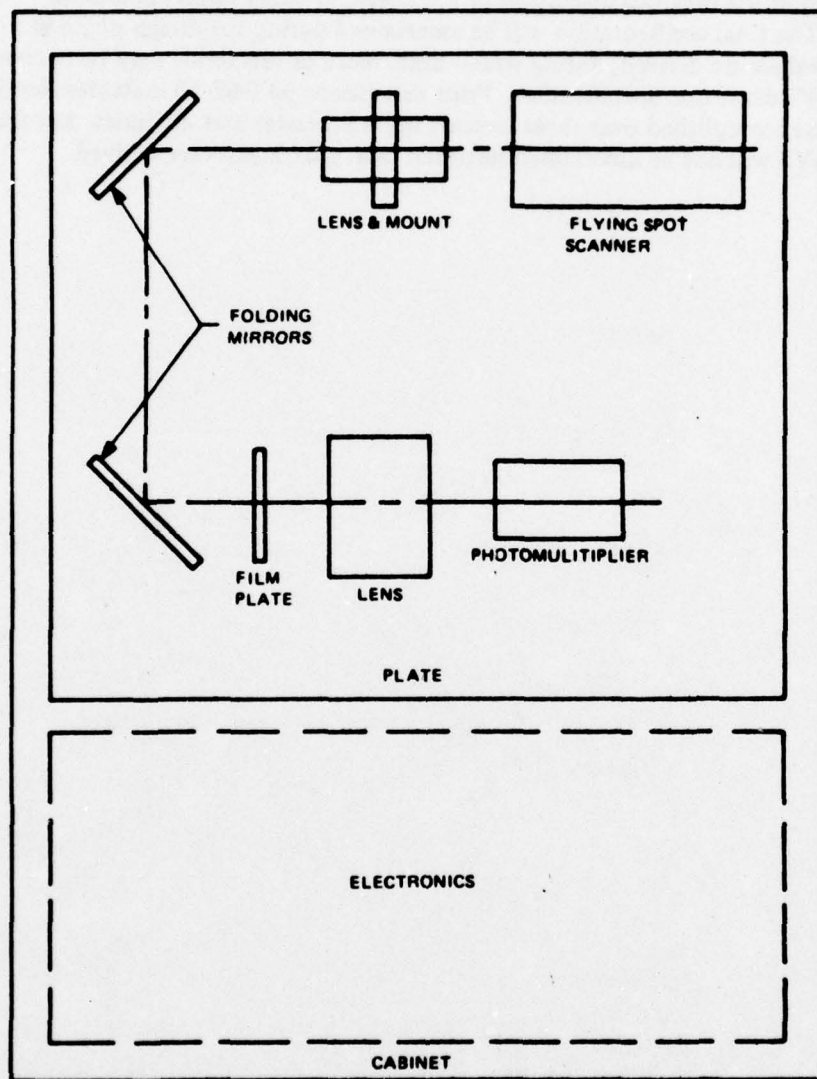


Figure 50. BACKGROUND IMAGE GENERATOR

The individual coefficient gain term is controlled by the system digital computer. This system, using sufficient terms in each equation, has provided a sweep waveform signal-to-noise ratio in excess of 80 db. Calculation of the individual coefficients incorporates the method of least squares, to minimize truncation errors.

It must be recognized that the previous discussion of the DARC is based upon experience gained from F4E-18. The final configuration will be ascertained during the design phase in which the coefficient values are derived; during which time, more or less terms may be necessary to insure meeting the 4% distortion specification. Prior experience on F4E-18 indicates that less than 2% distortion was accomplished over those aircraft flight attitudes and altitudes, but final system errors on AWAVS will not be ascertained until the final coefficients are derived.

FSS Raster Shape Derivation. This section derives the relationship between points on the Eidophor raster on the oil film and the corresponding points on the flying spot scanner, which will provide the correct seascape image elements to be projected.

First, the background image projector lens mapping must be taken into account. The lens is a combination of an f - θ lens with anamorph. It can be approximately represented by an f - θ lens projecting from a plane raster of altered aspect ratio.

For an f - θ projection lens, if points in the raster plane are given polar coordinates r, ϕ with the origin at the on-axis point, then the projection direction is described in spherical coordinates θ, ϕ , where θ is the polar angle from the lens axis and ϕ is the azimuth. The same symbol ϕ is used for the azimuth in both the plane, polar coordinates in the object plane and in image space, since (for appropriately-chosen axes) they are equal. The polar angle θ satisfies the relation:

$$(1) \quad (r = f \theta)$$

where f is the lens focal length, and θ is in radians.

If we appropriately scale the dimensions in the object plane, we may use a unit focal length. Then:

$$(2) \quad \theta = r = \sqrt{x^2 + y^2}$$

Where x and y are respectively the horizontal and vertical coordinates in the raster plane of altered scale and aspect ratio. Also:

$$(3) \quad \phi = \begin{cases} \arctan(y/x), & x \geq 0 \\ \arctan(y/x) + \pi, & x < 0 \end{cases}$$

We then find the direction cosines K_{BP}, L_{BP}, M_{BP} of the projection direction with (respectively) the X, Y , and Z Background Projector axes. Discussion of Frames of Reference:

$$(4) \quad \begin{cases} K_{BP} = \cos \theta \\ L_{BP} = \sin \theta \cos \phi \\ M_{BP} = \sin \theta \sin \phi \end{cases}$$

The next step is to refer K_{BP} , L_{BP} , M_{BP} to the display axes. In position 1 the projector field is shifted to the left ($\psi_s = -38.1^\circ$), then tipped down 4.8° . In position 2, the first rotation is zero degree, and the second rotation is again -4.8° . The sequence of rotations is the same as the standard yaw, pitch, roll sequence, so that, in analogy to the transformation from aircraft to inertial axes, we obtain the direction cosines K_D , L_D , M_D referred to the Display axes:

$$(5) \quad \begin{cases} K_D = [\cos \psi_s \cos (-4.8^\circ)] K_{BP} - [\sin \psi_s] L_{BP} + [\cos \psi_s \sin (-4.8^\circ)] M_{BP} \\ L_D = [\sin \psi_s \cos (-4.8^\circ)] K_{BP} + [\cos \psi_s] L_{BP} + [\sin \psi_s \sin (-4.8^\circ)] M_{BP} \\ M_D = [-\sin (-4.8^\circ)] K_{BP} + [\cos (-4.8^\circ)] M_{BP} \end{cases}$$

where $\psi_s = \begin{cases} -38.1^\circ, & \text{position 1} \\ 0 & , \text{position 2} \end{cases}$

Let X_1 , Y_1 , Z_1 be the coordinates in the display frame of the projection point. In position 2 the point X_1 , Y_1 , Z_1 is -11, 0, -24 in inches, but the rotation ψ_s for position 1 is taken about the center of the screen, so that:

$$(6) \quad \begin{cases} X_1 = (-11) \cos \psi_s \\ Y_1 = (-11) \sin \psi_s \\ Z_1 = -24 \end{cases}$$

Where $\psi_s = -38.1$ for position 1, and

$\psi_s = 0$ for position 2.

Let us now consider the point X_D , Y_D , Z_D (referred to Display axes) on the screen to which the projector is projecting the raster point. This is given by:

$$(7) \quad \begin{cases} X_D = K_D D + X_1 \\ Y_D = L_D D + Y_1 \\ Z_D = M_D D + Z_1 \end{cases}$$

Where D is the (as yet) undetermined distance from the projection point to the point X_D, Y_D, Z_D . Substituting eq (6) into the equation of the spherical screen surface,

$$(8) \quad X_D^2 + Y_D^2 + Z_D^2 = R^2 \quad (\text{where } R = 120 \text{ inches}), \text{ one obtains a quadratic of the form:}$$

$$(9) \quad A D^2 + B D + C = 0.$$

Where:

$$(10) \quad \begin{cases} A = K_D^2 + L_D^2 + M_D^2 \equiv 1 \quad (\text{since } K_D, L_D, M_D \text{ are direction cosines}) \\ B = 2(K_D X_1 + L_D Y_1 + M_D Z_1) \\ C = X_1^2 + Y_1^2 + Z_1^2 - R^2 \end{cases}$$

Since we desire a positive solution for D , and since $C < 0$, the correct sign for the square root in the quadratic formula is positive. Exploiting the fact that $A \equiv 1$, we write:

$$(11) \quad D = (-B + \sqrt{B^2 - 4C})/2.$$

In the display frame, the position of the observer is X_2, Y_2, Z_2 , where:

$$(12) \quad \begin{cases} X_2 = 6 \\ Y_2 = 0 \\ Z_2 = 15 \text{ in inches.} \end{cases}$$

Hence, the position on the screen, X_{OB}, Y_{OB}, Z_{OB} , in the Observer frame of reference can be obtained by subtracting X_2, Y_2, Z_2 from X_D, Y_D, Z_D as given by eq. (6), yielding:

$$(13) \quad \begin{cases} X_{OB} = K_D D + (X_1 - X_2) \\ Y_{OB} = L_D D + (Y_1 - Y_2) \\ Z_{OB} = M_D D + (Z_1 - Z_2). \end{cases}$$

We now refer these coordinates to an Inertial frame centered at the observers origin, obtaining:

$$(14) \quad \begin{cases} X_1 = T_{11} X_{OB} + T_{12} Y_{OB} + T_{13} Z_{OB} \\ Y_1 = T_{21} X_{OB} + T_{22} Y_{OB} + T_{23} Z_{OB} \\ Z_1 = T_{31} X_{OB} + T_{32} Y_{OB} + T_{33} Z_{OB}. \end{cases}$$

Where:

$$(15) \quad \left\{ \begin{array}{l} T_{11} = \cos(\text{heading}) \cos(\text{Pitch}) \\ T_{12} = \cos(\text{Heading}) \sin(\text{Pitch}) \sin(\text{Roll}) - \sin(\text{Heading}) \cos(\text{Roll}) \\ T_{13} = \cos(\text{Heading}) \sin(\text{Pitch}) \cos(\text{Roll}) + \sin(\text{Heading}) \sin(\text{Roll}) \\ T_{21} = \sin(\text{Heading}) \cos(\text{Pitch}) \\ T_{22} = \sin(\text{Heading}) \sin(\text{Pitch}) \sin(\text{Roll}) + \cos(\text{Heading}) \cos(\text{Roll}) \\ T_{23} = \sin(\text{Heading}) \sin(\text{Pitch}) \cos(\text{Roll}) - \cos(\text{Heading}) \sin(\text{roll}) \\ T_{31} = -\sin(\text{Pitch}) \\ T_{32} = \cos(\text{Pitch}) \sin(\text{Roll}) \\ T_{33} = \cos(\text{Pitch}) \cos(\text{Roll}) \end{array} \right.$$

Projecting the line from the observer to the screen onto a horizontal plane (representing the Seascape) a distance H below the observer, one obtains the plane coordinates X_S, Y_S :

$$(16) \quad \left\{ \begin{array}{l} X_s = \frac{X_I}{Z_I} \quad H \\ Y_s = \frac{Y_I}{Z_I} \quad H \end{array} \right.$$

The seascape transparency is a rectilinear projection of the seascape, and the flying-spot scanner lens projects the CRT rectilinearly onto the transparency, so that, except for a scale change, the motion of the point X_S, Y_S describes the required raster for the CRT of the flying-spot scanner.

If, at the Maximum altitude H_M that the flying spot-scanner simulates, the seascape coverage goes to θ_H below the Horizon, the coverage on the seascape lies inside a circle of radius R_{θ_H} , where:

$$(17) \quad R_{\theta_H} = H_M \cot(\theta_H).$$

(Note: $\cot 5^\circ = 11.430$, and $\cot 10^\circ = 5.671$.)

The proper scale factor is determined by the fact that R_{θ_H} , after scaling, should equal R_{CRT} , the radius of the useable area of the CRT. Applying this scale factor to equation (16), we obtain the coordinates X_{CRT} , Y_{CRT} on the CRT face:

$$(18) \begin{cases} X_{\text{CRT}} = \frac{X_I}{Z_I} \left(\frac{H}{H_M \cot \theta_H} \right) R_{\text{CRT}} \\ Y_{\text{CRT}} = \frac{Y_I}{Z_I} \left(\frac{H}{H_M \cot \theta_H} \right) R_{\text{CRT}} \end{cases}$$

Raster Shapes. Raster shapes have been determined for preliminary analysis. Section X discusses the math model that was included, but a list of the summary points are as follows:

- 1) Screen: A sphere with radius of 120"
- 2) Eyepoint: Located 15" below center and 6" forward of sphere center
- 3) Background Projector:

Position 1: Projector tilted towards projection center down 4.8° . Projector set at 38.1° to from view, rotated about the spherical pole axis. Locate 7" behind the center and 24" above.

Position 2: Projector tilted forward 4.8° , set at 0° azimuth. Located 7" behind and 24" above the screen center.
- 4) Projector Lens: $f(\theta)$ lens, with proper anamorph of 1.5 to projector raster plane orthogonal to projector axis
- 5) Film Plate: Vertical overhead projection
- 6) FSS Lens: $f \tan \theta$
- 7) FSS Crt: Flat face screen, orthogonal to optical path.

A series of raster plots have been generated to show the raster on the flying spot scanner desired to faithfully reproduce the image to the viewer. Position 1 and 2 refer to the position of the background projector. Position 2 represents symmetrical background of $\pm 80^\circ$ while position 1 represents the background image offset by 40° . Figure 51 (6 sheets) shows Position 2. The radiating lines are equal azimuth lines. The two concentric circles represent 5° below the horizon (outside circle) and 10° below the horizon (inside circle). The lines orthogonal (more or less) to the azimuth lines in the non-roll cases are equal television spaces of 16 TV lines per space. There are 51 lines overall, as seen in the 60° roll case, figure 51, sheet 6.

AWAYS RASTER PLOT

OFFSET=0.0 TILT= -4.8 HEAD= 0.0 PITCH=0.0 ROLL= 0.0
10/21/74

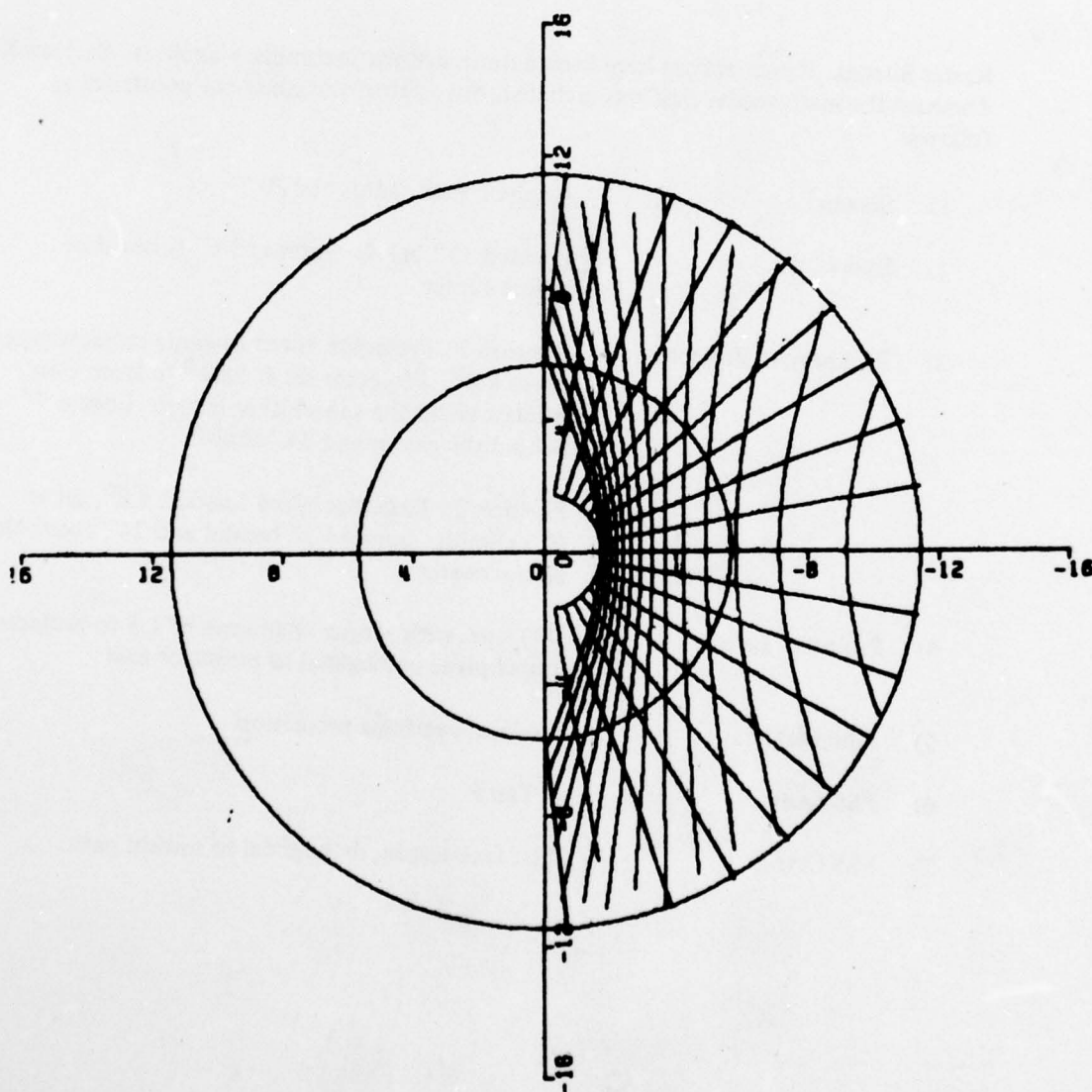


Figure 51. BACKGROUND PROJECTOR, POSITION 2 (PART 1 OF 6)

AWAVS RASTER PLOT

OFFSET=0.0 TILT= -4.8 HEAD= 0.0 PITCH=-15.0ROLL= 0.0
10/21/74

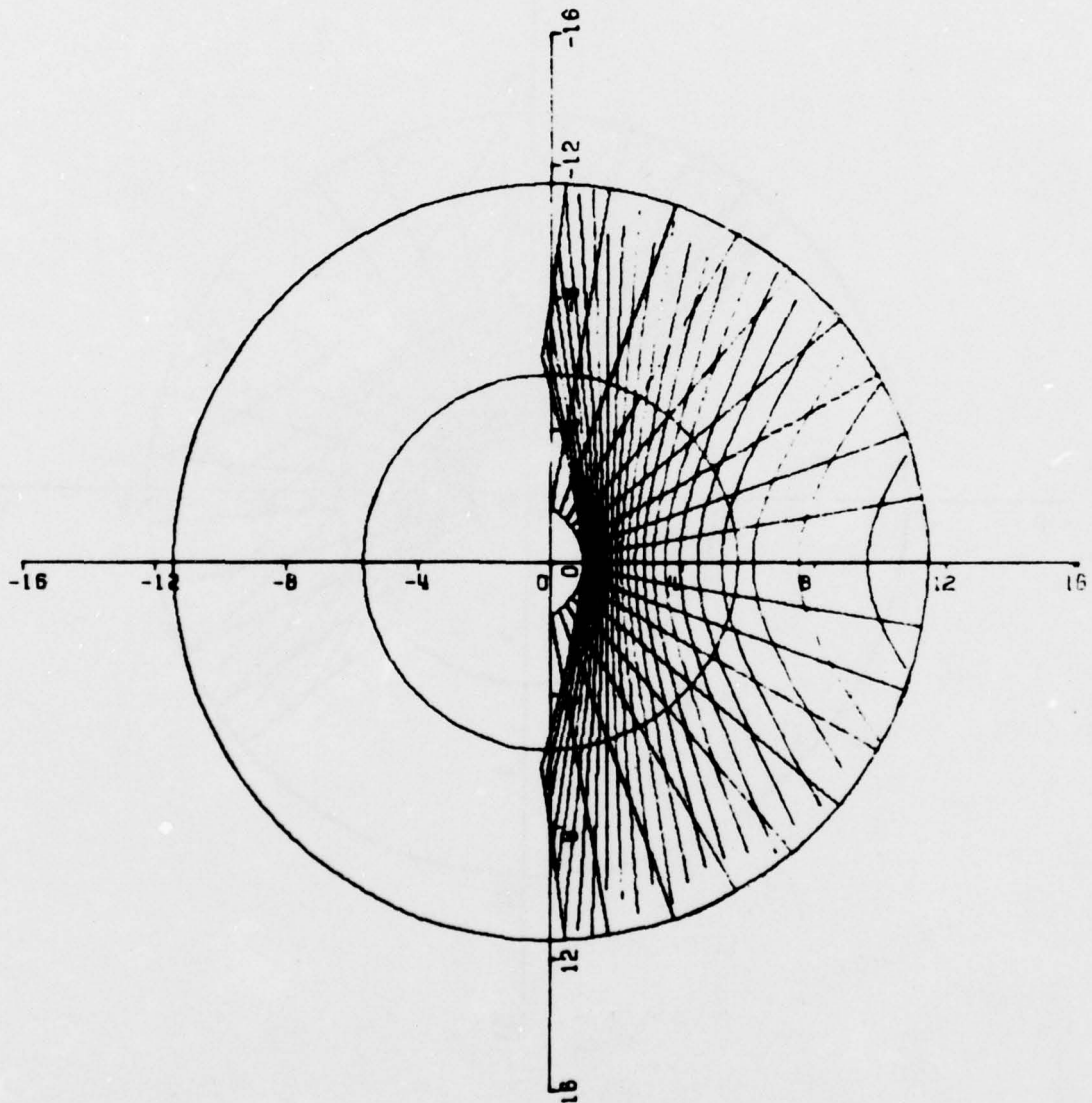


Figure 51. BACKGROUND PROJECTOR, POSITION 2 (PART 2 OF 6)

NAVTRAEQUIPCEN 75-C-0009-1

AWAYS RASTER PLOT

OFFSET=0.0 TILT=-4.8 HEAD=45.0 PITCH=0.0 ROLL=0.0
10/21/78

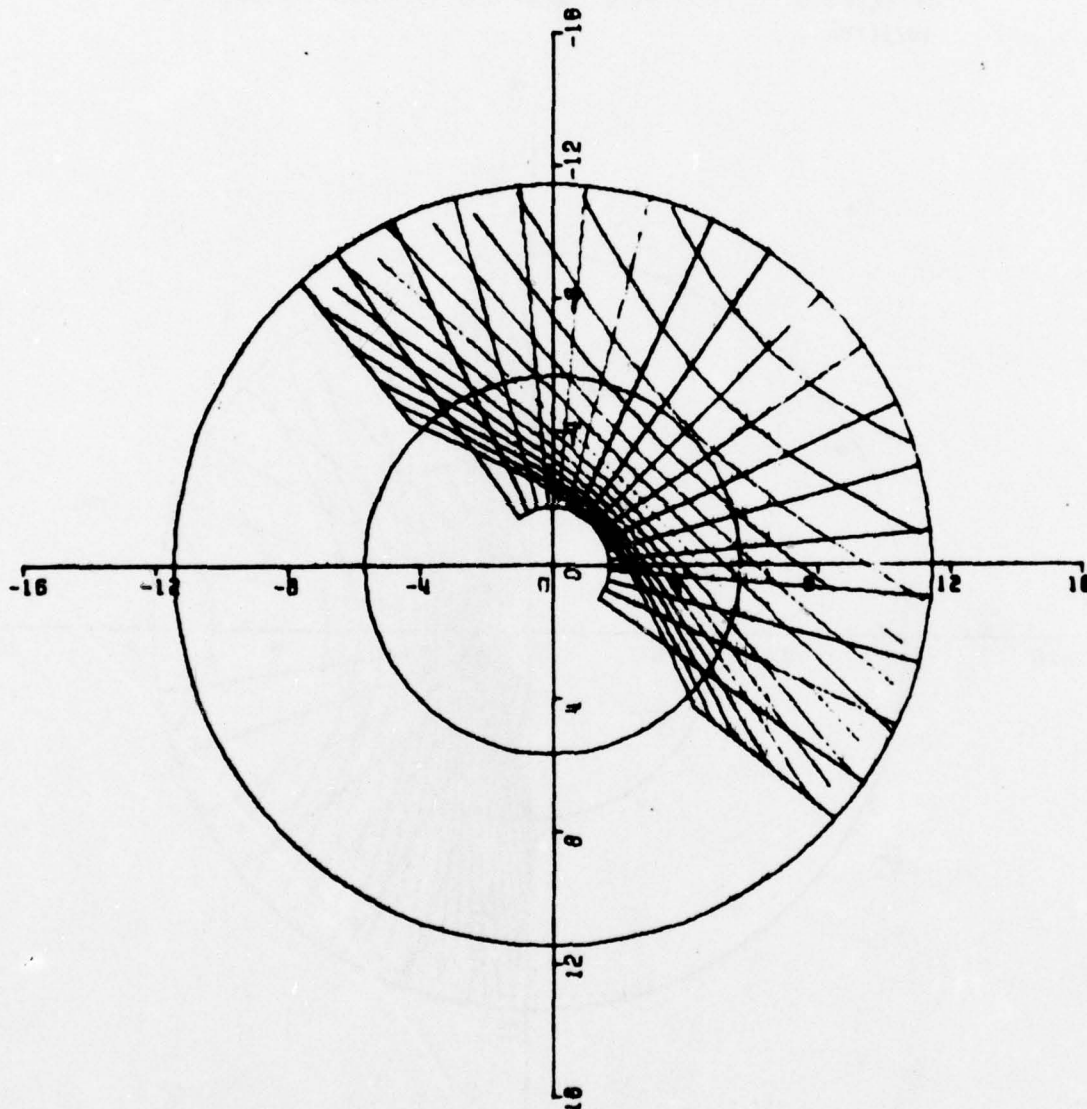


Figure 51. BACKGROUND PROJECTOR, POSITION 2 (PART 3 OF 6)

NAVTRAEQUIPCEN 75-C-0009-1

AWAVS RASTER PLOT

OFFSET=0.0 TILT= -4.8 HEAD= 0.0 PITCH=0.0 ROLL= -10.0
10/21/74

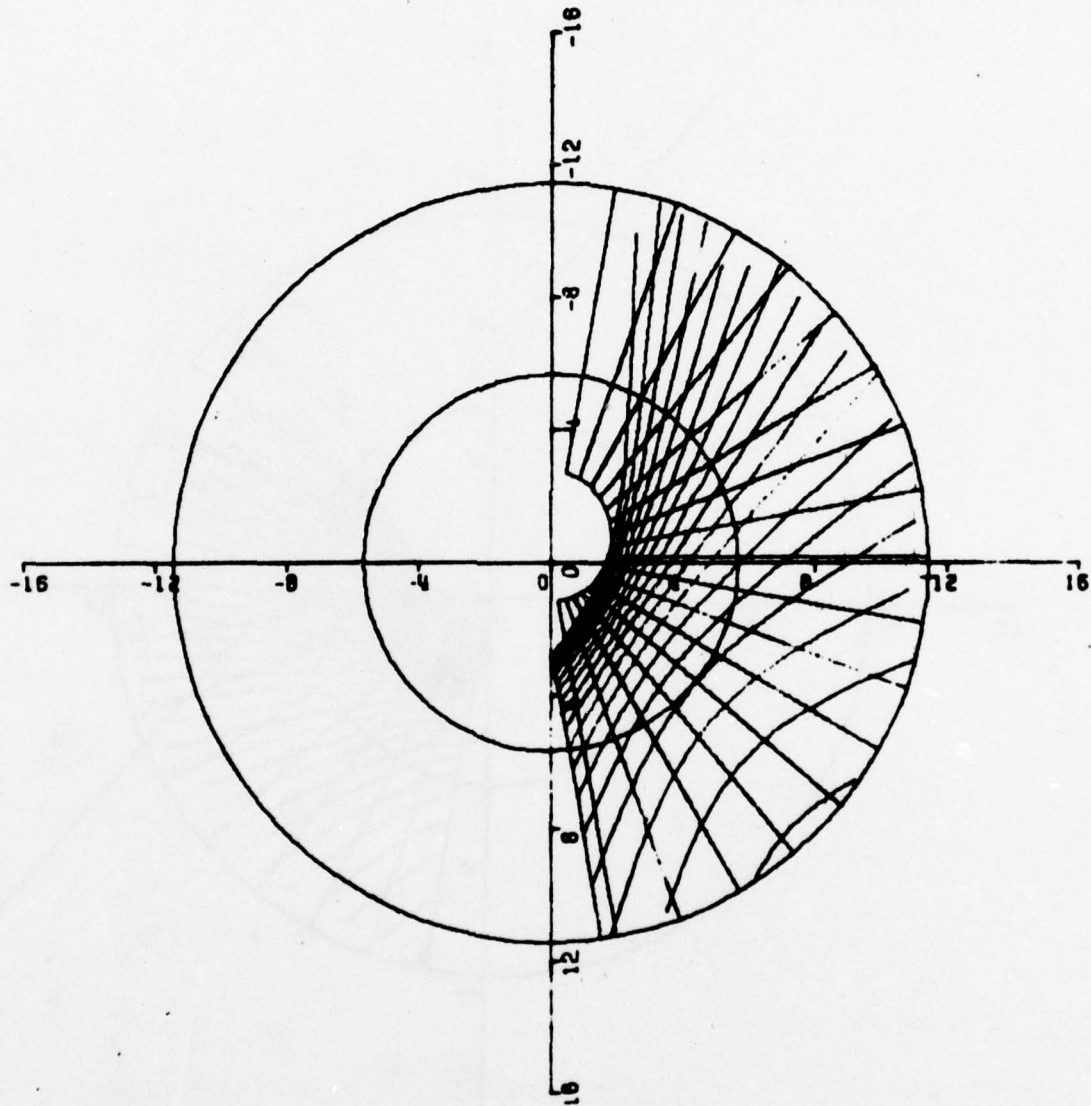


Figure 51. BACKGROUND PROJECTOR, POSITION 2 (PART 4 OF 6)

AWAVS RASTER PLOT

OFFSET=0.0 TILT=-4.8 HEAD=0.0 PITCH=0.0 ROLL=30.0
10/21/74

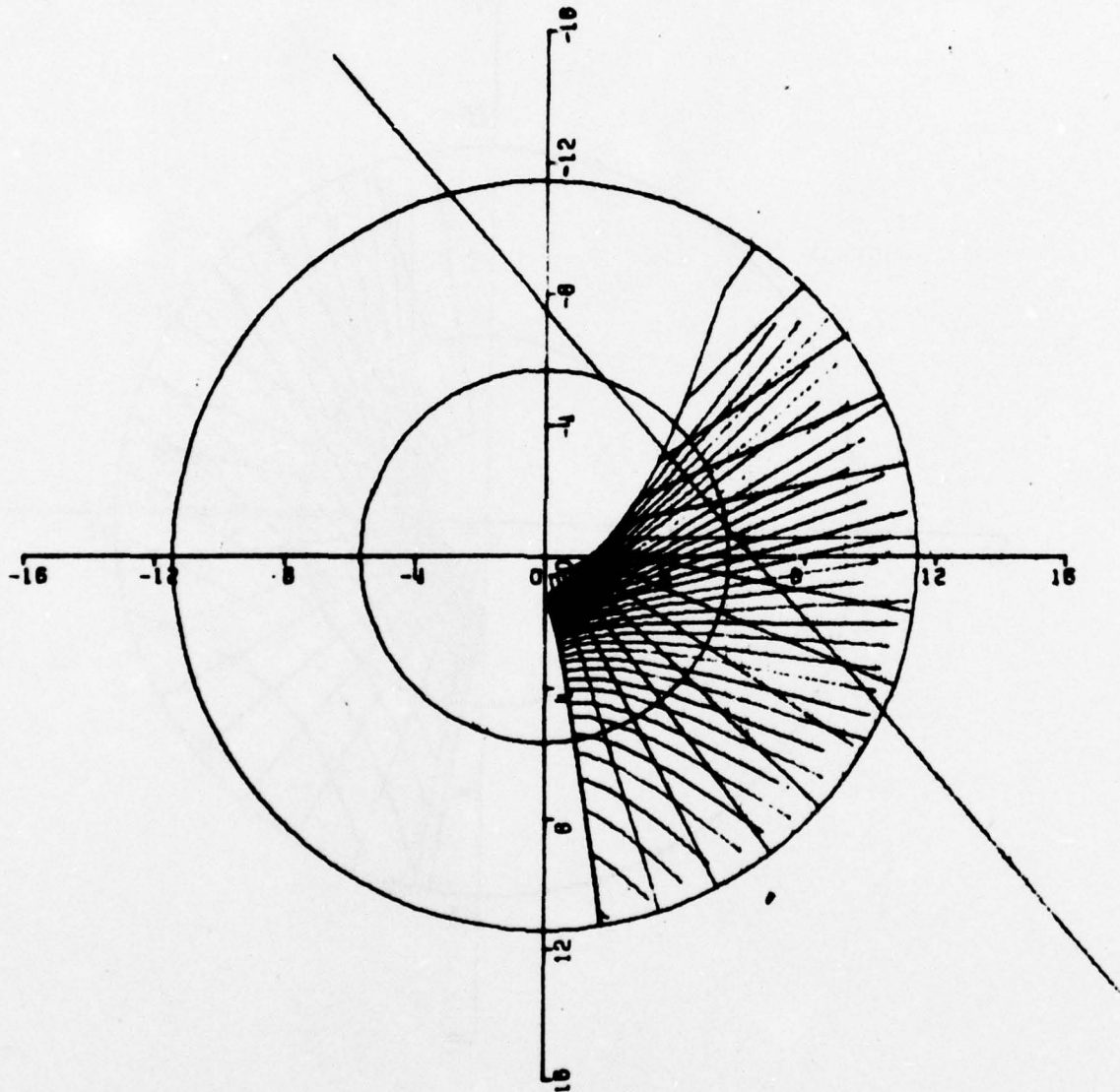


Figure 51. BACKGROUND PROJECTOR, POSITION 2 (PART 5 OF 6)

ANAVS RASTER PLOT

Offset=0.0 TILT=-4.8 HEAD=0.0 PITCH=0.0 ROLL=-80.0
10/21/74

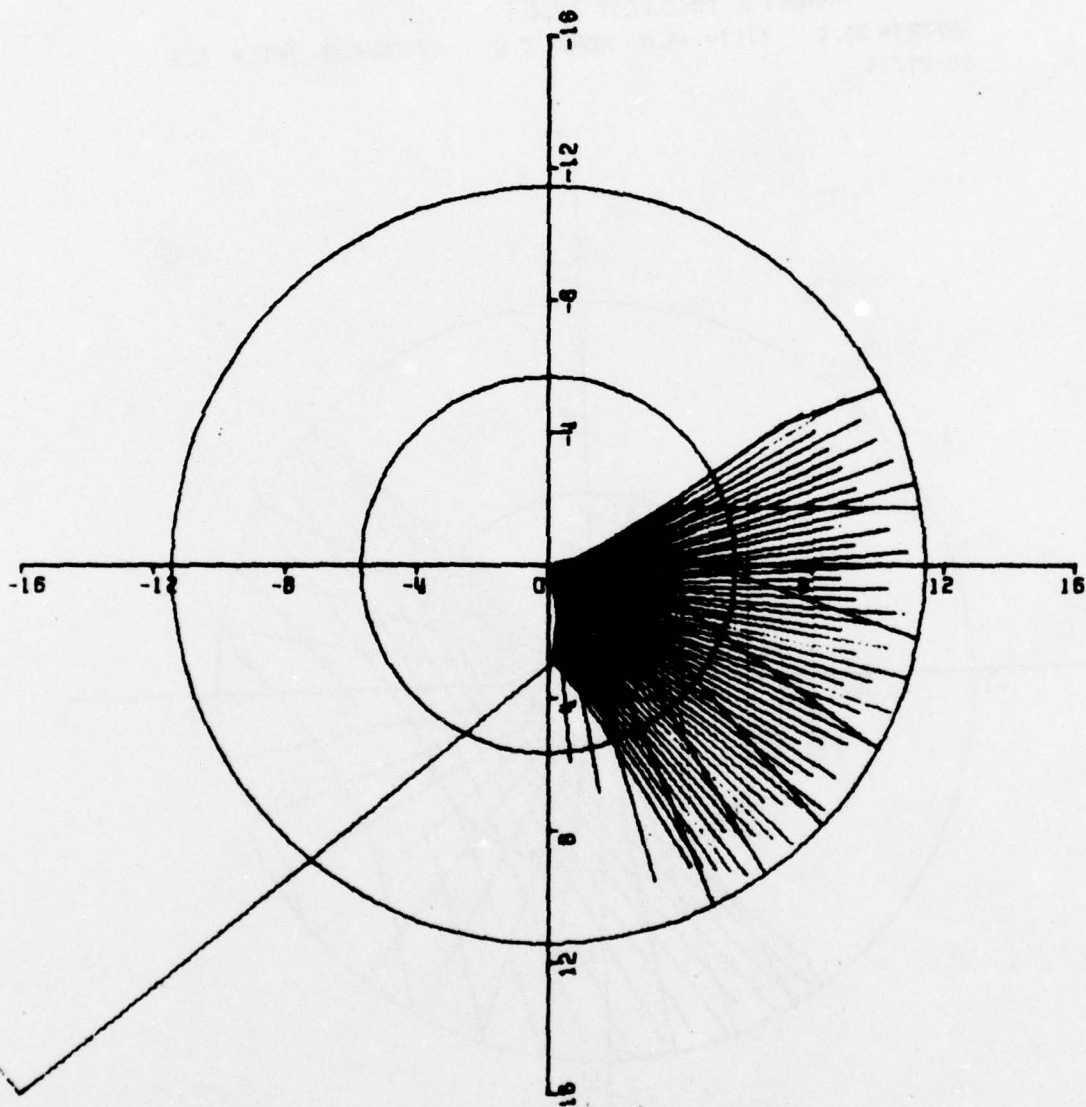


Figure 51. BACKGROUND PROJECTOR, POSITION 2 (PART 6 OF 6)

NAVTRAEQUIPCEN 75-C-0009-1

Figure 52 (8 sheets) represents in the required raster for position one. The details of the plots are the same as in position 2. Sheets 7 and 8 of figure 52 represent the same aircraft attitudes as sheets 1 and 2 respective but are taken to be one-half the altitude.

In the proposed system, the 10° circle (inner circle) represents the outer diameter of 5-inch cathode ray tube.

AWAVS RASTER PLOT

OFFSET=38.1 TILT=-4.8 HEAD=0.0 PITCH=0.0 ROLL=0.0
10/21/74

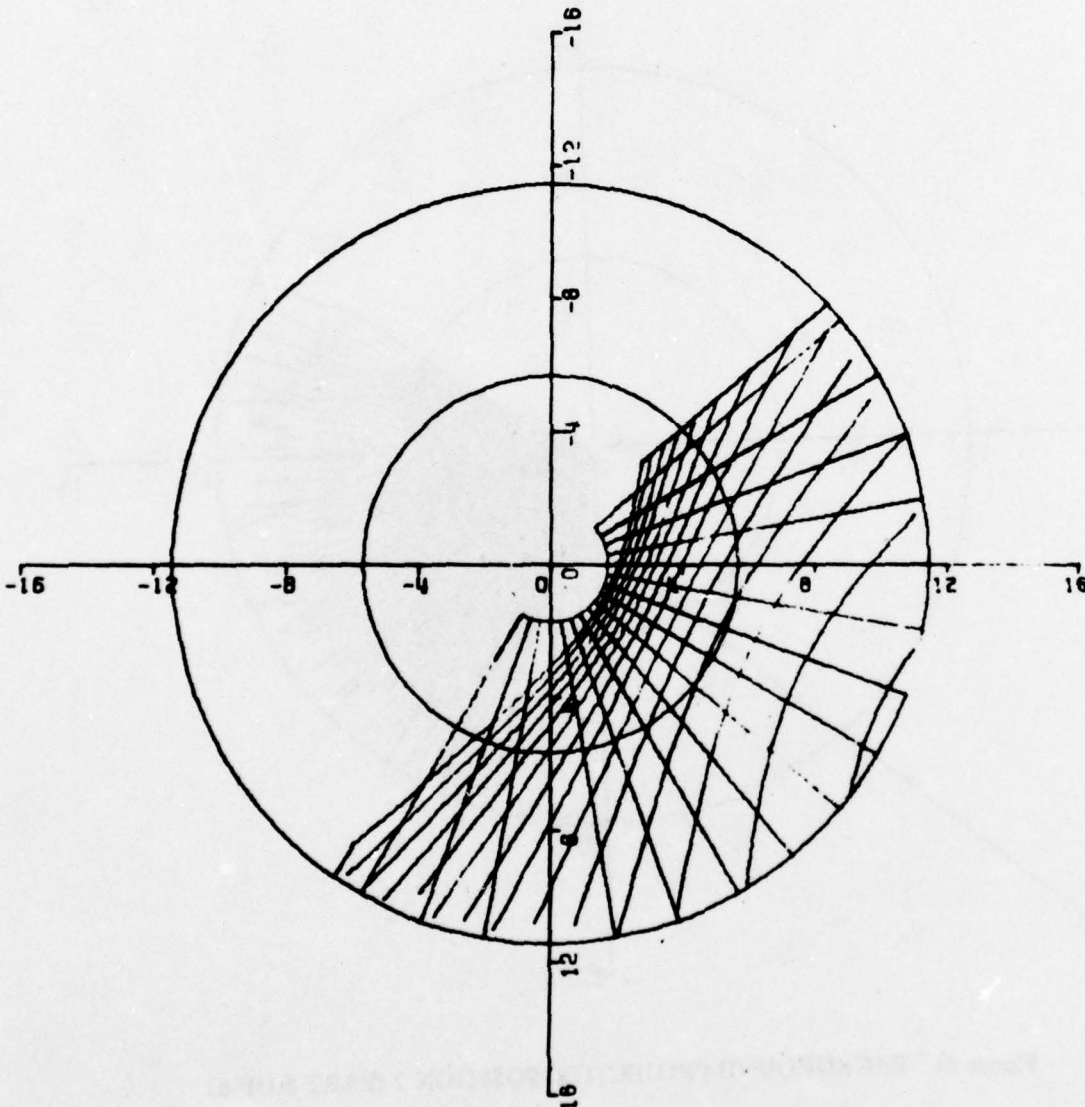


Figure 52. REQUIRED RASTER FOR POSITION ONE (PART 1 OF 8)

AWAYS RASTER PLOT

OFFSET=38.1 TILT=-4.8 HEAD=0.0 PITCH=-15.0ROLL=0.0
10/21/74

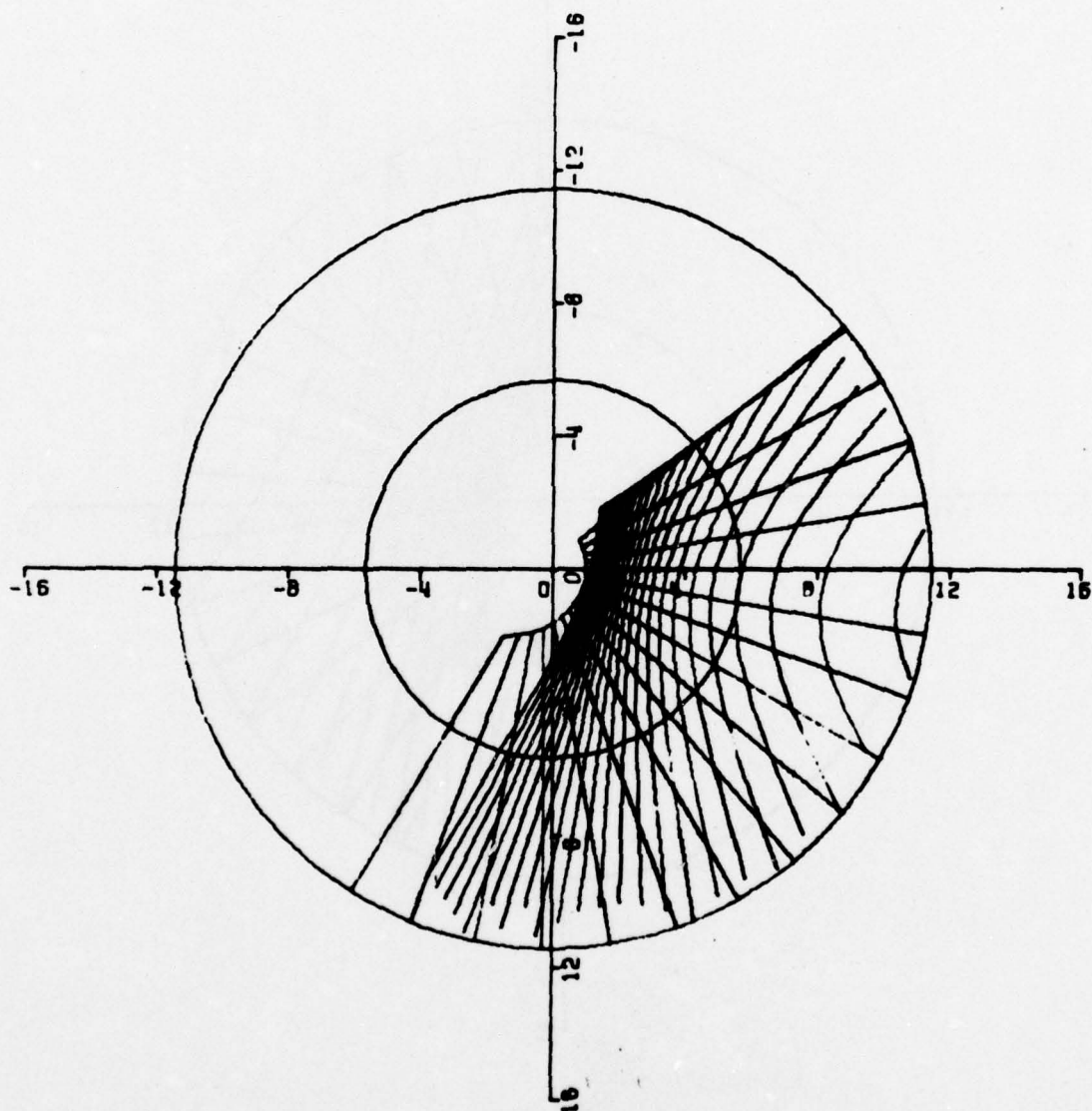


Figure 52. REQUIRED RASTER FOR POSITION ONE (PART 2 OF 8)

AWAVS RASTER PLOT

OFFSET=30.1 TILT= -4.0 HEAD= 45.0 PITCH=0.0 ROLL= 0.0
10/21/74

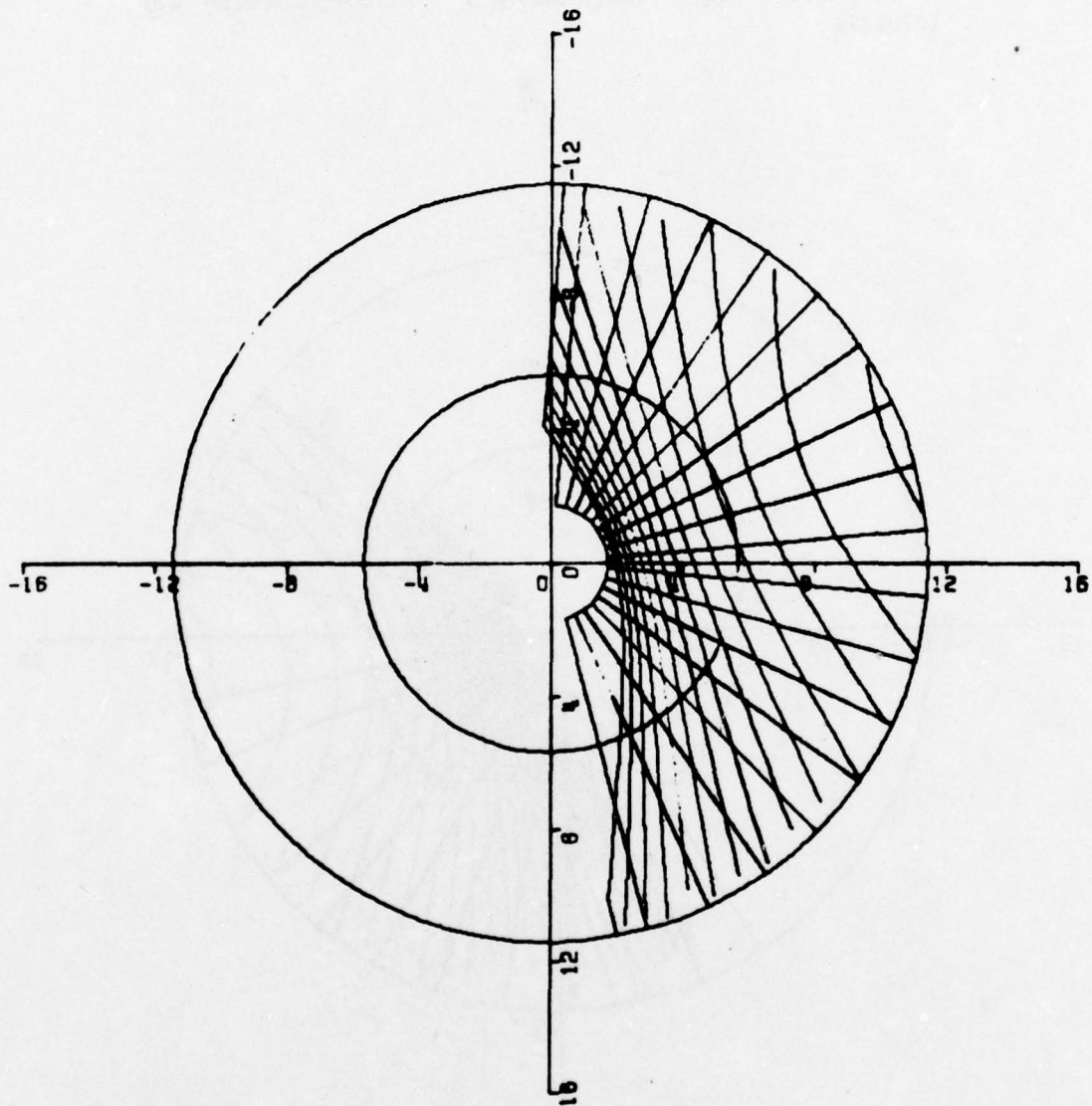


Figure 52. REQUIRED RASTER FOR POSITION ONE (PART 3 OF 8)

AWAVS RASTER PLOT

OFFSET=30.1 TILT= -4.0 HEAD= 0.0 PITCH=0.0 ROLL= -10.0
10/21/74

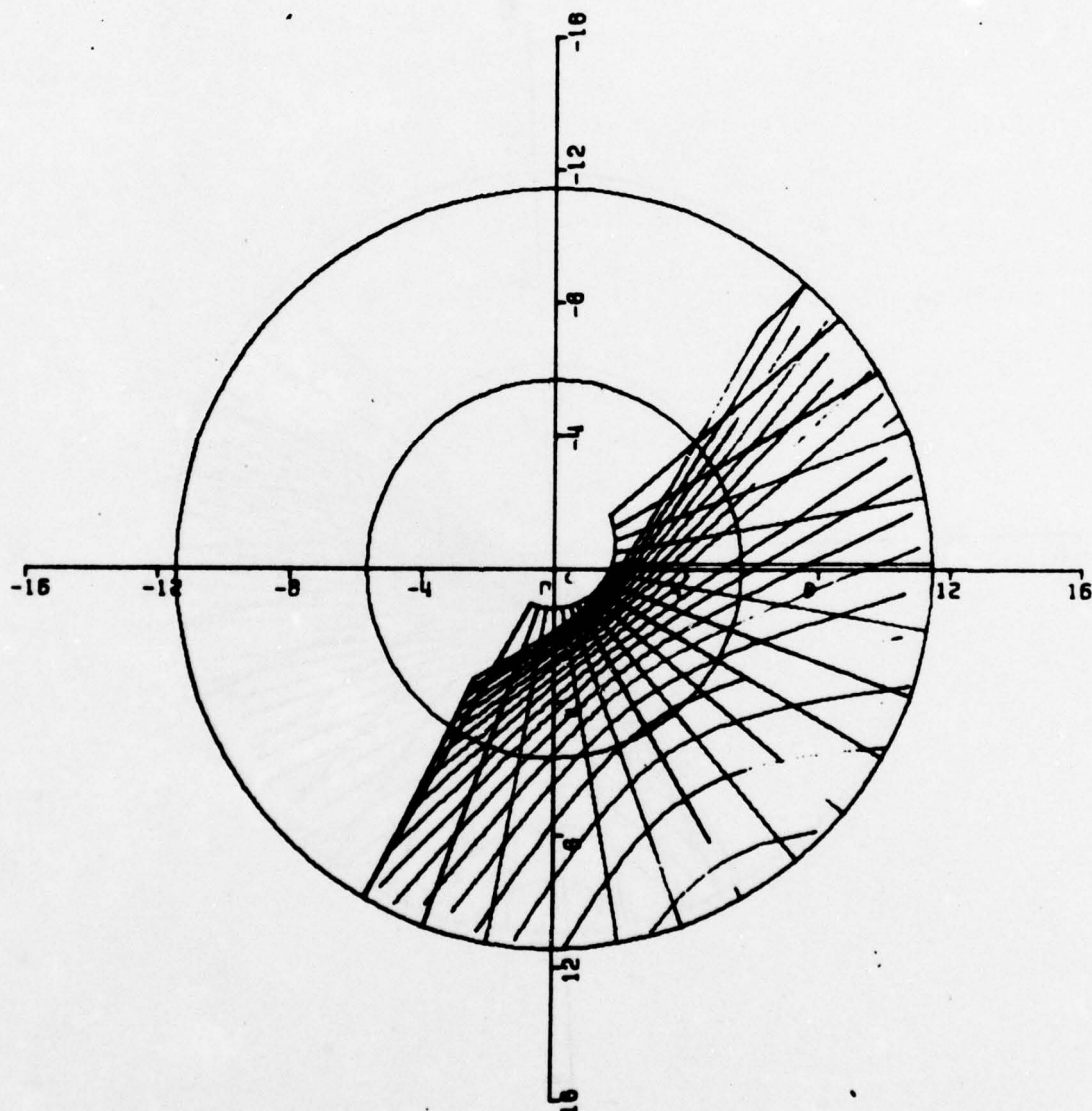


Figure 52. REQUIRED RASTER FOR POSITION ONE (PART 4 OF 8)

AWAVS RASTER PLOT

OFFSET=38.1 TILT=-4.8 HEAD=0.0 PITCH=0.0 ROLL=-30.0
10/21/74

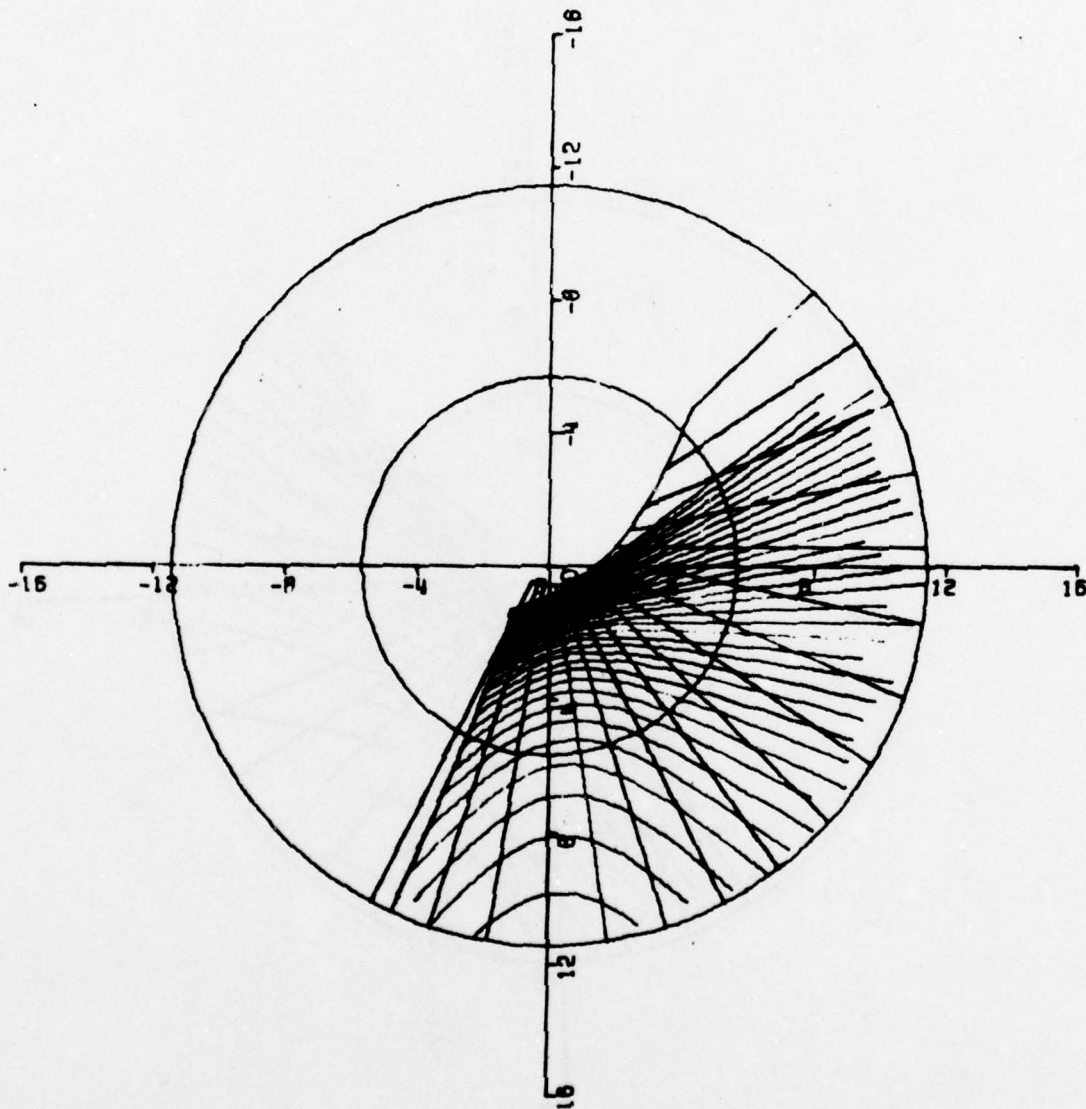


Figure 52. REQUIRED RASTER FOR POSITION ONE (PART 5 OF 8)

AWAVS RASTER PLOT

OFFSET= 35.1 TILT= -4.8 HEAD= 0.0 PITCH=0.0 ROLL= -60.0
10/21/74

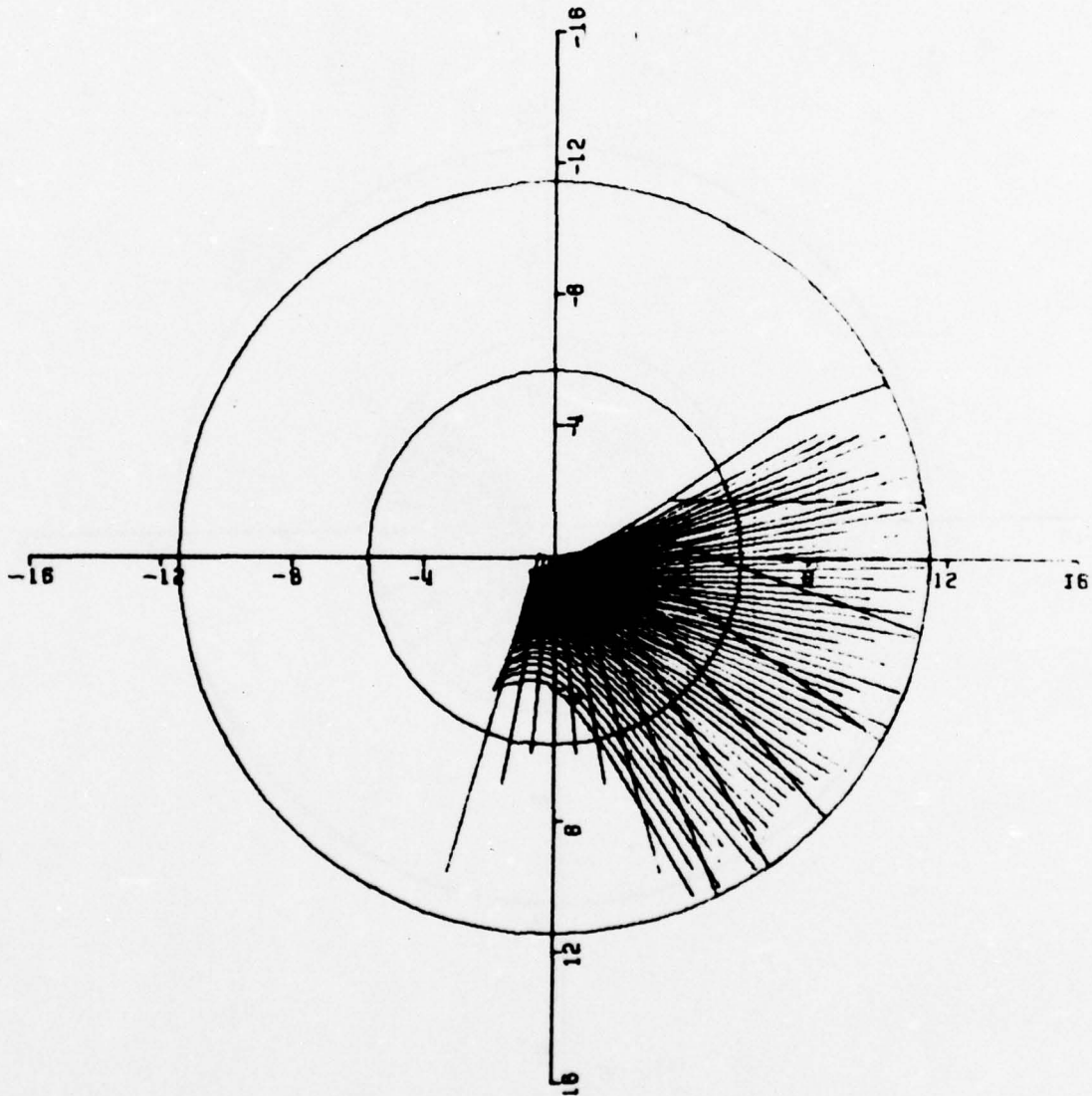


Figure 52. REQUIRED RASTER FOR POSITION ONE (PART 6 OF 8)

AWAYS RASTER PLOT

OFFSET=38.1 TILT=-4.8 HEAD=0.0 PITCH=0.0 ROLL=0.0
10/21/74

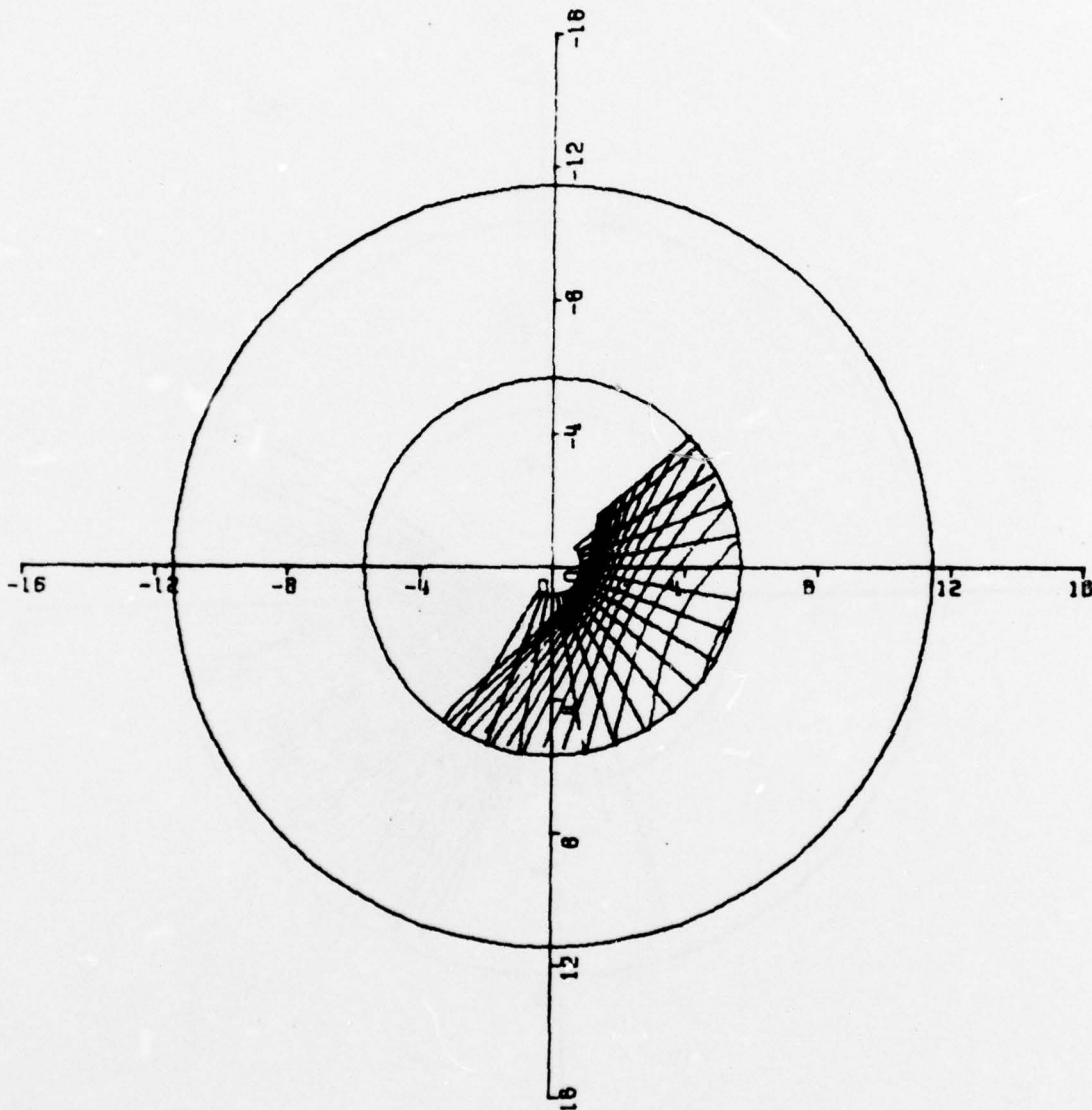


Figure 52. REQUIRED RASTER FOR POSITION ONE (PART 7 OF 8)

AWAVS RASTER PLOT

OFFSET=38.1 TILT=-4.8 HEAD=0.0 PITCH=-15.0ROLL=0.0
10/21/74

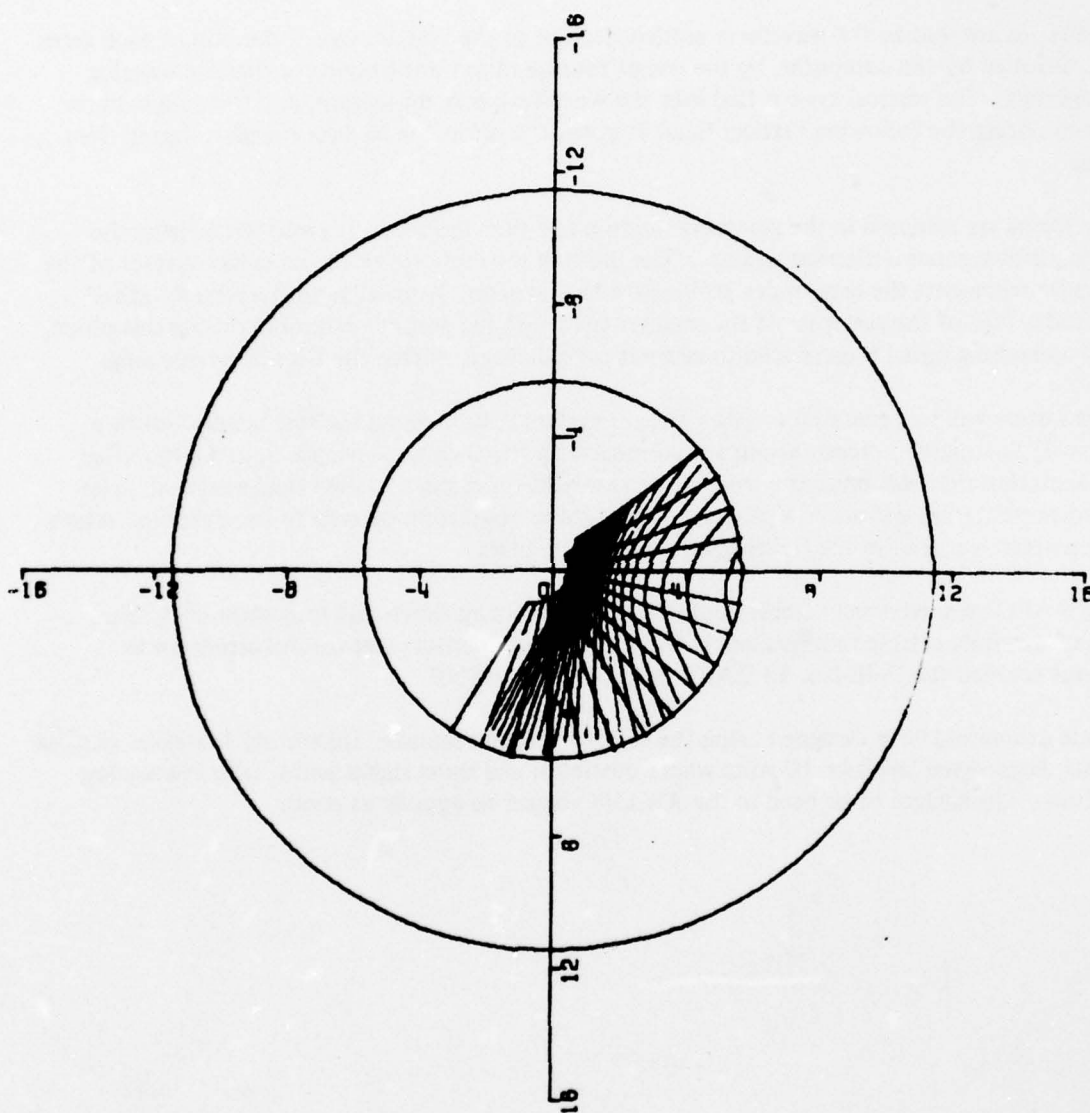


Figure 52. REQUIRED RASTER FOR POSITION ONE (PART 8 OF 8)

FSS, DARC Functional Hardware. A function block diagram is shown in figure 53. The system will be expanded if necessary to achieve the 4% distortion figure. The vertical and horizontal sync pulses drive the waveform generator, which produces the waveforms indicated by successive integrations. Thus, ψ and θ are linear ramp signals representing the fast and slow time functions. (Since V_k or V_y may be either fast or slow, that is, representative of the display fast sweep, and the display slow sweep, the terms horizontal or vertical are only relative.)

The terms are sent to the waveform control section of the system, where the gain of each term is controlled by the computer, by the use of four-quadrant multiplying or digital-to-analog converters. The vertical sync is tied into the waveform control section, and the data is transferred during the following vertical field, to prevent a jump due to data transfer, during field time.

The terms are summed in the summing module and then limited to prevent overdriving the flying-spot-scanner deflection system. The limiting is necessary, since the entire surface of the scanner represents the area under 10^0 , below the horizon. Normally, with a straight-ahead attitude, 75% of the raster is off the scanner tube, and the scanner is limited during this phase, and a blanking signal is generated to prevent tube damage, during the time of overdriving.

Test rasters will be generated to allow proper system test. Among the test rasters will be a normal, North-going presentation, a rectilinear scan for alignment purposes, and a modified presentation that will present a transformed straight-on picture to the visual eyepoint. The third presentation will show a proper grid pattern or resolution pattern to the eyepoint, when the pattern is placed in the flying-spot-scanner film plate.

The DARC uses extremely stable components, minimizing short- and long-term drift. The use of carefully selected integrators in the waveform generators and careful attention to layout enabled the F-4E No. 18 DARC to exceed 80 db SNR.

These generators were designed using the following requirements: Inherently low-noise components; large signal levels (± 10 volts where possible); and short signal paths, with few analog circuits. The system to be used in the AWAVS should be equally as good.

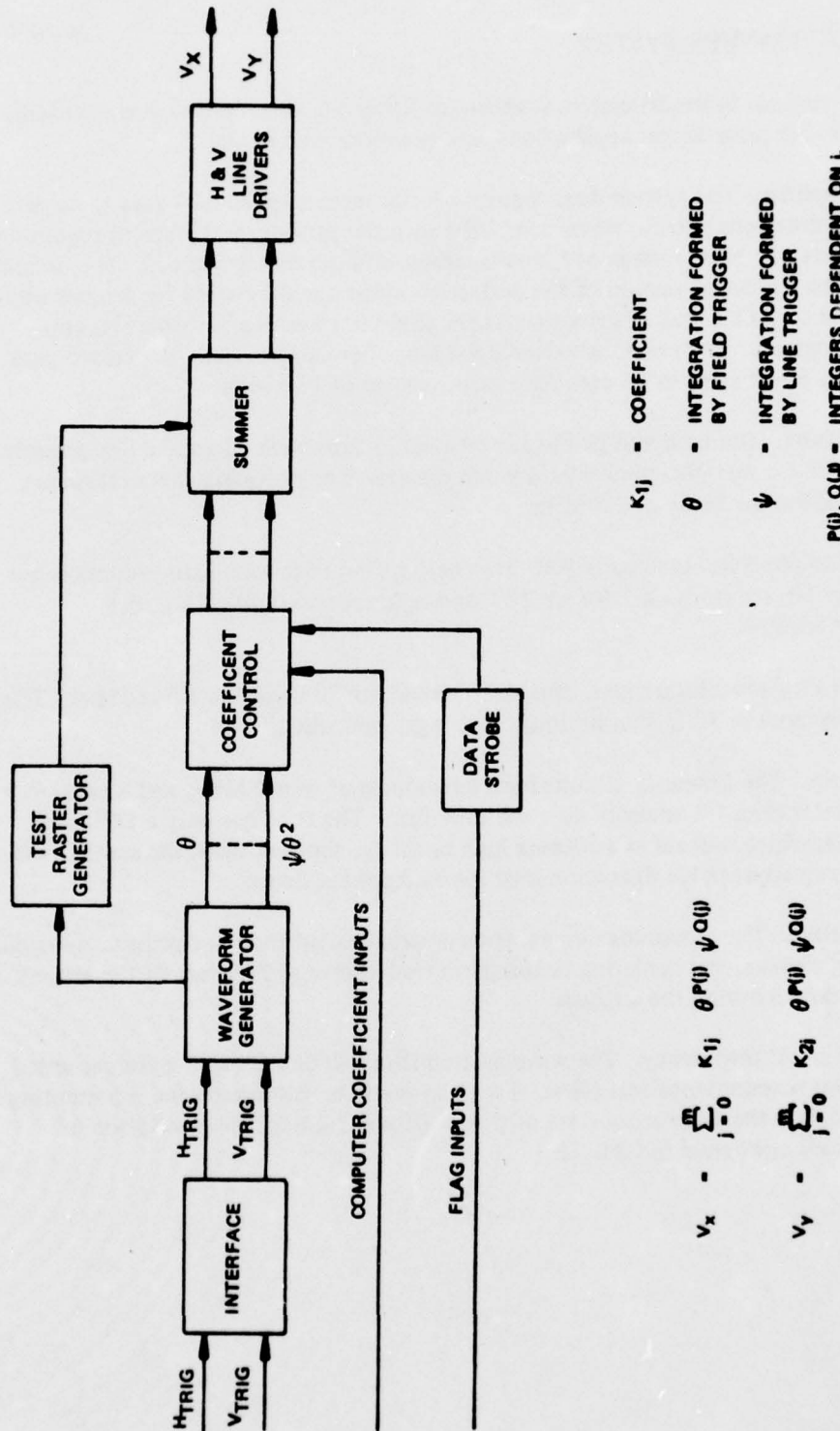


Figure 53. FSS DARC FUNCTIONAL BLOCK DIAGRAM

FLYING-SPOT-SCANNER SYSTEM.

The FSS (Flying-Spot-Scanner) system is shown in figure 54. The hardware is essentially the same as used in prior Singer applications, and is well-proven in use.

Deflection Amplifier. The system does require a faster retrace speed of 4 μsec to achieve of the unusual situations, which, when combined with the peak-to-peak current requirement of 5.4 amp, gives a flyback voltage of 80 volts, across a 60 μh -deflection coil. The deflection amperage will be a reduced version of the deflection amperage developed for Singers display CRT's and used on AOI (Area of Interest), SAAC (Simulated Air-to-Air Combat) and F4E No. 18 programs. The previously-developed amplifier can drive 30. A peak-to-peak current across a 60- μh yoke in 12 μsec for a peak voltage of 150 volts.

Cathode Ray Tube. The tube will be the Litton L-4125 tube with "S-gun." The phosphor will be the LP-202, a fast phosphor with a green spectra. The phosphor has a frequency break, due to phosphor decay at 2.5 MHz.

The aging due to phosphor-loading is 100 times better than P16, with light reduction less than 10%, after 10 coulombs/cm² for LP 202, and light reduction of 50% at 0.1 coulombs/cm² for P16.

The "S-gun" is a high-resolution gun, capable of delivering 20 ua into a 1.5-mil spot. The resolution of the spot in 32 lp/mm limiting, with a gaussian distribution.

Linearity Circuits. The Linearity circuits have a bandpass of over 1 MHz, and a capability of achieving better than 1% linearity over the tube face. The tube has only a 24° total deflection angle, which will aid in achieving high linearity. On this basis, the scanner will not introduce any appreciable distortion into the background image.

Remaining Circuits. The remaining circuits (power supplies, protection circuitry, dynamic focus, blanking circuits, and centering circuits) are well-known in the state of the art and will not be described during the analysis.

Wave Pattern Film Transparency. The wave pattern film will be a 9" x 9" plate mounted in the flying spot scanner lens focal plane. Two plates will be furnished, one representing a sea state of two, and the other a sea state of three. (Code 2 and 3). A description of these sea states are contained in table 15.

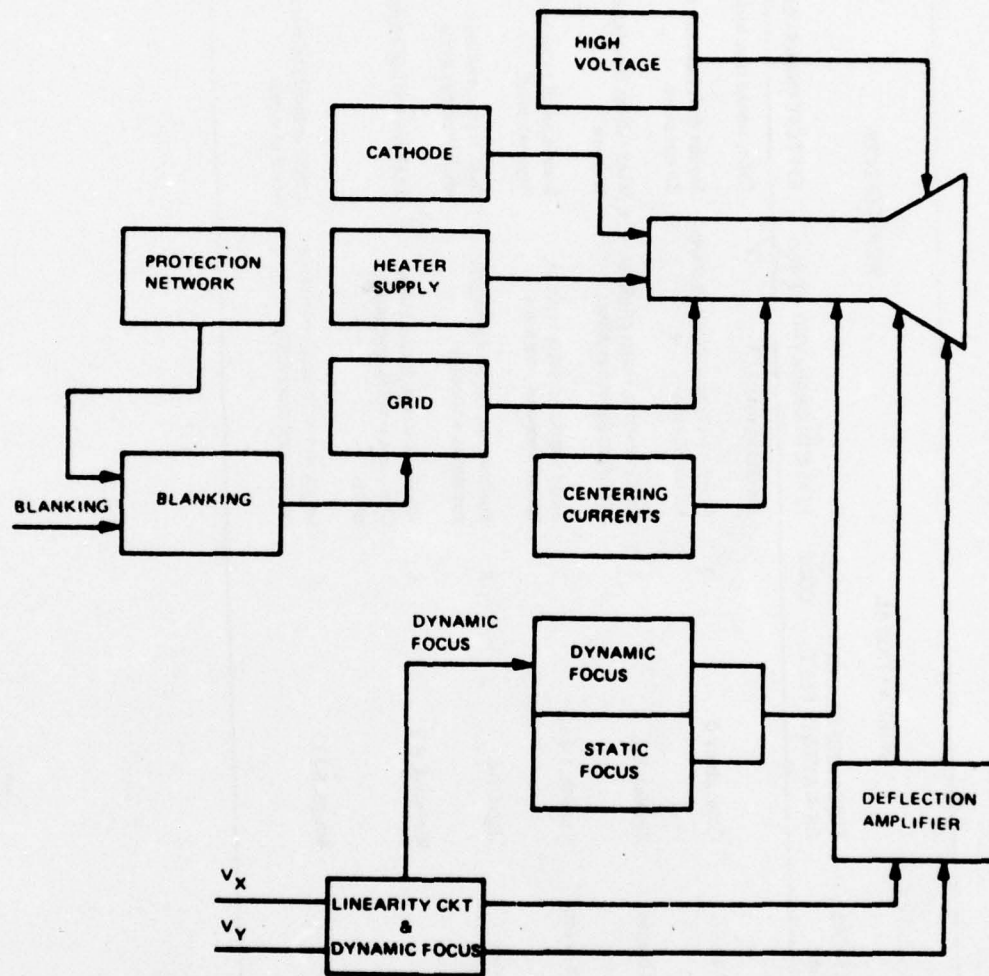


Figure 54. FLYING SPOT SCANNER SYSTEM

Table 15. STATE OF SEA DESCRIPTION

MODERN BEAUFORT SCALE			INTERNATIONAL		WIND EFFECTS	
BEAUFORT NUMBER	WIND KNOTS	NAUTICAL TERM	FORM AND HEIGHT OF WAVES IN FEET	CODE	EFFECTS OBSERVED AT SEA	EFFECTS OBSERVED ON LAND
0	under 1	Calm			Sea like mirror.	Calm; smoke rises vertically
1	1-3	Light air	Calm, glassy 0	0	Ripples with appearance of scales; no foam crests.	Smoke drift indicates wind direction; vanes do not move.
2	4-6	Light breeze	Rippled, 0-1	1	Small wavelets; crests of glassy appearance, not breaking.	Wind felt on face; leaves rustle; vanes begin to move.
3	7-10	Gentle breeze	Smooth, 1-2	2	Large wavelets; crests begin to break; scattered whitecaps.	Leaves, small twigs in constant motion; light flags extended.
4	11-16	Moderate breeze	Slight, 2-4	3	Small waves, becoming longer; numerous whitecaps.	Dust, leaves, and loose paper raised up; small branches move.
5	17-21	Fresh breeze	Moderate, 4-8	4	Moderate waves, taking longer form; many whitecaps; some spray.	Small trees in leaf begin to sway.
6	22-27	Strong breeze	Rough, 8-13	5	Larger waves forming; whitecaps everywhere; more spray.	Larger branches of trees in motion; whistling heard in wires.

Obviously, any desired sea state plate could be used, as long as a film plate could be obtained.

Investigations into sources indicated that two possible sources of film. One was the United States Department of Commerce Coast and Geodetic Survey, and the other was to contract an aerial survey to obtain the desired film.

Three cases were investigated for their feasibility. The three cases are:

- 1) Obtain the desired photograph directly on 9" x 9" film, representing the desired sea state over an effective 4250' x 4250', or 5000:1 scale. The photographs would be obtained from the U. S. Dept. of Commerce Coast and Geodetic Survey and would have the following characteristics:
 - a) Film Type: Anscochrome D 500 Resolution 100 lp/mm
 - b) Lens Resolution: 68 lp/mm
- 2) Obtain the desired film as in case 1), but at 10:000:1 scale, their normal photographic scale for coastlines. This would entail an enlargement of the negative, and would result in a 2:1 resolution loss.
- 3) Obtain a special film of the sea under a subcontract, Preliminary discussion with Simulation Systems Inc. Huntingdon Valley, Pa., who has had extensive experience in aerial photography, advise that a photograph taken on a 18" x 18" negative would have a resolution 60-70 lp/mm limiting, and when reduced to a 9" x 9" transparency would achieve over 100 lp/mm.

Analysis of the cascaded system through the 2:1 lens onto the CRT faceplate has indicated that very little difference appears in the resultant modulation transfer function curves (MTF), since the limiting item is the flying-spot-scanner spot size of 1.5 mil. Farther on in this section can be found greater detail on this analysis¹⁴. Therefore, effort will be made to obtain the film by the most cost-effective means.

The Coast and Geodetic Survey have been very cooperative, but they indicate that open sea shots are only incidental to coastal surveys, and are, therefore, not cataloged, but must be searched out. Thus, we are not positive at this time that a suitable photograph of the desired sea state, without any vessels visible, is obtainable from the coastal surveys.

The positive transparency used in the system will have enhanced contrast, obtained by special processing. The photograph would be of a continuous, grey scale, but the enhanced contrast, when combined with proper video processing, will have a range of grey levels representative of the open sea.

System Scaling. The proposed system will include imagery out to 10° from the horizon. Thus, the film plate can now be examined for the fixed altitude in relation to the wave scaling. The fixed altitude to be simulated calculated as follows:

$$h = r (\tan 10^\circ)$$

$$r = \frac{4250}{2} \times \frac{8}{9}$$

where lens $M = 2$
 usable CRT diameter = 4 inches
 $r \approx 1890$ ft.

$$\begin{array}{ll} \text{thus} & h = 1890 (\tan 10^\circ) \\ \text{or} & h = 333 \text{ ft.} \end{array}$$

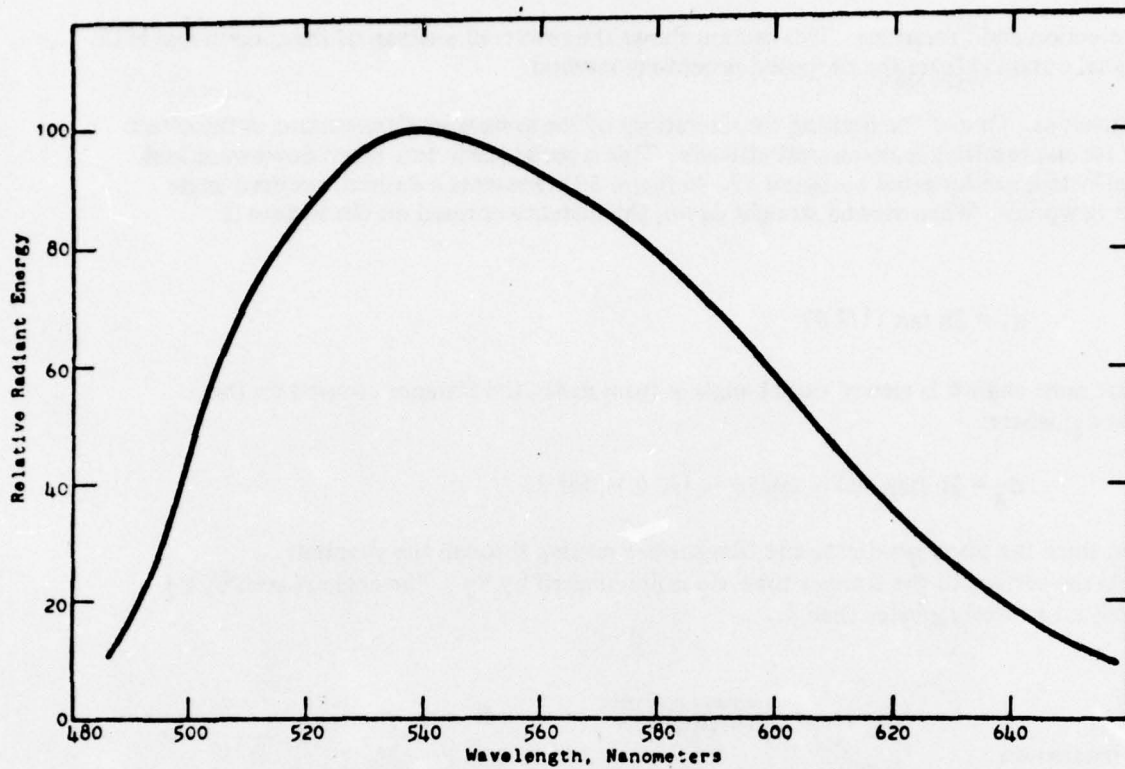
Thus the visual presentation will represent a fixed altitude of 316 ft to the pilot's eye.

Background Optics. The imaging lens will be essentially a scaled version of a Singer-designed lens used in a previous program designated as EPT. This lens has an almost immeasurable distortion and adequate speed, and when combined with the collecting optics, they produce an adequate signal at the photomultiplier to minimize the noise problem. The original EPT lens was designed for a 3.59:1 conjugate ratio. For the AWAVS application, the proposed ratio is 2:1. The proposed FSS uses an LP 202 phosphor which peaks at a wave length of approximately 540 nanometers. Figure 55 illustrates the spectral content of LP 202, which is within the range of conventional achromatic lenses. No unusual spectral requirements or achromatic correction is required. The spectral range is within that normally used in conventional visual optical systems.

A search will be made of off-the-shelf lenses, to determine if any commercially-available lenses can meet the requirements for the AWAVS program.

Figure 60 illustrates the optical layout for the background image generator.

It should be noted that the optical components after the image plane, i.e., the collecting optics and the photomultiplier, bear no relationship to the resolution or MTF of the system, since they are imaged on the exit pupil of the image lens, and their only function is to collect the light as efficiently as possible.



TENTATIVE SPECTRAL ENERGY DISTRIBUTION FOR LP202 PHOSPHOR

Figure 55. TENTATIVE SPECTRAL ENERGY DISTRIBUTION FOR LP202 PHOSPHOR

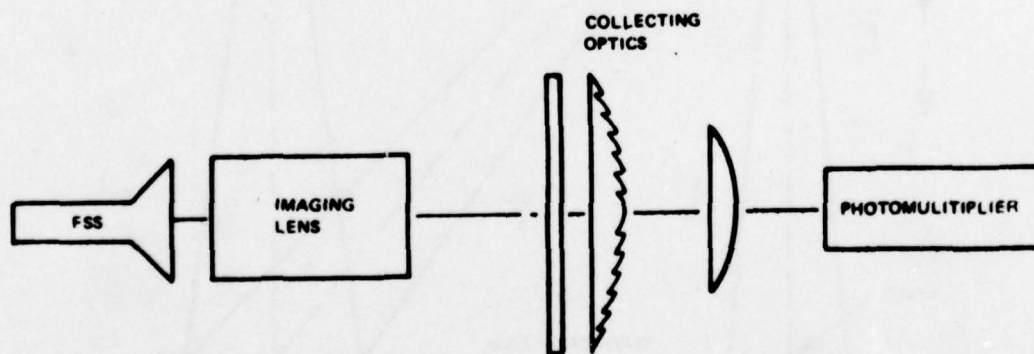


Figure 56. BACKGROUND OPTICS SCHEMATIC

Signal Detection and Processing. This section shows the results of analysis of the quality and MTF of the signal obtained from the proposed processing method.

Flight Envelope. One of the limiting considerations of the system implementation is the effect of raster format resulting from aircraft attitude. This is particularly true when downward look angle is effected, as illustrated by figure 57. In figure 57 represents a desired, resolved angle from the viewpoint. When viewed straight down, the distance covered on the surface is d_1 , or:

$$d_1 = 2h \tan (1/2 \theta)$$

When that same angle θ is viewed out at angle ψ from nadir, the distance covered on the surface is d_2 , where:

$$d_2 = 2h (\tan (\psi) - \tan (\psi - 1/2 \theta)), \text{ for } \theta.$$

However, since the plane parallel to the film surface passing through the eyepoint represents the surface of the scanner tube, d_2 is illuminated by P_2 . The angle as seen by P_2 is θ' , which is obviously greater than θ .

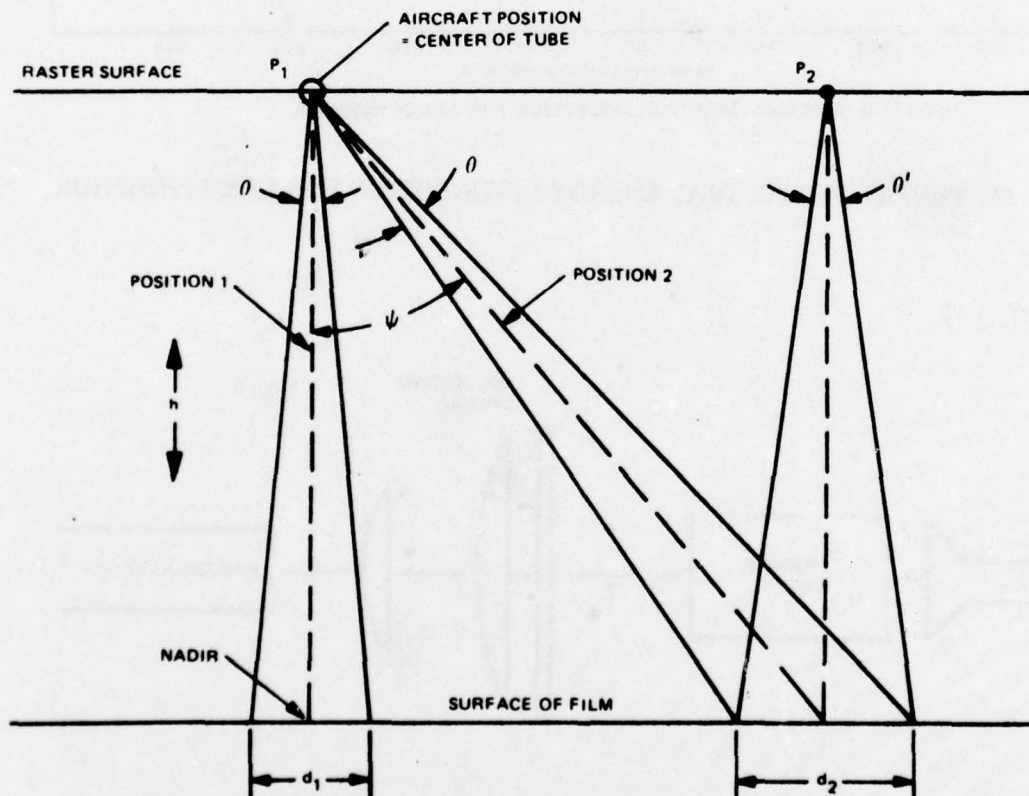


Figure 57. SCANNER RECTIFICATION

It follows that resolution capability of the scanner system is reduced as the look angle approaches the nadir. Figure 58 is a plot illustrating resolution improvement compared with nadir requirements, as the angle increases from nadir.

In order to properly define the image quality that will be generated by the background image generator, the flight pattern followed by NATOPS, NAVAIR 01-245FDD-1 will be used as bases. The points analysed will take worst case excursions in pitch and roll (heading does not effect the resolution on MTF of the system), and choose those area which are poorest in resolution. In addition to the points covered in NATOPS analysis, two additional points are covered, namely, straight ahead and 90° roll.

The system will be capable of any attitude desired, since restricting to flight envelope would not be tolerable. However, under severe attitude changes, such as 90° pitch down, degradation of the system may be expected. The -90° pitch down condition is also analysed to determined the MTF that will be generated.

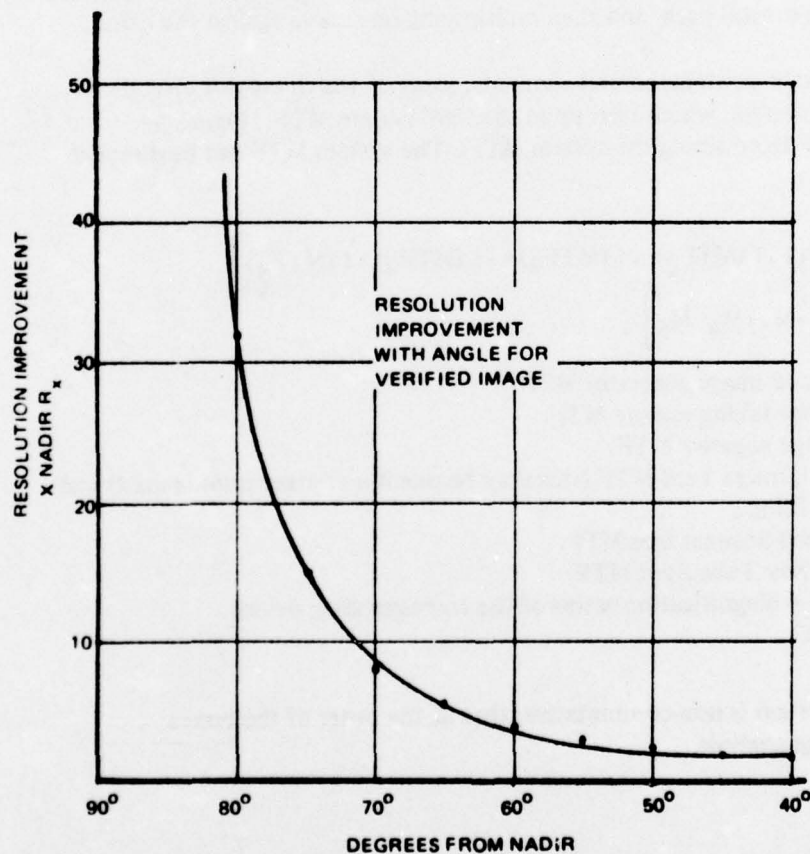


Figure 58. RESOLUTION IMPROVEMENT/NADIR REQUIREMENTS COMPARISON

The following data summarizes the NATOPS manual of flight and the points of interest in the attitude formulations:

- 1) Roll: Maximum Roll: $\pm 60^\circ$ at an altitude between 600 ft. to 800 ft.
 $\pm 30^\circ$ roll at an altitude between 450 ft. and 600 ft. $\pm 10^\circ$
 below 400 ft.
- 2) Pitch: Maximum pitch down: 15° between 600 and 1000 ft. altitude.
 5° between 300 and 600 ft. 0° below 300 ft.

No pitch down exceeding 5° during the 30 or 60° roll.

Take off: $+12^\circ$ to 300 ft.

- 3) Yaw: Unlimited.

Background Image Generator Modulation Transfer Function. The modulation transfer function (MTF) of the background image generator can be determined by obtaining the transfer function of each of the modules in the optical path, and then multiplying one curve against the other.

The background image generator contains several elements, some of which are not directly associated with the delivered system, which bear upon the final system MTF. Figure 59 illustrates the system flow for determining the system MTF. The system MTF can be directed as follows:

$$f(\text{MTF}_B) = \left[f(\text{MTF}_1) \cdot f(\text{MTF}_2) \cdot f(\text{MTF}_3) \cdot f(\text{MTF}_4) \cdot f(\text{MTF}_5) \right] \\ \left[M_1 \cdot M_2 \cdot M_3 \cdot M_4 \cdot M_5 \right];$$

where: $f(\text{MTF}_B)$ = Background image generator MTF.
 $f(\text{MTF}_1)$ = Wave image taking camera MTF.
 $f(\text{MTF}_2)$ = Wave image negative MTF.
 $f(\text{MTF}_3)$ = Process Camera Lens MTF (this may be one if a contact print is used) and Process Film.
 $f(\text{MTF}_4)$ = Flying-Spot-Scanner lens MTF.
 $f(\text{MTF}_5)$ = Cathode Ray Tube Spot MTF.
 M_1, M_2, M_3, M_4, M_5 = Magnification ratios of the corresponding device which effect the scale.

It should be noted that the system is non-commutative; that is, the order of the boxes can not be interchanged during analysis.

Image Film Transfer Function. The films being examined during the analysis assumed the following three cases ¹⁵.

Case 1) directly on 9" x 9" plate from 9" x 9" film, using contact method:

$f(MTF_1)$: limiting resolution 68 lp/mm, assume straight, line function.

$f(MTF_2)$: film type Anscochrome D500 resolution, 100 lp/mm.

$M1 = M2 = 1.0$.

$f(MTF_3) = 1$ [contact print; Kodalith Film MTF > 200 lp/mm.

Case 2) same as case 1, but $M = 0.5$: $f(MTF_3) = 1$.

Case 3) derived from information supplied by Simulation Systems Inc., Huntington Valley, Pa:

$f(MTF_1) f(MTF_2) f(MTF_3) = 60$ lp/mm limiting, straight line approximation:

$M = 2X$.

Figure 61 illustrates the cascaded results of:

$$f(MTF) = (M_1 M_2 M_3) f(MTF_1) f(MTF_2) f(MTF_3)$$

Flying-Spot-Scanner Lens (MTF_4). A possible lens that may be used (even though the f number is $F/3.0$, and the spectral transmission of the lens must be analyzed is a lens produced by Pacific Optical, their model 34489. The MTF points given on for this lens are as follows:

$M = 2X$.

8 lp/mm - 85%

12 lp/mm - 70%

85 lp/mm - limiting.

These points are referenced to the film plane. The resultant curve (MTF_3) is also illustrated in figure 60.

The compound MTF curve, relative to the flying-spot-scanner faceplate, is illustrated in figure 61 for the three film cases.

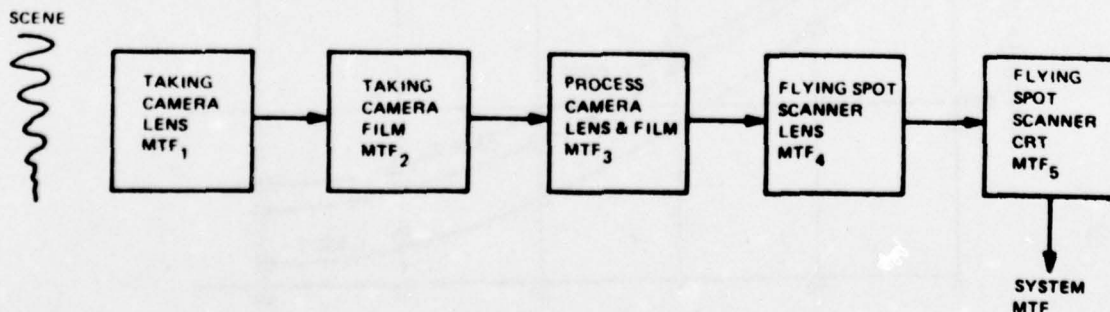


Figure 59. BACKGROUND IMAGE GENERATOR MODULATION TRANSFER FUNCTION FLOW DIAGRAM

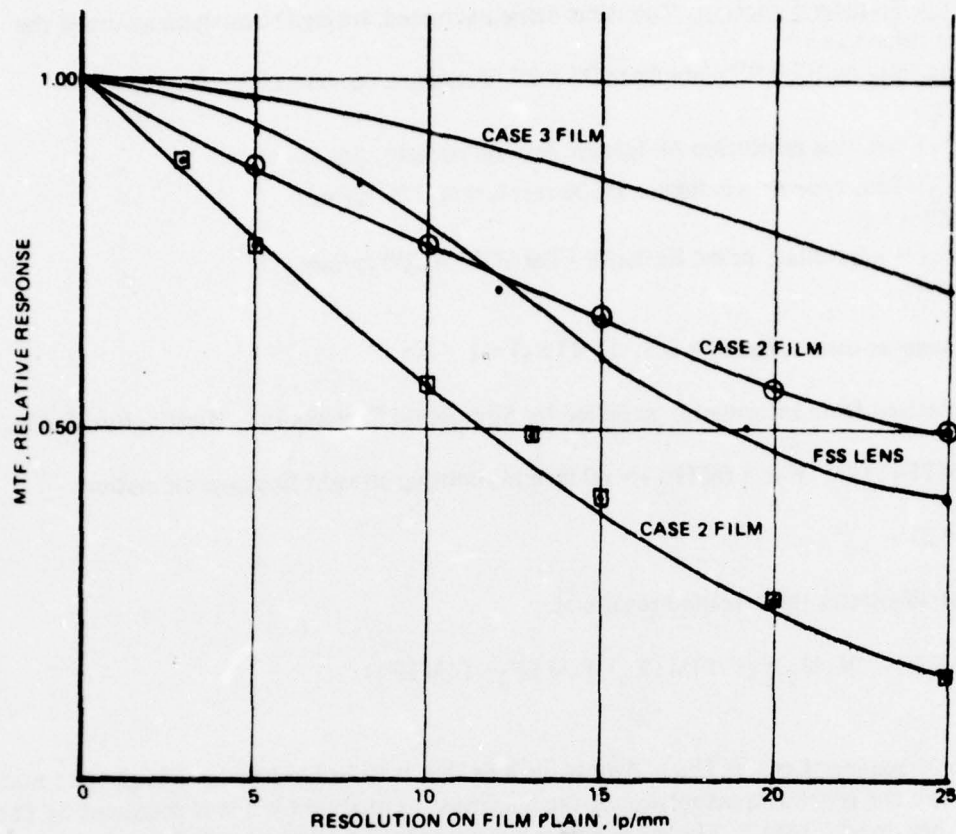


Figure 60. CASCADED RESULTS OF F(MTF) EQUATION

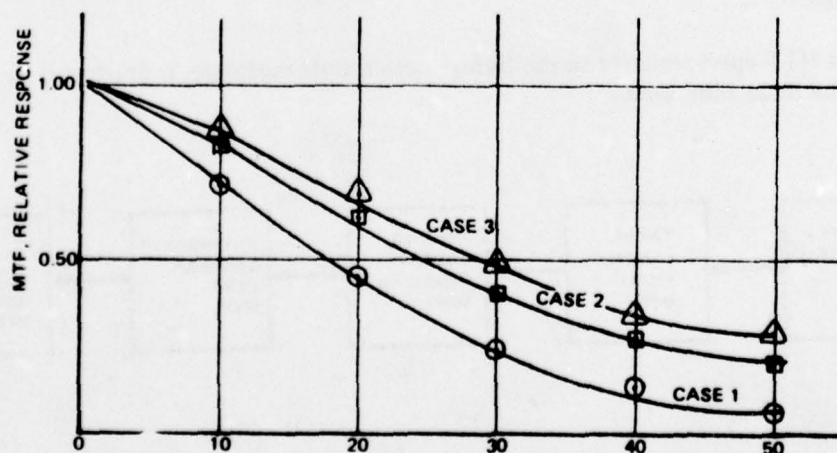


Figure 61. RESOLUTION ON CRT FACE OF FILM

Cathode Ray Tube (MTF_s). The cathode ray tube spot of 1.5 mil. has a Gaussian intensity distribution. The limiting resolution is 32 lp/mm, and the curve is shown in figure 62.

Photomultiplier and Collecting Optics. Since the purpose of these items are to collect the light that passes through the image plane, the collecting optics are focused on the exit pupil to the imaging optics. Thus the MTF of the collecting optics do not affect the system optical transfer function, or: $MTF_{CO} = 1.00$.

The photomultiplier likewise does not affect the optical transfer function, since the light received is the image of the EXIT pupil of the imaging lens, or constant diameter, chosen to optimize the working surface of the photomultiplier. The purpose of the photomultiplier is to transfer the image from the optical frame of reference to the temporal frame of reference. It is well within the state of the art to construct 20-MHz, photomultiplier systems, using low-capacitance photomultipliers. Systems well in excess of 20 MHz have been constructed for photon counting, in certain application. Thus, the photomultiplier MTF, MTF_p is set at unity, and is not further considered.

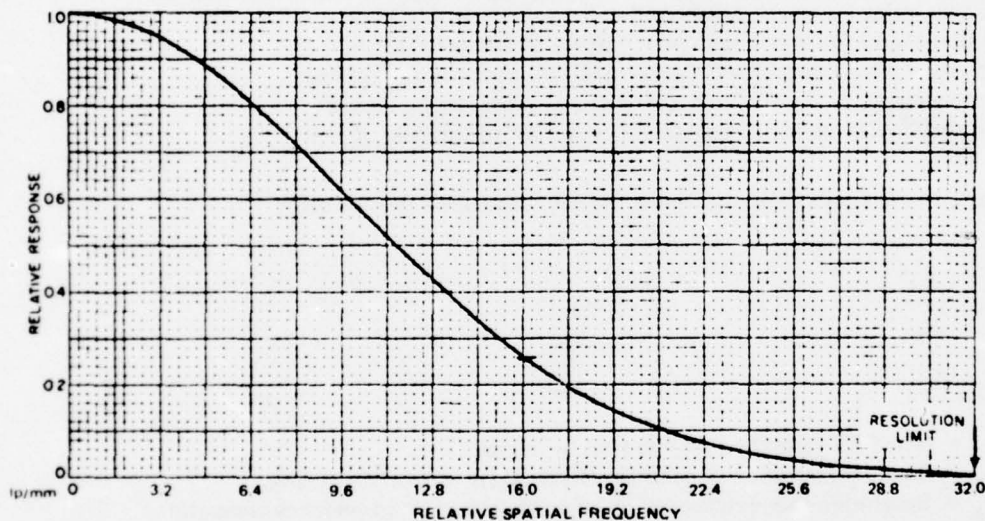


Figure 62. MODULATION TRANSFER FUNCTION OF CATHODE RAY TUBE SPOT

System Modulation Transfer Function - MTF_B. Figure 63 gives the background image generator MTF curves for three cases with different films. It is of interest to note that the final resultant depends primarily on the flying-spot-scanner CRT spot size, and that the results of the three films are almost identical. Selection of the film to be used will be based on availability and economics.

BIG System Visual Resolution. The required system resolution in the display center is 15 arc-min, and 30 arc-min elsewhere. Normal television practice holds that the requirement for center resolution holds for, 80% of the raster height. Figure 68 shows the area of concern. Thus to determine the system resolution, we must examine the edge of the circle of $r = 32^\circ$ to determine the worst case MTF for the center resolution requirements of 15 arc-min, and examine the remaining portion of the system for MTF relative to 30 arc-min resolution. The basic approach is as follows:

- 1) Determine the required resolution at nadir on the film image from the CRT face for 30 arc-min and 15 arc-min. Nadir is the most demanding area, assuming $h = 333$ ft. $r = 1890$ ft¹⁶.
- 2) Determine the angle from nadir for the worst case for 30 arc-min and 15 arc-min, using the envelope of flight indicated¹⁷. It should be noted that the 15 arc-min area shown in figure 68 lies such that it would take a pitch down of 68° for the nadir to reach the edge of the 15 arc-min circle, or at a 90° roll, a pitch down (down being toward nadir) of 60° . The center of the raster lies at $+10^\circ$ in the field of view.
- 3) Use the curve in figure 58 to determine the CRT resolution requirement:

$$R_c = \frac{R_n}{R_x}$$

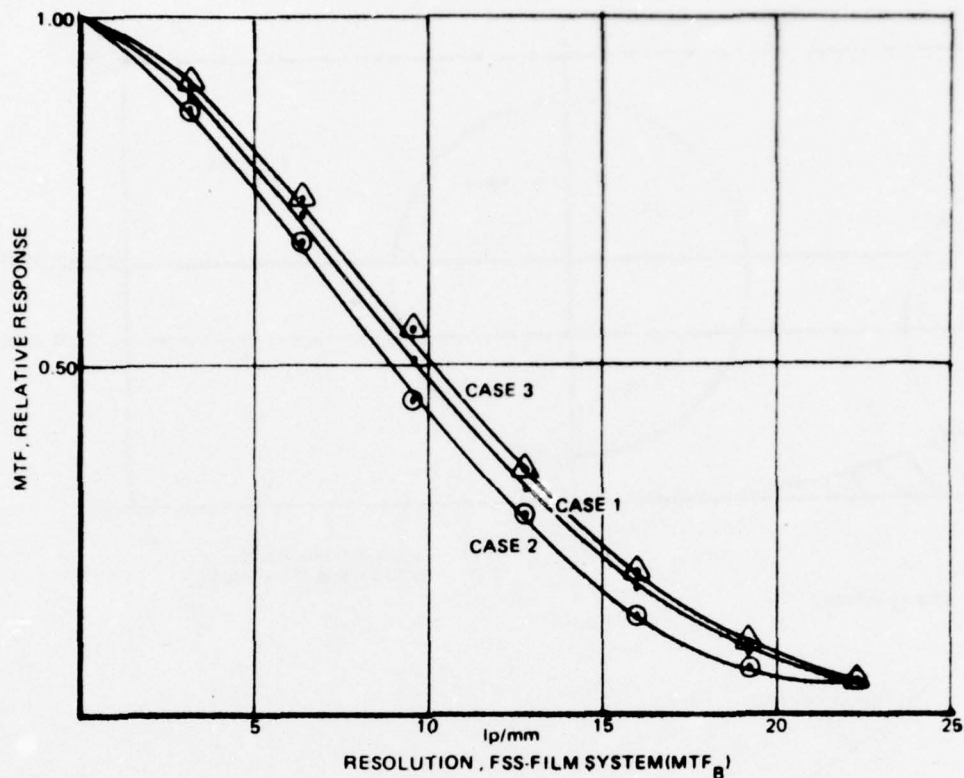
where:

- R_c = New CRT resolution requirement in lp/mm.
 R_n = Required resolution at nadir for either 30 arc-min or 15 arc-min.
 R_x = Resolution gain determined by angle of view of point under consideration and figure 58.

- 4) Using figure 63, determine modulation of the point in question.

Now we know all that is necessary to determine system resolution at various points of the display, under various modes of operation:

- 1) required resolution at nadir:
 - a) r of tube = 2.000 in.
 r of film = 1890 ft.
 Thus, $\frac{2.000}{1890} = \text{in./ft.} = 0.00106 \text{ in./ft.}$

Figure 63. RESOLUTION' FSS FILM SYSTEM (MTF_B)

b) $h = 333$ ft.

Desired angular subtense = 15 arc-min.

Thus, one element - $2 [333 \tan (\frac{1}{2} 15 \text{ arc-min})] = 1.45$ ft. on surface of water.

Converting to the CRT face: ,

CRT faceplate distance = $(1.45 \text{ ft./element}) (1.06 \text{ mil/ft.}) = 1.54 \text{ mil/element}$.

Converting to millimeters:

$$\frac{39.4 \text{ mil/min}}{1.46 \text{ mil/element}} = 25.58 \text{ elements/mm.}$$

Thus since the center resolution = 15 arc-min resolution we have:

$$R_{n15} \cong 26 \text{ lp/mm;}$$

and

$$R_{n30} \approx 13 \text{ lp/mm on CRT face.}$$

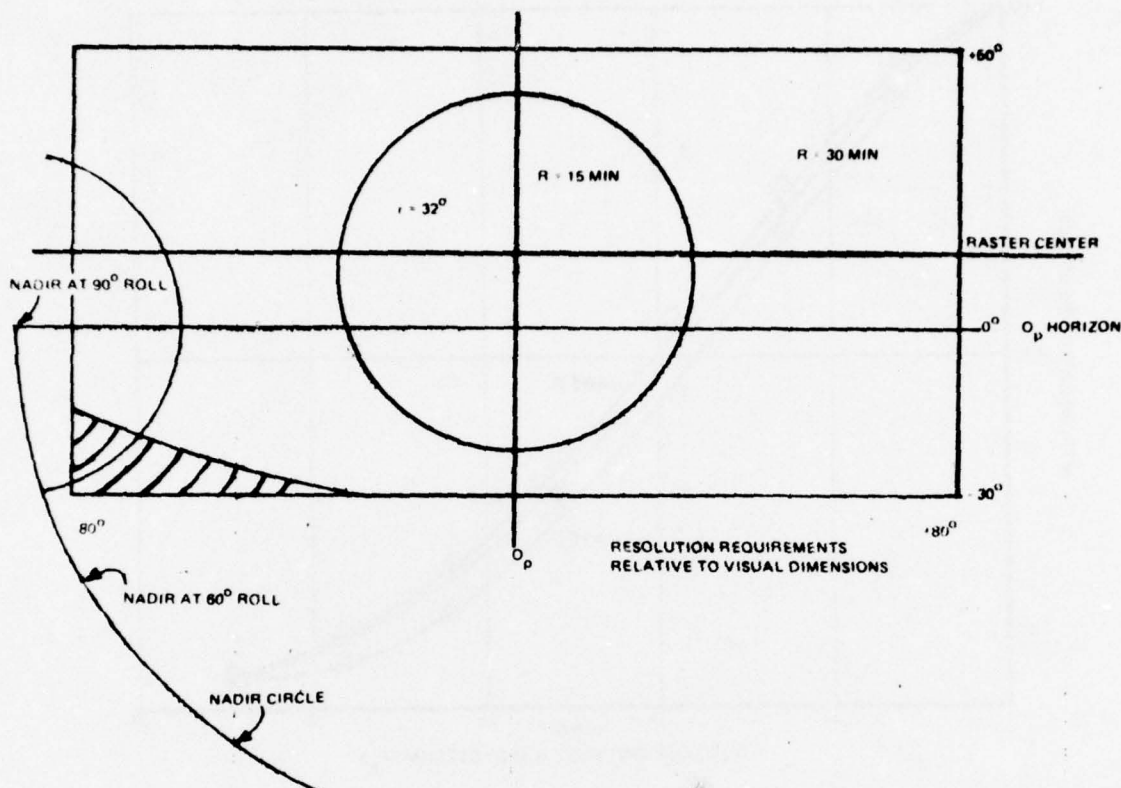


Figure 64. RESOLUTION REQUIREMENTS RELATIVE TO VISUAL DIMENSIONS

- 2) Flight attitude resolution (worst case for each attitude, within the 32° circle for 15 arc-min, and remaining scene for 30 arc-min):
 - a) Aircraft attitude = straight ahead:
 - (1) Referring to figure 64, the greatest angle of depression occurs at -22° from horizon look angle for the 15 arc-min requirement. Referring to figure 58, $R_x = 7$, for 68° from nadir.

Thus:

$$R_x = 7, \text{ for } 68^\circ \text{ from nadir.}$$

thus:

$$R_c = \frac{R_n}{R_x}; \text{ or,}$$

$$(1) \quad R_{c15} = \frac{26}{7} = 3.7 \text{ lp/mm, on CRT.}$$

Refer to figure 63, the MTF at 4 lp/mm exceeds 80% for all film cases.

- (2) Referring to figure 64 again, the greatest visual down angle is -30°
From figure 58, $R_x = 4$.

Thus:

$$R_{c30} = \frac{13}{4} \approx 3.3 \text{ lp/mm.}$$

Which is less than 4 lp/mm, thus assuring an MTF of greater than 80%.

- b) Aircraft attitude = pitch down -15°

- (1) The new angle of depression for the 15 arc-min circle is $22 + 15 = 37^\circ$
from horizon, or 53° from nadir.
From figure 58, $R_x = 2.8$.

$$\text{Thus: } R_{c15} = \frac{26}{2.8} = 9.3 \text{ lp/mm.}$$

From figure 63, the MTF_{15} at 9.3 lp/mm

Case 1 (film 1) $\cong 50\%$

Case 2 (film 2) $\cong 45\%$

Case 3 (film 3) $\cong 53\%$

- (2) 30 arc-min: $30^\circ + 15^\circ = 45^\circ$ down

$$R_x = 2,$$

$$\text{or: } R_{c30} = \frac{13}{2} = 6.5 \text{ lp/mm.}$$

Thus for figure 63:

$$MTF_{30} \cong 65\% \text{ for all cases}$$

- c) Aircraft attitude = Roll 90° :

- (1) Under roll of $\pm 90^\circ$, with no pitch, the worst the 15 arc-min can reach down
towards the nadir from nadir. Thus for figure 58 $R_x = 3.5$;
or $R_{c15} = \frac{26}{3.5} \cong 7.4 \text{ lp/mm.}$

at 7.7 lp/mm, the MTF_{15} is:

$$\text{Case 1 - } MTF_{15} \cong 63\%$$

$$\text{Case 2 - } MTF_{15} \cong 60\%$$

$$\text{Case 3 - } MTF_{15} \cong 66\%$$

Therefore, the center MTF at 15 min will always be 60% or better at any roll not exceeding 90° .

- (2) During a 90° roll the edge of the visual scene is within 10° of nadir. At this point, the factor $R_x = 1$. Thus at worst case,

$$R_{c30} = 13 \text{ lp/mm}$$

we have (from figure 63:

$$\text{Case 1 - } MTF_{30} \cong 30\%.$$

$$\text{Case 2 - } MTF_{30} \cong 25\%.$$

$$\text{Case 3 - } MTF_{30} \cong 32\%.$$

It should be noted that this is the worst case analysis for 30 arc-min under any condition. The circle around the nadir, wherein $R_x \cong 1$ is a radius of 30° , thus reaching 60° down from the horizon. Below 60° look down, $R_x \cong 1$.

Figure 65 illustrates the MTF curves for each of the points analysed.

- d) Pitch down -90° center resolution, same as nadir at 30° or at center, $MTF_{30} = 25\%$, case 2.

The following data summarize the results of the MTF discussion of the BIG:

- 1) Level Flight, Pitch = and Roll = 0

$$\begin{aligned} MTF_{15} &\geq 80\% \text{ all cases} \\ MTF_{30} &\geq 80\% \text{ all areas} \end{aligned}$$

- 2) 15° Pitch down, Roll = 0

$$\begin{aligned} \text{Lower edge of circle } MTF_{15} &\geq 45\% \text{ for all cases} \\ \text{Lower edge at raster } MTF_{30} &\geq 65\% \text{ for all cases} \end{aligned}$$

- 3) Roll $\pm 90^\circ$, no pitch down

$$\begin{aligned} MTF_{15} &\geq 60\% \text{ all cases} \\ \text{Outside } 30^\circ \text{ circle } MTF_{30} &= 30\% \text{ case 1 film} \\ \text{centered on nadir} &= 25\% \text{ case 2 film} \\ &= 32\% \text{ case 3 film} \end{aligned}$$

- 4) Pitch -90° , center $MTF = 25\%$ @ 30 min, case 2

Note that these results are only for a specific location on the screen, and is the worst case for that particular aircraft attitude. Figure 65 illustrates the MTF curves for each of the points analyzed. These curves give the MTF function of the worst-case points inside the 32° resolution circle (RC_{30}), using the specified attitudes.

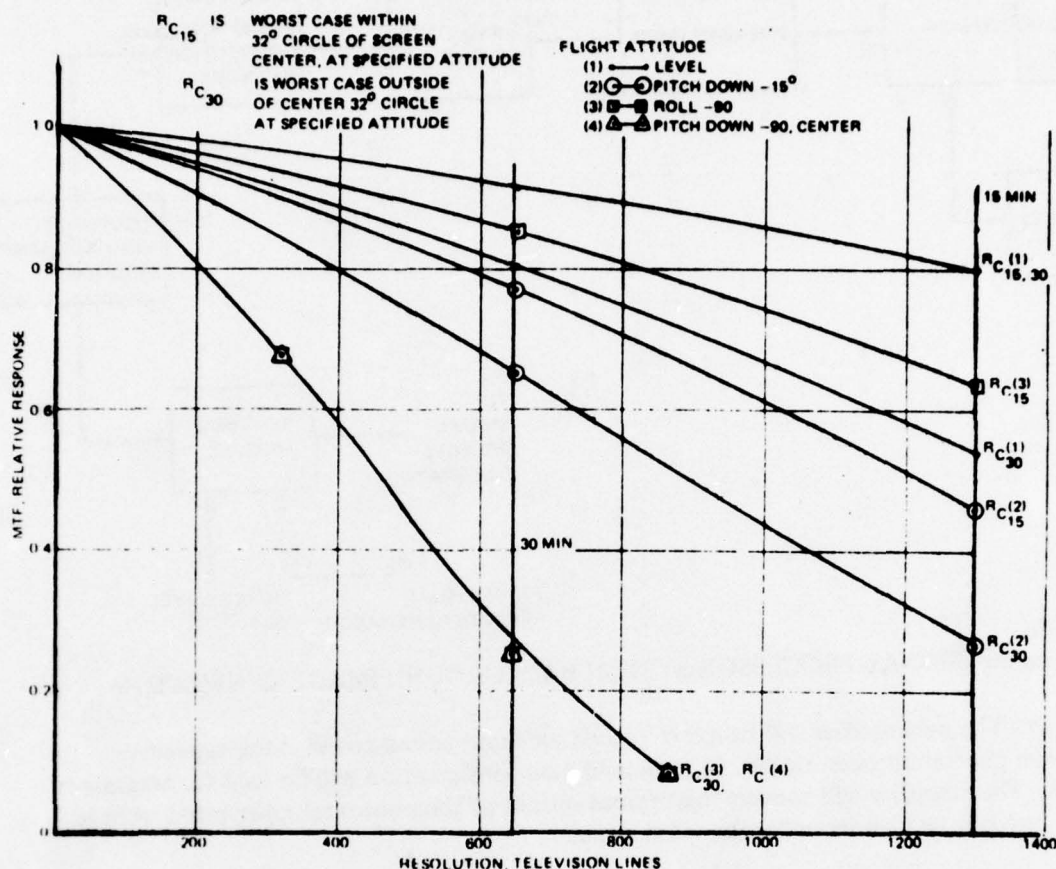


Figure 65. BACKGROUND IMAGE GENERATOR SYSTEM RESOLUTION VS. MTF

Video Signal Processing. Figure 66 is a flow diagram of the background image generator signal processor.

Photomultiplier. The photomultiplier will be a low-capacitance unit, so as to minimize capacitive loading. The incident light will be unusually high, and the tube linearity, under these conditions, will be an area under observation during tube selection.

Since the lens for the flying-spot-scanner has not been chosen at this point, the final signal-to-noise, out of the photomultiplier, has not been calculated. The calculation will be done as soon as a final lens is decided upon.

The preliminary analysis of the system SNR, based upon a similar system which had a 7.5 MHz bandwidth, indicates that the expected SNR over the 20-MHz, before boost, is 36 db, based upon the f/3 lens used in the MTF calculation. The calculation is based upon the standard television of SNR, peak-to-peak signal-to-(rms) noise.

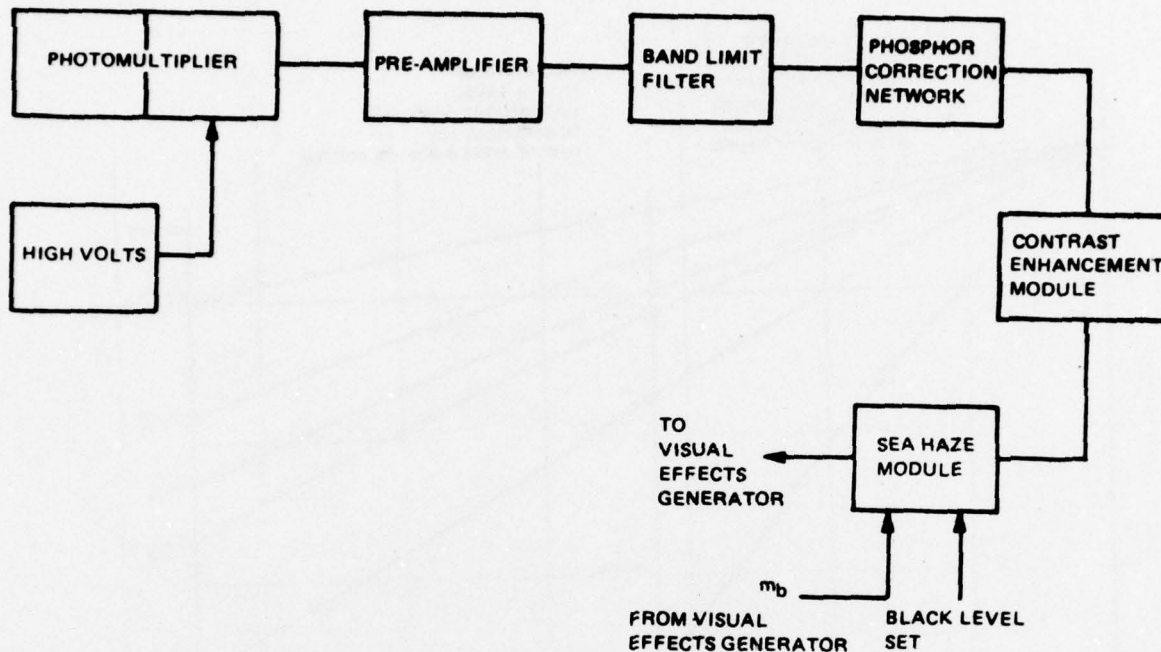


Figure 66. SIGNAL PROCESSOR SYSTEM BACKGROUND IMAGE GENERATOR

Preamplifier. The preamplifier will be a low-impedance input circuit to avoid the capacitive effects of the photomultiplier output. A grounded base configuration will be used for maximum bandwidth. The amplifier will convert this current output of the photomultiplier into a voltage signal and provide the line-driver for the video signal.

Band Limiting Filter. A 5-pole linear phase Thompson filter will be used to limit the noise content of the video bandwidth. The 3-db point will be set at 20 MHz. The linear-phase filter has been chosen over other filter types to provide a truly linear phase network, which prevents unwanted edge effects.

Phosphor Correction Network. The phosphor decay of the Litton LP 202 phosphor is a natural period that acts like a band limiting filter on the optical information in the horizontal direction. The decay period of the phosphor is approximately 130 ns. The equation for the primary correction point is:

$$\text{Fall time} = 0.32 \frac{1}{f} ;$$

or,

$$f = \frac{0.32}{\text{fall time}} ;$$

or,

$$f = \frac{0.32}{130 \times 10^{-9}} = 2.5 \text{ MHz.}$$

Thus, the primary peaking break will occur at 2.5 MHz.

The decay period is a natural phenomenon of the material which comprise the phosphor, and therefore, is not a highly-repeatable occurrence. A variable network will be used in the phosphor correction circuit. Since the expected bandwidth will be 20 MHz, the need of additional breaks will be examined and implemented as needed. It has been found through experience that a single 6-db octave boost, at 2.5 MHz, will extend the optical bandwidth beyond 10 MHz; but we can not tell at this time beyond 10 MHz what additional correction (if any) is needed to achieve 20 MHz.

One of the unfortunate results of the phosphor peaking is an increase in system noise, and a corresponding loss of signal-to-noise ratio. This loss is because the optical information loss is due to the natural optical filter of the phosphor, but the noise content is flat across the photomultiplier output. Therefore, the noise will be on a rising slope, during the peaking process. Since the signal peaking will be at least 18 db to correct the optical filtering, the noise, based upon normal S. N. R. calculations, is expected to increase by approximately 9 db, but the result is a marked increase in high-frequency noise. The decrease in SNR must be figured into the final SNR analysis, at that time. Based on the preliminary analysis, using an f/3 lens, the SNR after boost will be 27 db¹⁸. The peaking will be such that 100% video modulation is achieved for 100% modulated signal source.

The ability to achieve a 20-MHz signal with 100% usable video content is not known at this time. The bandwidth of 20 MHz represents approximately twice the boost capability than we have previously done. The system is a black and white system, and therefore, more light is available than before (increasing SNR), thus creating the necessity to boost to almost 10 times the original, which carries with it many areas of concern. The risk is considered reasonably low; but the risk increases rapidly with any further bandwidth boost.

Phosphor noise (i.e., the noise associated with phosphor thickness, etc.) is expected to be very low because of the extremely fine grain of the phosphor.

Effects of Contrast Enhancement of Film. Contrast enhancement of the wave image will be used¹⁹. The contrast enhancement has the advantage of increasing the signal content with respect to the signal noise. Thus, if the signal content normally has a range of 20% of the video content, and by contrast enhancement it could be increased to 80%, the respective signal-to-video content will have been increased by a factor of 4, or 12 db. The signal can then be compressed and added on a pedestal to recreate the desired signal with a 12-db increase in signal-to-noise ratio. Figure 67 illustrates the results, and also gives the block diagram for the enhancement system. A peak detector detects the presence of a white cap and injects a white pulse at that time to give the strong, visual indication of a white area in the sea.

Estimating about a 2-db SNR loss in the contrast reconstitution method, the expected SNR of the video into the visual effects generator will be $27-2 + 12 = 37$ db; or, $SNR_V = 37$ db, using an f/3 lens.

Sea Haze Module. The sea haze module will supply the effect of sea or sea haze from -10° below the horizon to the horizon. The circuit is similar to the circuit used in the background video effects generator, using the same m_p signal from the visual effects waveform generator. The circuit has been previously implemented in the F4-E No. 18 program Synthetic Terrain Generator (STG), where it proved highly-successful. The bandwidth was measured to be flat to beyond 30 MHz. A 75-ohm driver on the output will send the signal to the visual effects generator.

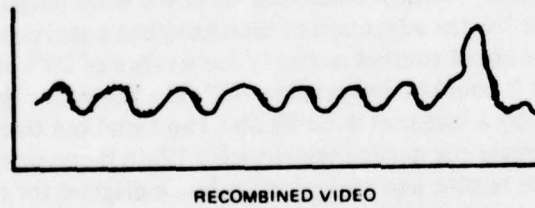
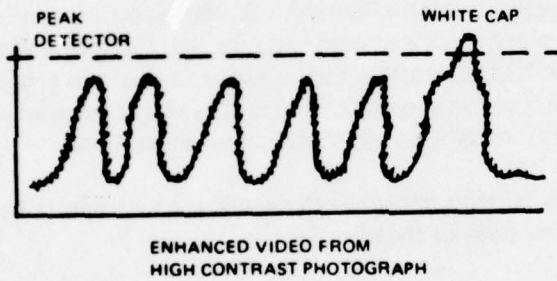
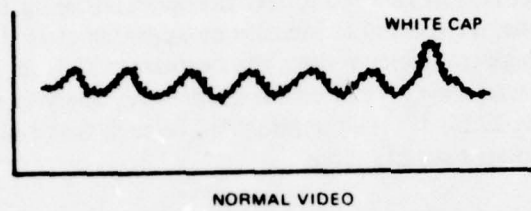
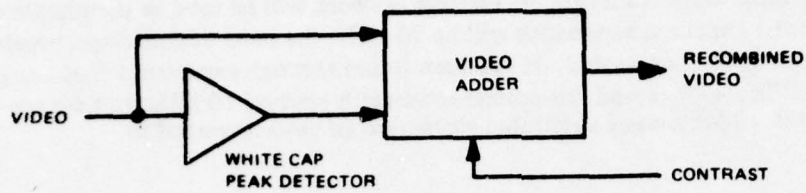


Figure 67. ENHANCED VIDEO EFFECTS

ALTERNATES.

The description and analysis methods used in this paragraph for alternates to the proposed flying-spot scanner system utilizes the analytical methods described ²⁰. Therefore, it is recommended that the reader become familiar with that paragraph before reading this one.

Altitude Cues. The proposed method of altitude cues makes use of several key analysis results. These are:

- 1) The Mission profile, including the aircraft attitude-altitude relationships ²¹. The system analysis will make use of these flight envelopes when describing and analyzing the system image quality.
- 2) For sea states 2 and 3, wave length or separation will be in the order of 21 feet. An analysis of the resolution capability was made to determine the resolvability of the 21-foot wave separation is a 15 arc-min system. The analysis used a separation of 25 feet, and then computed the limiting angle and distance from nadir in which the waves could be resolved. Beyond this angle, the sea will blend and become a homogenous scene, with very little detail present. Figure 68 illustrates the resultant curve, and is utilized in the alternate systems discussion.
- 3) The math model of the FSS raster computer, or DARC, notes that altitude functions only as a scaler of the raster plots ²². Thus, the raster plots shown in sheets 7 and 8 of figure 52 are the same as the plots in sheets 1 and 2 of the same figure, but scaled to one-half the size, or diameter.

Functional Analysis. The proposed method of altitude representation makes use of the same hardware that is used in the method analysed previously ²³. The hardware and the system consequences are listed below:

- 1) Film: One of three all 9 x 9 inches, representing 4250 ft. real world, using an 8" circle or 3780 ft ²⁴.
- 2) FSS 5" diameter, 4" usable face area, spot size of 0.0015 inches.
cathode
ray tube:

Note that previously the sea scene extending to 10° below the horizon, covering a diameter of 3780 ft, meant that the constant altitude would be set at 333 ft. ²⁵. All image quality discussion and MTF computations were made at the constant altitude of 333 ft. But in referring to figure 68, with an altitude of 333 ft., it is seen that beyond 77° or 1250 ft from nadir, no definition of the waves can be seen. This means that very little definition will appear more than 13° below the horizon.

A further examination of figure 68 shows that for a 3780 ft. diameter image, we could extend the altitude to almost 750 ft. and extend the sea haze to 21° below the horizon and retain the image information, but have the added realism of altitude cues. The raster on the scanners would become correspondingly larger, and therefore, capable of achieving even higher MTF's shown in the MTF analysis ²⁶.

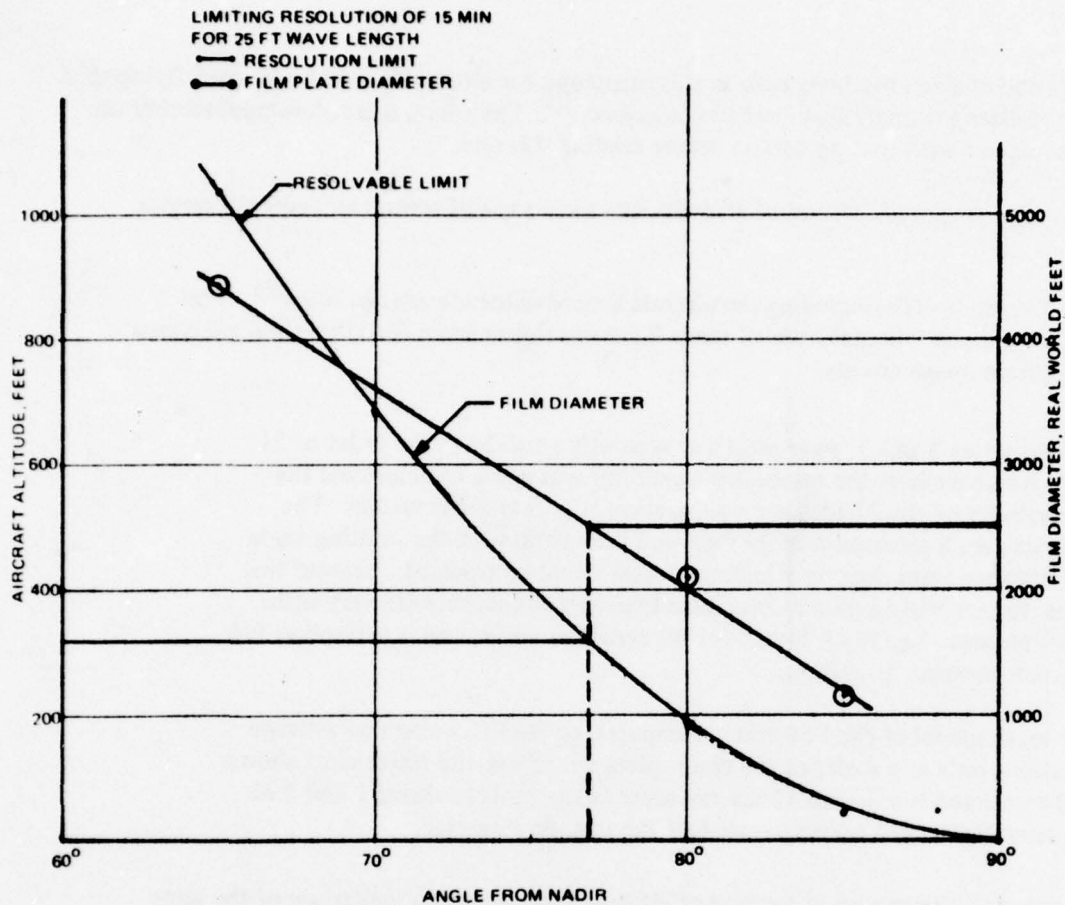


Figure 68. ANGLE FOR NADIR VS. AIRCRAFT ALT AND FILM DIAMETER. 25-FT. WAVES

For this option, it is proposed that no altitude variation be shown above 750 ft. Thus, until the aircraft has descended to an altitude of 333 ft or lower, the analysis, cited above, is met or exceeded. At 300-foot altitude, during landing, the aircraft is in the final approach. According to the flight profile, roll never exceed 10° and there is no down pitch because of the low speed.

At an altitude of 156 ft., the raster has reduced to approximately 1/2 in size, and the plate size allows a presentation out to 5° below horizon. At 156 ft., from figure 72, the visual angle is 9° below horizon for any detail at all at 15 arc-min, but the scanner will still show the 5° from horizon point at this time.

An MTF analysis at the nadir at this altitude reveals that:

- 1) A resolution of 54 lp/mm is needed at nadir.

$$R_{n15} = 54 \text{ lp/mm at this time;}$$

$$\text{and } R_{n30} = 27 \text{ lp/mm.}$$

- 2) An examination of the 0° pitch condition shows that:

$$R_c = \frac{R_n}{R_x}; \text{ and,}$$

$$R_{x15} = 7 \text{ from figure 58; or, } R_{c15} = \frac{54}{7} = 8 \text{ lp/mm; and,}$$

at 8 lp/mm, $MTF_{15-1} = 61\%$ at 15 arc-min, as shown in figure 63.

$$MTF_{215} = 58\% @ 15 \text{ arc-min.}$$

$$MTF_{315} = 64\% @ 15 \text{ arc-min.}$$

For 30 arc-min resolution, worst case:

$$R_{x30} = 4 \text{ at } -30^\circ.$$

Thus,

$$R_{c30} = \frac{27}{4} = 6.8 \text{ lp/mm;}$$

or,

$$MTF_{30} \cong 70\%.$$

- 3) If 5° pitch down were achieved, then the angle for 15 arc-min is $22 + 5 = 27^\circ$;
or,

$$R_{x15} \cong 5.$$

Thus:

$$R_{c15} = \frac{54}{5} \cong 11 \text{ lp/mm;}$$

$$MTF_{115} = 44\%;$$

$$MTF_{215} = 38\%;$$

$$MTF_{315} = 46\%;$$

$$\text{and, } R_{x10} = 2.7, R_{c30} = \frac{27}{2.7} = 10 \text{ lp/mm, } MTF_{30} = 50\%.$$

The 10° roll angle does not affect the system.

At an altitude of 100 ft, the new, required resolution is $\frac{316}{100} 27 = 83.7 \text{ lp/mm} = R_{n15}$ and $42 \text{ lp/mm} = R_{n30}$.

1) Straight and level flight:

$$R_{x15} = 7$$

$$R_{c15} = \frac{83.7}{7} = 11.9 \cong 12 \text{ lp/mm};$$

or,

$$\text{MTF}_{115} = 38\%;$$

$$\text{MTF}_{215} = 32\%;$$

$$\text{MTF}_{315} = 40\%;$$

and, for 30 arc-min:

$$R_{x30} = 4;$$

or,

$$R_{c30} = \frac{42}{4} = 10.5 \text{ lp/mm};$$

$$\text{MTF}_{130} = 47\%.$$

$$\text{MTF}_{230} = 41\%.$$

$$\text{MTF}_{330} = 49\%.$$

2) At an angle of attack of $+5^\circ$, the new angle from horizon, for 15 arc-min circle = $22.5^\circ = 17^\circ$; or, $R_{x15} = 12$; and for, 30 arc-min area, $30^\circ - 5^\circ = 25^\circ$; or, $R_{x30} = 5$.

Thus:

$$R_{c15} = \frac{83.7}{12} \cong 7 \text{ lp/mm}; \text{ and } \text{MTF}_{15} \cong 65\% \text{ for all cases.}$$

Thus:

$$R_{c30} = \frac{42}{5} \cong 8.5 \text{ lp/mm};$$

and,

$$\text{MTF}_{30} \cong 58\% \text{ for all cases.}$$

NAVTRAEQUIPCEN 75-C-0009 -1

At an altitude equal to 10 ft. over the flight deck, $h_e = 63 + 10 + 8 = 81$ ft., pitch = $+5^\circ$, or the altitude, when the aircraft passes over the edge of the carrier:

h_e = (height of flight deck over water) + (aircraft altitude) + (distance of eye height over wheels).

$$R_{n15} = \frac{316}{81} 27 = 104 \text{ lp/mm.}$$

$$R_{n30} = 52 \text{ lp/mm.}$$

$$R_{x15} = 12.$$

$$R_{x30} = 5.$$

Thus:

$$R_{c15} = \frac{104}{12} = 8.7 \text{ lp/mm; and, } MTF_{15} = 57\%; \text{ and, } R_{c30} = \frac{52}{5} = 10.4 \text{ lp/mm.}$$

$$MTF_{30} = 46\%.$$

Thus, the basic system proposed can be modified to meet the requirements for adding the limited altitude cues described in the previous paragraph ²⁷.

Figures 69, 70, and 71 illustrate the MTF curves at selected worst case points under the attitudes indicated, at 156 ft altitude, 100 ft altitude, and 81 ft altitude.

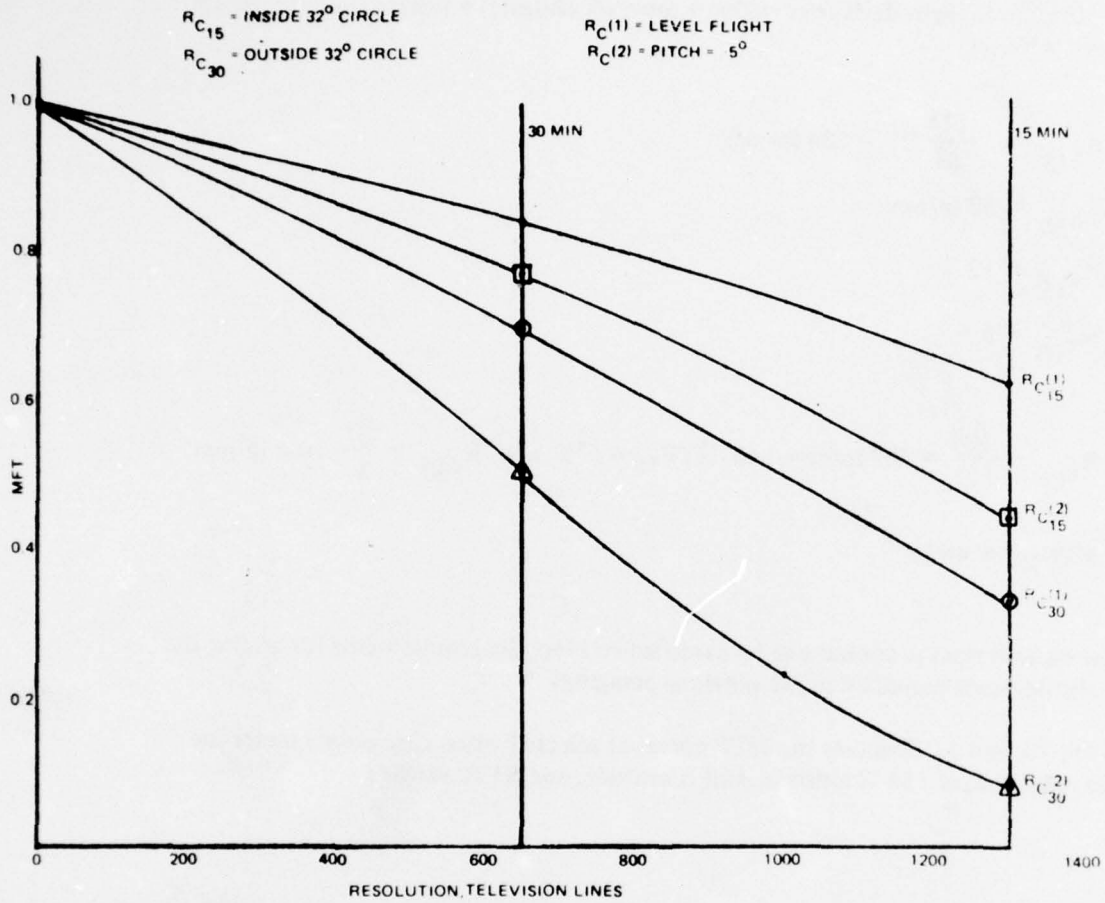


Figure 69. SYSTEM RESOLUTION VS. MTF, @ 156 FT.

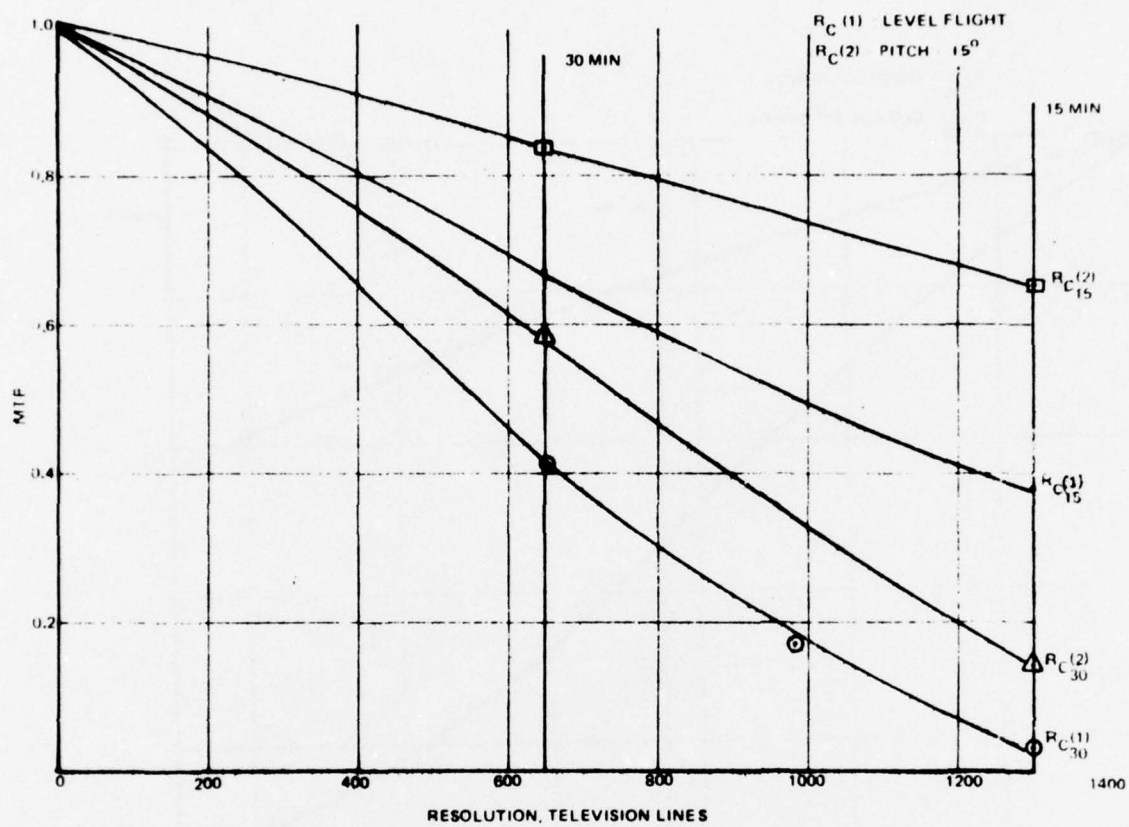


Figure 70. SYSTEM RESOLUTION VS. MTF, @ 100 FT.

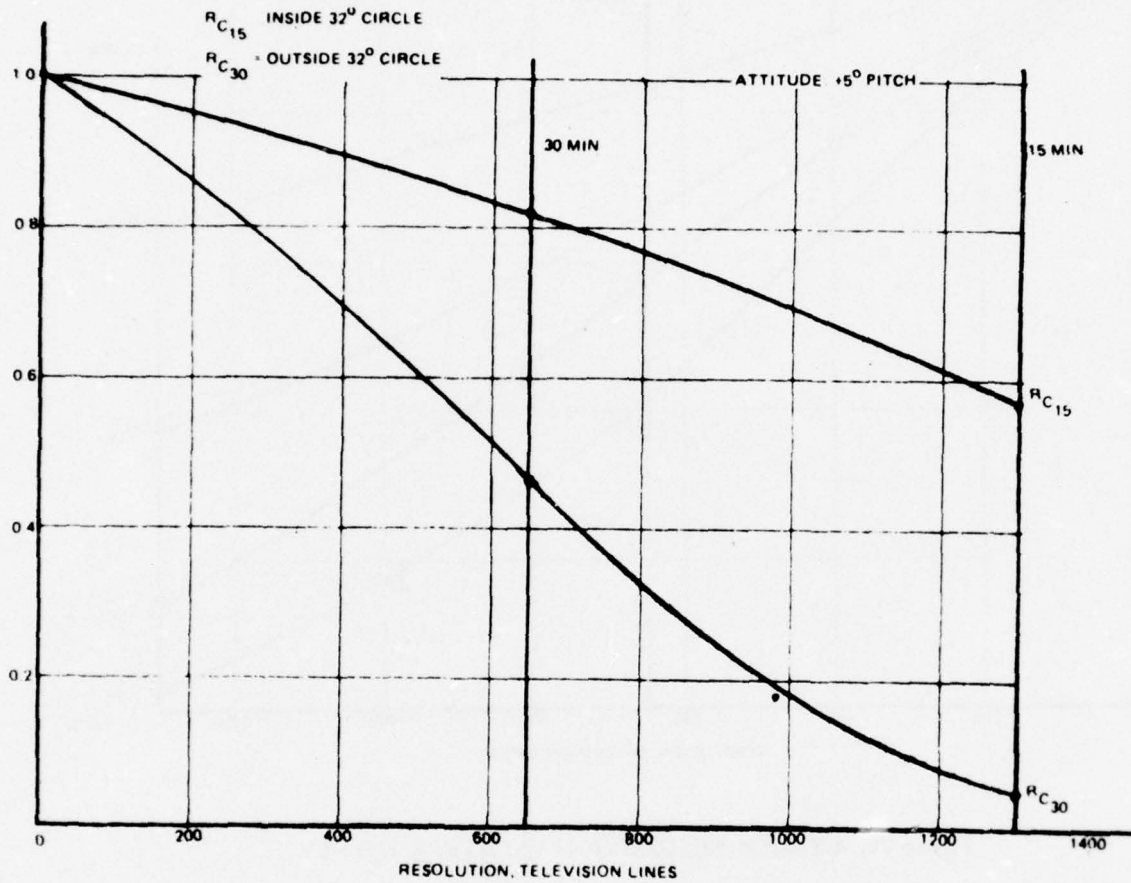


Figure 71. SYSTEM RESOLUTION VS. MTF, @ 81 FT.

Hardware Changes. The addition of altitude cues to the proposed system will require two more scaling multiplying, digital-to-analog converters, similar to those used in the DARC (raster computer). Additionally, more visual realism can be gained by adding a computer-controlled contrast input to vary contrast to the video signal. Also, the sea haze generator would have to be more sophisticated to allow the variable sea haze location.

Software Changes. Some modification of the software would be required to implement the software addition of altitude and variable sea haze.

Velocity Cues. The addition of velocity cues to the proposed system is a much more complex problem than altitude. In the analysis of velocity requirements, use is made of a previously shown analysis²⁸.

Moving Map. If a large area transparency could be generated, then velocity could be cued into the system, if the transparency could be moved. The size of the map obviously has some limitation. Discussions with Simulation Systems of Huntingdon Valley, Pa. has indicated the possibility of making a montage of a series of films of an area and filling in the seams, such that a map of 40" by 40" could be generated, with the resolution of the 9 x 9 inch map. The system would be of a 10,000:1 scale, covering 38,000 x 38,000 feet, or 6.3 x 6.3 nm.

During maneuvering, care must be taken so as to not use up the 6 nm of space before landing, and give some space for a bolter to be accomplished.

The hardware configuration would contain the 5-inch flying-spot-scanner and 1:1 lens specifically set to use the higher 10,000:1 film scale. The biggest change would be the addition of the 40 x 40-inch, moving X-Y drive. The system work would be an enlarged version of the radar landmass simulators now being built by Singer-SPD. Additional impact on software would be required to develop the drive algorithm. The system MTF would be equivalent to the use of a case-2 film.

Reset Raster Cue. A second method of adding velocity cues would be to have a large flying-spot-scanner surface, and fly the raster over the map. Since high-resolution flying-spot-scanners are limited at this time to about an eight-inch working diameter, with the same spot size as the four-inch working diameter type, the general approach of flying the raster must be modified. The method studied during this phase of the AWAVS program was to use a repeat-pattern film and fly the raster from one pattern to the next by moving the raster over the face of the CRT, and then jump the raster to be in the starting location on the first pattern, and repeat the sequence. The pattern could be as small as four repeat pattern, each one being an exact duplicate of the others, but blended into each other, so as to not be visible within the CRT. The raster would be flown over the maps, until one of the edges encroach on the edge of the CRT. Then the raster would be jumped to a new pattern, and the flight would continue. Thus, the velocity cue would be continuous at all times.

In general, several major problems remain in such a system. The film could be developed, and the scanner tube does exist; time/temperature change, etc. would have to be dealt with. The best linearity possible over the tube probably would be $\pm 0.2\%$, or perhaps 0.024 inches (or 16-spot diameters) on the tube. Thus, the reset jump would be noticeable. On the positive side, most of the time, the scanner could be defocused to reduce the jump error, but the reset would always be noticeable. Since the scale factors would be equivalent to the 5000:1 scale discussed, the average reset would be after a travel of about 4000 feet, or every 12-20 seconds over most of the travel time.

A sophisticated drive approach must be developed to take advantage of the flight path, to predict the best reset point, to diminish the number of resets. (Once a reset is initiated, the choice is among any of the three, remaining patterns: only one has the best chance to have the longest travel time, before the next reset.) The accuracy of detection and location is very important to achieve the best systems with the least amount of unwanted motion.

The use of the nine-inch CRT (eight-inch working diameter) would need the design of a high resolution, fast, large-format lens to meet these requirements. The larger CRT increases the mounting requirements of the optical path and impacts the collection optics but the remainder is essentially the same as the proposed systems modified by altitude.

The system MTF would be equivalent to those MTF's previously discussed ²⁹.

Analysis of 1023-Line System. The addition of more TV line necessarily increases bandwidth of the video and deflection systems. The deflection bandwidth required to settle by the end of a 7 usec retrace, which is a nominal increase from the proposed 8-usec retrace, should present no problem.

The increase of video bandwidth from 20 MHz to 27 MHz now requires that the system exceed the state-of-the art in flying-spot-scanners, which is 20 MHz. Beyond a 20-MHz bandwidth the picture quality deteriorates rapidly, because of the required high-frequency boost to compensate for the phosphor decay ³⁰. Therefore, it is recommended at this time, unless a breakthrough in high-speed phosphors is achieved that 20 MHz be the upper limit for video bandwidth. Thus 1023 lines is beyond the state of the art for flying spot scanners, unless a reduced horizontal resolution is implemented.

Synthetic Wake Generation. Two methods were analyzed for inserting a synthetic wake into the background image.

Analog STG generation. Singer Simulation Products has produced several Synthetic Terrain Generators, or (STG). The STG is basically an analog computer with parameters, controlled by the system digital computer. The resultant picture is a set of squares of proper perspective for the altitude and attitude of the system. A modified form of the basic STG could be produced to make a video insert to follow behind the carrier, at the proper length and attitude for the carrier parameters of distance, speed, direction, and location.

However, an analysis of the errors involved in the high-speed, analog computations used in the STG have given undesirable results. Thus, the basic analog STG approach to wake generation is not recommended, due to lack of accuracy of placement, relative to the carrier.

Digital Derivation and Insertion. Section 9 analyzes the system to be designed for elliptical blanking in the background and target generators. A similar system could be designed to provide an insert for the wake. The mathematics would be a straight-line outline of the wake. The math model and hardware could be made as sophisticated as desired to generate different patterns outline, stern wave effect, etc.

NAVTRAEQUIPCEN 75-C-0009-1

The video would be inserted by techniques used in the visual effects generator to switch from one level to another. The basic system would provide a constant, grey level in the wake area. Contrast could be controlled by the computer to add realism to the wake.

The errors associated with wake insertion would be those determined in section 9. The wake generator could be locked onto the elliptical blanking within 5 arc-min. rms, so that the remainder of the errors would be contributed as described in the elliptical blanking section.

Therefore, the digital approach of synthetic wake insertion is recommended over the analog STG system.

SECTION VI

BACKGROUND PROJECTOR

The requirements for the background projection system outlined in Specification 212-102 are as follows:

- 1) An instantaneous field of view, measured relative to the aircraft body axes, from $+50^{\circ}$ to -30° vertical and $\pm 80^{\circ}$ horizontal or optionally 120° to the left and 40° to the right is required. In both arrangements, the corners of the display may be rounded to a maximum of 15° arc.
- 2) A real image projected onto the screen by refractive optics shall be used.
- 3) Mapping from the projector image surface to the screen shall be such that equal displacements on the projector image surface are viewed as equal angular segments across the screen, as closely as possible.
- 4) Effective resolution, measured in TV lines, shall be such that 1300 TV lines per picture width are obtained horizontally and 600 TV lines per picture height vertically. With a Kell factor of 0.75, 800 active scan lines are required to obtain 600 scan lines of effective resolution. Also, the minimum resolution per optical pair must be 30 arc minutes or better, anywhere within the field of view.
- 5) An overall image brightness of 6 foot-lamberts is required with a design objective of 12 foot-lamberts.
- 6) The system shall be compatible with the requirements of the motion system, which are 12.75 inches of heave, 22° upward and 11.5° downward pitch, a $\pm 16.5^{\circ}$ roll capability, a $\pm 18^{\circ}$ yaw capability, and up to a 4g acceleration. Since the 4g acceleration is assumed to occur only during emergency shutdown conditions, it is not considered necessary for the image to show no degradation during this time, rather that no permanent damage be done to the equipment. In addition, the weight of the equipment shall be as low as possible.
- 7) The equipment shall be reliable.

Besides these requirements, additional features are desired for the initial design configuration to provide for future growth objectives. These may be summarized as the ability to mate with another, similar projection system to provide an overall field of view of 240° horizontal and -30° to $+60^{\circ}$ vertical. It is also desired to have the capability of replacing the image generators proposed for the initial system with Computer Generated Imagery (CGI) equipment. Since it is impossible to obtain the equivalent of a fully flexible camera raster computer within computer image generation equipment, it is necessary to provide some portions of the mapping within the display equipment. Therefore, the projectors chosen must be capable of providing mapping in response to a computed display raster format. By mapping is meant the ability to shape the TV scan lines and to modify the scanline velocities so that the position of the information viewed from the observer's eye point via the display screen is at the same angular position at which it would appear if the computed image plane were viewed from the CGI design perspective point. If possible, it would also be desirable to permit replacing a CGI system with a system in which the information is stored directly on movie film. If

the information stored on the movie film were to be projected by film-to-video conversion techniques, such as used in Singer's Scamp (Scanned Vamp) system, then it would merely be necessary to be able to modify the field of view of the display image to be compatible with that which could be provided by the Scamp system.

METHODS CONSIDERED.

Proposed Method. The technique used in selecting the image display system is broken down into three areas: first, the basic system configuration was established so that the two optional, desired fields of view could be obtained; second, a suitable background projector was selected; and third, the wide angle projection lens requirements were determined.

The basic, proposed system configuration resulting from the preliminary design analysis is shown in figure 72. Position 1 which results in the -120° by $+40^\circ$ view, locates the nominal projection pupil 6.8 inches to the right and 8.7 inches behind, in a plane 24 inches above the screen center. Position 2 locates the projector's pupil 11 inches behind and 24 in. above the screen center. In both cases the projection axis is tilted 4.8° downward. This tilt results in the optimum mapping of the elevation angles between $+50^\circ$ and -30° as viewed at the pilot's eyepoint, onto the projector raster plane, thru the $f \theta$ lens function. In moving from position one to position two, the projection pupil is rotated about the center of the screen and therefore, the mapping is essentially constant.

The EP8 Eidophor system was selected for the initial application. It provides the basic light output of 4,000 lumens for TV line scan systems, up to 800 lines. The design analysis has shown that this will allow the system to meet the display brightness specification requirement of 6 foot-lamberts.

To adapt the Eidophor to the AWAVS application, it is necessary to reinforce the projector structure so that it can be safely mounted on the motion system. At the present time, it has not been possible to establish what projector attitudes (pitch or roll) or accelerations would produce a failure of the projector. It has been established by the Eidophor projector manufacturer that at roll angles of greater than $\pm 8^\circ$ and pitch angles of greater than $+10^\circ$ or -24° objectionable effects in the controlled-oil layer, and therefore, the projected image will take place. Furthermore, the manufacturer has stated that, the projector may be operated up to a displacement of $\pm 20^\circ$ of pitch and $\pm 15^\circ$ of roll with up to 2g acceleration for 6 milliseconds without equipment failure but with some picture degradation. However, these are short of the specified roll and acceleration specifications. A study has shown that little if anything can be done in the way of repackaging the Eidophor to reduce its volume or weight.

It has been established that little if anything can be changed in the TV raster format. The ability to shape the raster has been ruled out by the manufacturer of the Eidophor. Thus the possibility to expand into the CIG applications appears slim.

The design analysis reaffirmed the position that the best lens for the wide angle projection application is the asymmetrical single lens design available from the Willey Optical Co. The resolution of the lens will be 10 Lp/mm horizontally and 6 Lp/mm vertically in the center of the field and no worse than 5-horizontal by 3-vertical Lp/mm everywhere within the field of view. These figures refer to 35% modulation.

Figure 73 gives the total background projector system (projector plus lens) MTF. The resolution analysis of the background image generator involves an extensive investigation into raster plots and flight attitude. The total system MTF, therefore, requires the generation of complex data surfaces, or equal resolution curves over the field of view. Current estimates of the total background image system are also provided ³¹.

Alternate Methods. Alternate methods are described in beginning page 186.

TV PROJECTOR.

The projector chosen is an Eidophor model EP8. This includes two assemblies, the projector housing, and the power supply for the projector lamp. The standard magnetic deflection electronics provide a uniform rectangular raster capable of static keystone correction for projection angles between +10 and -20 degrees. As a result of the design analysis, Singer intends to use this raster without modification in the initial configuration and to provide necessary mapping modification for the entire system in the raster computer equipment which is associated with the background image generator. An analysis has been made of the $f \theta$ mapping of the field of view of the observer back onto the Eidophor raster surface plane. It demonstrates that in order to meet the 1300 horizontal by 600 vertical resolution elements, the full 160° by 80° field of view, will have to be compromised. Figures 74 and 75 illustrate the mapping for the two different projector positions.

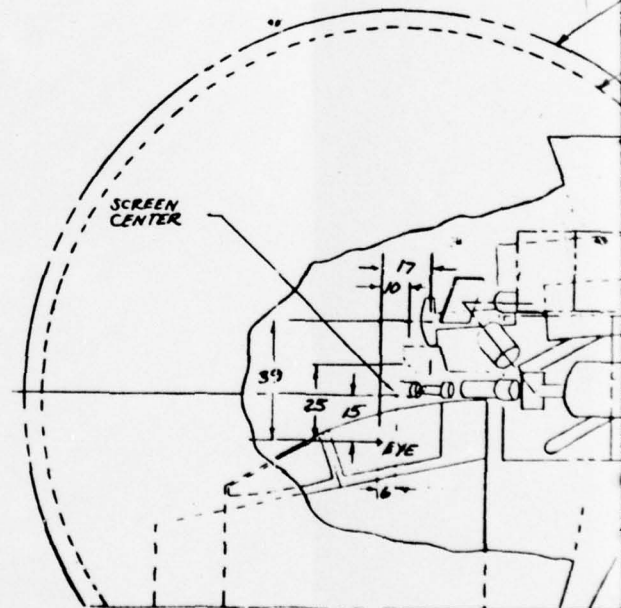
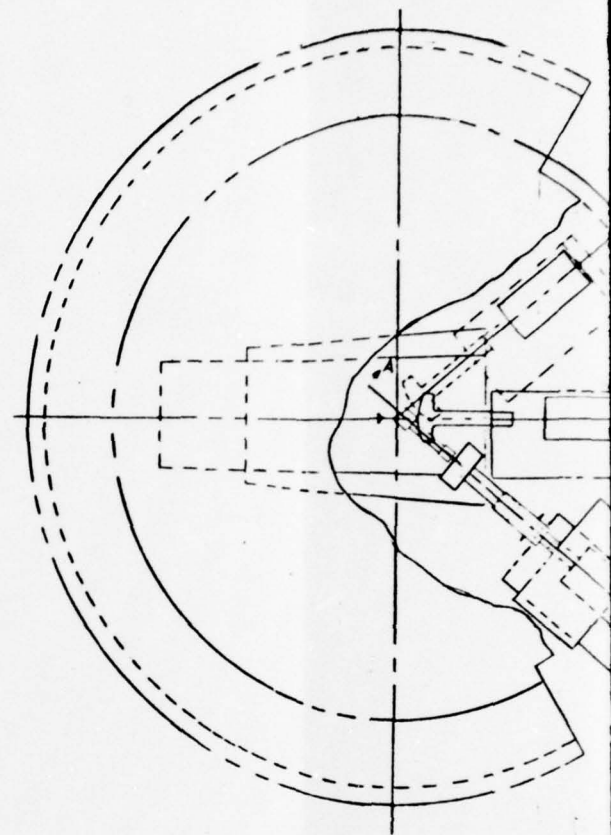
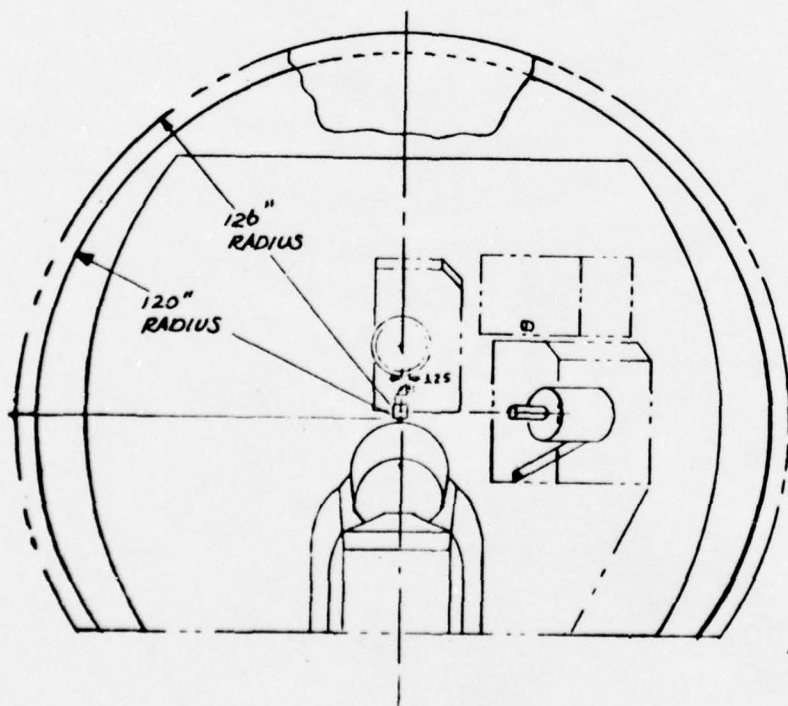
The amount of FOV clipping involves a compromise between FOV and the required number of scan lines and video bandwidth. Since an increase in bandwidth is accompanied by a reduction of signal to noise ratio, we would recommend limiting the bandwidth for the required resolution and still meet the maximum permissible FOV requirement. Figure 76 shows how the raster rounds off the FOV in an attempt to provide the necessary center resolution. It is felt that overscanning is not possible to achieve the required FOV because of the reduced-light output that would occur. Also, the bandwidth requirements would increase, and this would appear intolerable for the background image generator.

The projector resolution requirements is 1300 horizontal by 600 vertical resolution elements. Taking into account a 0.75 kell factor and 25 lines for vertical retrace, a total scan-line count of 825 lines would be required in order to attain 600 vertical resolution elements. The horizontal frequency is 24,750 Hz and allows for a 7 or 8 μ sec retrace line. An active scan time per horizontal line is 33.4 μ sec. Thus the minimum bandwidth requirement is given by

$$\begin{aligned} \beta\omega &= \frac{\text{Horizontal resolution}}{2X \text{ Active scan time}} \\ \beta\omega &= \frac{1300}{2X 33.4} = 19.5 \text{ MHz} \end{aligned}$$

the projector bandwidth is 20 MHz. Figure 77 shows the modulation transfer function of an Eidophor projector derived from actual measurements. It should be noted that the plotted MTF includes the effects of an unknown lens. The projector MTF for 1300 resolution elements per picture width is 0.09.

To accomplish target insertion into the background, special projector blanking is applied. This is discussed in detail in section 9.



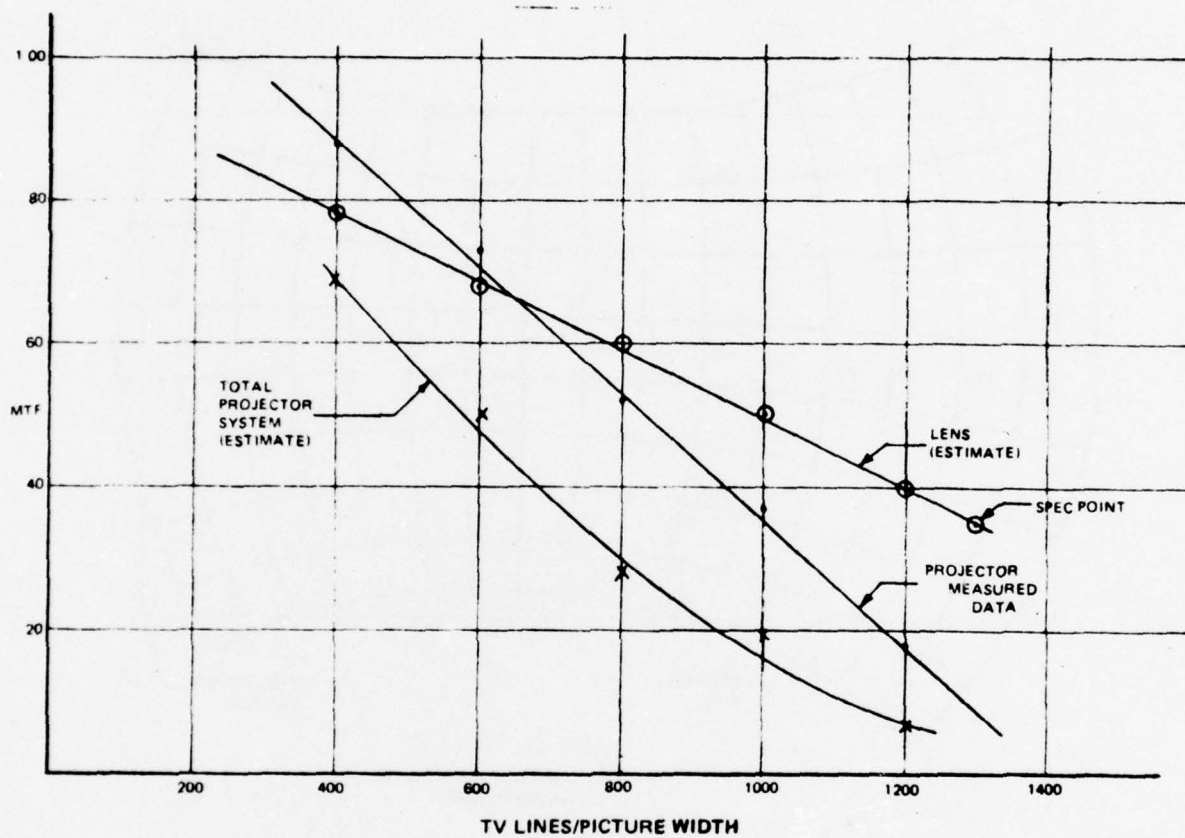


Figure 73. PROJECTOR SYSTEM - MTF

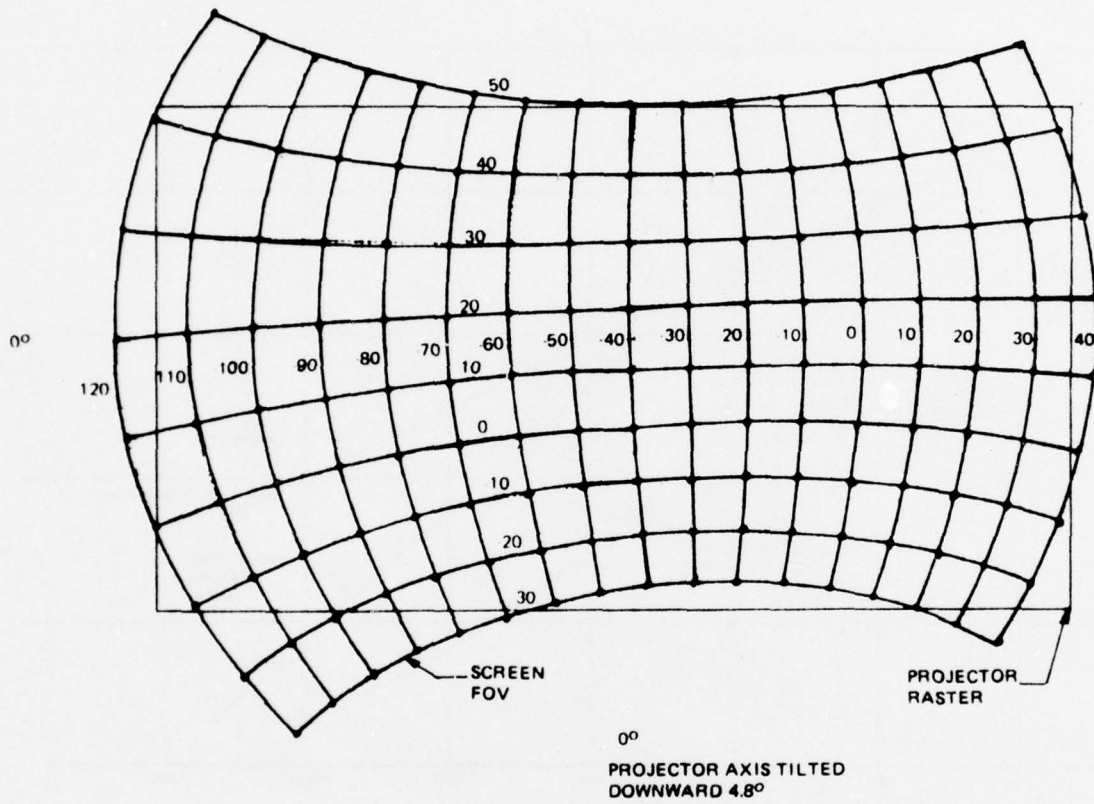


Figure 74. IMAGE PLOT FOR PROJECTOR POSITION NO. 1

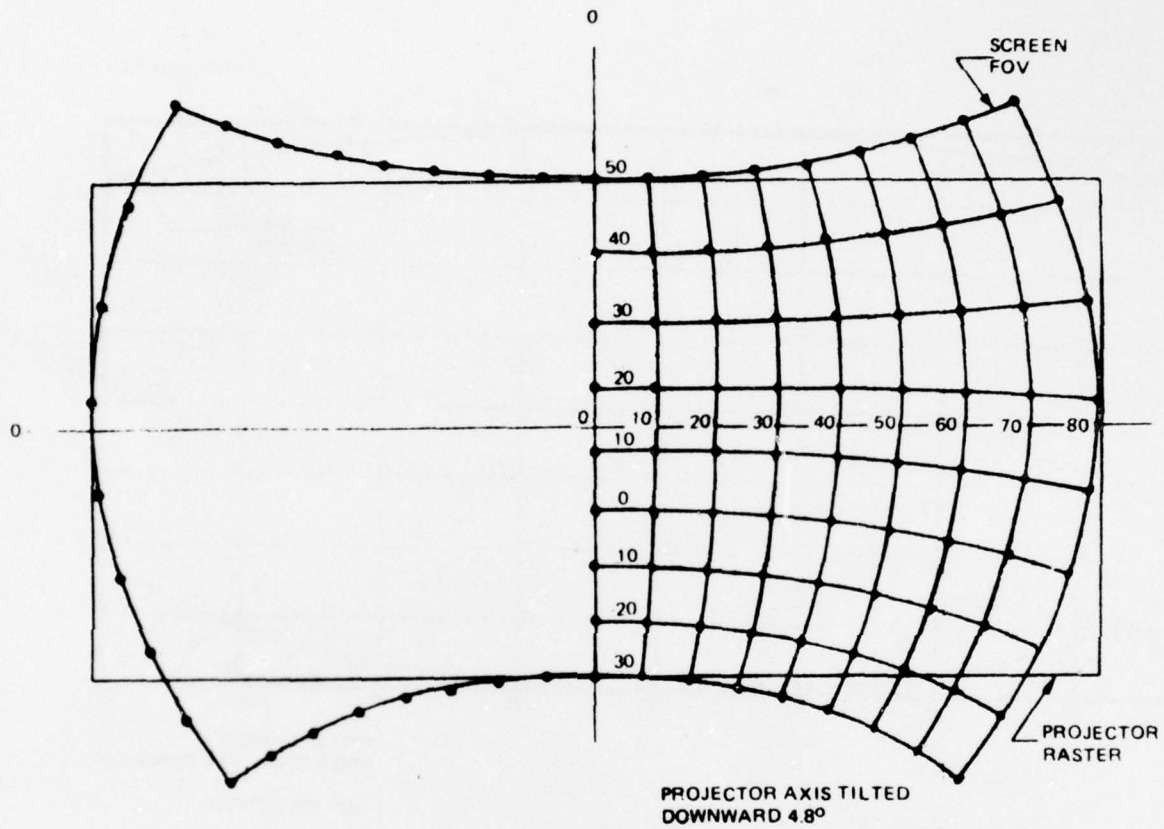


Figure 75. IMAGE PLOT FOR PROJECTOR POSITION NO. 2

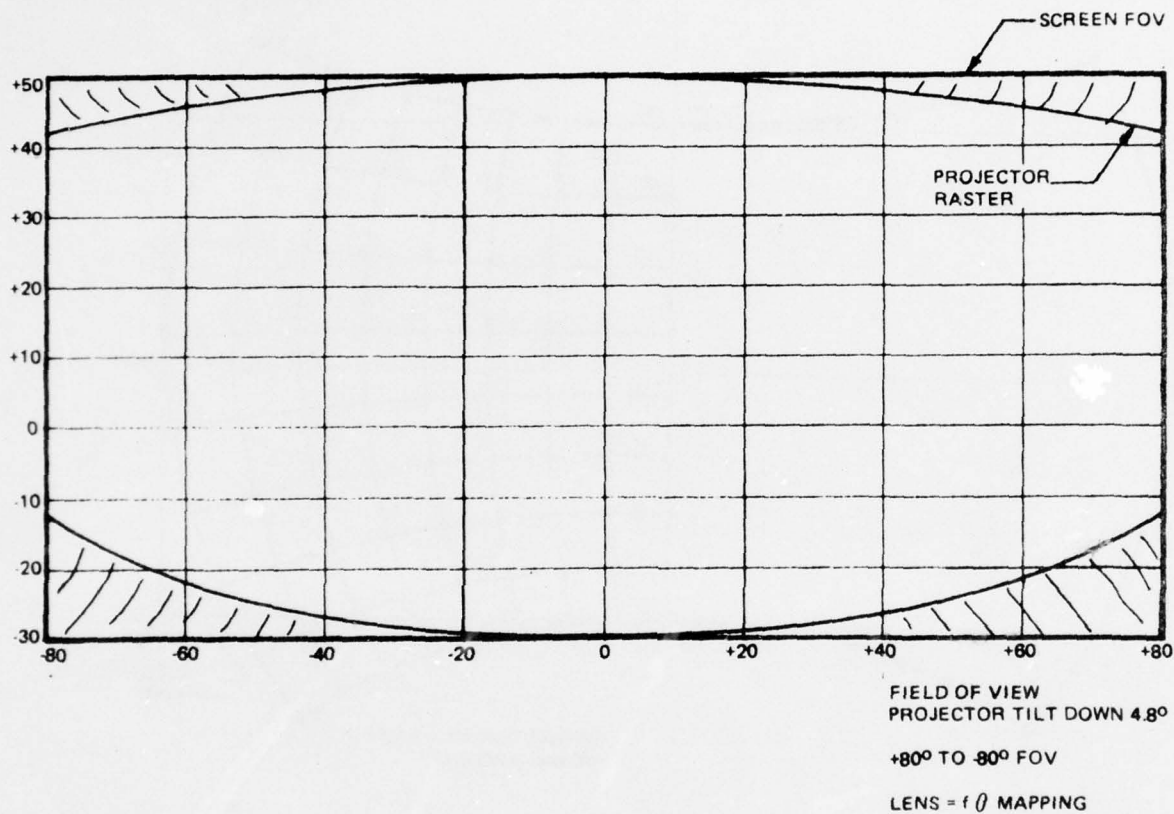


Figure 76. SCREEN FOV FOR PROJECTOR POSITION NO. 2

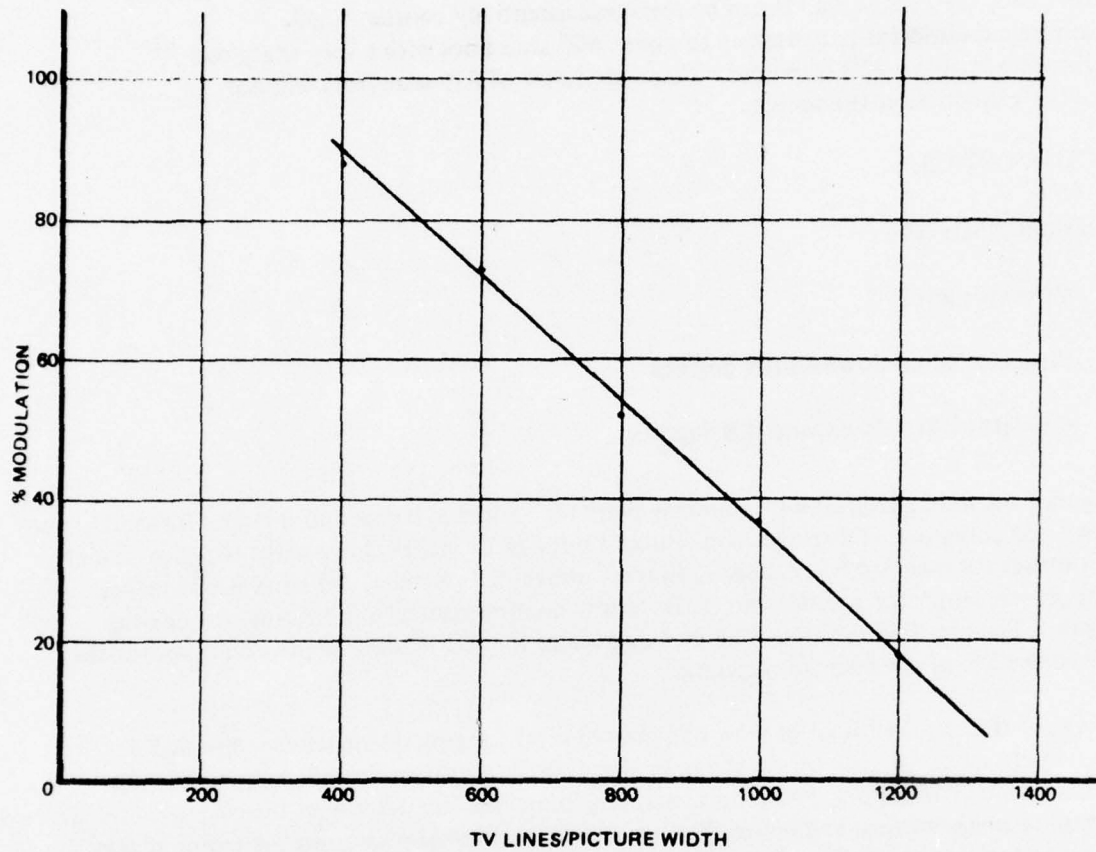


Figure 77. EIDOPHOR MTF DATA

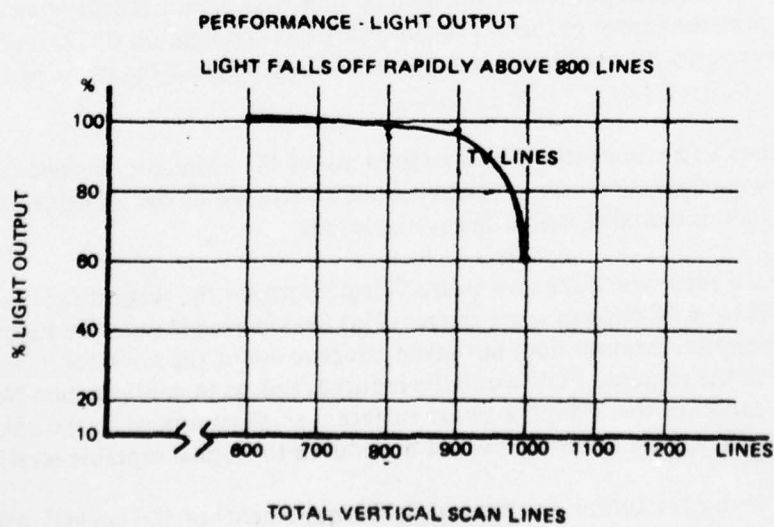


Figure 78. LIGHT OUTPUT AND TOTAL SCAN LINES RELATIONSHIP

Figure 78 shows the relationship between light output and total scan lines. The light output is specified as 4000 lumens \pm 10% at the raster center with less than 35% brightness distribution over the raster area. It can be seen that essentially constant light output can be expected for line rates up to about 800 scan lines with a very sharp roll off in light output above 900 scan lines. Thus the choice of 825 scan lines will not influence the brightness at the screen.

PROJECTOR OPTICS.

Configurations Analyzed:

- 1) Projector level
- 2) Projector tilted downward 9 degrees
- 3) Projector tilted downward 4.8 degrees

All configurations were analyzed with nominal eyepoint 15 inches below and 6 inches forward of the screen center of curvature. The projection lens exit pupil is 24 inches above and 11 inches behind the screen center for position No. 2, and 24 inches above, 6.794 inches right and 8.651 inches behind the screen center for position No. 1. Rotation about a vertical axis passing through the screen center. The required rotation is 38.144 degrees to the left to aim the projection axis at the point 40° to the left of the normal eyepoint.

The mapping of the required field of view was plotted after imaging through a lens having $f \theta$ mapping characteristics for each of the above configurations. Initially the lens was considered without anamorphic correction. From these mapping plots one can determine the effective area utilized of the Eidophor image surface and hence the flux available for projection onto the required area. Also one can determine the TV resolution capability for a given area of the projected scene. $f \theta$ mapping of a sphere onto a surface produces pin cushion shape lines of latitude and barrel shaped lines of longitude.

If one chooses to include the required corners of the field of view within the available area of the Eidophor image surface, then the center portion is considerably less in height on the Eidophor image surface and would not be covered by a sufficient number of TV lines to meet the required resolution in the center of the field.

Configuration No. 1 requires an unsymmetrical vertical field out of the projector lens and consequently a larger vertical field. This configuration also does not make effective use of the available Eidophor image surface if the total field is included within the available area.

Configuration No. 2 with the projector tilted downward 9 degrees makes the vertical field requirements of the projection lens equal to \pm 40 degrees when the required field is imaged onto the Eidophor image surface. This configuration however does not make effective use of the available image surface area, hence the brightness in the required FOV would be reduced, and, as in configuration No. 1, the height of the image in the center of the Eidophor image surface is small compared to the height at the edges and consequently the center resolution would be reduced to an unacceptable level.

To provide the maximum center resolution, the vertical field requirements of 50° up and 30° down require that the Eidophor image surface be tilted in the vertical direction. Configuration No. 3 with the projector axis tilted downward 4.8 degrees fulfills the requirement for the required 50°

up and 30° down to represent equal vertical distances on the Eidophor image surface. It is essential that the 80 degrees vertical field be imaged onto the Eidophor image surface at the full extent of the vertical raster to approach the required resolution and modulation. When this choice is made the full 80° degree vertical field is available only at the horizontal center of the displayed scene. This is because the lines of latitude are pin cushioned at the Eidophor image surface and thus require a greater vertical dimension than is available.

This configuration does not provide the full vertical field at other positions off axis horizontally but the lens type required has inherent rounding of the extremes anyway. Since the lens does not see these points it is unnecessary to include them within the available Eidophor image surface area. One possible means to cover greater vertical field at horizontal off axis positions is to have a lens of mapping form:

$$H = f \cdot \theta^P$$

Where H is the distance off axis in the image plane, f is the lens focal length, θ the field angle and P is a number less than one. Willey Corp. is investigating this possibility. This type of mapping, if possible, would make the requested FOV map more nearly into a rectangle by essentially pulling in the corners of the field, thus, putting more of the desired FOV onto the Eidophor image surface.

In any of the configurations investigated, lines of equally spaced latitude do not map into equally spaced lines on the Eidophor image surface. This results in unequal resolution depending upon the elevation angle. One possible means to equalize the spacing is by the inclusion of an achromatic wedge or prism within the projection lens. This type of device produces an anamorphic action whose power varies. If oriented correctly it could equalize the spacing on the Eidophor image surface of the lines of elevation. Willey is also investigating this possibility.

Several figures are shown which show some of the characteristics of the configuration considered.

1) Figure 79.

This figure shows arbitrary units of length surface when the required FOV for position No. 2 is imaged by a non anamorphic $f\theta$ lens. The lens axis is level.

2) Figure 80.

This is equivalent to figure 79 except that the projection lens axis has been tilted downward 4.8°. This tilt of 4.8 degrees makes the 30 degree down and 50 degree up point, at zero azimuth, equal distances at the image surface.

3) Figure 81.

This figure applies to position No. 1 of the projector. In this figure the projector is tilted down 4.8 degrees and then rotated 34.366 degrees to the left. Both rotations are about the exit pupil of the projection lens. This figure also shows arbitrary units of length at an image surface when the required FOV for position No. 1 is imaged by a non anamorphic $f\theta$ lens tilted as described above.

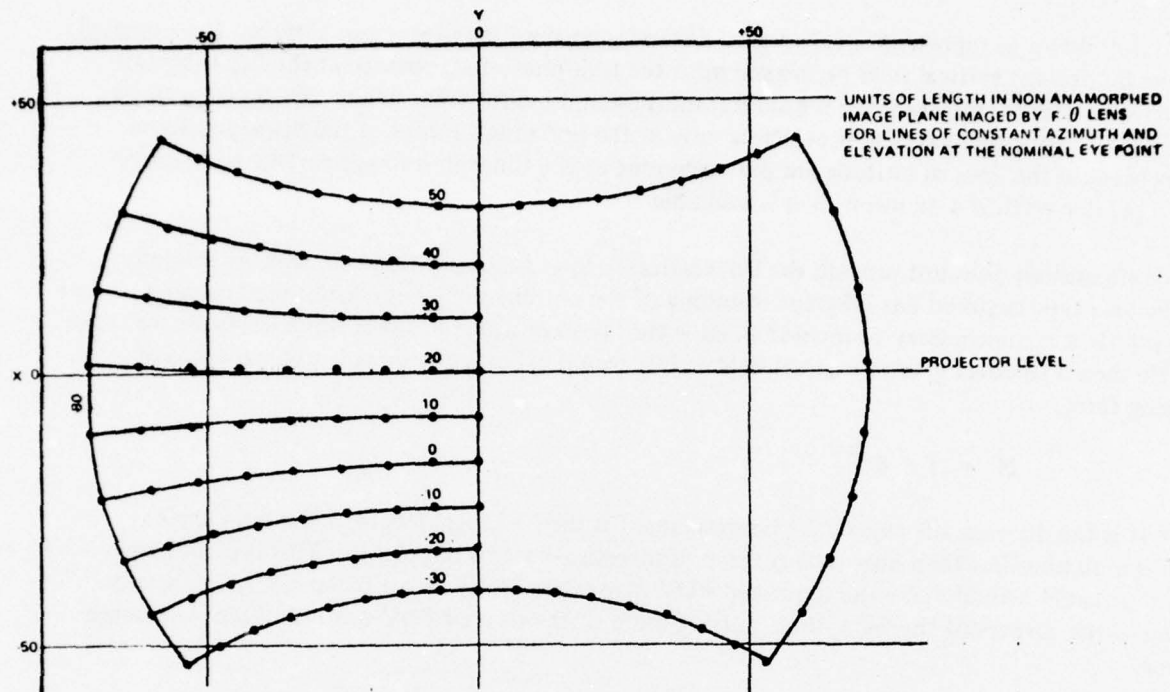


Figure 79. PROJECTOR LENS AXIS LEVEL

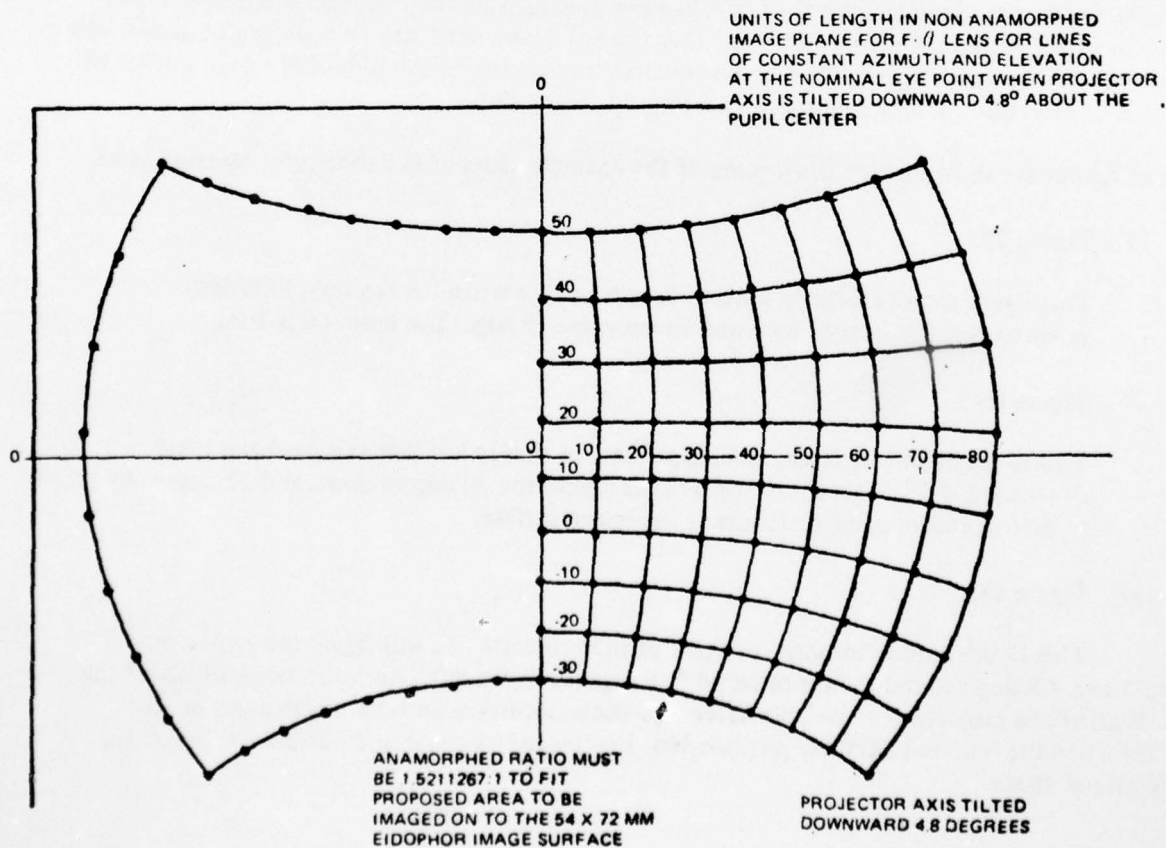


Figure 80. PROJECTION LENS AXIS TILTED DOWN

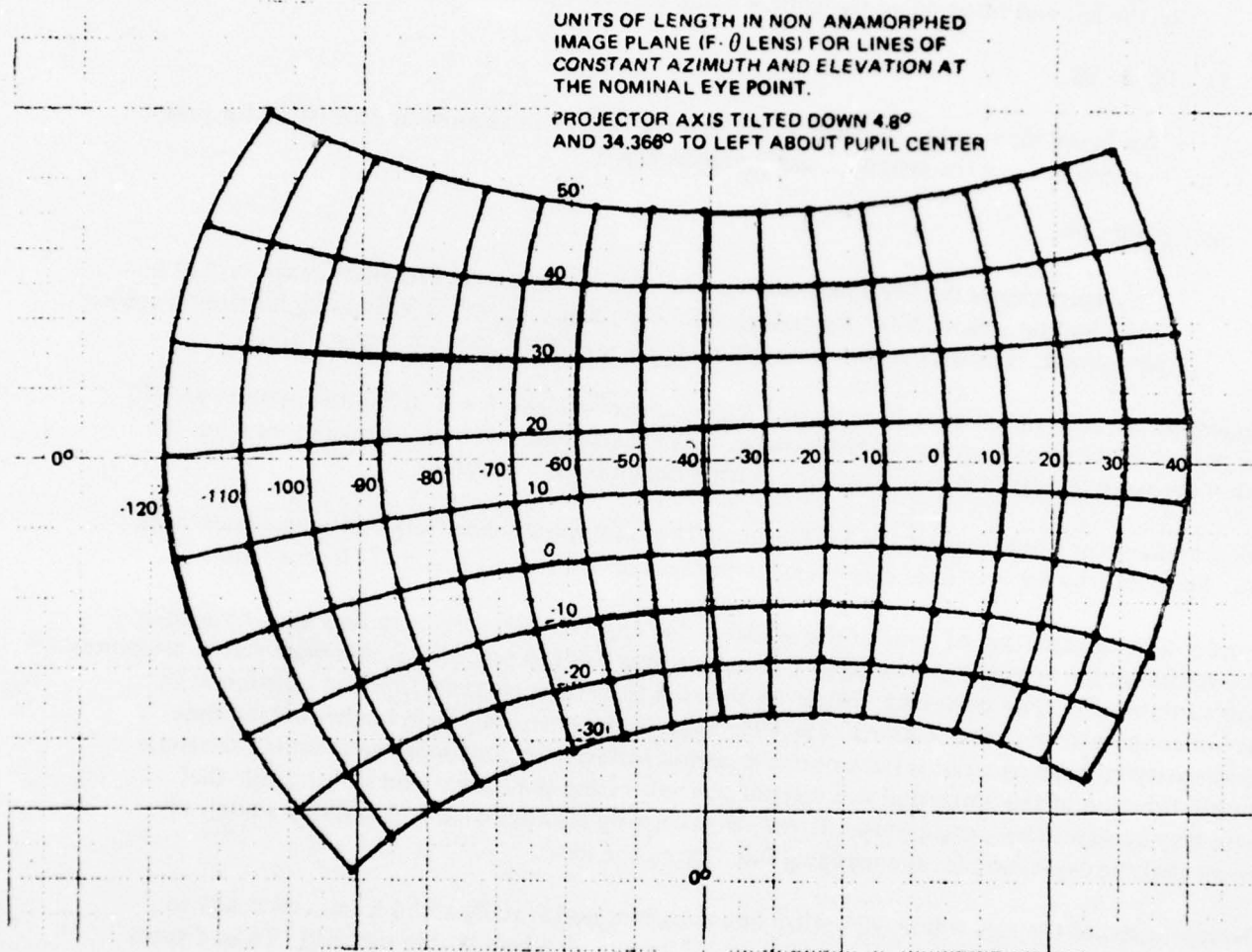


Figure 81. PROJECTOR POSITION NO. 1

4) Figure 82.

This figure applies to position No. 1. In this figure the projector was rotated in azimuth about a vertical axis through the center of the spherical screen an angle of 38.1437 degrees to the left and tilted down the same 4.8 degrees as for position No. 2.

5) Figure 83.

This figure shows what the field to the observer will be in azimuth and elevation for position No. 2, using the proposed configuration No. 3.

6) Figure 84.

This figure shows the horizontal and vertical dimensions on the Eidophor image surface in mm when the desired FOV for position No. 2 is imaged by an $f\theta$ lens having horizontal anamorphic power. The dark rectangular outline is the available Eidophor image surface.

The lens to be used is a natural extension of a lens system developed for NTEC in the period 1969-70. The present requirements are somewhat more stringent than those met by the previous lens, but are within the range of what can be achieved by further design improvements.

The proposed lens would project the conventional 72 x 54mm Eidophor format into an angular field of 160° horizontal by 80° vertical. This format will focus on a spherical screen of 10-foot radius.

In order to take advantage of most of the available flux from the Eidophor, the lens must be anamorphic to change the normal 3 x 4 format. The anamorphic lens has potentially 50% more screen brightness than a rotationally symmetric lens. However, this means that the mapping function is different in the horizontal and vertical directions. The wide angle of the horizontal field further causes some nonlinearity in mapping a flat surface onto a spherical surface. This mapping function is a relatively smooth function of the horizontal and vertical position within the format, but it is possible that there may be significant cross product terms. No difficulty is anticipated in describing a relatively simple analytic expression for the mapping function of the lens.

The resolution of the lens will be 10 optical line pairs/mm horizontally and 6 lp/mm vertically in the center of the field and no worse than 5H by 3V lp/mm anywhere within the field. These figures refer to 35% modulation, and 50% MTF will be the design goal. These values of resolution at 35% modulation will ensure that the combined system of FSS, transparency photomultiplier, Eidophor projector, and projection lens will provide a background scene where the angular resolution does not exceed 30 minutes of arc at the generally accepted minimum of 5% modulation.

The lens is expected to have approximately 20 optical surfaces, most of which will be appropriately coated to reduce surface reflections. Previous experience indicates that approximately 50% transmittance can be readily achieved. Vignetting within the lens is negligible due to the nature of the wide-angle lens. It is a fortunate circumstance that pupil aberrations in lenses of this general design actually enhance the uniformity of illumination vs. field angle. The entrance pupil of the lens grows in size as the angle from the optical axis is increased and therefore, the usual cosine effect is compensated.

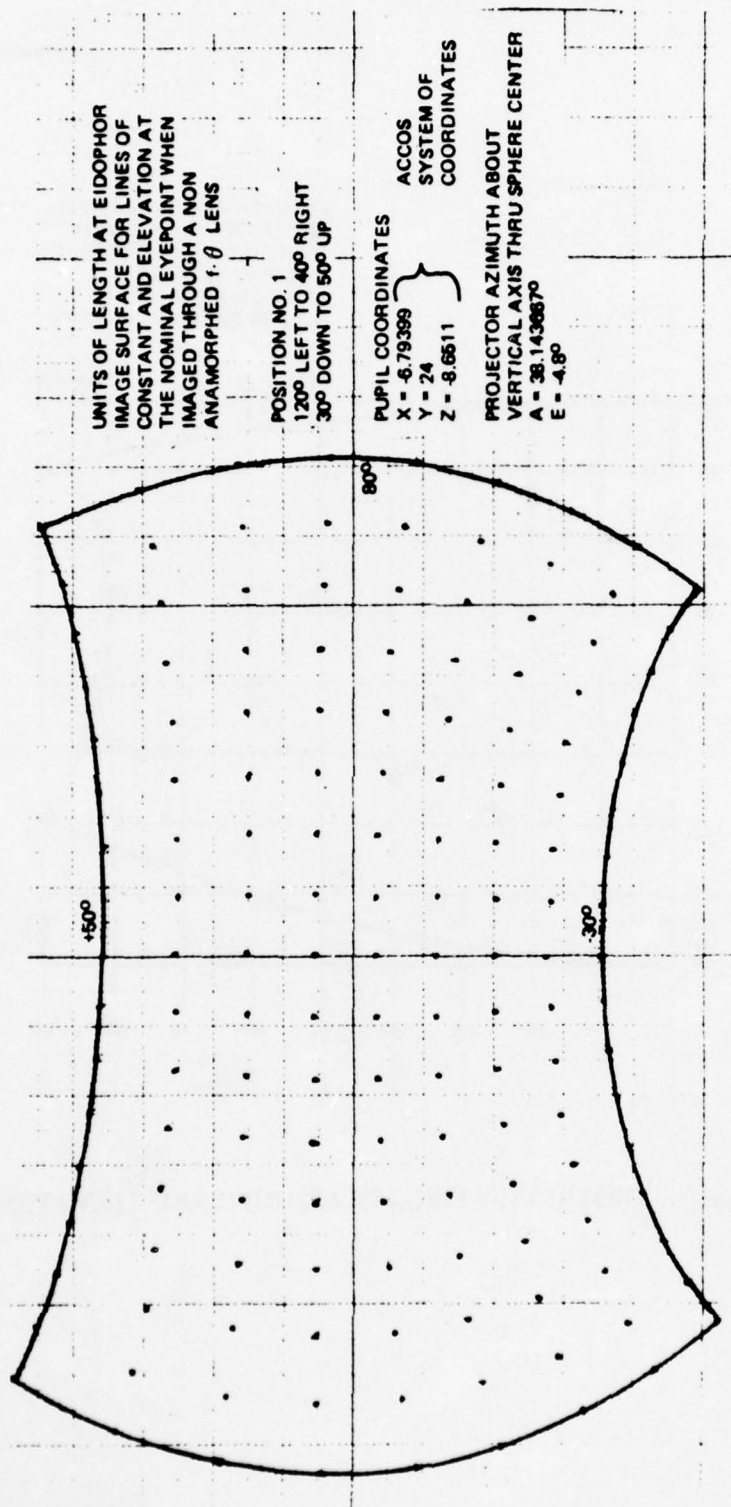


Figure 82. POSITION NO. 1 WITH AZIMUTHAL ROTATION

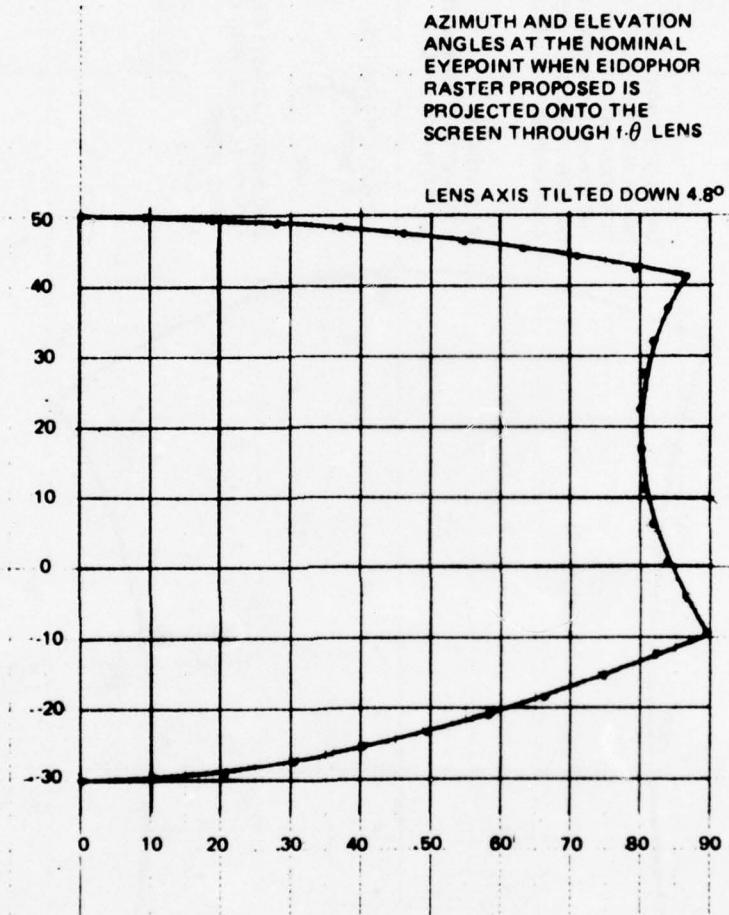


Figure 83. OBSERVER'S FIELD IN AZIMUTH AND ELEVATION

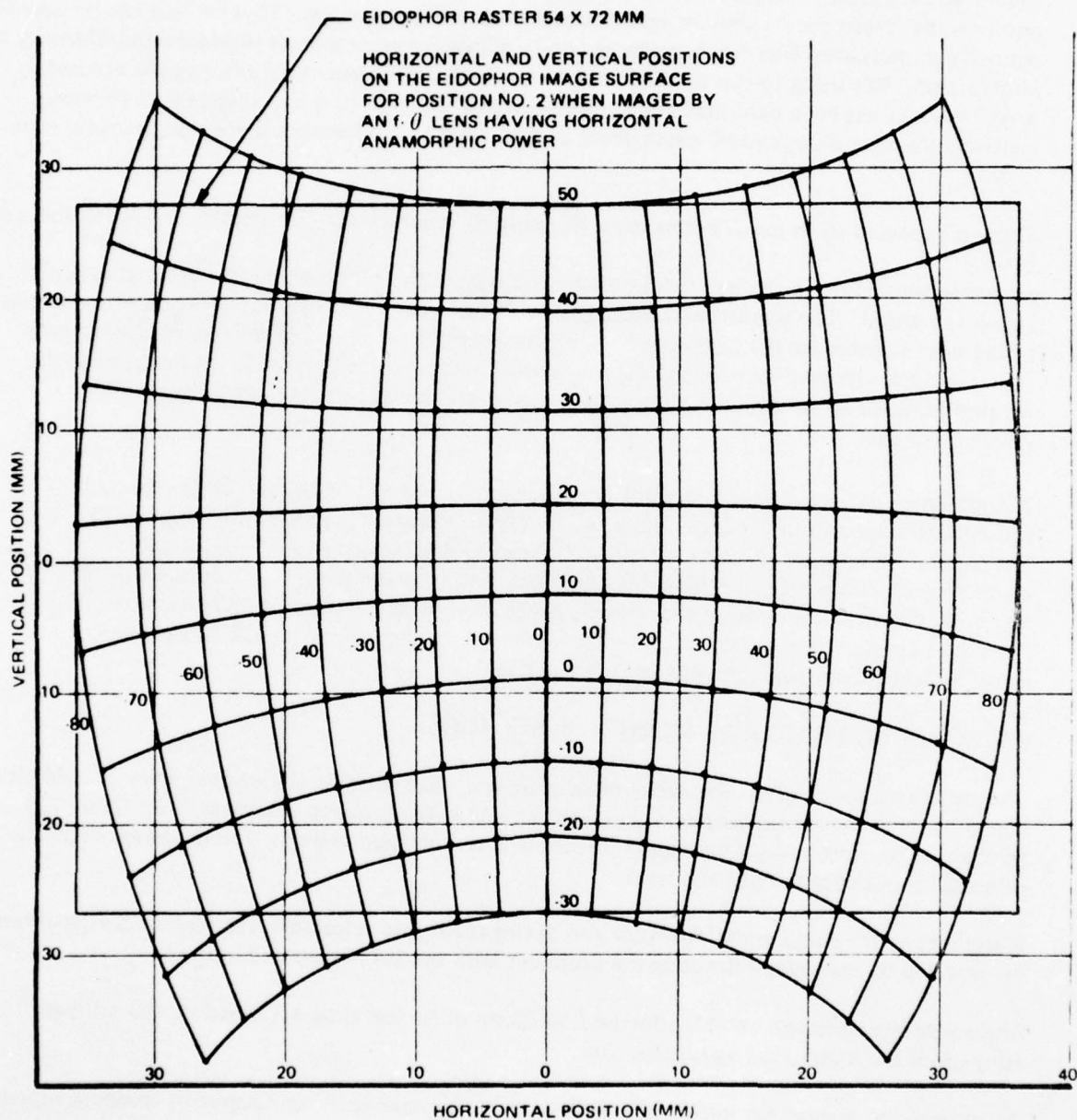


Figure 84. IMAGE PLOT ON PROJECTOR RASTER

Another consideration that is of importance in the projector lens is the uniformity of flux distribution over the field-of-view. The requirements of the specification for a uniformity within 25% over the total field is very stringent and probably cannot be met without the use of a special coating on the last element of the projection lens. At this point in the optical system, the beam going to any point on the screen has its smallest aperture and most unique position. That surface can be used to control the amount of flux reaching the screen to adjust for any inherent residual nonuniformity of illumination. Resorting to this method is of course undesirable because it reduces the average brightness. As has been described above, the nature of this type of a lens system is to provide relatively uniform illumination, particularly as compared to a symmetrical wide-angle lens system.

There is expected to be much better than 4% mapping accuracy match between computed and actual angle.

As previously indicated the lens will be above and behind the center while the nominal eyepoint is below and ahead. The significant advantage of this placement of projection lens and observer relative to the screen center are the negligible bend angles between the reflected rays from various image points and the observer's line of sight to the corresponding image points. Since the bend angles are negligible for all field points, there will be essentially no brightness falloff due to the screen or its gain.

The minimum expected light output of the Eidophor and proposed background projection lens is 2000 lumens over the area of approximately 300 square ft (as shown by figure 76). The resultant brightness is 6.67 lumens/sq ft. The required screen gain for the target image projector to achieve a 6-ft-lambert highlight is 4.3. If the Eidophor output were not modified, this would produce a background image brightness in excess of 28 ft-lamberts. Thus the Eidophor modulation must be altered to reduce the output for the background image to keep all images at the proper, relative level.

BACKGROUND PROJECTOR SUPPORT STRUCTURE.

The structure that supports the background projector must provide sufficient rigidity to hold all components in the required optical alignment as well as the required electronics (see figure 72). In addition, it must be light enough to be installed on a motion system. The truss-type construction proposed is both lightweight and rigid.

Placement of the background projector and optics at the two selectable horizontal FOV positions, will be provided by manually relocating the projector with the aid of pins and bolts.

The entire structure will exhibit a final safety factor of no less than 4:1 based on the ultimate strength of the material at 4g acceleration.

All optical component mountings will be designed to provide sufficient degree-of-freedom adjustment for purposes of alignment.

BACKGROUND IMAGE SYSTEM MTF ANALYSIS.

BIGSystem MTF Analysis. Preliminary data has analyzed the image generator modulation transfer function for the worst case points, within two areas of the field of view, for various aircraft attitudes³². The first area considered points inside a 32-degree radius circle at the center of the FOV, where the specified resolution is given as 1300 resolution elements per picture width. This resolution corresponds to approximately 15 arc-min per optical-line pair. The second area considered point outside the above circle that is within the required FOV. The required resolution is 30 arc-min per optical-line pair in this area.

Analysis shows that the point analyzed would change with aircraft attitude in order to reflect worse-case conditions³³. The total system performance is analysed for the conditions of aircraft attitude limited to a 15-degree pitch down attitude and a roll angle of 90 degrees. The total NATOPS flight profile is within these limits. The 15° pitch down condition is the most stringent shown in figure 89³⁴. The figure also includes the projection system MTF (projector and lens) curve, and the resultant background image system MTF reflected by the 15-degree pitch downward flight attitude. At an MTF of 5%, the TV resolution is shown to be 1150 lines. This is 88 percent of the required, 1300-TV-line resolution. It should be noted that the projector system alone does not meet the total requirement of 1300 TV lines at 5% modulation. The Eidophor projector is the weakest link in the background image system. The analysis has concluded that 1150-TV-line resolution represents the state of the art for the combined system of FSS image generator, wide angle optics design, and Eidophor projector technology.

ALTERNATES.

Background TV Projector. This alternate deals with operating the background projector at 1023 scan lines. Using the target television camera equation, table 16, below results³⁵.

Table 16. SCAN LINE DATA

SCAN LINE	NV	NH	NR	λ_T	λ_d	BW
825	600	1300	13	40.4	33.4	19.46
1023	715	1549	35	32.6	25.6	30.25

The problems with operation at 1023 scan lines are great. First, the available light output is only 50% of the 825 line rate, or about 2000 lumens at the center of the raster. Secondly, the modulation transfer function is well beyond limiting at the 1549 expected horizontal resolution, corresponding to 1023 scan lines and 30.25 MHz bandwidth. Finally, the required 30-MHz bandwidth is well beyond the capabilities of the background image generator as proposed.

Since increasing the background projector line scan rate does not improve the system resolution or performance, it is recommended that the proposed 825-line scan system be used.

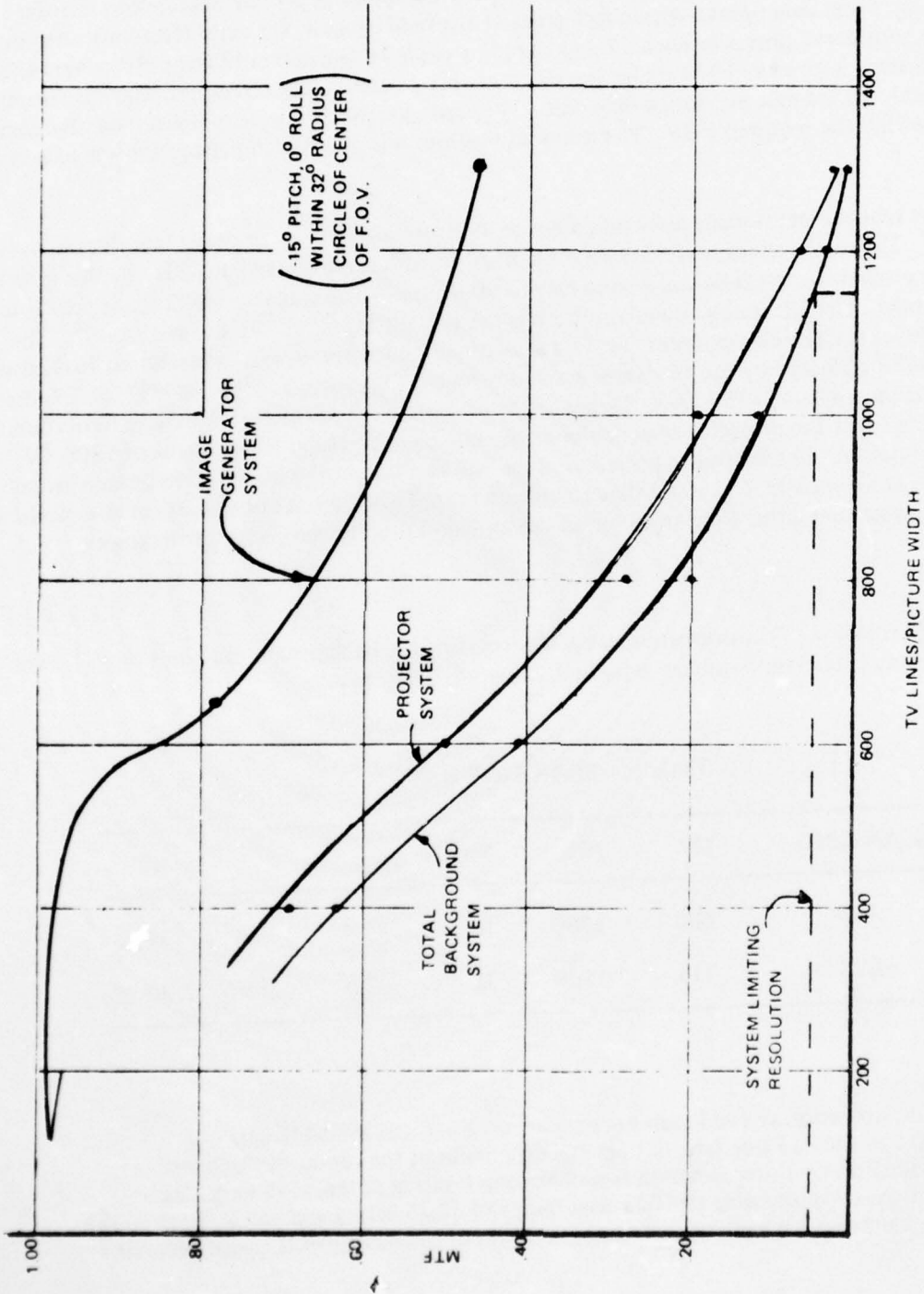


Figure 85. BACKGROUND SYSTEM

SECTION VII

DISPLAY SCREEN

The display screen will be spherical, with an inside radius of 10 feet, held to within ± 0.5 inches.

METHODS CONSIDERED.

Proposed Method. The screen consists of formed, spherical sections of aluminum which are fastened together to form a partial sphere.

Alternate Methods. The only alternate method considered was to develop the spherical screen using light-weight, fiberglass, honeycomb modules which could be bolted together.

DISPLAY SCREEN DETAILS.

Spherical sections of aluminum are sprayed with a reflective coating to obtain the required screen gain and then fastened together to form a partial sphere.

Once the spherical sections have been bolted together, the seams will be covered with thin tape, prior to painting, so they will not be apparent to the viewer when the visual scene is projected on the screen. The lightweight, self-supporting, partial sphere structure will be mounted to and supported by the mechanical structure of the motion platform. If necessary, the motion platform will be extended by means of outrigger supports.

The screen will be rigidly supported so that no movement of the displayed image is observable under normal, simulated-vehicle, acceleration cues. The structure will be designed to withstand a 4g acceleration.

The outside dimensions of the screen support structure will be contained within a diameter no greater than 21 feet. To provide for future extension of the simulated field of view, the spherical display screen will provide a minimum unobstructed field of view of $240^\circ (\pm 120^\circ)$ horizontal and $120^\circ (+90^\circ, -30^\circ)$ vertical, measured from the pilot's design eye position.

The maximum weight of the display screen and supporting structure will not exceed 2,000 pounds, with the weight distributed.

It has been determined in the design analysis study that a gain of 4.3 is adequate to meet the worst case luminance requirements of Specification 212-102, as discussed in the previous paragraphs.

The paint for the display screen will be of a resin base with suspended aluminum particles. The panels will first be cleaned to remove any grease and/or oil deposits, then rinsed and dried. The concave surface will then be sprayed with horizontal overlapping strokes; the gain will be controlled by the number of coats applied.

AD-A037 223

SINGER CO BINGHAMTON N Y SIMULATION PRODUCTS DIV

F/G 1/2

AVIATION WIDE-ANGLE VISUAL SYSTEM (AWAVS). DESIGN ANALYSIS REPO--ETC(U)

APR 75

N61339-75-C-0009

UNCLASSIFIED

AWAVS-1

NAVTRAEQUIPC-75-C-0009-1

NL

3 OF 5
AD
A037223



Either construction method (explained in the first paragraph) provides a screen with a structural and performance capability that satisfies the AWAVS specification. However, final selection of whether to use aluminum or fiberglass should not be made until the flight simulator specification is defined. Then, the type of screen can be selected with regard to taking maximum advantage of the configuration of the simulator motion platform.

SCREEN GAIN.

The minimum screen gain is determined by the transmission of the various projectors and the required minimum 6 ft.-lambert highlight brightness. The background and FLOLS systems require very low gains to meet the minimum requirements. The background projector would require a gain of only one to meet 6 ft.-lamberts minimum and the FLOLS required an even lower gain. With a gain of one, there would be no variation in luminance with either a change in field or viewing position. The target projector however, because of its low transmission requires a screen gain of 4.3 to meet the 6 ft.-lambert requirement. For field points within the required field of view, the maximum bend angle between the observers line of sight and the reflected ray is approximately 6° . For any point in the field, the variation with head motion is approximately 2° .

For a nominal gain of 4.3, the gain at bend angles of 6 and 8 degrees will be approximately 3.8 and 3.5, respectively. Thus, the ratio of minimum to maximum gain is approximately 81%. This percentage would imply that the luminance would vary by approximately 1.25 ft.-lamberts, which exceeds the 1 ft.-lambert variation requirement. Since this variation is both smooth and continuous, it should not detract from the training value. If strict adherence to the one ft.-lambert variation is required, it can be accomplished by a varying neutral density coating on the last element of the background projection lens and suitable modulation of the target projector Eidophor. It should be pointed out, however, that there would be considerable difficulty in obtaining a highly uniform display coating at this gain value which contains no false orienting cues within the pilot's field of view.

SECTION VIII

SERVO SYSTEMS

All servo systems will be designed to meet the requirements of Specification 212-102.

METHODS CONSIDERED.

Proposed Methods. The proposed methods are described below, beginning after Alternate Methods paragraph.

Alternate Methods. All proposed servo design meets the previously cited specification and has been proven on previous simulators (e.g. F-4E-18), therefore, no alternative methods were considered.

MODEL SERVOS.

The Pitch, Roll, Heave - model positioning servomechanisms will be dc-position servos, utilizing dc torque motors with infinite-resolution, follow-up potentiometer. DC tachometers will be utilized to stabilize the loop. In order to provide accurate positioning, minimum gearing will be utilized between load and follow-up potentiometer. Any gearing used will be anti-backlash gearing.

The maintenance control panel located on the gantry, probe, model control cabinet will contain local manual-control potentiometers to position each axis independently. Control mode switches will be located on this panel to select computer or local inputs. The roll, pitch and heave servos will be limited rotation devices and will include electrical switches and mechanical limit stops.

Heading - The heading servo will be larger and will have unlimited rotation and no limit switches. This servo will have an overspeed sense and trip circuit to prevent a runaway disc, should there be an amplifier failure, and will utilize 16-bit digital encoder for the position feedback device. This axis will require two motors to accelerate the large inertia of the 16 ft. dia. disc. Initial layouts utilize a honeycomb construction disc with a central hollow hub with bearings. The light fibers used for deck lighting, as well as control signals for pitch, roll, and heave servos, will pass through this hollow hub. (See figure 86).

Performance Requirements are: (Referenced to scaled values.)

<u>AXIS</u>	<u>RANGE</u>	<u>PERIOD</u>	<u>RATE</u>	<u>ACCEL</u>	<u>ACCURACY</u>
Pitch	$\pm 5^{\circ}$	10 sec	$3.14^{\circ}/\text{sec}$	$1.98^{\circ}/\text{sec}^2$	0.1% of 10°
Roll	$\pm 12^{\circ}$	16 sec	$4.7^{\circ}/\text{sec}$	$1.85^{\circ}/\text{sec}^2$	0.2% of 24°
Heave	± 30 ft	10 sec	18.8 ft/sec	$11.9 \text{ ft}/\text{sec}^2$	0.2% of 60 ft
Heading	Continuous	NA	$42^{\circ}/\text{sec}$	$26^{\circ}/\text{sec}^2$	0.01% of 360°

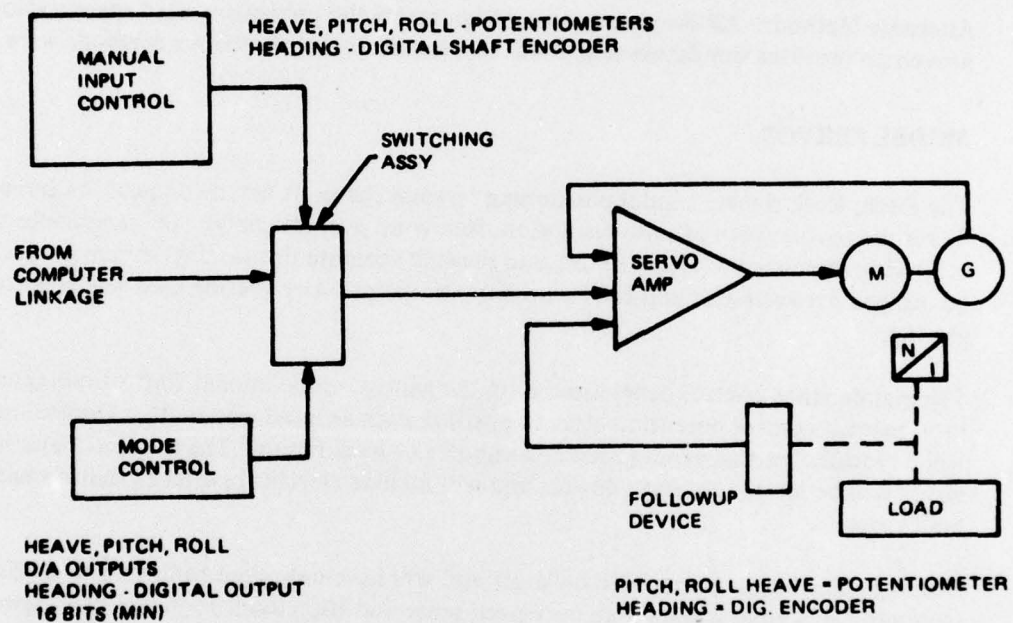


Figure 86. TYPICAL MODEL SERVOS SIGNAL FLOW DIAGRAM

PROBE SERVOS.

The probe assembly will contain 8-position servo mechanisms. These servos will use 400 Hz. motor generators with gear head assemblies geared to 400 Hz resolvers for the followup sensor and the load. In order to increase the accuracy of the heading, derotation, relay azimuth, servos, the resolver element is geared 4:1 to the output shaft. The resolver is therefore excited with 4 x the output angular rotation required. A synchronization system will be utilized to keep these servos in the correct revolution. This synchronization system, when first enabled, drives the output to a known position. It then compares the known position with required position and steps the servo in 45° increments of resolver signal, until it is in the correct revolution. At this time, the resolver drive is switched to the normal drive signal and drives to the proper position in the revolution.

The estimated range of required performance parameters for these servos located on table 17.

Table 17. PROBE REQ'D PERFORMANCE (ESTIMATED)

FUNCTION	PITCH	HEADING	DEROTATE	RELAY AZIM	*TILT/FOCUS	ZOOM	IRIS
RANGE Posit. Tol.	(-90° to +20° ± 0.43 Mins	Continuous ± 0.43 Mins	Continuous ± 0.43 Mins	Continuous ± 6 Mins	Functions of 7.5 to 20.3 Ft. Alt and ± 15° Pitch	Ratio 1:1 to 6.36:1	0.5 to 2.0 Dia. = 4:1 Ratio
VEL	10.6°/Sec	43°/Sec	53.6°/Sec	53.6°/Sec	10°/Sec Alt and 10.6°/Sec Pitch	0.4/Sec	0.25 Dia/Sec
ACCEL	14°/Sec ²	25.6°/Sec ²	39.6°/Sec ²	53.6°/Sec ²	10 Ft/Sec ² and 15°/Sec ²	1.6/Sec ²	1.0 Dia/Sec ²

Pitch = Elevation of LOS Relative to Gantry Axis System
 Heading = Azimuth of LOS Relative to Gantry Axis System
 Derotate = Pitch + Heading + Roll (LOS Roll, if required - Assumed Zero
 Ry Azim = Pitch + Heading

*Actual Servo Drives have Non Linear Mechanisms Requiring Function Storage in Drive Equation

$$\text{Tilt Lens Angle} = \left[\frac{K_1}{\text{Alt}} (\text{Cos Pitch}) + K_2 \right]$$

Tilt Servo Drive = Tilt Lens Angle

Derived for Condition of Max. Rates (For Required Fly By Carrier at 800 Ft. Alt. Passing 500 Ft. Abeam of Carrier at 250 Kts. With Carrier at 30 Kts.)

Requmts Increase - For: Higher A/C Velocity

- Lower Altitude

- Closer Range to Carrier

- Derivation of Math Model for Gantry and Probe will probably Revise These Reqmt's

NAVTRAEQUIPCEN 75-C-0009 -1

The performance available in the Farrand Probe is included in the performance requirements section of the preliminary Probe Specification LR-632 Rev. A as follows (and will be included in the procurement specification for the probe):

<u>Pitch</u>	<u>Pitch Rate</u>	<u>Pitch Accel.</u>
$\pm 135^\circ$	$\omega_\theta = 60^\circ/\text{sec LOS}$	$\alpha_\theta = 80^\circ/\text{sec}^2 \text{ to } 60^\circ/\text{sec } \omega$
<u>Yaw</u>	<u>Yaw Rate</u>	<u>Yaw Accel.</u>
$360^\circ \text{ Unlimited}$	$\omega_\psi = 60^\circ/\text{sec LOS}$	$\alpha_\psi = 80^\circ/\text{sec}^2 \text{ to } 60^\circ/\text{sec } \omega$
<u>Derotate (Roll)</u>	<u>Derotate Rate</u>	<u>Derotate Accel.</u>
Unlimited	$\omega_{\text{DER}} = 360^\circ/\text{sec}$	$\alpha_{\text{DER}} = 150^\circ/\text{sec}^2 \text{ to } 180^\circ/\text{sec}$

GANTRY SERVOS.

The gantry servos will be velocity servos with an outer position loop closed thru the computer. The flow diagram and interfaces are shown on figure 87.

The servos will use dc torque motors and dc tachometer with a minimum gearing between motor and load. Gearing unit used on the Y and Z axes will be Barry Controls Rohlix Rotary-to-Linear Motion converters to provide stepless transmission of force to the loads. The velocity command to the servo itself consists of two components; a) the computed axis velocity based on the flight parameters resolved into the model axis and b) the position error of the gantry relative to commanded position divided by the update computation time period multiplied by a constant to reduce the position error. Thus, inaccuracies in the tachometer feedback will be removed by the position loop. A geared, 17-bit encoder for the X and Y axis feedback is capable of providing greater than 1/7 ft. resolution.

The gantry X and Y servos must be capable of providing the scaled 4-g acceleration imparted to the aircraft during catapult and landing operations. The max. velocity has been set at 400 kts max differential between carrier and aircraft (350 kts aircraft +50 kts carrier or wind).

The servo amplifiers will be dc power amplifiers with adjustable current limit to enable the motor power rate to be limited to safe values. Each axis will contain electrical limit switches to stop the drive (before it reaches the mechanical limit stops) and overspeed sense circuitry to protect the motors and hardware from full command amplifier failure. These limit and overspeed circuits will disconnect the amplifier from the motor and close the motor armature circuit through a resistor, thus providing dynamic braking.

The servo systems stability networks will be included in the amplifier assembly.

Predicted Performance (Scaled in Parens):

<u>AXIS</u>	<u>RANGE</u>	<u>VELOCITY</u>	<u>ACCEL</u>	<u>RESOLUTION</u>	<u>HIGH SPEED TRACKING ERROR</u>
X	28 FT (8343)	2.186 FT/SEC (400 KTS)	0.4168 FT/ SEC ² (4G)	0.000427 FT ≅ (1/8 FT)	0.028 FT @ 2.186 FT/ SEC
Y	14 FT (4326)	2.186 (400 KTS)	0.4168 (4G)	0.000427 ≅ (1/8 FT)	0.014 FT @ 2.186 FT/ SEC
Z	2.912 FT (900 FT)	0.260 (6100 FT/MIN)	0.3126 (3G)	0.000427 ≅ (1/8 FT)	0.0029 FT @ 0.26 FT/ SEC

FLOLS Δ X, Δ Y DISPLACEMENT SERVOS.

Due to the extremely high accuracy requirements of the Δ X, Δ Y, displacement servo, all efforts will made to reduce servo errors. The torque motor will be of the brushless type, thus eliminating torque ripple and greatly reducing the friction. The feedback transducer will be an optical encoder or a precision film potentiometer. Figure 88 shows a schematic for a typical ΔX, ΔY, servo configuration.

Because of the high precision, a brushless tachometer will be used to provide sufficient stability with high-loop gain. A precision gear, gear box is required inside the feedback loop to allow the torque motor to cover a larger excursion. Both rate and position are sensed at the load to insure the best control of the mirror displacement. Care will be taken to minimize the friction in the gear box to assure smooth motion with high displacement resolution.

Because of the high resolution and linearity requirements, a linearity of 0.05% will be assumed with a resolution of at least 0.01%. The position feedback for these servos could be a precision film potentiometer of a type similar to CIC series 300 which is a 3-inch film pot with infinite resolution. A brushless-torque motor similar to the Kearfott CV 9600 series. These motors have no torque ripple (no brushes) and have limited rotation capability.

The use of an optical encoder may also be applicable here. A 13-bit encoder has accuracy of 2.63 arc-min., and a resolution of $1/8, 192 = 0.01\%$. These encoders are available from a few sources with reasonable size and electronic service requirement.

FLOLS Zoom Servo. The zoom servo does not have the stringout requirements that the ΔX, ΔY displacement servos have.

Therefore, a more conventional type of servo will be used. A ring on the zoom lens will be driven by a gear through a gear box to a motor. The feedback will be taken from the output to provide the best resolution and repeatability. A film pot will be used to sense the position information the rates and acceleration requirements can be met with readily available servo components.

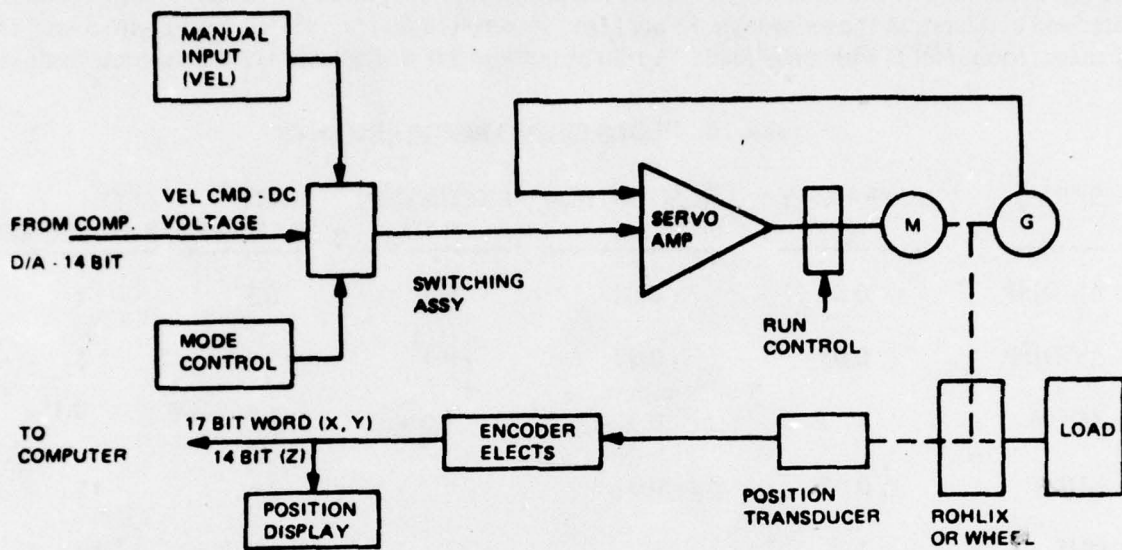


Figure 87. XYZ SERVO SIGNAL FLOW DIAGRAM

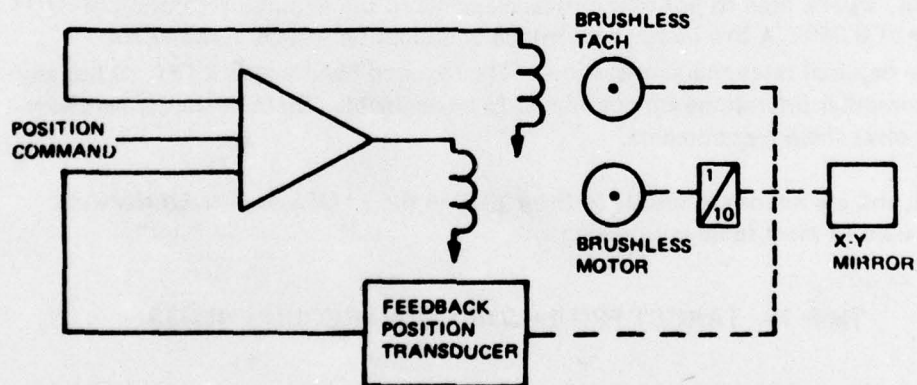


Figure 88. $\Delta X, \Delta Y$, DISPLACEMENT SERVO

FLOLS Iris Control. The iris control will require less design effort, because of reduced system requirements. The rates and acceleration shown in table 18 are high. However, a geared, printed motor with a tach should satisfy these requirements with small loads. A film potentiometer will be used for the position feedback.

Table 18. FLOLS SERVO REQUIREMENTS

SERVO	LINEARITY %	RESOLUTION %	EXCURSION RAD	RATE RAD/SEC	ACC RAD/SEC SEC
ΔX DISP	0.05	0.01	0.1	0.5	1
ΔY DISP	0.05	0.01	0.1	0.5	1
ZOOM	1	0.3	1.0	1.0	0.1
ROLL	0.05	0.01	π	2π	15
IRIS	1	1	2	10	40

TARGET PROJECTOR SERVO SYSTEMS.

The target projector servos are described in section 3. Table 19 shows a summary of the target projector servo requirements. The azimuth and elevation servos will be considered to be the same type of servo, even though azimuth drives a slightly larger inertial load than elevation. Optical encoders (13-bit) will be used to position optical elements to the required resolution of 0.01% with a linearity of 0.05%. A low inertia motor-tach combination will be used to drive the loads at the required rates and accelerations. The required band width is 1 Hz. Thus any errors due to computer iterations are considered to be negligible. State-of-the-art hardware will be used to meet these requirements.

The zoom, roll, and iris servos are similar to those used in the FLOLS and straightforward designs will be used to meet these requirements.

Table 19. TARGET PROJECTOR SERVO REQUIREMENTS

SERVO	LINEARITY %	RESOLUTION %	EXCURSION RAD	RATE RAD/SEC	ACCELERATION RAD/SEC SEC
AZ	0.05	0.01	5	5	15
EL	0.05	0.01	3	5	15
ZOOM	1	0.1	π	1	0.1
ROLL	0.1	0.01	π	π	15
IRIS	1	1	$\pi/2$	10	30

SECTION IX

TARGET INSETTING

The object of this section is to present proposed and alternate methods of system design to accurately generate a "hole" in the background raster into which the independently projected, high-resolution target image will fit. This system must work from a target image which subtends 60 degrees out to a simulated range of 6 nautical miles where the carrier end view will subtend only about 20 minutes of arc.

METHODS CONSIDERED.

Proposed Methods. The proposed visual system employs separate image generation devices and image projectors for both the background and the model (target).

Alternate Methods. Alternate methods are discussed beginning page 216.

PROPOSED TARGET INSETTING DESIGN.

The overall accuracy on target video inseting can be divided into three section as follows:

$$\begin{array}{ccccc} \text{Accuracy of Computer} & & & & \text{Accuracy of} \\ \text{Outputs Containing} & & & & \text{Target Insetting} \\ \text{Elliptical Information} & + & & + & \text{Accuracy of} \\ \text{at any given Time} & & & & \text{Projectors} \end{array}$$

The purpose of this analysis is to determine the exact accuracy and method of blanking with given conditions of projectors and computer outputs.

Integration of the above three parts can be made after studying individual portions. The following analysis is for the target inseting module alone on a X-Y plane coordinate system, the coordinate system on the projector plane.

METHOD OF BLANKING.

"FOV" elliptical blanking can be realized physically in two ways:

- 1) By employing analog computing circuitry ³⁶.
- 2) By using digital computing circuitry as shown in this report.

SYSTEM TOLERANCE.

Before attempting to make any analysis of blanking methods it is desirable to note required system blanking accuracy in terms of various system variables.

For background video:

Horizontal resolution:	1300 TV elements
Scanning time per horizontal line:	33.4 microseconds
Display Screen width:	$(\pi r) \frac{160}{180} = (10' \pi) \frac{160}{180} = 27.925' = 335.103''$
Projector viewing angle horizontally:	160 degrees

Therefore,

$$\frac{33.4}{1300} = 25.69 \text{ nanoseconds/horizontal TV element}$$

$$\frac{335.103''}{1300} = 0.257''/\text{horizontal TV element}$$

$$\frac{335.103''}{160 \times 6} = \frac{335.103''}{960} = 0.349''/10 \text{ arc-minutes}$$

25.69 nanoseconds horizontal scanning time is equivalent to 0.257 inches on the display screen.

The accuracy of the inseting techniques will be 48 arc-minutes horizontally and 24 arc-minutes vertically. A design goal will be ± 20 arc-minutes in both directions, and the design analysis will be presented with the design goal in mind. Thus 20 arc-minutes is equal to $0.349 \text{ in.} \times 2 = 0.698 \text{ in.}$ on the display screen. 0.698 in. on the display screen is:

$$0.698 \times \frac{100}{33.5103} = 0.21\% \text{ of display screen width; and } 25.69 \text{ ns} \times \frac{0.698}{0.257} = 69.77 \text{ ns}$$

of one horizontal line scanning time.

ANALOG ELLIPTICAL BLANKING.

Figure 89 shows a simple analog blanking circuit, and figure 94 represents error terms in 93 circuit.

As derived later on in this section, the design goal of the target inseting accuracy is ± 20 arc minutes or $\pm 0.21\%$ of screen width.

Figure 90 shows that an analog blanking circuit generates considerably more than 0.21% error.

In summary, an open loop analog blanking circuitry cannot meet the background raster hole positioning design goal accuracy requirements.

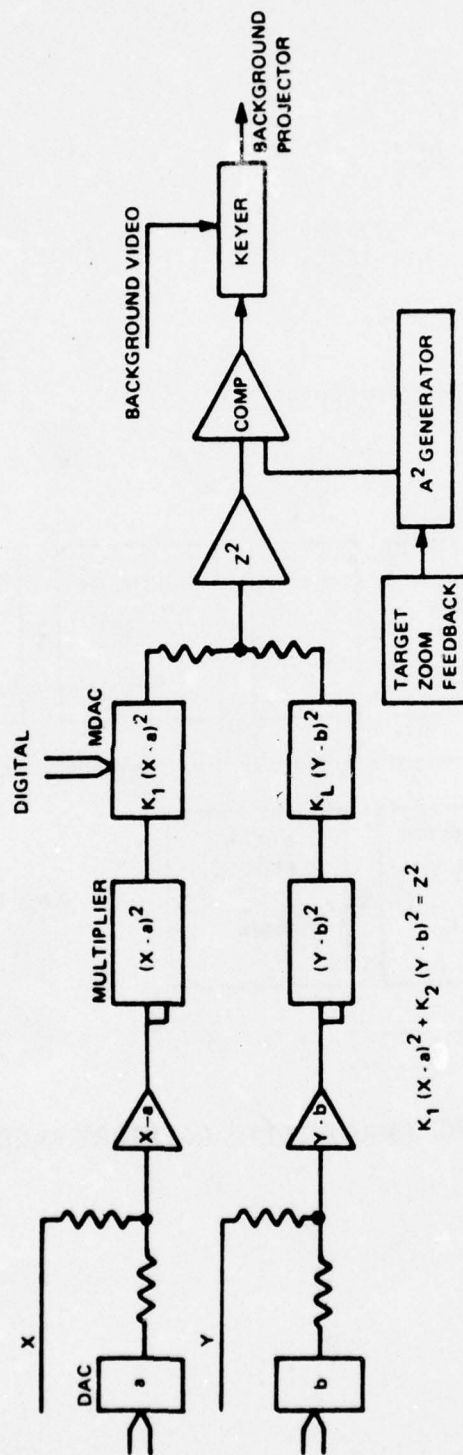


Figure 89. SIMPLE ANALOG CIRCULAR BLANKING CIRCUIT FUNCTIONAL BLOCK DIAGRAM

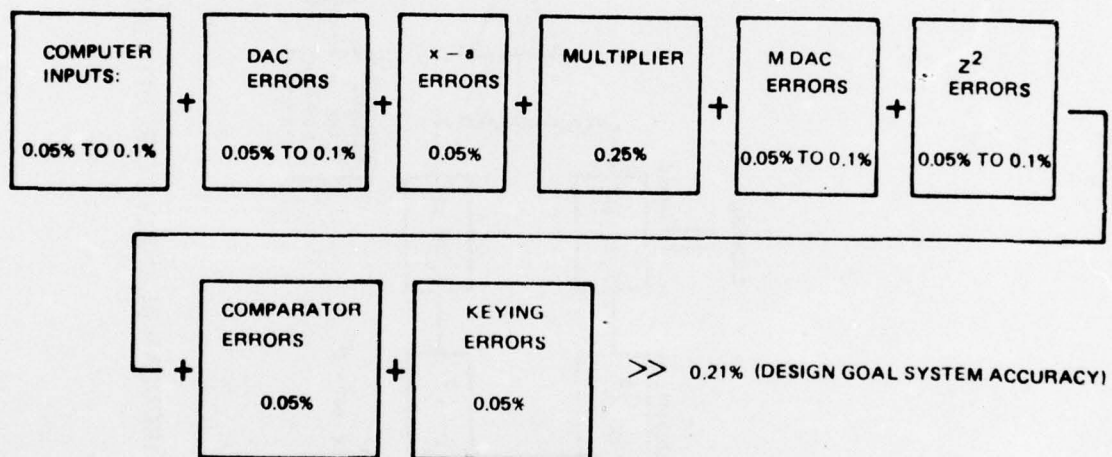


Figure 90. ERROR TERMS IN FIGURE 93 CIRCUIT

DIGITAL ELLIPTICAL BLANKING.

The following analysis will show that digital blanking circuits meet the accuracy requirements of the design goal.

Figure 91 of this analysis illustrates a block diagram of "FOV" blanking which is applicable to the digital approach.

The positional information in a video signal is contained implicitly in time domain, that is, to the time taken to arrive at a given position. Therefore, elliptical blanking coordinates may be calculated and expressed in time domain.

A video signal in time domain is shown in figure 92.

An ellipse on a X-Y plane coordinate system with given center position, elevation and azimuth is illustrated in figure 93.

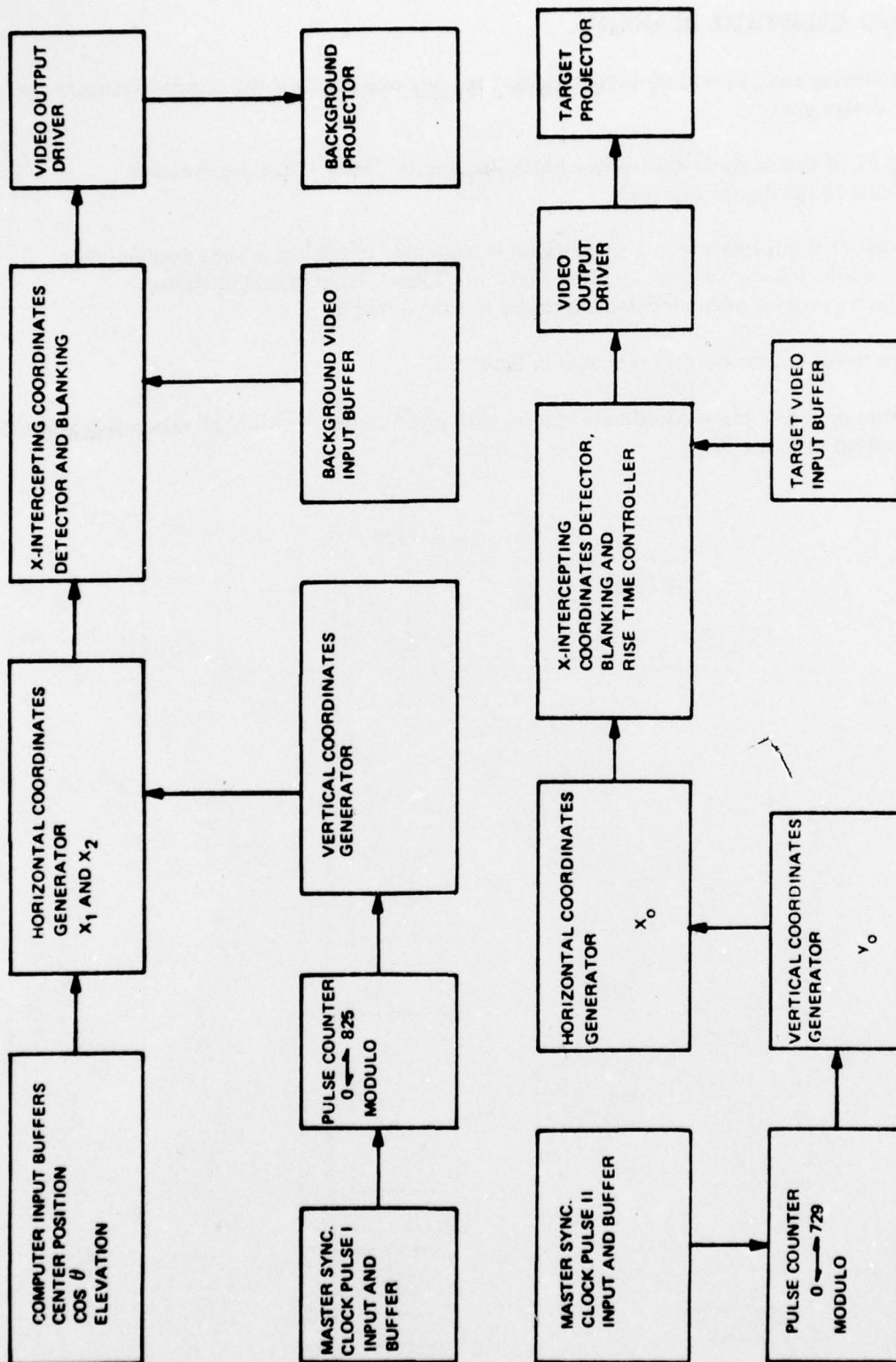


Figure 91. FOV ELLIPTICAL BLANKING BLOCK DIAGRAM

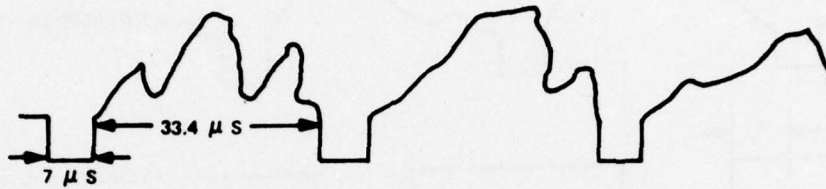


Figure 92. A VIDEO SIGNAL

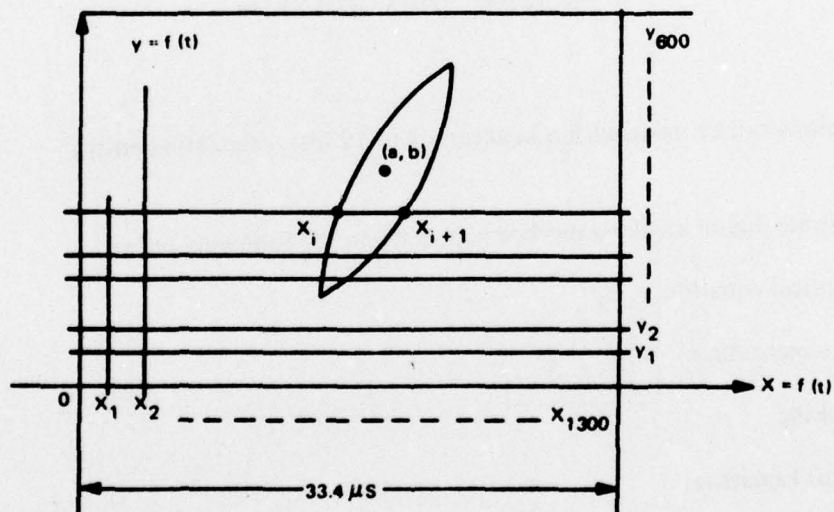


Figure 93. TIME DOMAIN ELLIPSE ON X-Y PLANE

By calculating $x_i = f(t)$ and $x_{i+1} = f(t)$ accurately, the desired blanking signals can be generated.

Figure 94 represents unchopped video, blanking and blanked video signals.

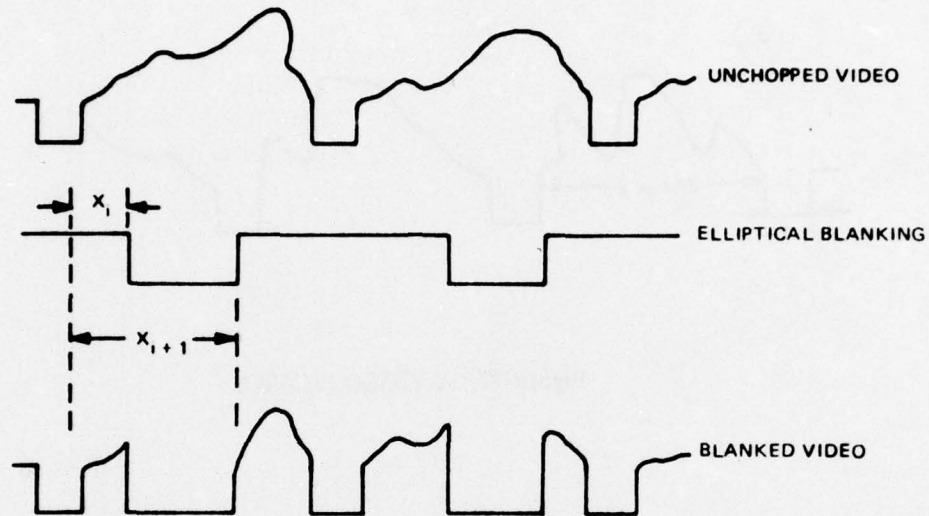


Figure 94. VIDEO BLANKING

Since calculations can be made within an accuracy of 12 bits, calculating errors are negligible.

Studies of possible digital blanking methods are made in the following order:

- 1) Elliptical equation
- 2) Implementation
- 3) Blanking

9.4.1 Elliptical Equation.

A general elliptical function located in a plane may be expressed by the equation

$$\begin{aligned}
 &A \left[(x \cos \theta + y \sin \theta) - a \right]^2 + \\
 &B \left[(-x \sin \theta + y \cos \theta) - b \right]^2 = C^2
 \end{aligned}$$

The equation represents an ellipse with the major axis rotated by θ when referenced to the raster plane X - Y coordinates. The equation for an ellipse may be rewritten in the following form on an X - Y plane (see section 10.6 for the math model discussion):

$$K_1(X)^2 + K_2(X) + K_3(XY) + K_4Y + K_5Y^2 + K_6 = 0$$

The system computer will calculate the values for K_1 through K_6 and feed the high speed special purpose processor to be developed for this purpose.

For each value of Y, or each horizontal line value, the equation reduces to

$$Ax^2 + Bx + C = 0$$

where

$$\begin{aligned} A &= K_1 \\ B &= K_2 + K_3Y \\ C &= K_4Y + K_5Y^2 \end{aligned}$$

Implementation. The system will be implemented with a special purpose high speed processor. The equation will be solved during one horizontal line time, the answer stored, and used during the next horizontal line. Thus the time available is $40 \mu \text{ sec}$. It is well within the state of the art to perform the necessary calculation of multiplications, addition, and square root using dedicated hardware to an accuracy of 12%, bits in the $40 \mu \text{ sec}$ available.

Figure 95 illustrates a simple video chopper circuit.

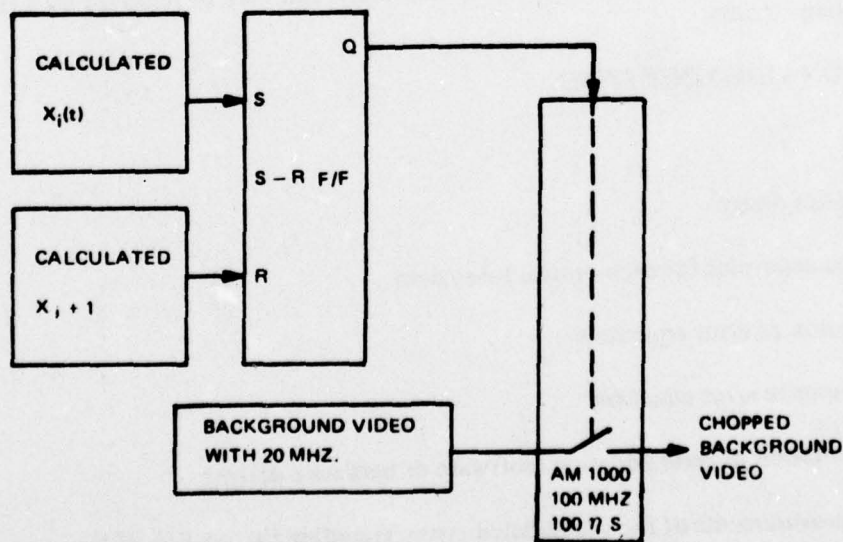


Figure 95. SIMPLE VIDEO CHOPPER CIRCUIT

NAVTRAEQUIPCEN 75-C-0009-1

Switching time error of AM 1000 is 26 nanoseconds for the worst case. Hence, the worst condition error of the entire inseting module is: calculating error and switching error = inseting error.

calculating error = 0.025% or 2 arc-minutes for 12 bit for background

switching error = 26 ns or 7.5 arc-minutes for background

or

inseting error = $2 + 7.5 = 9.5$ arc minutes for background

Therefore, worst case error would be opposite errors in the target and the background projectors, or:

Target error + projector error = total worst case error.

Thus:

Target projector error = 3 arc minutes out of 60° FOV

Background projector errors = 9.5 arc minutes out of 160° FOV

Total error = $9.5 + 3 = 12.5$ arc-minutes

which is within the 20 arc-minute error goal set as a design goal.

Since the errors are caused by the two similar devices, the AM 1000, running in parallel, it is expected that they will tend to cancel each other out, and reduce the error from the worst case analysis. The RMS error expected should not exceed 10 arc minutes for the combined systems. The error, due to the AM 1000, is a fixed time delay, and may be removed by a time delay in the inseting circuits.

ERROR TERMS ON VIDEO INSETTING.

Steps to be taken:

- 1) Final optics design
- 2) Predicted error plot for each optical subsystem.
- 3) Formulation of error equations
- 4) One composite error equation
- 5) Implementation of error equation (software or hardware design)
- 6) Actual measurements of the unpredicted errors including the portion of the predicted error plots which can not be formulated in equational forms. These measurements will be done on the final system and interpolated in the computer.

Assumption. Eidophor projectors are devices of linear transformation; that is video scanning time is a linear function of physical distance on the display screen. Any deviation from the above assumption will be corrected by error equations defined in item c) below.

$$t = f(X) = a x + b$$

t = scanning time

x = distance proportional to t

a, b = constants

From the above assumption, it can be seen that an ellipse input to the projectors will be displayed on the spherical display screen without any distortion, provided physical arrangements introduce no errors. This is true without respect to video image inputs to the projectors.

There are four major error terms on video inseting:

- a) Errors introduced by a wide angle lens of $160^{\circ}\text{H} \times 80^{\circ}\text{V}$ where the error function can be represented as $x_e = f(t)$; i.e.

x_e = error distance projected on the display screen proportional to the scanning time on the projector.

- b) Projector and eyepoint off-axis error due to the actual locations on the cockpit where the (for illustration, see figure 96) error position of background projector on the display screen relative to the target projector on the display screen can be represented as:

$$x_B = f(x_T, t)$$

x_B = displayed error position of background projector relative to the target projector position x_T at a given scanning time t.

- c) Errors on the display screen due to physical nonuniformity: These errors can not be formulated as a functional equation because they are randomized errors. These errors must be interpolated in the computer by actual measurements on the final system, if errors, due to the display screen, are significant.
- d) Errors on target projector optics: These are the most troublesome errors. Errors in the above a), b) and c) are static errors, and relatively easy to formulate in the form of equations. Errors on the target projector optics are the combination of static and dynamic conditions with four optical variables.

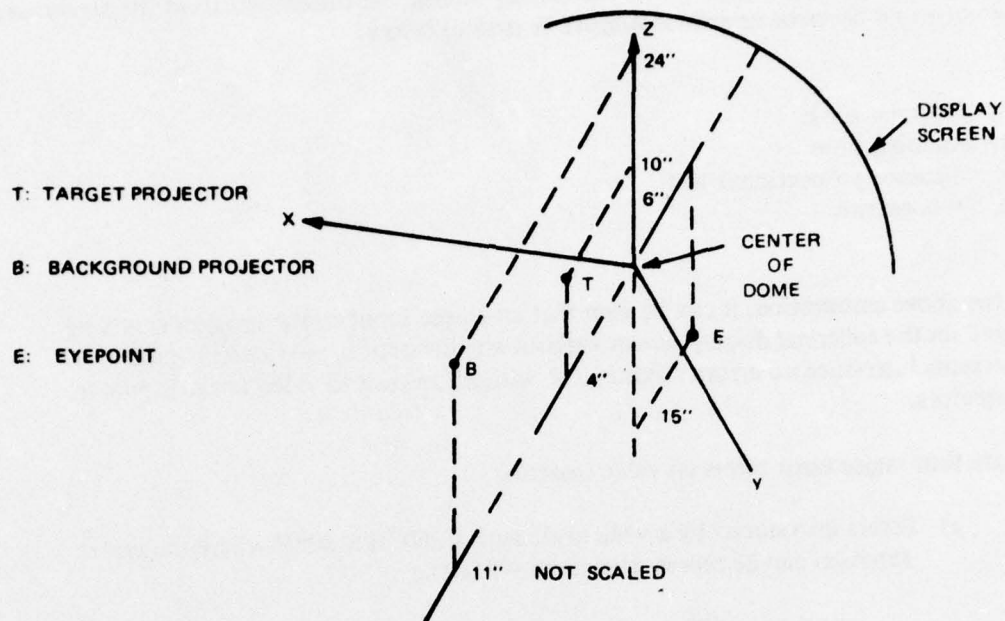


Figure 96. POSITION OF PROJECTOR RELATIVE TO THE DISPLAY SCREEN

The error functions of the optics are approximated as follows:

x_z = amplification error due to zoom change input $Z_r = f(Z_r)$.

x_r = azimuth error due to azimuth input $A_r = f(A_r)$.

x_y = yaw error due to yaw input $y = f(y)$.

x_p = pitch error due to pitch input $p = f(p)$.

ERROR ANALYSIS.

Error sources on video inseting were previously examined ³⁶. The following are the initial approximations. **Figure 97** illustrates the effects of system mapping errors of a target projector circular pattern onto the background projector image plane.

Mapping Errors. Initial, graphical analysis, using a circular target blanking, projected on a coordinate of $+30^\circ$ and -50° of the background, using maximum, circular blanking on the target, and matched with an ellipse on the background raster, indicates a maximum error of $\pm 1^\circ$, due to fitting errors. The error will diminish as the target is moved to the center. The maximum error derived is approximately $\pm 2.5\%$, of the projected target FOV diameter, and is probably a constant with target size in a given location. Therefore, with zoom the absolute error due to mapping will diminish.

The analysis at this time has indicated a need for further analysis, and an analytical analysis of the mapping error is continuing for a more precise answer.

Before proper analysis can be completed, the elliptical fitting function must be derived, and used in the final system configuration.

The errors, due to mapping of the projector surface, can be ascertained accurately knowing the mathematical relationships of the system. These errors will be a linear function that, if necessary, can be derived using the digital approach, previously described.

Time and Temperature Projector Mapping Errors. The Eidophor mapping surface has a mechanical-optical tolerance that shifts with time and temperature. Experience with Gretag's Eidophor projector, indicates a stability of 0.3 to 0.5%. The long-term drift is unknown at this point, but it seems reasonable that if the center of the raster can be aligned with the center of the display, and the size adjusted at the edges on a periodic basis, the long term drift should be minimized.

Analyzing the 0.3 to 0.5% errors over the 160° background gives an error of 0.5° to 0.8° or as much as 30 arc-min to 48 arc-min, due to the time and temperature drifts.

The target projector errors, over the 60° field of view, amount to 12 arc-min to 18 arc-min. It is recognized that the system will be on a motion system, and that the dynamics involved in a moving and accelerating field will change the structure of the oil surface and cause additional error of unknown amount.

The combination of the errors could involve as much as 42 arc-min to 66 arc-min. Under worst case conditions, the average error will be less. And since target projector error is a percentage of the target projector, the error decreases as the zoom is activated.

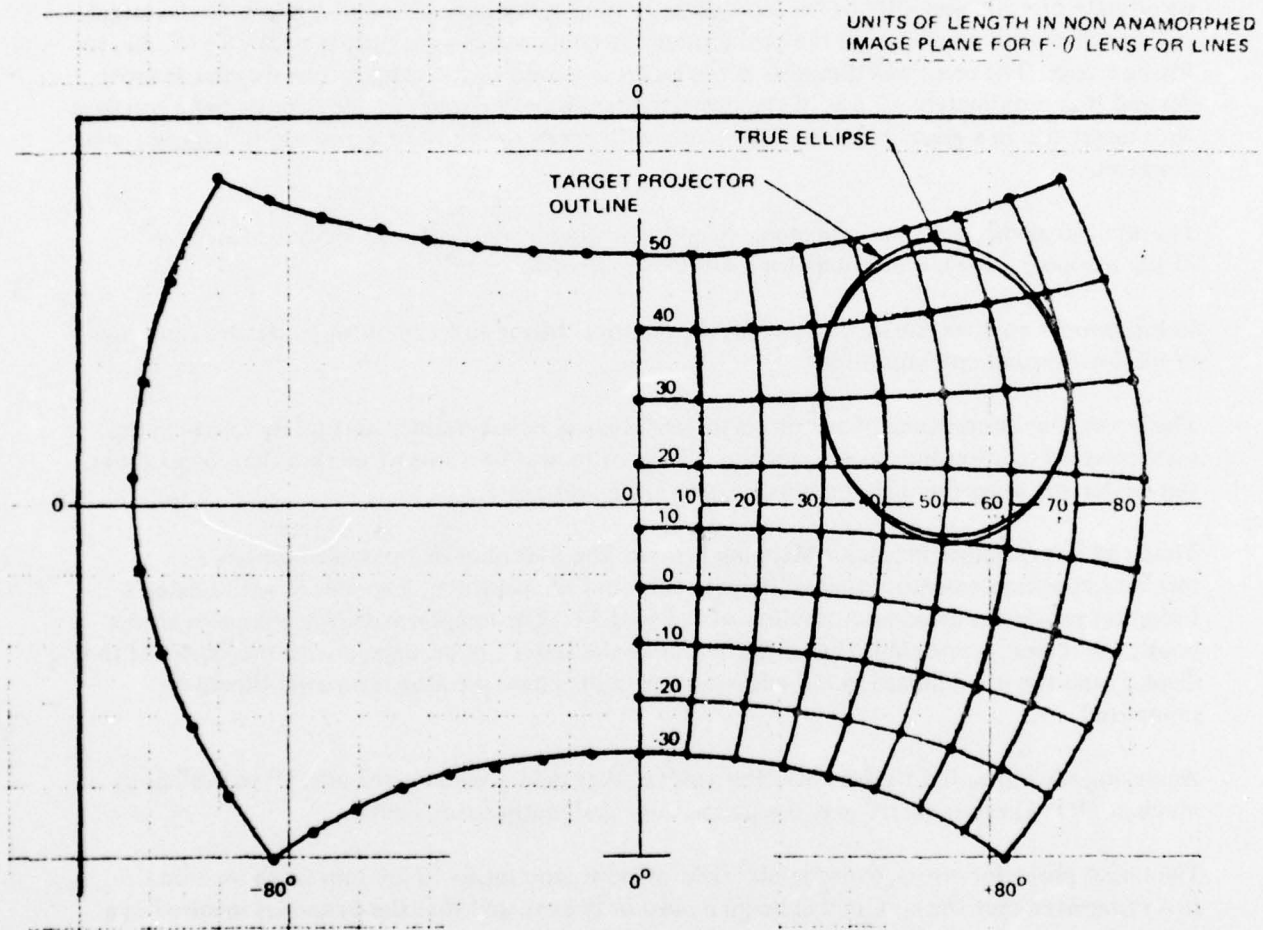


Figure 97. SYSTEM MAPPING ERROR

Target Projector Servo Pointing Error. The error involved with the target projector servo pointing capability was previously ³⁷. A summary of the error analysis is as follows:

Elevation and azimuth pointing errors = 10 arc-min

Zoom = 2 arc-min

Roll = 20 arc-min

The roll error of 20 arc-min translates to 6.7 arc-min of motion with respect to the eyepoint target projector image for the 30-degree half-angle field of view.

The zoom error of 2 arc-min is due to the wandering of the center, during the zoom travel.

Summations. Summing up the errors we have:

1) Error from mapping: mathematically desired, $\pm 1^\circ$ for maximum target and displacement.

2) Error due to Time and Temperature:

Background: ± 30 arc-min to 48 arc-min

Target: ± 12 arc-min to 18 arc-min (60° FOV)

3) Target projector servo pointing errors:

Elevation and azimuth error: ± 10 arc-min

Zoom center: ± 2 arc-min

Roll: ± 6 arc-min

4) Target inseting module error (rms): 0 to 10 arc-min

Insetting Method. Assumption:

The contrast ratio between carrier and seascape is a minimum of 20 mv for all simulated conditions.

$$V_S + 20 \text{ mv} \leq V_C$$

Where: V_S = Video amplitude of seascape

V_C = Video amplitude of carrier

For the target video:

Horizontal resolution is 700 TV elements.

Viewing angle horizontally is 60° .

One horizontal line scanning time is $38.7 \mu\text{s}$

Target video signal is 9.1 MHz.

$$\therefore \pi \times 10' \left(\frac{60}{180} \right) = 10.47' = 125.66'' : \text{display screen width for } 60^\circ \text{ width}$$

$$\frac{125.66''}{700} = 0.1790''/\text{TV horizontal element}$$

$$\frac{38.7 \mu\text{s}}{60^\circ \times 6} = 107.50 \text{ ns}/10 \text{ arc-min}$$

$$\frac{38.7 \mu\text{s}}{700} = 55.28 \text{ ns}/\text{TV horizontal element}$$

$\therefore 0.179''$ on the display screen is equivalent to 55.28 ns of scanning time.

The extent of the degraded picture quality of the carrier image due to the special effects video insetting is:

$$\frac{10 \text{ ns}}{55 \text{ ns}} (\text{one horizontal TV element}) \approx 1/5 \text{ TV element for the worst case.}$$

With the special effects video insetting accuracy of 1/5 horizontal TV element (worst case) derived above, no significant errors are expected for all simulated conditions.

Figure 98 Shows the Simple Blanking Circuit.

The worst case of video blanking is represented by figure 99.

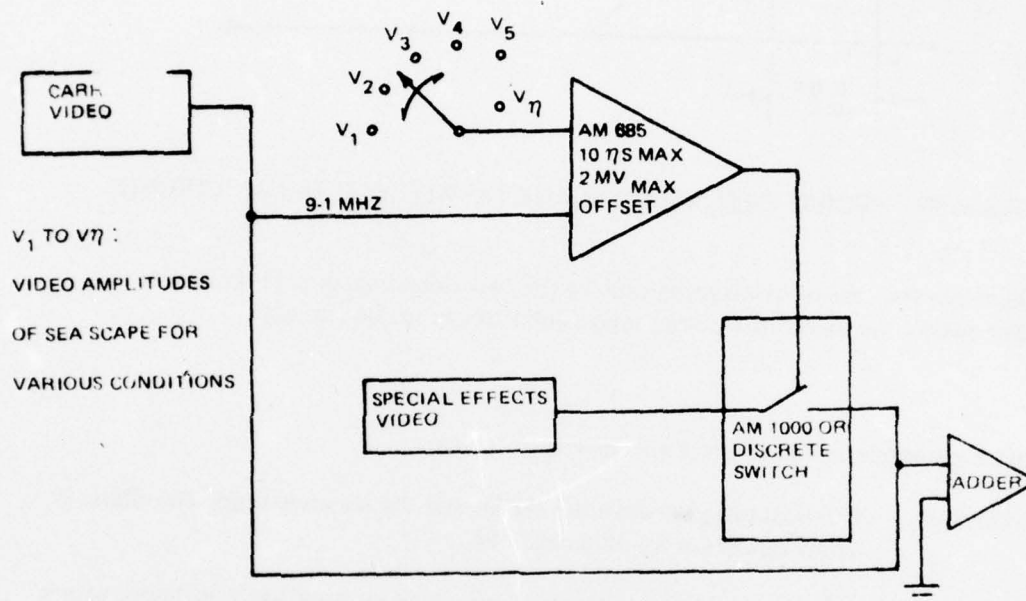


Figure 98. A SIMPLE BLANKING CIRCUIT

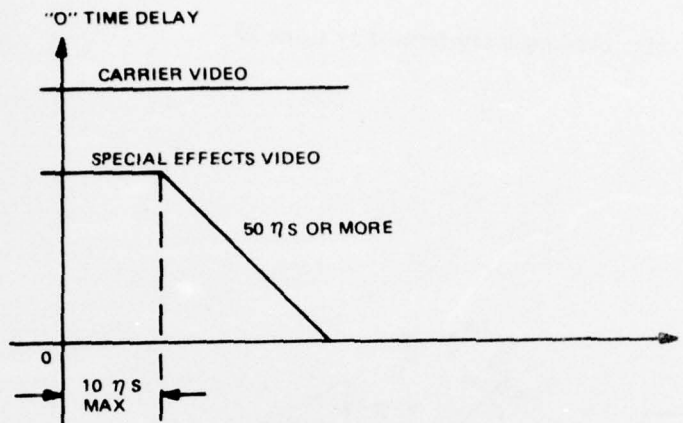


Figure 99. WORST CASE VIDEO BLANKING WITHOUT DELAY CIRCUIT

As seen above, the worst case of overlapping time of the two video images is 10 ns. due to the comparator delay time (without a carrier image delay device in the circuit).

SUMMARY.

The following is a summarization of the above proposed system:

- 1) Condition: Contrast ratio between the carrier and the seascape inside the ellipse is 20mv minimum for all conditions.
- 2) Accuracy:
 - a) Proposed digital blanking generator by itself has a negligible effect on inseting accuracy.
 - b) Overall major inseting error is introduced by the 4 optical components placed in front of the target projector, and will be compensated for in the error correction generator which acts on the blanking generator output.
 - c) Other system errors which can not be formulated in equational forms will be measured on the final system and be interpolated in the computer.
- 3) Perspective quality: The nature of "FOV" elliptical blanking itself generates an unrealistic view on the display screen due to the difference of contrast, wave pattern, etc. between the background seascape and fixed seascape surrounding the carrier model inside the ellipse.

Magnitude of possible errors introduced by the whole system is an open question. To what extent the errors can be corrected by actual measurements on the final system and interpolating those in computer is also an open question. We will attempt to answer these questions when vendors supply the actual hardware.

ALTERNATES.

Background Seascape Scanning. To surmount the errors in the optical components and to reduce the perspective problem, installation of one background seascape scanning system in the target generator is a solution.

It does not eliminate optical errors, but eliminates the unmatched seascape problem. Insetting inaccuracy effects due to optics have little affect on the inseting quality.

Figure 100 shows the inseting accuracy and the improved perspective quality of the seascape along the edge of the ellipse.

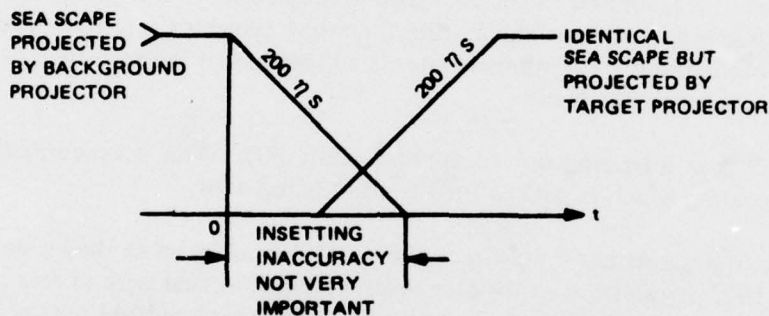


Figure 100. INSETTING OF SEASCAPE ALONG THE ELLIPSE

Addition of scanner also simplifies the elliptical blanking circuitry. Since there is no need to change the size and shape of ellipse, an ellipse with fixed size and shape can be used for blanking the target and background projectors. This reduces the variables of elliptical equation, simplifies the equation, and hence, the inseting hardware.

In summary, an additional background seascape scanner in the target image generator system a digital blanking generator for target and special effects image as described elsewhere in this report shows promise of providing a superior method of video inseting.

Scene Keying Design Considerations. In the projected scene-keying approach, a keying signal is developed from the projected target image. This technique has the advantages of including all anomalies within the blanking, and being able to blank just where the carrier is located. The technique utilizes an image Isocon camera and lens, positioned next to the background projector. The camera will produce a signal only when its scan line crossed the carrier image.

The camera lens is a scaled version of the background projector lens. This lens makes the geometry of the scan on the camera tube nearly identical to that of the Eidophor. Both the background projection lens and scene-keying camera lens will have filters in them. They will have opposite transmission from each other. This will prevent the background image from reaching the camera tube. The target image will get through because it is not filtered.

The optical filters will be located in the least-divergent area of the lens, because the dielectric type of filter's transmission spectrum is very sensitive to incidence angle.

The keying camera raster will be calibrated to the background projector. It is done by removing the optical filter in the background projector and leaving the target projector off, while projecting a reference pattern in the background. The camera raster is adjusted until the reference pattern is detected at exactly the conjugate scan point.

The lens on the camera will have a transmission of approximately 80%. This is accomplished by utilizing an antireflection coating which is peaked for the band being used.

The Isocon (RCA 4807 or equivalent) has a peak response at 440 nanometers as shown on figure 101. By consulting figure 102, it can be seen that the visual response is near zero at this point. Therefore, it appears that this is a good, central point to pick for the narrow-band optical filter. However, one other thing needs consideration before making the choice: the spectral transmission of the target lenses.

Since the target projector contains many lenses, it will probably have reduced transmission in blue, since the off-the-shelf lenses will have coatings optimized for the green region, and flint glasses generally have lower blue transmission. However, these are usually not more than 1/2 of the green transmission. The arc lamps higher blue content, the Isocon's higher responsivity and negligible effect on the background image colorimeters makes 440 a good choice for the center of the band.

The net result of the Isocon's sensitivity and target projector image's spectral energy distribution is about a uniform signal with wavelength from 400 to 470 nanometers.

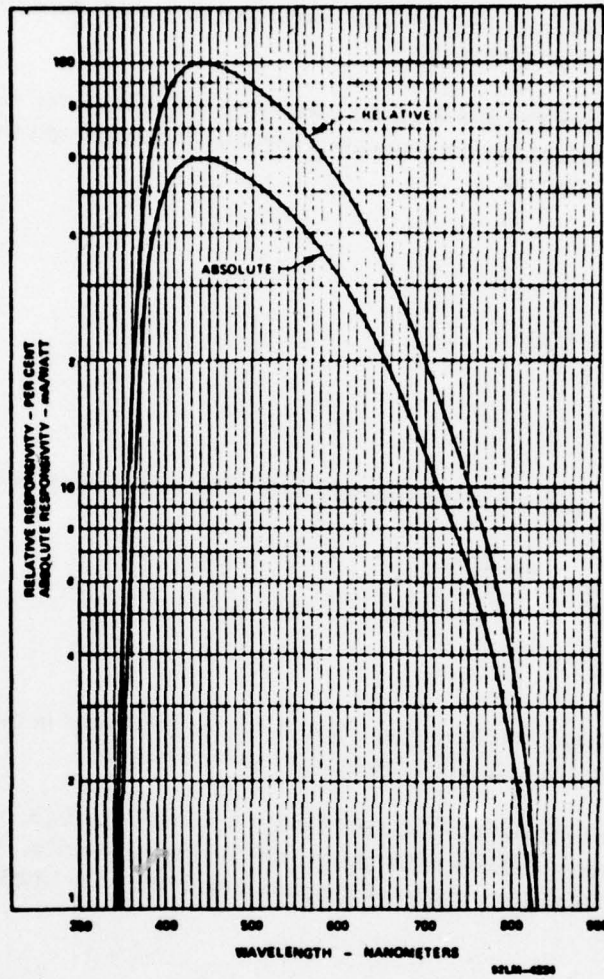


Figure 101. TYPICAL S-20 SPECTRAL RESPONSE

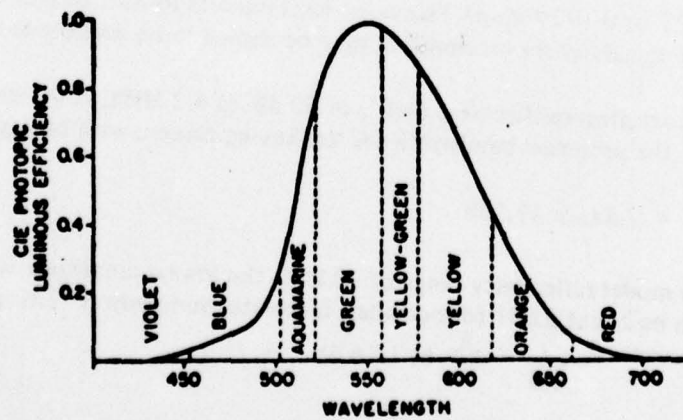


Figure 102. VISUAL RESPONSE

For estimation purposes, a band from 400 to 470 is considered to provide about 70/300 of the energy output of the target projector.

As an estimate, the luminosity of the screen can be used. At $B = 6$ ft-lamberts, the fraction accepted is $w = 7/30$. The required Isocon luminance is $I_f = 0.01$ ft-candles, and the $f/\text{No.}$ can be determined from the equation:

$$N^2 = \frac{0.2 BW}{I_f}$$

$$= \frac{0.2 \times 6 \times 7/30}{0.01}$$

$$N = 5.3$$

The transmission of the keying lens is approximately 80%. This will decrease N by the square root of 0.8:

$$N_{\text{required}} = 5.3 \sqrt{0.8} ;$$

$$= 4.7 ;$$

Thus it may be concluded that a lens having an $f/\text{No.}$ of 4.7, when utilized in the above-described system, will provide sufficient light level on the faceplate of the Isocon.

For the conditions described above the RCA 4807 Isocon has a S/N of 33 db, over a 4.2-MHz bandwidth, which will degrade to 27 db at the proposed, 16-MHz bandwidth. The implication of this is that the noise in the white portions of the picture will be due to Isocon photon noise and equal to:

$$\frac{0.7v \text{ video output}}{27 \text{ db}} = \frac{0.7}{22} = 0.032v_{\text{rms}},$$

Which equals $6 \times 0.032V$ or $0.192V$ vp-p. This noise level reduces to near zero at the low amplitude levels of the signal, where preamplifier, may be shown to be negligible as follows:

- 1) State of the art preamplifier have SNR 's of 52 db, at 4.2 MHz, at $0.3 \mu a$.
At 16 MHz, the proposed bandwidth for the keying camera will be degraded by

$$\left(\frac{16}{4.2}\right)^{3/2} = 7.5x, \text{ or } 17.5\text{db.}$$

- 2) Assuming a model reflectivity range of 10 to 1, the lowest amplitude signal from the Isocon will be $2\mu a$ at 0.001 foot-candles, faceplate illumination. This provides an improvement of $\frac{2}{0.3} = 6.7$, or 16.6 db.

Thus, the preamplifier S/N equals $52 \text{ db} - 17.5 \text{ db} + 16.6 \text{ db} = 51.1 \text{ db}$, and may be disregarded, considering the development of a keying signal from a video signal having such a S/N. The worst case for developing a keying signal is when the video signal has a S/N of 27 db due to Isocon, photon noise. As stated previously, this noise level is 0.192 vp-p. It will be shown in the following paragraphs that a signal having this amount of noise is adequate to reliably operate the blanking generator for day and dusk illumination conditions.

Blanking Method. The blanking circuitry in this method is very simple, because the inseting module does not require any carrier image information from the computer (except distortion information).

This section can be divided into two subsections; electronic blanking and carrier image detection by the added TV camera.

- 1) **Blanking Generator.** The coordinate information of the carrier on the display screen is taken directly by a TV camera (on the cockpit) for all simulated conditions.
- 2) **Inseting.** Two generalized conditions of inseting are shown in figure 103.

As seen in figure 104, the worst inseting accuracy will be due to a 25-ns, max switching time, which is equal to approximately one horizontal TV element 25.7 ns, derived in the elliptical blanking analysis report). A typical switching time error of the above circuit is 10 ns, or approximately 4 arc-min. Operation of the circuit of figure 104 is as follows:

- a) For case A: $y_0(t)$ input to F/F II makes a transition of F/F II output from low to high output. This high output, in turn, shuts off F/F I, and hence, the background video signals (including special effects) between $y_0(t)$ and $y_1(t)$ coordinates will pass MC1545 and be displayed on the screen. When $y_1(t)$ input is made to F/F II, the above circuit conditions are reversed and the background video, including special effects will be cut along the remaining edge of the carrier image.
- b) For case B: The strobe will prevent any inputs to F/F II, indicating that a mode of placing the special effects image behind the carrier image has been selected in the special effects generator. This strobe input freezes F/F II and SN5400 and this frozen portion of the circuitry does not affect the rest of the circuits. Hence, the background video including special effects video will be cut along the complete edge of the carrier displayed.

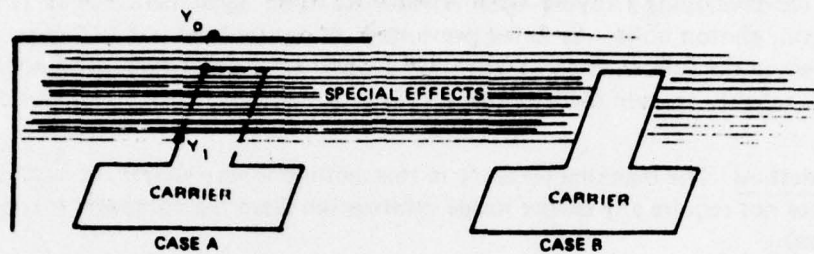


Figure 103. POSSIBLE CONDITIONS

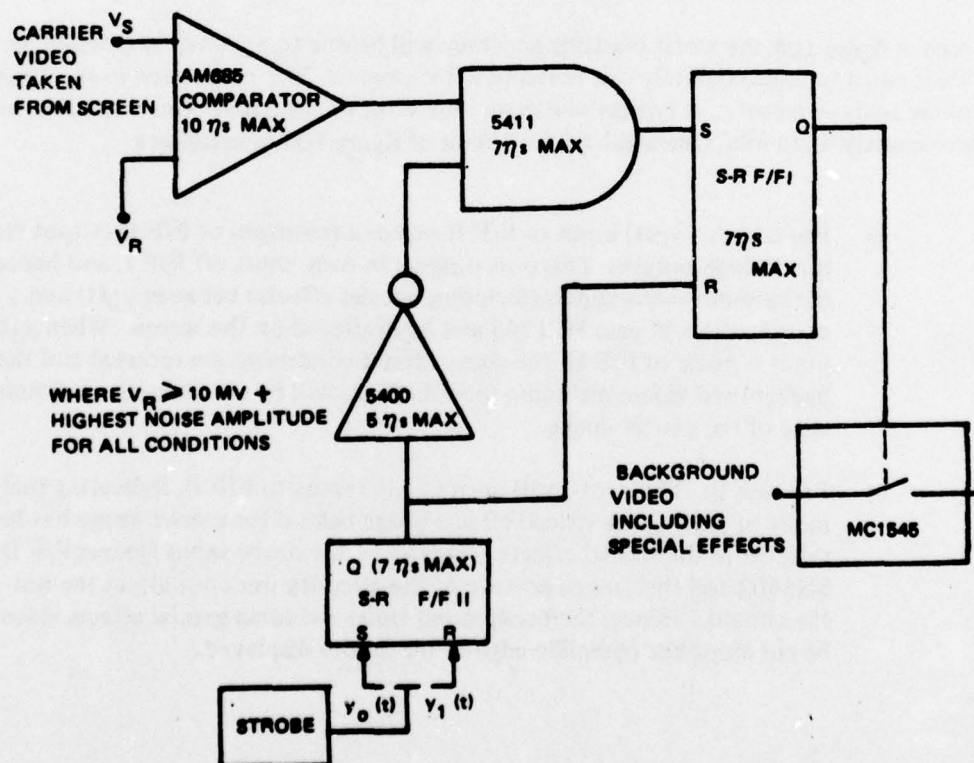


Figure 104. BLANKING CIRCUIT

SECTION X

MATHEMATICAL MODELS.

The system software function is to provide the outputs from central, digital data processing which are required for proper control of the visual hardware.

METHODS CONSIDERED. Only the proposed method was considered.

NOTE

Symbol dictionary for math model symbols can be found in the reference section of this document.

Summary. The AWAVS programs can be conveniently grouped into system program modules. The following program modules are associated with the AWAVS.

- 1) Carrier Model Drive Signal Module
- 2) Wake Disc Drive Signal Module
- 3) Gantry Drive Signal Module
- 4) Probe Drive Signal Module
- 5) Camera Raster Signal Module
- 6) Point of Interest Module
- 7) Target Projector Drive Signal Module
- 8) FLOLS Drive Signal Module
- 9) Background Image Generation Drive Signal Module
- 10) Target Insetting Drive Signal Module
- 11) Special Effects Drive Signal Module

The names which have been chosen for these modules indicate the function of the module. For example, the function of the point of interest module is to define the point of interest and, hence, the orientation of the probe in heading and pitch and the orientation of the target projector optics in azimuth and elevation.

The carrier model drive signal module's drive signal outputs are the drive signals to the carrier model's pitch, roll and heave servos. The inputs to this module are the desired pitch, roll, and heave will be based on sea state, pitch, roll, and heave inputs from the simulator operator's station, and will be done by the carrier model motion module. The carrier model drive signal module will also evaluate the carrier model to wake frame direction cosines, using carrier pitch and roll angle inputs from the carrier model motion module.

The wake disc drive signal module's outputs are the drive signals required to drive the wake disc servo system and the desired angular orientation of the wake disc. The desired angular orientation of the wake will be an output from the wake disc algorithm. The wake disc and an associated probe point position by giving considerations to the problems of keeping the probe away from those corners of the model board which are nearest the model and the use of wake disc rotation to present relative translation between the nominal viewing point and the carrier model. It is desired to keep the probe away from the corners which are close to the wake disc in order to maintain the operational envelope of the probe (i.e., in order to prevent the probe from being positioned such that it is required to instantaneously drive the probe to the other side of the model board). In order to achieve the goal of keeping the probe away from the "near" corners, it is, of course, necessary to simulate relative translation between the nominal viewing point and the carrier model by using wake disc rotation, since the gantry will be driven to simultaneously present the proper range and aspect to the carrier and to attempt to minimize the translational accelerations imparted to the gantry.

The gantry drive signal module's function is to control the gantry's translational servo systems. The gantry's X, Y, and Z servo systems will be velocity servo systems in the sense that the control inputs to these systems will be interpreted as velocity signals. In the actual formulation of these X, Y, and Z translational outputs, a linear combination of the appropriate gantry translational velocity component and its associated translational position component will constitute an output to a given gantry servo system. The translational velocity component will, of course, predominate when the desired probe translational velocity component is large and the associated position component error is small. The translational position component will only predominate when the translational velocity component is small and the associated position component error is significant. This situation will occur, for example, when it is desired to reset the gantry to some new position relative to the model board. The inputs to the gantry drive signal module will be desired gantry position and velocity components from the wake disc drive signal module during an actual simulation exercise and desired simulated aircraft position with respect to the simulated carrier during a simulator reset.

The probe drive signal module's function is to provide digitally computed heading, pitch, derotation, relay azimuth, iris, tilt, focus, and zoom outputs of the probe. Since the AWAVS system is an area of interest system, the attitude of the probe's central axis will always be driven to that orientation which is associated with the defined point of interest. The derotation prism will be driven such that the proper orientation of the projected target image is presented in the display. This must take the attitude of the simulated aircraft, the orientation of the probe's central axis, and the image roll associated with the heading and pitch of the probe into account. Tilt is used to keep the near foreground in focus as the carrier is approached, and is a function of both simulated aircraft altitude and pitch. Focus is a function of the distance from the probe point to the carrier/wake model when tilt is ineffective, and primarily a function of tilt when tilt is effective.

The camera raster shaping drive signal module's outputs are digital words which are used to scale the voltage outputs from waveform generators. This scaling is a function of the position of the point of interest in the displayed field of view, since the mapping of the projected area of interest onto the spherical screen will depend on the orientation of the target projector optics (i.e., the azimuth and elevation of the projected area of interest). The

voltage outputs from the waveform generators will be scaled such that summations of these scaled voltage outputs will cause the camera raster to be shaped such that the proper distortion correction of the displayed area of interest image is presented when viewed from the nominal viewing point. The procedure which will be used to determine a set of scaling words for a given orientation of the target projector optics is to start with a given set of target projector reference sweep values, then determine the direction numbers of the associated ray in target projector space (this mapping is fixed), next determine the direction numbers of this same ray in target projector optics space (this mapping is also fixed), find the associated display screen intersection point, find direction numbers of this screen intersection point with respect to the nominal viewing point in the area of interest coordinate system, next find the corresponding camera vidicon coordinates of this same ray, determine the corresponding camera vidicon raster voltages which are necessary to cause the camera vidicon's electron beam to be positioned at those camera vidicon raster coordinates, and finally to determine the scaling words by using the method of least squares on a network of points which cover the entire field of view of the area of interest for given values of target projector optics azimuth and elevation. Once the scaling words associated with required raster shapes have been determined over the limits of travel of the target projector's azimuth and elevation optics, these words can be stored in terms of mixed polynomials in azimuth and elevation. If these words are stored as data points, values of these words at given values of azimuth and elevation can be determined by means of interpolation. If they are stored in terms of mixed polynomials, then the mixed polynomials can be evaluated for the desired azimuth and elevation angles of the target projector's optics.

The output of the point of interest module is the point of interest. The point of interest is at the geometric center of the area of interest. It is natural to let the selection of the point of interest depend on the position of the simulated aircraft with respect to the carrier and wake models. For example, when the FLOLS is either visible or nearly visible, the FLOLS is selected as the point of interest. This selection will occur most often during a landing approach. However, once the simulated aircraft crosses the ramp of the carrier, the angular orientation of the FLOLS with respect to the cockpit changes vary rapidly, and is, in fact, lost from the simulated field of view. Therefore, whenever the aircraft is over the carrier, the point of interest will be fixed with respect to the simulated cockpit. Fixing the point of interest with respect to the simulated cockpit amounts to a fixed display of the area of interest. Such a fixed display is also appropriate during carrier launches. Whenever the simulated aircraft is operating in general space (i.e., neither over the carrier nor near the nominal glide slope) the point of interest is chosen to maximize the amount of carrier and wake which is capable of being displayed within the area of interest. The transition from one point of interest reference to another point of interest reference will be by moving from one reference to another through equal angular increments in equal times.

The target projector drive signal module will provide the required control outputs to the target projector optics' servo systems: zoom, roll, azimuth, and elevation. Target projector zoom will be driven such that the displayed image is presented at a scale which is realistic for the range to the carrier.

Target projector roll will be driven to that position which exactly cancels the image roll introduced by the azimuth and elevation optics. This has two obvious advantages: 1) the image presented to the pilot will correspond to the image at the Eidophor projector, and, hence, to the image presented on the monitor at the simulator operators' station and 2) the probe's dynamic capability in rotation need only account for those rotations introduced by the combination of aircraft dynamics and angular orientation of the point of interest and need not include additional image rotations introduced by the target projector azimuth and elevation optics. The target projectors azimuth and elevation optics will be driven such that the point of interest is properly positioned on the display screen, i.e., its position with respect to the nominal viewing point must correspond to the position of the point of interest with respect to the nominal viewing point in the real world counterpart of the simulated mission.

The FLOLS drive signal module will determine: when the FLOLS is visible, the position of the meatball, with respect to the FLOLS display; and the roll orientation of the FLOLS, with respect to the chosen area of interest. Basically, the FLOLS is visible 20° on either side of the nominal 4° glideslope and 1.25° above and below the nominal glideslope. The display of the wave-off and cut lights depend on inputs from the simulator operator's station. The position of the meatball with respect to the FLOLS depends on the position of the aircraft above or below the nominal 4° glideslope. When the FLOLS is the area of interest, the FLOLS will be centered at the point of interest. When some other point interest is chosen, the FLOLS will not be displayed. The roll orientation of the projected FLOLS image will always be proper with respect to the projected image of the carrier, since FLOLS image roll is controlled by a separate roll prism.

The background image generation drive signal module controls the raster shaping of the background image generation flying spot scanner. The digital computer control of this system is similar to the control described previously for the camera raster, i.e., the scaling of waveform generator outputs is controlled by digital word outputs. The inputs to the waveform generators are the fast and slow reference sweeps for the background Eidophor projector. In this case, however, the values of the digital word outputs depend on the attitude of the simulated aircraft rather than the attitude of the projector. In this case, of course, the attitude of the background projector is fixed in either of two fixed positions. Flying spot scanner positions can be found, as in the case of camera raster positions, by starting with Eidophor projector reference sweep values and tracing the corresponding ray through the system to the corresponding film plate coordinates. The film plate coordinates, in turn, determine the desired flying spot scanner coordinates, and, hence, the required flying spot scanner deflection voltages.

The target inseting drive signal module is responsible for the control of both target image elliptical unblanking and background image elliptical blanking. This control is done by means of digital word outputs to high speed special purpose, digital data processing hardware which computes the positions of the desired video blanking on a line by line basis. The digital word outputs from central digital data processing determine the size, position, shape, and orientation of the desired ellipse. In general, the desired ellipse will be the smallest ellipse which contains the maximum amount of carrier and wake visual information which can be displayed in the field of view of the area of interest. The center of the ellipse will, in general, not be coincident with the point of interest. However, in most cases, the center of the ellipse will be close to the point of interest. In the case of the target projector video unblanking, video information outside the chosen elliptical area will be

blanked. In the case of the background image projector, the video information inside the elliptical area will be blanked. In general, the reference ellipse for the target projector's video blanking computation will differ with respect to the reference ellipse for the background projector's video blanking. This is because an ellipse of given size, position, shape and/or orientation on the target projectors raster will not project onto the same ellipse as an ellipse of the same size, position, shape, and/or orientation on the background projector's raster. For example, the projected fields of view of the two projectors differ, and the center of the target projector does not, in general, correspond to the center of the background projector.

The special effects drive signal module's outputs consist of controls for visibility effects for the area of interest image and the background image. The visibility effects requires visibility range divided by altitude above the sea, the area of interest (or background projector) axes direction cosines with respect to the local vertical, altitude above clouds, and special two state variables describing special conditions such as in clouds.

Software System Flow Chart.

Figure 105 presents an overall software system flow chart. This flow chart encompasses all the software modules and their interfaces. It indicates the sources and destinations of the information required to develop the AWAVS hardware drive signals. The drive signals to each hardware component are explicitly shown on this overall visual system flow chart.

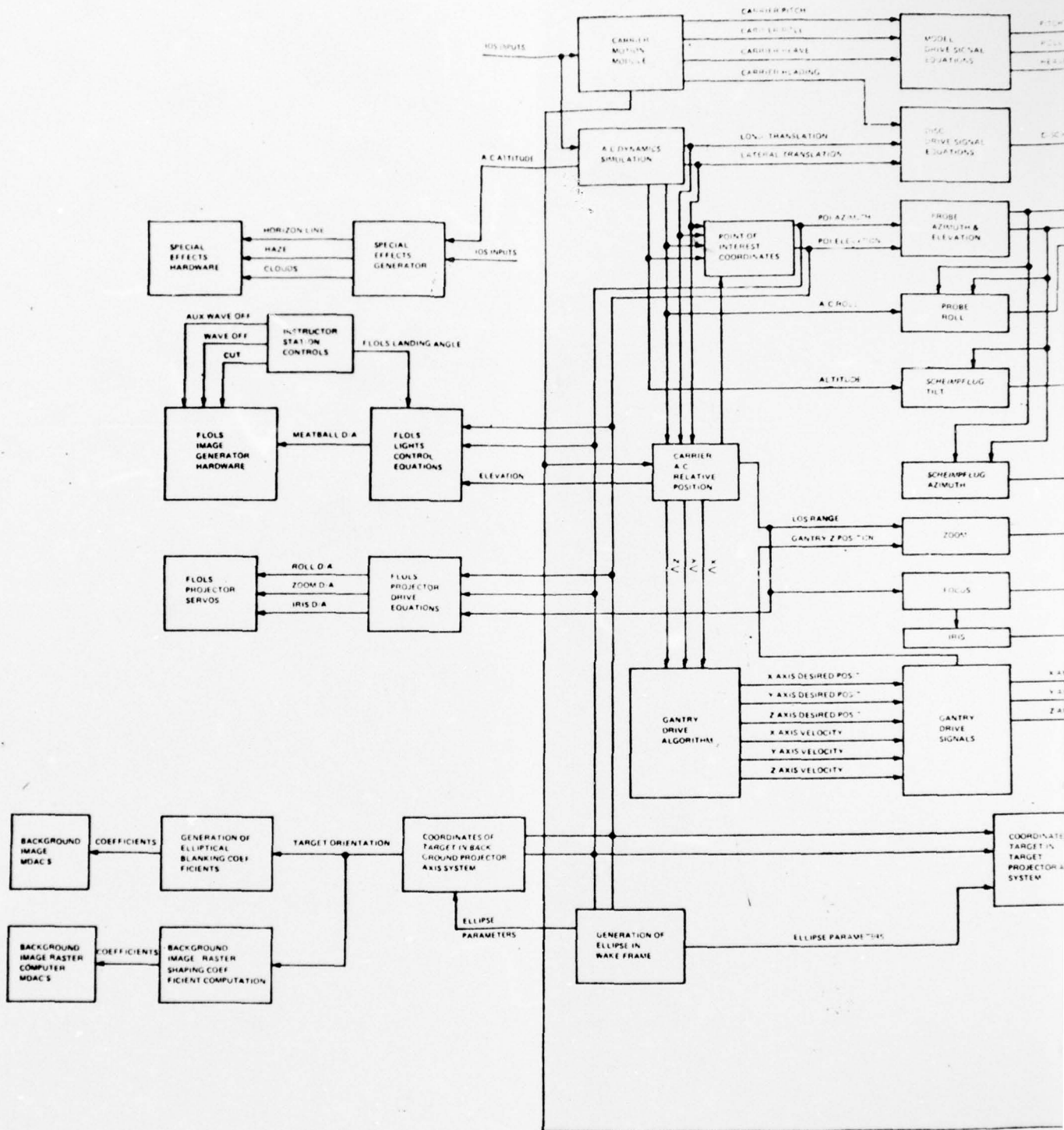
Discussion of Frames of Reference.

The following system of axes forms the basis for the AWAVS visual software system:

- 1) Display Axes - Origin at the center of curvature of the spherical screen. Orientation parallel to cockpit axes (i.e., aircraft body axes).
- 2) Observer Axes - Origin at the nominal viewing point. Orientation parallel to cockpit axes (i.e., aircraft body axes).
- 3) Background Projector Axes - Origin at the projection point. X coincident with the central axis of projection. Y constrained to be in a plane parallel to the X-Y display axes plane. X positive in the direction of projection. Y positive in the positive direction of the Y display axis when the background projector axes are parallel to the display axes. The Z background projector axis is determined by the right hand rule.
- 4) Target Projector Axes - Origin at the projection point of the target projector. X coincident with the central axis of projection. Y constrained to lie in a plane parallel to the X-Y display axes plane. X positive in the direction of projection. Y positive in the positive direction of the Y display axis when the target projector axes are parallel to the display axes. Z determined by the right hand rule.

- 5) Aircraft Body Axes - Origin at aircraft center of gravity. X parallel to fuselage reference line, positive out nose. Y perpendicular to plane of symmetry, positive out right wing. Z determined by right hand rule.
- 6) Carrier Axes - Origin at center of carrier model rotation. X parallel to the hull reference line, positive toward bow. Y perpendicular to hull plane of symmetry, positive toward starboard side. Z determined by right hand rule.
- 7) Wake Axes - Origin at center of wake disc. X coincident with wake centerline. positive toward the front of the wake. Y perpendicular to X in the plane of the wake, positive toward the right when facing in the direction of positive X. Z determined by the right hand rule.
- 8) Area of Interest Axes - Origin at the nominal viewing point. Positive X directed toward the point of interest. Y constrained to lie in the X-Y observer axes plane. Z determine by the right hand rule. The area of interest axes are defined to be parallel to the observes axes when the X area of interest axis is coincident with the X observer axis.
- 9) Probe Axes - Origin at the probe point. X coincident with the central axis of the probe, positive outward from the probe. The probe axes are parallel to the area of interest axes.
- 10) Gantry Axes - Origin at same, as yet unspecified, gantry reference point. Y axis vertical, positive away from the earth's center. Z axis perpendicular to the plane of the model board, positive toward the back side of the model board. Positive X defined such that the gantry axes are right-handed and mutually orthogonal.

The display axes, observer axes, background projector axes, and target projector axes are used to map rays of light defined by the fast and slow reference sweeps of the background projector's raster and target projector raster through the real world counterpart object space of the simulated mission in order to determine the corresponding flying spot scanner raster and camera vidicon raster locations. The display axes and the observer axes are fixed in both position and orientation. The background projector axes are also fixed in position and orientation, but for either a front projection or a side projection of the field of view of the background image. However, the orientation of the field of view of the background projector is fixed in only one of its two allowable positions during a given simulated mission. The target projector axes both rotate and translate. The rotation is intentionally introduced in order to properly place the area of interest in the displayed field of view. The translation of the origin occurs as a result of the design of the target projector's optics; the target projector azimuth drive carries the target projector pitch prism in a circular arc of radius 3.25. This translation of the origin of the target projector axes must be considered in the Target Projector Drive Signal Module.



NAVTRAEQUIPCEN 75-C-0009-1

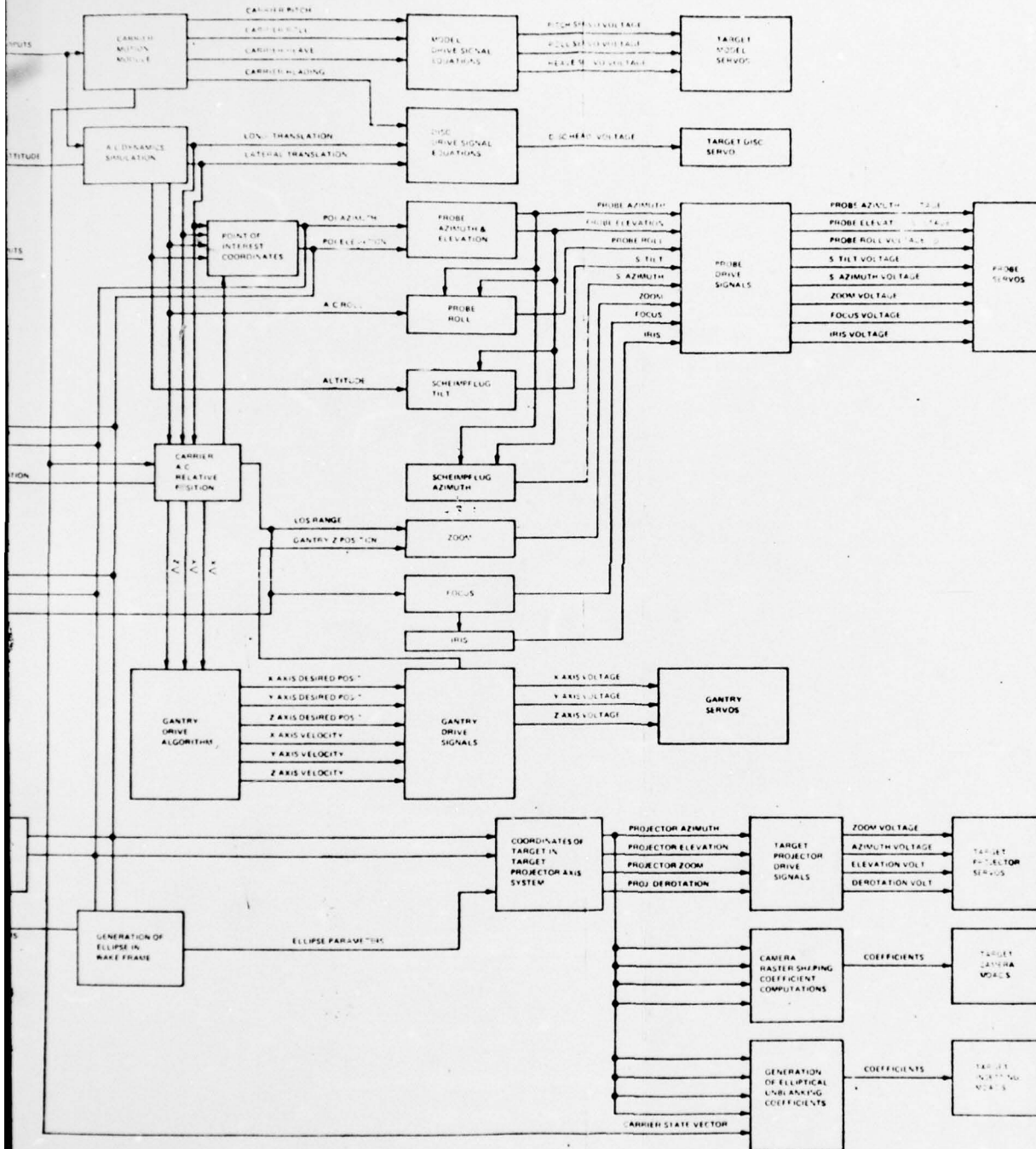


Figure 105. AWAVS SOFTWARE SYSTEM
FLOW CHART

2

The aircraft body axes are the reference axes for the motion of the simulated aircraft. Hence, the outputs of the flight computation, aircraft center of gravity translation and aircraft body axes orientation, are referenced to the aircraft body axes. The translation and orientation of the observer axes with respect to the wake requires aircraft center of gravity and aircraft body axes orientation as inputs. This computation is required in order to provide the drive signals to most of the visual system servo systems.

The carrier axes are the moving frame of reference in the determination of carrier position relative to the wake frame. The coordinates of carrier features are constant in the carrier axes system, since the carrier axes system is fixed with respect to the carrier. The coordinates of carrier features in other frames of reference are determined by first transforming carrier frame coordinates into wake frame coordinates and, hence, into a frame of reference of interest. For example, the FLOLS reference point must be mapped into the observer frame in order to determine the azimuth and elevation angles of the target image projection.

The wake axes provide a reference for wake disc rotation with respect to the gantry axes. The probe must be translated and rotated such that its position and orientation corresponds to the desired position and orientation of the area of interest axes with respect to the real world counterpart of the wake axes system. These requirements, in turn, define the desired position of the probe point with respect to the gantry axes system.

TARGET IMAGE GENERATOR.

Overall Description. The Target Image Generator subsystem is comprised of the software modules which drive the target image generation hardware. The modules which are encompassed in this section are:

- 1) The carrier model drive signal module.
- 2) The wake disc drive signal module.
- 3) The gantry drive signal module.
- 4) The probe drive signal module.
- 5) The camera raster shaping module.

The carrier model drive signal module provides the drive signal voltages to the carrier model roll, pitch and heave servos. The actual carrier motion is computed in the carrier motion module.

The wake disc model drive signal module computes the drive signals to the wake disc servos. These drive signals provide the model with the desired angular orientation to provide heading cues and in some cases translational cues.

The gantry drive signal module provides drive signals to the gantry X, Y, and Z servos. These servo systems require velocity commands. The velocity commands are computed as a function of the gantry position error and the aircraft velocity vector relative to the carrier.

The probe drive signal module provides drive signals to the various probe servos. These servos control probe pitch, heading, derotation, Scheimpflug tilt, Scheimpflug azimuth, zoom, focus and the iris.

The camera raster shaping module provides the raster shaping coefficients. These coefficients are dependent upon the azimuth and elevation angles of the target model image and projector.

Carrier Model Drive Signal Module. The purpose of this module is to determine the target model servo drive signals based on the carrier dynamics as specified by the carrier motion module. The target model is capable of excursions of $\pm 12^\circ$ in roll, $\pm 5^\circ$ in pitch and ± 1.17 inches in heave. The heave excursion of ± 1.17 inches corresponds to ± 30 feet in the real world.

Under normal operating conditions the model pitch, roll and heave drive signals are scaled voltage outputs of the carrier pitch, roll and heave as computed by the carrier dynamics model. These drive signals are computed in the following manner. All servos have a ± 10 volt input range. The requirement on pitch is $\pm 5^\circ$ and this provides a ratio of 2 volts per degree of pitch. The equation for the pitch drive signal is then:

$$VTPM = 2 (VTPC). \text{ (A symbol dictionary appears at the end of this section)}$$

The requirement on roll is $\pm 12^\circ$ this provides a ratio of 0.833 volts/degree of roll. The equation for the roll drive signal is then:

$$VTRM = 0.833 (VTRC).$$

The requirements on heave are ± 30 feet this translates into ± 1.17 inches on the model which combines to give a ratio of 0.333 volts 1/ft of carrier heave. This gives a heave drive signal equation of:

$$VTHM = 0.333 (VTHC).$$

When the aircraft is on the deck it is undesirable to drive the carrier because it may strike the optical probe. For this reason as the aircraft approaches the carrier the model motion will be attenuated and the background image will begin to be driven in the opposite direction to provide the illusion of carrier motion. This will be done only when the aircraft is in the landing approach pattern. The point at which this transition will begin is determined by the response characteristics of the model servos and the background image generation hardware.

If the aircraft is in the landing approach pattern the transition range will be computed by:

$$VTRT = f(VTPM, VTRM, VTHM, VTPSR, VTRSR, VTHSR, VTBIGR).$$

Once the aircraft has reached this transition range the attenuation of the carrier model motion is accomplished by driving the voltage output signal to each of the servos toward zero. The drive signals to the servos would then be of the form:

- 1) $VTPM = VTPM - (VTK1) (VTPM).$
- 2) $VTRM = VTRM - (VTK2) (VTRM).$
- 3) $VTHM = VTHM - (VTK3) (VTHM).$

These computations continue until:

$$VTPM = VTRM = VTHM = 0.$$

The effects introduced by the background image generation system during this phase are discussed in the section on background image generation.

Wake Disk Drive Signal Module. In order to limit the acceleration requirements of the gantry, the disk containing the carrier and wake will be rotated to simulate translational motion of the aircraft. The angle the wake axis makes with the display axis will depend on the aircraft position with respect to the carrier and the probe position on the display axis:

$$\frac{VTYAC}{VTXAC} = \frac{-VTXG \sin(VTAWD) + VTYG \cos(VTAWD)}{VTXG \cos(VTAWD) + VTYG \sin(VTAWD)}.$$

The drive signal to the disk is a voltage which is proportional to the velocity of disk. This velocity is a function of the aircraft position and velocity, the probe position and velocity and the angle calculated in the above equation.

On the display, the angle the aircraft line of sight makes with the carrier x axis must be the same as the real angle. In addition the time rate of change of these angles must be the same. This angular velocity on the display depends not only on the velocity of the probe on the gantry, but also on the angular velocity of the disk.

The angle between the A/C to carrier line and the carrier x axis is:

$$VTACA = \tan^{-1} \left(\frac{-VTYAC}{VTXAC} \right) \quad , \text{ in carrier frame;}$$

and,

$$VTACA = \tan^{-1} \left(\frac{VTXG \sin(VTAWD) - VTYG \cos(VTAWD)}{VTXG \cos(VTAWD) + VTYG \sin(VTAWD)} \right) ;$$

in display frame.

The time rate of change of this angle is:

$$\left(\frac{d(VTACA)}{dt} \right)_{\text{carrier}} = \left(\frac{d(VTACA)}{dt} \right)_{\text{display}}$$

Therefore:

$$\frac{d}{dt} \left(\tan^{-1} \left(\frac{-VTYAC}{VTXAC} \right) \right) = \frac{d}{dt} \left(\tan^{-1} \left(\frac{VTXG \sin(VTAWD) - VTYG \cos(VTAWD)}{VTXG \cos(VTAWD) + VTYG \sin(VTAWD)} \right) \right)$$

Since $\left(\frac{-VTYAC}{VTXAC} \right) = \left(\frac{VTXG \sin(VTAWD) - VTYG \cos(VTAWD)}{VTXG \cos(VTAWD) + VTYG \sin(VTAWD)} \right)$;

$$\frac{d}{dt} \left(\frac{-VTYAC}{VTXAC} \right) = \frac{d}{dt} \left(\frac{-VTXG (\sin(VTAWD)) + VTYG (\cos(VTAWD))}{VTXG (\cos(VTAWD)) + VTYG (\sin(VTAWD))} \right)$$

Therefore, let:

$$VTRW = \frac{d}{dt} \left(\frac{VTYAC}{VTXAC} \right) = \frac{VTVYA (VTXAC) - VTVXA (VTYAC)}{VTVXA^2}$$

All the variables in the above equation are known, so VTRW can be calculated, and

$$VTRW = \frac{d}{dt} \left(\frac{-VTXG \sin(VTAWD) + VTYG \cos(VTAWD)}{VTXG \cos(VTAWD) + VTYG \sin(VTAWD)} \right)$$

This equation is of the form:

$$VTRW = \frac{d}{dt} \left(\frac{A}{B} \right) = \frac{BdA - AdB}{B^2}$$

where A represents $-VTXG \sin(VTAWD) + VTYG \cos(VTAWD)$, and B represents $VTXG \cos(VTAWD) + VTYG \sin(VTAWD)$. A and B can both be calculated, because VTXG, VTYG and VTAWD are known.

If:

$$VTC1 = \frac{1}{B} \quad \text{and} \quad VTC2 = \frac{-A}{B} ;$$

then,

$$VTRW = (VTC1) \frac{d(A)}{dt} + (VTC2) \frac{d(B)}{dt} ;$$

$$\frac{d(A)}{dt} = \frac{d((-VTXG) \sin(VTAWD) + (VTYG) \cos(VTAWD))}{dt};$$

and,

$$\frac{d(B)}{dt} = \frac{d((VTXG) \cos(VTAWD) + (VTYG) \sin(VTAWD))}{dt}.$$

If:

- 1) $VTC3 = (VTXG) \cos(VTAWD);$
- 2) $VTC4 = (VTXG) \sin(VTAWD);$
- 3) $VTC5 = (VTYG) \cos(VTAWD);$
- 4) $VTC6 = (VTYG) \sin(VTAWD);$
- 5) $VTC7 = (VT'XG) \cos(VTAWD);$
- 6) $VTC8 = (VT'XG) \sin(VTAWD);$
- 7) $VTC9 = (VT'YG) \cos(VTAWD);$

and 8) $VTC10 = (VT'YG) \sin(VTAWD);$

then:

$$\frac{d(A)}{dt} = -VTC3 (VT'AD) - VTC8 - VTC6 (VT'AD) + VTC9;$$

and

$$\frac{d(b)}{dt} = -VTC4 (VT'AD) + VTC7 + VTC5 (VT'AD) + VTC10.$$

Where: $VT'AD = \frac{d(VTAWD)}{dt}.$

- If:
- 1) $VT'KD1 = VTC1 (-VTC3 - VTC6);$
 - 2) $VT'KD2 = VTC1 (-VTC8 + VTC9);$
 - 3) $VT'KD3 = VTC2 (-VTC4 + VTC5);$
- and 4) $VT'KD4 = VTC2 (VTC7 + VTC10);$

then the equation:

$$VTRW = (VTC1) \frac{d(A)}{dt} + (VTC2) \frac{d(B)}{dt}$$

becomes:

$$VTRW = (VTKD1 + VTKD3) (VTVAD) + (VTKD2 + VTKD4);$$

and

$$VTVAD = \frac{VTRW - (VTKD2 + VTKD4)}{(VTKD1 + VTKD3)}$$

VTVAD is the disk velocity, (the time rate of change of VTAWD). This velocity is then modified by a scaling constant to get the voltage needed to turn the disk.

$$VTDV = VTA (VTVAD).$$

Gantry Drive Signal Module. The gantry drive signal module is employed to provide the proper translational positioning of the probe opposite the model board based on the relative positions of the carrier and aircraft. In general the gantry will be used to provide translational cues except when the limits of the gantry capabilities will be exceeded. In these cases the gantry motion will be augmented by the probe zoom and wake disc rotation.

For certain conditions such as "fly-by" disc rotation will be combined with gantry motion to provide the proper translational cue. This will involve developing an algorithm to combine these to motions. As yet no suitable algorithm has been developed for the gantry Y axis servo drive for these conditions. For the present the Y axis position is kept on the center of the board. Two possible approaches are discussed in the Target Image Generation section of this report.

The first set of computations involves determining the aircraft coordinates in the gantry frame of reference. This is done by taking the aircraft coordinates in the carrier frame and transforming them into the gantry frame:

$$\begin{bmatrix} VTXAG \\ VTYAG \\ VTZAG \end{bmatrix} = [VTTCG] \begin{bmatrix} VTXAC \\ VTYAC \\ VTZAC \end{bmatrix}$$

Both the X and Z axes desired gantry positions are computed as a function of the respective components of simulated range and the zoom ratio. These relationships are:

$$VTXAGD = (VTSF) (VTXAG) \left(\frac{\text{PROBE ZOOM}}{\text{DISPLAY ZOOM}} \right);$$

and
$$VTZAGD = (VTSF) (VTYAG) \left(\frac{\text{PROBE ZOOM}}{\text{DISPLAY ZOOM}} \right).$$

The gantry position error is now computed by:

- 1) $VTXGPE = VTXAGD - VTXAGA;$
- 2) $VTYGPE = 0;$
- and 3) $VTZGPE = VTZAGD - VTZAGA.$

The desired gantry velocity is now computed as a function of relative velocity between the carrier and the aircraft and the position error:

- 1) $VTXVD = (VTXVC) (VTXVCA) (VTXGPE);$
- 2) $VTYVD = (VTYVC) (VTYVCA) (VTYGPE);$
- 3) $VTZVD = (VTZVC) (VTZVCA) (VTZGPE).$

Another function of the camera gantry drive software is to provide redundant protection to the optical probe from striking any portion of the target model. A relatively conservative model will be used to compute impending impact. First a circle called the outer limit circle will be circumscribed about the carrier with radius equal to half the carrier length. A check will be made to determine if the desired probe position is within this circle. If it is not there is no concern of striking the target. If it is another circle will be circumscribed around the island of the carrier. This circle is called the inner circle. If the desired probe position is within the outer limit circle but not within the inner limit circle a check will be made on the desired probe height. If it is lower than the carrier deck, then the gantry will be stopped, and the Z axis driven to clear the deck. If the desired probe position is within the inner limit circle a check will be made on the desired probe height. If it is lower than the top of the island the gantry motion will be terminated and the Z axis driven to clear the island. The equations used in this algorithm are presented below.

First the coordinates of the carrier center of rotation must be transformed from the wake frame to the gantry frame:

$$\begin{bmatrix} VTXCRG \\ VTYCRG \\ VTZCRG \end{bmatrix} = \begin{bmatrix} VTTWG \end{bmatrix} \begin{bmatrix} VTXCRW \\ VTYCRW \\ VTZCRW \end{bmatrix}$$

Now the distance between the desired probe position and the carrier center of rotation projected into the XY gantry plane must be computed:

$$VTRCRC = \left[(VTXAGD)^2 + (VTYAGD)^2 \right]^{1/2} - \left[(VTXCRG)^2 + (VTYCRG)^2 \right]^{1/2}$$

Then the distance to the outer limit circle is computed by:

$$VTDOLC = VTRCRC - VTROLCL$$

If $VTDOLC \geq 0$ the desired probe position is within the outer limit circle. Then a check must be made to determine if the desired probe position is within the inner limit circle. First the distance to the island from the desired probe position is computed:

$$VTRI = \left[(VTXAGD)^2 + (VTYAGD)^2 \right]^{1/2} - \left[(VTXCRG + VTXI)^2 + (VTYCRG + VTYI)^2 \right]^{1/2}$$

Now the distance to the inner limit circle is computed by:

$$VTDILC = VTRI - VTRILC.$$

If $VTDILC \geq 0$ the desired probe position is within the inner limit circle.

If the desired probe position is within the outer limit circle but not within the inner limit circle then a check is made to determine if the probe height is sufficient to clear the deck:

$$VTZPMD = \frac{VTLC}{2} \tan(VTPC) + 0.039(VTHC) + VTCRWL.$$

If $VTZAGD \leq VTZPMD$;

then set 1) $VTXVD = 0$.

2) $VTYVD = 0$.

3) $VTZVD = (VTZPMD - VTZAGD) VTZVCM$.

Now if the desired probe position is within the inner limit circle, a check is made to determine if the probe will clear the island:

$$VTZPMI = VTHIWL + 0.039(VTHC).$$

If $VTZAGD \leq VTZPMI$:

the set 1) $VTXVD = 0$.

2) $VTYVD = 0$.

3) $VTZVD = (VTZPMI - VTZAGD) VTZVCM$.

Once the probe is sufficiently high to clear the model the X and Y gantry drives may resume.

When in the reset mode the Z axis position will be driven to its maximum height until the X-Y drive has correctly positioned the probe then the probe will be lowered to its proper height. The Z axis equation is:

$$VTZVD = (VTZMAX - VTZAGA) (VTZVCM).$$

and the X-Y drives are computed based on the position error as before, but they are driven at maximum velocity:

$$VTXVD = (VTXGPE) (VTXVCM);$$

and $VTYVD = (VTYGPE) (VTYVCM).$

Once the desired velocity components have been computed the voltage output signals must be computed as a function of the servo characteristics. The three drive signal voltage equations are:

$$VTXVGX = (VTXVD) (VTXGSC);$$

$$VTYVGX = (VTYVD) (VTYGSC);$$

and $VTZVGX = (VTZVD) (VTZGSC).$

Probe Drive Signal Module. The probe Drive Signal Module's outputs are probe heading, pitch, derotation, relay azimuth, tilt, focus, zoom and iris control. In order to eliminate the perspective transformation between the probe frame of reference and the area of interest frame of reference, the probe point will be made to correspond to the nominal viewing point and the attitude of the probe will be made to correspond to the attitude of the area of interest. Therefore, if the gantry frame to probe frame direction cosines are denoted by VTP [VTI, VTJ], the circular functions associated with desired probe pitch, heading, and relay azimuth are:

$$1) \quad \sin(VTTP) = -VTP [1, 3], \\ \cos(VTTP) = (VTP [1, 1]^2 + VTP [1, 2]^2)^{1/2}$$

$$2) \quad \sin(VTSP) = VTP [1, 2] \div \cos(VTTP); \\ \cos(VTSP) = VTP [1, 1] \div \cos(VTTP).$$

$$3) \quad \sin(VTHP) = VTP [2, 3] \div \cos(VTTP); \\ \cos(VTHP) = VTP [3, 3] \div \cos(VTTP).$$

The drive signals required by the probe servo systems are related to the servos system resolver angles of the probe heading, pitch derotation, and relay azimuth servo systems for the F4E No. 18 as shown by the following dependencies:

$$1) \quad VTSR = f(VTSP).$$

$$2) \quad VTTR = f(VTTP).$$

$$3) \quad VTDR = f(\pm VTSP, \pm VTTP, \pm VTHP).$$

$$4) \quad VTAR = f(\pm VTSP, \pm VTTP).$$

Where VTSR, VTTR, VTDR, and VTAR are the respective resolver angles in the probe heading, pitch, derotation, and relay azimuth servo systems. The tilt angle is dependent on desired probe point altitude and probe pitch. This dependency is symbolically shown below:

$$VTTA = f(VTVP, VTTP).$$

Where VTVP and VTTP are the desired probe altitude and probe pitch. The focus position is dependent on described probe tilt and the range to the point of interest. The symbolic representation of this dependency is:

$$VTZ = f(VTTA, VTR).$$

Where VTTA and VTR are the respective tilt angle and distance to the point of interest. Zoom position is a function of the distance to the point of interest and iris position is a function of zoom position. If zoom position is denoted by VTW, the respective resolver angles for the tilt, focus, zoom and iris servo systems can be symbolically denoted:

- 1) VTTAR = f(VTTA).
- 2) VTZR = f(VTZ).
- 3) VTRR = f(VTR).
- 4) VTWR = f(VTW).

The gantry frame to probe frame direction cosine matrix is simply the matrix product of the real world counterpart of the gantry frame to aircraft body axis direction cosine matrix and the aircraft body axes to area of interest axes direction cosine matrix:

$$[VTP] = [VTAL] [VTB].$$

Where VTAL is the aircraft body axes to area of interest axes direction cosine matrix and VTB is the gantry axes system to aircraft body axes direction cosine matrix. The values of the VTAL matrix depend on the point of interest in the observes axes system. The values of the VTB matrix are determined by the aircraft body axes to sea reference frame direction cosines supplied by flight, and the orientation of the gantry with respect to the sea reference frame.

Camera Raster Shaping Module. The target image on the display screen will be generated by scanning the target projector with a horizontal fast scan and a vertical slow scan. If the image in the camera were sent to the target projector in the same way, severe distortion on the display screen would occur because of the spherical shape of the display screen, the off axis location of the projector, and optical distortion. Any point on a raster is a function of the X voltage which bends the electron beam through a horizontal angle and a Y voltage which bends the beam through a vertical angle. The X voltage is usually referred to as the "fast" voltage and the Y voltage is referred to as the "slow" voltage because:

$$\frac{dV_x}{dt} \gg \frac{dV_y}{dt}$$

$$VTXC = VTFC1 (VTVFC)$$

$$VTYC = VTFC2 (VTVSC)$$

If the relationship between a point on the projector raster and a point on the camera raster is known then a relationship between the voltages can also be found. Since the projector voltages can not be modified the camera voltage must be changed (i.e. the camera raster will not be scanned with a horizontal fast scan and a vertical slow scan) to send the proper image to the projector.

To find the correspondence between points the mapping from the camera raster to the area of interest is found first:

$$VTXA = VTMCA (VTXC, VTYC).$$

Then these points are transformed to the observer frame;

$$VTXO = [VTTHO] [VTXA].$$

From the observer frame they are transformed to the display frame:

$$\begin{pmatrix} VTXD \\ VTYD \end{pmatrix} = [VTOD] \begin{pmatrix} VTXO \\ VTYO \end{pmatrix}.$$

and from there, mapped back to the target projector:

$$\begin{bmatrix} VTXP \\ VTPP \end{bmatrix} = [VTMDP] \begin{bmatrix} VTXD \\ VTYD \end{bmatrix}.$$

$$\begin{aligned} VTVFP &= [VTFP1] [VTPP] \\ VTVSP &= [VTFP2] [VTPP] \end{aligned}$$

By substituting the voltage functions into the above equation in place of the coordinates, equations of the form below result.

$$\begin{aligned} VTVSC &= VTF2 (VTVFP, VTVSP); \\ \text{and} \quad VTVFC &= VTF1 (VTVFP, VTVSP). \end{aligned}$$

Each voltage is a function of time. VTF1 and VTF2 are very complex functions therefore the camera voltages were not calculated during the design analysis. Rather, VTVSC and VTVFC are expressed as:

$$\sum_{VTI=1}^{VTN} \sum_{VTJ=1}^{VTN} VTK(VTI, VTJ) VTVFP^{VTI-1} VTVSP^{VTJ-1}$$

where the VTK's are constants and VTN is a limit imposed by the digital to analog converter which will continuously modify the above expression with respect to time.

The VTK's will be determined for specific azimuth and elevation angles. These constants will then be stored in the simulation computer. The VTK's for intermediate angles will be interpolated from the measured values.

TARGET PROJECTOR OPTICS.

Overall Description. The target projector optics subsystem involves determination of the center of the area of interest and the target projector drive signal module.

The point of interest selection module defines the geometric center of the area of interest based on the relative positions of the simulated aircraft and the carrier. There are three spaces defined for area of interest. Carrier space, cone space and general space. In carrier space, the point of interest is defined by a fixed, angular orientation with the observer axis system. In cone space the point of interest is defined as the center of the FLOLS system. In general space the point of interest is the center of the ellipse which maximizes the view of the carrier and wake. The point of interest module also provides for smooth transition among these spaces.

The target projector drive signal module provides the drive signals to drive the target projector servos. These servos control the zoom lens and the roll, elevation and azimuth prisms. The azimuth and elevation prisms are used to correctly position the center of the area of interest on the display screen. The roll prism is used to de-rotate the error in roll introduced by the azimuth and elevation prisms. The zoom lens is employed to present the image in the proper scale as a function of range to the carrier.

Point of Interest Selection. The point of interest is chosen dependent upon the particular portion of the simulated flight envelope in which the simulated aircraft is operating relative to the carrier. Consider three spatial volumes to be defined for the purpose of specifying the AWAVS point of interest.

First, the carrier space is defined as that spatial volume directly above the simulated carrier. Second, the cone space is defined as that space which lies outside the carrier space and lies within a right circular cone of 20° half angle, with its apex at the intersection of a 4° glide slope and the carrier centerline, and further whose axis of symmetry is coincident with the 4° glide slope. The third space, referred to as general space, is the remaining space not included in the above two spaces.

The point of interest, when the simulated nominal viewing point is in carrier space, is defined by a fixed angular orientation with respect to the observer axis system. The coordinates of the point of interest, in the observer frame, for this case are:

- 1) $VPXPI = (VPHNEC) \tan (VPFPIA).$
- 2) $VPYPI = 0.$
- 3) $VPZPI = VPHNEC.$

If the simulated, nominal viewing point is in cone space, the point of interest will be the center of the FLOLS system. Then to compute the coordinates of the point of interest in the observer frame, first the position of the aircraft relative to the FLOLS is computed in the carrier frame. These components are given by:

$$1) \quad VPXFC = VPXFOC - VPXAC.$$

$$2) \quad VPYFC = VPYFOC - VPYAC.$$

Now the coordinates of the point of interest in the observer frame may be computed by rotating the above coordinates into the aircraft body axes, and then translating into the observer frame. This can be accomplished by:

$$\begin{bmatrix} VPXPI \\ VPYPI \\ VPZPI \end{bmatrix} = - \begin{bmatrix} VPTCB \\ VPTCB \\ VPTCB \end{bmatrix} \begin{bmatrix} VPXFC \\ VPYFC \\ VPZFC \end{bmatrix} - \begin{bmatrix} VPTBO \\ VPTBO \\ VPTBO \end{bmatrix}$$

The third case is to determine the point of interest when the simulated nominal viewing point is in general space. This point is defined as that point which allows the maximum amount of carrier and wake visual information to be presented within the area of interest. This point is the center of the ellipse which can be generated in the observer frame which maximizes the area. This is accomplished in much the same way as the target inseting ellipse was generated. First take the components of each of the selected points in the field as defined in the observer frame [VIXO] and use the algorithm of the target inseting module to fit an ellipse and find its center. The components of the center of this ellipse will be VPXPI, VPYPI and VPZPI.

The elevation angle of the point of interest is:

$$VPEAPI = \tan^{-1} \left(\frac{VPZPI}{VPXPI} \right);$$

and the azimuth is given by:

$$VPAAPI = \tan^{-1} \left(\frac{VPYPI}{VPXPI} \right).$$

When the simulated nominal viewing point leaves one space, there will be a smooth transition to the new space. This will be done by first computing the difference between the azimuth and elevation angles of the new and old points of interest:

$$1) \quad VPEAPD = VPEAPI - VPEAPP.$$

$$2) \quad VPAAPD = VPAAPI - VPAAPP.$$

The sign of these computed differences will determine which direction the point of interest will be driven to reach the new point of interest. Each iteration, the point of interest will be incremented as a function of the maximum velocity of the servo. These increments are given by:

$$VPEAI = \text{sign}(VPEAPD) f(VPPPMV);$$

and,

$$VPPAAI = \text{sign}(VPAAPD) f(VPPAMV).$$

These values are added to the old angles until the difference is within some ϵ of zero by using the following equations:

- 1) $VPEAPP = VPEAPP + VPEAI.$
- 2) $VPAAPP = VPAAPP + VPAAI.$

Target Projector Optics Drive Signal Module. The target projector optics system has 4 degrees of freedom, roll, azimuth, elevation and zoom. The zoom is used to simulate slant range. The azimuth and elevation prisms correctly position the point of interest on the display screen. The roll is used to correct for rotations introduced by the rest of the optical system.

The zoom is a function of slant range to the carrier and varies only when the range is greater than 1000 feet and less than 2 nm. At ranges outside these limits range is simulated by changes in gantry position and/or probe zoom only. Within these limits the function of zoom vs. range is not linear because the gantry and probe zoom are being used in combination with projector zoom to simulate the range. The function will depend upon hardware characteristics such as the zoom lenses chosen and the maximum acceleration of the gantry:

- 1) $VPFZR = f(VPH).$
- 2) $VPPZ = VPFZR(VPSR).$
- 3) $VPPZV = VPPZC(VPPZ).$

The probe roll will be used to simulate the aircraft roll. Therefore, the projector roll will be used only to correct any extraneous roll introduced into the image as a result of imperfections in the lens system and by rotation of the azimuth and elevation prisms:

- 1) $VPPR = VPFRA(VPPL, VPAP, VPEP).$
- 2) $VPPRV = VPPRC(VPPR).$

The azimuth prism is rotated to position the point of interest at the correct azimuth angle in the observer frame, and the elevation prism is rotated to provide the correct elevation. Neither of these angles will be the same as the angles in the observer frame because of the location of the projector with respect to the nominal viewing point.

Inputs available from the POI selection module are the real-world coordinates of the POI in the observer frame, and the azimuth and elevation angles. The simulator observer frame coordinates are proportional to the world observer frame coordinates.

That is:

- 1) $VPXPID = (VPC) (VPXPI).$
- 2) $VPYPID = (VPC) (VPYPI).$
- 3) $VPZPID = (VPC) (VPZPI).$

where

$$VPC = VPCF (VPDR, VPDXNC, VPDZNC, VPAAPI, VPEAPI)$$

These coordinates are only different from coordinates in a parallel axis frame, with center at the projection point, by translation factors:

- 1) $VPXPIP = VPXPID + VPDXP.$
- 2) $VPYPIP = VPYPID.$
- 3) $VPZPIP = VPZPID + VPDZP.$

These coordinates can then be used to find the azimuth and elevation angles for the projector:

- 1) $VPAP = \arctan \left(\frac{VPYPIP}{VPXPIP} \right)$
- 2) $VPEP = \arctan \left(\frac{VPZPIP}{\sqrt{VPXPIP^2 + VPYPIP^2}} \right)$
- 3) $VPAPV = VPAPC (VPAP).$
- 4) $VPEPV = VPEPC (VPEP).$

FLOLS.

Overall Description. The only time that the FLOLS image is presented is when the center of the FLOLS is the point of interest. There is no requirement to drive the X-Y mirror in the FLOLS projector. The cut lights, wave off lights and auxiliary wave off lights are controlled from the instructor station. The datum lights and the meatball are illuminated at all times that the FLOLS is on. The FLOLS lights will always be displayed with proper relative orientation. The only exception to this is that there is no capability to roll stabilize the meatball. Pitch stability is taken care of by the shutters on the meatball.

Meatball Drive Signal Module. This module provides the drive signal to control the aperture over the meatball lenses. This aperture is on a rotating cylinder which provides the pilot of the simulated aircraft with a display of the proper portion of the light box based on his relative elevation angle.

First the glide slope angle of the FLOLS must be computed. This is simply the basic angle, which is the pitch angle of the lens box as determined by the hook-to-eye distance of the particular airplane being recovered. The basic angle is an input from the instructor's station. As a function of desired hook-to-eye distance, the lens box is rolled to maintain the proper projection of the glide slope on the vertical plane over the angled deck centerline. The glide slope angle measured in the angled deck centerline vertical plane is:

$$VFGSA = VFBA.$$

The next step is to compute the angle between the glide slope angle computed above and the line of sight from the nominal viewing point to the center of the FLOLS projected onto the deck centerline plane. The coordinates of the nominal viewing point in the carrier frame or VFXEC, VFYEC, VFZEC and the coordinates of the FLOLS center point in the carrier frame are VFXFC, VFYFC, VFZFC.

The line of sight range from the nominal viewing point to the center of the FLOLS is:

$$VFREF = [(VFXEC - VFXFC)^2 + (VFYEC - VFYFC)^2 + (VFZEC - VFZFC)^2]^{1/2}$$

The angle that the line of sight makes with the carrier deck is:

$$VFALC = \cos^{-1} \left[\frac{VFZEC - VFZFC}{VFREF} \right]$$

Then the angle between the glide slope and the line of sight is:

$$VFAGL = VFGSA - VFALC.$$

Since the FLOLS system is pitch stabilized the pitch angle must be subtracted out and the resulting angle is:

$$VFLOLS = VFAGL - VTPC.$$

The meatball drive signal voltage then is:

$$VFMBV = VFSVC (VFLOLS).$$

Wave-Off Lights Drive Signal Module. Both the wave-off lights and the auxiliary wave off lights are under control of the instructor. It is his responsibility to turn them on or off. Therefore, a signal will be transferred directly from the instructor station to the wave-off lights hardware and the flashing of these lights will be accomplished by hardware.

Cut Lights Drive Signal Module. The cut lights are also under the control of the instructor and will, therefore, be handled in the same manner as the wave-off lights.

Optics Drive Signal Module. Since the X-Y tilt mirror is to be stationary the only optical components which require drive signals are the zoom lens, the iris and the roll prism.

The zoom lens will be driven strictly as a function line of sight range. It's output voltage is given by:

$$VFZLV = VFZSVC (VFREF):$$

The iris controls the intensity of the image. It is controlled both from the instructor's station and from the computer based on various parameters. If the FLOLS is turned off at the instructor's station the iris will be stopped down so no light passes through. If the FLOLS is not the center of the area of interest the iris again will be stopped down to zero. The brightness thumbwheel at the IOS will establish a base intensity which is further adjusted by range.

The equation used to compute the output voltage to the iris servo based on the above conditions is:

$$VFISV = [(VFFIS) (VFPIF)] [(VFIRC) (VFREF) + (VFIISC) (VFIIS)].$$

The roll prism is used to properly align the FLOLS image in roll with the target image. The drive signal to the FLOLS roll servo must provide the same roll angle as the target image at the combining mirror in the target projection system. Therefore the FLOLS roll servo drive signal equation must be of the form:

$$VFRSV = VFRSC (VFRTI).$$

BACKGROUND IMAGE GENERATOR.

Overall System Description. The background image generator is to provide a seascape image in the proper perspective for the attitude and heading of the aircraft. This will be done by projecting the image of a seascape on the face of a flying spot scanner. The scanner raster will then be shaped to show the attitude and heading changes of the aircraft. The raster plots are presented in section 538.

Desired FSS Raster Shapes. The Flying Spot Scanner raster shapes will depend on the aircraft attitude and heading and the distortions in the optical and projection systems. This raster will be shaped in the same manner as the target projector raster. That is, a correspondence between display screen points and background projector points will be determined for various attitudes of the aircraft. This mapping is then used to determine the raster shaping needed at the FSS.

The raster voltages of the FSS can be expressed as a function of the background projector voltages:

- 1) $VB'VF = VBF1 (VBBVF, VBBVS).$
- 2) $VB'VS = VBF2 (VBBVF, VBBVS).$

These functional relationships are very complex and are best represented by truncated series:

$$\begin{aligned}
 1) \quad VBFVF &= \sum_{VBI=1}^{VBN} \sum_{VBJ=1}^{VBN} VBK1[VBI, VBJ] (VBBVF)^{VBJ-1} (VBBVS)^{VBI-1} \\
 2) \quad VBFVS &= \sum_{VBI=1}^{VBN} \sum_{VBJ=1}^{VBN} VBK2[VBI, VBJ] (VBBVS)^{VBI-1} (VBBVF)^{VBJ-1}
 \end{aligned}$$

These constants (VBK's) will be used to drive the raster shaping circuitry.

BIG Drive Signal Development. The constants (VBK's) used to drive the background image generator will have values which depend on the aircraft attitude. These constants will be determined for a series of aircraft attitudes. The constants for intermediate values needed during simulation can be calculated by two possible methods.

The first method is to store the measured constants in the computer. To find the constants for an intermediate attitude, a set or sets of constants for attitudes near that attitude are taken from storage. The constants needed would then be calculated from these values by a linear or higher order interpolation.

The second method is to express the constants as functions of the aircraft attitude. These functions would also be expressed as truncated series:

$$VBK = \sum_{VII=1}^{VIN} (VBC[VII]) (VBAAB)^{VII-1}$$

These new constants (VBC's) would be stored and the VBK's could be calculated directly from those constants and the aircraft attitude.

TARGET INSETTING.

Overall System Description. The projection system consists of 2 projectors, a target projector and a background projector. The target projector projects an elliptical image which contains as much of the carrier and wake as possible at a given range. It should contain the smallest possible amount of seascape. The background projector projects a generated background image with an elliptical "hole" cut into the image which must coincide with the target ellipse.

The ellipse is of variable size, shape and orientation. Therefore, five parameters will be needed to describe the ellipses, the x and y coordinates of the center, the magnitudes of the major and minor axes and θ the angle through which the axes are rotated from a fixed axis system. Because θ only appears as $\sin \theta$ and $\cos \theta$ it can be treated as 2 parameters, making six in all. These parameters are functions of the slant range of the aircraft, the nominal viewing point, and the aircraft heading with respect to the carrier heading.

In order to determine these parameters, a set of points on the carrier and wake are selected. These points should be indicative of the carrier shape (e.g. top of the tower, tip of the bow, end of the wake etc.) once these points are known in the carrier axis frame, they can be transformed to the observer frame. They can then be mapped to the projectors axis frames. By the following statistical analysis, the ellipse parameters can be determined.

First the "center of mass" is found. This point is determined by finding the average X value and the average Y value of the points. Second, the most distant point from this "center of mass" is found. This point becomes one end of an axis (not necessarily the major axis) the most distant point from this end point becomes the other end of the axis. This axis defines the center of the ellipse (the point half way between the ends), the length of the axis, and sine θ and cosine θ . The only remaining parameter is the length of the second axis. By putting each point into the ellipse equation one at a time and solving for the eccentricity of the ellipse, the maximum value needed for eccentricity, such that all the points fall within the ellipse, can be found.

The final values for the lengths of the axes is the calculated value plus a 10% margin.

For each iteration of the computer, the ellipse parameters are constant. The ellipse equation can be rewritten in the form:

$$K_1 X^2 + K_2 X + K_3 XY + K_4 Y + K_5 Y^2 + K_6 = 0.$$

Where the K_i 's are functions of the ellipse parameters. These constants will be calculated and passed to the hardware elliptical blanking equipment.

Determination of Desired Target Projector Video Blanking. In order to determine the ellipse on the projector it is necessary to locate the carrier and wake on the projector raster. To do this, key points on the carrier are chosen as discussed in section 6³⁹. The carrier points are first transformed to points in the wake frame by using information about the roll, pitch and heave of the carrier obtained from the carrier model drive signal module.

$$[VIXW] = [VITCW] [VIXC].$$

These points, together with significant wake points are then transformed to the observer frame using the nominal viewing point and the direction cosines between the wake and aircraft frames obtained from flight computations:

$$[VIXO] = [VITWO] [VIXW].$$

The last coordinate transformation is done from the observer frame to the area of interest frame using the direction cosines from the target image generator math model:

$$[VIXA] = [VITOA] [VIXO].$$

Next, the points are mapped to the target camera:

$$[VIXM] = [VIMAC] [VIXA];$$

and then, from the camera to the projector:

$$[VIXT] = [VIMCT] [VIXM].$$

These points are then analyzed as previously described ⁴⁰. To find the ellipse parameters, first the center of mass is found:

$$1) \quad VIYTC = \left(\frac{VIN}{\sum_{VII=1} VIXT [2, VII]} \right) \div VIN.$$

$$2) \quad VIZTC = \left(\frac{VIN}{\sum_{VII=1} VIXT (3, VII)} \right) \div VIN.$$

Then the two end points are found:

$$1) \quad \begin{bmatrix} VIYTE1 \\ VIZTE1 \end{bmatrix} = VIMAX (VIYTC, VIZTC, VIXT).$$

$$2) \quad \begin{bmatrix} VIYTE2 \\ VIZTE2 \end{bmatrix} = VIMAX (VIYTE1, VIYTE2, VIXT).$$

From these end points, the length:

$$VIAT = \frac{1}{2} \sqrt{(VIYTE1 - VIYTE2)^2 + (VIZTE1 - VIZTE2)^2};$$

Center:

$$VIYTO = (VIYTE1 + VIYTE2) \div 2 \quad VIZTO = (VIZTE1 + VIZTE2) \div 2$$

and the sine and cosine of the angle:

$$1) \quad VITTC = (VIYTE1 - VIYTE2) \div 2(VIAT)$$

$$2) \quad VITTS = (VIZTE1 - VIZTE2) \div 2(VIAT).$$

can be calculated.

By using these values and calculating the length of the other axis for each point, the maximum values for this axis can be found. Each axis will be the calculated value plus a 10% margin.

$$VIAT = 1.1 \times VIAT$$

$$VIBT = 1.1 \times VIBT$$

Determination of Desired Background Image Generator Video Blanking. Because of the locations of the two projectors an ellipse in one projector (the target projector) will not be the same shape if it were mapped to the other projector (the background projector). The closest "fit" between the two ellipses can be achieved by mapping the points used to generate the ellipse from the target projector to the background projector.

$$[VIXB] = [VIMTV] [VIXT]$$

Once these points have been found in the background frame, the same analysis will be done to find the parameters of the ellipse at the analysis previously described in detail⁴¹.

Video Blanking Drive Signal Module. The ellipse equation can be written in the form:

$$K_1X^2 + K_2X + K_3XY + K_4Y + K_5Y^2 + K_6 = 0.$$

Where the K_i 's are functions of the ellipse parameters. The following expressions are based on the target ellipse, but the same relationships hold true for the background ellipse.

These constants are output to the hardware. For one scan line on the projector raster, Y is a constant. For each Y value the ellipse equation reduces to:

$$AX^2 + BX + C = 0.$$

A special purpose computer will substitute Y values for each scan line into the ellipse equation and solve for X . The two X values will give the points on the scan line between which the ellipse appears. These X values will be fed to the blanking equipment.

SPECIAL EFFECTS GENERATOR.

Overall System Description. The special effects generator accepts inputs, which indicate visibility range, time of day, cloud cover and aircraft attitude and altitude. This information is used to generate the appropriate visibility and sky conditions on the display screen. The inputs from the operator's console are visibility range (from 0 to 99,000 feet in 1,000 foot increments), cloud base (height of cloud top from 0 to 9,900 feet in 100 foot increments) and 3 position switch for day, dusk, and night. All these parameters, nominal viewing point altitude, and appropriate direction cosines of the local vertical are input to the special effects generators.

Visibility Effects Drive Signal Module. Inputs to the visibility effects drive signal module are those inputs from the operator's console described above, simulated aircraft attitude, area of interest attitude, and nominal viewing point altitude. The outputs from the visibility effects generators consist of the following two state variables: in clouds, above clouds, day/dusk, and night/day; and the following 12 bit word outputs: visibility range divided by nominal viewing point altitude, altitude above the clouds, observer frame direction cosines of the local vertical to the special effects generator for the background image generator, and polynomial coefficient outputs to the special effects generator for the target image generator.

The visibility range divided by nominal viewing point altitude is obtained directly from a division of available quantities. The altitude above the clouds is obtained by subtracting cloud altitude from nominal viewing point altitude. Observer frame direction cosines are three of the simulated aircraft body axes to horizontal reference frame direction cosines evaluated by the simulation of the flight characteristics. The polynomial coefficient outputs to the special effects generator for the target image generator will be evaluated off-line and stored as functions of area of interest frame azimuth and elevation.

OTHER PROGRAM MODULES.

Aircraft Position and Altitude Module. The function of this module will be to extrapolate aircraft position and altitude at the AWAV system rate from the VTFS program.

The inputs to the program will be aircraft altitude and X, Y position. The module will use past values to extrapolate the 20/sec. VTFS data to 30/sec. for the AWAV system. (See figure 106).

Ground Track Module. The ground track computation module will use as inputs aircraft velocity and velocity vector orientation. It will generate as outputs aircraft X and Y position. (See figure 107.)

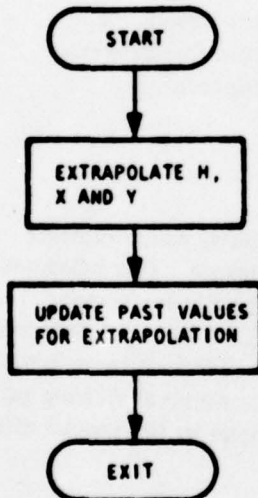


Figure 106. AIRCRAFT POSITION AND ALTITUDE MODULE

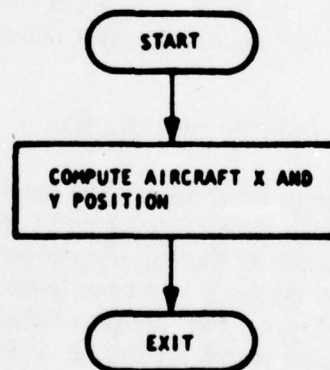


Figure 107. GROUND TRACK MODULE

Carrier Simulation. This module will compute the carrier data from instructor-controlled inputs. The inputs will be carrier speed and heading and sea state.

The module will generate carrier position, roll, pitch, heave, and deck height above sea level as outputs. (See figure 108.)

Arresting Hook Module. The function of this module will be to generate a boolean for arresting hook position. The boolean will be "true" for the arresting hook extended.

After the pilot input to extend the arresting hook is recognized, a timer will be incremented. When the correct delay is reached, the boolean for arresting hook extended will be set. (See figure 109.)

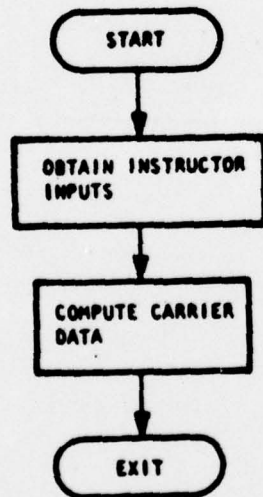


Figure 108. CARRIER SIMULATION MODULE

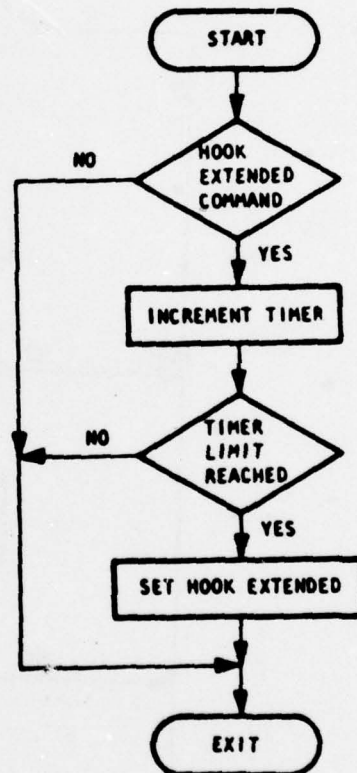


Figure 109. ARRESTING HOOK MODULE

Arrested Landing Module. The function of this module is to provide the parameters required to simulate hook capture landings and bolters. The inputs to the module will be aircraft and carrier position and altitude, arresting hook position, instructor input (for a bolter), and carrier landing system data.

The module will compute arresting hook forces and moments to be included in the simulation of aircraft forces and moments and the motion system cues as outputs. Hook capture, zone, and wire numbers will be available for printout if requested by the instructor. The visual system will use the outputs to provide visual cues. (See figure 110.)

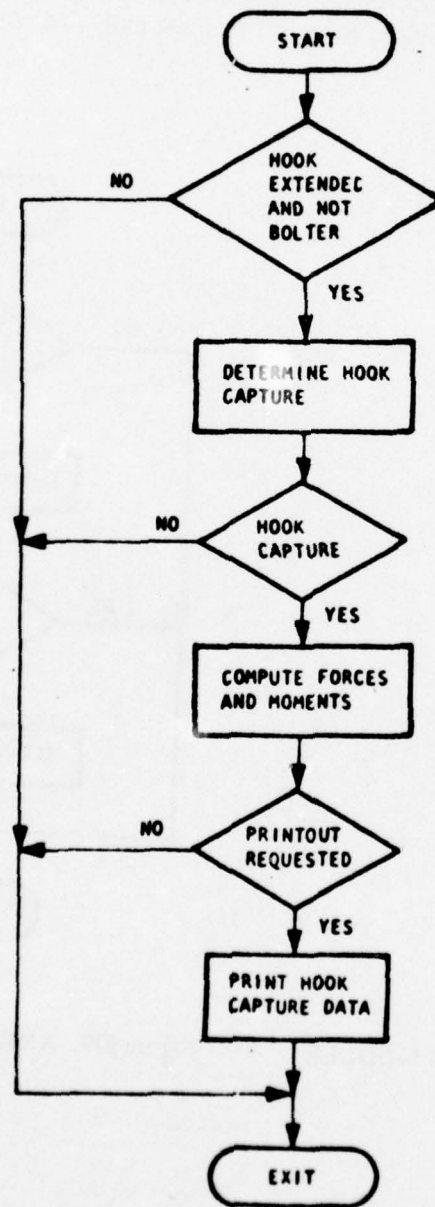


Figure 110. ARRESTED LANDING MODULE

Crash Conditions Module. This module will provide additional crash indications representative of carrier operations. The inputs will be aircraft and carrier positions and attitudes.

The module will generate a crash indication for landing on the carrier outside the landing area, ramp strikes, and crashes into the water as outputs. The simulator will freeze when a crash occurs. (See figure III.)

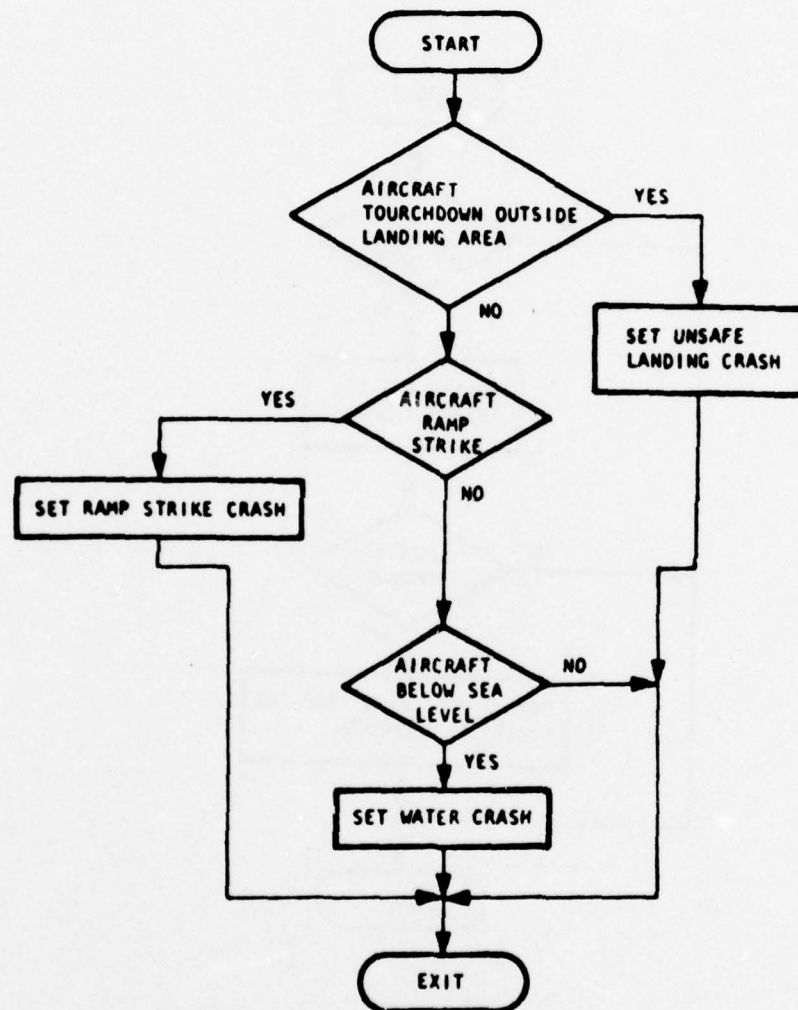


Figure III. CRASH CONDITIONS MODULE

Catapult-Launch Module. The function of this module will be to compute the forces and moments applied to the aircraft by the catapult launch system. After initializing for a catapult-launch, the input to the module will be a command to launch.

Catapult applied forces and moments will be generated as outputs for the computation of motion and visual system cues and the summation of forces and moments in the aircraft equations of motion. (See figure 112.)

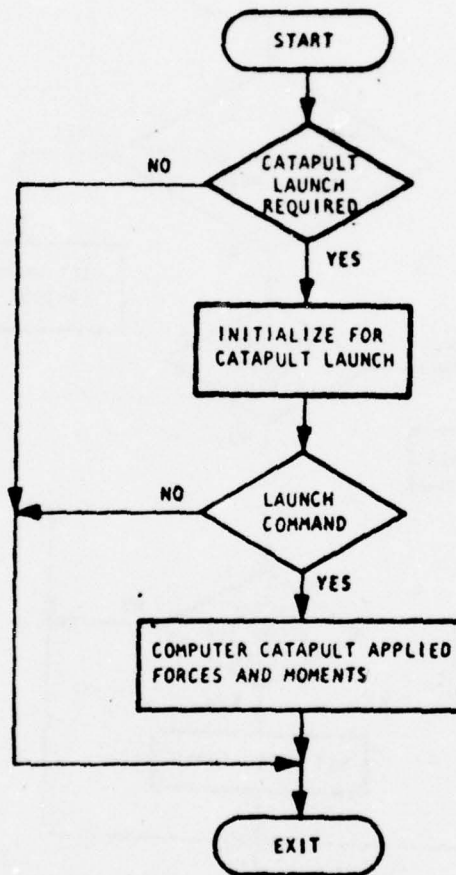


Figure 112. CATAPULT LAUNCH MODULE

SECTION XI

SPECIAL EFFECTS GENERATORS

The special effects generator (SEG) will electronically modify an input video signal to realistically create the impression of overcast ceiling, restricted visibility, and above-cloud flight. Two SEG's will be used: one for the background display system and one for the target display system. Since the SEG systems are so similar, only one discussion is presented for both.

METHODS CONSIDERED.

The special effects generators (SEG) are, in general, similar to the SEG systems that have a proven performance capability record garnered in a number of previous programs. This section on the SEG will examine in detail the features of the already existing special effects generators and the modifications necessary to implement them for the AWAVS program. No alternatives were considered.

SYSTEM BLOCK DIAGRAMS.

Figure II3 represents a simplified block diagram, and figure II4 (sheets 1 and 2) show a detailed block diagram of the SEG.

Inputs. (For figure II3.) Mode selections (visibility conditions are as follows):

- 1) daylight/dusk/night
- 2) above/below cloud
- 3) flight above cloud
- 4) in-cloud conditions

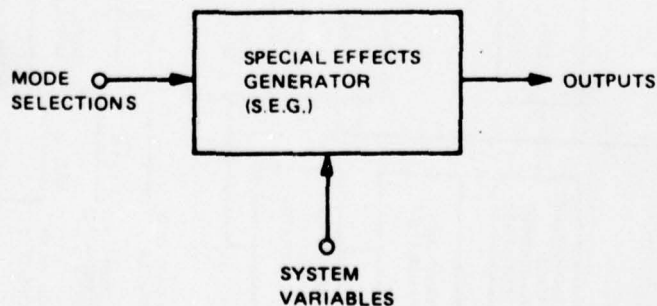


Figure II3. SPECIAL EFFECTS GENERATOR, SIMPLIFIED BLOCK DIAGRAM

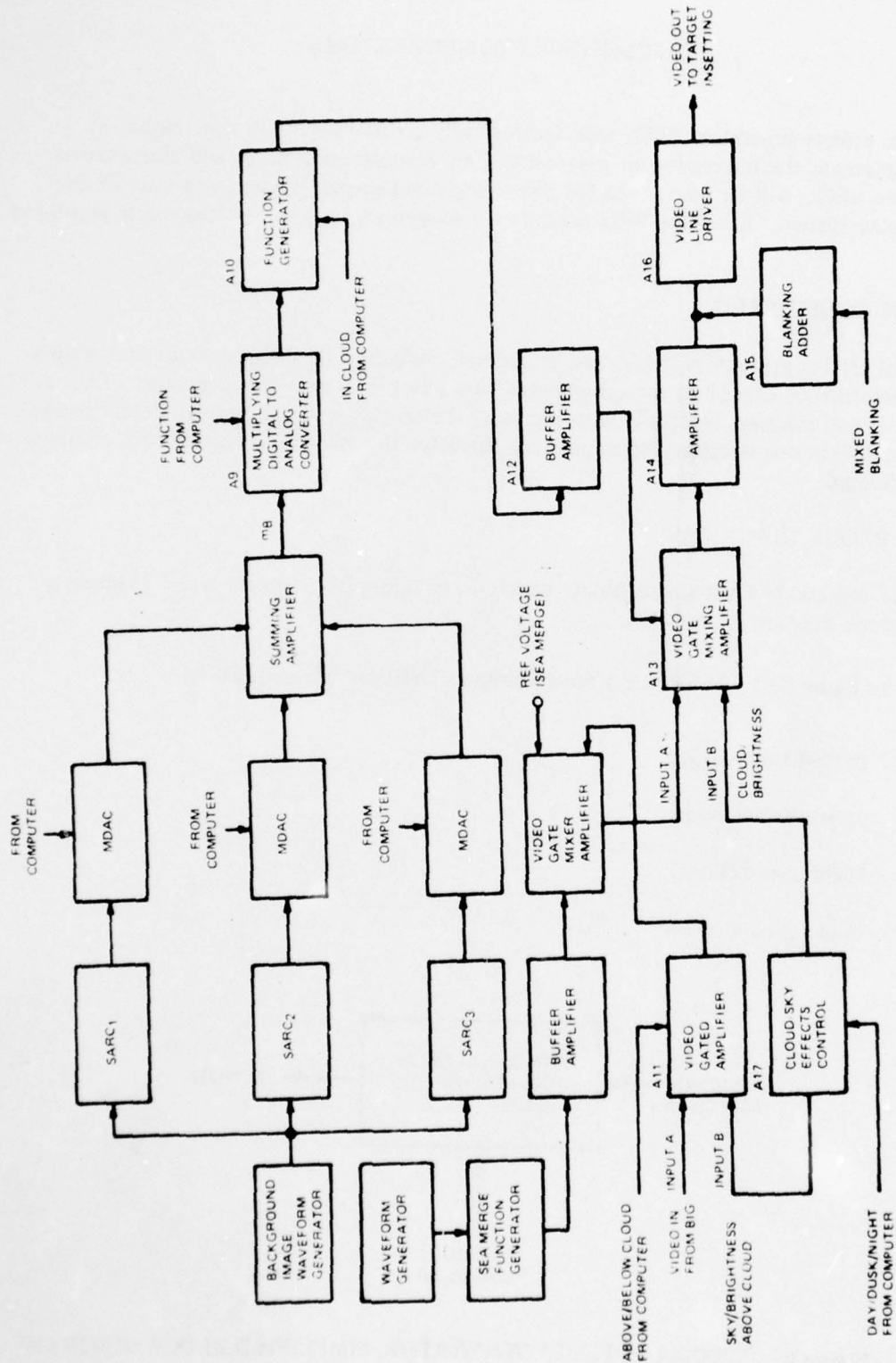


Figure 114. VISIBILITY AND SPECIAL EFFECTS GENERATOR BLOCK DIAGRAM (PART 1 OF 2)

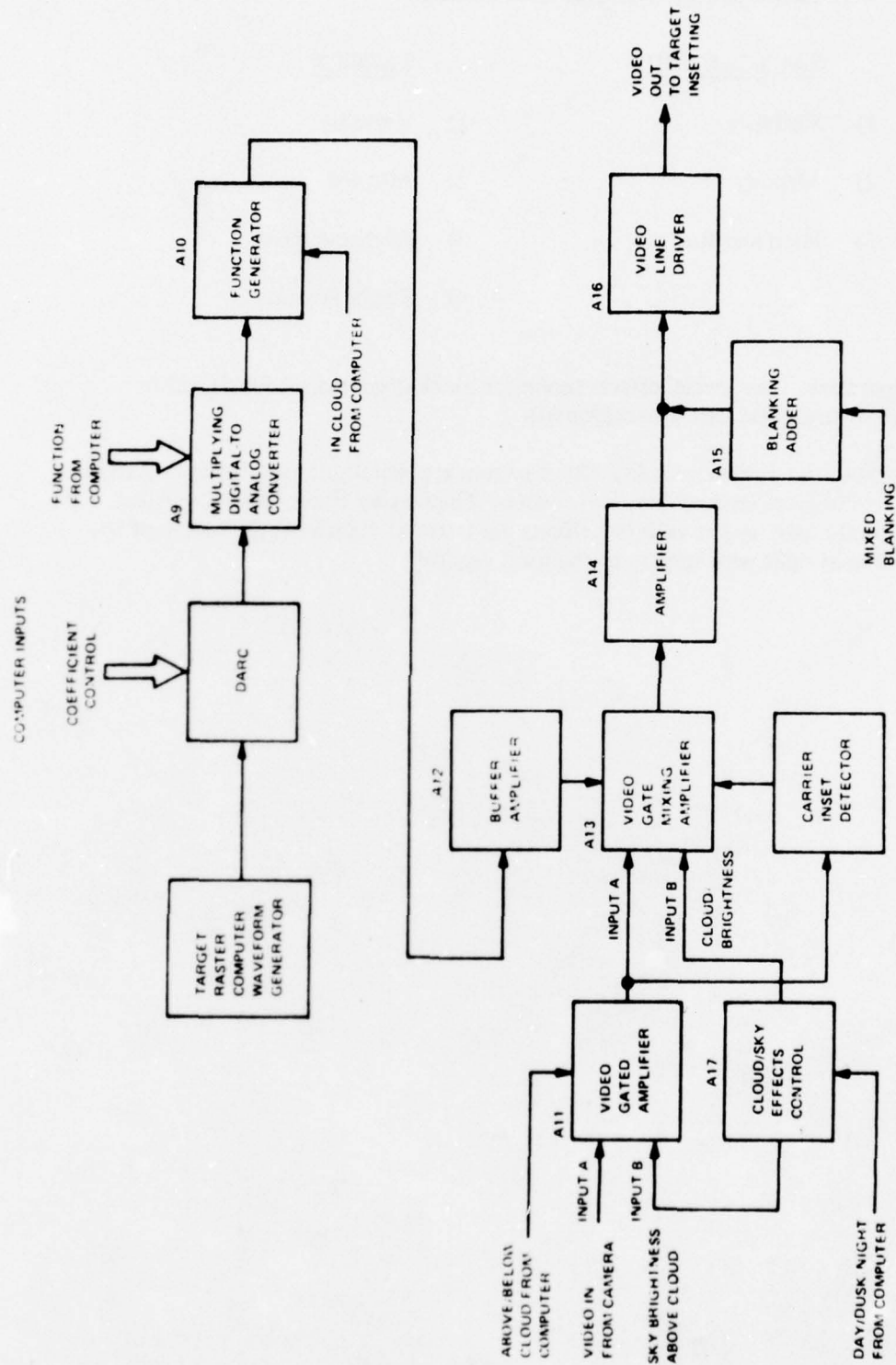


Figure 114. VISIBILITY AND SPECIAL EFFECTS GENERATOR BLOCK DIAGRAM (PART 2 OF 2)

System variables (relative aircraft positioning information):

<u>BACKGROUND</u>	<u>TARGET</u>
1) Visibility	1) Visibility
2) Altitude	2) Altitude
3) Pitch and Roll	3) Pitch and Roll
	4) Target Position

Principle of Operation. The special effects generator block diagrams are illustrated in figure 114 (part 1 target and part 2 background).

The major inputs to the present visibility effect system are visibility range divided by altitude and display frame to local vertical direction cosines. The display frame to local vertical direction cosines are used by the visibility effects hardware to determine the cosine of the instantaneous line of sight with respect to the local vertical.

The target mapping function is a dynamic system, dependent on location and zoom. Therefore, a term will be generated by a DARC, or digital-analog raster computer similar to the system described in section 5. Only a single expansion need be generated; thus requiring only one-half the control signals used in the raster computers.

The background projector mapping is a fixed function for a given projector orientations. The generator will utilize a Static-Analog Raster Computer (SARC).

The SARC is a fixed version of the DARC, using fixed resistors to determine the signal rather than computer controlled amplifiers, or MDACS, as used in the dynamic raster computer DARC. A plug-in replacement will be used for the second position.

The remaining portion, after the production of the term "m", is common to all of Singer's special effects generators, and constitute the heart of the performance proven SEG systems.

The camera is fed to the "A" input of A11 and the "sky brightness above the clouds" signal is fed to the "B" input of A11. The computer generated signal "above cloud/below cloud" switches the output of A11 to provide the proper signal into the "A" input of A13. The "cloud brightness" signal is fed into the "B" input of A13.

Selection between inputs A and B in amplifier A13 is controlled by the gating waveform from A10. One of the very desirable features of these switching amplifiers is their "soft" transition between inputs A and B. This characteristic permits the gradual (and realistic) blending of the lower and upper parts of the picture. The "sharpness" of the transition is controlled directly by the "steepness" of the negative-going edge of the gating waveform.

The simulation of scud is created by varying the gating function in a pattern so as to give the effect that the aircraft is flying in and out of varying levels of cloud. The rate of change is a computer pseudo-random signal varied over the closest 100 foot level of cloud base or cloud top. The signal is changed from normal picture to full cloud as the aircraft goes into the cloud. The converse occurs during the exit from the clouds.

NAVTRAEQUIPCEN 75-C-0009-1

Selection "dusk" energizes two relays in the cloud/sky effects control module. Selection of "night" similarly operates a relay. Operation of these relays switches in different controls so that the "cloud brightness" and the "above cloud sky brightness" signal levels are different for "day," and "night" operation.

Thus the pictorial presentation may be described as follows, under the condition of below cloud, above cloud, and in cloud:

- 1) Below Cloud: Carrier image from model board in lower portion and cloud cover or sky in the upper portion of the picture when flying below ceiling altitude.
- 2) Above cloud: Cloud cover undercast in the lower portion and sky in the upper portion of the picture when flying above cloud top altitude.
- 3) In cloud: Plain gray - white over entire picture when flying above ceiling and below cloud top.

The addition of carrier inseting will be made to the SEG. The carrier inseting is described in section 9. The signal generated by the carrier inset detection will modify the gating function for proper presentation of the carrier during final approach and on the landing deck, when the carrier will be visible above the horizon line normally presented by the SEG.

Proper detection of the carrier is dependent on contrast difference between the carrier and other video. Therefore, the choice of paints and lighting arrangements must be made to assure the minimum signal difference necessary to accurately detect the carrier against the seascape.

OPERATIONAL CONTROLS.

RVR - Visibility range will be adjustable from 0 to 99,000 ft in 1000-ft increments.

Cloud Base - The height of the cloud cover will be continuously adjustable from 0 to 9,900 ft above sea level in 100-ft increments.

Ambient - Three-position switch for day, dusk and night.

Cloud Top - The thickness of the cloud layer may be established by the instructor by adjusting the height of the top of the clouds. Adjustable from 0 to 9,900 ft in 100-ft increments.

CONCLUSION.

The addition of modified waveform generators to the basic special effects system allows the performance-proven existing concept for the Singer SEG to meet the requirements of the AWAVS SEG.

SECTION XII

FUTURE ADDITION

Growth potential requirement of the procurement specification is discussed in this section.

REQUIREMENTS.

The AWAVS design concept permits adding to the basic configuration to permit evaluation of many visual system configurations. The required characteristic of each module to be added depends on the AWAVS configuration prior to the proposed modification, and the anticipated growth objectives as they may then be defined. To simplify the analysis of possible approaches, it is assumed that the sequence of the additions will be as described at the orientation conference; namely air-to-air combat and formation flight, shore airport operations, and air-to-ground weapon delivery.

Since detailed visual system specifications for each of these operational equipments have not been defined, appropriate visual cue requirements are assumed for this analysis.

Air to Air Combat. Provision for this capability requires very large fields of view with the capability to display the target anywhere in the field of view. The target aircraft attitude should be observable to permit the pilot to anticipate its future flight path. Likewise, it is desirable to be able to observe an indication of the operation of speed brakes or booster to anticipate speed changes. These requirements indicate the need for a range of 100 ft. to 36000 ft., or from about 50° to 3 arc-minutes, dependent on the aircraft size and attitude. The horizon is also needed for attitude reference and the earth imagery is required for altitude cues. Inclusion of the sun, missile, and cloud formations is desirable to permit training and maneuvering evaluation under realistic conditions. Realism of the scene content is desirable to permit establishing and maintaining the maximum mental stress and pilot loading conditions, but may be omitted for laboratory type evaluation of aircraft maneuverability or the development of some tactics maneuvers.

Formation flying. Formation flight requires most of the same visual system capabilities, except that a FOV 60° or larger may be required for tight formations. In both cases, monochrome images are adequate.

These requirements indicate that a visual system with the following characteristics should be provided:

1) **Background FOV**

-30° to $+60^{\circ}$ vertical, with -120° to $+120^{\circ}$ horizontal. If possible, the vertical FOV should be increased to $+90^{\circ}$.

2) **Earth Image**

Altitude range 500 ft. to 20,000 ft.

Heading freedom - 360° .

Ground velocity cues.

Unique landmarks for position reference.

Maneuvering range - 10 nm square.

3) Haze and horizon

From edge of earth image to horizon.

4) Cloud formation

Open layers of clouds, with altitude range selectable from 2000 to 20,000 ft.

5) Sun

As bright on image as feasible, with selectable position in the sky.

6) Target Aircraft

Range - 100 to 36,000 ft.

Resolution - to permit attitude determination at ranges up to 18,000 ft.

Shore-Based Airport Operation. This includes training in conducting airport flight patterns, with approach, landing, and takeoff, and includes practice in the use of the VASI visual landing aids, under various weather conditions. It does not include navigation to the base so that an operating volume of 6 x 10 nm x 1200 ft. height is adequate. During the VFR approach traffic pattern, it is necessary to be able to keep the airport continuously within the field of view. For the usual counter-clockwise patterns, a 120° horizontal FOV or larger is required. The 120° FOV may be marginal if the display cannot be smoothly rotated to keep the touch-down point approximately centered. Discrete display FOV shifts are undesirable, since they will provide an unnatural position cue. A vertical FOV maximum of 80° will be adequate. Final analysis of the maximum expected bank angles may determine that a somewhat lower FOV will be adequate. As usual, reducing the FOV permits increases in brightness and resolution, so the display should be kept as low as possible without losing imagery effectiveness. The critical visual scene characteristics are shown below:

1) Display FOV

-30° to +50° vertical, with 120° horizontal: A full 240° horizontal FOV with the airport Area-Of-Interest (AOI) image inset and moveable within the larger FOV. The display FOV should be able to be shifted from full left, to center or to forward, as required by the flight pattern. A full 240° of horizon is desirable.

2) Image Content

Airport - area 6 x 10 nm; image content - runway with texture, runway lights with controllable brightness.

Operating altitude range, touchdown to 1200 ft. colored, VASI lights and airport runway lights.

Visibility control, clear to CAT II condition.

Imagery - except as noted, monochromatic, but color is desirable.

Time of Day simulation - day, dusk, night.

Air-to-Ground Weapon Delivery. The image requirements here are similar to those for airport operations, if the requirements for target location and identification are omitted. The inclusion of these two training objectives appear to be beyond the capabilities of extension of the AWAVS capabilities, because in the ultimate, it is desired that the pilot ferret out small or camouflaged objects. If the kind of detail required for this were included in the system performance objectives, the object would tend to be included in a spotlight-type of inset, thereby providing unacceptable, unreal conditions. The AWAVS can, however, be upgraded to provide training in approach pattern selection, based on terrain and cover conditions, and in weapon delivery procedures, to both flat ground and hillside targets.

A large variety of potentially-acceptable TV techniques is available to satisfy the above objectives. Since they may be used in many combinations, the definition or analysis of specific system configurations will be omitted. Instead, a definition of the various subsystems will be given, together with their advantages, limitations, and interface considerations. A matrix of the cues required, and the capabilities of various image generators, to provide these cues is provided in table 20. Analysis of the display system design considerations and potential solutions follows the analysis of the image generation design approach. Unless specifically discussed otherwise, it may be assumed that any image generator may interface with any of the recommended projector subsystems.

CAMERA MODEL GROUND IMAGE GENERATORS.

Camera model systems have the following characteristics.

Advantages. The models may contain any of the following features: realism, with controllable ground light patterns; texture; recognizable features for altitude and range cues; 3D objectives, for fine translational cues during landing; presentation of geographical and/or cultural features to be considered in tactical selection; training in recognition of features of a specific airport or area; readily-relocatable objects such as targets. Models are relatively inexpensive to modify.

Flexibility may also be obtained in optical probe and cameras in the following areas:

Field of view - 60° or 120° using existing designs.

Optical characteristics - conventional or Scheimpflug-compensated (the latter permits lower eyepoint and smaller model sizes) rectilinear or spherical mapping.

Cameras - Monochromatic or color cameras with a wide variety of resolution sensitivity, image stickiness, and noise characteristics.

Application. Camera sweeps may be driven from camera raster computers to provide true eyepoint simulation, even though neither the observer nor the projector is at the screen center. When the system also includes display raster computers, it is possible to move the inset within the background image, to permit the inset to provide an area of interest function with only fixed functions raster computers, a very desirable feature. With dynamic raster computers it also appears feasible to inset the camera model into CGI imagery with image correlation between the two sources. In either case, this permits combining the wide area of the CGI with the excellent characteristics of the CM imagery in a selected ground area. The choice between the 120° to 60° probes depends on the training maneuver requirements, and whether the model scene is alone, or if it is inset into a wide FOV image generator. Improved resolution, image brightness and cost reductions are possible with the low FOV and non Scheimpflug probes.

Limitations. The area which may be included on the model is equal to the product of the scale factor and permissible model size. The scale factor selected ranges between 50 to 90 times the minimum eyeheight to be simulated. The value selected for this latter factor depends on the type of terrain, resolution and contrast requirements. The 90X factor may be used with flat terrain such as runways, with Scheimpflug corrected probes and where the contrast requirements of the image generator subsystem are not severe.

CAMERA MODEL (GIMBALLED AIRCRAFT MODEL).

This subsystem approach is useful for air to air and formation flight simulation. The equipment includes a 3-axis, gimballed model and gantry, a camera, a camera optical system, and sometimes additional range simulation features. These would be required to satisfy the 100 to 36,000 ft. range. Consider the requirements for a 40-ft. aircraft scaled to 1 ft.; 100 ft. would correspond to 2.5 ft. from probe entrance to model center. A typical breakdown of range simulation functions may be as follows:

Model gantry (motion 100 to 500 ft.)	- 5X
Projection zoom optics	- 10X
Display raster shrink	- up to 15X

$(5X)(10X)(15X) = 750X$, largest possible product using this method.

Other options include camera zoom lens addition and/or camera raster expansion, or in various combinations. If Eidophor projectors are used, raster shrinking is not feasible, so one of the other techniques could be applied.

EXPANDED CAPABILITY AND ADDITIONAL VISUAL SYSTEM CHARACTERISTICS	CAMERA MODEL			FILM BASED		
	TERRAIN IMAGE		FULLY GIMBALED AIRCRAFT MODEL 80° FIELD	SCANNED VAMP	COMPUTER GENERATED IMAGE	DAY/NIGHT CALLIGRAPHIC
	120° PROBE	80° PROBE				
<u>AIR TO AIR AND FORMATION FLYING</u>						
A. BACKGROUND IMAGE ATTITUDE CUE (E.G. HORIZON) ALTITUDE CUE (E.G. GROUND OBJECT SIZE) CLOUDS	POSSIBLE, BUT FOV IS INADEQUATE FULL HORIZON MUST BE PROVIDED	SAME AS 120° FOV PROBE BUT CONDITION IS MORE SEVERE	NOT APPLICABLE	NOT APPLICABLE	VERY GOOD COST EFFECTIVE IF CGI IS ALSO USED FOR OTHER APPLICATIONS	VERY GOOD AND COST EFFECTIVE
B. INSET DETAIL IMAGE RELATIVE BEARING AND DISTANCE DIRECTION OF TRAVEL DISTANCE (30 FT - 30,000 FT)	NOT APPLICABLE	NOT APPLICABLE	GOOD COULD BE ADDED TO AIRCRAFT CARRIER GANTRY SUBSYSTEM	NOT APPLICABLE	VERY GOOD LIGHTS ON AIRCRAFT MAY BE ADDED	COULD PROVIDE A SILHOUETTE WITH SOME SHADING, LIGHTS AND LINE OVERLAY MOST ECONOMICAL
C. SUN IMAGE EFFECT	NOT APPLICABLE	NOT APPLICABLE	NOT APPLICABLE	NOT APPLICABLE	OK AS PART OF BACKGROUND GENERATOR	PROBABLY COULD BE PROVIDED
<u>SHORE AIRFIELD</u>						
A. BACKGROUND IMAGE ATTITUDE CUES ALTITUDE CUES CLOUDS	MARGINALLY ALL RIGHT WITHOUT AREA OF INTEREST DISPLAY INSET INTO HAZE HORIZON GENERATOR	ONLY MARGINALLY ACCEPTABLE WITH AOI OPERATION	NOT APPLICABLE	OK - PROBABLY MOST EFFECTIVE FOR MULTIPLE UNIT PRODUCTION	VERY GOOD, COST EFFECTIVE IF CGI IS ALSO USED FOR OTHER APPLICATIONS	VERY GOOD AND COST EFFECTIVE
B. INSET DETAIL IMAGE AIRFIELD DETAILS LIGHTS (INCH VAS) CIRCLING APPROACH (WITH AIRFIELD IN SIGHT) LANDING/T.O. LIMITED VISIBILITY EFFECTS	GOOD WITH AOI TYPE GENERATION	VERY GOOD FOR INSET WITH AOI TYPE GENERATION	NOT APPLICABLE	ALL RIGHT - PROBABLY MOST EFFECTIVE FOR MULTIPLE UNIT PRODUCTION	VERY GOOD COST EFFECTIVE IF CGI IS ALSO USED FOR OTHER APPLICATIONS	VERY GOOD AND COST EFFECTIVE

Table 20. REQUIRED CUES FOR
IMAGE GENERATORS

ELECTRONIC IMAGE GENERATION					OPTICAL IMAGE GENERATION	
COMPUTER-GENERATED IMAGE	DAY/NIGHT CALLIGRAPHIC	SYNTHETIC TERRAIN GENERATOR	SCANNED TRANSPARENCY	ELECTRONIC HAZE AND HORIZON GENERATOR	VASI PATTERN GENERATOR	GIMBALED SPOTLIGHT
GOOD EFFECTIVE IF ALSO USED FOR APPLICATIONS	VERY GOOD AND COST EFFECTIVE	VERY GOOD AND COST EFFECTIVE	GOOD, BUT LIMITED TO 10:1 ALTITUDE CHANGE, WITHOUT EQUIPMENT CHANGE OR 20:1 WITH CHANGE OF FSS CRT	REQUIRED FOR HORIZON BUT PROVIDES NO ALTITUDE OR HEADING CUES	NOT APPLICABLE	NOT APPLICABLE
GOOD ON AIRCRAFT & ADDED	COULD PROVIDE A SILHOUETTE WITH SOME SHADING, LIGHTS AND LINE OVERLAY MOST ECONOMICAL	NOT APPLICABLE	NOT APPLICABLE	NOT APPLICABLE	NOT APPLICABLE	NOT APPLICABLE
AS PART OF BACKGROUND GENERATOR	PROBABLY COULD BE PROVIDED	NOT APPLICABLE	NOT APPLICABLE	NOT APPLICABLE	COULD BE MODIFIED AS SUN IMAGE GENERATOR	MOST ECONOMICAL AS ADDITIONAL GENERATOR
VERY GOOD, COST EFFECTIVE IF CGI, SO USED FOR APPLICATIONS	VERY GOOD AND COST EFFECTIVE	GOOD	NOT COST EFFECTIVE COMPARED WITH HAZEL HORIZON GENERATOR FOR AOI TYPE BACKGROUND	USE FOR HORIZON AND CLOUD GENERATION	NOT APPLICABLE	NOT APPLICABLE
GOOD EFFECTIVE IF ALSO USED FOR APPLICATIONS	VERY GOOD AND COST EFFECTIVE	NOT APPLICABLE	NO GOOD FOR LIGHTS, ALSO ALTITUDE IS RANGE LIMITED	USE FOR HORIZON AND LIMITED VISIBILITY GENERATION	MODIFY FLOLS GENERATOR FOR VASI	NOT APPLICABLE

TV SCANNED VAMP.

This is another TV technique used by Singer, called Electronic Perspective Transformation. This system makes use of information stored on a movie film, but processes the data on the film by electronic image scanning techniques, so that the apparent eyepoint may be moved around within a large maneuvering volume. This maneuvering volume well meets the maneuverability objectives of airport approaches, landings, and takeoffs under all kinds of weather conditions. Basically different problems may be simulated via different films. This system may also be suitable for air-to-ground weapons delivery, since the desired flight paths for this maneuver are relatively well defined. This system has the very great advantage that optimal scale factors are employed over a full range of operation, since effectively, a new scale factor is in effect for each film frame. Thus, this TV-type system permits the greatest resolution over the largest potential maneuvering path. The only constraint of the system is that it is limited to providing maneuvering routes which must follow reasonably well-defined flight paths. Generally, the degree of freedom provided by the equipment exceeds that which is permissible under approved flight path patterns.

SCANNED TRANSPARENCY.

The scanned transparency system used in the initial configuration could be modified to provide earth, rather than a sea image. An additional channel is required for each background projector. The image would also be mapped to provide a full 240° display.

ELECTRONIC IMAGE GENERATION.

Each of the electronic TV scanned transparency image generators (i.e., CGI, Calligraphic Day/Nite Visual (CDNV), Synthetic Terrain Generation (STG), and Haze/Horizon generators) are capable of generating scenes covering a full sphere about a single design point. Thus they are especially adapted for generating the wide angle displays required for the growth requirements. For image quality, brightness, and equipment flexibility reasons, an image generator channel is recommended for each display channel. Each of these systems, except for CGI and CNDV can be designed to provide almost any desired scan line mapping, thus they may be readily used with either CRT or Eidophor projectors. The choice between these is determined primarily by image content and display system interface considerations.

COMPUTER-GENERATED IMAGERY.

The CGI approach offers the greatest image flexibility. It may be used to generate imagery which will provide all of the cues, both ground and flying aircraft, required for each of the proposed growth applications. The image is computed from a stored 3D environment, to form an image on a plane, as if the image were photographed onto a plane ahead of each projector. In this system, the scan lines can only be straight and parallel, containing no mapping function. Therefore, all mapping must be provided in the projector, or via intermediate equipment. When projection CRT's are used, the mapping may be incorporated in them. If it is decided to match the Eidophor with a DIG, it will be necessary to provide a scan converter between them. With the 100% MTF (Modulation Transfer Function) output of the CGI equipment, it is possible to obtain a monitor display with almost the same MTF and with a resolution of 1000 lines per picture height, yet with no effective noise. Thus a bright dynamic scene is available on a CRT. This would be viewed by a high resolution camera, to provide the necessary mapping and scan conversion.

CALLIGRAPHIC DAY/NITE VISUAL SYSTEM.

The Calligraphic Day/Nite Visual system is a new Singer development. It provides some of the flexibility of a CGI system with the STG type simplicity. It portrays only a ground plane. However, the patterns may be made up of various sizes of straight-sided shapes on the ground plane. This gives much greater flexibility than the STG in the provision of heading and position cues. It also can provide textured runway surface and excellent day or night runway lights. However, like the CGI system, the image is defined as the projection of a segment of the earth onto the window plane. Thus the image element edges are straight, without the flexibility of mapping. Its interface with the displays would then be the same as the CGI system. However, as the name indicates, it will work only with a display capable of Calligraphic presentations. Thus it is limited to the CRT projectors. If colored lights are required, the necessary colored CRT channels could be provided.

SYNTHETIC TERRAIN GENERATOR.

The synthetic terrain generator provides an image representing a checkerboard earth that is viewed from the correct eye point height, and along the simulated lines of sight of the associated projector. It is possible to include eight unique patterns, inserts, etc. into the pattern of uniform squares, so that position and heading references are obtainable. The checkerboard squares provide very effective altitude, velocity, and attitude change cues. It is very useful as a ground plane for air to air formation and combat, and flight maneuvers. It has also been used as a background, with a camera model image inset into it, for an AOI type presentation. Any required mapping can be provided, so it may be fed directly to either Eidophors or CRT's.

HAZE/HORIZON.

The haze horizon generator is generally used only for limited visibility effects on landing and takeoff, and for providing a haze band between the edge of the image provided, by one of the methods outlined above, and the proper horizon position.

Any of these systems can be used for the background image generator. Only the CGI system would be effective for the inset image for a target or formation flight aircraft. The optimum configuration must be defined after an analysis of the equipment then available, as well as the anticipated requirements at the time of the analysis.

SUN IMAGE GENERATOR.

A spot projector, with the scanning position capability of the inseting projector, will be required for this. It also must respond to computer control.

VASI GENERATOR.

A modification of the FLOLS design approach should be suitable for this.

BACKGROUND PROJECTOR.

Background Projector growth requirements include the following:

- 1) Increasing the FOV from $80^{\circ} \times 160^{\circ}$ to $90^{\circ} \times 240^{\circ}$

- 2) Providing a continuous image across the full FOV, with a minimum of gap at the upper and lower edges, at the joint between channels.
- 3) Compatibility with the Image Generator subsystems, past and future.
- 4) Provision for area of interest operation or image movement within the FOV.
- 5) Retaining or improving resolution and brightness.

Additional characteristics which may be added include the following:

- 1) Conversion to color.
- 2) Compatibility with CGI without the need for intermediate scan conversion.
- 3) Provision for relaxing the motion and shock limits.

INSET PROJECTOR.

Inset projector growth requirements include the following, in addition to the applicable requirements listed above:

- 1) Required additions:

None.

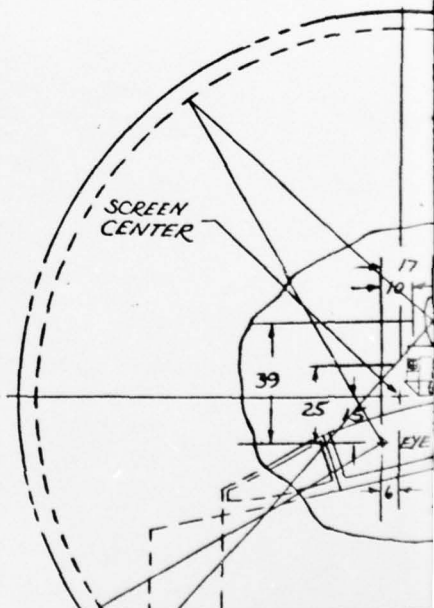
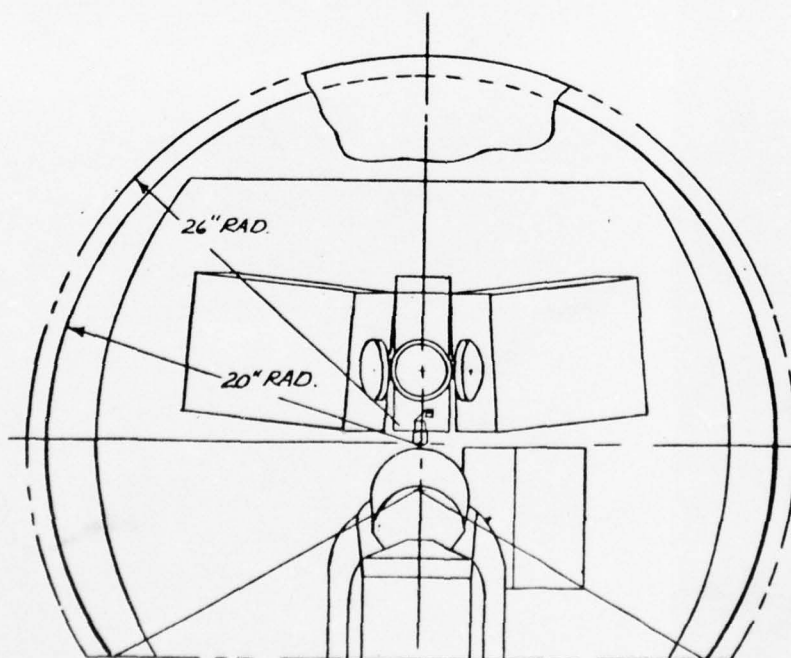
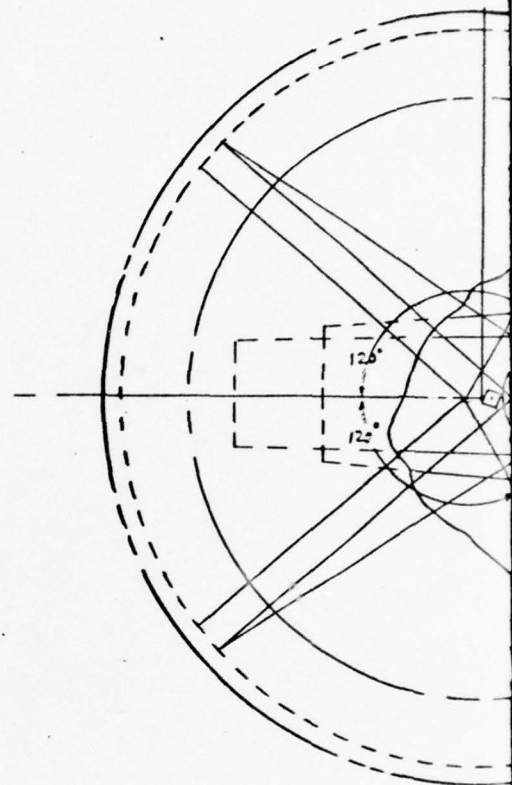
- 2) Desirable Additions:

Incorporation of raster shrink to replace and/or supplement the zoom lens in the projection optical system.

Increasing the FOV will require a new lens and projector arrangement. Consideration of the objective to use a CGI input indicates the desirability of decreasing the FOV, per image generator. This is desirable to provide a adequate resolution. Since the CGI image is generated on a plane with equally-spaced resolution elements on that plane, the resolution element becomes very widely spread in the center of the field of view. It is, therefore, recommended that a layout configuration with three $80^{\circ} \times 90^{\circ}$ displays be used as shown on figure 115.

Vertical scan lines are desirable to permit smoother joints between windows, to permit moving images about between windows, including the condition when they span windows, and to permit integration of camera model and CGI images in a moveable area of interest type of operation. Vertical scan lines could be provided by rotating the image plane, via optical image rotations, if Eidophor projectors are used, or by vertical scan lines, if projection CRT's were used. Anamorphic lenses could be used to optimize the 3 to 4 Eidophor image format to the 3×3.4 ($80^{\circ} \times 90^{\circ}$) display format. With projection CRT's the scan lines could be initially generated vertically, and with the desired format.

In order to provide an essentially-continuous FOV, it appears that a 95° diagonal FOV lens would be required, if 3 projectors are used. For the inset projector, the Eidophor projector optical system incorporates both an image rotation prism and a varifocal lens system. Using a telecentric lens system design, such as in the Fairchild 160 $^\circ$ lens, it should be possible to insert a Pechan prism and varifocal lens between the input and output elements, so that an f2 system may be achievable. This would require complete redesign of the inset projector lens system, including replacement of the Schleiren mirror, with a low loss beamsplitter. Even with optimum design, this system would have somewhat greater loss than that of the background projector. However, the screen area to be illuminated is less than half of that per background channel, so that approximately-equal brightness levels should be obtainable with the insert and background projectors.



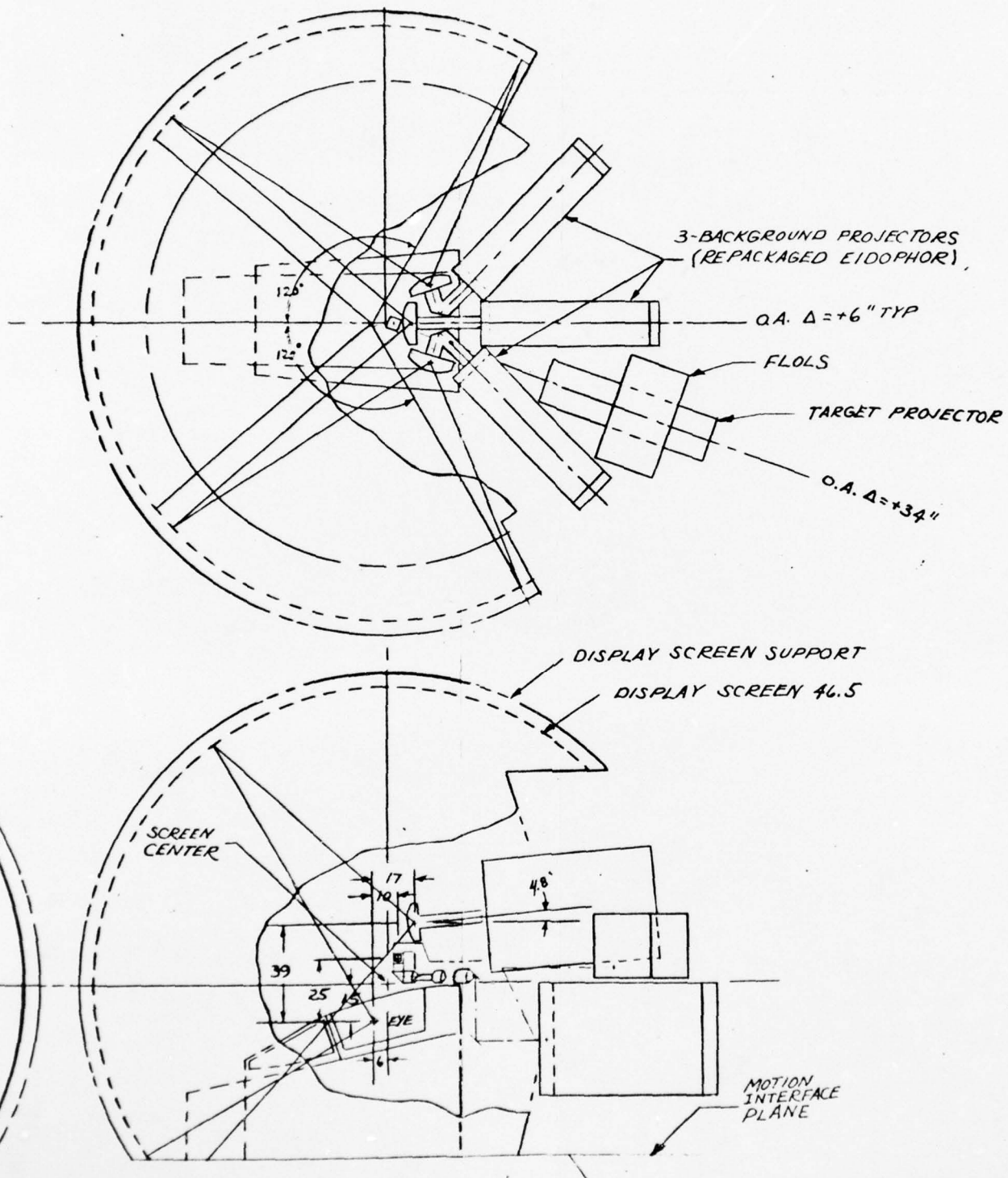


Figure 115. AWAVS DISPLAY SYSTEM,
FUTURE ADDITION

SECTION XIII

SYSTEM CONTROLS

The AWAVS, to be used in conjunction with an operational flight simulator, is intended as a feasibility model or a training device, "to provide an experimental basis for the development of future advanced flight simulators and visual systems." The requirement for system controls at the instructor station of such an experimental training device differs in two important ways from those of an operational training device:

- 1) In the experimental training device, flexibility — the ability to vary any of a wide range of parameters — is of utmost importance; in operational training devices, standardization of training dictates comparatively narrow limits to the variation of parameters by the instructor.
- 2) System controls on operational training devices must be designed for error-free use by a large number of instructors whose prior familiarity with the training device may be slight. Simulator instructor stations to be used by instructor pilots, for example, must be designed for easy use by instructors, familiar with teaching from the back seat (or copilot's seat) of the aircraft, who often lack the time and motivation to master a complex instructor console. It has been noted that when instructor consoles are complex, flight instructors do not exploit the full capability of the simulator. By way of contrast, the experimenters using the instructor console of an experimental training device are few in number, and motivated to accept the chore of learning a more complex console if the console provides needed experimental flexibility.

Thus, the system controls of the AWAVS should provide flexibility and easy change of any parameter even at the cost of added complexity. Analysis indicates that such flexibility is best attained by use of dedicated controls for most, if not all, parameters — i.e., a separate knob or switch for each item to be controlled.

METHODS CONSIDERED. No alternate methods were considered. The only method considered is the one discussed in the following paragraphs.

LOCATION AND GENERAL ARRANGEMENT.

In addition to controls at the instructor station, a significant number of operating and maintenance controls, including those exercising system servos, will be located in the maintenance area.

Details of instructor station controls, along with other controls and displays (including those for servo systems), are discussed in this section⁴².

INSTRUCTOR STATION CONTROLS AND DISPLAYS.

The instructor station console contains a CRT television monitor that provides an integrated display of the target image presented to the pilot; appropriately colored and shaped indicators, in the pattern of FLOLS, that illuminate to provide a display of the FLOLS image presented to the pilot; and the controls needed to operate the feasibility model and to control, monitor, and record the subject's performance. A sketch of that panel is shown in figure 116; a tabulation of the controls and indicators thereon (other than the television monitor and FLOLS "repeaters") is provided in table 21. Notes to that table describe the functioning of these controls and indicators, and point out the rationale for their selection.

SERVO SYSTEMS.

The servo systems are directly controlled by the computer for normal on-line operation of the visual system. This includes position or velocity commands and freeze commands, if required, in the hardware. The instructor console has control switches and/or keyboards to introduce the required conditions into the computer to establish the proper parameters for the simulation problem. Computed functions control the various servos for reset, freeze, or operate modes. Instructor controls do not directly control any servo in the system. (All servo drive signals originate in the computer.)

In the off-line mode (maintenance) each subsection of the visual system has controls and/or displays as necessary to test, calibrate, and isolate problems in that subsection.

Morning readiness tests that specify "off-line" program control of the visual system control the hardware via the computer and normal linkage signal paths.

OPERATING AND MAINTENANCE.

An indicator light is provided on the instructor (operator) console visual system control panel to indicate the operational or maintenance status of the visual scene generation and display system.

Controls and displays are provided at the subcomponent control cabinets for use in maintenance operations. These control-display systems provide for isolation of the visual hardware from the computer and substitution of individual manual control inputs to control the subsystem performance for alignment or test, and to isolate faults.

Each subcomponent maintenance control panel includes controls and displays to enable maintenance personnel to isolate problems with power supplies or electronics packages, selectively freeze and position each servo. The target generation panel includes means to control the ambient lighting, control the intensity of carrier lights, adjust the TV camera system, and monitor the TV picture.

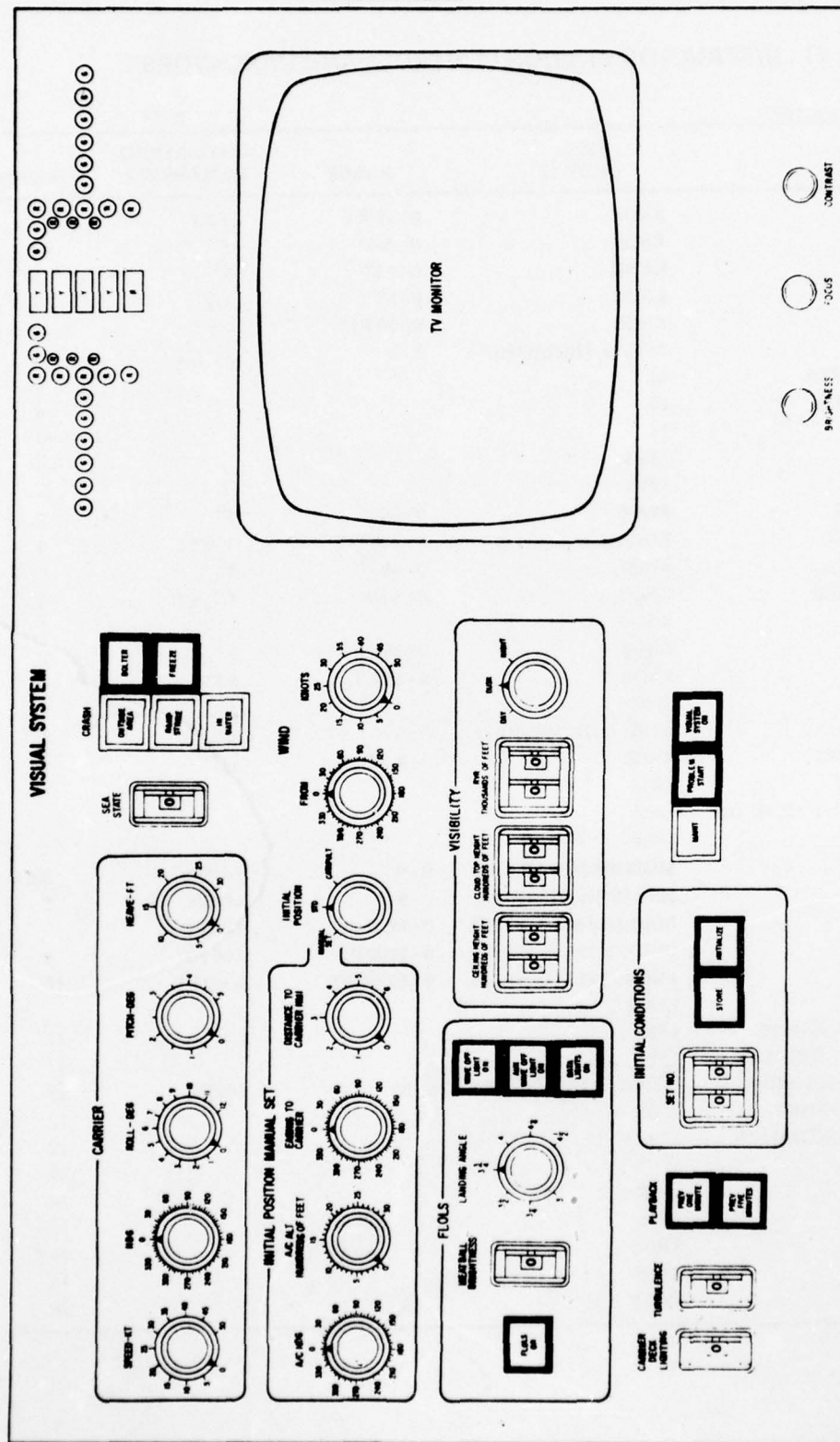


Figure 116. INSTRUCTOR STATION PANEL

Table 21. INSTRUCTOR STATION CONTROLS AND INDICATORS

FUNCTION/TITLE	TYPE (NOTE 1)	RANGE	GRADUATIONS/ INCREMENTS	NOTE(S)
CARRIER SPEED	KNOB	0 - 50 KT	5 KT	2
CARRIER HEADING	KNOB	0 - 360°	5°	2
CARRIER ROLL	KNOB	0 - 12°	1°	2, 3
CARRIER PITCH	KNOB	0 - 5°	1/2°	2, 3
CARRIER HEAVE	KNOB	0 - 30 FT	5 FT	2, 3
SEA STATE	SINGLE THUMBWHEEL	0 - 9	UNITS	3
CRASH - OUTSIDE AREA	LI			4
CRASH - RAMP STRIKE	LI			4
CRASH - IN WATER	LI			4
BOLTER	LPBS			5
FREEZE	LPBS			
AIRCRAFT HEADING	KNOB	0 - 360°	5°	2, 6
AIRCRAFT ALTITUDE	KNOB	0 - 3000 FT	100 FT	2, 6
BEARING TO CARRIER	KNOB	0 - 360°	5°	2, 6
DISTANCE TO CARRIER	KNOB	0 - 6 NM	1/2 NMI	2, 6
INITIAL POSITION	KNOB			7
WIND FROM	KNOB	0 - 360°	5°	2
WIND KNOTS	KNOB	0 - 50 KT	5 KT	2
FLOLS ON	LPBS			
FLOLS BRIGHTNESS	SINGLE THUMBWHEEL	0 - 4	UNITS	8
FLOLS LANDING ANGLE	KNOB	3 - 4.5°	1/4°	2
WAVE OFF LIGHT ON	LPBS			
EMERGENCY WAVE OFF LIGHT ON	LPBS			
DATUM LIGHTS ON	LPBS			
CARRIER LIGHTING	SINGLE THUMBWHEEL	0 - 9	UNITS	8, 17
TURBULENCE	SINGLE THUMBWHEEL	0 - 9	UNITS	8
CEILING HEIGHT	DOUBLE THUMBWHEEL	0 - 9900 FT	100 FT	
CLOUD TOP HEIGHT	DOUBLE THUMBWHEEL	0 - 9900 FT	100 FT	9
RVR	DOUBLE THUMBWHEEL	0 - 99000 FT	1000 FT	10
DAY-DUSK-NITE	KNOB			
PLAYBACK PREV ONE MINUTE	LPBS			11
PLAYBACK PREV FIVE MINUTES	LPBS			11
INITIAL CONDITIONS SET NUMBER	DOUBLE THUMBWHEEL	0 - 99	UNITS	12
INITIAL CONDITIONS STORE	LPBS			12
INITIAL CONDITIONS INITIALIZE	LPBS			12
MAINT	LI			13
PROBLEM START	LPBS			14
VISUAL SYSTEM ON	LPBS			15
BRIGHTNESS	KNOB			16
FOCUS	KNOB			16
CONTRAST	KNOB			16

Table 21. INSTRUCTOR STATION CONTROLS AND INDICATORS (Cont)

- NOTE 1: LIGHTED PUSHBUTTON SWITCHES (LPBS) AND LIGHTED INDICATORS (LI) WILL BE SIMILAR UNITS, DISTINGUISHED BY BEZEL COLOR.
- NOTE 2: A MULTIPOSITION ROTARY SWITCH WILL BE USED HERE, RATHER THAN A POTENTIOMETER OR SERVO. INCREMENTS WILL BE CHOSEN TO PROVIDE SUFFICIENTLY FINE CONTROL; INCREMENTS INDICATED ON THE TABLE REPRESENT CURRENT ESTIMATES OF REQUIREMENTS.
- NOTE 3: WITH THE "SEA STATE" THUMBWHEEL SWITCH SET AT "0," CARRIER ROLL, PITCH, AND HEAVE ARE CONTROLLED BY THE KNOBS SO LABELED. WITH SETTINGS OTHER THAN "0" ON THE "SEA STATE" THUMBWHEEL SWITCH, THOSE OF THE "ROLL," "PITCH," AND "HEAVE" SWITCHES THAT ARE SET AT "0" ARE DEACTIVATED, AND THESE CARRIER MOTIONS (ONES WITH CONTROLS SET AT "0") ARE CONTROLLED BY A STOCHASTIC PROGRAM THAT CALCULATES APPROPRIATE INSTANTANEOUS VALUES OF ROLL, PITCH, AND/OR HEAVE, BASED UPON WIND AND CARRIER VELOCITIES. (SUCH PROGRAMS HAVE ALREADY BEEN DEVELOPED BY SINGER-SPD IN CONNECTION WITH F-4J AND S-3A SIMULATOR PROGRAMS.) CARRIER MOTION IN AXES WHOSE THUMBWHEEL POSITION IS SET AT VALUES OTHER THAN ZERO WILL BE CALCULATED IN ACCORDANCE WITH THE THUMBWHEEL VALUE.
- THIS APPROACH PERMITS EXCURSIONS IN ANY OF THE THREE DEGREES OF FREEDOM - ROLL, PITCH, AND HEAVE - TO BE CONTROLLED EITHER WITH THE FULL REALISM OF THE STOCHASTIC PROGRAM OR WITH THE DIRECTNESS OF A FRONT PANEL SETTING.
- NOTE 4: LIGHTS ARE EXTINGUISHED WHEN SIMULATED AIRCRAFT IS REPOSITIONED.
- NOTE 5: WITH THIS SWITCH IN THE ACTIVATED (ILLUMINATED) STATE, A MISSED HOOK, OR BOLTER, WILL OCCUR IRRESPECTIVE OF HOW THE SIMULATED AIRCRAFT IS FLOWN.
- NOTE 6: THE PROVISION OF THE FOUR CONTROLS "BEARING TO CARRIER," "DISTANCE TO AIRCRAFT," "AIRCRAFT HEADING," AND "AIRCRAFT ALTITUDE" PROVIDES A MUCH GREATER DEGREE OF FLEXIBILITY THAN REQUIRED BY THE SPECIFICATION, WHICH REQUIRES LAUNCH FROM ONLY TWO POSITIONS: CARRIER LAUNCH AND AN INITIALIZATION "AT THE BEGINNING POSITION OF THE FINAL APPROACH TO LANDING." LAUNCH CAN BE MADE FROM EITHER OF THESE POSITIONS, WITHOUT SETTING THESE FOUR CONTROLS, USING THE "LAUNCH POSITION" SWITCH AS DESCRIBED IN NOTE 7.
- NOTE 7: THIS SWITCH ENABLES THE POSITION OF THE AIRCRAFT TO BE INITIALIZED AT THE "CATAPULT" LAUNCH POSITION ON THE AIRCRAFT CARRIER, OR AT THE "STD" BEGINNING POSITION OF THE FINAL APPROACH TO LANDING, OR AT SOME OTHER POSITION DETERMINED BY THE SETTINGS OF THE CONTROLS LABELED "A/C HDG," "A/C ALT," "BEARING TO CARRIER," AND "DISTANCE TO CARRIER." NO SEPARATE CONTROLS FOR AIRCRAFT ROLL AND PITCH ARE PROVIDED; ROLL WILL BE SET AT ZERO AND PITCH AT ZERO OR SOME NOMINAL NEAR-ZERO VALUE UPON INITIALIZATION, WHEN THE "INITIAL POSITION" SWITCH IS SET TO "MANUAL SET" OR "STD."
- NOTE 8: ZERO SETTING IS "OFF;" OTHER NUMBERS REPRESENT ARBITRARY VALUES, INCREASING IN MAGNITUDE WITH HIGHER NUMBERS.
- NOTE 9: A SETTING OF 9,900 FT ELIMINATES CLOUD TOP.
- NOTE 10: A SETTING OF 99,000 FT PROVIDES UNLIMITED VISIBILITY.
- NOTE 11: BLINKING WILL OCCUR (AFTER DEPRESSION) WHILE THE SIMULATOR IS BEING PREPARED FOR PLAYBACK; THE SWITCHLIGHT WILL ILLUMINATE STEADILY WHILE THE REPLAY IS IN PROGRESS.
- NOTE 12: THESE CONTROLS ENABLE THE INSTRUCTOR TO STORE UP TO 99 SETS OR COMBINATIONS OF INITIAL CONDITIONS, AND TO INSERT ANY SET WITH MINIMUM EFFORT. DEPRESSION OF THE "STORE" SWITCH CAUSES THE VALUE OF ALL INITIALIZATION PARAMETERS, SET BY THE VARIOUS CONTROLS ON THE PANEL, TO BE STORED IN A SET OF REGISTERS IDENTIFIED BY THE "SET NUMBER" THUMBWHEEL SWITCHES. DEPRESSION OF THE "INITIALIZE" SWITCH CALLS UP THE PARAMETER VALUES THUS ASSOCIATED WITH THE NUMBER ON THE "SET NUMBER" SWITCH. WHEN THE "SET NUMBER" SWITCH IS SET ON "00," THE "STORE" AND "INITIALIZE" SWITCHES ARE DISABLED IN FUNCTION, AND WILL NOT ILLUMINATE; WITH THIS "00" SETTING, LAUNCH WILL BE BASED UPON PARAMETER VALUES INDICATED BY INDIVIDUAL PANEL CONTROLS, RATHER THAN STORED VALUES.

Table 21. INSTRUCTOR STATION CONTROLS AND INDICATORS (Cont)

- NOTE 13: ILLUMINATES TO INDICATE THAT, BECAUSE OF MAINTENANCE IN PROGRESS, AWAVS IS NOT AVAILABLE.
- NOTE 14: IF THE SIMULATOR IS NOT READY, THE LIGHT WILL BLINK. WHEN THE AIRCRAFT IS STARTED, BY DEPRESSION OF THE "PROBLEM START" SWITCH WHEN ITS LIGHT IS OUT, THE LIGHT WILL COME ON TO VERIFY START.
- NOTE 15: WITH THIS SWITCH IN THE "ON" POSITION, AWAVS INPUTS, SUCH AS THOSE AFFECTING AIRCRAFT POSITION, WILL OVERRIDE ANY CONFLICTING OFT DATA INPUTS. IN THE "OFF" POSITION, THE OFT WILL OPERATE AS A FLIGHT SIMULATOR WITHOUT VISUAL SIMULATION.
- NOTE 16: THESE ARE CONVENTIONAL CRT CONTROLS.
- NOTE 17: INCLUDES CENTERLINE, VERTICAL DROP, RUNWAY EDGE, ATHWARTH SHIP AND DECK EDGE LIGHTS

SECTION XIV

RECOMMENDED SYSTEM

In previous sections of this report, various alternate subsystems are described. In this section, selected subsystem alternates are combined and analyzed as a complete system. This recommended system differs from the proposed basic system as described in this section.

GENERAL DESCRIPTION.

Target Image Generator. A 24' x 24' model board, without a rotating disk, and a 370:1 scale factor are utilized. This allows the use of straightforward gantry positioning algorithms for the simulation of all flight paths that are near to the carrier, and does not require excessive gantry accelerations. Correct placement of the probe pupil is maintained for simulated ranges up to 2300 ft., and perspective distortion of the canted deck is less than 2 arc-minutes for all simulated ranges.

A conventional probe provides reduced probe complexity with an improvement in vertical object definition while causing some degradation of picture quality for near objects at minimum altitude. A closed-loop probe pointing system is also used to provide improved, FLOLS registration during FLOLS operation.

Model illumination requirements are reduced because of the projected scene keying method used for target inseting. Only the model and wake need be illuminated because there is no seascape on the model board.

Selectable sweep rates are available in both the target and the background systems to allow for controlled variation of system resolution.

Target Projector. A new target projector optics design approach, including the removal of the Fresnel mirror, provides improved light transmission, thereby requiring a screen gain of 1.5 to meet the light-level requirements.

FLOLS. The FLOLS analysis has resulted in a design approach which is compatible with the target projector optics and which will also provide a FLOLS system of smaller size.

Background Image Generator. The background image generator analysis includes the provision of altitude and velocity cues, as well as the incorporation of a wake image generator (WIG). The wake image signal is electronically added to the background image signal prior to projection, resulting in a combined seascape and wake image being projected by the background projector.

The background system includes the capability of selecting sweep rates to allow for controlled variation of system resolution.

Background Projector. The method of providing variable-light output by partial spectrum removal and inserting complementary filters is recommended.

Target Inseting. The method of projected scene keying is utilized for target inseting. The requirement for, and the analysis of, a closed-loop raster registration technique is presented.

Special Effects Generator. The complexity of the target special effects generator is reduced because of the method used for target inseting.

The following paragraphs detail the recommendations for the subsystems.

TARGET IMAGE GENERATOR.

Target Model Board Assembly. The target model board assembly (figure 117) will be 24 ft. by 24 ft. mounted on a framework approximately 3 1/2 ft. off the floor. The support assembly will be approx. 8 ft. longer (total 32 ft.).

The carrier model will be installed at the center of the model board with a wake astern of the carrier in a fixed position. The carrier model will be driven in pitch, roll, and heave relative to the model board assembly. The deck lighting system will be simplified to use standard light boxes for the light source as described herein.

Perspective Distortion Analysis. The following analysis has been performed to determine the range at which the probe can be stopped and range effects simulated by the use of probe zoom and target projector zoom without introducing perspective error greater than 3 resolution elements. (Reference is 700 lines for the 60 degree field of view of the probe.)

For this analysis the perspective distortion is computed for the extreme right edge of the painted deck edge line of the canted-deck as viewed from astern at points along the extended, canted-deck center line at deck level. The range measurement is from the intersection of the canted-deck centerline and the amid ship position of the hull. (See figure 118 for values and reference dimensions.)

The equations for the difference angles for probe view and world view are as follows:

$$a_1 = \tan^{-1} Z_T \left(\frac{c}{R_p - b} \right) - \tan^{-1} Z_T \left(\frac{c}{R_p + a} \right) \text{ (radians)}$$

probe

$$a_2 = \tan^{-1} \left(\frac{c}{R - b} \right) - \tan^{-1} \left(\frac{c}{R + a} \right) \text{ (radians)}$$

world

$$\begin{aligned} \text{Perspective error} &= a_2 - a_1 \\ &= \left[\tan^{-1} \left(\frac{c}{R - b} \right) - \tan^{-1} \left(\frac{c}{R + a} \right) \right] - \left[\tan^{-1} Z_T \left(\frac{c}{R_p - b} \right) - \right. \\ &\quad \left. \tan^{-1} Z_T \left(\frac{c}{R_p + a} \right) \right] \end{aligned}$$

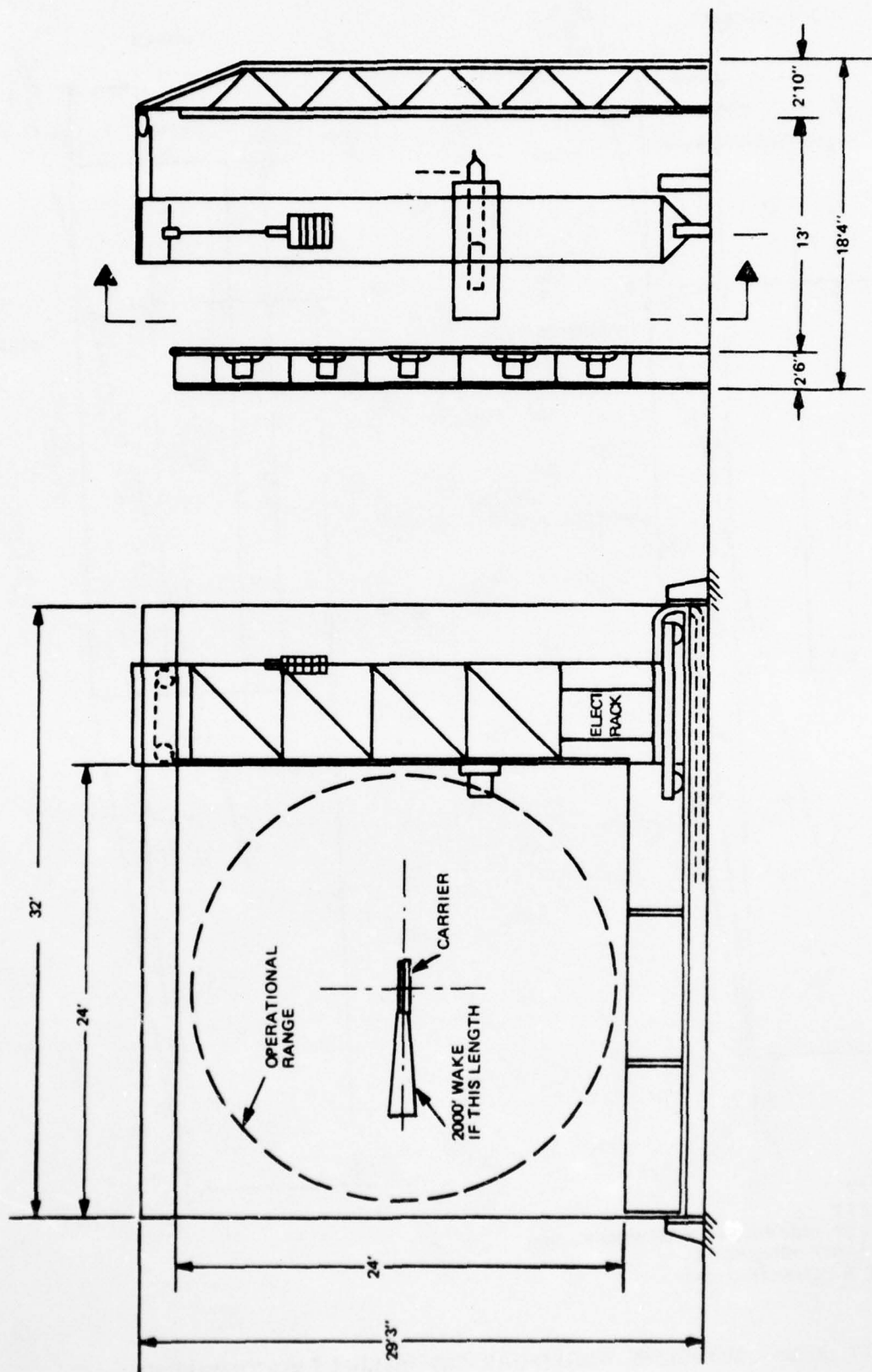


Figure 117. MODEL BOARD ASSEMBLY, CORRECTED VIEW

One resolution element is required at 700 elements per 60 degrees FOV.

$$\begin{aligned}
 1 \text{ Res Element} &= \frac{60}{700} (Z_D) \text{ (degrees)} & Z_D &= \text{Display Zoom} \\
 &= \frac{60}{700} (Z_D) \frac{\pi}{180} \text{ (radians)} \\
 &= \frac{Z_D}{668.45} \text{ (radians)}
 \end{aligned}$$

$$\text{Relative Error in Resolution Elements} = \frac{\text{Diff. Angle (radians)}}{1 \text{ Resolution Element (rad)}}$$

$$\begin{aligned}
 &= \frac{668.45}{Z_D} \left\{ \left[\tan^{-1} \left(\frac{c}{R-b} \right) - \tan^{-1} \left(\frac{c}{R+a} \right) \right] - \left[\tan^{-1} Z_T \left(\frac{a}{R_p-b} \right) \right. \right. \\
 &\quad \left. \left. - \tan^{-1} Z_T \left(\frac{c}{R_p+a} \right) \right] \right\}
 \end{aligned}$$

To evaluate limits, the ranges are defined as follows:

R_1 = Scaled slant range below which probe is moving at correct velocity.

r_1 = Scaled probe range below which probe is moving at correct velocity.

R_2 = Scaled slant range at which probe stops.

r_2 = Scaled probe range at which probe stops.

R_p = Scaled probe range.

R = Scaled slant range.

R_3 = Scaled slant range at which Z_D stops changing as range increases and further zoom is done with probe zoom.

AD-A037 223

SINGER CO BINGHAMTON N Y SIMULATION PRODUCTS DIV
AVIATION WIDE-ANGLE VISUAL SYSTEM (AWAVS). DESIGN ANALYSIS REPO--ETC(U)
APR 75

F/G 1/2

N61339-75-C-0009

UNCLASSIFIED

AWAVS-1

NAVTRAEQUIPC-75-C-0009-1 NL

4 OF 5
AD
A037223



$Z_T = Z_P Z_D$ The parameters of zoom and R_p vary as defined below:

Parameter	Scaled Slant Range (R)				
	0-1000 Ft.	1000- R_1 Ft.	R_1-R_2	R_2-R_3	$R_3-36,457$ Ft.
R_p	R	R	$*R - \frac{R_2 - r_2}{(R_2 - R_1)^2} (R - R_1)^2$	r_2	r_2
Z_T	1.0	$\frac{R_p}{R} = 1.0$	$\frac{R_p}{R}$	$\frac{R_p}{R} = \frac{r_2}{R}$	$\frac{R_p}{R} = \frac{r_2}{R}$
Z_p	1.0	$\frac{R_p}{1000} = \frac{R}{1000}$	$\frac{R_p}{1000}$	$\frac{R_p}{1000}$	$\frac{R_p}{R} \frac{1}{Z_D} = \frac{r_2}{R} \quad (10)$
Z_D	1.0	$\frac{1000}{R}$	$\frac{1000}{R}$	$\frac{1000}{R}$	$\frac{1}{10}$

*This relationship is derived below.

The displacement of a body subjected to a constant acceleration is given by:

$$R_p = R_1 + v_1 t + 1/2 a t^2$$

where $t = 0$ at $R = R_1$, v_1 is the velocity of the body when $R = R_1$, and a represents the constant acceleration of the body. When the velocity of the simulated viewing point is constant, $R - R_1 = v_1 t$ and the above equation for R_p becomes:

$$\begin{aligned} R_p &= R_1 + R - R_1 + 1/2 a \frac{(R - R_1)^2}{v_1^2} \\ &= R + 1/2 \frac{a}{v_1^2} (R - R_1)^2 \end{aligned}$$

At $R = R_2$, $R_p = r_2$. Therefore at $R = R_2$:

$$r_2 = R_2 + \frac{a}{2v_1^2} (R_2 - R_1)^2$$

or,

$$\frac{a}{2v_1^2} = \frac{r_2 - R_2}{(R_2 - R_1)^2}$$

Therefore:

$$R_p = R - \frac{R_2 - r_2}{(R_2 - R_1)^2} (R - R_1)^2$$

Taking the derivative of this equation:

$$\dot{R}_p = \dot{R} - \frac{R_2 - r_2}{(R_2 - R_1)^2} (2) (R - R_1) \dot{R}$$

Substituting at $R = R_2$, $R_p = 0$ (stopped)

$$0 = \dot{R} \left| 1 - \frac{R_2 - r_2}{(R_2 - R_1)} \right| \quad (2)$$

$$\therefore R_2 - R_1 = 2(R_2 - V_2)$$

$$\text{also} \quad = 2(r_2 - R_1)$$

To evaluate the Relative Error equation over the various ranges of interest, the small angle = tan angle approximation and a use of the first two terms of the expansion for the fraction have been made. This reduces the Relative Error equation to:

$$\begin{aligned} \text{Relative Error} &= \frac{668.45}{Z_D} (a+b)(c) \left(\frac{R_p - R}{R_p R^2} \right) \\ &= \frac{668.45}{Z_D} (682.5)(40) \left(\frac{R_p - R}{R_p R^2} \right) \\ &= \frac{18.248 \times 10^6}{Z_D} \left(\frac{R_p - R}{R_p R^2} \right) \frac{V_2}{Z_D} \left(\frac{R_p - R}{R_p R^2} \right) \end{aligned}$$

This general equation can be analyzed at the various ranges to determine the trends and error curve shapes.

For Large Ranges $R > R_3$

$$Z_D = \frac{1}{10} \quad R_p = r_2$$

$$\therefore \text{Rel Error} = K_2 \left(\frac{10}{1} \right) \left(\frac{r_2 - R}{r_2 R^2} \right) = \frac{K_2 10}{r_2} \left(\frac{r_2 - R}{R^2} \right)$$

A plot of error vs. R crosses zero at r_2 , increases negative to a max, and then decreases to zero at very large ranges.

The max. error occurs at

$$\frac{d(\text{Rel Error})}{dR} = \frac{K_2(10)}{V_2} [r_2(-2)R^{-3} + R^{-2}]$$

$$0 = -2r_2 + R$$

$$R = 2r_2$$

For the range $R > R_2$ (up to R_3)

$$Z_D = \frac{1000}{R}, R_p = r_2$$

$$\therefore \text{Rel Error} = K_2 \left(\frac{R}{1000} \right) \left(\frac{r_2 - R}{R^2 r_2} \right) = \frac{K_2}{1000} \frac{r_2}{R} - 1$$

A plot of this error curve vs. range crosses zero at r_2 , increases negative and approaches $-K_2$ as R increases.

Since this range is bounded by the Z_D range (at R_3), the value of R_3 can be computed.

$$\frac{1}{10} = \frac{1000}{R_3} \quad \therefore R_3 = 10,000 \text{ ft.}$$

For the range of R between R_1 and R_2

$$Z_D = \frac{1000}{R}, R_p = R - \frac{(R_2 - r_2)}{(R_2 - R_1)^2} (R - R_1)^2$$

$$\text{Rel Error} = \frac{r_2}{1000R} \left[\frac{-(R_2 - r_2) (R - R_1)^2}{R(R_2 - R_1)^2 - (R_2 - r_2) (R - R_1)^2} \right]$$

A plot of this error curve vs. range has been analyzed and does not get as large as the values for the other ranges so they are predominate.

Based on the curve and limits defined, the perspective error will increase through the R_1 - R_2 range up through the $R > R_2$ until $R = R_3$ where the error will decrease. By equating the relative error to $(-).3$ and setting the range to R_2 , it is possible to solve for r_2 . Using the approximate equation, this condition is:

$$Z_D = \frac{1}{10}, R_p = r_2, R = R_3 = 10000 \text{ ft.}$$

$$-.3 = 18,248 \times 10^{-6} \left(\frac{10000}{1000} \right) \left(\frac{r_2 - 10000}{10000^2 r_2} \right)$$

$$r_2 = 3872 \text{ ft.}$$

Using the exact, initially derived equation with only the small angle = tangent angle approximations, the r_2 range can be determined as follows:

$$-.3 = 668.45 \times 10^{-6} \left(\frac{10}{1} \right) \left\{ \left[\frac{40}{10000 - 498.5} - \frac{40}{10000 + 184} \right] - \left[\frac{r_2}{10000} \left(\frac{40}{(r_2 - 498.5)} - \frac{r_2}{10000} \left(\frac{40}{(r_2 + 184)} \right) \right) \right] \right\}$$

Reducing and clearing:

$$0 = r_2^2 - 4050 r_2 - 91724$$

Solving for r_2

$$r_2 = 4070, 22.5. \text{ (22.5 is below range of consideration)}$$

The plots of α_1 , α_2 , difference, Z_D and resolution elements error have been computed and are plotted in a subsequent section.

Scale Factor of Model. Based on using 22 ft. of the 24 ft. model structure (i.e., 11 ft. radius and the requirement for a 4-G acceleration factor required for catapult launches, the scale factor has been determined to be 370:1 for an r_2 dimension of 4070 ft. For this scale factor, the gantry will accelerate to 400 kts. (max velocity required) in 1770 ft. (scaled).

$$R_1 = r_2 - \text{Deceleration} = 4070 - 1770 = 2300 \text{ ft.}$$

$$R_2 = R_1 + 2D = 2300 + 3540 = 5840 \text{ ft.}$$

For this scale factor new tables of probe and display parameters vs. slant range have been computed and are included along with a plot of the zoom powers and RP. (See tables 22 and 23, and figure 119.)

In addition, the exact perspective error equation has been used to compute the angles, α_1 and α_2 , difference, and the display resolution and perspective error in resolution elements and plotted vs. slant range. (See figure 120.)

The probe and target projector zoom ratios at the limits of their ranges will be slightly modified as necessary to allow the servos to dynamically position the lens to the required zoom ratio without hitting the mechanical limit stops in the lens assemblies. The detailed system design will also round off the sharp breaks in the zoom curves to reduce the acceleration requirements. These changes will cause small variations to the data tables.

Range vs. Altitude for Correct Aspect Angle. The revised model board structure extends the altitude over which the aircraft can maneuver around and about the carrier with no aspect distortion. For this analysis, it is assumed that the gantry (probe) will operate within a circular area around the carrier of 11 ft. radius ($R_p = 4070$ ft. scaled).

The Z motion of the gantry (probe) in the Z dimension will be less than the 3 ft. excursion by the small distance required to install limit switches and stop the motion before the carriage hits the bearings or framework. Assuming 1000 ft. usable, scaled motion above the water level, the Z motion is $1000/370 \times 12 = 32.4$ inches.

At this scale factor the aspect angle will be correct if the aircraft is directly over the carrier at up to 1000 ft. altitude. This altitude will hold out to a slant range of 2300 ft. As slant range increased to 5840 ft. ($R_p \text{ slant} = 4070$), the altitude increases to 1437 ft. From this point on out, the altitude is a straight line function out to 8963 ft. altitude at a slant range of 6 miles (36480 ft.). (See figure 121.)

Table 22. PROBE PARAMETERS VS. SLANT RANGE SIMULATED

R Simulated Range (NM)	R _p Probe Range Ft.	θ_p Carrier Length Angular Width	40 x V ₀ FOV Probe Degrees	\mathcal{L} TV Lines Over Angular Width	ω Fractional Width of Carrier Length on Camera	Z _p Probe Zoom
6	4070	14.54	54.5x36.4	150	.248	1.12:1
4	4070	14.54	38.1x25.4	200	.369	1.67:1
3	4070	14.54	29.0x19.4	300	.493	2.23:1
2	4070	14.54	19.6x13.0	400	.741	3.35:1
10,000 ft.	4070	14.54	16.2x10.8	600	.900	4.07:1
9120 ft.	4070	14.54	16.2x10.8	600	.900	4.07:1
7600 ft.	4070	14.54	16.2x10.8	600	.900	4.07:1
6080 ft.	4070	14.54	16.2x10.8	600	.900	4.07:1
5840 ft.	4070	14.54	16.2x10.8	600	.900	4.07:1
4070 ft.	3627.5	16.30	18.1x12.1	600	.900	3.63:1
2300 ft.	2300	25.5	28.2x18.8	600	.900	2.30:1
1000 ft.	1000	54.9	60 x 40	600	.900	1.00:1
0 ft.	0	NA	60 x 40	NA	NA	1.00:1

Probe starts moving at 5840 ft. scale slant range when approaching carrier.
Probe moving at correct velocity at 2300 ft. scale slant range.

Table 23. DISPLAY PARAMETERS VS. SLANT RANGE SIMULATED

<u>"R"</u> <u>Simulated</u> <u>Range (NM)</u>	θ <u>Carrier Length</u> <u>Angular Width</u>	Display			Z_D <u>Display Zoom</u> <u>Power</u>
		ℓ <u>TV Lines Over</u> <u>Angular Width</u>	<u>R-Resolution</u> <u>Per TV Line</u> <u>(Arc Minutes)</u>		
6	1.6	150	.64		1:10.0
4	2.4	200	.72		1:10.0
3	3.3	300	.66		1:10.0
2	4.9	400	.74		1:10.0
10000 ft.	6.0	600	.60		1:10.0
9120 ft.	6.5	600	.65		1:9.12
7600 ft.	7.8	600	.78		1:7.60
6080 ft.	9.8	600	.98		1:6.08
5840 ft.	10.2	600	1.02		1:5.04
4070 ft.	14.6	600	1.46		1:4.07
2300 ft.	25.5	600	2.55		1:2.30
1000 ft.	54.9	600	5.49		1:1.00
0 ft.	NA	NA	5.49		1:1.00

Probe starts moving at 5840 ft. scale range when approaching carrier.
Probe moving at correct velocity at 2300 ft. scale slant range.

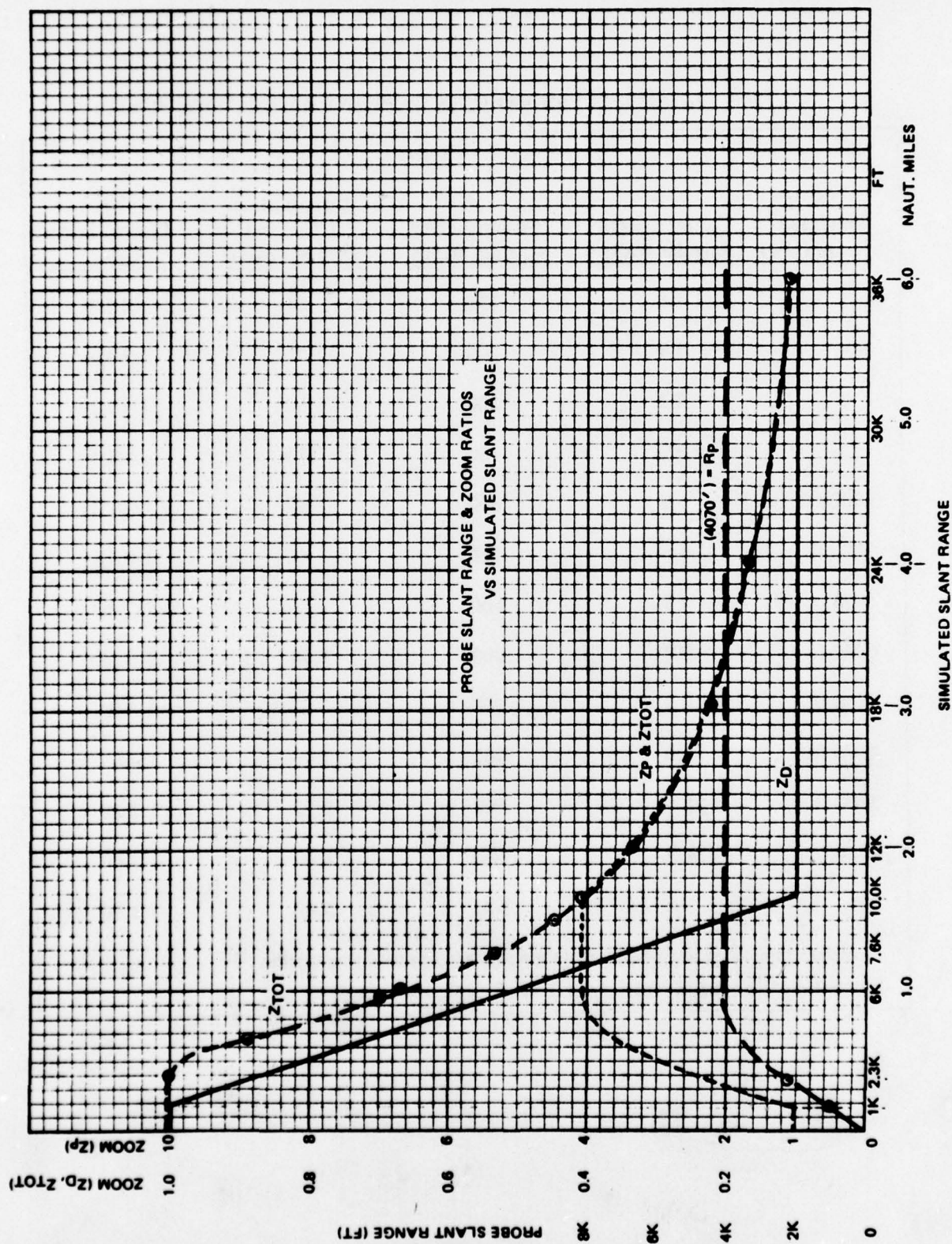


Figure 119. PROBE SLANT RANGE VS. SLANT RANGE SIM.

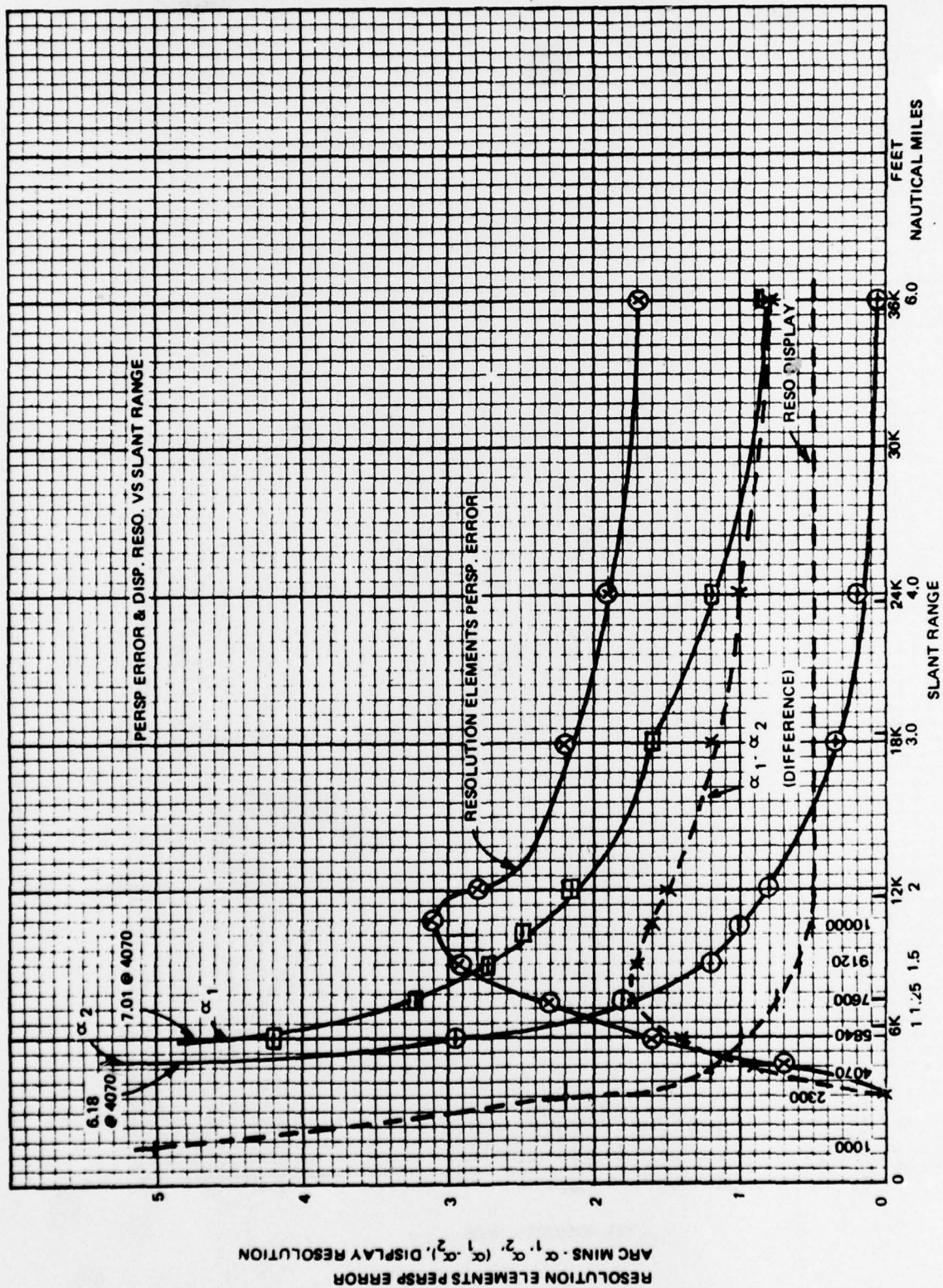


Figure 120. PERSP. ERROR & DISP. RESO. VS. SLANT RANGE

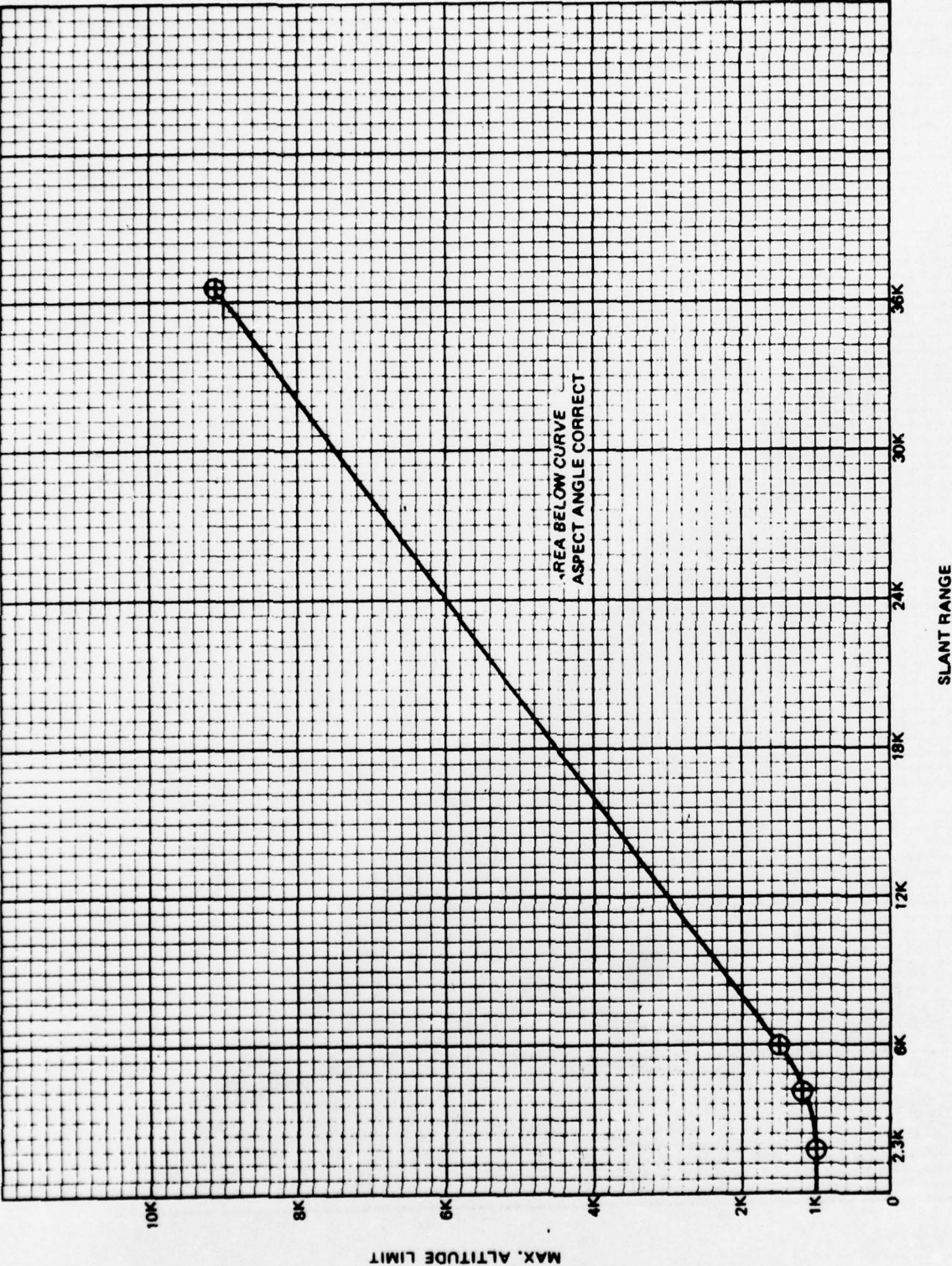


Figure 121. MAX. ALTITUDE VS. SLANT RANGE

Wake Cutoff Analysis. The wake cutoff and field of view have been recomputed for the same conditions of relative aircraft to carrier positions. In this analysis six points on the carrier wake are compared with the probe field of view for four aircraft locations in the turn to final approach.

A 2,000 ft. wake length is used, with a width of 250 ft. at the carrier stern and 500 ft. at the aft end. The six wake points, in the wake frame offset to the FLOLS location, are (in feet):

$$1) \text{ stern port corner} = \begin{bmatrix} -407 \\ 15 \\ 62 \end{bmatrix} = \underline{a_1}$$

$$2) \text{ stern center} = \begin{bmatrix} -407 \\ 140 \\ 62 \end{bmatrix} = \underline{a_2}$$

$$3) \text{ stern starboard corner} = \begin{bmatrix} -407 \\ 265 \\ 62 \end{bmatrix} = \underline{a_3}$$

$$4) \text{ aft port corner} = \begin{bmatrix} -2407 \\ -110 \\ 62 \end{bmatrix} = \underline{a_4}$$

$$5) \text{ aft center} = \begin{bmatrix} -2407 \\ -140 \\ 62 \end{bmatrix} = \underline{a_5}$$

$$6) \text{ aft starboard corner} = \begin{bmatrix} -2407 \\ 390 \\ 62 \end{bmatrix} = \underline{a_6}$$

The four aircraft locations, in the wake frame offset to the FLOLS location are (in feet):

$$1) \text{ } 90^\circ \text{ turn point} = \begin{bmatrix} -7380 \\ -5334 \\ 438 \end{bmatrix} = \underline{b_1}$$

(R = 1.5 nm, h = 500 ft.)

$$2) \text{ FLOLS entry} = \begin{bmatrix} -7771 \\ -1370 \\ -388 \end{bmatrix} = \underline{b_2}$$

(R = 1.3 nm, h = 450 ft.)

$$3) \text{ Wake crossing} \quad (R = 1.25 \text{ nm, } h = 425 \text{ ft.}) \quad = \begin{bmatrix} -7587 \\ 140 \\ -363 \end{bmatrix} = \underline{b}_3$$

$$4) \text{ Line-up} \quad (R = 1.0 \text{ nm, } h = 400 \text{ ft.}) \quad = \begin{bmatrix} -5965 \\ 1105 \\ -338 \end{bmatrix} = \underline{b}_4$$

For each aircraft location, the transformation from the wake frame orientation to the area-of-interest frame orientation (FOV is centered about the FLOLS location) is:

$$\underline{T} = \begin{bmatrix} \cos \psi & \cos \theta & \sin \psi & \cos \theta & -\sin \theta \\ -\sin \psi & & \cos \psi & & 0 \\ \cos \psi & \sin \theta & \sin \psi & \sin \theta & \cos \theta \end{bmatrix};$$

where:

$$\psi = \tan^{-1} (b_y/b_x)$$

$$\theta = -\tan^{-1} (b_z / \sqrt{b_x^2 + b_y^2})$$

Each carrier wake point, in the area-of-interest frame located at the pilot's eyepoint, is:

$$\underline{c} = \underline{T} (\underline{a} - \underline{b})$$

and, from the center of the field of view, the horizontal and vertical viewing angles are:

$$\alpha = \tan^{-1} (c_y/c_x)$$

$$\gamma = -\tan^{-1} (c_z / \sqrt{c_x^2 + c_y^2})$$

Table 24 shows the computed viewing angles for the six wake points for each of the four aircraft locations.

The field of view half-angles are determined by probe zoom (Z_P). Probe zoom and display zoom (Z_D) are constrained such that total system zoom (Z_T) is:

$$Z_T = Z_P Z_D = \frac{R_P}{R};$$

where:

$$\begin{aligned} R_P &= \text{probe slant range (scale ft.)} \\ R &= \text{simulated slant range (ft.)} \end{aligned}$$

Table 24. VIEWING ANGLES

<u>A/C Location</u>	<u>Wake Point</u>	<u>α (Deg.)</u>	<u>γ (Deg.)</u>
1	1	1.63	-0.50
1	2	2.27	-0.48
1	3	2.90	-0.45
1	4	10.53	-1.26
1	5	11.86	-1.17
1	6	13.13	-1.09
2	1	0.65	-0.62
2	2	1.59	-0.62
2	3	2.52	-0.60
2	4	3.21	-1.86
2	5	5.71	-1.82
2	6	8.14	-1.77
3	1	0.06	-0.65
3	2	1.06	-0.65
3	3	2.05	-0.65
3	4	-1.70	-1.95
3	5	1.05	-1.95
3	6	3.81	-1.95
4	1	-0.60	-0.85
4	2	0.64	-0.87
4	3	1.90	-0.88
4	4	-8.32	-2.92
4	5	-4.06	-3.01
4	6	-0.86	-3.10

In our simulation approach,

$$\begin{aligned} Z_D &= 1.0 & R < 1,000 \text{ ft.} \\ Z_D &= \frac{1000}{R} & 1,000 \text{ ft.} < R < 10,000 \text{ ft.} \\ Z_D &= 0.1 & R > 10,000 \text{ ft.} \end{aligned}$$

Therefore, the probe zoom is:

$$\begin{aligned} Z_P &= \frac{Z_T}{Z_D} \\ Z_P &= 1.0 & R < 1,000 \text{ ft.} \\ Z_P &= \frac{R_p}{1000} & 1,000 \text{ ft.} < R < 10,000 \text{ ft.} \\ Z_P &= 10 \frac{R_p}{R} = \frac{10r_2}{R} & R > 10,000 \text{ ft.} \end{aligned}$$

where, in our approach:

$$\begin{aligned} R_p &= R & R < R_1 \\ R_p &= R - \left(\frac{R-R_1}{R_2-R_1} \right)^2 (R_2-r_2) & R_1 < R < R_2 \\ R_p &= r_2 & R > R_2 \\ R_1 &= 2300 \text{ ft.} \\ R_2 &= 5840 \text{ ft.} \\ r_2 &= 4070 \text{ ft.} \end{aligned}$$

The distance subtended by the probe horizontal field of view half-angle, in the object plane, is:

$$d = \frac{R_p}{Z_P} \tan 30^\circ.$$

At the eyepoint, this distance subtends a horizontal field of view half-angle of:

$$\begin{aligned} \alpha' &= \tan^{-1} \frac{d}{R} \\ &= \tan^{-1} \left(\frac{R_p}{Z_P R} \tan 30^\circ \right); \end{aligned}$$

since:

$$\begin{aligned} Z_P &= \frac{Z_T}{Z_D} = \frac{R_p}{Z_D R} \\ \alpha' &= \tan^{-1} (Z_D \tan 30^\circ); \end{aligned}$$

and, by the same process, the vertical field of view half-angle, at the eyepoint, is:

$$\gamma' = \tan^{-1} (Z_D \tan 20^\circ).$$

For the four aircraft locations used:

$$Z_D = \frac{1000}{R} ;$$

and:

$$\alpha' = \tan^{-1} \left(\frac{1000}{R} \tan 30^\circ \right)$$

$$\gamma' = \tan^{-1} \left(\frac{1000}{R} \tan 20^\circ \right).$$

Table 25 shows the simulated slant ranges, probe slant ranges, display zoom ratios, and FOV half-angles (from the eyepoint) for the four aircraft locations used.

Figure 122 shows, for the four aircraft locations, the shape of the carrier wake together with the FOV limit frame. Perspective distortion is not included in this analysis.

Table 25. FIELD OF VIEW

<u>R</u> (ft.)	<u>R_p</u> (scale ft.)	<u>Z_D</u>	<u>α' (deg.)</u>	<u>γ' (deg.)</u>
9120	4070	1/9.12	3.62	2.29
7904	4070	1/7.90	4.18	2.64
7600	4070	1/7.60	4.34	2.74
6080	4070	1/6.08	5.42	3.43

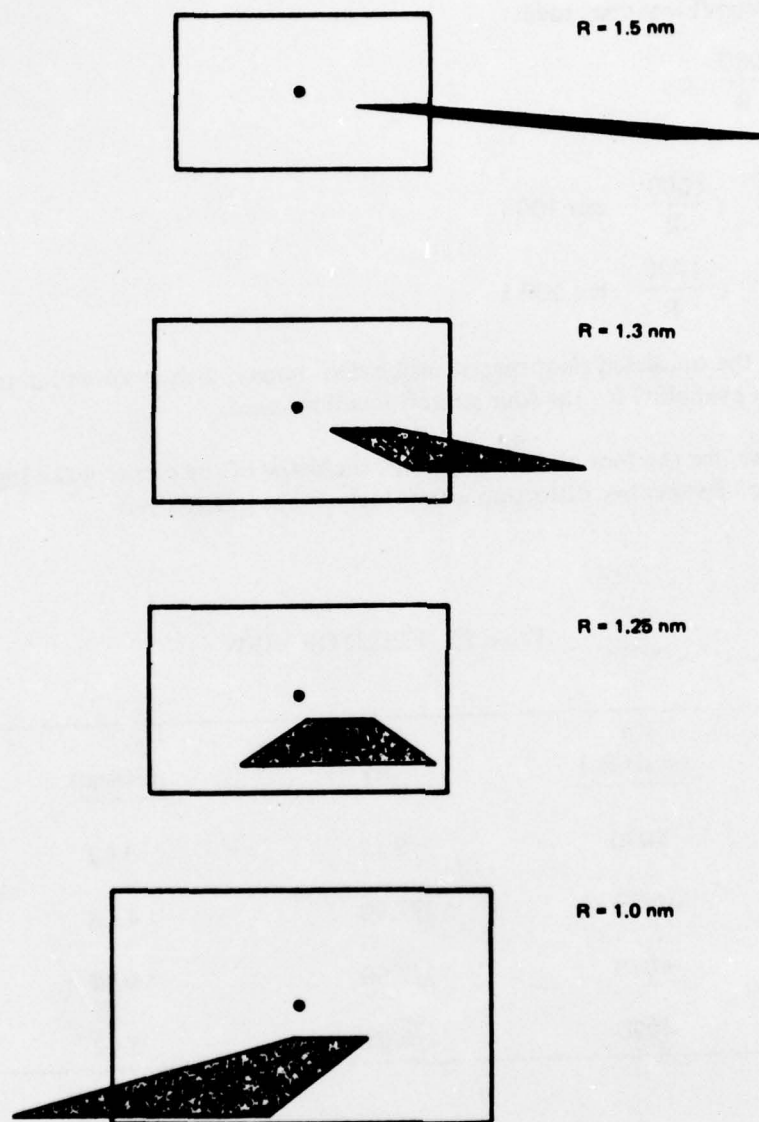


Figure 122. CARRIER WAKE AND FIELD-OF-VIEW

XYZ Performance Requirements. The performance requirements for the gantry will change to reflect the revised gantry model board configuration and scale factor. The scaled velocities, accelerations, resolution and high speed tracking error will remain the same but the ranges will change.

Table 26 displays some examples of this.

Table 26. GANTRY PERFORMANCE REQUIREMENTS

	<u>Range</u>	<u>Velocity</u>	<u>Acceleration</u>	<u>Resolution</u>	<u>High Speed Tracking Error</u>
X	22 ft. (8140)	1.826 ft/sec (400 kts.)	0.348 ft/sec ² (4G)	0.000354 ft. ≅(1/8 ft.)	0.022 ft. @1.826 ft/sec
Y	22 ft. (8140)	1.826 ft/sec (400 kts.)	0.348 ft/sec ² (4G)	0.000354 ft. ≅(1/8 ft.)	0.022 ft. @1.826 ft/sec
Z	2.7 ft. (1000)	0.274 ft/sec (6100 ft/min)	0.261 ft/sec ² (3G)	0.000354 ft. ≅(1/8 ft.)	0.0027 ft. @0.274 ft/sec
() = scaled values					

Deck Lighting. The scale factor change to a larger value (smaller model) and a review of the drawings supplied for the carrier have made it evident that it will be difficult if not impossible to utilize fiber optics for the deck edge lights on the carrier model. The fibers would be visible below the deck and/or hangar deck level of the model, as they cannot be bent too sharply.

It is proposed to use the small (0.030") diameter pin-lights recessed in the deck but protruding slightly above the deck level. These light bulbs have been used before and have good life, if used at reduced voltage. The light intensity can be varied by controlling supply voltage applied to them. The light output level of these lights on the carrier are at a much lower level than the deck C/L, edge and athwartship lights. (Mfg. by Pinlites Div. of Refac, Caldwell, N. J. - Type L-15 or L-12 series.)

Runway center line, edge athwartship and vertical drop lights will be fiber optics, as previously discussed.

The elimination of the rotating disc will allow the use of the previously designed and utilized light boxes to supply the light to the optic fibers. These light boxes have a 300-watt bulb, cooling air fans, an optics assembly to direct the light onto the fibers, and an iris assembly driven by a dc servo to control the light intensity.

The light box has a provision to mount a motor driven disc assembly to provide flashing lights. This provision will be used to provide variable rate runway center line strobe lights. Variable intensity controlled from the instructor's station will be provided for the following light

groups: center line lights, runway edge and athwartship lights, vertical dropline lights and deck edge lights. The light box also has the provision to mount a solenoid-driven mask that can block the light to part of the fibers.

The number of light boxes required will depend on how many fibers can be held by each box and still have even lighting at the output end of the fiber.

Model Illumination. Now, since it is only necessary to illuminate the carrier and a smaller wake instead of the larger area of the original design report, it is now possible to reduce the number of lamps and power requirements. All lights will point straight ahead and will not be directed at the carrier model. This straight-ahead pointing is to allow for future expansion of the lighting system to illuminate the whole 24 ft.² model board.

The f/No. of the probe has been changed to 39.97, and this will stay constant with zoom. Since Scheimpflug correction will no longer be used in the probe, the transmission has gone up to 32%. An additional factor must now be inserted into the lighting calculations that was not included in the original design analysis report. This factor is to account for the loss of light going to the camera, due to the presence of the spectrally selective beamsplitter, that must be inserted between the probe and the camera to provide light for the FLOLS position sensing detector. Part of the light coming from the probe will be split off from the camera bundle with this spectrally selective beamsplitter and then will be sent through a narrow bandpass filter before going onto the position detector. Because of insufficient information at this time as to the spectral and absorption characteristics of the beamsplitter and bypass filter and as to the requirements of the position detector, it cannot be determined at this time exactly how much the position detector will affect the lighting requirements. However, it is estimated that the detector will increase the lighting requirements by no more than a factor of two. To compute the new illumination required on the carrier model, the following formula is used:

$$I_m = \frac{4I_i N^2 F}{R T M}$$

- Where:
- I_m = Illumination required on the carrier model.
 - I_i = Illumination required on the camera tube faceplate = 0.074 foot candles for a highlight signal current of 0.75 μ a at an 825 television line rate.
 - N = f/No. = 39.97.
 - F = Estimated factor to account for light loss due to the beamsplitter needed for the position detector = 2.
 - R = Average highlight reflectance of the carrier model = 0.60.
 - T = Probe transmission = 0.32.
 - M = Maintenance factor to allow for lamp and camera tube aging = 0.8.

Using these numbers, the carrier initial illumination requirement (I_m) is 6160 foot-candles.

To determine the number of lights needed on the model board, a computer program that was developed for the F-4E No. 18 system was used. This program adds up the contribution of each light (all lights are aimed straight ahead) at the points of interest on the model board, using the formula:

$$I_m(13, y, z) = \sum_{i=1}^n \frac{c(\theta_i) \times \cos \theta_i}{R_i^2} ;$$

Where: $I_m(13, y, z)$ = Total illumination on the model (in foot-candles) at the point P with coordinates (13, y, z). The 13 is the approximate x value for all points on the model; i.e., the model is 13 feet from the lighting board and parallel to it. The lighting board is the same size as the model board.

θ_i = Angle between the normal to the i^{th} lamp and the line from the i^{th} lamp to the point P.

$c(\theta_i)$ = Candlepower (lumens/steradian) of the fixture as a function of angle.

R_i = Distance from the i^{th} lamp to the point P in feet.

n = Number of lamps on the lighting board.

These variables are shown in figure 123.

From this program, it was determined that 32, 1000-watt metal halide lamps in fixtures with a NEMA-5 distribution will provide sufficient illumination. These lights will be arranged in an 8 x 4 matrix with a 2-foot horizontal by 4-foot vertical spacing. These 32 lights will uniformly illuminate only the carrier and its wake, and these 32 lights will be the only ones supplied by Singer-SPD with the system. If the lighting were expanded in the future to illuminate the whole 24 ft. x 24 ft. model board, an additional 50 lights (same type) would be required for a total of 82 lights in the lighting bank. Figure 124 shows the configuration of both the initial lighting system (32 lights) and the expanded system (82 lights).

Figure 125 also shows illumination levels for both the initial and expanded systems. In the expanded system, the illumination at the corner point would be only 30% of the highest illumination point on the model. However, these calculations do not take into account the contributions from any reflectorized scene extenders that could be added for future expansion. Also, at a point 2 feet up and 1 foot over from the corner, the illumination would be already up to 50% even without scene extenders. The highest illumination point in the expanded system would be 7850 foot-candles.

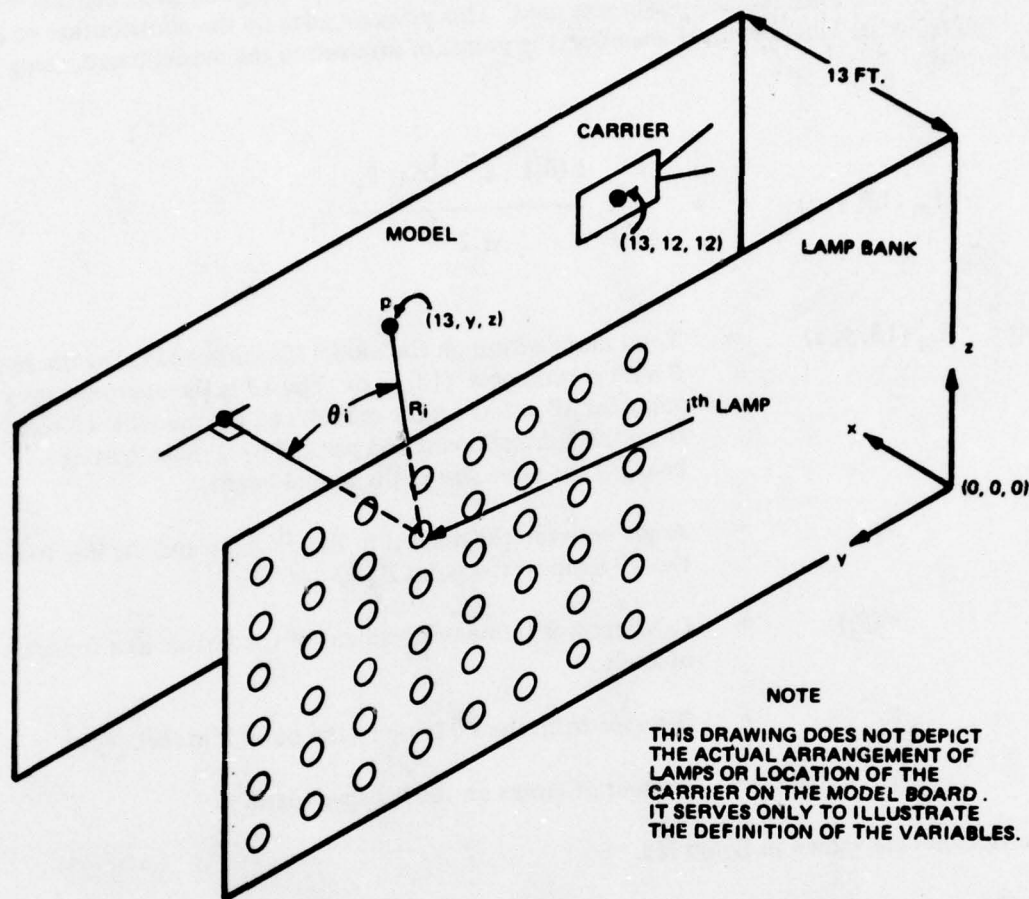


Figure 123. DEFINITION OF VARIABLES FOR ILLUMINATION PROGRAM

In the initial lighting system, the illumination at the center of the carrier model will be approximately 6200 foot-candles with a negligible fall off to the corners of the carrier. This illumination level and the levels discussed below are with new lamps. The initial illumination on the sides of the carrier will be 610 foot-candles on the two short sides (ends), and 740 foot-candles on the two long sides. If the sides of the ship were painted a normal battleship gray of approximately 19.5% reflectance, this means that only 119 foot-lamberts would come off the short side. If the average highlight of 60% were located at the center of the ship, then 3720 foot-lamberts would be reflected at this point. This would mean a contrast ratio of $3720:119 \approx 31:1$, and the blacks would be too black for reliable scene keying in the visual display. In order to avoid this problem, the sides of the ship could be painted with a 90% white so that the short side reflects 549 foot-lamberts, yielding a contrast ratio of $3720:549 \approx 6.8:1$ from the carrier model.

This contrast ratio must be raised to a power equal to the target camera/target T.V. projector system gamma in order to calculate the contrast ratio on the display screen. At this point, a final determination has not been made as to what this system gamma will be. Therefore, in order to continue the carrier model analysis, an assumption of the final system gamma will have to be made. It will be assumed that the system gamma will be 1.35.

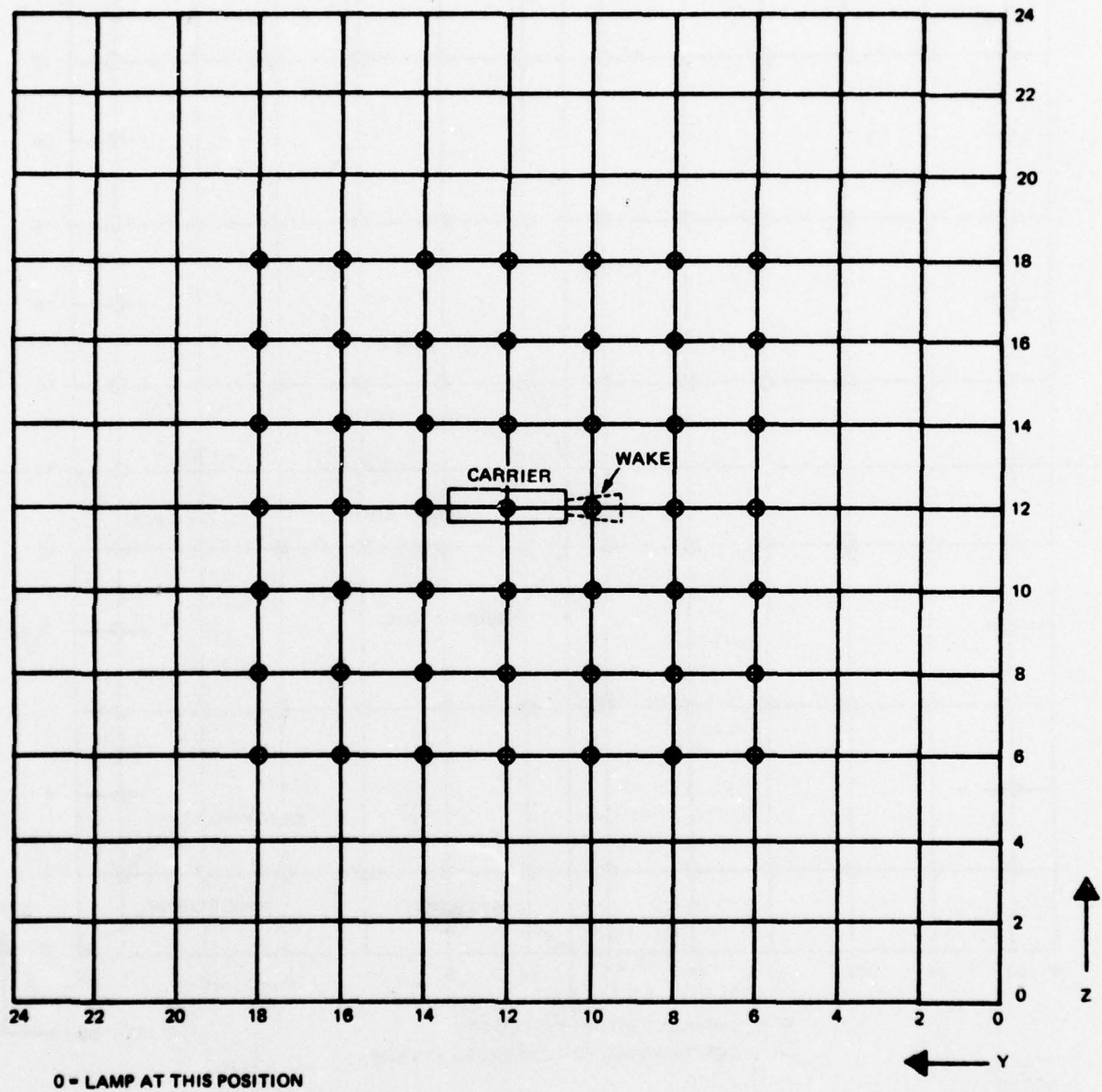
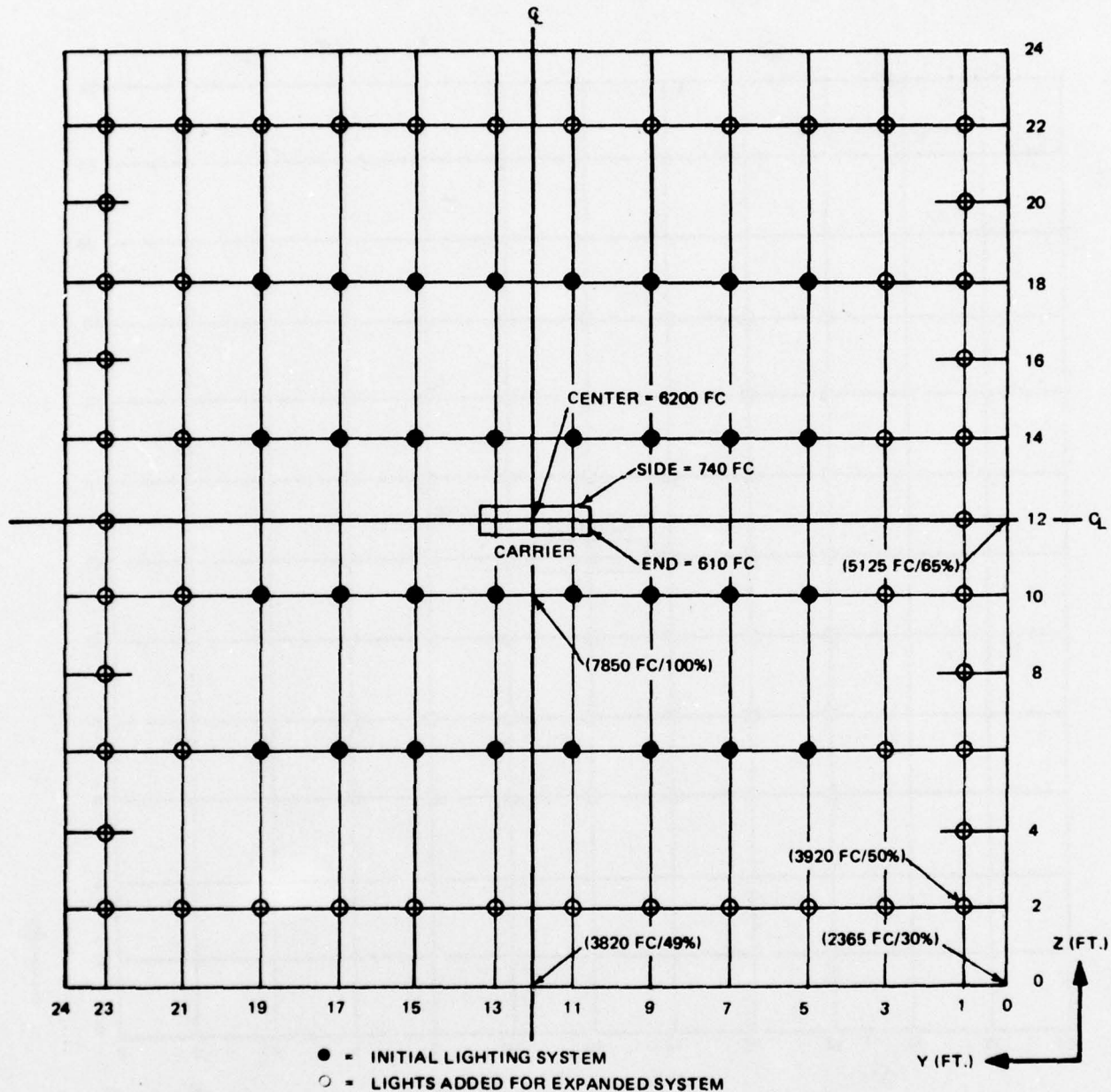


Figure 124. LIGHTING CONFIGURATION



NOTES:

1. NUMBERS IN PARENTHESES INDICATE ILLUMINATION LEVEL AT INDICATED POINT AFTER EXTRA LIGHTS HAVE BEEN ADDED FOR THE EXPANDED SYSTEM. THE PERCENTAGE INDICATES THE PERCENTAGE OF HIGHEST ILLUMINATION LEVEL ON MODEL.
2. NUMBERS WITHOUT PARENTHESES LABELED "CENTER", "SIDE", AND "END" INDICATE ILLUMINATION IN INITIAL SYSTEM BEFORE IT IS EXPANDED.
3. ALL INDICATED ILLUMINATION LEVELS DO NOT TAKE INTO ACCOUNT CONTRIBUTIONS FROM REFLECTORIZED SCENE EXTENDERS WHICH COULD BE ADDED BY NTEC IN THE FUTURE.
4. ALL ILLUMINATION LEVELS ARE WITH NEW LAMPS, THE LAMPS DECREASE IN LIGHT OUTPUT WITH AGE.

Figure 125. ILLUMINATION LEVELS

Raising the carrier contrast ratio to the system gamma power yields a contrast ratio on the display screen of $6.8 \exp(1.35) = 13.3:1$. This is the desired ratio for obtaining 8 shades of gray on the screen. The 8 shades of gray on a logarithmic chart correspond to a contrast ratio of 13.75:1, which is very close to the 13.3:1. If the final system gamma turns out to be higher than 1.35, then supplemental lighting can be added to the lighting system to increase the illumination on the sides of the carrier. A combination of increased reflectivity and supplemental lighting might also be used even if the system gamma is 1.35 or below.

Night will be simulated with all the lights on the lighting board off. Dusk will be simulated either by shutting off half the lights or by keeping them all on and closing down the probe pupil one stop. The latter has two advantages: 1) the 20-minute cycle time for full operational level from a hot start is eliminated for the day to dusk or night and then immediately back to day cycle, and 2) the hot spots that might occur when half the probe fill-in lights are turned off are eliminated.

For the initial lighting system, the 32 lamps and ballasts on the main lighting bank will draw approximately 34.6 kilowatts (36.3 KVA) during day simulation. Gantry and probe fill-in lighting should draw no more than 5 kilowatts. In addition, some additional power may be needed for the extra lights that may be needed to increase the illumination on the sides of the carrier.

For the expanded lighting system, the 82 lamps and ballasts would draw approximately 88.6 kilowatts (93.1 KVA) during day simulation. Gantry and probe fill-in lighting should draw no more than 10 kilowatts.

Television Line Scan Rates. This section describes the incorporation of multiple television line scan rates into the AWAVS systems concept. Due to limitations of the Eidophor projector, the range of line rates will be limited to the range between 525 to 825 scan lines. The complexity of the AWAVS image system dictates that the television systems be switched between discrete line rates within this range, as opposed to considering system operation over all rates within the range. The setup time and technical skill required to align each subsystem as the line rate is changed can be reduced by employing sets of prealigned circuit card modules. The set of modules can be interchanged at the desired time by replacing modules or switching between preinstalled modules under the control of a remote switching function. Each desired line rate would employ a separate set of circuit modules, and therefore, the number of line rates should be minimized. The AWAVS subsystems affected are:

- 1) Target image camera
- 2) Target image camera raster computer
- 3) Target image camera special effects generator
- 4) Target image synchronous pulse generator
- 5) Target image projector
- 6) Background image flying spot scanner (FSS)
- 7) Background image FSS raster computer
- 8) Wake image FSS
- 9) Background image synchronous pulse generator
- 10) Background image projector
- 11) Scene keying camera raster
- 12) Scene keying raster correction circuits

The following discussion of the impact of multiple-line rate on the target image generator is applicable to the background and wake image generators, and to the key camera raster.

Figure 126 shows the four, major elements of the target image generator which are impacted by the decision to operate at multiple, television-line rates. The television camera employs linear deflection amplifiers which are under the control of the camera dynamic raster computer, and therefore, the camera deflection circuits are unaffected by the multiple-line rates. However, the sweep protection circuits, employed by the camera to protect the vidicon image tube from damage due to raster underscan, is sensitive to the period of the deflection waveforms. Therefore, the dynamic range of this circuit function must be expanded to cover the total 525 to 825 line scan range.

Section 2 describes the relationship between line rates, resolution, and video bandwidth in detail⁴³. The video bandwidth of the camera output will be varied as the line rate is changed, in order to maintain the desired relationship between horizontal and vertical resolution. A separate video circuit module or filter assembly will be employed for each standard line rate. The camera video blanking function will be derived from the magnitudes of the x and y deflection currents, and therefore, they do not require modification as the line scan rate is varied.

The target image camera raster computer employs successive integrations, in order to generate the required term for the raster wave shape as outlined in section 5⁴⁴. It will be necessary to use a different set of integration modules for each line scan rate employed. However, the summing and scaling section will be common. The modular construction of the camera raster computer will allow multiple line rates to be implemented.

The special effects generator accepts the horizontal and vertical synchronous pulses from the pulse generator. The linear sweep generator module generates linear sweep waveforms from these pulses for use by the special effects generator and camera raster computer. This module will be replaced for each standard line scan rate employed.

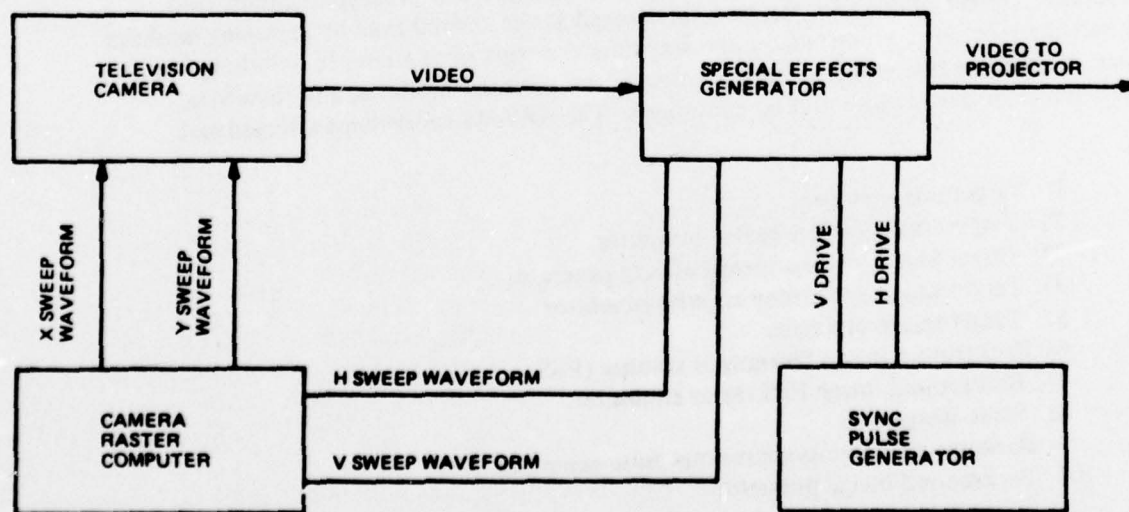


Figure 126. TARGET IMAGE GENERATOR TELEVISION FUNCTIONAL DIAGRAM

The programmable television synchronous pulse generator supplies the required horizontal and vertical drive pulses to the special effects generator and target image projector. Operation of the synchronous pulse generator at various, standard, television line rates is achieved through the generator program switches and the proper selection of the crystal oscillator frequency. This procedure can be performed by technicians with nominal skills in television maintenance.

Target Television Camera. The target image camera will employ the Westinghouse intensified WX-31836/WX5168 2-inch vidicon, because its superior resolving power and sensitivity provide optimum performance in a very critical area. The target image generator will employ dynamic raster shaping at the camera raster to compensate for system distortions, resulting from the target projector pointing.

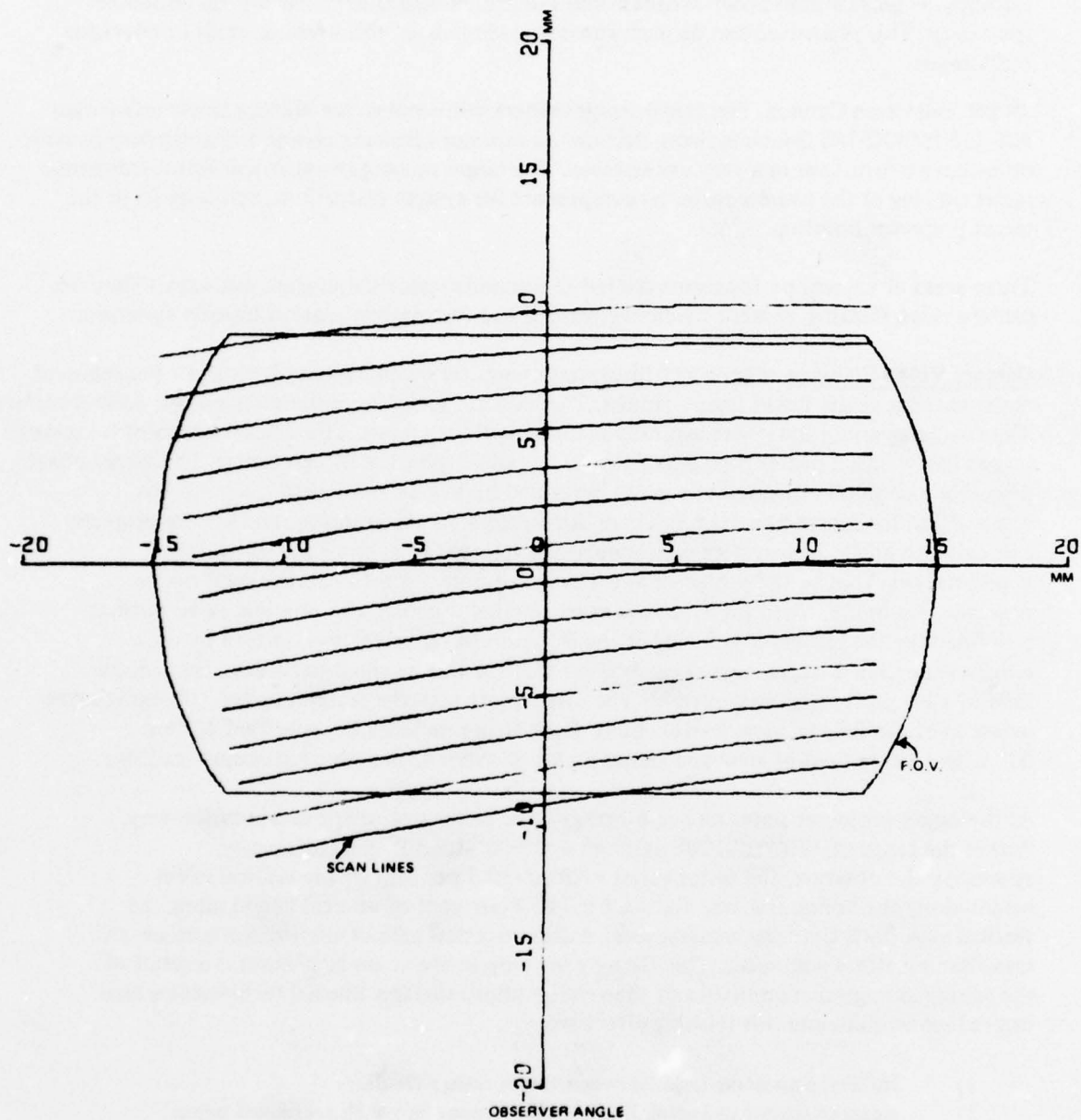
Three areas of camera performance related to dynamic raster shaping are discussed. They are camera video flashing, camera lag characteristics and camera modulation transfer function.

Camera Video Flashing. Figure 127 illustrates computer output plots which show the required raster shaping at the target image camera. The axes are scaled in millimeters on the vidicon surface. The following conditions were assumed in deriving these rasters. The normal eyepoint is located 15 inches below and 6 inches forward of the 10 ft. radius spherical screen center. The target image projector exit pupil is located at a point described by $x = -(4 + 3.5 \sin \theta)$; $y = 3.5 \cos \theta$; $z = -10$ in the screen axis frame: where the dimensions are in inches, and θ is the projector axis azimuth angle. This system configuration is referred to as the 3.5, right-offset configuration. That is, the projector axis frame is 3.5 inches offset to the right of the observer axis frame, when the two frames are parallel. Further, the nominal raster format is defined for the projector pointing at the 0° azimuth - 0° elevation, as seen by an observer. Section 3 of this report established that for this nominal condition, the required field of view must be overscanned⁴⁵. The raster plots take the recommended 10% horizontal overscan of the field of view into account. Each figure includes the specified 40° by 60° target image field of view and shows a plot of every 45th active horizontal scan line.

As the target projector pointing angle changes, the raster size, shape and rotation vary. Within the range of $+80^\circ$ to -120° azimuth and $+50^\circ$ to -30° elevation angle, as seen by the observer, the raster varies $+7.8$ to -20.2 per cent of the vertical raster height along the horizontal axis and $+4.4$ to -11.4 per cent of vertical height along the vertical axis. Each time the camera raster writes on a new area of the vidicon surface, an area flashing effect will occur. This flashing or jump in the video brightness is a result of the energy storage characteristics of the vidicon photo surface. Special techniques which can reduce or eliminate this flashing effect are:

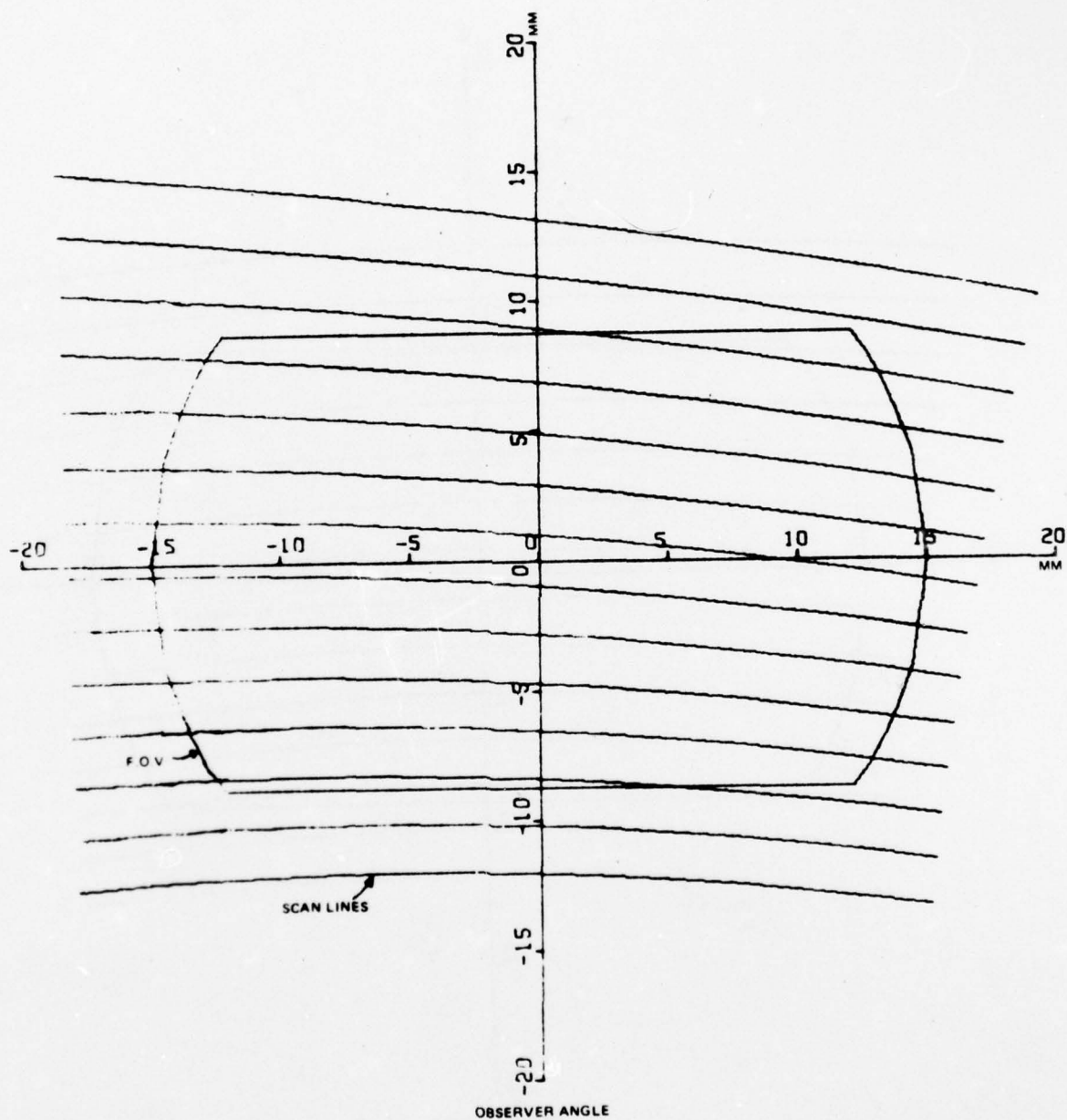
- 1) Interlace an erase field between target image fields.
- 2) Retrace scanning during horizontal retrace time with increased beam current to further discharge the photo surface.
- 3) Overscan the required field of view.

The technique of employing an erase field prior to each image field has been successfully employed with this image tube on the SAAC program. This method does require twice the video and deflection system bandwidth as the standard two fields per frame system, along with the accompanying reduction in signal-to-noise ratio. This technique will not be considered for the AWAVS application, since the Eidophor projector would be unable to meet the required light output at these increased scan rates.



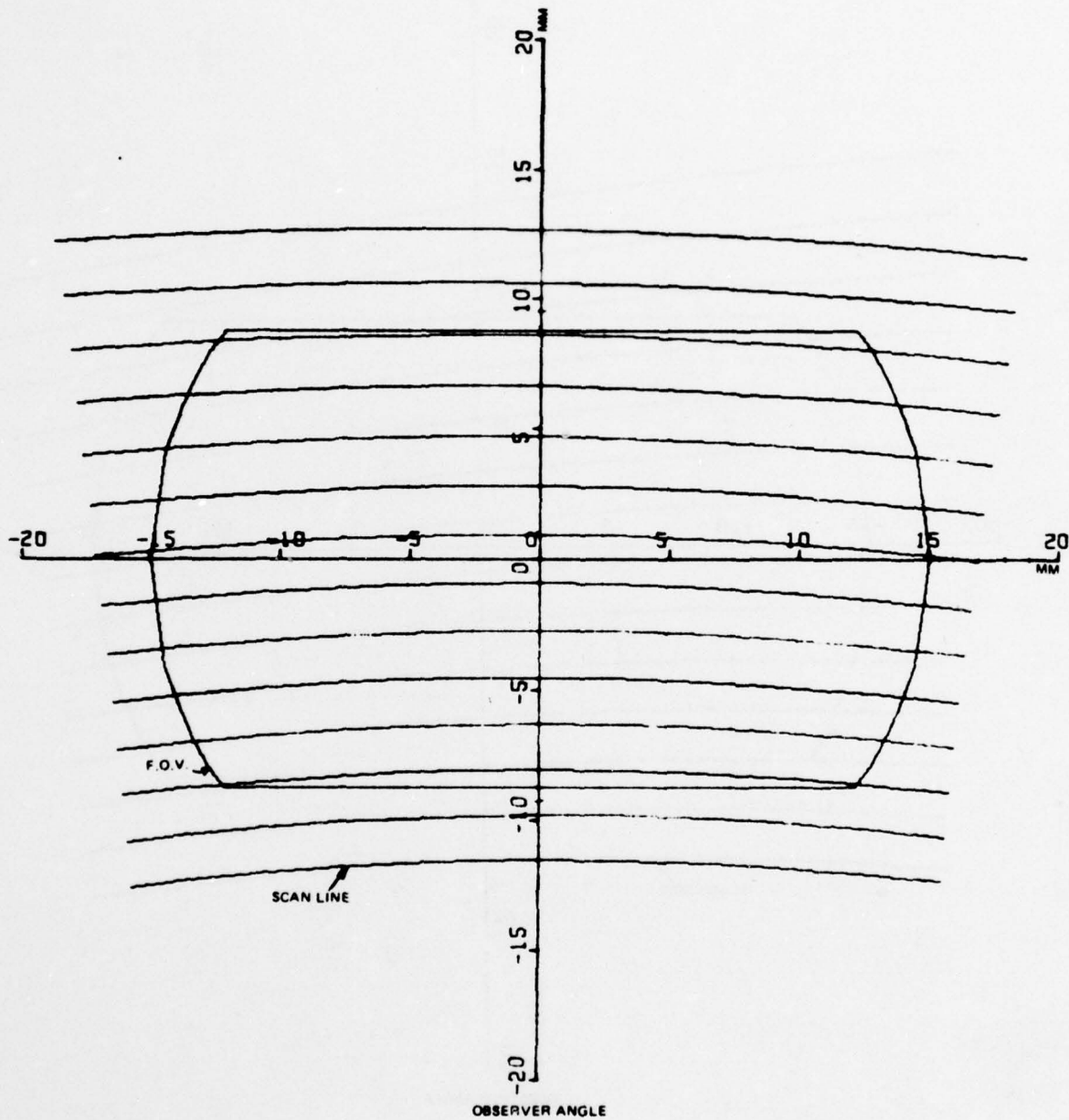
AZIMUTH=80. ELEVATION=50.

Figure 127. CAMERA RASTER PLOTS (PART 1 OF 8)



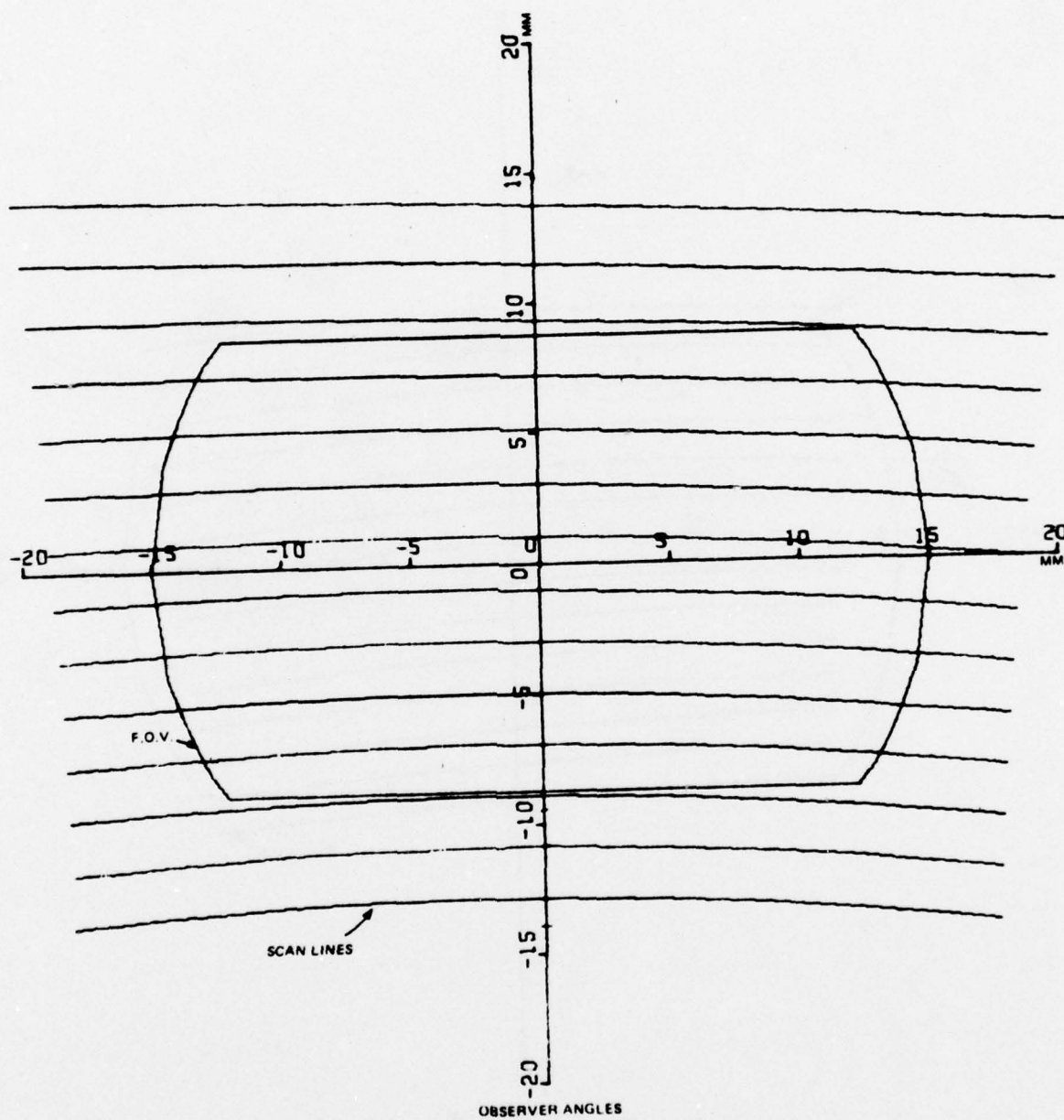
AZIMUTH=80. ELEVATION=-30. -

Figure 127. CAMERA RASTER PLOTS (PART 2 OF 8)



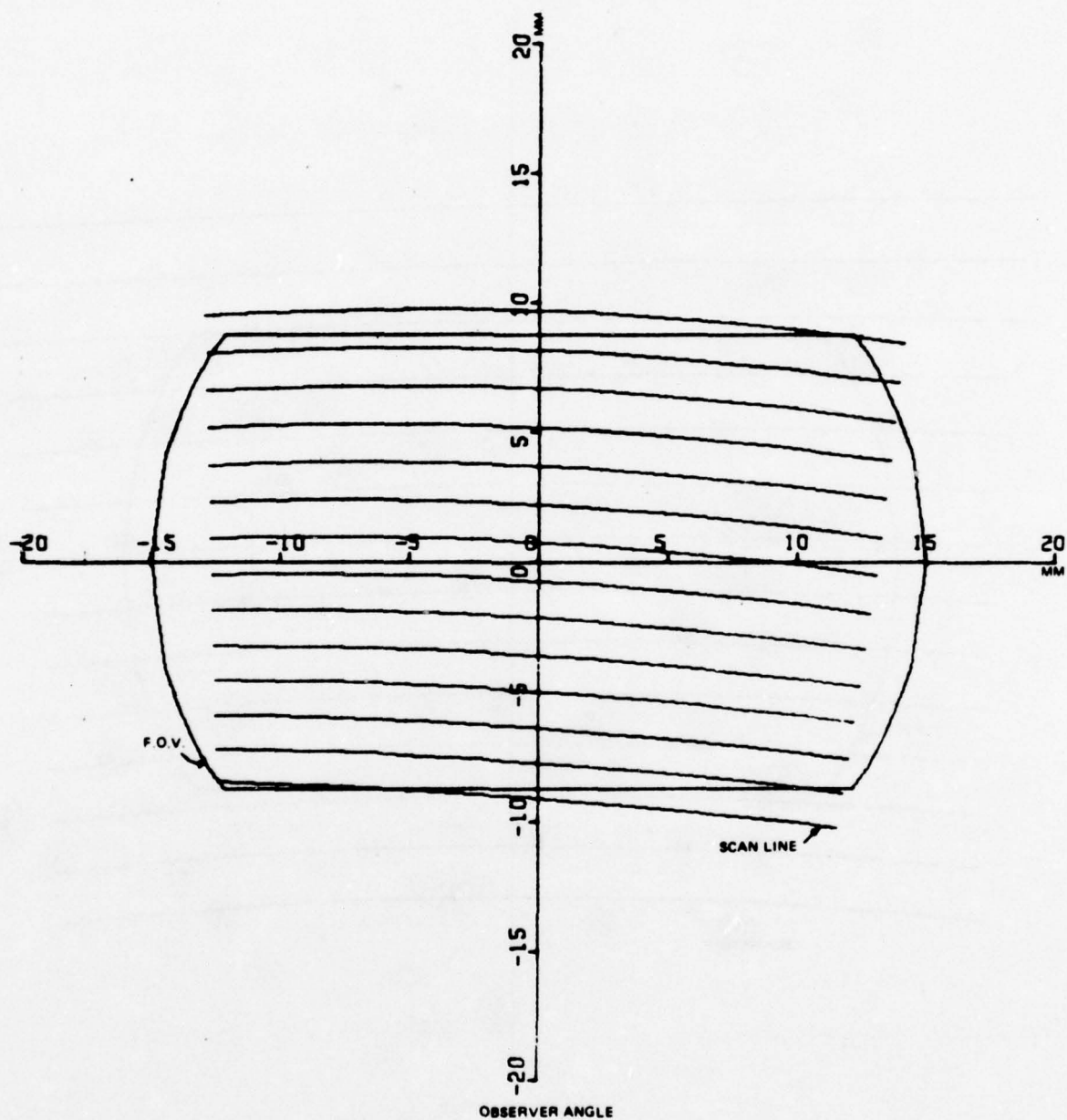
AZIMUTH=0. ELEVATION=0.

Figure 127. CAMERA RASTER PLOTS (PART 3 OF 8)



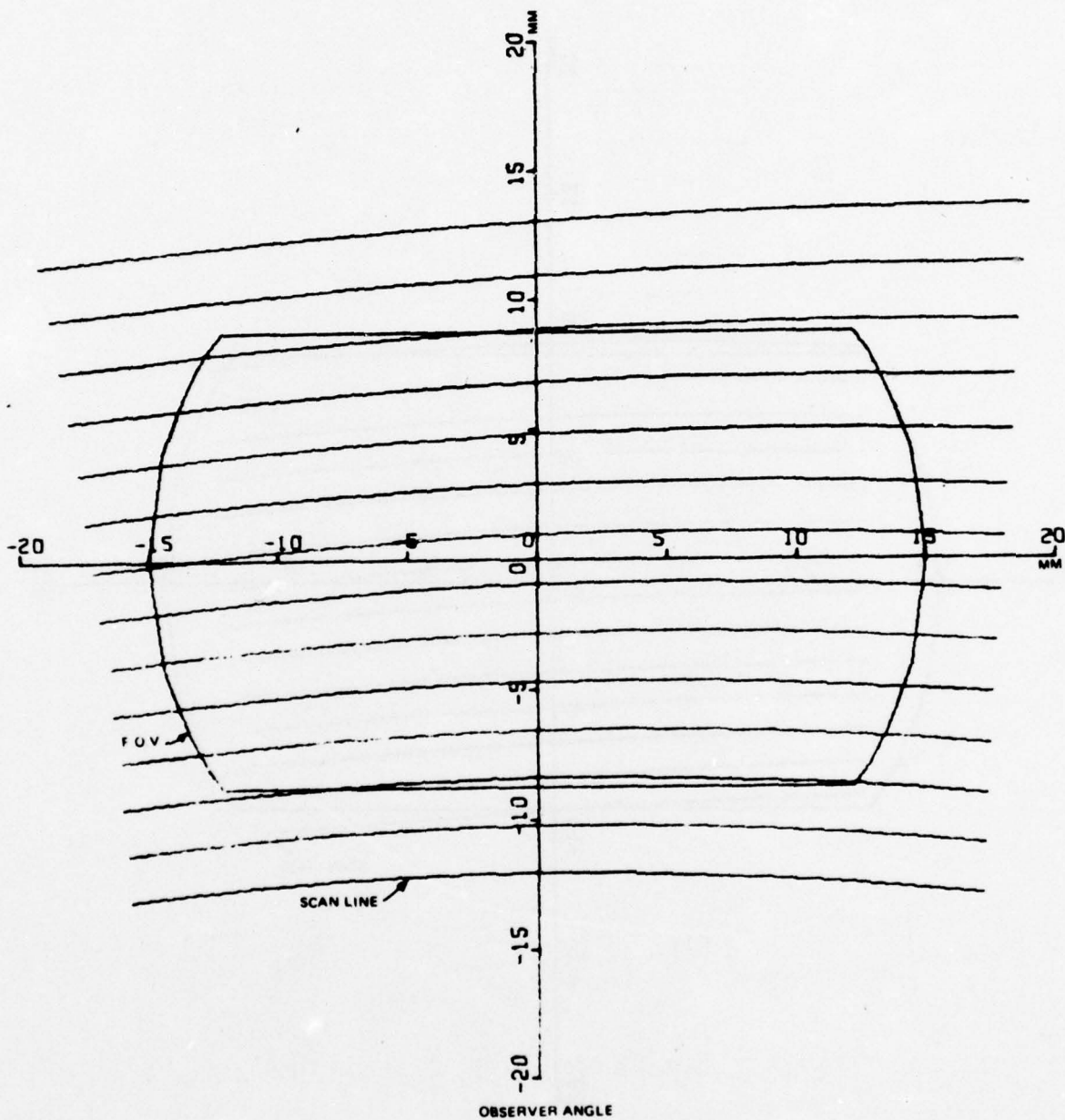
AZIMUTH=0. ELEVATION=-30.

Figure 127. CAMERA RASTER PLOTS (PART 4 OF 8)



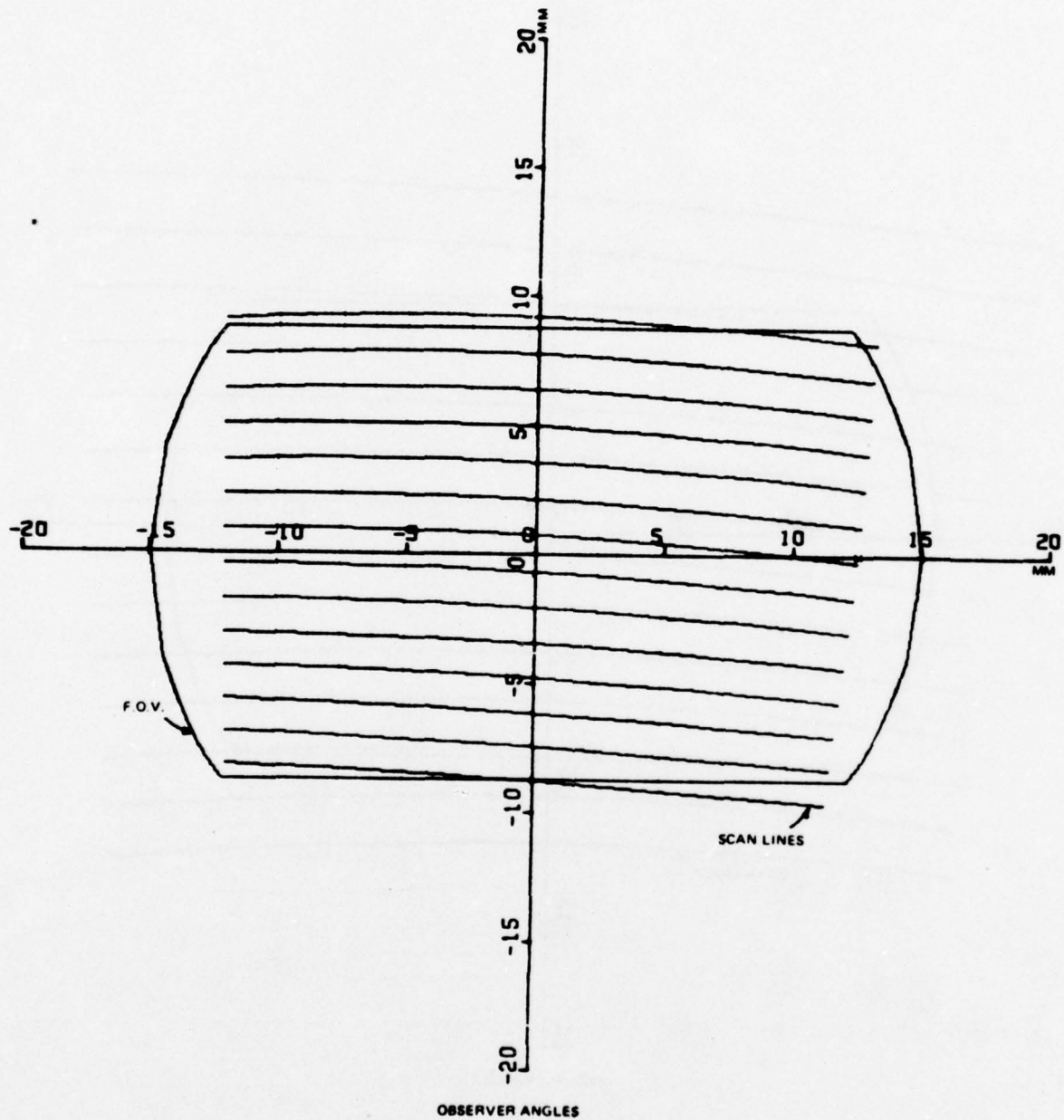
AZIMUTH=-80. ELEVATION=50.

Figure 127. CAMERA RASTER PLOTS (PART 5 OF 8)



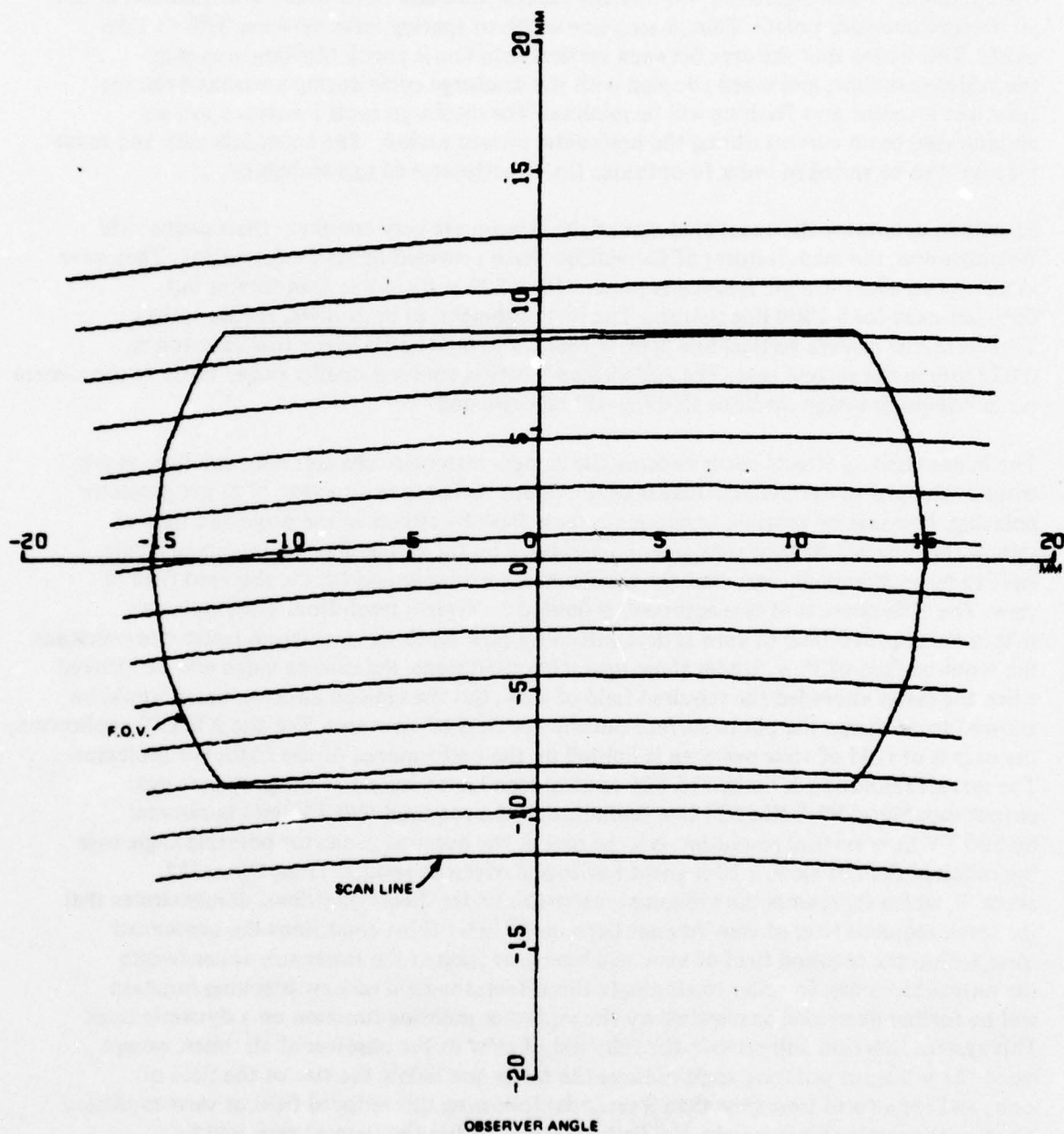
AZIMUTH=-80. ELEVATION=-30.

Figure 127. CAMERA RASTER PLOTS (PART 6 OF 8)



AZIMUTH=-120. ELEVATION=50.

Figure 127. CAMERA RASTER PLOTS (PART 7 OF 8)



AZIMUTH=-120. ELEVATION=-30.

Figure 127. CAMERA RASTER PLOTS (PART 8 OF 8)

The spacing between vertical scan lines is a source of area flashing effects. Assume the active vertical scan lines are uniformly distributed across the Eidophor raster surface, and therefore, the line density is 15 lines per millimeter. The camera raster plots show the camera vertical line density to vary between 0.022 mm to 0.039 mm. The vidicon specification gives the limiting resolution as 2000 TV lines over a 0.84 inch height. This reduces to 93.7 TV lines per millimeter. From figure 128 we find the vidicon spot size to be 0.025 mm diameter at the 50 percent intensity points. Thus, a scan line width to spacing ratio between 0.88 to 1.56 exists. This means that the area between vertical scan line is partly discharged during the active scan time, and when coupled with the discharge cycle during horizontal retrace time, the intraline area flashing will be minimal. The discharge cycle involves applying an increased beam current during the horizontal retrace period. The beam intensity and focus may have to be varied in order to optimize the effectiveness of this technique.

Efforts to determine the exact spot size of the vidicon are very complex. Discussions with Westinghouse, the manufacturer of the vidicon, have provided limited information. They have in test noted that intraline flashing is present for a 525 vertical line scan format but does not exist for a 1000 line pattern. The vertical height, in both cases, is 0.85 inches. Therefore, the camera vertical line density reduces to 0.041 mm in the first case and to 0.022 mm in the second case. The AWAVS application covers a smaller range. Early in the camera raster computer design intraline flashing will be evaluated.

The major flashing effects occur because the camera raster size changes and scan lines move from discharged to undischarged areas of the photo surface as a function of target projector pointing. It would be possible to eliminate these flashing effects in the projected field of view if the required field of view were overscanned by the raster. The overscanning would have to be great enough such that the minimum raster size would fill the required field of view. The effectiveness of this approach is limited by system resolution. The resolution within the required field of view is determined by how much the maximum raster size overscans the required field of view. Under these operating conditions, the camera video will be blanked when the raster exceeded the required field of view, but the vidicon electron beam would be allowed to discharge the photo surface outside the field of view area. For the AWAVS application, the extent of field of view overscan is limited by the performance of the Eidophor projector. The system resolution is limited to 825 vertical scan lines because of the projector light output capability. With this 825 line limitation, if the required 700 TV lines horizontal by 500 TV lines vertical resolution is to be met at the nominal projector pointing angle over the required field of view, a 10-percent horizontal overscan results. Thus, figure 127, sheet 7, which represents the minimum raster size under these conditions, demonstrates that the total, required field of view has not been met. Under these conditions the unscanned areas within the required field of view will bloom or flash as the raster size expands into the unscanned areas. In order to eliminate this effect, the field of view blanking function will be further decreased as required by the projector pointing function on a dynamic basis. This system function will provide the full field of view to the observer at all times, except when the projector pointing angle reduces the raster size below the size of the field of view, and for a fixed time (less than 3 seconds) following this reduced field of view condition. Thus, as the raster size increases, the flashing effect within the field of view will be blanked out. Preliminary calculation indicates that this reducing blanking will occur at elevation angles greater than 30° and the minimum observer field of view will be 51.3° horizontal by 40° vertical. Thus, the requirements of dynamic raster shaping present difficult but manageable problems for the AWAVS camera design.

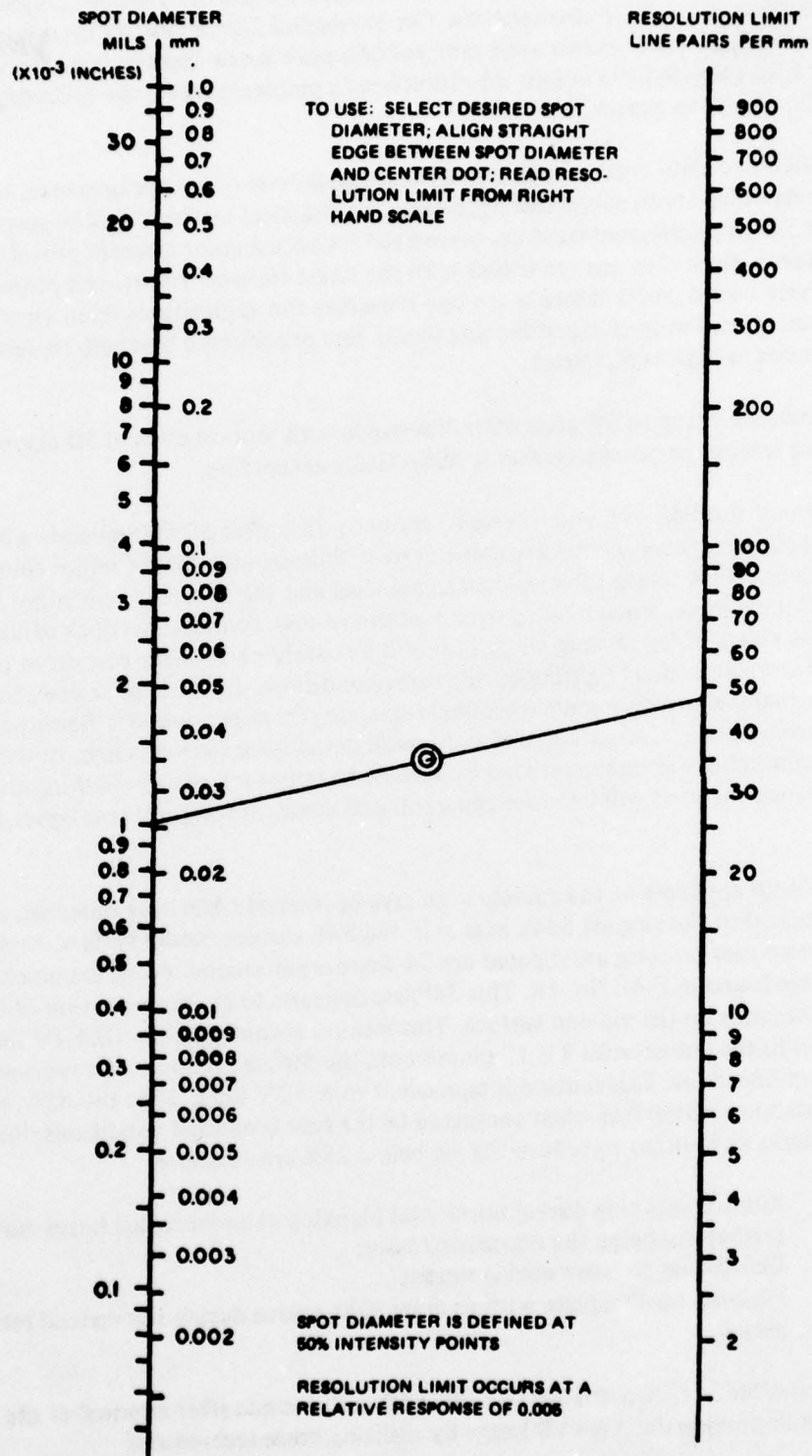


Figure 128. SPOT SIZE VS. RESOLUTION

Camera Lag Characteristics. A discussion of camera performance is not complete without consideration of the lag characteristics. The intensified 2-inch vidicon lag is specified at 25 percent, 50 milliseconds after removal of a peak white illumination. Since numerical values of lag provide little insight into its effect in picture quality, the following discussion has been prepared.

It is difficult to state what constitutes an acceptable level of lag performance, since the effects of lag are so subjective. However, as a practical matter it will be assumed that the 1-inch plumbicons used in commercial broadcast color cameras provide acceptable lag performance, since they are consistent with the latest state-of-the-art, and provide subjectively useful performance when one considers the applications from an image-motion standpoint; (i.e., the tracking of moving racing cars or a thrown baseball, representing motion rates as high as $50^{\circ}/\text{sec.}$)

The plumbicon decay to 5% after 50 milliseconds with motion rates of 50 degrees per second provides a level of performance that is subjectively acceptable.

In the case of the F4E #18 visual system, decay to 25% after 50 milliseconds with motion rates of 120 degrees per second are encountered. This causes a loss of image contrast which is dependent on the image tube residual signal level and the nature of the image being viewed. For example, when moving over medium or low contrast portions of the terrain model, the effect of lag causing image blur will be barely perceptible compared to moving over high contrast airfield lighting during night conditions. In the former case, the residual signal from the luminance channel remaining from previous TV fields will be masked by the chrominance information, and only small detail information is lost. In the latter case, where bright lights will be surrounded by a black background, the residual signals from the luminance channels will be more apparent, and some blurring of these lights will be visible.

In the AWAVS application, the camera is an area of interest (AOI) presentation, as opposed to being locked to the aircraft body axis as in the F4E camera model system. In AWAVS, the maximum motion rates anticipated are 34 degrees per second which are much smaller than motion rates found in F-4E No. 18. This $34^{\circ}/\text{sec}$ converts to an image motion of 0.495 mm in 50 milliseconds on the vidicon surface. This motion is equivalent to 10.4 TV lines. In comparison to the commercial TV 1" plumbicon, the $50^{\circ}/\text{sec}$ reduces to a motion of 0.275 mm in 50 milliseconds. This motion is equivalent to 8.7 TV lines. Thus the AWAVS lag characteristics are reasonable when compared to the best broadcast conditions. However, special techniques in order to reduce the lag below 25% are available:

- 1) Retrace scanning during horizontal blanking at an increased beam current to further discharge the photoconductor.
- 2) Defocusing of beam during retrace.
- 3) Flashing the faceplate with an erase light source during the vertical retrace period.

It appears possible to reduce the lag to 12% in 50 milliseconds after removal of the illumination, thus further improving the AWAVS image by utilizing these techniques.

Camera MTF. The camera raster plots contain the information required to specify the camera modulation transfer function. At the time of the AWAVS design analysis report the best estimate of the camera raster format was a linear 5:8 aspect TV raster. The actual raster density function is contained in the raster plots which show the nominal resolution is 11.5 LP/mm horizontal. Variation between 10.8 to 15.3 LP/mm horizontal occurs due to the raster computer shaping. Figure 129 gives the camera modulation transfer function as a function of television lines. There are three curves presented which represent three conditions. The first curve represents a 1:1 aspect ratio where TV lines per picture height equal TV lines per picture width. The two other curves represent a standard 3:4 aspect ratio. One curve represents TV lines per picture height and the other TV lines per picture width. The right-hand vertical scale is expression in LP/mm. Thus, knowing LP/mm MTF can be read directly from the left-hand vertical scale. The normal MTF is 0.77 horizontal while variations between 0.79 to 0.64 occur at the raster center due to the raster computer shaping.

Conventional Probe.

Probe Analysis and Pitch. An analysis has been made to determine the performance requirements for the revision to the probe specification. The probe will be centered on a fixed point on the center of the carrier deck until acquisition of FLOLS, after which it will be centered on the FLOLS, and then held at a fixed attitude during the final seconds of approach and landing. The maximum probe pitch and heading drive ratio will therefore occur during the initial carrier fly-by on the upwind leg, where airspeed is maximum and range to carrier is small.

Equations developed cover this situation as follows:

$$\theta = \tan^{-1} \frac{H}{R_{\text{gnd}}} = \tan^{-1} \frac{H}{\sqrt{(Vt)^2 + R^2}}$$

$$\dot{\theta} = \frac{-HV^2t}{(V^2t^2 + R^2 + H^2)(V^2t^2 + R^2)^{1/2}}$$

$$\ddot{\theta} = \frac{HV^2 (V^2t^2 + R^2 + H^2)(V^2t^2 + R^2)^{1/2} - V^2t^2 (V^2t^2 + R^2 + H^2)(V^2t^2 + R^2)^{-1/2} + 2(V^2t^2 + R^2)^{1/2}}{(V^2t^2 + R^2 + H^2)^2 (V^2t^2 + R^2)}$$

$$\psi = \tan^{-1} \frac{R}{Vt}$$

$$\dot{\psi} = \frac{-RV}{V^2t^2 + R^2}$$

$$\ddot{\psi} = \frac{2RV^3t}{(V^2t^2 + R^2)^2}$$

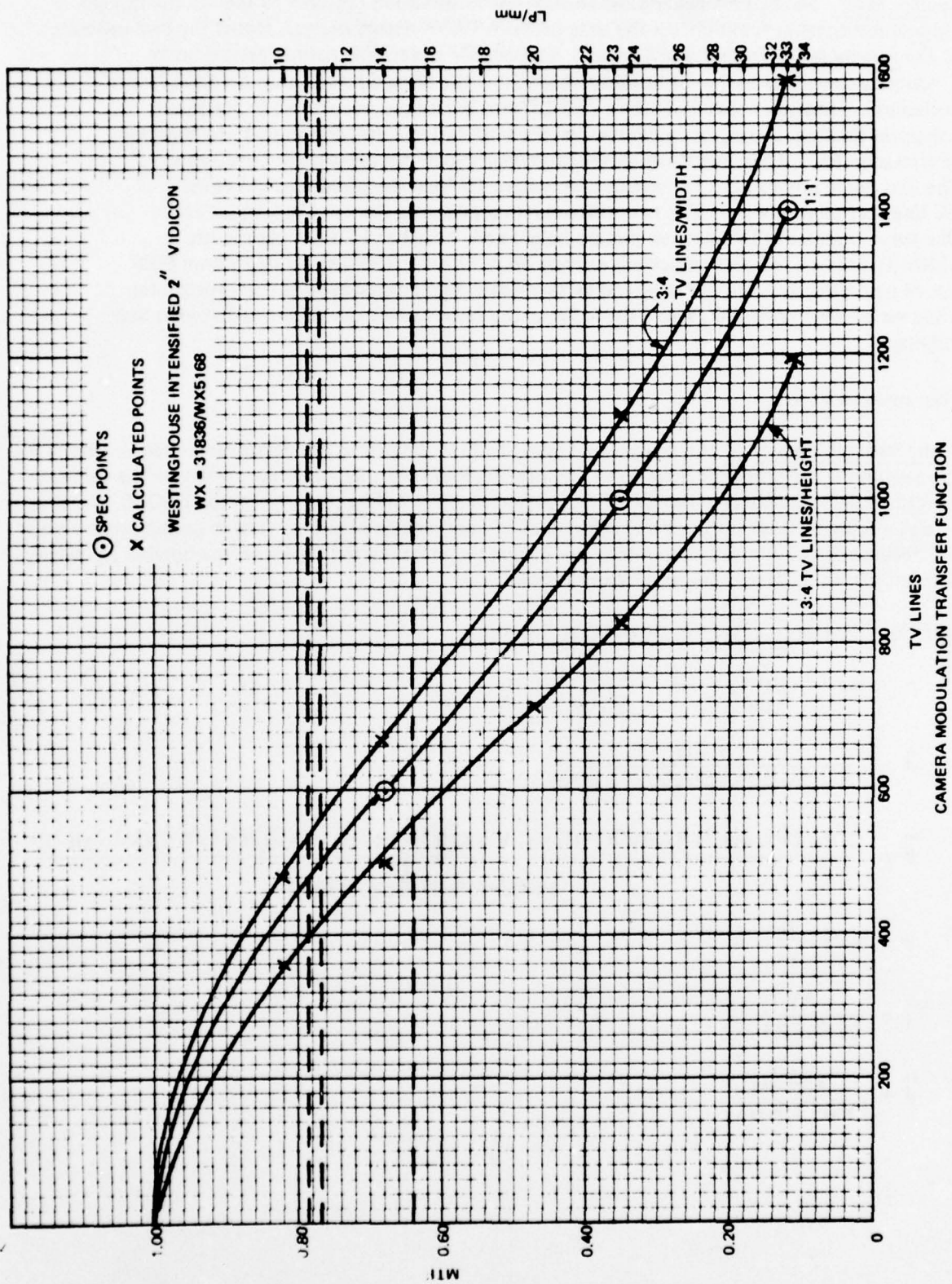


Figure 129. CAMERA MODULATION TRANSFER FUNCTION

NAVTRAEQUIPCEN 75-C-0009 _1

where: V = difference velocity between carrier and aircraft (x axis)
 H = altitude difference between aircraft and carrier deck
 R = distance aircraft is abeam of carrier
 θ = elevation angle of OS = probe pitch angle
 ψ = azimuth angle of carrier relative to aircraft = probe heading
 R_s = slant range to carrier
 R_{gnd} = ground range to carrier
 t = time, $t = 0$ at abeam position

These have been evaluated for the following conditions:

V = aircraft velocity - (carrier + wind velocity)
 = 250 kts - 30 kts = 220 kts = 371.6 ft/sec
 H = altitude aircraft - altitude carrier deck
 = 800 ft - 62 ft = 738 ft
 R = distance abeam of carrier
 = 500 ft

$\theta_{\text{max}} = -55.8^\circ$ $\psi_{\text{max}} = \pm 180^\circ$ (i.e., continuous rotation)
 $\dot{\theta}_{\text{max}} = \pm 10.6^\circ/\text{sec}$ $\dot{\psi}_{\text{max}} = \pm 42.6^\circ/\text{sec}$
 $\ddot{\theta}_{\text{max}} = \pm 14.7^\circ/\text{sec}^2$ $\ddot{\psi}_{\text{max}} = \pm 20.6^\circ/\text{sec}^2$

The probe derotation (roll) prism must be driven to rotate the image back to correct attitude for each of the above rotations.

$\phi_{\text{derotate}} = -(\theta + \psi) = \pm 180^\circ$ (i.e., continuous rotation)
 $\dot{\phi}_{\text{derotate}} = -(\dot{\theta} + \dot{\psi}) = \pm 53.2^\circ/\text{sec}$
 $\ddot{\phi}_{\text{derotate}} = -(\ddot{\theta} + \ddot{\psi}) = \pm 35.3^\circ/\text{sec}^2$

The actual image must drive at the above rates and positions but the prism rotation will be half this value.

Probe Zoom and Iris Parameters. The probe zoom power ratios have been computed in the gantry analysis section. Slant range as a function of time can be expressed as a function time for this maneuver as follows:

$$R_s = \sqrt{V^2 t^2 + R^2 + H^2}$$

For each range where probe zoom is changed, the equation for slant range has been substituted into the probe zoom equation and evaluated for maximum requirements for the set of velocities and displacements of the fly-by.

Range - 1000 ft. → 2300 ft.

$$Z_p = \frac{R_p}{1000} \text{ where } R_p = R_s$$

$$= \frac{1}{1000} (V^2 t^2 + R^2 + H^2)^{1/2}$$

$$\dot{Z}_p = \frac{V^2 t}{1000 (V^2 t^2 + R^2 + H^2)^{1/2}}$$

Range - 2300 ft. → 5840 ft.

$$Z_p = \frac{1}{1000} \left[R_s - \frac{R_2 - r_2}{(R_2 - R_1)^2} (R_s - R_1)^2 \right] = \frac{1}{1000} [R_s - K (R_s - R_1)^2]$$

$$\dot{Z}_p = \frac{V^2 t}{1000} \left[\frac{1}{(V^2 t^2 + R^2 + H^2)^{1/2}} - 2K \left\{ 1 - \frac{R_1}{(V^2 t^2 + R^2 + H^2)^{1/2}} \right\} \right]$$

$$= \frac{V^2 t}{1000} \left[\frac{1}{(V^2 t^2 + R^2 + H^2)^{1/2}} - 2 \left(\frac{R_2 - r_2}{(R_2 - R_1)^2} \right) \left\{ 1 - \frac{R_1}{(V^2 t^2 + R^2 + H^2)^{1/2}} \right\} \right]$$

Range - 5840 → 10,000 ft.

$$Z_p = 4.07 = \text{constant}$$

Range - 10,000 ft. → 36,480 ft.

$$Z_p = \frac{r_2}{R_s} (10) = 40700 (V^2 t^2 + R^2 + H^2)^{-1/2}$$

$$\dot{Z}_p = \frac{-40700 V^2 t}{(V^2 t^2 + R^2 + H^2)^{3/2}}$$

Substituting in the same values for R, H, V: R = 500 ft., V = 371.6 ft/sec, H = 738 ft. and values of: R₂ = 5840, r₂ = 4070, R₁ = 2300 and solving for maximum values of Z_p provides the following:

	<u>Ranges</u>		
	<u>1000 - 2300</u>	<u>2300 - 5840</u>	<u>10000 - 36480</u>
$\dot{Z}_p =$.3425 pwr ratio/ sec @ Z _p of 2.30 R _s = 2,300 ft.	.3425 pwr ratio/ sec @ Z _p of 2.3 R _s = 2300 ft.	-0.14 pwr ratio/ sec @ Z _p of 4.07 R _s = 10,000 ft.

Zoom acceleration rate will be determined by the actual hardware design capability. For this analysis, it is assumed that the sharp break in Z_p at the 1000 ft. range will be rounded in 1/4 second.

$$\therefore \ddot{Z}_p = \frac{\dot{Z}_p}{.25} = \frac{.1683}{.25} = .673 \text{ zoom range/sec}^2$$

For the probe specification, these values have been increased by a minimum of 50% to allow a safety factor and also to provide a margin of safety if the aircraft is below 800 ft. altitude, closer than 500 ft. to the carrier when abeam, or at higher velocity.

TARGET PROJECTOR SYSTEM

In an attempt to increase the target projector system light transmission to 6 ft-lamberts with a screen gain of 1.5, an experiment was made to determine the amount of light from the Eidophor within the light-gathering area. In addition, the target projector optics was reviewed to see what changes could be made to improve transmission. As a result, the target projector optics has been modified resulting in light output which has been determined to be in excess of 6 ft-lamberts.

Eidophor Light Output. An experiment was performed on an EP8 (5080) Eidophor to determine the variation in light level as a function of $f/\#$. As a result, it was determined that the output from the Eidophor does not vary inversely with the $f/\#$ squared. In fact, it deviated quite markedly from this. A series of known apertures was inserted immediately after the bar mirror, and the luminosity was measured on a screen with a Pritchard digital photometer. The photometer was calibrated before and after the measurements were made and the drift was found to be imperceptible.

The screen was divided into 24 regions, with 4 rows by 6 columns. The luminosity of each region was measured. The area of integration covered about 35% of each region. The measurements were performed with full aperture (90 mm) and the lamp current at 60 amps rather than 90 amps, which is the normal operating current. The cover had to be removed to insert the various apertures and without the cover, the lamp overheats at 90 amps. The measurements were made on a signal lambertian reference card which was moved to each region. Its reflectance was calibrated.

A control area was selected near the center for making luminosity measurements as the aperture size was changed. It was assumed that the total flux on the screen would vary as the flux in the reference area. The projector was adjusted so that the field was full white with no pattern.

The covers were replaced, and the lamp current was raised to 90 amps. The luminosity was then measured in the reference area. The light distribution was the same for 90 amps as 60 amps. Only the light intensity changed. The above data was used to convert the screen luminosity to a level resulting from 90 amps and at the various apertures. The luminosity was integrated for each aperture so that a single flux value could be associated with each aperture. These were plotted, and figure 130 shows that the measured level was 3250 lumens, not the 4000 lumens advertised. It is assumed that this reduced output resulted because either the lamp originally did not meet spec, or the lamp is old. Two curves are plotted on figure 130, showing the measured value and the possible value, if 4000 lumens is provided. The AWAVS operating aperture will be 40.88 mm which gives an available flux of 1900 lumens.

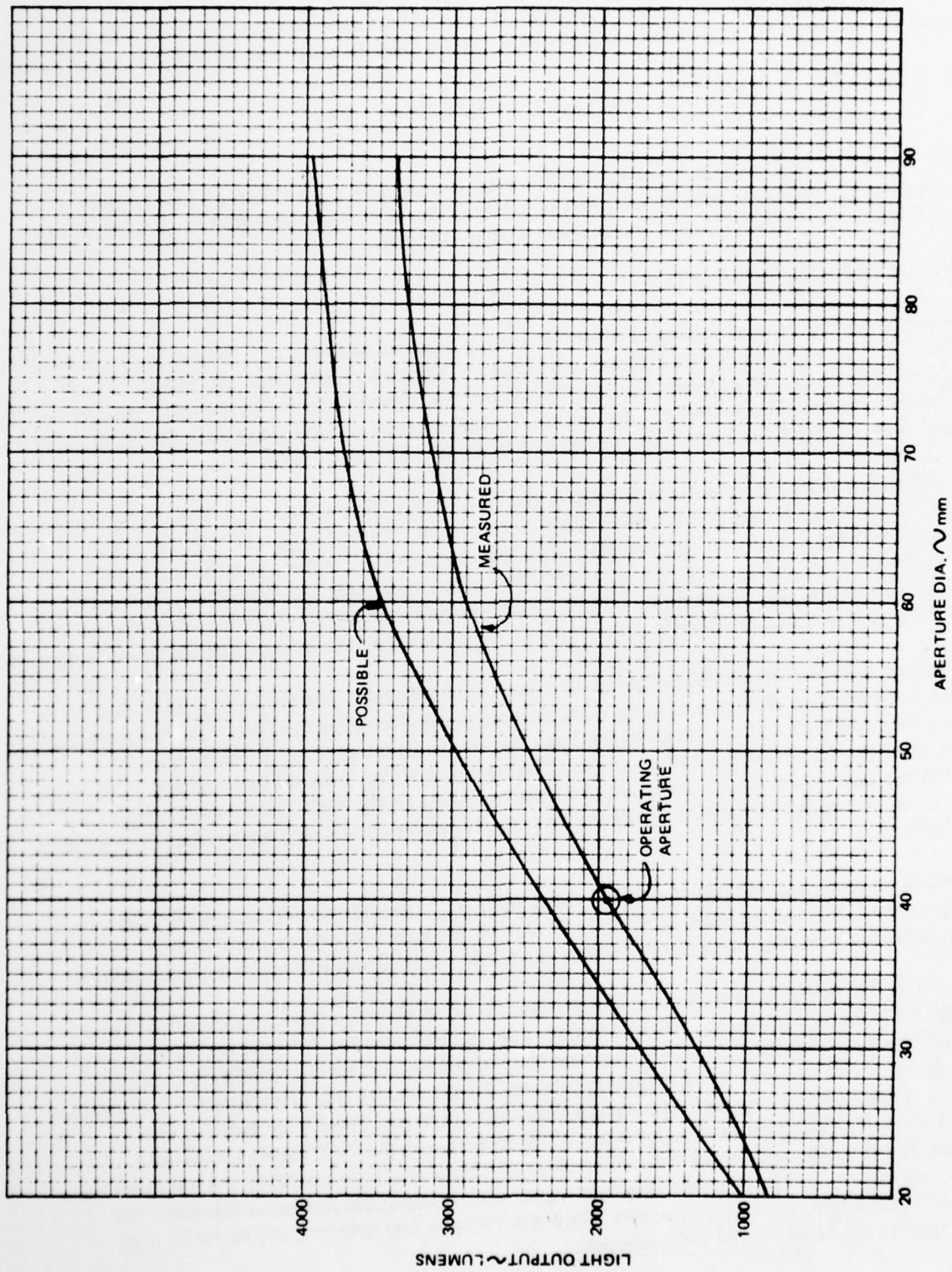


Figure 130. LIGHT OUTPUT VS. APERTURE SIZE

Table 27 shows the luminosity in foot-lamberts, after background is subtracted, before 90 amp and reflectivity calibration is applied. The second group of data shows the area of the various regions in inches squared. The lumens per each region was calculated as follows (using 85% for reflectivity and 80% for Eidophor lens transmission):

$$\text{lumens/region} = \frac{(\text{area of region in inches}^2) (\text{raw data in ft-lamberts})}{(.80) (.875) (144 \text{ inches}^2/\text{foot}^2)}$$

$$\text{Total lumens (for 60 amps)} = \Sigma \text{lumens/each region}$$

Target Project Zoom Optical Invariant. Since the zoom lens is the limiting aperture in the system, many zooms were reviewed (table 28) to find the one which has the greatest invariant (image diagonal / f/#). Three lenses have the greatest invariant. They are the Angenieux 10 x 35 and 10 x 28 and the Cannon 8 x 15. Since the Cannon is only an 8 x 15 and a zoom of 10 is required, it cannot be used. The Angenieux 10 x 28 (zoom rates x focal length) has too large a field. So the 10 x 35 is the choice. The latest data from Angenieux, which is contrary to catalog (and table) data, indicates that the f/# has become 3.92 with a pupil distance of -865.9 mm with a 221.207 mm diameter.

Target Projector System Optics. In the present configuration, shown in figure 131, a single lens is used to relay the Eidophor image to the target projection zoom image plane. The FLOLS image is combined by a beamsplitter, and the Pechan prism has been replaced with a different type roll prism. The roll prism is within the long conjugate of this relay (lens L1). This roll prism consists of two right-angle prisms cemented to a corner cube prism,

Table 27. REGION AREA VS. LUMINOSITY

75	87	100	90	89	75		
84	100	115	106	93	87		
88	112	109	93	75	67		
78	93	84	70	62	40		
Luminosity in Ft-Lamberts (Subtracted Background, 60 Amps, 90 mm Aperture)							
	7-11/32	10-25/32	11-3/32	11-3/16	10-7/16	4-7/8	
10-11/16	78	115	119	119	111	52	10.688
11-3/32	81.5	119	123	124	116	54	11.094
10-3/4	79	116	119	120	112	52.5	10.750
10-1/8	74.5	109	112	113	106	49.5	10.125
	7.344	10.781	11.094	11.188	10.438	4.875	
Region Area (Inches ²)							

and all reflections are total, internal reflections. The only losses in this type of prism are the reflection losses at the entrance and exit faces, and the internal glass absorption. The computed transmission for this prism is greater than that of a K mirror, having 97% reflection for each of the 3 reflection surfaces. In the short conjugate path of relay L1 is the combining cube beamsplitter. This arrangement puts one glass path in diverging light and one in converging light, thus helping to nullify the chromatic aberrations introduced by glass paths. Because of the position of the Angeneux zoom exit pupil the field lenses F1 and F2 both have negative focal lengths for proper relaying of the pupils. Negative focal length field lenses are unusual in optical systems. Usually we have positive field lenses which cause an increase in the field curvature, whereas in the proposed system, the negative field lenses can be used to actually flatten the field at the zoom image planes. The proposed system has no elements requiring design which is beyond the state-of-the-art.

Slope u on the Eidophor side of L1 is determined from the Angeneux exit pupil data and the magnification between the Eidophor image and zoom lens image.

Table 28. COMPARISON OF AVAILABLE ZOOM LENSES

	Zoom Ratio	Short Focal Length	f/#	Image Diag	OI	Smallest Field Angle
Zoomar	10x	135	8	25	3.1	5.33
Angeneux	10x	24	2.6	28	10.75	50.5
	15x	18	2.0	21	10.5	50.3
	18.5x	27	2.0	21	10.5	34.1
	15x	14	1.6	16	10.0	49.3
	18.5x	20	1.6	16	10.0	34.1
	10x	35	3.8	43	12.3	52.5
	10x	28	3.8	43	12.3	63.7
	18.5x	55	4.0	43	10.8	
Cannon	8x	15	1.3	16	12.3	56.8
Rank	10x	12	2.0	16	8.0	

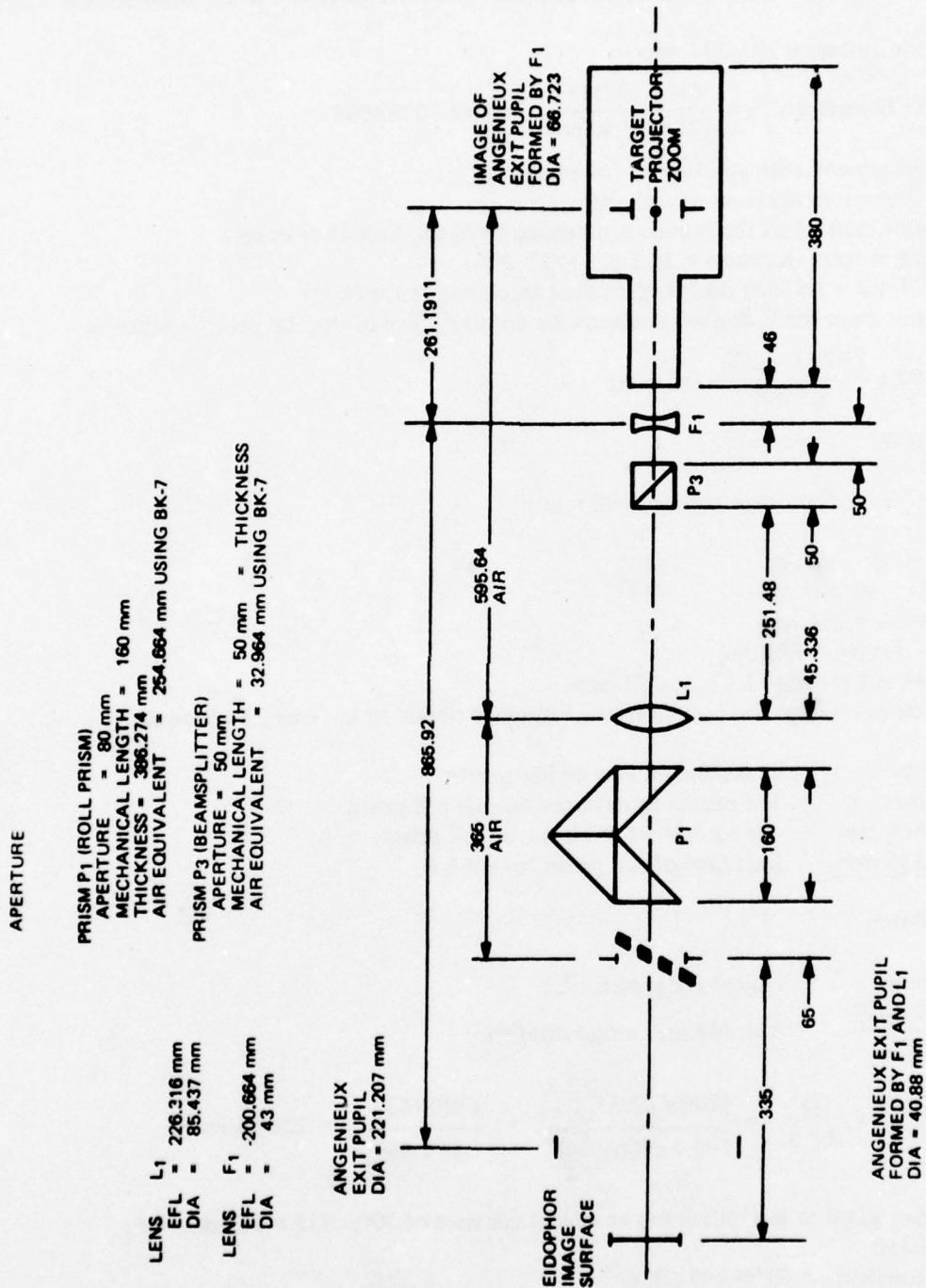


Figure 131. PROJECTOR OPTICS

Eidophor image diagonal = 90 mm

Zoom lens diagonal = 43 mm

Zoom lens exit pupil distance = -865.92 mm from zoom image (away from zoom behind image plane)

Exit pupil diameter = 221.207 mm

$$\text{Slope } u \text{ on Eidophor side} = \frac{(221.207)43}{(2)(865.92)90} = 0.0610263008$$

A1 = minimum entrance aperture of roll prism

A2 = minimum exit aperture of roll prism

A2 is greater than A1 as the bundle is diverging from the Eidophor image.

The roll prism total thickness = $2A2(1 + \sqrt{2}) = t$

Using BK-7 ($n_d = 1.5168$) the air equivalent thickness becomes t/n .

The distance from the Eidophor image to the entrance face of the roll prism = 400 mm.

$$2\left(400 + \frac{2A2(1 + \sqrt{2})}{1.5168}\right)u = A2$$

Solving for A2

$$A2 = 79.842 \text{ mm minimum; use } 80 \text{ mm}$$

Prism aperture = 80 mm

Thickness = 386.274

Air equivalent = 254.664

Mechanical length = 160 mm

Exit face of roll prism to L1 = 45.336 mm

The total air equivalent distance from the Eidophor object to the lens L1 becomes

335 mm	Eidophor oil film to bar mirror
65 mm	Bar mirror to entrance face of roll prism
254.664 mm	Air equivalent thickness of roll prism
<u>45.336 mm</u>	Exit face of roll prism to lens L1

700.0 mm

S = 700 mm Object distance for L1

$$S' = \frac{(700)(43)}{90} = 334.444 \text{ mm image distance}$$

$$\text{required EFL} = \frac{SS'}{S + S'} = \frac{(700)(700)\left(\frac{43}{90}\right)}{700 + (700)\left(\frac{43}{90}\right)} = \frac{(700)(43)}{43 + 90} = 226.316 \text{ mm}$$

The Eidophor pupil or bar mirror has an object distance of $700 - 335 = 365 \text{ mm} = P1$.

EFL = 226.316

Pupil image distance = $P1' = 595.6356$

For the field lens F1, the pupil object distance

$$P2 = P1' + S' = -.595.6356 + 334.444 = -261.1912$$

$$P2' = \text{image distance} = -865.92 \text{ mm}$$

The required focal length is computed from $\frac{1}{f} = \frac{1}{P2} + \frac{1}{P2'}$

$$f = 200.66405 \text{ mm for lens F1}$$

The Angeneux exit pupil diameter is 221,207 mm; therefore, at the bar mirror, the image of the pupil as formed by F1 and L1 equals

$$\text{DIA} = \frac{(221.207) (P2) (P1)}{(P2') (P1')} = 40.88 \text{ mm}$$

With this diameter, we can collect 1900 lumens of the total available.

Lens L1

$$\text{EFL} = 226.316$$

$$\text{Dia} = 85.437$$

$$f/\# = 2.648$$

Lens F2

$$\text{EFL} = -200.664 \text{ mm}$$

$$\text{Dia} = 43 \text{ mm}$$

$$f/\# = 4.6666$$

Estimated target projector transmission total system

.90	roll prism
.80	relay
T_B	beamsplitter transmission
.90	field lens
.70	zoom
.80	1st projection lens
.95	prism
.80	2nd projection lens
.95	prism
.95	prism

$$\text{target projector transmission} = 0.2488 T_B$$

$$\frac{(1900 \text{ lumens}) (0.2488) (T_B) (\text{screen gain})}{73 \text{ ft}^2} = \text{ft. lamberts}$$

Screen gain = 1.5 and minimum level = 6 ft-lamberts; therefore T_B minimum =

$$T_B \text{ min} = \frac{(6) (73)}{(1.5) (.2488) (1900)} = 0.6177$$

if $T_B = .8$, then we would obtain 7.77 ft-lamberts.

Television Line Scan Rates. The Eidophor television projector can be operated at multiple line scan rates as outlined in section 3.6.1 of the design analysis report.

Target System Resolution. Figure 132 shows the MTF curves (probe and target projector optics MTF are design goals) for the Target System Components and the Total Target System.

Large field of view displays have a special problem from extra image illumination from the remainder of the image. This tends to reduce contrast. Thus, the contrast of the observed target projected image will be degraded. Figure 133 shows a screen which is illuminated uniformly from the center of curvature "c". An arbitrary area d"A0" is illuminated by the screen. In particular, an area dA is shown contributing to the illumination of dA0. The surface dA is assumed to be a lambertian radiator. The luminance B is thus independent of the angle α .

The illumination of dA0 is proportional to the relative solid angle subtended by dA0:

$$\frac{dA_0 \cos \alpha}{s^2}$$

and the projected area of dA:

$$\cos \alpha$$

and proportional to the luminance B of the area dA.

The illuminance dE0 of dA0 from dA is:

$$\begin{aligned} dE_0 &= B \frac{dA \cos \alpha}{s^2} \cos \alpha \\ &= B \frac{\cos^2 \alpha}{s^2} dA \end{aligned}$$

"s" can be expressed as:

$$s = 2 r \cos \alpha$$

Substituting:

$$dE = B \frac{\cos^2 \alpha}{4 r^2 \cos^2 \alpha} dA.$$

The surface area dA is:

$$dA = r^2 d\theta d\phi.$$

Substituting dA and simplifying:

$$\begin{aligned} dE &= B \frac{r^2 d\theta d\phi}{4 r^2} \\ &= B \frac{d\theta d\phi}{4} \end{aligned}$$

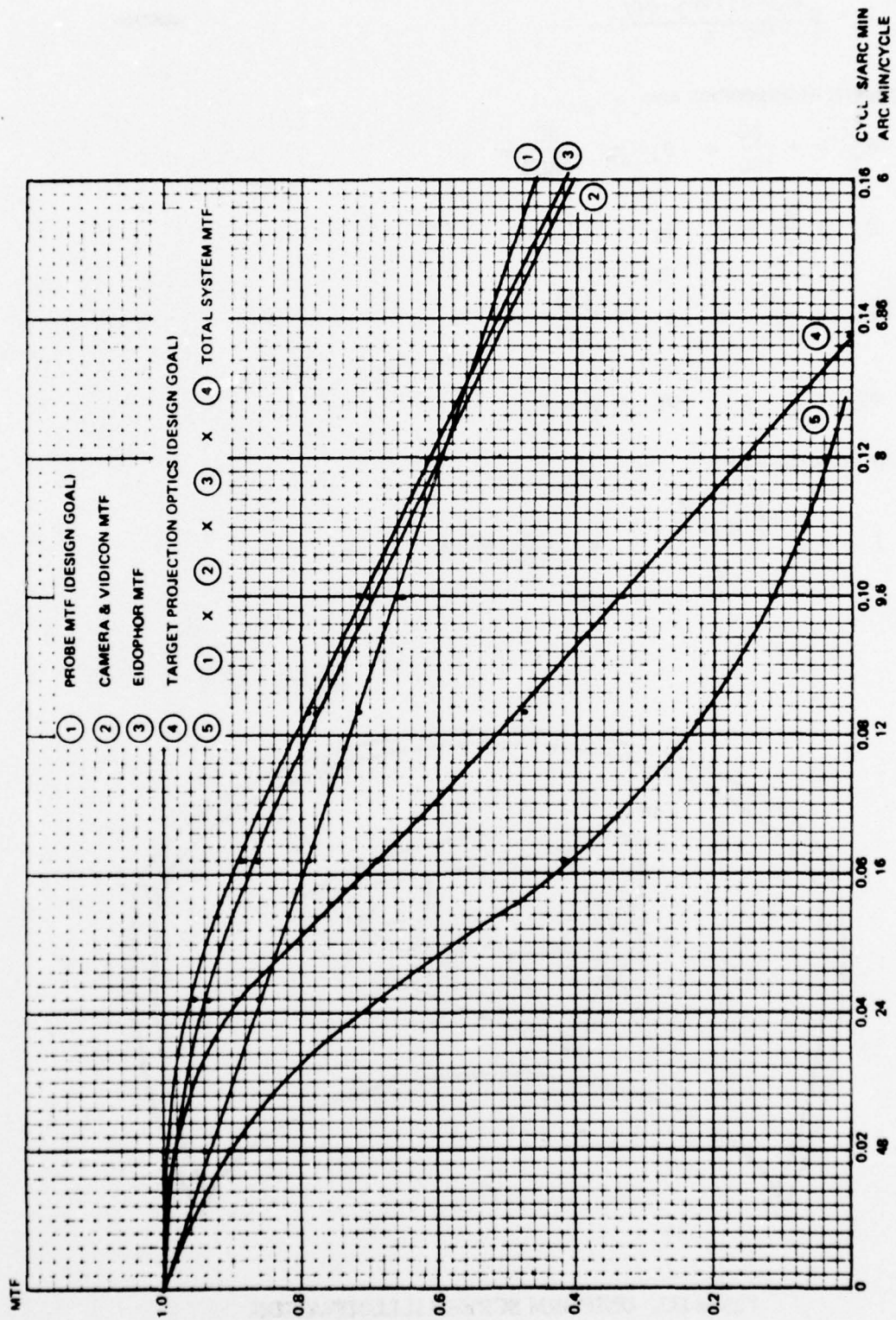


Figure 132. AWAVS TARGET PROJECTION SYSTEM MTF

Integrating:

$$E = B \frac{(\theta_2 - \theta_1)(\phi_2 - \phi_1)}{4}$$

The limits of integration are:

$$\theta_2 = + \frac{80}{180} \pi \quad \theta_1 = - \frac{80}{180} \pi$$

$$\theta_2 = \frac{4}{9} \pi \quad \theta_1 = - \frac{4}{9} \pi$$

$$\phi_2 = \frac{40}{180} \pi \quad \phi_1 = \frac{120}{180} \pi$$

$$\phi_2 = \frac{2}{9} \pi \quad \phi_1 = \frac{2}{3} \pi$$

Substituting the limits:

$$E = B \frac{\left(\frac{8}{9} \pi\right) \left(\frac{4}{9} \pi\right)}{4} = \frac{32}{324} \pi^2 B$$

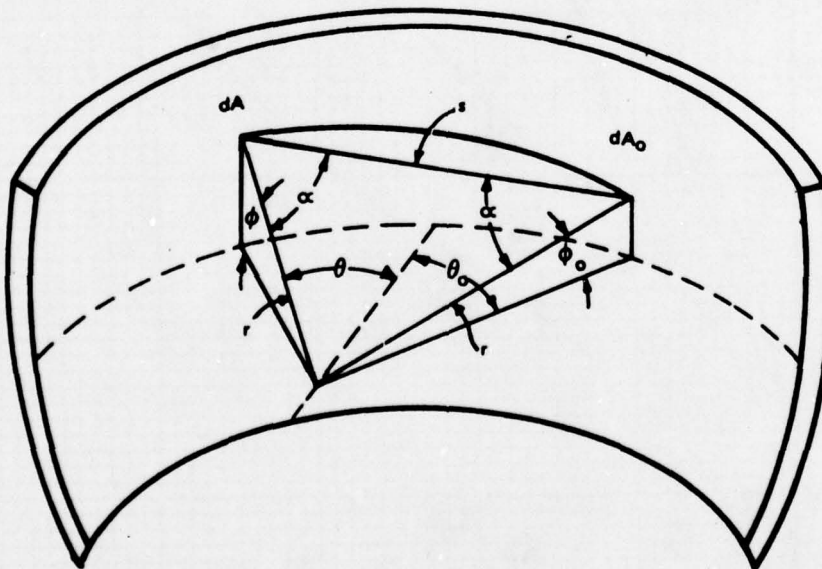


Figure 133. UNIFORM SCREEN ILLUMINATION

The screen brightness, due to E from the screen is:

$$\bar{B} = \frac{E}{\pi}$$

$$\bar{B} = \left(\frac{32}{324} \pi^2 / \pi \right) B$$

$$= \frac{32}{324} \pi B$$

The change in brightness is $\frac{32}{324} \pi$.

The above is for one perfect reflection. Since an infinite number takes place at a reflectivity of R, the result is expressed as a geometric progression:

$$\begin{aligned} \bar{B} &= B \left(1 + \left(\frac{32}{324} \pi \right) R + \left(\frac{32}{324} \pi \right)^2 R^2 + \dots \right) \\ &= B \frac{1}{1 - \frac{32}{324} \pi R} \end{aligned}$$

An experiment to measure cross screen reflectance was set up as shown on figure 134. The screen was painted matte white and covered $\pm 90^\circ$ by $+50^\circ$ to -30° . The remaining area was painted black. A small hole was placed in the screen to measure the brightness of the screen. Two diffusers of opal glass were placed at the hole to essentially integrate all light incident on the surface. A mask of black was made to cover the entire screen except the hole. The measurements were made with this in and out. The meter was a Pritchard digital photometer. The source was a 110 volt lamp located at the center of curvature. It was powered by a regulated supply. The lamp output was constant during the measurement.

The average measurement with cross screen reflectance is 1.35 times larger than the brightness without it. However, the analysis shows that it should be 1.42. This is calculated from the equations:

$$E = B \frac{(\theta_2 - \theta_1)(\phi_2 - \phi_1)}{4}$$

$$\bar{B} = \frac{E}{\pi}$$

The limits are:

$$(\theta_2 - \theta_1) = \left(\frac{90}{180} \pi + \frac{90}{180} \pi \right) = \pi$$

$$(\phi_2 - \phi_1) = \left(\frac{40}{180} \pi + \frac{120}{180} \pi \right) = \frac{4}{9} \pi$$

$$\bar{B} = B \frac{(\pi) \left(\frac{4}{9} \pi \right)}{4 \pi}$$

$$= B \left(\frac{1}{9} \pi \right)$$

With multiple reflection and reflectivity of 0.85:

$$\overline{B} = \frac{1}{1 - \left(\frac{1}{9} \pi\right) (0.85)} \quad B = 1.42 B.$$

FLOLS.

FLOLS Optics. Because of the reconfiguration of a portion of the target projection optics, a change is necessary in a portion of the FLOLS optics. Previously, the two paths were combined by a Fresnel bar mirror, whereas now they are combined by a cube-type beamsplitter.

At the target projector zoom, the maximum diameter of the FLOLS image is 1.519 mm. The FLOLS zoom operates only over a 5:1 range, so some latitude is available to choose its operating range out of the 10:1 range available. By choosing a range in the middle, we have the ability to extend the range at either end of the zoom. Therefore, we shall operate with a maximum diameter of the FLOLS image at the FLOLS zoom of 30 mm. This implies that we need a magnification of $30/1.519 = 19.7498$ between the target projector zoom and the FLOLS zoom. Lens L2 will produce a magnification of -4.4441 and lens L3 will provide a magnification of +4.4441 (figure 139).

Field lens F1 EFL = -200.664 mm
 Pupil object distance = -865.92 mm, diameter = 221.207 mm
 Pupil image distance = -261.1911 mm, diameter = 66.7236 mm
 Object distance for L2 = 100 mm
 Magnification to be -4.4441 mm
 Image distance therefore = 444.41 mm
 EFL = 81.63 mm

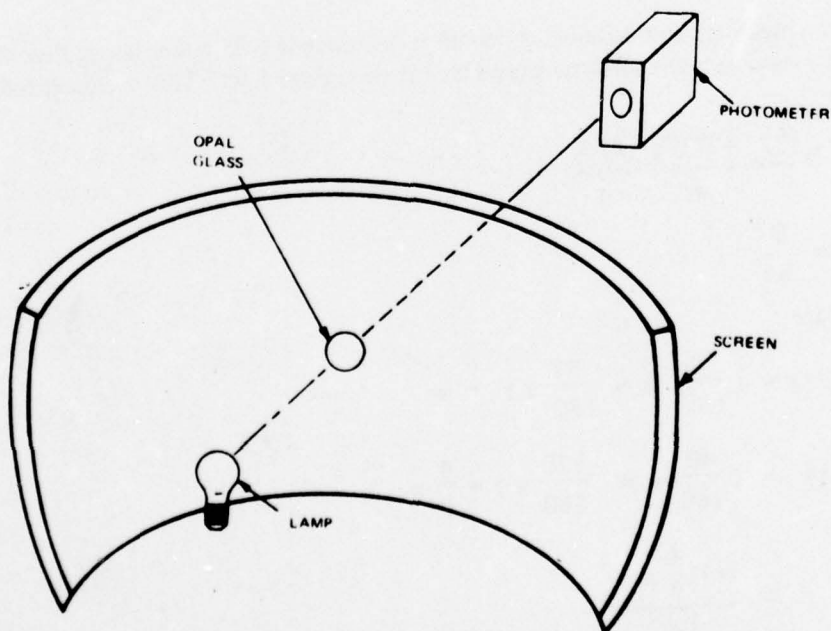


Figure 134. CROSS-SCREEN REFLECTANCE MEASUREMENT EXPERIMENT

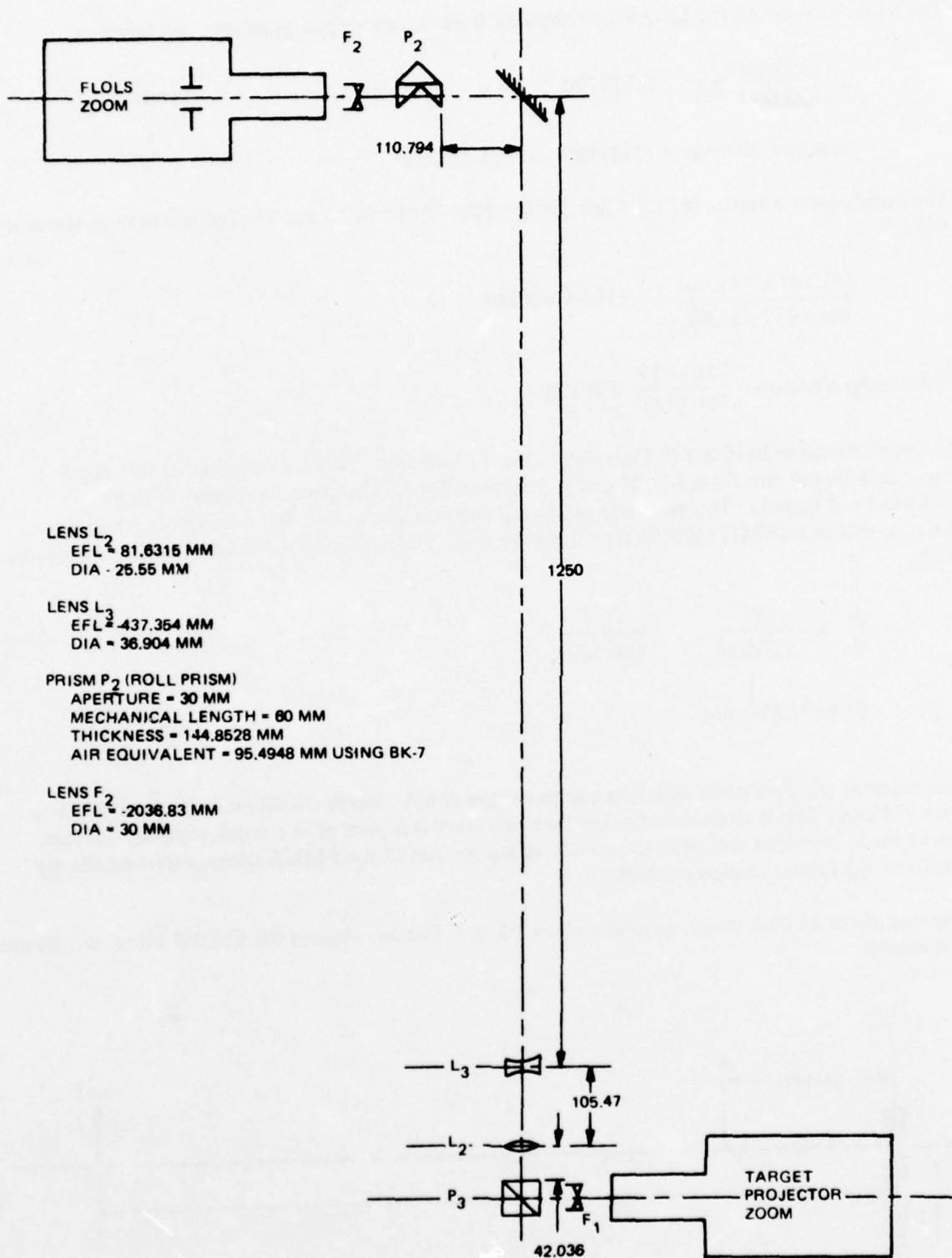


Figure 135. FLOLS OPTICS (CORRECTED)

The required aperture for L2 can be computed from the zoom exit pupil size and location.

$$u = \frac{221.207}{(2)(865.92)} = 0.127729$$

$$\text{required diameter} = (2)(100)(u) = 25.546 \text{ mm}$$

The pupil object distance for L2 = 261.1912 + 100 = 361.1912 mm. The image distance, therefore, will be:

$$\frac{(61.1912)(81.63)}{361.1912 - 81.63} = 105.4679 \text{ mm}$$

$$\text{The demagnification} = \frac{105.4679}{361.1912} = 0.292$$

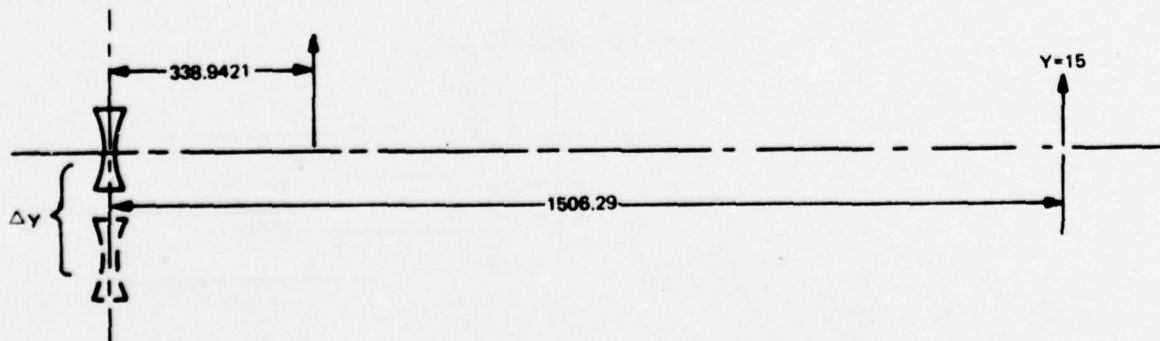
The pupil diameter becomes $(0.292)(66.7236) = 19.48$ mm. Lens L3 is located at this pupil image or 105.468 mm from L2. The object distance for L3 therefore, becomes $-(444.41 - 105.468) = -338.942$. This lens is to produce a magnification of +4.4441; therefore, the image distance will be $(4.4441)(338.9421) = 1506.29$ mm. The required focal length for L3 is computed from:

$$\frac{1}{f} = \frac{1}{1506.29} - \frac{1}{338.9421}$$

$$f = -437.354 \text{ mm.}$$

The required pupil diameter of L3, as computed previously, is only 19.48 mm; thus, the effective $f/\# = f/22.44$. This is an extremely slow lens, and since it is located at a pupil position, this lens can be made oversized and used to provide an x-y motion of the FLOLS image, replacing the x-y mirror of the original design concept.

The size of the FLOLS image, as produced by L2, is 6.75 mm; while at the FLOLS zoom, it is 30 mm in diameter.



The diameter of the field at the FLOLS zoom image plane is 30 mm. In order to move the FLOLS image out of the field, the center of the field must move 30 mm off axis at the FLOLS zoom image plane. The required movement ΔY of lens L3 is computed from:

$$\frac{\Delta Y}{338.9421} = \frac{30}{1506.2926 - 338.9421}$$

$$\Delta Y = 8.71 \text{ mm}$$

Thus, the additional diameter requirements of L3 = $2 \Delta Y = 17.42$ mm. The total diameter now becomes equal to the instantaneous diameter requirement of 19.48 plus the xy additional of 17.42 = 36.9 mm.

The f/# of L3 now becomes $437.354/36.9 = f/11.85$. The field lens F2 at the FLOLS zoom must image the zoom exit pupil onto L3. The pupil object distance for F2 = -865.92 mm. The pupil image distance = 1506.2926. The required focal length, therefore, becomes:

$$\frac{1}{f} = \frac{-1}{865.92} + \frac{1}{1506.2926}$$

$$f = -2036.83 \text{ mm}$$

Field lens F2

$$\text{EFL} = -2036.83 \text{ mm}$$

$$\text{Diameter} = 30 \text{ mm}$$

$$f/\# = f/67.89$$

The useful instantaneous diameter at L3 = 19.48 mm. The distance to the FLOLS zoom image plane = 1506.2926 mm.

$$u = \frac{19.48}{(2)(1506.2926)} = 6.4662 \times 10^{-3}$$

The effective $f/\#$ at the FLOLS zoom = $1/2u = f/77.3$. Estimated FLOLS transmission:

.65	condenser
.80	insertion factor
.80	fiber transmission
.85	FLOLS condenser
.90	FLOLS field lens
.70	FLOLS zoom lens
.90	field lens F2
.90	roll prism
.90	lens L3
.80	lens L2
R_B	beamsplitter reflection
.90	field lens F1
.70	target projector zoom lens
.80	1st projection lens
.95	prism
.80	2nd projection lens
.95	prism
.95	prism

FLOLS projector transmission = $0.0449 R_B$

Since the beamsplitter transmission was chosen for the target projector as 0.80, the remainder is available for the FLOLS reflectance. Considering absorption within the cube prism at the dielectric surface and the surface reflection losses, a reasonable value for $R_B = 0.15$. Therefore, the FLOLS system transmission becomes $(0.0449) (.15) = 6.735 \times 10^{-3}$.

From a drawing by Osram⁴⁵ of the typical radiation pattern from their Xenon arc lamp, the following analysis was made. The drawing shows the relative intensity as a function of angle in a plane. The total area of this was measured. Then the areas were determined of the pattern contained within 20, 40, 60, 80 and 100 degree segments equally divided about a horizontal axis. The ratios of the segment areas to the total area were determined.

A_θ = ratio of an area to total area. The steradians into which the lamp radiates for a $1/2$ plane angle of $\theta = 4 \sin \theta$. The steradians picked up by a condenser system subtending a $1/2$ plane angle of $\theta = 2 \pi (1 - \cos \theta)$. The ratio of the steradians collected to the total in a zone =

$$R_\theta = \frac{1 - \cos \theta}{2 \sin \theta}$$

1/2 Plan Angle θ	Area Ratio A_θ	Steradian Ratio R_θ	$*P_\theta =$ $\frac{A_\theta}{R_\theta}$
10	.16355	.0437444	7.15×10^{-3}
20	.376168	.08816349	.03316
30	.560747	.13397	.075125
40	.745327	.181985	.135638
50	.92056	.2331538	.214632

* P_θ represents total lumens output of lamp = lumens collected by condenser having $1/2$ plane angle θ .

As shown in the design analysis, the maximum area of a meatball image on the screen is 0.00236 ft². Also shown was the excess luminous requirement for angular alignment =

$$\left(\frac{1.4}{.25}\right)^2 = 31.36$$

Screen gain = 1.5

$$\frac{(\text{lumens})(6.735 \times 10^{-3})(1.5)}{(31.36)(.00236 \text{ ft}^2)} = 100 \text{ desired ft-lamberts}$$

This implies that the collected lumens must be 732.587. If a condenser subtending 60° is used, then the total lamp output must be:

$$\frac{732.587}{.075125} = 9751.57 \text{ total lumens}$$

A 450 or 500 watt Xenon source is sufficient to provide the necessary lumens.

FLOLS Range Simulation. With the new range at which target zoom can begin, and the resulting new zoom tables, the FLOLS range simulation can now be done completely with the FLOLS zoom. Range simulation of the FLOLS is determined by the relative powers of the FLOLS zoom and the target projection zoom. The projection zoom operates in conjunction with the probe zoom to provide a carrier image of proper angular subtent. In order to obtain maximum resolution as quickly as possible for the carrier image, the projection lens zoom relative power remains at a minimum for long simulated ranges while the probe zoom operates until the carrier subtends its maximum size on the vidicon. At this position, the probe zoom has reached its maximum power. Further changes in the simulated range are now made by the projection zoom until the simulated range where the probe begins to move. The total power in the target projection system is the product of the probe and display zoom relative powers. At the position where the probe begins to move, the probe zoom relative power is decreased while the projection zoom power continues to increase. At all times the product of their relative powers equals the ratio of the probe range to the simulated range.

The FLOLS image must change in size down to the limit of 500 ft. where the FLOLS is no longer useful. Since the FLOLS zoom is used in conjunction with the projection zoom to display the FLOLS image, the product of their relative powers must equal the ratio of 500 ft. to the simulated range. This ratio divided by the projection zoom power equals the relative FLOLS zoom power.

Table 29 shows the relationship between the relative zoom powers over a range from 6 nm to 500 ft.

Light-Emitting Source with Position-Sensitive Detector. A method of reducing optical probe pointing errors was introduced in section 4⁴⁶. This section will expand and analyze the suggested approach in more detail. A more detailed system block diagram of the system was designed. A math model for the system was constructed with the simplifying assumptions listed such that a computer program could be used to explore the pertinent performance characteristics of the system. The program was expanded to include such nonlinearities as deadband in the probe servos and the nonlinear transfer function of a quadrature detector. A sweep generator

Table 29. FLOLS ZOOM

<u>Simulated Range Ft.</u>	<u>Probe Range Ft.</u>	<u>Relative Power Probe Zoom</u>	<u>Relative Power Display Zoom</u>	<u>Relative Power FLOLS Zoom</u>
36480	4070	1.1157	0.1	0.137
24320	4070	1.6735	0.1	0.206
18240	4070	2.2315	0.1	0.274
12160	4070	3.3470	0.1	0.411
10000	4070	4.07	0.1	0.5
9120	4070	4.07	0.10965	0.5
7600	4070	4.07	0.13158	0.5
6080	4070	4.07	0.16447	0.5
5840	4070	4.07	0.17123	0.5
4070	3627.5	3.6275	0.24570	0.5
2300	2300	2.30	0.43478	0.5
1000	1000	1.0	1.0	0.5
500	500	1.0	1.0	1.0

was modeled to simulate the gantry motion for dynamic error analysis. Several computer runs were made varying the deadband level, initial step error and the sweep rate.

The total integration of the tracker was not completed at this time. The range of operation and maximum rates of tracking should be reviewed during the design phase to insure consistent assumptions. Special care will be taken to insure that the error integrators are initialized by command such that a minimum of discontinuity exists when the command is transferred from computer to the tracker.

Figure 136 is a simplified system diagram, showing the fundamental approach. The light-emitting source is matched to the beamsplitter, between the optical probe and the TV camera, in such a way that the light source emission is reflected into the detector and removed from the transmitted image. The beamsplitter will not appreciably affect the transmission image to the TV camera. The image of the source may be brought into sharp focus at the detector, so that the positional sensitivity may be in the order of 2 or 3 arc-minutes.

The addition of this suggested control loop, which is essentially another feedback path around the probe control system, will reduce the system error not sensed by the optical element servos in the probe. Since the suggested system will compensate for errors in the gantry position and in the probe pointing by closing the control loop around these subsystems, significant improvements should be realized in the FLOLS registration on the carrier.

The detector has to sense the position of the emitted spot and generate error signals to drive the pitch and heading servos in the optical probe. The detector is assumed to be a simple four-quadrant detector, which will drive the decode electronics in the classical "bang-bang" mode. More complex position-sensitive, or scanning techniques were not considered in this analysis.

Figure 137 shows a detailed system diagram. A light source is mounted at the center of the FLOLS board on the carrier model. It is assumed that the intensity of the light source is much brighter than any reflected light from the scene in the spectrum of light reflected off the beamsplitter into the detector. The light from the light source is transmitted through the optical probe and deflected along within the added errors of those elements in pitch and azimuth by the optical elements. Just before the total image enters the TV camera, the matched beamsplitter, with a very narrow reflective notch, removes the source light and passes the image from the model, with very little attenuation. The light source spot is imaged on a four-quadrant photo detector which detects the spot location and outputs a four-bit digital coded word.

The output of the detector is a series of four bits which is decoded in the quadrature detector logic. This logic determines if the spot is within capture range of the tracker. If the spot is out of range of the tracker, the OR output of the quadrature detector switches (R_1 and R_2) the inputs to the pitch servo and azimuth servo to the computed pitch and azimuth from the computer. A block with servo compensation was included to optimize the performance of the servo loops in the tracker mode.

The pitch and azimuth servos are the high-quality position servos in the optical probe. Any secondary servo drives (such as derotation) are derived from the position signal or the actual optical element motion. The servo drives the position of the pitch and azimuth elements such that the spot is centered in the quadrant detector. When this is accomplished, the quadrature detector senses the on track and is nulled to very near zero; that is, pointed straight at the light source on the FLOLS board on the model within the friction level of the servos.

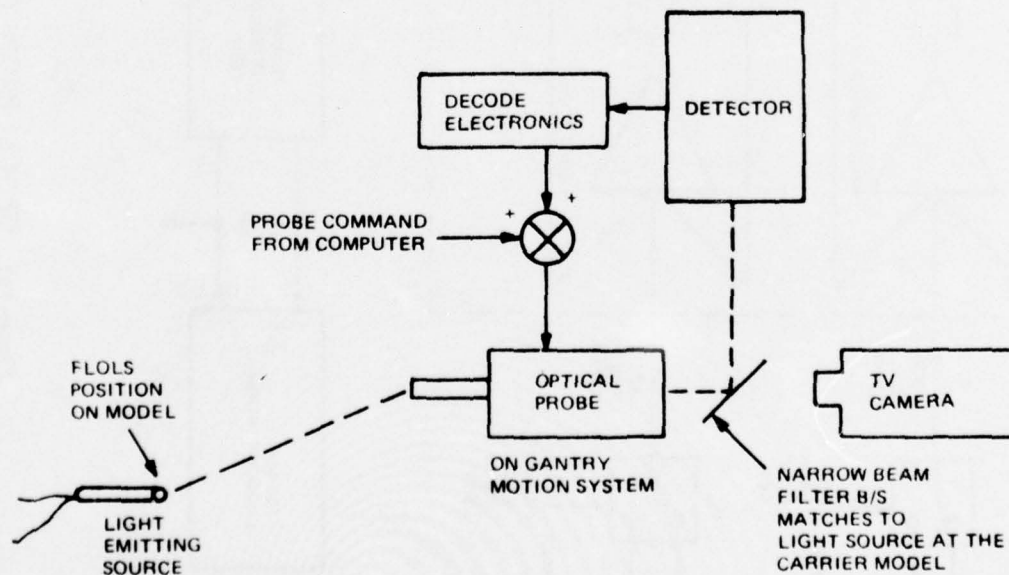


Figure 136. PROBE-POINTING SYSTEM, SIMPLIFIED

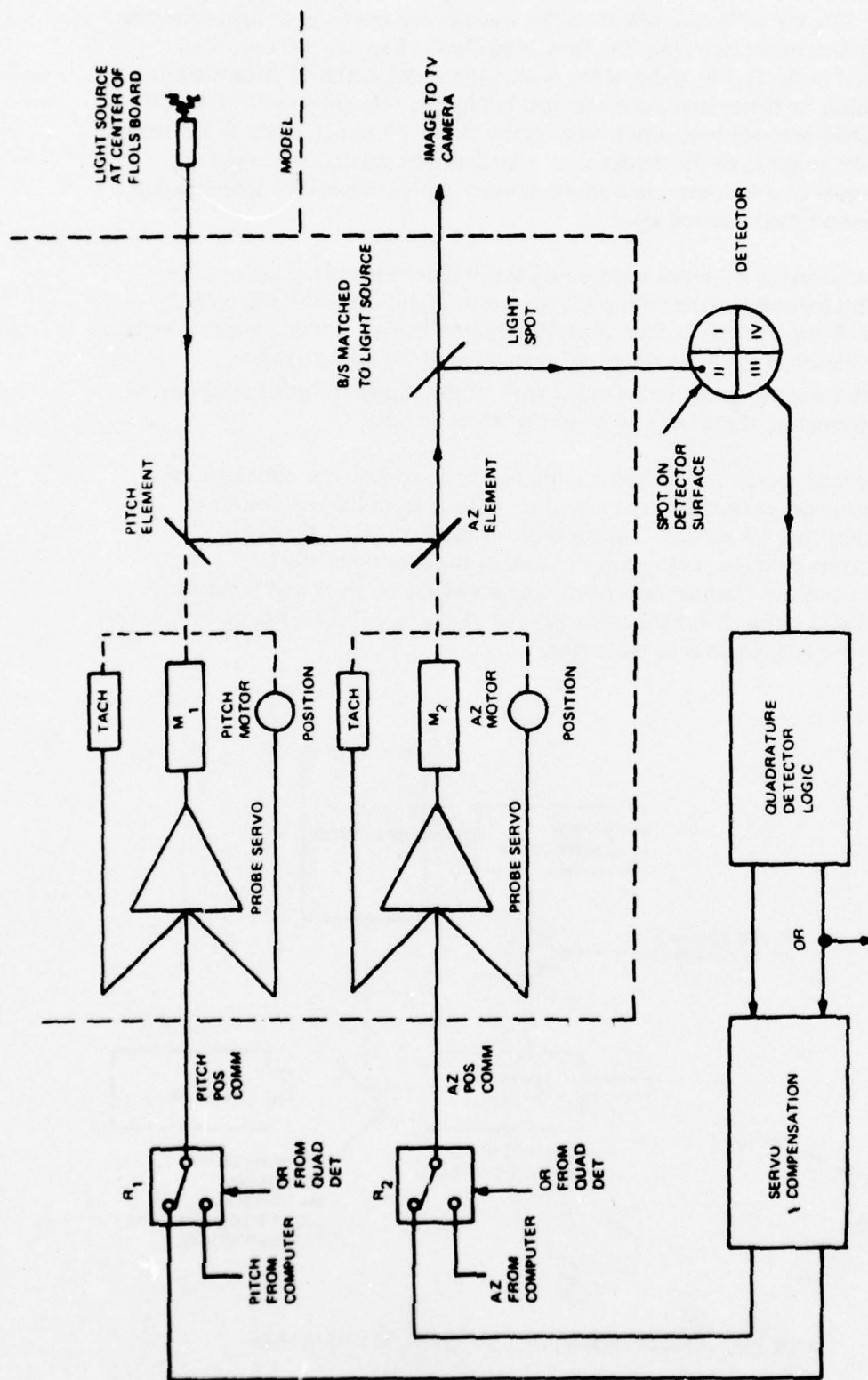
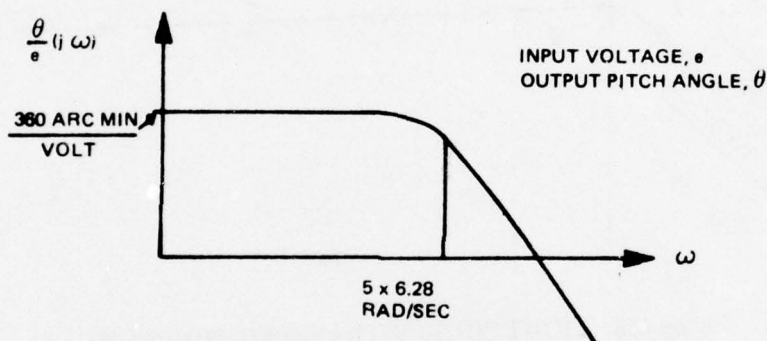


Figure 137. OPTICAL PROBE TRACKING OF IR SOURCE, BLOCK DIAGRAM

To construct a math model of the system for analysis, the following list of assumptions are given:

1. Design goal of tracker ± 3 arc minutes pointing accuracy reference to FLOLS board center.
2. Computer pointing capability of probe (open loop) 1 degree (60 arc minutes) which is considered adequate for tracker acquisition.
3. The probe threshold of sensitivity is 1 to 2 arc-minutes.
4. Input voltage scaling to probe servos $\pm 10V$.
5. Assume the pitch and azimuth servos are independent of each other. Only the pitch servo will be considered for analysis. Since other servo is independent, the same analysis applies. It is assumed that any auxiliary drives (such as roll with pitch) are derived from the input command signal or from the optical element motion itself.
6. Pitch servo function is:



$$\text{TRANSFER FUNCTION } \frac{\theta}{e} = \frac{360}{(1 + j \frac{\omega}{31.4})}$$

$$\text{Transfer function } \frac{\theta}{e} = \frac{360}{(1 + j \frac{\omega}{31.4})}$$

Note that 360 arc minutes/volt scaling, 1 arc min = 3×10^{-3} volts.

7. Transfer function of the light source spot through probe.
8. System reference is position of detector which is assumed to be centered on center of optical probe. (See figure 138.)
9. Assume integrator is needed to null out position errors. (Get very high gains at low frequency.) This is a $K/j\omega$ in the servo compensation box.
10. Quadrature Detector Logic: Assume the detector output is a digitized output. The cases exhibited in figure 139 exist.
11. Assume effective control from detector is a function as shown in figure 140. This combines the M+ and M- functions together since they are mutually exclusive.
12. The deadband will be of the form shown in figure 141.
13. The gantry motion appears to be a linear ramp at the pitch output. A linear ramp generator will be used to drive the system at the detector input for dynamic error analysis.

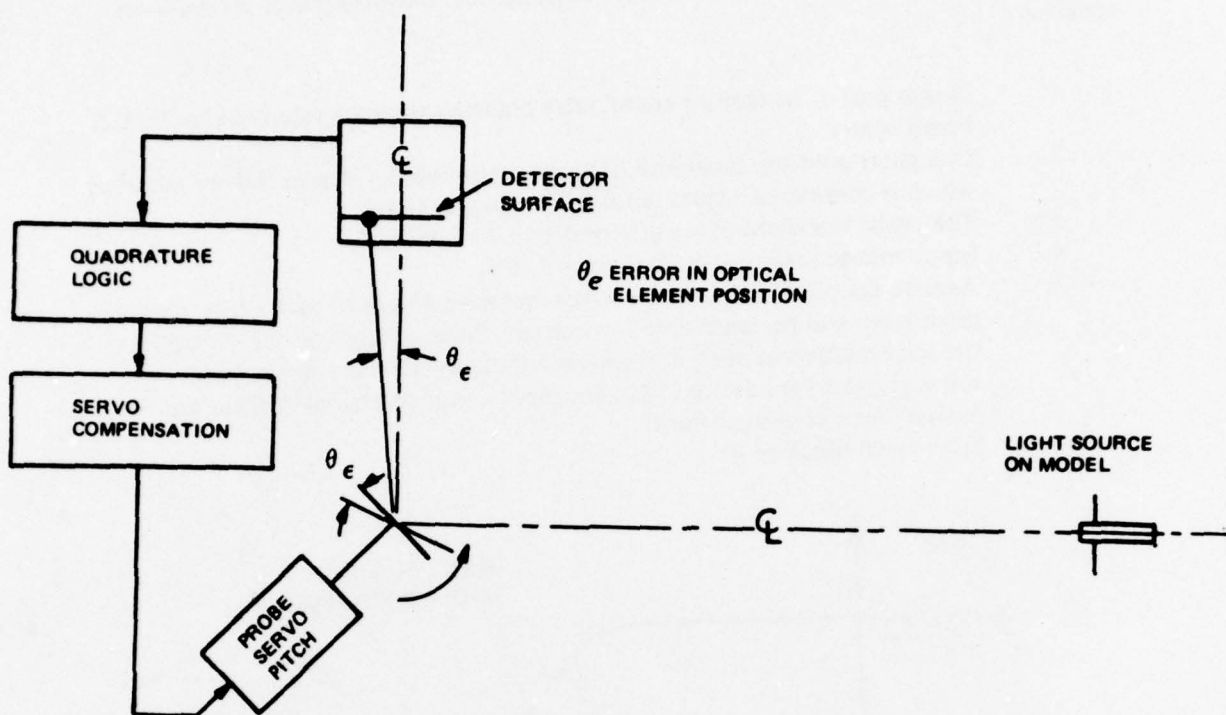


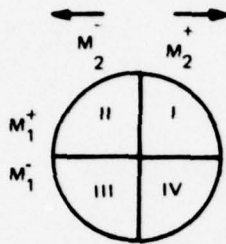
Figure 138. LIGHT SOURCE TRANSFER FUNCTION

Using the assumption listed on page 344 to simplify the system represented in figure 137, the simplified block diagram was arrived at in figure 142. This block diagram was used to develop the math model for a computer simulation.

The computer simulation was set up such that the rate on the sweep generator was varied for different values of deadband in the system. The performance criterion was the value of system error, ϵ , as shown in figure 142.

The composite simulation is shown in figure 143.

The GE timeshare system Mark II was used to run the simulations. The sweep generator was changed from 200 arc minutes per sec up to value of 3600 arc minutes per sec. The deadband was varied from +1 arc min to +12 arc min. The output of block (28) was plotted as a measure of the system error. The transient error was measured and compared.



CASE	QUADRATURE DETECTOR OUTPUT				PITCH		AZIMUTH		OUT OF RANGE
	I	II	III	IV	M_1^+	M_1^-	M_2^+	M_2^-	
0	0	0	0	0	0	0	0	0	1
1	0	0	0	1	1	0	0	1	0
2	0	0	1	0	1	0	1	0	0
3	0	0	1	1	1	0	0	0	0
4	0	1	0	0	0	1	1	0	0
5	0	1	0	1	0	0	0	0	0
6	0	1	1	0	0	0	1	0	0
7	0	1	1	1	0	0	0	0	0
8	1	0	0	0	0	1	0	1	0
9	1	0	0	1	0	0	0	1	0
10	1	0	1	0	0	0	0	0	0
11	1	0	1	1	0	0	0	0	0
12	1	1	0	0	0	1	0	0	0
13	1	1	0	1	0	0	0	0	0
14	1	1	1	0	0	1	1	0	0
15	1	1	1	1	0	0	0	0	0

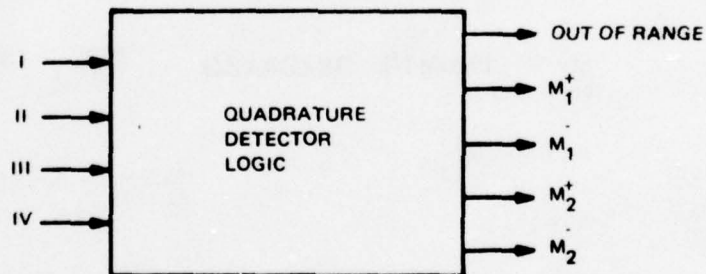


Figure 139. ILLUSTRATION OF QUADRATURE DETECTOR LOGIC

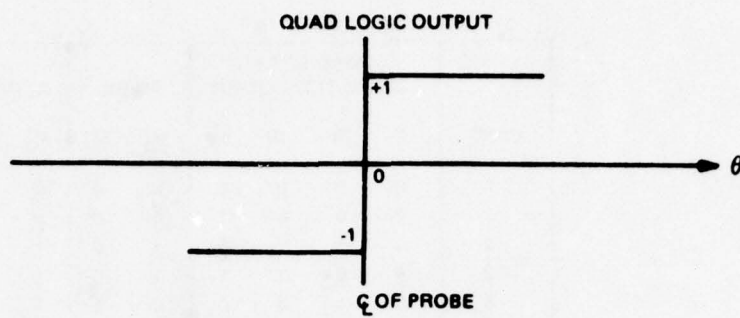


Figure 140. COMBINING M+ AND M- FUNCTIONS

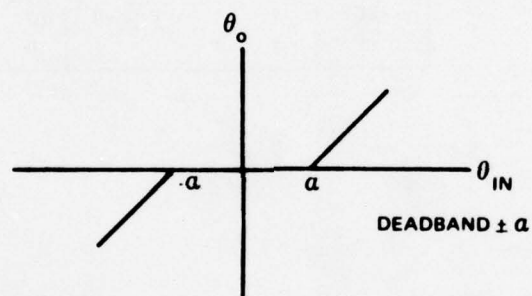


Figure 141. DEADBAND

Figure 144 shows a plot of ϵ for a sweep of 2700 arc min/sec with a deadband of ± 6 arc min. Since each run looked basically the same in shape, the comparison characteristics of p , the peak to peak transition and t_s , the time to settle within 10% of p , was chosen to be listed for comparison.

Table 30, Simulation Results, shows the results of multi-runs. It appears that settling time, t_s is about constant in the 0.1 sec to the 0.2 sec range for all cases tested. The height of transition, p , appears to be proportional to the sweep rate as expected. Case 9 would be considered to be a most likely condition on approach, with 200 arc min/sec and a deadband of ± 6 arc min. This has a peak swing of 6.6 arc and settles within 0.11 sec, which should not degrade the TV image.

In case 11, (above) the sweep was raised to 3600 arc-min/sec, which is a little over 1 rad/sec. The system was able to track, but not converge. An error of 120 arc-min. existed, even at the end of 0.3 sec. of sweep. No attempt was made to accommodate this condition since the input rate is so high.

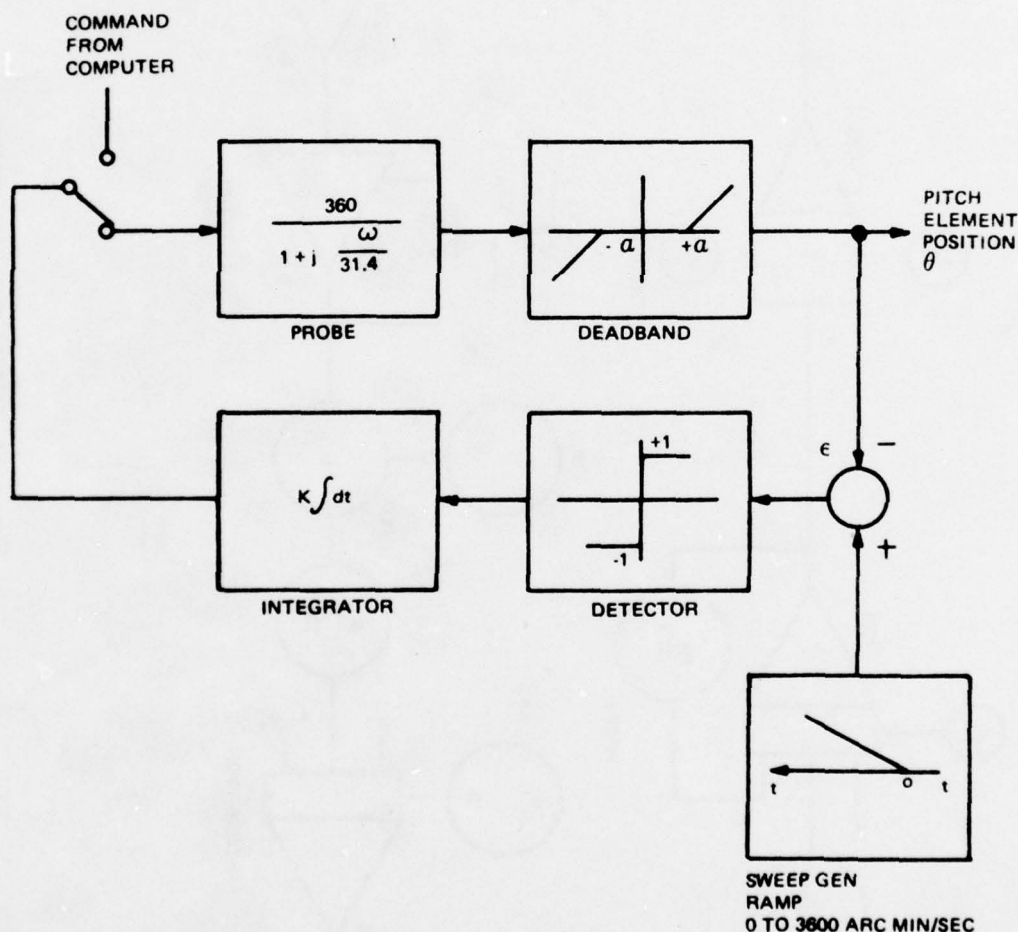


Figure 142. BLOCK DIAGRAM FOR COMPUTER SIMULATION

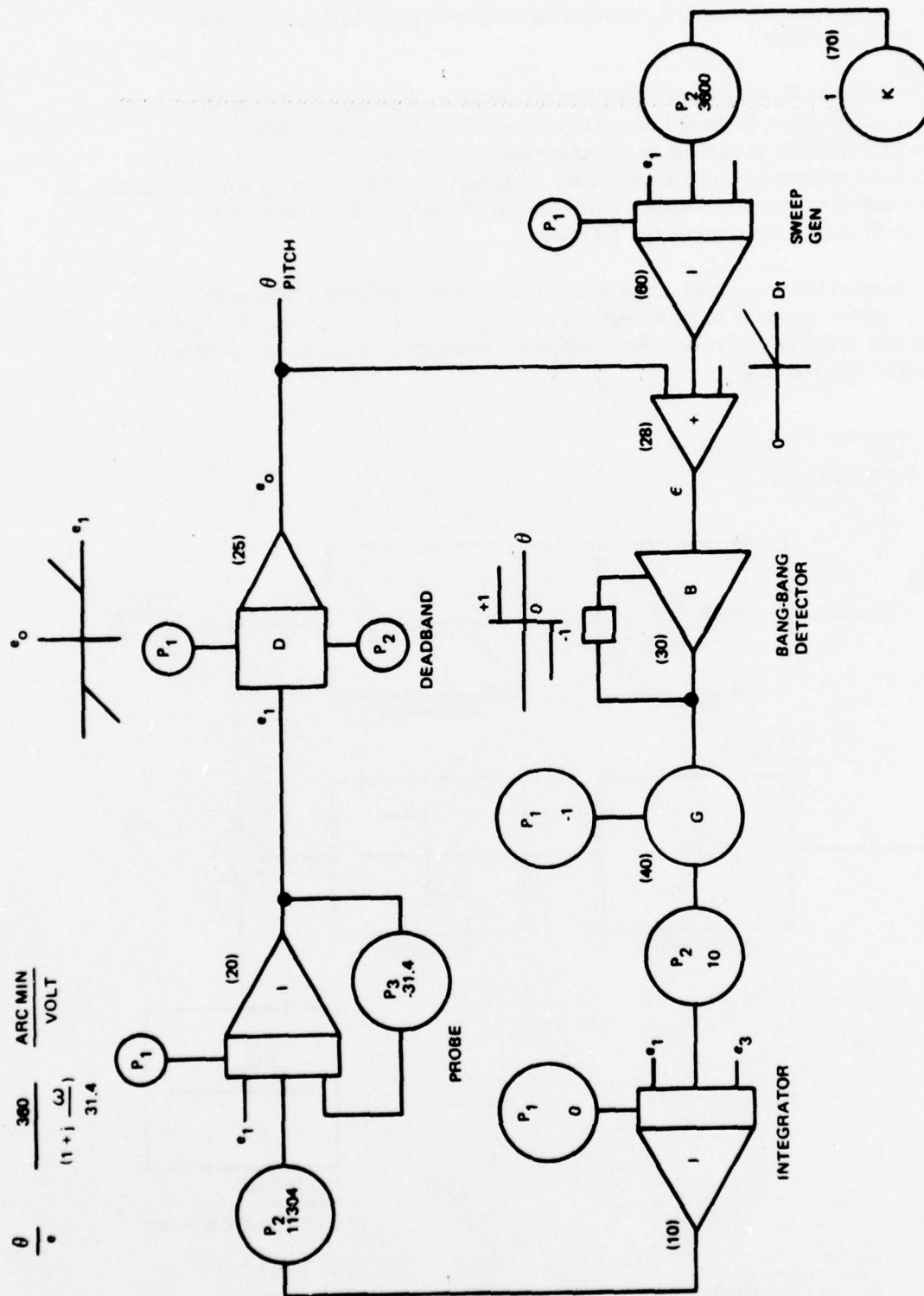


Figure 143. COMPUTER SIMULATION

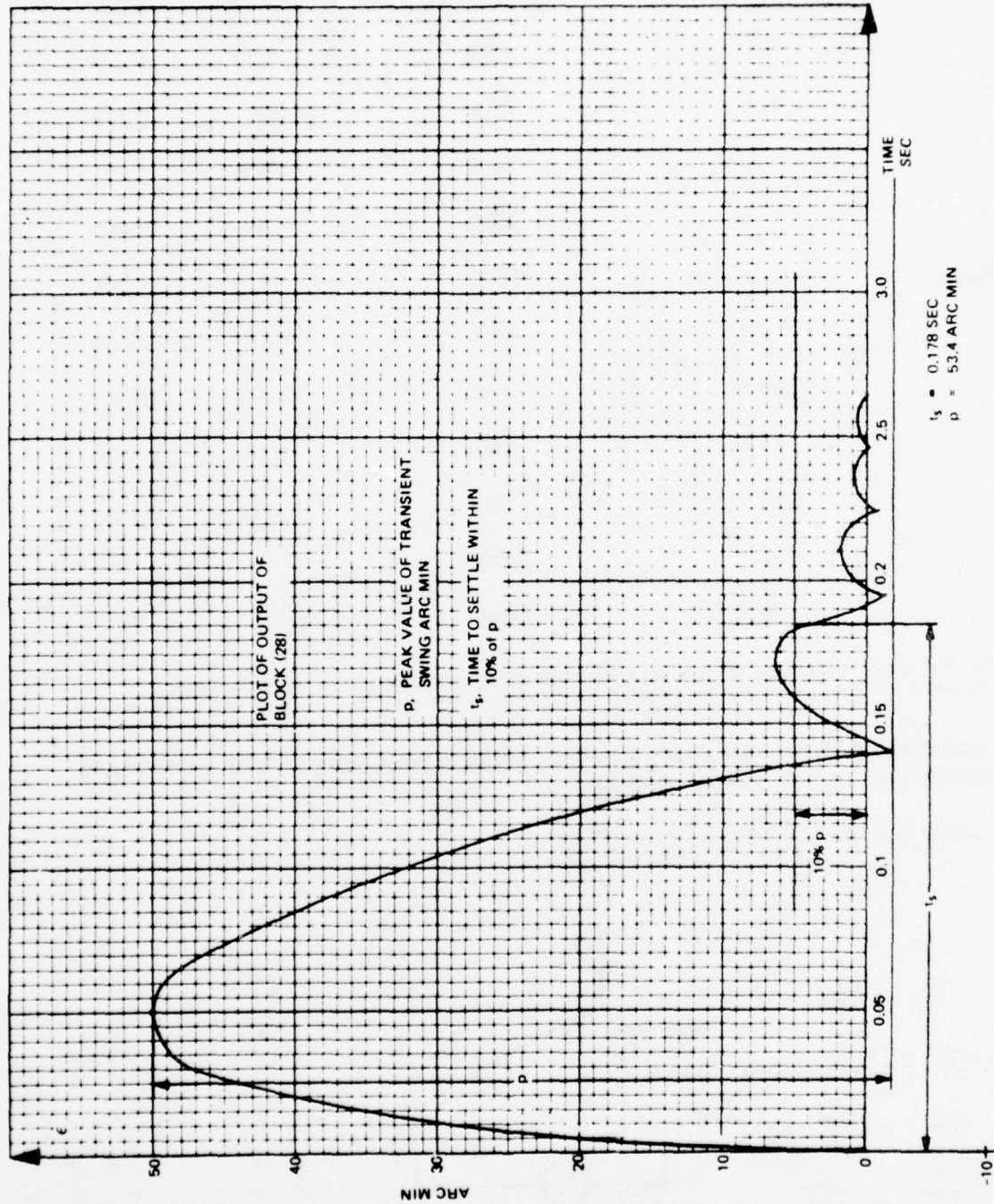


Figure 144. ERROR PLOT FOR SWEEP OF 2700 ARC-MIN/SEC DEADBAND OF ± 6 ARC-MIN

Table 30. SIMULATION RESULTS

CASE	INITIAL CONDITIONS	SWEEP RATE ARC MIN/SEC	p	t _s
	DEADBAND ARC MIN		ARC MIN	SEC
1	± 6	2700	53.4	0.178
2	± 3	2700	50	0.174
3	± 1	2700	48.6	0.17
4	± 12	2700	59.6	0.185
5	± 12	1800	33	0.135
6	± 12	900	18.7	0.115
7	± 12	450	12.4	0.13
8	± 12	200	10.4	0.15
9	± 6	200	6.6	0.115
10	± 6	900	12	0.12
11	± 6	3600	120	—*

*did not settle; exceeded the rate at which the servo could catch up with the spot.

Development of Simulation. Figure 145 exhibits a model of probe using DYSIM, GE MARK II. Transfer function equation is stated as follows:

$$\text{Transfer function} = \frac{e_o}{e_i} = \frac{360}{(1 + j \frac{\omega}{31.4})}$$

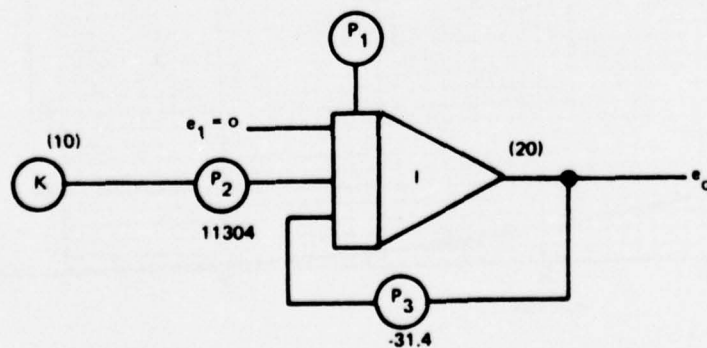


Figure 145. PROBE FRICTION LEVEL

Expanding the simulation to include a representation of the probe friction level is shown in figure 146.

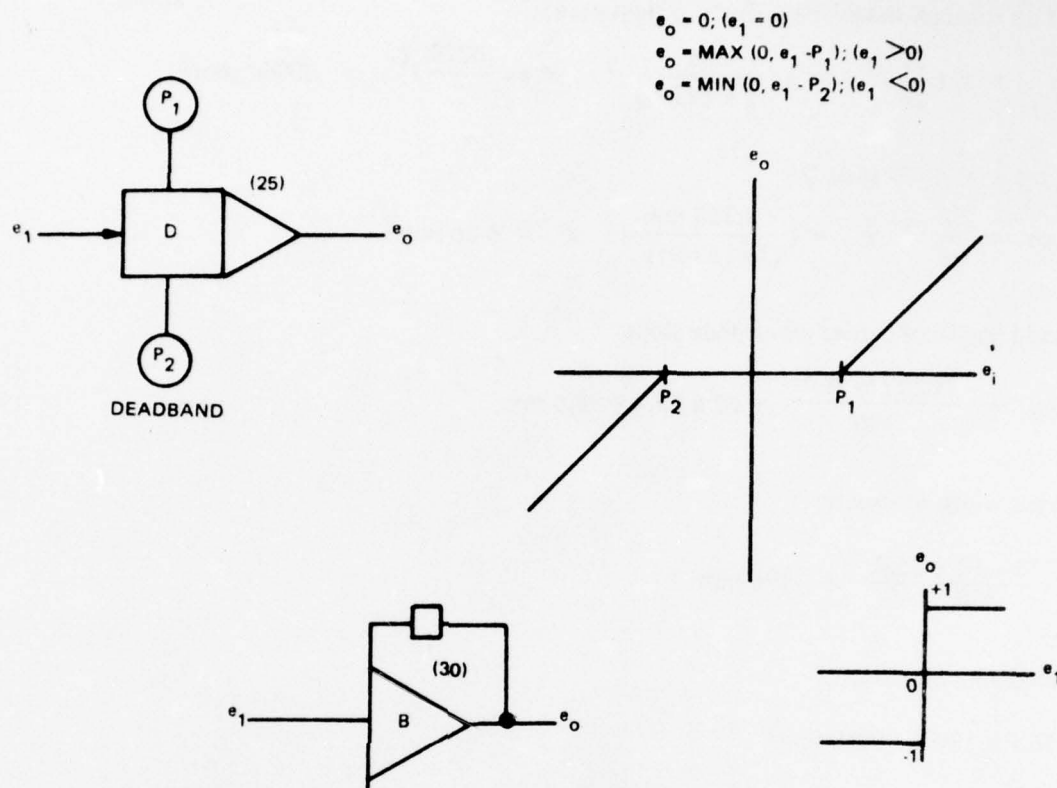


Figure 146. REPRESENTATION OF PROBE FRICTION LEVEL

Simulation of gantry velocity input is illustrated in figure 147.

NOTE

Assume max velocity of 1 rad/sec \approx 3600 arc min/sec.

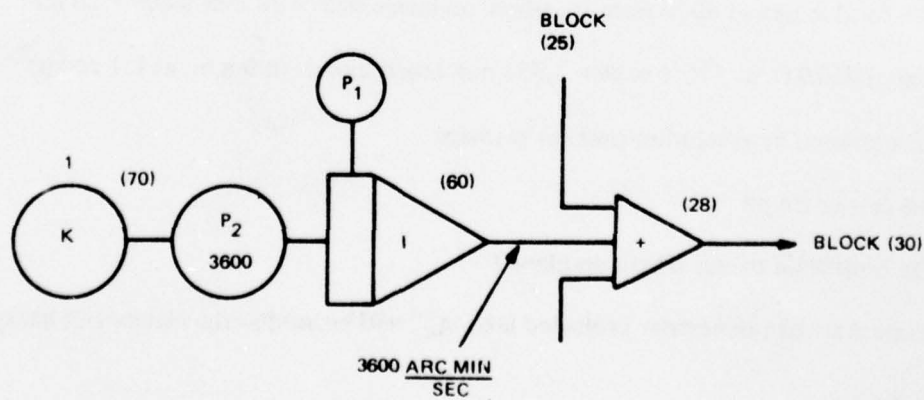


Figure 147. SIMULATION OF GANTRY VELOCITY INPUT

FLOLS Tracker Light-Emitting Source. Two sources of light for the FLOLS tracker detector were considered: one was a light-emitting diode; and the other a laser source, piped through fiber optics. The following calculations evaluate the two source signals, compared with the background signal, picked up through the probe (reference figure 148).

$$a' = \pi \left(\frac{f_6}{2\delta} \right)^2 = \pi \left(\frac{26}{2 \times 1134.5} \right)^2 = \pi \left(\frac{.0229}{2} \right)^2 = .00041 \text{ mm}^2$$

Projected a' at 4070 scale ft:

$$A_o = \left(\frac{S_6}{2\delta} \right)^2 \pi = \left(\frac{3,353 \text{ mm}}{(2)(1134.5)} \right)^2 \pi = 6.86 \text{ mm}^2$$

Projected length of carrier along glide slope:

$$A_c' = \frac{1020 \cos 86^\circ}{370} \times 12 \times 25.4 = 58.6 \text{ mm}$$

Projected width of carrier:

$$\frac{238 \times 12 \times 25.4}{370} = 196 \text{ mm}$$

Projected area of carrier:

$$58.6 \times 196 = 11489 \text{ mm}^2$$

Projected area of 1° quadrature detector is:

$$A_c'' = \left(\frac{\frac{1^\circ}{57.3} \times 3,353}{2} \right)^2 \pi = 2688 \text{ mm}^2$$

$\delta \equiv$ Angular resolution element = .33 cyc/min = 1134.5 cyc/rad

$f_6 \equiv$ Probe focal length at 4070 scale ft., where on image size of 30 mm $\Rightarrow 60^\circ = 26 \text{ mm}$

$S_6 \equiv$ Range at 4070 ft. at 370:1 scale = 3,353 mm (corresponds to 6 n.m. at 1:1 zoom)

$a' \equiv$ Is area covered by resolution element at image

$A_c \equiv$ Is the carrier length

$A_c' \equiv$ Is the projection of this length on plane P

Since A_c'' is smaller than the carrier projected area, A_c'' will be used as the element of background area.

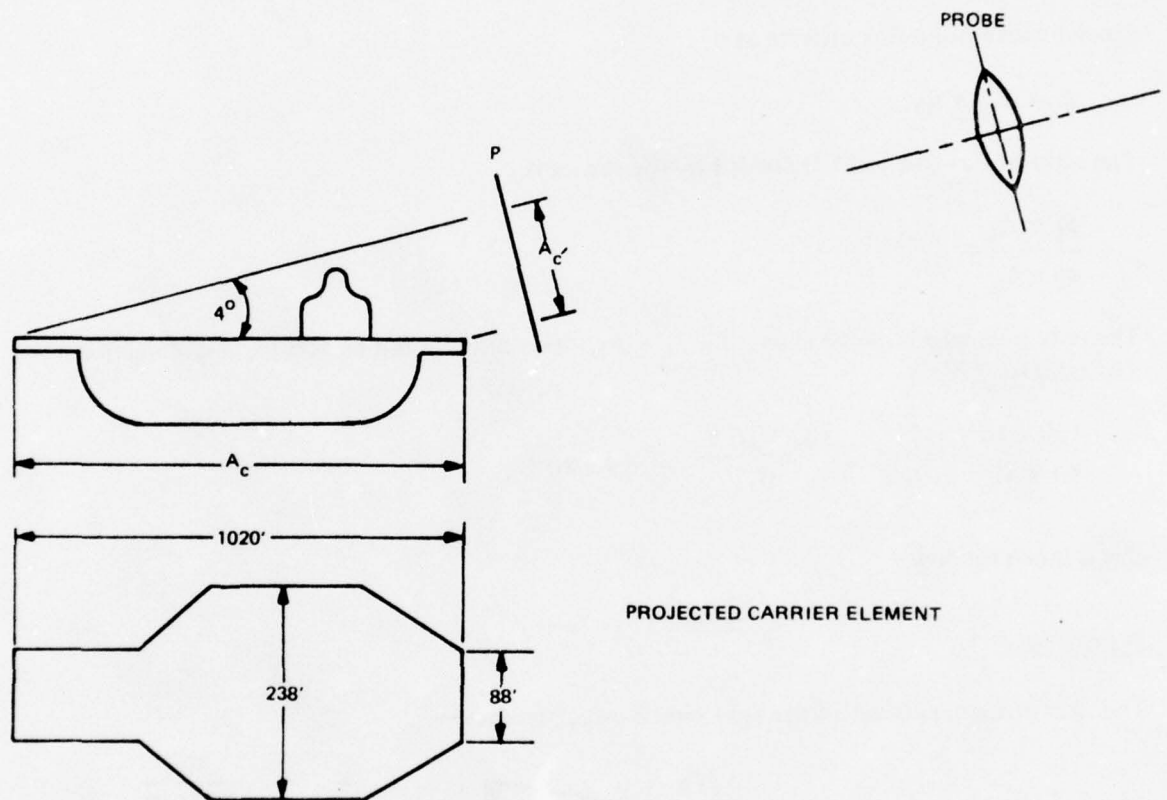
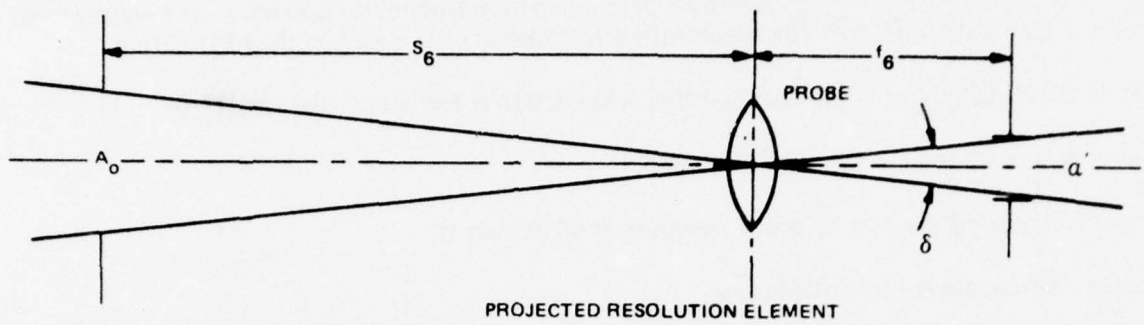


Figure 148. COMPARISON OF TWO LIGHT SOURCES

ϕ_c is the watts/ft²/sr due to integrated carrier illumination from 620 + 680 nm = .381 watts/ft²/sr = 4.1×10^{-6} watts/mm²/sr. This bandwidth is required to collect 85% of the LED output.

ϕ_L is the watts/cm²/sr of the light-emitting diode = .016 $\equiv 160 \times 10^{-6}$ watts/mm²/sr

A_L = area of LED = 2×10^{-3} cm² $\equiv .2$ mm²

r_D = solid angle picked up by probe aperture at 4070 scale ft.

Light emitting diode flux arriving at α'

$$\phi_L \times A_L \times r_D$$

Carrier background flux arriving at α'

$$\phi_c \times A_c'' \times r_D$$

The ratio of flux due to LED divided by the carrier is

$$\frac{\phi_L \times A_L}{\phi_c \times A_c''}$$

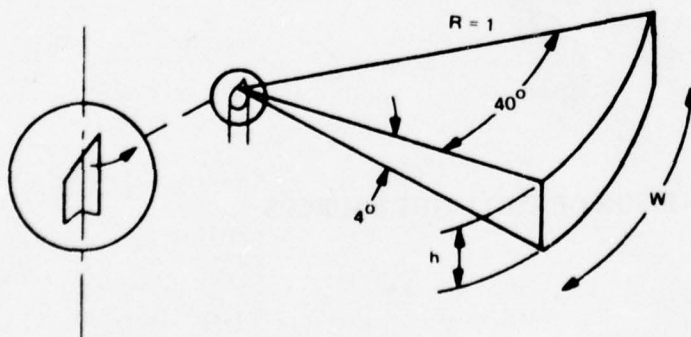
The only item which can be changed is $\phi_L \times A_L$. This ratio should be 100 for easy detection. The ratio for LED is:

$$\frac{160 \times 10^{-6} \times .2}{4.1 \times 10^{-6} \times 2688} = \frac{32 \times 10^{-6}}{.011} = 2.9 \times 10^{-3}$$

this is much too low.

Using a laser:

The laser output angle with fiber light pipe is calculated below:



$$W = \frac{40^\circ}{57.3^\circ/R}$$

$$h = \frac{4^\circ}{57.3^\circ/R}$$

$$sr = \frac{40 \times 4}{(57.3)^2} \approx .05$$

Let J = laser flux in watts

$$K_s = \text{laser output watts/sr} = \frac{J}{.05} = 20J$$

Using the previously stated criteria, the ratio of beacon watts/sr should be 100 times the carrier watts/sr and choosing an 8 nm band filter located at 632.8 nm which is the helium-neon wavelength. This gives a carrier watts/sr of $.419 \times 10^{-6}$ watts/mm²/sr. This width collects 100% of the laser output.

$$100 = \frac{K_s}{\phi_c \times A_c} = \frac{20J}{.419 \times 10^{-6} \times 2688} = .0178 \times 10^6 J$$

$$J = \frac{100}{.0178 \times 10^6} = 5.63 \times 10^{-3} \text{ watts}$$

Small, economic lasers exist with 3×10^{-3} watt CW output. Since this is not quite enough with losses which are estimated at 50%, additional refinement will be done during the design to decrease the required 5.63 milliwatts. It will optimize the detection circuits so that less than 100:1 is required: use a smaller bandwidth than 8 nm; use a more expensive but higher power laser; combine several 3 mw lasers; or decrease acquisition range.

BACKGROUND IMAGE GENERATOR.

The basic background image generator outlined in section 5 of this report has been expanded in order to provide aircraft altitude and velocity visual cues in the seascape imagery, in addition to the heading and attitude cues. Two approaches employing the basic flying spot scanner have been analyzed; the recommended raster reset method and the alternate X-Y motion table method. Both BIG systems employ raster size modulation to simulate altitude changes, as outlined in section 547. The basic difference between raster reset and the X-Y motion table method is in the approach used to achieve velocity cues.

The raster reset method employs a 5-inch fiber optic faceplate cathode ray tube which covers a seascape image film plate made up of four identical images in a square two by two pattern. The velocity cue is created by moving the BIG raster across the CRT until the edge of the tube is reached. At this point, the raster is reset to a duplicate pattern on a different image and the flight is allowed to continue.

The X-Y table method employs a 7-inch cathode ray tube in conjunction with an imaging lens system and an 18-inch by 18-inch seascape image film plate. The film plate is moved by an X-Y table in order to give relative velocity between the aircraft and seascape.

Raster Reset. The system studied for use is shown in figure 149. The system consists of a flying spot scanner having a fiber-optic faceplate, a contact repeat pattern film plate, collecting optics, video processor, CRT deflection drive system, linearity correction network, and the sweep generation system made up of the computer interface, DARC, X-Y drive digital smoother and summer.

Cathode Ray Tube. The advantages of a fiber optics faceplate scanner tube stem from the nature of the fiber optics used in the faceplate. The tube is unique, since the spot size obtainable on the faceplate surface is 20 microns, or about 0.008 inches. The fibers themselves are of 7-micron diameter, such that approximately 9 fibers are used to cover any one spot, thus minimizing phosphor noise due to fiber breakage.

A second advantage of the fiber optics faceplate cathode ray tube stems from the fact that the interior of the faceplate may be optically ground with a radius to eliminate the normal pincushion effects of a flat-face cathode ray tube. Since the primary problem in implementing

the raster reset technique of background image generation was a resultant jump due to the inability to completely eliminate the pincushion effects, the expected jump of 0.024 inches, given in section 5, would be considerably reduced⁴⁸.

Discussions have been held with the suppliers of the fiber-optics faceplates used by Litton Corporation in the manufacturing of the tube L-4199. Due to manufacturing techniques of the fiber-optics, the pincushion effects are changed to a slight barrel effect of 0.004 inches over a centrally located circle having a 2-inch diameter and a maximum of 0.010 to 0.015 inches over the entire 4.5-inch faceplate. Since this effect is concentric with the center of the tube, normal techniques used in linearity correction are expected to reduce these effects to less than 0.001 inch, or one spot size, over the useful area of the tube.

Further, since the techniques that will be used to reduce or eliminate the noise effects which effectively increase the spot size as the distance from the nadir is increased, the picture jitter due to reset is expected to be unnoticeable and should effectively be masked by the pictorial noise of the system.

A third advantage is the ability to use contact film on the cathode ray tube face. Discussion with the manufacturer, Litton Corporation, discloses that the effective $f/\text{no.}$ for the direct contact fiber optics faceplate is $f/0.7$. This extremely low $f/\text{no.}$, combined with the higher beam loading allowed in this particular tube design, for a given beam size, indicates that the expected SNR will be 40 db out of the complete system, using the techniques described in section 5.

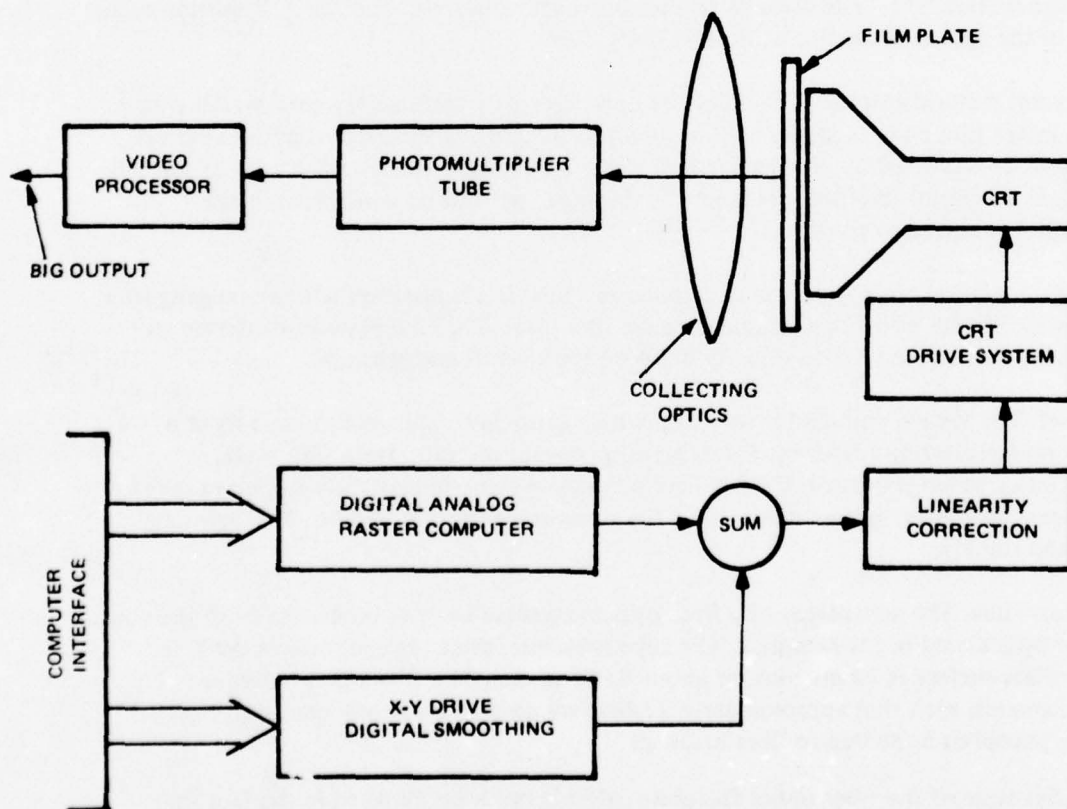


Figure 149. RASTER RESET BIG BLOCK DIAGRAM

Film Plate. The seascape film plate, figure 150, contains four, identical seascape images obtained from a high precision step and repeat printing process. The patterns will be overlapped in order to smoothly integrate the wave pattern in the area of the film junctions. The picture area to be scanned is of the same magnitude described in section 5 of this report, or 3,775 feet per side of each seascape image. The film is half the size, as outlined in section 5⁴⁹, but due to the superior optical efficiency of the fiberoptic faceplate over the CRT, compared to the efficiency of a lens which was required for the FSS system, the beam current can be reduced and hence spot size will also be half the size outlined in section 5. Therefore, the criteria for the resultant television picture quality is the same as analyzed in section 5 of this report. No deviation is expected from the MTF curves and signal-to-noise derived from the original system, except a slightly improved SNR of 3 db due to the increased optical efficiency. It should be clearly understood that the raster reset is concerned only with the seascape image background. Any anomalies present due to offset jitter or MTF response, if present, would not be a part of the target, target inset, or the wake inset.

The film plate will contain registration marks on the outer edge of the picture for alignment purposes. The film plate will not include the nadir locus perimeter outline included in the figure as a broken line. This is an invisible boundary which, when intersected by the aircraft nadir, will cause a raster reset to an identical image pattern on one of the other three film images. The reset will be controlled by the computer and will occur during the flying spot scanner vertical retrace period. It is therefore possible to fly over a seascape of unbounded size and almost unlimited velocity range. For example, if the aircraft is flying along with an airspeed of 300 knots (500 ft/sec), any motion between TV fields would be 8-2/3 ft. Since techniques are being developed to increase the rate of digital integration, the expected motion of the reset due to digital instability will be less than one resolution element. The methods of digital integration, or digital smoothing, use the horizontal retrace

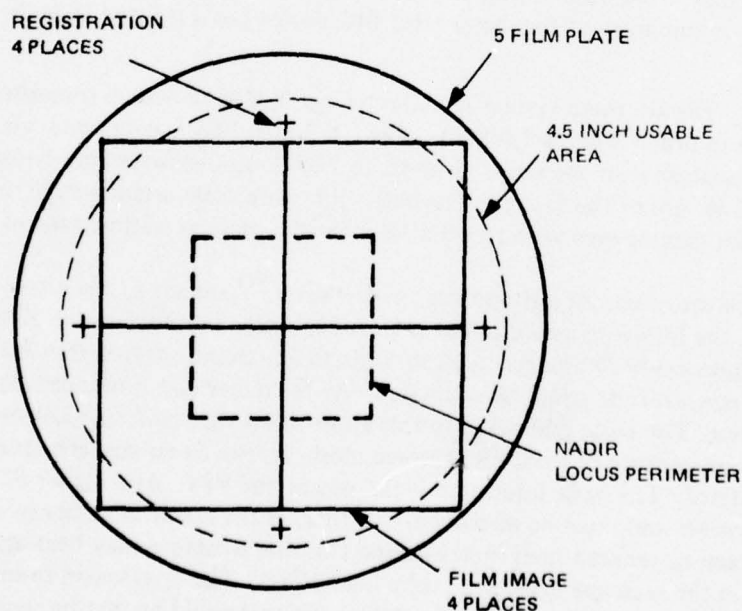


Figure 150. BIG FILM PLATE

time of the scanner to effect a slight forward motion of the resultant raster to eliminate (or lessen) the effect of the digital stepping as would usually be found in digital motion systems, particularly with simulation systems having update rates of only 20 cycles per second or less. The use of high speed counters, digital-to-analog converters, and fast settling yokes allow sufficient time during the 7- μ sec retrace time for adequate forward motion to be obtained and settled out since the expected forward motion will be very small between lines.

During the raster reset, which occurs during vertical retrace time, the intersymbol shift; that is, the actual motion caused by the difference in the output of the computer and the time interval of the next vertical retrace would be retained and added to the reset value to eliminate any additional offset due to the time differential from computer output to vertical retrace timing.

Thus on an approach to the carrier, when the pilot's sight is concentrated on the FLOLS, the carrier, wake, horizon, and sea merge would appear as steady as the entire servo system would allow. It should also be stressed that the reset, when it does appear, is at a random time base occurring from 6 to 12 seconds apart, depending on aircraft speed. The drive algorithm will be such that no raster reset will occur during the last 1/2 mile of the carrier approach.

Collecting Optics. The collecting optics will be designed to make most effective use of the f/0.7 lens of the cathode ray tube. The collecting optics housing shall form a light tight package connecting the CRT faceplate to the photomultiplier cathode, thus eliminating the need for the large light tight housing of the FSS system.

DARC. The digital-analog raster computer, outlined in section 5, will be expanded to include the X-Y drive and digital smoothing circuits required to impart the velocity cues. This technology is presently being used in SPD's synthetic terrain generator and, therefore, is readily available. A summary of the raster reset BIG design goals is listed in table 31.

X-Y Motion Table. The alternate system includes a large X-Y table which translates the seascape film plate in order to impart velocity cues. A 7-inch FSS is employed which allows altitude simulation over the range of 68 ft. to 720 ft. and velocity simulation of up to 400 kts within 1 1/4 nm of the carrier. The basic film plate scale factor was reduced in order to provide sufficient gaming area with an 18 x 18 inch film plate as outlined below.

Altitude Cues. The discussion of altitude cues in section 5⁵⁰ applies to the raster reset method, however, the following analysis was required in order to optimize the X-Y table application. The previously referenced section 5 discussion demonstrated that by scaling of the FSS raster size, altitude could be simulated. As the raster size is reduced, lower altitude is simulated. The basic limitation to this approach is the resolution achieved because of the small percentage of total FSS surface used. As the raster size is increased, higher altitudes are simulated. The basic limitation is the size of the FSS. At a higher altitude, more seascape is visible and must be displayed. Further, as the raster increases in size, the distance between raster scan lines increases and this line structure may beat against the wave pattern in the seascape causing a moire beat effect. The conclusion found in section 5 was that for altitudes above 316 ft., the resolution analysis could be met or exceeded and that performance below 316 ft. was reasonable.

Table 31. RASTER RESET BIG DESIGN GOALS

Film Scale Factor	22,000:1
Altitude Cues	760' to Deck
Velocity Cues	Up to 400 Knots
Gaming Radius	Unlimited
BIG MTF @ 316 ft.	.70
FSS	5" - 4.5" Usable
Visibility to Horizon	Up to 5°
CRT L 4199 (Litton Corporation)	
· Spot Size	.0008 inches
· Fiber Size	.0003 inches
· Deflection Angle	40° total
· CRT Linearity (inside radius)	.004 inches over center 2" of tube
	.015 inches over usable 4.5" of tube
· CRT + Correction	
Circuits	
Linearity	< .001 inches over usable 4.5" of tube
· Deflection Yoke	
Linearity	.1% guaranteed
· Correct Deflection	
Yoke Linearity	.02% or .001 inches over useful tube area
· RSS Error Over	
Useful Tube Surface	0.0014" or less than 2 spot sizes

This analysis extends the performance to altitudes below 316 ft. On final approach at altitudes below 300 ft., the analysis is restricted to a flight profile where roll never exceeds 10° and there is no pitch down. A 7-inch FSS will be used in place of the 5-inch FSS. The original analysis showed that at 158 ft., the raster was half the size used at 316 ft. This analysis, for convenience of rounding off numbers, will set the raster size at 150 ft., equal to the size at 316 ft. in the original analysis. One further difference relates to the visibility to the horizon. The original analysis restricted visibility to angles up to 10° below the horizon. The present analysis will vary the visibility angle to the horizon in accordance with figure 151.

This figure shows that at 150 ft. altitude, visibility to within 7° of the horizon is desired. Setting the system scale factor for the above condition, we have:

$$R = \frac{h}{\tan \sigma}$$

where R = range to visibility limit

h = aircraft altitude

σ = seascape visibility limit below horizon

$$R = \frac{150}{\tan 7^\circ} = 1221.7 \text{ ft.}$$

Thus, FSS scaling will be 1333.3 ft. = 2 inches or 1 inch = 666.7 ft.

Applying the MTF analysis developed in section 5, the MTF analysis at the nadir for the 150 ft. altitude is:

Given: 6 in. usable FSS tube diameter

$$R = 3 \text{ in.}$$

Scale on FSS is 1 in. = 666.7 ft. real world

1 mm = 26.25 ft. on the FSS

Thus: 150 ft. = 5.71 mm scaled

$$R_{n15} = 2 h_o \tan \left(\frac{\theta}{2} \right) = 2 \times 5.71 \tan \left(\frac{.25}{2} \right) = .02491 \text{ mm/Lp}$$

$$R_{n15} = 40.14 \text{ Lp/mm}$$

Referring to figure 04 of this report, the greatest angle of depression occurs at -22° from the horizon for the 15 arc-min requirement. Referring to figure 151, $R_x = 7$ for 68° from nadir.

Thus: $R_x = 7$

$$R_{C15} = \frac{R_{n15}}{R_x} = \frac{40.14}{7} = 5.7 \text{ Lp/mm}$$

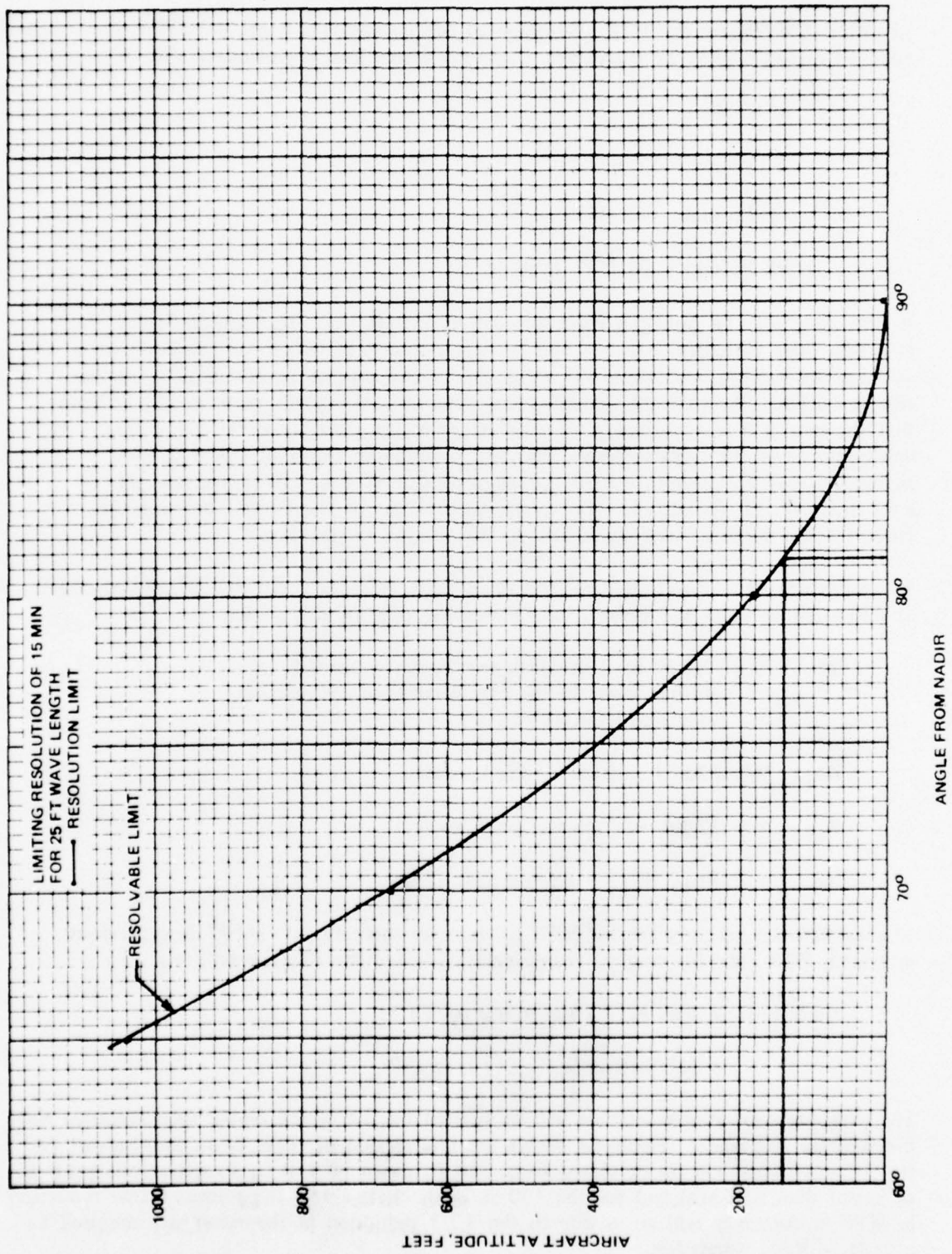


Figure 151. ANGLE FROM NADIR VS. AIRCRAFT ALTITUDE

Referring to figure 62, the FSS MTF is .82 at 5.7 Lp/mm.

In order to complete the MTF evaluation of the background image generator, the lens and film performance must be evaluated. The lens design goal performance will be:

$$M = .5X$$

$$8 \text{ Lp/mm} - .85 \text{ MTF}$$

$$12 \text{ Lp/mm} - .70 \text{ MTF}$$

$$85 \text{ Lp/mm} - .05 \text{ MTF limiting}$$

A film plate may be obtained from Simulation System, Inc., Huntington Valley, Pa., at a film scale factor of 1 in. = 1333 ft. or a nominal 16,000:1 scale factor with a 100 Lp/mm limiting resolution. If we assume a straight-line approximation for the film resolution, the resultant film plus lens performance is given in figure 152. Note that the lens is used to magnify the film image at the CRT faceplate rather than demagnify as in the original design analysis. Combining the film, lens and FSS performance at 5.7 Lp/mm we get a total generator MTF of .70 worst case for level flight at 150 ft. altitude. Following the analysis of the aircraft crossing the fantail of the carrier, found in section 5, the analysis is as follows:

At an altitude equal to 10 ft. over the flight deck, $h_e = 63 + 10 + 8 \text{ ft.}$, pitch = $+5^\circ$ at this altitude, when the aircraft passes over the edge of the carrier.

$$h_e = (\text{height of flight deck over water} + \text{aircraft altitude over the deck} + \text{distance of eye height over wheels}) = 81 \text{ ft.}$$

$$R_{n15} = 150/81 \times 40.1 = 74.3 \text{ Lp/mm}$$

$$R_{x15} = 12 \text{ for } +5^\circ \text{ aircraft pitch angle}$$

$$R_C = R_{n15}/R_{x15} = 6.2 \text{ Lp/mm}$$

or a background image generator MTF of .65* which represents a 14% improvement in system MTF over the original design analysis under the above conditions.

$$\begin{aligned} *.65 \text{ MTF} &= \text{FSS MTF (film + lens MTF)} \\ &= .81 \text{ (reference figure 62)} \times .80 \end{aligned}$$

The maximum, achievable altitude will be limited by the 6-inch usable tube diameter and the selected film scale. Figure 68 shows the intersection of these two conditions at 720 ft. Thus, altitude will be simulated from 720 ft. down to 150 ft. at resolutions equal to or better than that analyzed for the 150 ft. case. Below 150 ft., a small (10%) reduction in MTF performance will occur due to the 2.2:1 reduction in the raster size required by a 68-ft. altitude simulation.

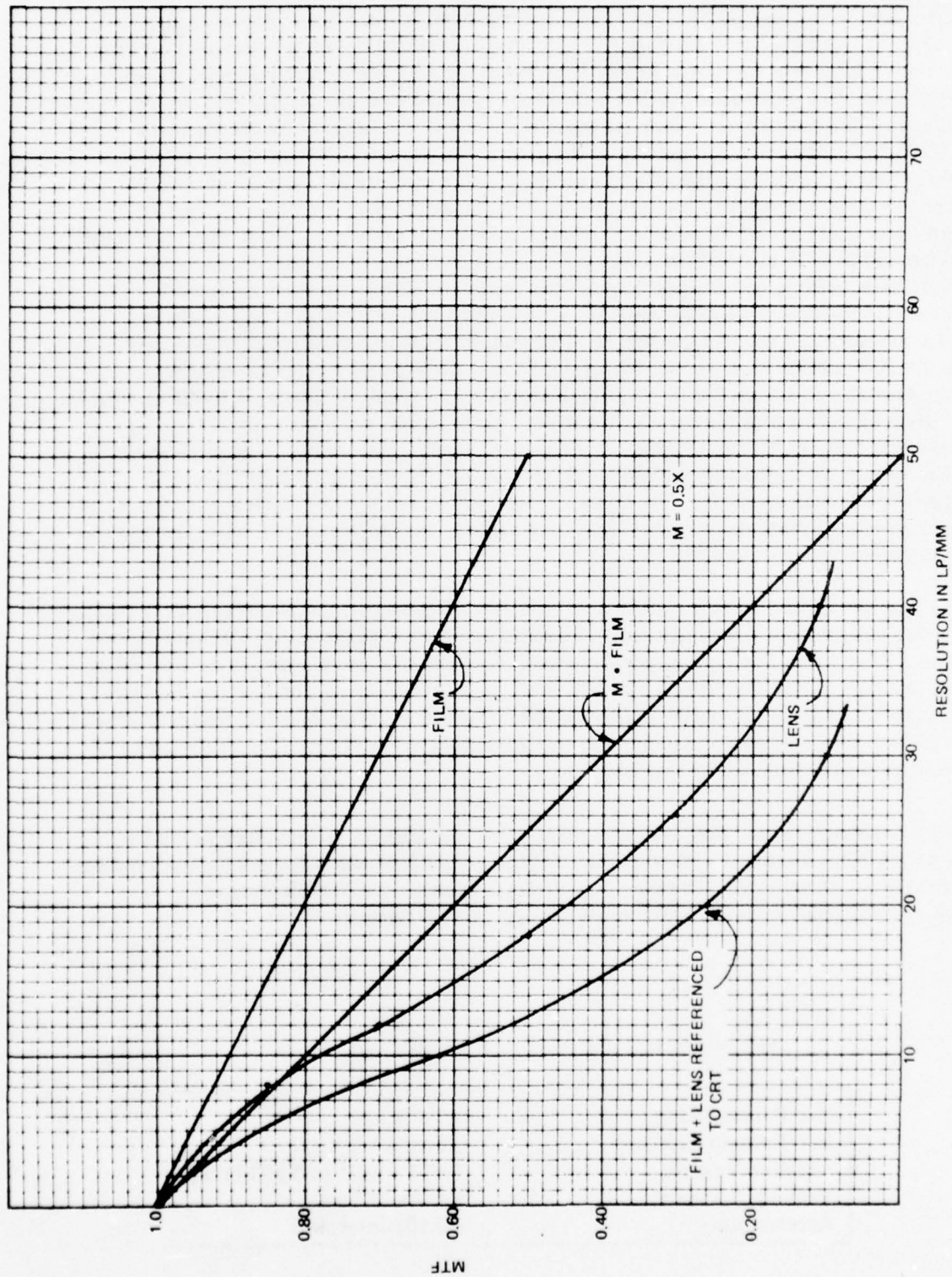


Figure 152. RESOLUTION OF FILM REFERENCED TO CRT FACE

Velocity Cues. An expanded film plate mounted on an X-Y motion table will allow realistic velocity cues in the immediate area of the aircraft carrier. A film scale factor of 1 inch = 1,333 feet was established Altitude Cues paragraph. Limiting the usable film plate to 18 x 18 inches, the plate would cover 23,994 x 23,994 ft. or 3.95 x 3.95 nautical miles. It will be established that the carrier position will always coincide with a point 2,000 ft. to the right of the film plate center, thus allowing sufficient seascape imagery for the standard NATOPS flight pattern in the vicinity of the carrier. See figure 153. No relative motion exists between the ship and the seascape except that the carrier will be capable of 360° heading changes in respect to the seascape. In order to insure that the 3-inch FSS raster radius never goes beyond the edge of the film, the X-Y motion of the 18-inch film plate must be restricted to ±7.5 inches. This allows the seascape to remain in the background such that attitude, heading and altitude cues are still provided. Thus, whenever the aircraft is within 1.6 nautical miles of the seascape center, some velocity cue will exist. Outside the 1.6 nm range, no velocity cue will be displayed. In order to simulate realistic velocity cues, the X-Y motion must be capable of duplicating the 4-g acceleration experienced during the catapult launch mode. The film plate must be capable of moving 0.130 inches within 1.57 seconds required by the launch. In addition to the launch mode, the aircraft will fly at velocities between 100 and 400 knots. Because of the limited size of the seascape image, a buffer region will be needed in order to accelerate the film plate from zero velocity to the properly scaled velocity. The seascape image will be replaced by the seamerger (constant gray tone) video during the transition from true velocity to zero velocity which will eliminate any potential false velocity cues.

The maximum velocity of 400 knots would require 1.45 inches of film plate in order to accelerate from 0 to 400 knots at 4 g acceleration. The transition from 0 to the scaled 400 knots would require 5.25 seconds. Thus, whenever the aircraft is within 6.05 inches or 1.33 nautical miles of the seascape center, the properly scaled velocity will be displayed. The X-Y motion table will be driven with velocity servos which incorporate position encoders which feed positional data back to the computer controlling the velocity inputs to the system. The performance of the X-Y motion system is shown in table 32.

Based on past experience, with large film plate flying spot scanner systems such as the F4 landmass system, it is reasonable to expect that the AWAVS system will meet the performance required in the above table. However, any effects to increase the film plate size will require further analysis in the servo design and system packaging areas.

Table 32. X-Y TABLE PERFORMANCE

X-Y Position Range	±7.5 in.
X-Y Position Accuracy	±0.10%
Absolute Velocity	0.533×10^{-3} to 0.533 in/sec
Velocity Accuracy	±1.0%
Acceleration	±0.105 in/sec/sec

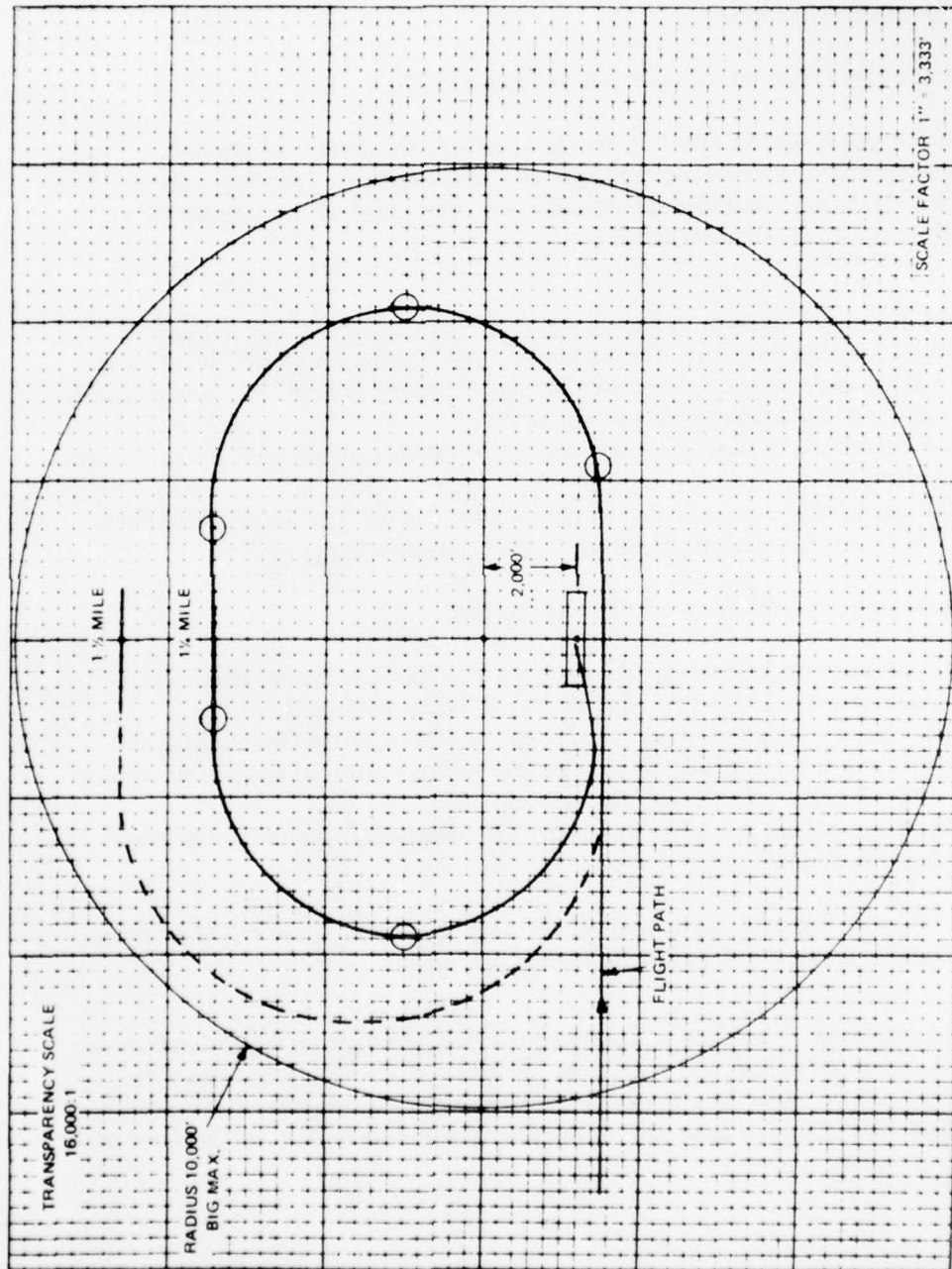


Figure 153. CARRIER CIRCLING PATTERN

WAKE IMAGE GENERATION.

Three categories of Wake Image Generation (WIG) were analyzed to determine the appropriate method for implementing the WIG system. These are:

1. Analog Method
2. Digital Method
3. Flying Spot Scanner

The Analog Method was rejected for the following reasons:

1. There was no visible way to generate a realistic appearance of texture. To implement texture required special processing tied to the raster rates. This means each new line rate requires incorporating new logic to create the texture for the new formats.
2. The technique requires designing a high speed analog processor (similar to Singer's analog Synthetic Terrain Generator). The processor circuits must be designed constrained to the raster timing. Thus, any line rate changes require redesign of the analog processor hardware.
3. The texture, as artificial as it will appear, is not changeable by manual/operator adjustments.
4. The analog system of calculations would result in registration errors of from 2° to 4° for the circuitry involved in its implementation.

The Digital Method was rejected for the following reasons:

1. This requires designing/adapting a special high speed processor that *requires much redesign for each line rate to be implemented.*
2. The texture simulation would require use of Digital Image Generator (DIG) techniques to create a texture that suffers from an artificial appearance similar to that resulting with the analog method.
3. This design would result in "staircasing" in the display. This would be most distracting to the pilot.

The Flying Spot Scanner method shows promise of being applicable to the WIG simulation implementation and is pursued more in the following paragraphs.

Method of Implementation. The wake image generator (WIG) will generate video which the background image projector (BIP) will project on the screen as a ship's wake. The video output of the WIG will be added to the output of the background image generator (BIG), processed by the visibility effects generator to provide appropriate haze at the horizon, and sent to the BIP.

The WIG employs a photographic transparency showing a wake in a straight-down projection. The transparency is opaque outside the boundaries of the wake. It is mounted on the fiber-optic faceplate of a flying-spot scanner (FSS) identical to that of the BIG. Proper drive of the FSS sweeps involves two tasks: (1) generation of a raster which shows the wake in correct perspective, and (2) registration of wake with the target image, to correct for accumulated system errors.

The texture of the attached, electronically generated wake is a fixed presentation, which is integral with the wake image film plate. While the texture content may be changed by changing the wake image film plate, the wake texture in a given flight configuration will remain almost constant, and will be fixed in relation to the aircraft carrier. That is, the wake itself, including the wake texture, will follow the ship. Thus, if the ship is moving at thirty knots, its wake and wake texture will also be moving at thirty knots. While some of the texture content will be modified by the technique involved in range setting, the majority of the wake scene's texture will be moving at the same rate of speed as the ship's.

In considering the first task, we note that the wake transparency represents a scaling of a portion of the sea plane. In this plane, there is a moving point which corresponds at each instant to the point being scanned on the oil film of the BIP Eidophor at that instant. The position on the BIP raster plane is a simply described function of time, since the sweeps are linear. From this position, the corresponding position on the screen can be calculated using the lens mapping. The direction cosines of the line from the eyepoint to the point on the screen can now be found. Application of a rotation transformation to account for the attitude of the simulated aircraft; and projection of the resulting direction line onto a plane an altitude h below, where h is the simulated altitude can also be accomplished. As a result, for a given time, the position of the desired, moving point on the sea plane, in coordinates with the origin at the simulated aircraft nadir is obtained.

The WIG raster should become active when this moving point enters the area of the sea plane covered by the WIG. The desired point on the WIG raster is obtained by adding a vector to the coordinates of this calculated point to shift the origin to the center of the area of the sea plane represented by the WIG FSS, and by multiplying by the appropriate scale factor. For both x and y an off-line fit to the desired function of time is made for a polynomial which is a function of generated, fast and slow sweep ramps. The coefficients of these polynomials are tabulated as a function of pitch, roll, heading, altitude, range to carrier, and azimuth of line of sight to the carrier. For each video frame, the main frame computer will interpolate from those tables and output coefficients to a DARC which will develop in real time, voltage analogs of the polynomials that were fitted off line. These voltage analogs will be a sufficient approximation to the x and y coordinates of the theoretical desired point on the FSS at a given instant, and they will be amplified to drive the FSS deflection coils.

Figure 154 shows the relationship of the areas of BIG and WIG coverage in the sea plane. The large circle has a radius of 6 nm and is centered at nadir and represents the limit within which a wake will be shown. The small circle represents the 3780 ft diameter circle covered by the BIG, the intermediate diameter circle represents the coverage of the WIG, and the trapezoid within this circle represents the wake. This circle can be moved anywhere within the 6 nm radius circle by appropriate alteration of the raster by the DARC.

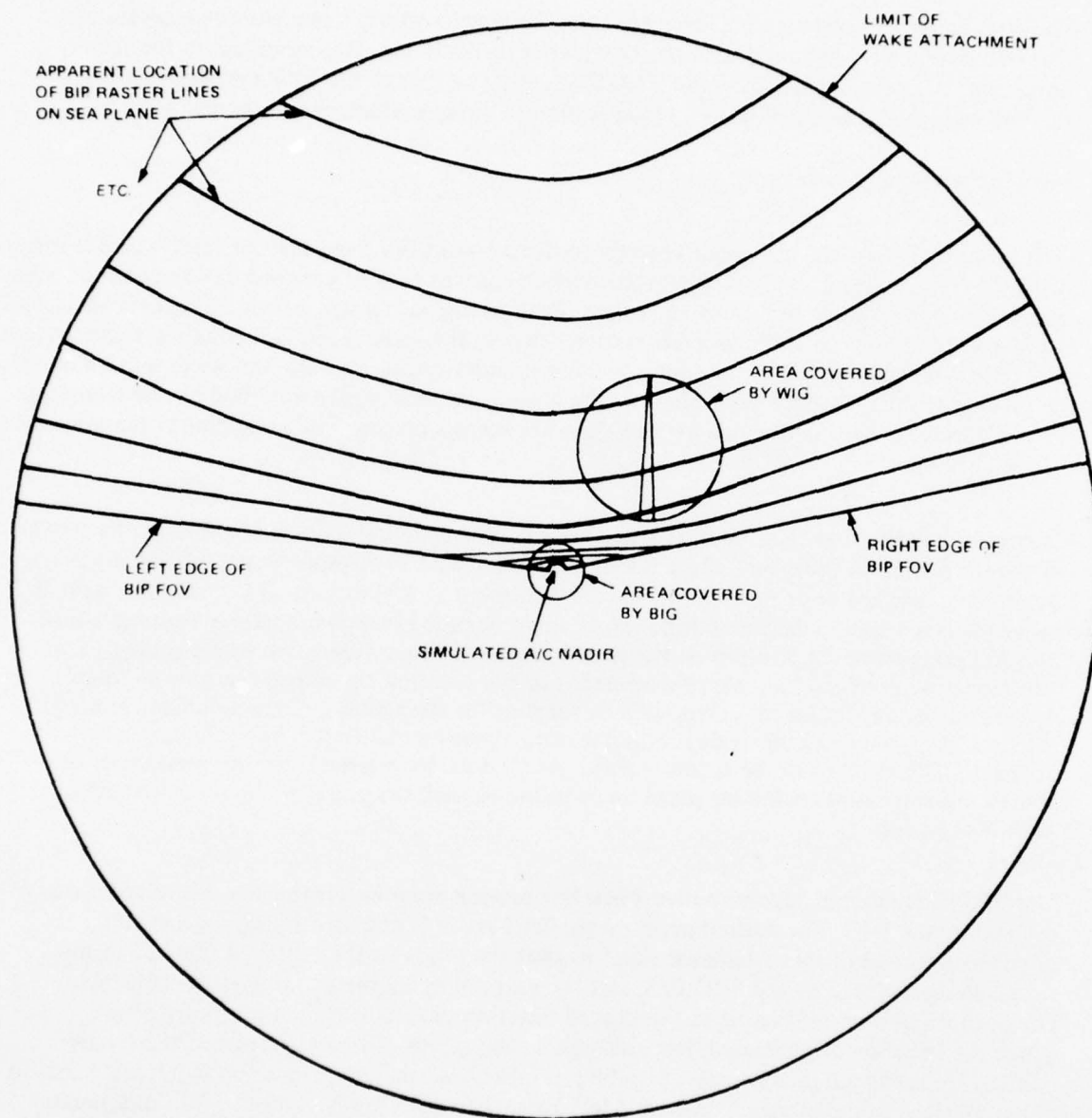


Figure 154. BIG AND WIG COVERAGE IN SEA PLANE

At 6 nm, the spot velocities on the WIG FSS are excessive (approximately 2.5 inches per μsec). This can be reduced by changing the scale factor of the WIG when the most-distant portion of the wake is at a range greater than 2 nm. By so doing, the maximum spot velocity can be reduced by a factor of three. The size of the effective portion of the wake transparency is changed in proportion to the raster scaling, so that the same real-world wake length is represented. This is done by gating off the WIG video on command from comparators sensing the CRT sweep along the axis parallel to the length of the wake. Figure 155 shows how this is done. For ranges up to 2 nm, the comparator levels are set at A and A'. At 2 nm the comparator levels shift continuously, reaching B and B' at 6 nm. The length of the effective portion of the wake transparency, (i.e., the distance between the comparator levels is inversely proportional to range from 2 to 6 nm). The actual, transmitting portion of the wake transparency extends from A to B'. Note that the width at the head and tail of the effective portion of the transparency is scaled in proportion to the length. Since the center of the effective portion of the wake transparency shifts as the comparator level moves, there must be an additive raster shift as well as a multiplicative scale change.

At the closer ranges, where detailed structure within the wake is apparent, the scale factor is constant. When the scale factor begins to change, the wake will be far enough away so that only the perspective of the wake outline will be important. When the most distant portion of the wake is at 2 nm, the nearest portion of a 1.5-nm. wake is no closer than 0.5 nm.

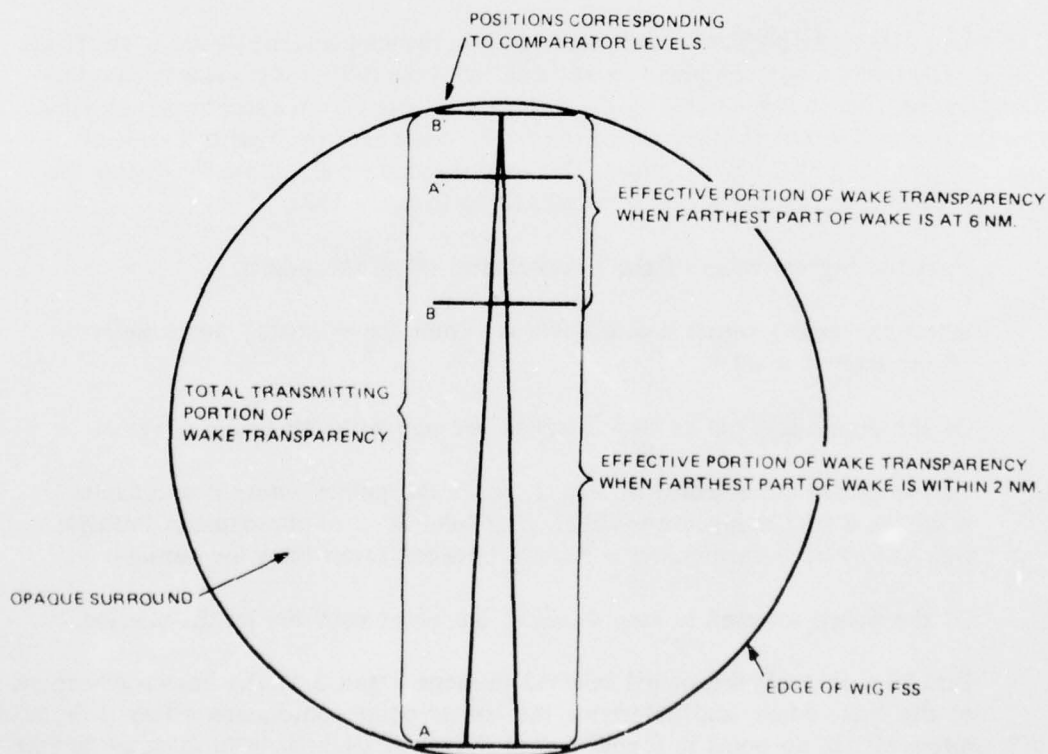


Figure 155. WAKE TRANSPARENCY

By altering the comparator level at the tail end of the wake, it will be possible to simulate shorter wake lengths than the maximum of 1.5 nm. However, the shorter wake will have a sharply clipped tail, instead of ending in a fade-out transition. Of course, this clipping will occur when scale change is being implemented to reduce FSS spot velocity; but in that case, the wake will be at such a range that the effect is minimally noticeable.

The task of registration is most accurately accomplished if closed-loop error correction can be made. The scene keying camera (SKC) is essential for this since it views the wake attachment point (target image) with a raster synchronized with the BIP raster, which is the raster with which the wake is projected.

In the normal wake registration method, we will in effect plot points in the sea plane for the individual keying pulses from the SKC for an entire TV frame at the outline of the target image. This will be done by digitizing the sweeps generated by the DARC for driving the WIG FSS at a time determined by the keying pulse. The coordinates of these sweeps are referred to as the CRT axes of the WIG FSS. The wake transparency is aligned with these axes. The axis, along the wake length, is called the axis. These DARC sweeps will be generated over a larger area than necessary to cover the FSS, in order to provide digitizer acquisition over a range of wake registration error (subsequently the sweeps will be limited to the area covered by the CRT before going to the deflection amplifiers).

Figure 156 shows how those digitized points would plot in the sea plane in relation to the target image outline. The target image contains a short "stub" of wake (500 ft is the length currently under consideration), which is generated by the target image probe from a short wake actually painted on the model. The points at the tail of the "stub" wake have the highest x value of those points plotted from SKC keying pulses. This suggests a simple algorithm for finding the coordinates of the left, rear corner of the stub wake (refer to figure 157):

1. Find the highest value of the x-coordinates of all the points.
2. Select the points whose x-coordinate is within the estimated digitizing error of the highest x value.
3. Of the points selected in step 2, select the one with the lowest y value.
4. Of the points not selected in step 2, select the points whose x coordinate is within 8 of the highest x value. The value 8 is an approximate multiple (say twice) of the estimated x interval between raster lines for constant y.
5. Of the points selected in step 4, select the point with the lowest y value.
6. Pass lines through the points selected in steps 3 and 5 in the known directions of the wake edges, and determine the corner point coordinates where these points intersect. If no point is found in step 5 (which might happen at large ranges), use the point found in step 3 as the corner point.

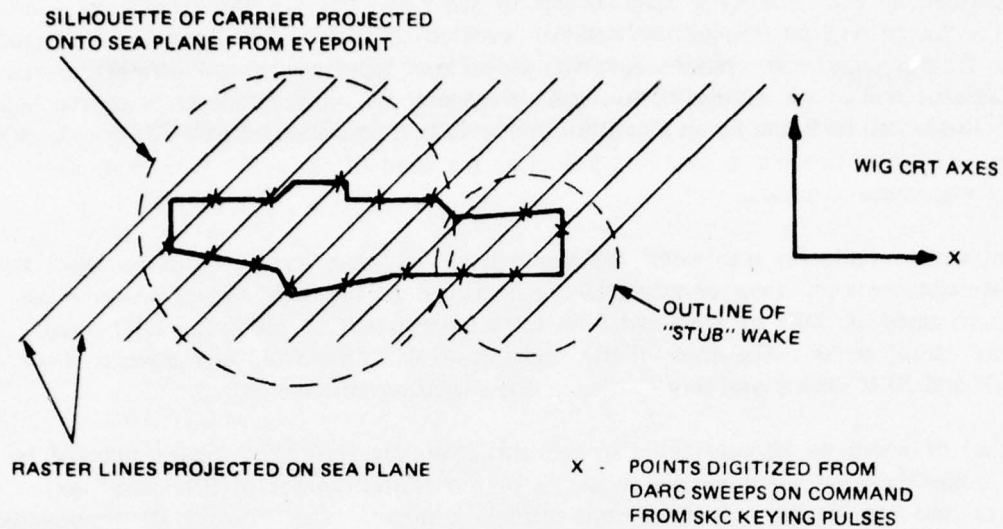


Figure 156. EXAMPLE OF PLOTTED DIGITIZED POINTS

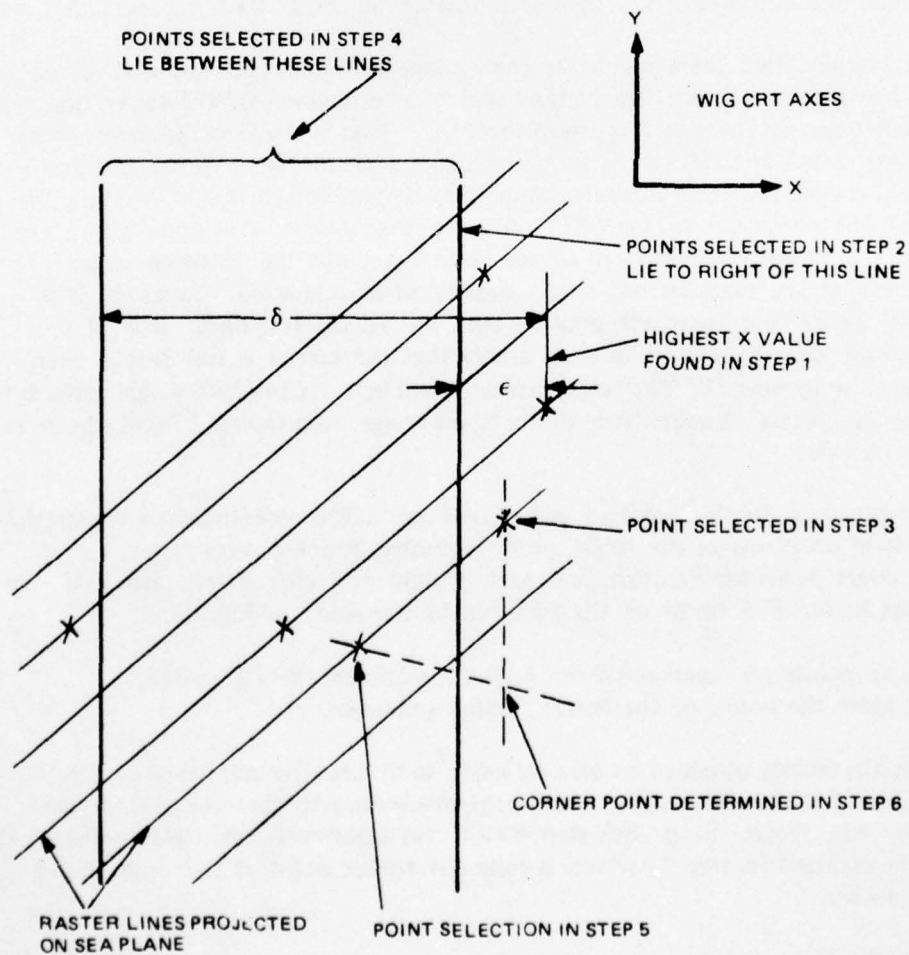


Figure 157. ALGORITHM TO FIND "STUB" WAKE CARRIER POINT

Points obtained by digitizing these same sweeps at the time that the FSS spot crosses the edge of the transparent portion of the wake are plotted similarly. The digitizing command will come from a comparator sensing the WIG video level from the photomultiplier of the FSS. This plot will be an outline of the wake transparency. The corner point at the head of the WIG wake can be found by an algorithm similar to that described on page 371 for the stub wake; the essential difference is that the points at the head of the wake have minimum instead of maximum x values.

When the corner points for the "stub" wake and the WIG wake have been determined, the vector difference between their coordinates can be added to the WIG sweeps to drive the difference to zero. A shift may be added to the x component to make the WIG wake overlap the "stub" wake. The error in this registration will arise from any asynchronism of the BIP and SKC rasters and any delays in the digitizing commands.

The number of points to be considered in the corner-finding algorithm can be reduced by drawing "boxes" around the expected locations of the desired corner of the "stub" and WIG wakes, and considering only the points inside the boxes. The "boxes" are constructed by using analog comparators sensing the sweeps that are digitized, and by having levels set by computer control. Limiting the number of points reduces the data storage requirements, the processing time, and the probability of a spurious, keying pulse resulting from SKC noise.

It was originally assumed that there would be some range beyond which the SKC could not be used, simply because there is a range beyond which superposition of the target image is more suitable than target image insetting using the SKC. This is because the target image becomes undesirably small at large ranges in comparison with the error in the position of the insetting edge. However, upon careful examination, it was found that a keying pulse always occurs on at least one raster line of the SKC. At very large ranges, this pulse may come from the edge of the carrier image instead of the stub wake, but the resulting error, although undesirable, is less than for any other method of attachment. Therefore, it is concluded that the closed-loop approach may be used out to the full 6nm. But if it is desirable to introduce visibility effects in such a way that the carrier is not visible, then use of the SKC must be abandoned. The target projector will be turned off when the carrier is to be fogged out so that the spectral characteristics of the target image, even though behind fog, do not give a false cue to the pilot.

For the obscured-target, visible near-end of wake condition. The recommended registration method is open loop on errors in the target probe pointing, target camera raster, target projector raster, target projector pointing, and back ground projector raster. However, the considerable errors in the BIG raster on the FSS can be corrected as follows:

1. Digitize points on command from edge detection of the FSS video. Also store the count of the master timing generator.
2. From the points obtained in step 1, begin to follow the algorithm already described (for the closed-loop attachment procedure) to find the corner point of the WIG wake. Stop with step #3 of that algorithm - this selects one of the points digitized in step 1, which is near the corner point at the head of the WIG wake.
3. Using the time recorded when the point selected in step 2 was recorded, and assuming linear sweeps, determine a point on the raster plane of the BIP.

4. As described at the beginning of this section (i.e. considering BIP lens mapping, simulated aircraft attitude) and projector-screen-observer geometry, calculate the point on the sea plane corresponding to the point found in step 3.
5. Compare the coordinates of the point obtained in step 4 with those of the point obtained (with the appropriate scaling and origin shift) from the point selected in step 2. The difference is the error originating in the DARC.
6. Apply this measured error as an additive correction to the open-loop WIG raster sweeps.

Error Involved with WIG Attachment. One of the prime sources of error in the WIG attachment technique lies in the errors involved with the scene keying detection implementation. A summary is given of these errors in table 33.

Table 33. SUMMARY OF SCENE KEYING ERRORS

<u>Condition</u>	<u>Center</u>	<u>Top</u>	<u>Bottom</u>
Target Detection			
Vertical	± 12 arc-min.	± 16 arc-min.	± 16 arc-min.
Horizontal	± 12 arc-min.	± 16 arc-min.	± 16 arc-min.
Alignment Error	± 6 arc-min.	± 8.4 arc-min.	± 8.4 arc-min.
Total System Errors			
	± 18 arc-min.	± 24.4 arc-min.	± 16 arc-min.
	$\pm 0.4\%$ vertical	$\pm 0.50\%$ vertical	± 16 arc-min.
	$\pm 0.2\%$ horizontal	$\pm 0.25\%$ horizontal	± 8.4 arc-min.

It should be noted that the method described for WIG attachment uses the scene keying camera for its prime source of carrier information.

One of the results of the summary table of scene keying errors is to determine the dimension of the zone box that will be generated by the computer for WIG attachment. The purpose of the zone box is to prevent large errors in WIG attachment by predicting all sources of error and building a zone within which a large certainty exists that the wake stub is present. The two sources of error that must be considered are the pointing error of the target projection as given in Section IX, target inseting, and the errors involved with table 33.

The target projection errors are noted to be ± 10 arc-min for elevation and azimuth errors, ± 2 arc-min for zoom center misalignment, and ± 6 arc-min roll errors. The RSS value of these three sources of target errors is ± 12 arc-min. Thus, the minimum size of the zone box that will be constructed around the predicted location of the WIG attachment center is as follows:

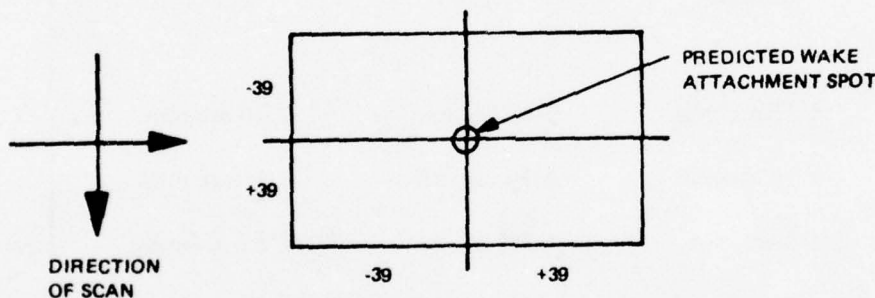
Horizontal: $[\pm 12 \text{ arc-min (target projector)}]$

or

Vertical: $+ [\pm 25 \text{ arc-min (scene keying)}]$

$= \pm 37 \text{ arc-min. (total)}$

It is recommended that an additional 5% of space be allocated to allow for maximum variation. Thus the generated software zone box, within which the WIG strobe will be attached, is shown in figure 158.



NOTE

● All numbers are in arc-minutes.

Figure 158. WAKE ATTACHMENT ZONE BOX

In addition to the errors of the scene keying camera, a certain error exists in the electronic closed loop for the WIG generator. This error is a combination of waveform and flying-spot-scanner signal noise and the spread function of the scanner, with the raster speed (which varies with range) determining the contribution of the errors due to each phenomenon. The average of such errors are approximately one part out of 700, or 15 arc minutes; or ± 8 arc minutes.

In addition to the static criteria described above, the error is effected during the dynamic change occurring when rapid attitude changes of the aircraft. Since the attitude changes are always done on a "predicted" basis, the predicted spot of WIG attachment is always known by the system computer. Thus the worst possible error is determined by the WIG software box described above. Thus the maximum possible error permissible, based upon an RSS computation of all system errors, is described by the box sketch given above and summarized below, assuming that the scene keying camera detects the carrier damage. (See table 35.)

Table 34. SUMMARY OF WIG ATTACHMENT ERRORS UNDER DYNAMIC CONDITIONS

Horizontal:	± 47 arc-minutes, or $\pm 0.5\%$
Vertical:	± 47 arc-minutes, or $\pm 1.0\%$

There may be certain times during high maneuverability modes (roll and/or pitch) that the error may momentarily exceed these values due to the time lag between image detection on the keying camera, computer iteration rates less than television frame rates and time lapse between television updates. These transport delays are a dynamic function of the image motion.

A modified table indicating the total errors of WIG attachment is shown in table 35, for the static case.

Table 35. STATIC ERRORS FOR WIG ATTACHMENT

<u>Vertical</u>	<u>Center</u>	<u>Top</u>	<u>Bottom</u>
Scene Keying	± 18 arc-min	± 25 arc-min	± 25 arc-min
WIG error (avg)	± 8 arc-min	± 8 arc-min	± 8 arc-min
Total	± 26 arc-min	± 33 arc-min	± 33 arc-min
% Error	$\pm 0.54\%$	$\pm 0.7\%$	$\pm 0.7\%$
<u>Horizontal</u>	<u>Center</u>	<u>Top</u>	<u>Bottom</u>
Scene Keying	± 18 arc-min	± 25 arc-min	± 25 arc-min
WIG error (avg)	± 8 arc-min	± 8 arc-min	± 8 arc-min
Total	± 26 arc-min $\pm 0.27\%$	± 33 arc-min $\pm 0.35\%$	± 33 arc-min $\pm 0.35\%$

Television Line Rates. Television line rates is discussed earlier within this section.

PROJECTED SCENE KEYING.

System Design. The method of projected scene keying is to spectrally code the background projector so that the scene keying camera, which has the same raster as the background projector, will not detect it. The keying camera will only detect the target and will blank the background projector whenever the target image is detected. This system requires a rotatable filter that is part of closing the loop. The camera has a conjugate raster to the background projector. Each point which is scanned in the projector is projected to the screen by a lens. The light reflects from the screen to the key camera. The lens on this camera is similar to the background projector so that with a small alignment of the camera raster, the point which is projected is simultaneously scanned by the camera.

The background projector is identified spectrally by a filter located as shown and spectrally described in figure 159. This filter has a notch, or band of no transmission. The keying camera filter is spectrally shown in figure 159. It is a band-pass filter which only transmits light in the notch band on the background projector. As a result, only light from the target projector gets into key camera. When the key camera develops a signal, it is processed and blanks the video in the background projector, so that the seascape will not bleed through the target.

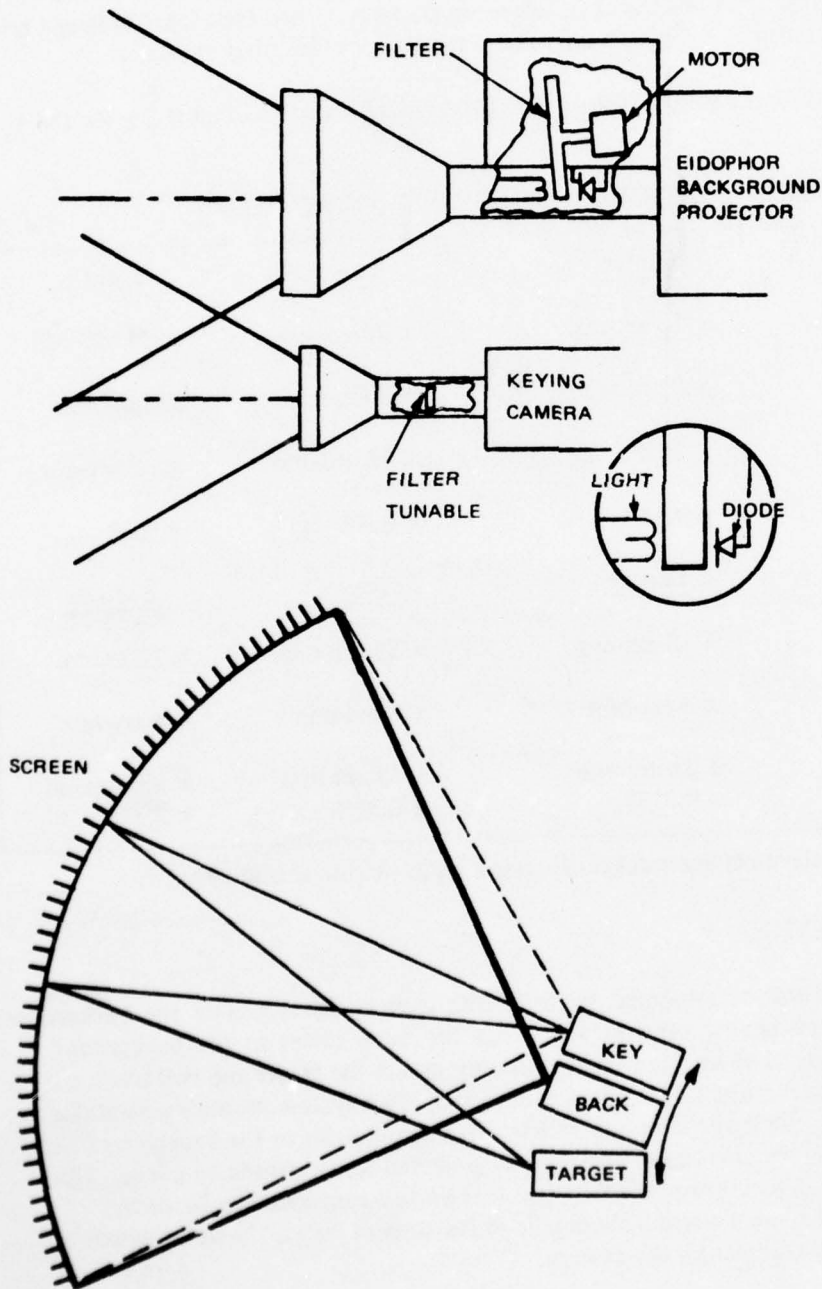


Figure 159. DISPLAY CONFIGURATION

The filter in the key camera is tunable, so that it can be made to match the background projector notch. Both filters are located in the optical path where there is the least divergence. This is required for spectral purity of the image. Otherwise, different parts of the image would have a different band or the band would be smeared and be larger than the background notch. This would allow background imagery into the key camera.

TV Camera and Optical Considerations.

Optics. The offset and separate camera system was chosen for three reasons. The first is the spectral purity which can be better controlled and tuned for transmissive filters. The second is that the Eidophor's output is about 4000 lumens whereas the received flux is about 4×10^{-5} lumens. This makes the image exactly like the Eidophor's except for a small error due to the small displacement between the two. This small error is compensated by a small adjustment of the camera raster.

The choice of the type of keying camera is dictated by the sensitivity and resolution requirements for detection of the projected carrier image. The image isocon camera best meets these requirements and approximate isocon signal levels of operation have been selected for the purposes of this analysis.

Exact camera light level requirements will be determined during the detail hardware design phase of the program. Then, camera keying irregularities can be evaluated as a function of isocon face plate light level. A minimum light level will be chosen that will provide acceptable levels of irregularities of the blanking signal which blanks the background image generator around the carrier outline.

Knowing the isocon signal current requirements, the spectral filter characteristics which incorporate the attenuation band into the background projector light output and the pass band into the keying camera light input can be selected to provide the required amount of isocon signal current. See figure 160 for illustration of spectral filter characteristics.

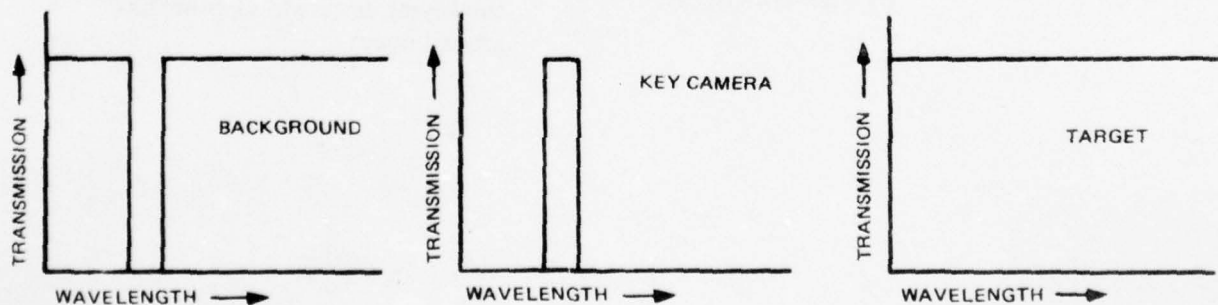


Figure 160. SPECTRAL CHARACTERISTICS OF VARIOUS DISPLAY COMPONENTS

The accuracy of the detected target image coordinates is dependent upon the following:

- 1) S/N ratio and signal amplitude level of the keying camera video output.
- 2) Rise and fall time of the carrier video signal.
- 3) Camera geometric distortion and sweep linearity.
- 4) Accuracy of the coordinate keying detector.

Signal Level of the Camera Video Output. The following equations were used to determine the highlight values of foot-lamberts and isocon anode current of the keying camera. Since the gamma of the isocon tube is not unity for all incident light levels, the tube characteristic curves must be used to determine the true anode current for levels above the knee ($4 \mu a$).

$$\sum_{n=1}^{n=31} \frac{L(n) * T(n) * V(n) * 680 * G * S1}{A1 * 10^6} = \text{Foot-lamberts from target projector on screen}$$

$$\sum_{n=1}^{n=31} \frac{L(n) * T(n) * B(n) * I(n) * F1(n) * S1}{A1 * 4 * M^2 * 1000} \approx \text{Total anode current in } \mu a \text{ out of keying camera}$$

$$\sum_{n=1}^{n=31} \frac{L(n) * C(n) * V(n) * F2(n) * 680 * G * S2}{A2 * 10^6} = \text{Foot-lamberts from background projector on screen}$$

$$\sum_{n=1}^{n=31} \frac{L(n) * C(n) * F1(n) * F2(n) * B(n) * S2 * I(n)}{A2 * 4 * M^2 * 1000} = \text{Total bleed through anode current of the keying camera in } \mu a \text{ from background image}$$

where:

$L(n)$	=	Lamp spectral characteristics in $\mu\text{watts}/10\text{ nm}$ / lumen in the n th wavelength interval
$T(n)$	=	Transmission of the target projection system in the n th wavelength interval
A_1	=	Area of projected scene by target projector in $\text{ft}^2 = 70$.
$B(n)$	=	Transmission of the keying camera lens in the n th wavelength interval
$I(n)$	=	Isocon response in $\text{na}/\mu\text{w}/\text{ft}^2$ in the n th wavelength interval
$J(n)$	=	Signal current with no filter in $\text{na}/10\text{ nm}$ per input lumen in the n th wavelength interval
G	=	Gain of screen
S_1	=	Total lumens entering target projection optics = 1900
M	=	$f/\#$ of keying camera lens
$F_1(n)$	=	Keying camera blocking filter transmission in the n th wavelength interval
$C(n)$	=	Background projection lens transmission in the n th wavelength interval
A_2	=	Background scene area in $\text{ft}^2 = 396$
$F_2(n)$	=	Background projector blocking filter transmission in the n th wavelength interval.
S_2	=	Total lumens entering background projection optics = 2630
n	=	n th 10 nm wavelength interval starting with $n = 1$ at 400 nm and ending with $n = 31$ at 700 nm, i.e., $n = 1$ corresponds to the interval 395 nm to 405 nm
680	=	Conversion constant from watts to lumens at a wavelength of 550 nm only
$V(n)$	=	Relative visibility of light to the human eye in n th wavelength interval.

With the key camera filters, the signal current for the carrier highlight is $12.5\ \mu\text{a}$, this considers all losses. The corresponding bleedthrough current is $0.25\ \mu\text{a}$.

AD-A037 223

SINGER CO BINGHAMTON N Y SIMULATION PRODUCTS DIV
AVIATION WIDE-ANGLE VISUAL SYSTEM (AWAVS). DESIGN ANALYSIS REPO--ETC(U)
APR 75

F/G 1/2

N61339-75-C-0009

UNCLASSIFIED

AWAVS-1

NAVTRAEQUIPC-75-C-0009-1 NL

5 of 5
AD
A037223



END

DATE
FILMED

4-77

Color Band Considerations. A number of visual tests were performed showing the appearance of the background sea when the blue portion of the spectrum was removed for scene keying. The yellow-green sea which resulted is unacceptable. Removal of the red portion was tested and found to produce a more acceptable appearance. As analyzed below, it is shown to be viable to remove the red even though the camera tube response is much lower.

Filter Considerations. The key camera filter design includes a temperature colored glass. This eliminates bleed-through in the blue-green seascape. The filter is a Schott RG610, or equivalent. The transmission at 600 nm is down to 0.01. At 590, it plummets to 10^{-3} and at 580, it drops to 10^{-5} , etc.

The anti-reflection coatings in the keying camera consist of a three-layer coating on the BK7, which is peaked at 700 nm, and a Mg F coating on the SF10 glass, which also peaked at 700 nm. These cause the lens surfaces to act as filters to block more the blue-green spectrum and enhance the transmittance in the red keying spectrum.

The lenses in the background projector are similarly coated but the peak was 500 nm. This causes greater rejection of the red signal in the background image. It is now felt that the peak should be closer to 450 to further enhance the red rejection.

The target projector transmission peaks at 26%. The high transmission improves the screen luminosity. This provides a high signal level for the scene keying camera.

Scene-Keying Camera Image Analysis. The scene keying camera image errors may be divided up into errors associated with the following problems:

- 1) Alignment and calibration errors due to accumulated spread function (projector and lens plus camera and lens) and noise.
- 2) Scene detection errors due to camera and lens spread function, noise, and gray level variation.

Noise and Discriminator Level. In order to insure that the scene keying circuit does not trigger on the background image, the threshold T (comparator reference voltage) must be set such that

$$T > S_B + N(S_B) / 2 + C \quad (1)$$

where S_B = the scene keying camera (SKC) signal current due to bleedthrough of the peak white (wave crests) in the background image (determined to be $0.25 \mu\text{a}$).

$N(S_B)$ = the peak-to-peak noise for the SKC current level = S_B

C = the triggering uncertainty of the comparator which generates the blanking = 0.07.

In order to insure that the scene keying circuit does not unblank over the carrier portion of the picture, the threshold level (T) must be set such that

$$T < S_C - N(S_C) / 2 - C \quad (2)$$

where S_C is the minimum allowable SKC signal developed from the carrier image plus bleedthrough. (Determined to be $20.7 \mu a$.)

$N(S_C)$ is the peak-to-peak noise for the SKC current level = S_C

C is the triggering uncertainty of the comparator which generates the blanking.

The noise level $N(S)$ can be determined from the equation

$$N(S) = \frac{S}{(S/N)_{PEAK}}$$

Where S/N is the signal to noise ratio. This ratio is found from charts supplied by RCA which are shown on figures 161 and 162.

The carrier will have a 13.75:1 contrast ratio. Therefore, the smallest signal is $1/13.75 \times 11.8$ or $0.858 \mu a$. The 11.8 is the maximum current previously calculated. This corresponds on figure 161 to a faceplate illumination of 3.8×10^{-4} lumens/foot². Then by using the figure 164B one finds the S/N_O is 2.3. However, this applies to a system of 4.2 MHz bandwidth. The system that is being proposed has a 16-MHz bandwidth. The S/N_O can be transformed to the 16-MHz bandwidth by the equation below.

$$(S/N)_{db} = (S/N_O)_{db} + 20 \log \left(\frac{BW_O}{BW} \right)^{1/2}$$

$$(S/N)_{db} = 23 + 20 \log \frac{(4.2)^{1/2}}{16}$$

$$= 23 - 5.8$$

$$= 17.2$$

The value for the peak signal to peak noise can be found from the equation:

$$(S/N)_{peak} = 1/6 \text{ antilog } (S/N)_{db}/20$$

$$= 1/6 \text{ antilog } (17.2/20) = 1.207$$

The S/N for the bleedthrough can be similarly determined. For it the equivalent faceplate illumination is 1.5×10^{-4} . This produces a value of 18 for S/N with a bandwidth of 4.2 MHz. The (S/N_O) can be factored to a 16-MHz bandwidth as before.

$$(S/N)_{db} = 18 + 20 \log \left(\frac{4.2}{16} \right)^{1/2}$$

$$= 12.2$$

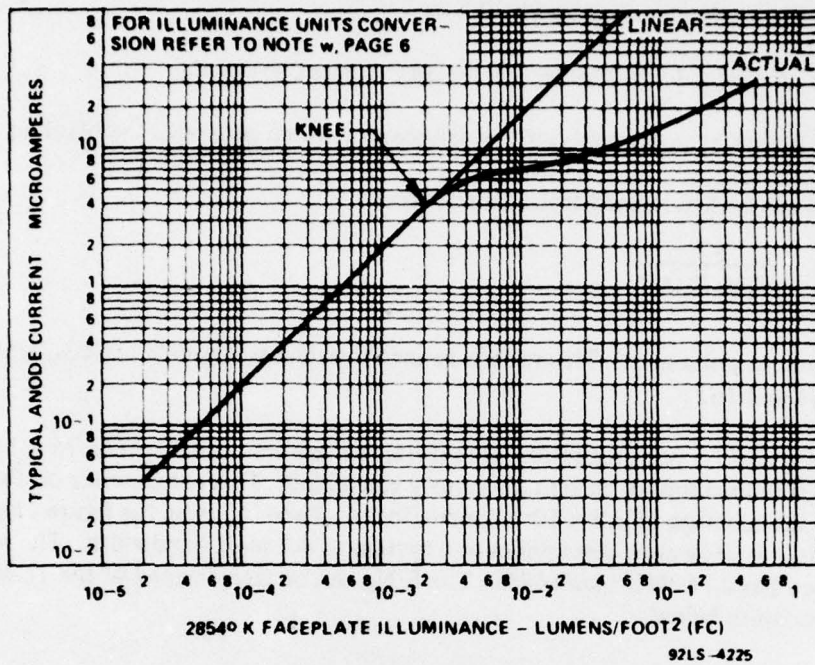


Figure 161. TYPICAL TRANSFER CHARACTERISTIC

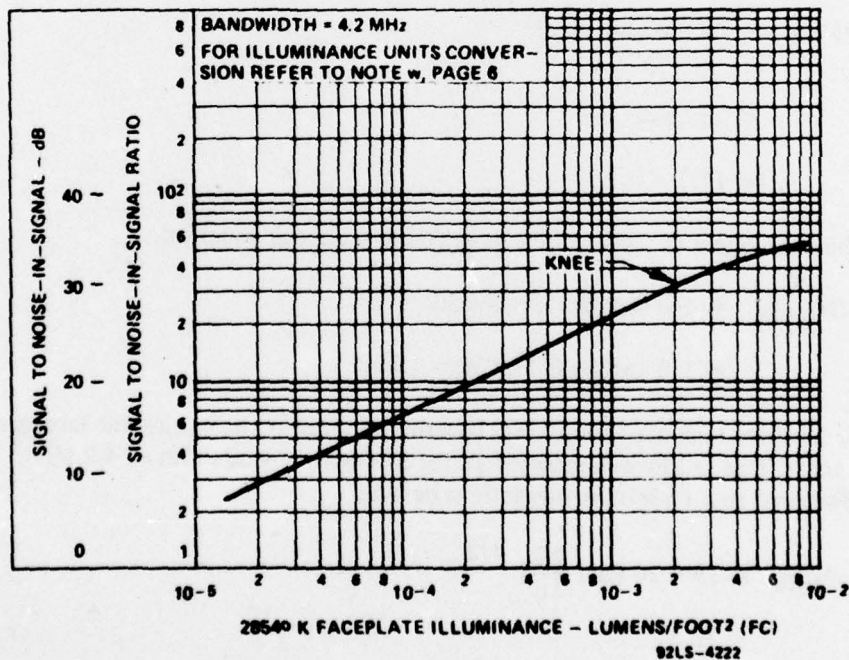


Figure 162. TYPICAL SIGNAL TO NOISE-IN-SIGNAL RATIO AS A FUNCTION OF FACEPLATE ILLUMINANCE OR IRRADIANCE FROM FLUX LEVELS WITHIN A GIVEN SCENE. (BEAM ADJUSTMENT FIXED AT 2 x KNEE SETTING)

The value of the peak signal to peak noise is found to be:

$$(S/N)_{PEAK} = 1/6 (\text{antilog } 12.2/20) \\ = 0.68$$

For the carrier signal, the noise is:

$$N(S_C) = \frac{0.858}{1.207} = 0.711$$

For the bleedthrough signal, the noise can be taken as 1/2 the signal since the $(S/N)_{PEAK}$ is less than one.

$$N(S_B) = 1/2 \cdot 0.25 = 0.125$$

The value of C is 0.1 μ a.

The value of the equation 1 is:

$$T > 0.25 + \frac{0.125}{2} + 0.07$$

$$T > 0.383$$

For equation 2:

$$T < 0.836 - \frac{0.692}{2} - 0.07$$

$$< 0.420$$

For dusk conditions, the carrier signal is 1/2 day = 0.418 Na the $(S/N)_{db}$ from figures 161 and 162 is 20. Converting to 16-MHz it is $20 - 5.8 = 14.2$.

The bleedthrough signal is 0.125 Na. The signal to noise is 14. Converted to 16-MHz, it is $14 - 5.8 = 8.2$.

The peak signal to peak noise is:

$$(S/N_c)_{PEAK} = 1/6 \text{ antilog } \left(\frac{14.2}{20} \right) = 0.86$$

Since both this and the background or less than 1, 1/2 of the signal will be used as the noise level.

$$DUSK N(S_C) = \frac{0.418}{2} = 0.209$$

$$DUSK N(S_B) = \frac{0.125}{2} = 0.063$$

The threshold is:

$$T > 0.125 + \frac{0.063}{2} + 0.07$$

$$T > 0.227$$

$$T < 0.418 - \frac{0.209}{2} - 0.07$$

$$T < 0.244$$

Figures 163 and 164 summarize this noise and discriminator level data.

Alignment Errors. The scene keyed inseting method has certain errors inherent due to the cascading of images from the background projector to the scene keying camera. These errors are due to alignment as well as target detection errors which are discussed below:

The two methods of alignment that were investigated are covering a single field flash of alignment points during one television frame, and a steady state measurement occurring during standby time wherein many measurements can be made.

The errors discussed in this section are derived from the approach using the first detected leading edge to predict the location of the projected calibration marks. Thus, the calibration location is defined, for the purposes of the following discussion on errors, as that location on the background projector corresponding to the initial turn-on of the projector.

Further discussion is presented using the results of a method which reduces the effects of the spread function and noise on the system.

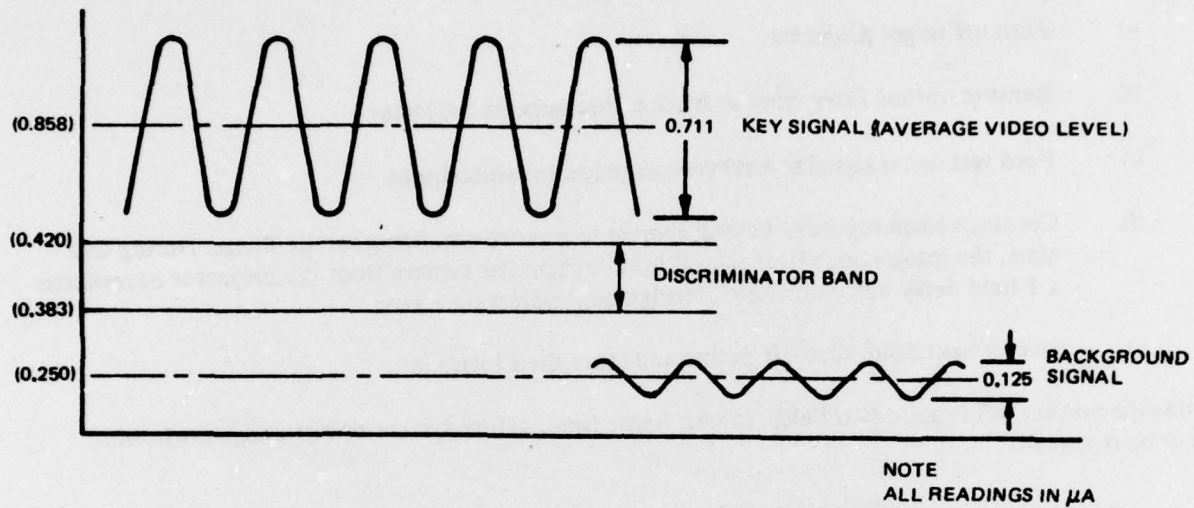


Figure 163. DAY SIGNAL & NOISE LEVELS AND DISCRIMINATOR

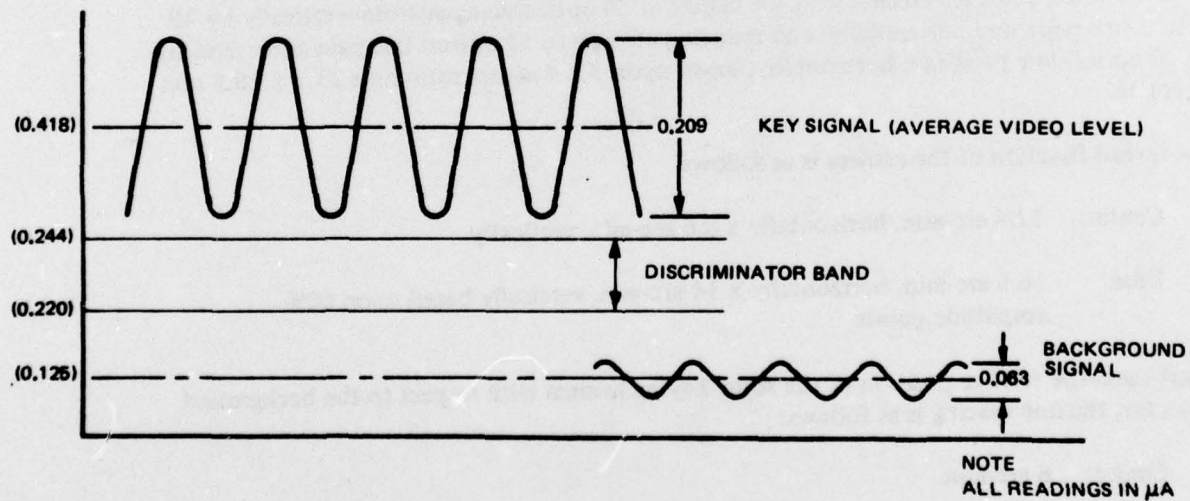


Figure 164. DUSK SIGNAL AND NOISE LEVELS AND DISCRIMINATOR

NAVTRAEQUIPCEN 75-C-0009 -1

Single-Field Calibration - If it becomes necessary to correct the raster alignment due to projector image drift during a mission, and a single television field were used, the following procedure should be followed:

- a) Turn off target projector.
- b) Remove optical filter from in front of background projector.
- c) Feed test raster signal to background projector video input.
- d) Continue scanning scene keying camera to remove remaining carrier image. During this time, the integrating effort (signal build-up) on the camera from the projector necessitates a 1-field delay before reading off alignment points on screen.
- e) During next field, read-off points and store their location.

Thus, the system will require two fields, or one frame time, before system carrier image projection may be resumed.

During the alignment procedure, the image on the scene keying camera will be the result of the cascaded images from the background projector to the camera. The alignment image will consist of a quantity of single lines drawn on the screen throughout the FOV of an arbitrary length so that the light output will have reached at least 70% peak level before the leading edge will be detected. In order to perform an error analysis, the spread functions of the image and the camera (including lens) at various places on the screen must be determined. An analysis of the scene keying camera indicates that the spread function is based on a limiting television response of 1000 TV lines, and a lens response at the center of 24 optical line pairs/mm vertically by 40 optical line pairs/mm horizontally; and reducing off axis to 12 optical line pair/mm vertically by 20 optical line pairs/mm horizontally, based upon 3 x 4 aspect ratio on a 21.3 x 28.5 mm faceplate.

The spread function of the camera is as follows:

Center: 12.4 arc-min. horizontally x 8.6 arc-min. vertically

Edge: 16.5 arc-min. horizontally x 14 arc-min. vertically based upon 60% amplitude points

Based upon the relative position of the scene keying camera with respect to the background projector, the line spacing is as follows:

Center: 6 arc-min.

Top: 6.9 arc-min.

Bottom: 5.1 arc-min.

An analysis of the background projector lens and Eidophor projector shows the screen displayed image spread functions to be the same as the camera spread functions.

Thus the combined spread function of the alignment spot on the face of the camera is as follows:

Center: 17.5 arc-min. horizontally x 12.2 arc-min. vertically

Edge: 23.3 arc-min. horizontally x 20 arc-min. vertically

An analysis of the response of the television system, assuming a comparator setting of 60% (which insures a detection of every point) gives an error function as follows:

Center: Center detection gives horizontal error of ± 5 arc-min. (delay compensated for) and a vertical error of +3 to -9 arc-min., or as expected, the line spacing due to single field determination, or sampling.

Edge: The spread function gives horizontal error of ± 8 arc-min. uncertainty and a vertical, top error of +3 to -14 arc-min. (2 lines), and a bottom error of -15 arc-min. (3 lines).

Further, since the spread function indicates that several lines will cross the image, circuits must be developed to mask off the areas to prevent multiple recording of points.

Standby Mode Calibration - In this mode of operation both fields can be used to detect the presence of the calibration points. One disadvantage of the standby mode is that repeated passes may be used to remove the major effects of signal noise on the point detection.

Assuming no noise in the signal, and a flat video output (i.e., the corrections for shading also correct for signal fall-off, due to enlarged spread function and change in line spacing), the uncertainty errors are as follows for a detection level set at 70%:

Vertical center:	1 line uncertainty	(0.125%)
Top:	1.8 lines uncertainty	(0.225%)
Bottom:	2.5 lines uncertainty	(0.31%)
Horizontal center:	5 arc-min.	(0.05%)
Top:	8 arc-min.	(0.084%)
Bottom:	8 arc-min.	(0.084%)

Effect of Noise - The effect of noise on a single field exposure is shown in the table below. The effect on the spread function errors, due to the broader image content, is also included in this table. These errors are in addition to the errors due to the spread function itself:

Vertical Top Corner:	6 arc-min.
Center:	6 arc-min.
Bottom Corner:	9 arc-min.

NAVTRAEQUIPCEN 75-C-0009-1

Horizontal:

- 1) Using first detection criteria the error is equal in magnitude to the length of calibration mark, or if a one-degree pulse is used, 60 arc-min.
- 2) Using the criteria that the detected pulse is at least 30 arc-min. long, the 90% error term is as follows:

Top Corner: -8 arc-min. + 30 arc-min.

Center: -6 arc-min. + 15 arc-min.

Bottom: -10 arc-min. + 30 arc-min.

with a 10% chance of missing the spot entirely.

The effect of noise on a standby calibration mode, wherein 20 fields were used, would reduce the error by $\sqrt{20}$ or 4.5. Thus the vertical errors due to noise would be reduced to ± 2 arc-min., and the horizontal errors due to noise would be reduced to:

Top Corner: -2, + 7 arc-min.

Center: -1.5, + 3 arc-min.

Bottom: -2, + 7 arc-min.

A summary of the errors due to spread function and noise alignment mode is shown in table 36.

Table 36. SUMMARY OF ERRORS (FIRST DETECTION CRITERIA)

<u>Vertical</u>	<u>Center</u>	<u>Top</u>	<u>Bottom</u>
Spread Function	+3, -9 arc-min.	+3, -14 arc-min.	+3, -15 arc-min.
Noise	± 6	± 6.9	± 7.6 arc-min.
TOTAL	+9, -15 arc-min. +0.2%, -0.3%	+9.9, -20.9 arc-min. +0.2%, -0.4%	+10.6, -22.6 arc-min. +0.22%, -0.5%
<u>Horizontal</u>	<u>Center</u>	<u>Top</u>	<u>Bottom</u>
Spread Function	+5 arc-min.	± 8 arc-min.	± 8 arc-min.
Noise	-6, +15 arc-min.	-8, +30	-8, +30
TOTAL	-11, +21 arc-min. -0.1%, +0.2%	-16, +38 arc-min. -0.2%, +0.4%	-16, +38 arc-min. -0.2%, +0.4%
with a 10% chance of no detection at all.			

The results of this study, together with the expected results if the alignment points were flashed on the screen for short but still recognizable time elements, has led to the recommendation that the single field exposure not be used to obtain system alignment unless all else fails as would be the case with large Eidophor surface defects. Since the Eidophor problems are unknown at this time, it is recommended the above concept not be implemented.

Recommended Alignment Procedure - The recommended alignment procedure is to align the system during the standby mode. During this time, a pattern assuring adequate detection would be deployed, being three resolution elements by three resolution elements wide. The outline of each calibration point will be stored and sent to the prime system computer, as further illustrated in the section Raster Pattern Generator for Error Sampling. During this mode the spread function of the scanning spot is the only source of error, since noise is averaged out and detection levels are removed. The alignment errors thus reduce to 1σ of the spot, or ± 6 arc minutes in the center, and ± 8.4 arc minutes at the edges. The errors are symmetrical for horizontal and vertical.

Target Analysis - The spread function of the camera is the key in determining errors in the scene key detection. The scene keying camera plus lens resolution element is assumed to be gaussian and is 12.4 arc-min. at the 60% point. The beam current varies, for 8 shades of gray, between $7 \mu\text{a}$ and $0.91 \mu\text{a}$ output. The effect of signal noise shows that the detection level must be set at $0.5 \mu\text{a}$, or $7/0.5 = 7.5\%$ of peak. The variation in detection due to the signal variation gives a spatial variation of $\pm 1.5 \sigma$; where:

$$\sigma = 6.22 \text{ arc-min. Thus the error due to detection is } \pm 1.5 \times 6.22 = \pm 9.5 \text{ arc-min.}$$

Thus on a dark image, the detection level in the center of the screen will be 9.5 arc-min. beyond the actual image; while in a bright scene, the detection level will be 9.5 arc-min. before. This error occurs in both the horizontal and vertical direction.

The spread function on the edges rises to 16.7 arc-min. at the 60% point, or $\sigma = 8.4$ arc-min.

Thus the error at the edge of the raster is $1.51 \times 8.4 = \pm 12.7$ arc-min.

Target Insetting Error Summary. The following is a summary of the various analysis due to image spread functions and scene gray levels. It should be noted that these figures assume a flat field for all video content. This means that great attention be paid to correct all shading effects. (See table 37.)

Smearing Effects Due To Isocon Lag.

Figure 165 is the lag characteristic of the isocon image tube, and table 38 represents a relationship between signal current and residual current after 1-1/2 frame time. All the data in that table is for a 2.5 KW bulb with 6 ft-lamberts representing the brightest spot on the carrier and 8 shades of gray or 1 to 13.7 signal range.

Table 37. TARGET INSETTING ERROR SUMMARY

<u>Condition</u>	<u>Center</u>	<u>Top</u>	<u>Bottom</u>
Target Detection			
Vertical	± 12 arc-min.	± 16 arc-min.	± 16 arc-min.
Horizontal	± 12 arc-min.	± 16 arc-min.	± 16 arc-min.
Alignment Error	± 6 arc-min.	± 8.4 arc-min.	± 8.4 arc-min.
Total System Errors			
	± 18 arc-min.	± 24.4 arc-min.	± 24.4 arc-min.
	$\pm 0.4\%$ vertical	$\pm 0.50\%$ vertical	$\pm 0.50\%$ vertical
	$\pm 0.2\%$ horizontal	$\pm 0.25\%$ horizontal	$\pm 0.25\%$ horizontal

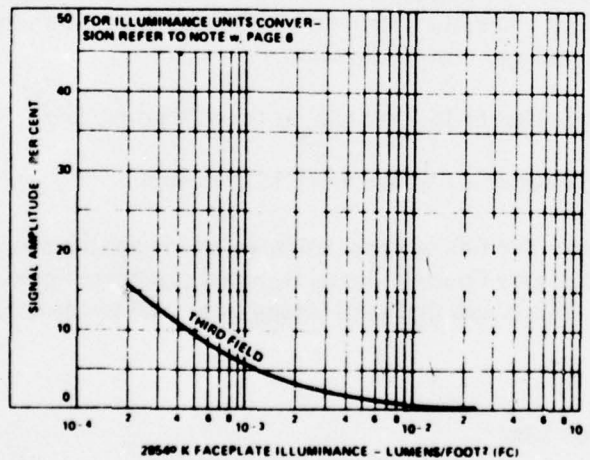


Figure 165. RESIDUAL SIGNAL (LAG) CHARACTERISTIC OF ISOCON IMAGE TUBE

Table 38. SIGNAL CURRENT VS. RESIDUAL SIGNAL AND S_B

Target Image: 8 Shades of Gray			I_S ; Signal Current μa	I_R ; Residual Current After 1½ Frame Time; μa	S_B ; Background Bleed Through (note 3) μa
Screen ft-lm	Isocon ft/c				
Day	6.0	0.01	7 μa (note 1)	1% of $I_S = 0.07$	0.25
	6/13.7 = 0.44	0.0005	12.5/13.7 = 0.91	8% of $I_S = 0.07$	
Dusk	6/2 = 3	0.003	5 μa (note 2)	3% of $I_S = 0.15$	0.13
	3/13.7 = 0.22	0.00025	12.5/2x13.7 = 0.46	13% of $I_S = 0.05$	

Note 1: 7 $\mu a \equiv$ isocon current corresponding to 12.5 μa with gamma 1.

Note 2: 5 $\mu a \equiv$ isocon current corresponding to 6.25 μa with gamma 1.

Note 3: S_B = bleed through for an average white crest.

As shown in table 38, the highest residual signal after one frame time is less than the signal detection reference level of the comparator ($> S_B$). Assuming the frequency of the system software outputs fed to the AWAVS hardware is once per frame time, there will be no false signal detection or smearing effects due to the isocon image tube lag.

In order to further insure against smearing effects, the keying camera will be turned off outside of the carrier edge as shown in figure 166.

Comparator Reference Levels without System Shading Considerations. Day Condition - As shown in table 38, the signal current range is 0.91 μa to 7 μa with $S_B = 0.25 \mu a$ or 0.46 μa peak min. to 3 μa peak min with $S_{B_{max}} = 0.38$.

Therefore, by choosing the comparator level of 0.42 μa , a reliable keying with 8 shades of gray (1 to 13.7 signal ratio) can be expected.

Dusk Condition - The signal range is $0.46 - \frac{1}{2} (0.46) = 0.23$ peak min. to 2 μa peak min with max peak $S_B = 0.19$.

Therefore, by choosing the comparator level of 0.21 μa , a reliable keying with 8 shades of gray can be expected.

Shading Effects.

Signal Detection Reliability due to the System Shading Effects. Table 39 is a collection of shading data taken from either a specification of the component or a vendor's best approximation at this point.

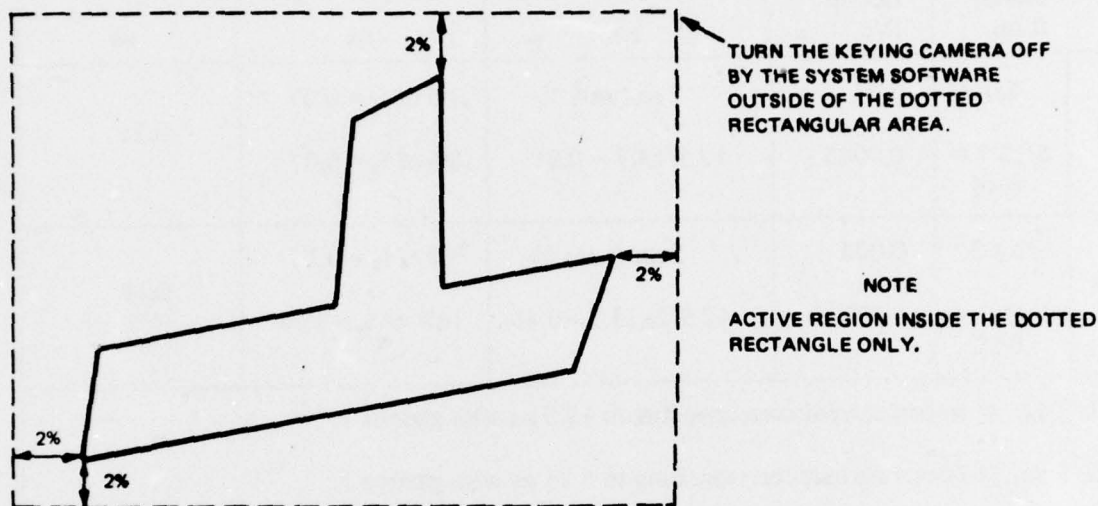


Figure 166. KEYING CAMERA ACTIVE REGION

Table 39. SHADING DATA ASSOCIATED WITH SKI

Component	Shading (%)	Approx. Shading Function
Eidophor	30%	$f_1 = a x^2 + b$
Eidophor Lens	50%	$f_2 = c x^2 + d$
SKC Lens	50%	$f_2 = c x^2 + d$
SKC	Negligible	—
Display Screen	30%	$f_1 = a x^2 + b$

* Shading means % functional transmission decrease around the edge of the raster plane compared to the center of the raster.

* $x \equiv$ position variable; $a, b, c, d \equiv$ constants.

Figure 167 is a pictorial representation of Table 39.

Table 40 is a modified table 38 in accordance with table 39 and figure 167 shading effects.

Comparator Reference Levels for Raster Edge. In Table 40, the minimum peak signal for day conditions is $0.27 - \frac{1}{2}(0.27) = 0.13$ with the maximum peak $S_B = 0.025 + \frac{1}{2}0.025 = 0.037$.

Therefore, by choosing the comparator level of $0.08 \mu a$, a reliable keying will be obtained.

For dusk conditions, the minimum peak signal is :

$$0.13 - \frac{1}{2}(0.13) = 0.07 \mu a \text{ with the maximum peak}$$

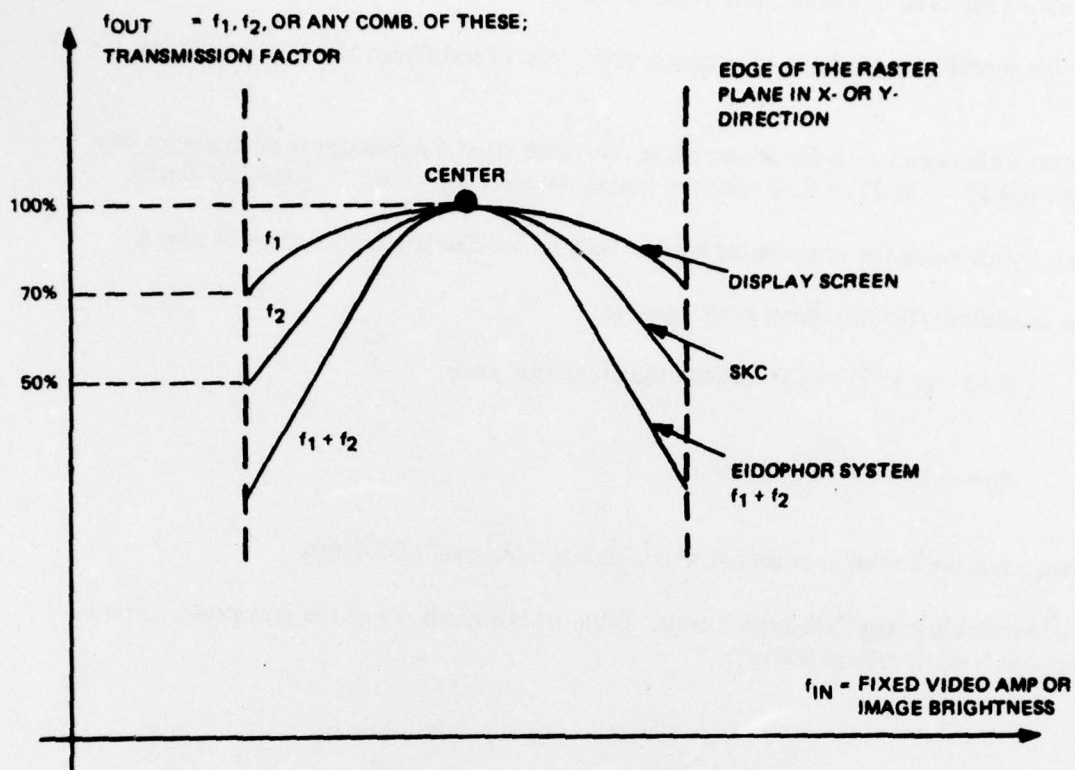
$$S_B = 0.013 + \frac{1}{2}(0.013) = 0.02.$$

Therefore, a reliable keying is expected with a comparator level of $0.04 \mu a$.

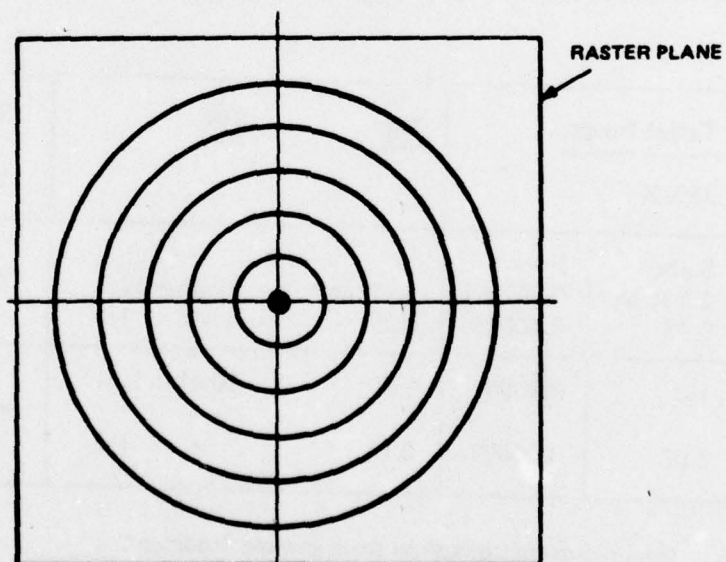
Total System Comparator Reference Levels. Table 41 is a summary of the previously derived comparator reference voltage levels.

Table 40. SIGNAL CURRENT (I_S) vs S_B FOR THE EDGE OF THE RASTER PLANE

	Target Image; 35% X		$*I_S$	S/N	S_B 10% X
	Screen 2.1 ft-lm 0.15	Isocon 0.002 ft/c 0.00015			
Day			3.75 μa 0.27	21 db = 12:1 — 1:1	0.025 μa
Dusk	1.0 0.08	0.0009 0.00007	1.87 0.13	20 db = 12:1 — 1:1	0.013 μa
* $I_S \equiv$ Isocon current converted from gamma 1 current.					



(A) GRAPHICAL REPRESENTATION OF SHADING



(B) CONTOUR OF SHADING; CENTER REPRESENTS 100% TRANS.

Figure 167. PICTORIAL REPRESENTATION OF TABLE 39

Table 41. COMPARATOR REFERENCE LEVELS

	Comparator Ref. Level Range	Approximated Shading Function
Day	0.08 μ a to 0.42 μ a	$*f_2 = c x^2 + d$
Dusk	0.04 μ a to 0.21 μ a	$*f_2 = c x^2 + d$
* f_2 is shown in table 38.		

The parabola function generator output, f_2 modulated in accordance with figure 167 (b) contour, will be fed to a comparator reference terminal. Two f_2 generators are needed: one for day conditions, and the other for dusk conditions.

Signal Detection for the Carrier Edge . (See figure 168.) Due to seawave interference, the background bleed-through current will be added up to the carrier edge signals. The amount of S_B to be added up is 0.25 μ a for day conditions and 0.13 μ a for dusk conditions.

This wave interference will further insure a more reliable keying for the carrier edge.

Raster Pattern Generator for Error Sampling The maximum brightness output from the proposed Eidophor projector is 6 foot-lamberts. As shown in the previous paragraph, 10% of 6 foot-lamberts or 0.6 foot-lamberts is only transmitted and picked up by the scene keying camera for the edge of the raster plane if an image is projected through the background projector. The signal-to-noise ratio associated with 0.6 foot-lamberts or 0.001 foot-candles is 21 db (= 1 to 12 ratio) with 2 μ a of I_S . Due to this low signal-to-noise ratio and the image spreading effects both on the display screen and the isocon faceplate, a reliable error sampling will not be accomplished for a test dot projected on the edge of the raster plane. A pictorial representation of this is shown in figure 169.

The technique for solving this problem is to employ a simple mini-raster generator instead of a dot pattern generator. The center of the distorted raster picked up by the keying camera can be found easily by the system software. By comparing the input raster center with the output raster center, a reliable error sampling will be achieved. This method is illustrated in figure 170.

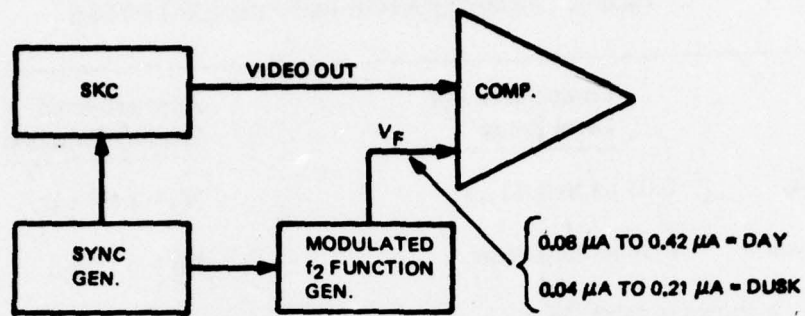


Figure 168. BLOCK DIAGRAM OF SIGNAL DETECTION

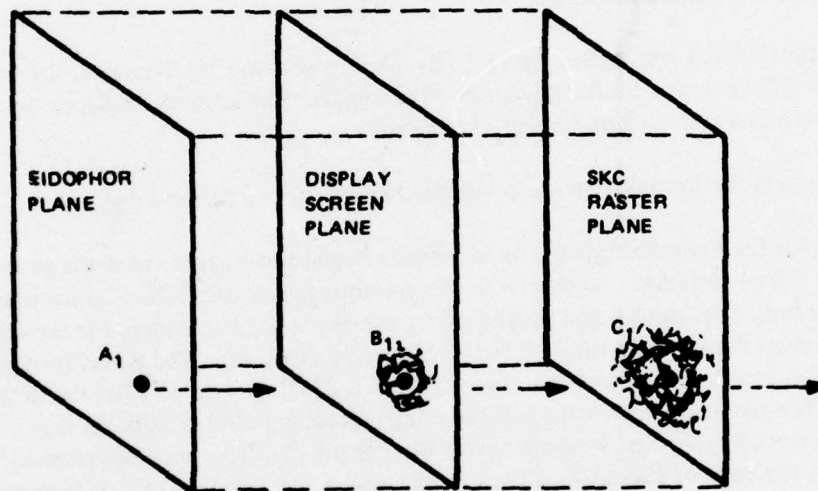


Figure 169. PROJECTED-DOT SAMPLING

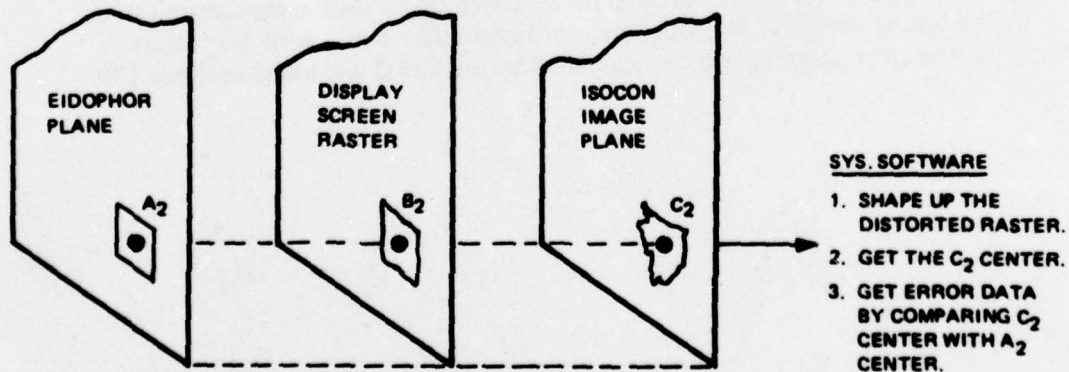


Figure 170. ERROR SAMPLING WITH MINI-RASTER GENERATOR

Summary on SKI. The following is a summary of scene keying inset:

- 1) Accuracy - On the order of 0.5%; this may not be significant from the pilot's viewpoint in a dynamic display condition.
- 2) 8 shades of gray will be achieved with a 2.5 KW bulb.
- 3) Red spectrum will be used for insertion.
- 4) Frequency of Error Sampling - The error circuit will be connected to the AWAVS "START" circuit so that the first few seconds can be devoted to error sampling and correction whenever "START" button is pressed down.
- 5) Error Correction - Will be implemented by a Singer CRC.
- 6) System Software will turn the keying camera off for the display region outside a calculated rectangular which encloses the carrier.
- 7) Signal detection reliability will not be degraded due to shading effects.
- 8) Two parabola function generator outputs will be used as the voltage reference levels for signal detection.

SPECIAL EFFECTS GENERATORS.

In Section 11 of this report, the features and operational controls on an existing SEG were described and it was concluded that the features of the existing SEG would meet all the AWAVS spec. requirements.

The SEG in the target image generator, except for fog effects, will not be required when video inseting by a projected scene keying technique is utilized.

Target SEG. The cloud effects on the carrier are done by the background SEG. For above and in-cloud conditions, the background cloud and the target image will be superimposed and the intensity of cloud will be varied for range simulation.

The target SEG in connection with the scene keying inseting system is solely for a fog simulation of the carrier when a pilot flies in from a long distance away (close to horizontally).

The target SEG for the scene keyed inseting system is a simplified version of the original target SEG for use in the elliptical target inseting and can be expanded to the original SEG without any complexity. (See figure 171.)

The special effects video output of A13 of figure 171 is a combination of the target camera video output fed to input A and a fixed reference dc voltage fed to input B. The simulation of fog conditions will be accomplished by varying the level applied to A13. This is known as the RVR/R function and is varied by system software. There will be no new hardware for this simulation.

Generation of Sea Merge. Figure 172 is a block diagram of the background SEG, modified for sea merge effects. A computer-controlled waveform generator 2, a sea merge function generator, and a video gate mixer have been added to the basic background SEG.

The circuitry and operation of the sea merge function generator are similar to those of RVR/R function generator.

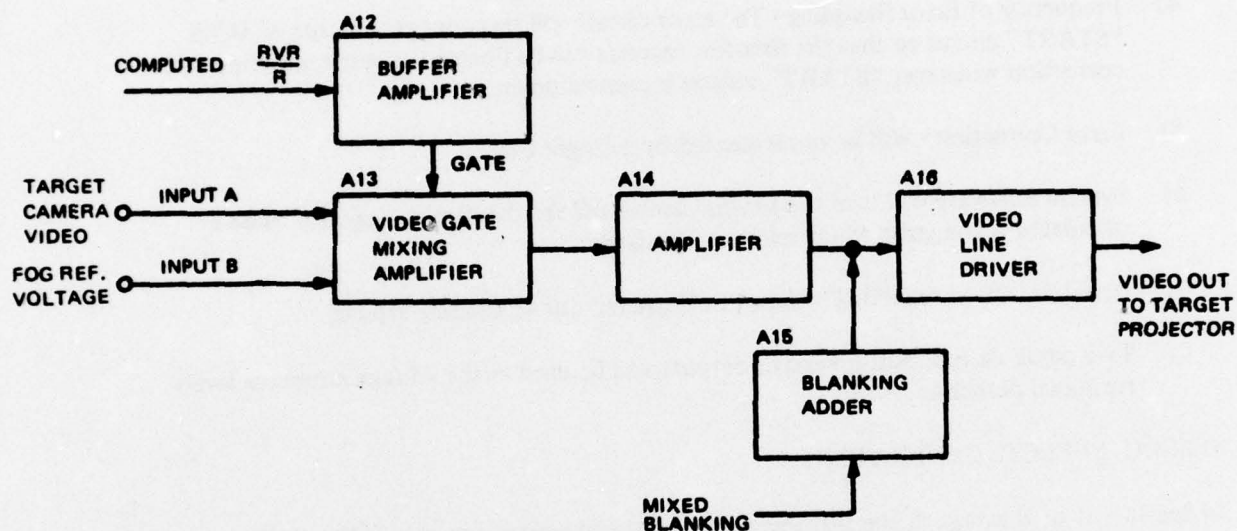


Figure 171. TARGET IMAGE SEG



SECTION XV

CONCLUSIONS

The following section summarizes the conclusions reached in the design analysis. Each subsystem is discussed in relation to the overall system goals.

TARGET IMAGE GENERATION.

A television camera model system is used as the target image generation subsystem. This subsystem consists of a Forrestal class aircraft carrier model, model illumination, optical probe, television camera and gantry system. A 370:1 scale factor was chosen for the design analysis. This scale factor provides for correct pupil placement for simulated range up to 2300 feet using a 24 x 24 foot model board. Simulation of ranges greater than 2300 feet is accomplished by a zoom lens in the optical probe. The analysis shows that perspective distortion of the canted deck for all simulated range will be less than 2 arc minutes.

In order to minimize the registration error of the Fresnel lens optical landing system on the carrier image, it has been concluded that closed loop probe pointing system must be employed.

Illumination of the model board will be uniform over the entire area to provide for future applications, however, some sections of lights can be extinguished to conserve power while still providing sufficient illumination on the carrier model to satisfy the signal requirements of the television camera.

An analysis of the optical probe indicates that a conventional probe, by virtue of its simplicity and ability to resolve vertical surfaces, is the most desirable configuration for the AWAVS application.

A television camera employing a 2-inch intensified vidicon will provide the necessary resolving power and sensitivity. Distortions, resulting from target projection pointing, must be compensated for by use of dynamic raster shaping. This shaping does affect camera performance in the areas of video flashing, lag characteristics, and modulation transfer function. Methods of compensating for these effects have been analyzed and, from this analysis, the effects are considered to be correctable.

Selectable TV sweep rates can be provided to allow for controlled variation of system resolution.

Projection of the target image onto the spherical screen is accomplished through a TV projector, a zoom lens and a set of optics. The 30:1 scale model of the FLOLS is projected through a zoom lens optical system and combined into the secondary image plane of the target projector by a beamsplitter. The target is projected with a highlight brightness of up to 7.7 foot-lamberts with a screen gain of 1.5.

This modest screen gain imposes severe limitations on the design of this subsystem. The analysis is based on a television projector which provides approximately 2,000 lumens into a 40 mm aperture. The required brightness would be obtained with a screen gain of 1.5. An eidophor EP-8 projector will satisfy the above requirements; however, some question remains regarding the ability for this projector to operate on the flight simulator motion system for some of the future applications. It may be necessary to make a compromise in screen gain and brightness requirements such that a projector more suitable to the flight simulator environment can be selected for use on the AWAVS.

BACKGROUND AND WAKE IMAGE GENERATION.

The background image will be generated using a flying spot scanner employing a 5-inch fiber optic faceplate and a contact seascape film plate. The raster reset method of providing velocity cues, up to 400 knots, gives an unlimited gaming area. The altitude cues from 760 feet to the deck are accomplished by raster size modulation. The 9,000 feet of wake will be generated by a separate flying spot scanner (FSS) which is identical to the background image FSS. The wake image video is added to the background image video. To provide correct registration of the wake to the target requires a closed loop system. The scene keying camera is used to close the loop by detecting the correct wake attachment point on the carrier image.

The projection of the background and wake images is accomplished using a TV projector identical to the target TV projector and a wide angle lens which provides the required FOV of 160° horizontal by 80° vertical. The background brightness, including the transmission loss due to the filter required for scene keying, is in excess of six foot-lamberts.

At an MTF of 5%, the TV resolution for the total background image system is 1150 TV lines, 88 percent of the 1300 TV line resolution required. The analysis has concluded that 1150 TV line resolution represents the state of the art for the combined system. The TV projector can be operated at multiple line scan rates.

SPECIAL EFFECTS GENERATION.

The target and background special effects generators will provide varying weather conditions and sea merge.

TARGET SCENE KEYING.

It was determined that reliable target scene keying can be obtained with the target contrast ratio up to 8 shades of gray.

The scene keying system consists of an Isocon camera for detecting the target, a complementary filter to that in the background projection lens and blanking electronics for blanking the background image where the target appears. The spectrum which will be removed from the background will be the red (from approximately 610 monometers) up to the infra-red. Removal of this spectrum will cause the background scene to appear blue-green.

It was concluded from the analysis that the keying system must be a closed loop system. This requires a test-raster pattern generator for the background projector and a dynamic raster computer to correct the system errors. However, the total errors, after correction, can still be as high as 0.5%.

SECTION XVI

RECOMMENDATIONS

The design analysis has explored several methods of implementation which would meet the objectives of the program. The system described under the heading "Recommended System" represents the optimum configuration. It is recommended that direction for implementation of the design be based on this recommended system.

One aspect of the recommended system is still undergoing evaluation. This aspect has to do with the suitability of the selected projector system for future applications. Empirical data in this area is required to define the extent of modifications, if any, to adapt the projector to these future applications.

SECTION XVII

SUMMARY

This section provides a synopsis of the approaches used in attacking the design of the AWAVS individual subsystems.

TARGET IMAGE GENERATOR.

The target image generator consists of a large, vertically-situated, three-dimensional model of an aircraft carrier viewed by a TV camera and optical probe. Both are mounted on a movable gantry that positions the camera and probe in accordance with the position and attitude of the simulated aircraft, when it is within 0.75 nautical miles of the carrier. Some of the features of the proposed design are described in the following paragraphs.

Target Model. The model scale will be 309:1. This is the largest size model that can be accommodated by the standard gantry. This scale minimizes the design difficulty of the probe. The model is to be built of wood or epoxy. The carrier wake is to be on the surface on the model board.

Target Model Illumination. The target model illumination source will be 1000-watt, Sylvania, metal, arc lamps. Illumination is 8500 foot-candles, giving a camera illumination of 0.075 foot-candles, which yields a signal-to-noise ratio (preamplification noise, plus photon noise) of 46 db.

Target Model Motion. Four servos will be used to provide roll, pitch, heave and rotation of the carrier model and rotation of the carrier wake.

Target Optical Probe. The 120° field-of-view probe which was built for Singer by Farrand Optical Company for the F-4E No. 18 will be modified for this project. Modification will consist of lengthening the focal length of the objective lens, adding a servo-controlled iris, and adding a zoom lens. Resolution is calculated to be adequate to meet the requirements of AWAVS. The zoom ratio of the baseline design is 6.36 to 1. The probe has $\pm 135^\circ$ of pitch freedom and continuous roll and yaw freedom.

Target Television Camera. The luminance channel of the F-4E No. 18 camera is used in conjunction with the Westinghouse intensified WX-31836/WX-5168 2-inch vidicon with selenium photoconductor. The line standard is 825 lines. Vertical resolution is 590 TV lines. At 10 arc-min. per line pair the MTF is 78 percent with a signal-to-noise ratio of 46 decibels for an illumination of the faceplate of 0.075 foot-candles.

Target Camera Gantry. The gantry has X, Y, and Z (altitude) ranges of 28, 14, and 2.9 feet, respectively. Response is representative of an F-4J aircraft traveling at up to 400 knots.

TARGET PROJECTOR.

The layout of the target and background projectors relative to the dome and the cockpit is such that the nominal eye position is 15 inches below and 6 inches ahead of the center of the dome. The nominal pupil of the target projector is 10 inches above and 4 inches behind the center of the dome. The following paragraphs describe the components of the target projector.

Projector. An Eidophor EP8 television projector is used. The line standard 825 lines; bandwidth is 15 mhz. The light output of the projector is 4,000 lumens. Vertical resolution is 590 TV lines. At 10 arc-minutes per line pair the MTF is 55 percent at the projector output.

Target Projector Lens. The target projector lens will consist of several, specially-designed field and relay lenses. Their design is straightforward and will present no problems. A commercially-available zoom lens is used to provide the specified 10:1 zoom range. The largest image format zoom lens is used; however, there will still be a considerable loss of light (64%) due to the mismatch between the Eidophor F number and the zoom lens F number. Since there is still enough light to meet specified performance, with the overall transmission of the projector lenses at 7.7%, it is not necessary to design a special zoom lens. At 10 arc minutes per line pair the MTF is 33 percent. The maximum field of view is 63° vignetting will be less than 15%. Illumination of the screen is 1.5 foot-candles. Thus, a minimum screen gain of 4 meets the minimum specification of 6 foot-lamberts brightness.

The angular relation between the pilot's field of view at the nominal eye position and the pupil of the target projector lens has been computed and includes the mappings due to the screen location, and projector optics. From this analysis has come the optimum pointing angles for the target projector.

Target Projector Gimbals. The target projector gimbal consists of an elevation prism gimbal and an azimuth prism gimbal. They are driven by low-inertia dc motor-tachometer assemblies. The elevation prism servo-tachometer will be mounted on the azimuth support frame in a similar manner to the design of the aircraft image generator of the Simulator for Air-to-Air Combat (SAAC). This design provides the advantage of placing the mass of the pitch motor-tachometer on the support frame rather than on the moving gimbals. Rates are 300° /second and acceleration is 15 rad/sec^2 . The design is such that it is physically impossible for the gimbals to make mechanical contact with other stationary components.

FLOLS (FRESNEL LENS OPTICAL LANDING SYSTEM) IMAGE PROJECTOR.

The FLOLS simulation system consists of a commercially-available, zoom lens optical system, which projects the image of a 30:1 scale model of a Mark 6 MOD 1 FLOLS into the secondary image plane of the target projector. A unique bar mirror is used to efficiently transfer the light into the target projector optical system. The FLOLS lights are operated under computer control to three servos.

FLOLS Motion System. The FLOLS image is adjusted in size using a commercially-available 4:1 zoom lens. The image is properly simulated from near the point of intended touchdown to 15nm. Field of view is $\pm 20^{\circ}$ of runway centerline. The rotation is accomplished using a Pechan prism. X-Y position is done by registering the probe carrier image on the FLOLS image. Tracking accuracy is within 5% of the carrier width, if the probe is operated in a closed loop mode.

FLOLS Illumination. Two 500-watt, xenon arc lamps with fiber-optic light guides will be used to light the lights on the FLOLS model. The estimated brightness of a white light projected on the screen is greater than 100 foot-lamberts. The various color filters will reduce this brightness. Dynamically, the brightness undergoes a hundredfold increase. A servo-controlled iris assembly will be used to compensate for this increase and maintain correct brightness of the FLOLS display.

BACKGROUND IMAGE GENERATOR.

The nominal position of the pupil of the background projector is 24 inches above and 11 inches behind the center of the dome.

The device consists of a flying-spot scanner, stationary film transparency, and photomultiplier sensor. Clouds will be amorphous and will be generated by a special effects generator.

Image Content. The background consists of Sea State 2 or 3 to within 10° of the horizon, haze to the horizon, and amorphous clouds. The proper mapping function is achieved by using a raster computer to shape the flying-spot scanner raster. The azimuth and elevation angles, measured at the nominal position of the background projector pupil for constant azimuth and elevation angles at the nominal eyepoint, are computer-generated.

The computer program used to generate these data is extended to include the mapping functions of the projector lens, Eidophor projector, and image generator in order to compute the coefficients for the raster computer.

In the basic system, only heading and attitude information is presented. However, alternate systems which do provide altitude and velocity information are described.

Background Projector. The background projector is an Eidophor EP8. It and the projection lens are mounted so that they can be easily rotated to position 1 or 2 without disassembling equipment.

The bandwidth of the Eidophor projector is 20 MHz. Scan line standard is 825 lines. The illumination on the screen is at least 6.7 foot-candles.

Background Projector Lens. The background projector lens is a modification of a wide-angle anamorphic $60^{\circ} \times 160^{\circ}$ lens developed for NTEC by Willey Optical.

The nominal 80° vertical by 160° horizontal coverage of the Willey lens is adequate for covering the $+50^{\circ}$ to -30° vertical by 160° horizontal field of view of the pilot.

Background Projector Support Structure. The background projector and lens assembly is mounted above the target projector. The construction is a truss-type, designed to withstand acceleration of up to 4g. The background projector and lens can be easily changed in position to provide the two difference fields of view in accordance with Specification 212-102.

DISPLAY SCREEN.

The display screen is an assembly of spherical sectors bolted together to form a partial sphere with a radius of 10 feet \pm 0.5 inches. It is designed to withstand a 4g acceleration with no detectable deformation. An optical-quality screen with a gain of approximately 4 will be provided over $\pm 120^{\circ}$ horizontal and $+90^{\circ}$, -30° vertical, as measured from the pilot's nominal eye position.

SERVO SYSTEMS.

All servo systems are designed to meet the AWAV system requirements. Their individual types and rates are presented later in this report.

TARGET INSETTING.

The recommended method of target insetting is a technique known as projected scene keying.

MATH MODEL.

Math models are provided with the visual system to drive the components of the AWAVS, in accordance with aircraft attitude and position, as obtained from the simulator equations of motion, and in accordance with the coordinate definitions provided in this report. The software required is based on proven software currently operating with the Singer-SPD Mark V, F-4E No. 18, and SAAC Systems.

SPECIAL EFFECTS GENERATOR.

The special effects generator electronically modifies an input video signal to realistically create the impression of: Overcast ceiling (stratiform clouds); Restricted visibility; Above-cloud flight (undercast stratus clouds); and scud above clouds.

Two special effects generators are used — one for the background display system and one for the target display system. Both systems are based on designs used on the F-4E No. 18 Simulator.

FUTURE ADDITIONS.

In the baseline design developed by Singer-SPD, the growth potential requirement of paragraph 3.2.7.2 of the procurement specification has been taken into account. The capabilities of growth options are compared with the operational requirements for them. These requirements are discussed in greater detail in the body of this report.

Design of the AWAVS was researched with the intent of maximum reuseability of visual/video designs that have been developed on other Singer-SPD programs. Therefore, if a system already existed, has proven itself successful, and was found to be compatible with AWAVS, then the system design was integrated into the AWAVS design, and no alternatives were considered.

REFERENCE FOOTNOTES LIST

1. L. Levi and R. H. Austing, Applied Optics 7 , 961 (1968).
2. Paragraph - TARGET TV PROJECTOR, Section 3.
3. Paragraph - DIGITAL-ANALOG RASTER COMPUTER.
4. Paragraph - TARGET TELEVISION CAMERA, Section 2.
5. Source Data: A. F. Collier memo No. VD/AFC/73-148, dated 9/07/73.
6. Source Data: Telephone Conversation with Eidophor, LTD, 9/12/73.
7. Paragraph Performance Requirements, Section 2.
8. Paragraph - FLOLS Image Movement, Section 4.
9. Paragraph - FLOLS Registration of Carrier, Subparagraph Optical Probe Pointing Errors, Section 4.
10. Paragraph - Closed-Loop Probe to Model, Section 4.
11. Paragraph - First Order Description, Section 4.
12. Paragraph - FLOLS Luminance, Section 4.
13. Paragraph - Closed-Loop Probe to Model, Section 4.
14. Paragraph - SIGNAL DETECTION AND PROCESSING.
15. Paragraph - Flight Envelope, Section 5.
16. Ibid.
17. Paragraph - Flying-Spot Scanner System.
18. Paragraph - Video Signal Processing, Subparagraph Photomultiplier, Section 5.
19. Paragraph - Background Image Generator Modulation Transfer, Section 5.
20. Paragraph - Signal Detection and Processing, Section 5.
21. Paragraph - Flight Envelope, Section 5.
22. Paragraph - Raster Shapes, Section 5.
23. Paragraph - Signal Detection and Processing, Section 5.
24. Paragraph - Flying-Spot Scanner System, Section 5.
25. Paragraph - Signal Detection and Processing, Section 5.
26. Paragraph - BIG System Visual Resolution, Section 5.
27. Paragraph - Altitude Cues, Section 5.
28. Ibid.
29. Paragraphs - Signal Detection and Processing, and Altitude Cues, Section 5.
30. Paragraph - Video Signal Processing, Section 5.
31. Paragraph - Background Image System MTF Analysis, Section 6.
32. Paragraph - BIG System Visual Resolution, Section 5.
33. Ibid.
34. Ibid.

35. Paragraph - Target Television Camera, Section 2.
36. Paragraph - ERROR TERMS ON VIDEO INSETTING.
37. Ibid.
38. Paragraph - DIGITAL-ANALOG RASTER COMPUTER (DARC).
39. Paragraph - TV PROJECTOR.
40. Paragraph - Overall System Description, Section 10.
41. Paragraph - Determination of Desired Target Projector Video Blanking.
42. Paragraphs - Instructor Station Controls and Displays, and Servo Systems.
43. Paragraph - TARGET TELEVISION CAMERA.
44. Paragraph - DIGITAL ANALOG RASTER COMPUTER.
45. Reference Osram Data Sheet L/5 5/62.
46. Paragraph - Light-Emitting Source With Position-Sensitive Detector.
47. Paragraph - Altitude Cues.
48. Paragraph - Velocity Cues; Subparagraph - Reset Raster Cue.
49. Paragraph - FLYING SPOT SCANNER SYSTEM.
50. Paragraph - Altitude Cues; Subparagraph - Functional Analysis.

LIST OF ABBREVIATIONS

AOI	- Area of Interest
AWAVS	- Aviation Wide Angle Visual System
BIG	- Background Image Generator
BIP	- Background Image Projector
B/S	- Beamsplitter
BW	- Bandwidth
CDNV	- Calligraphic Day/Night Visual
CGI	- Computer Generated Imagery
Q_c , C/L	- Centerline
CM	- Camera Model
CRC	- Camera Raster Computer
CRT	- Cathode Ray Tube
DARC	- Digital-Analog Raster Computer
DIG	- Digital Image Generator
EFL	- Effective Focal Length
FLOLS	- Fresnel Lens Optical Landing System
FOV	- Field of View
FSS	- Flying Spot Scanner
IR	- Infra-Red
LOS	- Line of Sight
LP	- Lumens Per
MDAC	- Multiplying Digital-to-Analog Converters
MTF	- Modulation Transfer Function
RSS	- Root Sum Squared
SARC	- Static-Analog Raster Computer
SEG	- Special Effects Generator
SKC	- Scene Keying Camera
SKI	- Scene Keying Inset
SNR	- Signal to Noise Ratio
STG	- Synthetic Terrain Generator
TVL	- Television Lines (?)
WIG	- Wake Image Generator

SYMBOL DICTIONARY.

VBBVF	-	Background projector fast scan voltage.
VBBVS	-	Background projector slow scan voltage
VBC	-	Constants
VBVFV	-	FSS fast scan voltage
VBVVS	-	FSS slow scan voltage
VPF 1 & 2	-	Functions of background projector voltages giving FSS voltages.
VBI	-	Counter
VBJ	-	Counter
VBK 1 & 2	-	Constants
VBN	-	Truncation limit for a series
VFALC	-	Angle between line of sight and carrier deck
VFAGL	-	Angle between the glide slope and the line of sight
VFBA	-	FLOLS lens box basic angle
VFFIS	-	Boolean indicating FLOLS turned on at instructors station
VFGSA	-	FLOLS glideslope angle
VFIIS	-	Brightness setting from instructor's station
VFIISC	-	FLOLS iris intensity constant
VFIRC	-	FLOLS iris range constant
VFISV	-	Iris servo drive signal voltage
VFLOLS	-	FLOLS viewing angle
VFMBV	-	meatball drive signal voltage
VEFIF	-	Boolean indicating FLOLS is the center of area of interest
VFREF	-	Line of sight range from the nominal viewing point to the center of the FLOLS

NAVTRAEQUIPCEN 75-C-0009-1

VFRSC	-	FLOLS roll servo voltage constant
VFRSV	-	FLOLS roll servo roll servo drive signal voltage
VERTI	-	Roll angle of the target image at the combining mirror
VFSVC	-	Meatball servo voltage constant
VFXEC	-	X coordinate of nominal viewing point in carrier frame
VFXFC	-	X coordinate of center of FLOLS in carrier frame
VFYCL	-	Perpendicular distance from angled deck center line to center of FLOLS measured in the plane of the deck
VFYEC	-	Y coordinate of nominal viewing point in carrier frame.
VFYFC	-	Y coordinate of center of FLOLS in carrier frame
VFZEC	-	Z coordinate of nominal viewing point in carrier frame
VFZFC	-	Z coordinate of center of FLOLS in carrier frame
VFZLV	-	Zoom lens drive signal voltage
VFZSVC	-	Zoom lens servo voltage constant
VIAB	-	"a" axis of the ellipse on background projector
VIAT	-	"a" axis of the ellipse on target projector
VIBB	-	"b" axis of the ellipse on background projector
VIBT	-	"b" axis of the ellipse on target projector
VIFBM	-	Function which finds the maximum value of b from the ellipse equation
VII	-	Counter
VIKB 1-6	-	The constants given to the hardware from which the ellipse is generated on the background projector
VIKT 1-6	-	The constants given to the hardware for the target projector
VIM	-	No. of points chosen from the carrier
VIMAC	-	Mapping function from the area of interest frame to the camera frame

NAVTRAEQUIPCEN 75-C-0009 -1

VIMAX	-	Function which finds the point in a set of points which is most distant from a given point.
VIMCT	-	Mapping from the camera to the target projector
VIMTB	-	Mapping from the target projector to the background projector
VIN	-	Total No. of points chosen to describe the carrier and wake
VITBC	-	$\cos \theta$ in background projector frame
VITBS	-	$\sin \theta$ in background projector frame
VITCW	-	Rotation-translation matrix from carrier to wake
VITOA	-	Rotation-translation matrix from observer to area of interest
VITTC	-	$\cos \theta$ in the target projector frame
VITTS	-	$\sin \theta$ in the target projector frame
VITWO	-	rotation-translation matrix from the wake to the observer frame
VIXA	-	X, Y, Z coordinates in the area of interest frame
VIXB	-	X, Y, Z coordinates in the background projector frame
VIXC	-	X, Y, Z coordinates in the carrier frame
VIXM	-	X, Y, Z coordinates in the camera frame
VIXO	-	X, Y, Z coordinates in the observer frame
VIXT	-	X, Y, Z coordinates in the target projector frame
VIXW	-	X, Y, Z coordinates in the wake frame
VIYBC	-	Y coordinate of the "center of mass" in the background projector frame
VIYBE 1-2	-	Y coordinate of the 1st and 2nd end points of the "a" axis in the background projector frame
VIYBO	-	Y coordinate of the ellipse center in the background projector frame
VIYTC	-	Y coordinate of the "center of mass" in the target projector frame
VIYTE 1-2	-	Same as VIYBE 1-2 in target projector frame

NAVTRAEQUIPCEN 75-C-0009-1

VITYO	-	Same as VIYBO in target projector frame
VIZBC	-	Z coordinate of the "center of mass" in the background projector frame
VIZBE 1-2	-	Z coordinates of the 1st and 2nd end points of the "a" axis in the background projector frame
VIXBO	-	Z coordinate of the ellipse center in the background projector frame
VIZTC	-	Same as VIZBC in target projector frame
VIZTE 1-2	-	Same as VIZBE 1-2 in target projector frame
VIZTO	-	Same as VIZBO in target projector frame
VPAAI	-	Incremental change in the point of interest azimuth angle
VPAAPD	-	Difference between the new and old azimuth angles of the point of interest in the observer frame
VPAAPI	-	Azimuth angle of the point of interest in the observer frame
VPAAPP	-	Old azimuth angle of the point of interest in the observer frame
VPAP	-	Target projector azimuth angle
VPAPC	-	Scaling factor of azimuth to voltage
VPAPV	-	Voltage driving azimuth prism
VPC	-	Constants of proportionality between coordinates in the real world and these in the simulator
VPCF	-	Function defining constants in terms of sphere radius, origin displacement and azimuth and elevation angles
VPDR	-	Display screen radius
VPDXNC	-	X displacement of nominal viewing point from sphere center
VPDXPN	-	X displacement of projector from nominal viewing point
VPDZNC	-	Z displacement of nominal viewing point from sphere center
VPDZPN	-	Z displacement of projector from nominal viewing point
VPEAI	-	Incremental change in point of interest elevation angle
VPEAPD	-	Difference between new and old elevation angles of the point of interest in the observer frame

NAVTRAEQUIPCEN 75-C-0009-1

VPEAPI	-	Elevation angle of the point of interest in the observer frame
VPEAPP	-	Old elevation angle of the point of interest in the observer frame
VPEP	-	Target projector elevation angle
VPEPC	-	Scaling factor of elevation to voltage
VPEPV	-	Voltage driving elevation prism
VPFPIA	-	Fixed point of interest angle relative to the X observer axis
VPFZR	-	Function of range which gives projector zoom
VPH	-	Relevant hardware characteristics
VPHNEC	-	Height of the nominal viewing point above the simulated carrier deck
VPPAMV	-	Maximum velocity of probe azimuth servo
VPPL	-	Relevant lens characteristics
VPPPMV	-	Maximum velocity of probe pitch servo
VPPR	-	Projector roll
VPPRC	-	Scaling factor of roll to voltage
VPPRV	-	Voltage which drives roll
VPPZ	-	Projector zoom
VPPZC	-	Scaling factor of zoom to voltage
VPPZV	-	Voltage which drives zoom
VPTBO	-	Aircraft body frame to observer frame transformation matrix
VPTCB	-	Carrier frame to aircraft body frame transformation matrix
VPXAC	-	X coordinate of the aircraft in the carrier frame
VPXFC	-	X coordinate of the aircraft relative to the FLOLS in the carrier frame
VPXFOC	-	X coordinate of the FLOLS in the carrier frame
VPXPI	-	X coordinate of the point of interest in the observer frame

NAVTRAEQUIPCEN 75-C-0009-1

VPXPID	-	X coordinate of the point of interest in the simulator observer frame
VPXPIP	-	X coordinate of the point of interest in a frame parallel to the observer frame with origin at the target projector
VPYAC	-	Y coordinate of the aircraft in the carrier frame
VPYFC	-	Y coordinate of the aircraft relative to the FLOLS in the carrier frame
VPYFOC	-	Y coordinate of the FLOLS in the carrier frame
VPYPI	-	Y coordinate of the point of interest in the observer frame
VPYPID	-	Y coordinate of the point of interest in the simulator observer frame
VPYPIP	-	Y coordinate of the point of interest in the same frame as VPXPIP
VPZAC	-	Z coordinate of the aircraft in the carrier frame
VPZFC	-	Z coordinate of the aircraft relative to the FLOLS in the carrier frame
VPZFOC	-	Z coordinate of the FLOLS in the carrier frame
VPZPI	-	Z coordinate of the point of interest in the observer frame
VPZPID	-	Z coordinate of the point of interest in the simulator observer frame
VPZPIP	-	Z coordinate of the point of interest in the same frame as VPXPIP
VSA	-	Aircraft altitude
VSDC	-	Transformation matrix from earth to aircraft
VSPC	-	Cosine of aircraft pitch angle
VSPS	-	Sine of aircraft pitch angle
VSRC	-	Cosine of aircraft roll angle
VSROA	-	Visibility range over altitude
VSRS	-	Sine of aircraft roll angle
VSRVR	-	Visibility range
VTA	-	Scaling factor

NAVTRAEQUIPCEN 75-C-0009-1

VTACA	-	Angle to the aircraft to carrier line makes with the carrier X axis.
VTAL	-	Aircraft body axes to area of interest direction cosine matrix
VTAR	-	Resolver angle of probe relay azimuth
VTAWD	-	Angle the wake is rotated with respect to the display
VTB	-	Gantry axes system to aircraft body direction cosine matrix
VTBGR	-	Background image generator response
VTC	-	"Constants"
VTCTWL	-	Height of the center of rotation of the carrier above the water line
VTDLCL	-	Distance from the desired probe position to the inner limit circle
VTDLCL	-	Distance to the outer limit circle
VTDR	-	Resolver angle of probe derotation
VTDV	-	Voltage needed to drive disk
VTFC1	-	The function of the fast camera voltage which gives the X coordinate of the point scanned
VTFC2	-	The function of the slow camera voltage which gives the Y coordinate of the point scanned
VTFP1	-	The function of the X coordinate of the point scanned which gives the fast projector voltage.
VTFP2	-	The function of the Y coordinate of the point scanned which gives the slow projector voltage.
VTF1	-	The function of the projector voltages which gives the X camera voltage
VTF2	-	The function of the projector voltages which gives the Y camera voltage
VTHC	-	Heave displacement as computed by the carrier dynamics module
VTHM	-	Heave drive signal voltage to the model
VTHP	-	Probe azimuth
VTHSR	-	Model heave servo response

NAVTRAEQUIPCEN 75-C-0009 -1

VTI	- Counter
VTJ	- Counter
VTK	- Constants
VTKD	- "Constants"
VTK1	- Attenuation constant for model pitch servo
VTK2	- Attenuation constant for model roll servo
VTK3	- Attenuation constant for model heave servo
VTMCA	- Mapping from camera to area of interest
VTMDP	- Mapping from display to projector
VTN	- Summation limit
VTP	- Gantry to probe direction cosine matrix
VTPC	- Pitch angle as computed by the carrier dynamics module
VTPM	- Pitch drive signal voltage to the model
VTPSR	- Model pitch servo response
VTR	- distance to point of interest
VTRC	- Roll angle as computed by the carrier dynamics module
VTRCA	- Range from carrier to aircraft
VTRCRC	- Distance from desired probe position to the carrier center of rotation projected onto the X-Y gantry plane
VTRI	- Distance to the island from the desired probe position
VTRILC	- Radius of inner limit circle
VTRM	- Roll drive signal voltage to the model
VTROLC	- Radius of outer limit circle
VTRR	- Resolver angle for zoom

VTRSR	-	Model roll servo response
VRTT	-	Transition angle for attenuating model motion
VTRW	-	Time rate of change of VTYAC + VTXAC
VTSF	-	Model scale factor
VTSP	-	Probe heading
VTSR	-	Resolver angle of probe heading
VTTA	-	Tilt angle
VTTAO	-	Transformation from area of interest to observer frame
VTTAR	-	Resolver angle for tilt
VTTCG	-	Carrier to gantry frame transformation matrix
VTTOD	-	Transformation from observer to display frame
VTTP	-	Probe pitch
VTTR	-	Resolver angle for probe pitch
VTTWG	-	Wake frame to gantry frame transformation matrix
VTVAD	-	Time rate of change VTAWD
VTVFC	-	X camera voltage
VTVFP	-	X projector voltage
VTVP	-	Probe height
VTVSC	-	Y camera voltage
VTVSP	-	Y projector voltage
VTVXA	-	X component of aircraft velocity
VTVXG	-	X component of probe velocity
VTVYA	-	Y component of aircraft velocity

NAVTRAEQUIPCEN 75-C-0009-1

VTVYG	-	Y component of probe velocity
VTW	-	Zoom position
VTWR	-	Resolver angle for iris
VTXA	-	X, Y, Z coordinates in area of interest frame
VTXAC	-	X coordinate of aircraft in carrier frame
VTXAG	-	X coordinate of aircraft in gantry frame
VTXAGA	-	Actual X coordinate of gantry
VTXAGD	-	Desired X coordinate of gantry in fantry frame
VTXC	-	X coordinates in camera frame
VTXCRG	-	X coordinate of carrier center of rotation in gantry frame
VTXCRW	-	Coordinate of carrier center of rotation in wake frame
VTXD	-	X, Y, Z coordinates in display frame
VTXDC	-	X axis deceleration constant
VTXG	-	X coordinate of the probe
VTXGPE	-	Gantry position error X coordinate
VTXGSC	-	X axis gantry servo constant
VTXI	-	X component of the island from the carrier center of rotation
VTXMVC	-	X gantry servo maximum velocity constant
VTXO	-	X, Y, Z coordinates in observer frame
VTXP	-	X coordinates in projector frame
VTXPE	-	Out of synchronization Boolean
VTXPEM	-	Maximum position error to remain in synch
VTXVC	-	X gantry velocity constant
VTXVCA	-	X component of carrier and aircraft relative velocity

NAVTRAEQUIPCEN 75-C-0009-1

VTXVCM	-	X component of maximum gantry velocity constant
VTXVO	-	X component of desired gantry velocity
VTXVGV	-	X axis gantry drive signal voltage
VTXVL	-	X axis model visual limit
VTXVLE	-	X coordinate of model visual limit exceeded
VTYAC	-	Y coordinate of aircraft in carrier frame
VTYAG	-	Y coordinate of aircraft in gantry
VTYAGA	-	Actual Y coordinate of gantry
VTYAGD	-	Desired Y coordinate of gantry in gantry frame
VTYC	-	Y coordinates in camera frame
VTYCRG	-	Y coordinate of carrier center of rotation in gantry frame
VTYCRW	-	Y coordinage of carrier center of rotation in wake frame
VTYDC	-	Y axis deceleration constant
VTYG	-	Y coordinate of the probe
VTYGPE	-	Gantry position error Y coordinate
VTYGSC	-	Y axis gantry servo constant
VTYI	-	Y component of the island from the carrier center of rotation
VTYMVC	-	Y gantry servo maximum velocity constant
VTYP	-	Y coordinates in projector frame
VTYVC	-	Y gantry velocity constant
VTYVCA	-	Y component of carrier and aircraft relative velocity
VTYVCM	-	Y component of maximum gantry velocity constant
VTYVD	-	Y component of desired gantry velocity
VTYVGV	-	Y axis gantry drive signal voltage

NAVTRAEQUIPCEN 75-C-0009-1

VTYVL	-	Y axis model visual limit
VTYVLE	-	Y coordinate of model visual limit exceeded
VTZ	-	Focus position
VTZAC	-	Z coordinate of aircraft in carrier frame
VTZAG	-	Z coordinate of aircraft in gantry frame
VTZAGA	-	Actual Z coordinate of gantry
VTZAGD	-	desired Z coordinate of gantry in gantry frame
VTZCRG	-	Z coordinate of carrier center of rotation in gantry frame
VTZCRW	-	Z coordinate of carrier center of rotation in wake frame
VTZDC	-	Z axis deceleration constant
VTZGPE	-	Gantry position error Z coordinate
VTZGSC	-	Z axis gantry servo constant
VTZMVC	-	Z gantry servo maximum velocity constant
VTZPMD	-	Minimum probe height to clear deck
VTZPMI	-	Minimum probe height required to clear the island
VTZR	-	Resolver angle for focus
VTZVC	-	Z gantry velocity constant
VTZVCA	-	Z component of carrier and aircraft relative velocity
VTZVCM	-	Z component of maximum gantry velocity constant
VTZVD	-	Z component of desired gantry velocity
VTZVGV	-	Z axis gantry drive signal voltage

DISTRIBUTION LIST

Defense Documentation Center (12)	Headquarters (1)
Cameron Station	U.S. Marine Corps
Alexandria, Virginia 22314	CMS A03C
	Washington, D.C. 20380
Commanding Officer (38)	
Naval Training Equipment Center	U.S. Army Training Device (4)
Orlando, Florida 32813	Agency
	Orlando, Florida 32813
Chief of Naval Education & (1)	
Training Support	AF HRL/ASM (1)
Code N-21	Attn: Mr. Don Gum
Pensacola, Florida 32508	Wright Patterson AFB, Ohio 45433
Chief of Naval Education & (1)	
Training	AF HRL (1)
Code N-331	Attn: Col. J.D. Boren
Pensacola, Florida 32508	Williams AFB, Arizona 85224
Naval Air Systems Command (6)	
AIR 340F	AF ASD/ENE (1)
Washington, D.C. 20350	Attn: Mr. A. Doty
	Wright Patterson AFB, Ohio 45433
Chief of Naval Operations (1)	
OP 59	Scientific Technical (1)
Washington, D.C. 20350	Information Office
	NASA
Chief of Naval Material (1)	Washington, D.C. 20546
Navy Department	
Code 0324	NASA Ames Research Center (1)
Washington, D.C. 20360	Moffett Field, California 94035
	Attn: Mr. J. Dusterberry
Commander (1)	
Naval Air Development	NASA Langley Research Center (1)
Center Library	Attn: Mr. Kurbjan
Warminster, Pennsylvania 18974	Hampton, Virginia 23365
Chief of Naval Research (1)	
ONR 461	
800 North Quincy Street	
Arlington, Virginia 22217	
Chief Naval Air Training (1)	
Training Research Department	
NAS Corpus Christi, Texas 78719	